TESIS DOCTORAL

Programa de Doctorado en Biología Fundamental y de Sistemas

Peroxisomal-dependent signalling in plant response to abiotic stress

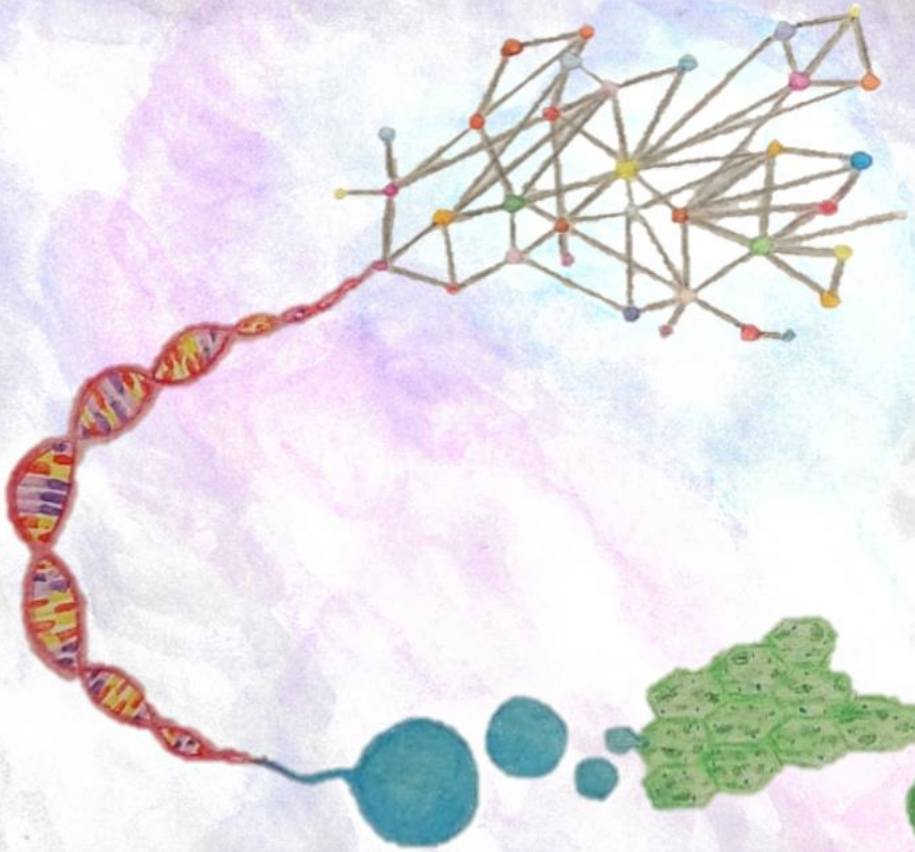

Mª Ángeles Peláez Vico

University of Granada

Doctoral Programme in Fundamental and Systems Biology

Consejo Superior de Investigaciones Científicas (CSIC)

Estación Experimental del Zaidín (EEZ)

Department of Biochemistry and Cellular and Molecular Biology of Plants

Ministerio de Ciencia, Innovación y Universidades

Peroxisomal-dependent signalling in plant response to abiotic stress

DOCTORAL THESIS

Mª Ángeles Peláez Vico

Granada, november 2021

Editor: Universidad de Granada. Tesis Doctorales
Autor: Mª Ángeles Peláez Vico
ISBN: 978-84-1117-199-1
URI: http://hdl.handle.net/10481/72323

Financiación

Esta Tesis Doctoral ha sido realizada en el Departamento de Bioquímica y Biología Celular y Molecular de Plantas de la Estación Experimental del Zaidín (EEZ), del Consejo Superior de Investigaciones Científicas (CSIC) de Granada, dentro del grupo de investigación de Señalización por especies de Oxígeno y Nitrógeno Reactivo en Situaciones de Estrés en Plantas.

/

This Doctoral Thesis has been performed in the Department of Biochemistry and Cellular and Molecular Biology of Plants, at Estación Experimental del Zaidín (EEZ), from the Spanish National Research Council (CSIC) of Granada, within the research group of Reactive Oxygen and Nitrogen Species Signalling under Stress Conditions in Plants.

La financiación para el trabajo realizado procede de las siguientes fuentes:

/

This work has been funded via:

- Programa Estatal de Promoción del Talento y su Empleabilidad en I+D+i. Subprograma Estatal de Formación de Personal Investigador (FPI). Referencia: BES-2016-076518
- Plan Nacional (BIO2015-67657-P), cofinanciado por Fondos FEDER
- Plan Estatal, Generación del Conocimiento (PGC2018-098372-B-I00), cofinanciado por Fondos FEDER

Publicaciones

Los resultados presentados en esta Tesis Doctoral han sido publicados en las siguientes revistas internacionales o estan en vías de publicación:

/

The results presented in this Doctoral Thesis have been published in the following international journals or are in the process of being published:

Sandalio LM, **Peláez-Vico MA**, Romero-Puertas MC. (2020). Peroxisomal metabolism and dynamics at the crossroads between stimulus perception and fast cell responses to the environment. Frontiers in Cell and Developmental Biology 8, 1-5. IF: 6,68; Q1.

Sandalio LM, **Peláez-Vico MA,** Molina Moya E, Romero-Puertas MC. (2021). Peroxisomes as redox-signalling nodes in intracellular communication and stress responses. Plant Physiology 186, 22-35. IF: 8,34; D1.

Romero-Puertas MC, Terrón-Camero LC, **Peláez-Vico MA,** Molina Moya E, Sandalio LM. (2021). An update on redox signals in plant responses to biotic and abiotic stress crosstalk: insights from cadmium and fungal pathogen interactions. Journal of Experimental Botany 72, 5857-5875. IF: 6,99; D1.

Romero-Puertas MC, **Peláez-Vico MA,** Pazmiño DM, Rodríguez-Serrano M, Terrón-Camero LC, Bautista R, Gómez-Cadena A, Claros MG, León J, Sandalio LM. (2021). Insights into ROS-dependent signalling underlying transcriptomic plant responses to the herbicide 2,4-D. Accepted in Plant, Cell and Environment (IF: 7,23).

Congresos

Asimismo, parte de los resultados obtenidos durante esta Tesis Doctoral han sido presentados en los siguientes congresos y reuniones científicas:

/

Also, part of the results obtained during this Doctoral Thesis have been presented at the following congresses and scientific meetings:

- II Young Researchers Science Symposium, 2017 (Granada, Spain). Comunicación oral: Caracterización funcional de *PEX11a* en la respuesta de los peroxisomas al estrés. **Peláez-Vico MA**, Sandalio LM, Romero-Puertas MC.

- Desgranando Ciencia, Hablando de Ciencia, 2017 (Granada, Spain). Póster I: Game of Plants. Terrón-Camero LC, Molina-Moya E, **Peláez-Vico MA**, Rodríguez V, Sandalio LM, Romero-Puertas MC. Póster II: Los peroxisomas, esos grandes desconocidos. **Peláez-Vico MA**, Terrón-Camero LC, Olmedilla-Arnal A, Sandalio LM, Romero-Puertas MC.

- Open European Peroxisome Meeting, 2018 (Groningen, The Netherlands). Póster: Insights into the peroxisomal *ACX1* ROS-dependent cell response to the

herbicide 2,4-D in plants. Romero-Puertas MC, Rodríguez-Serrano M, **Peláez-Vico MA**, Bautista R, Pazmiño DM, Claros MG, Olmedilla A, Sandalio LM.

- II Congreso/IV Jornadas de Investigadores en Formación: Fomentando la interdisciplinariedad (JIFFI), 2019 (Granada, Spain). Comunicación oral: Función de *PEX11a* durante la respuesta de los peroxisomas al estrés por cadmio. **Peláez-Vico MA**, Sandalio LM, Romero-Puertas MC.

- XV Meeting of Plant Molecular Biology, 2020 (online). Póster: Expression pattern and identification of key proteins involved in PEX11a regulation in plant response to cadmium. **Peláez-Vico** MA, Molina-Moya E, Terrón-Camero LC, Sandalio LM, Romero-Puertas MC.

Estancia

Parte de los resultados expuestos en la presente Tesis han sido logrados durante la estancia financiada por la ayuda FPI anteriormente citada, y desarrollada en el "Institut des Sciences de la Vie", de la Université Catholique de Louvain (UCL) en Louvain-la-Neuve (Bélgica), bajo la supervisión del Dr. Henri Batoko.

/

Part of the results exposed in this Thesis has been achieved during the stay granted by the above mentioned FPI Internship, and was carried out in the Institut des Sciences de la Vie, from the Université Catholique de Louvain (UCL) of Louvain-la-Neuve (Belgium), under supervision of Dr. Henri Batoko.

Agradecimientos

El camino no ha sido fácil. Ha habido resultados inexplicables, algún gen fantasma, plásmidos que no eran lo que decían ser, no *Agrobacteriums* que se creían *Agrobacteriums,* archivos de RNA-seq eliminados, digestiones de bandas mezcladas, complots de microscopios, discos duros retenidos en la aduana… Hasta aquí más o menos los problemas normales de un doctorando, pero ¿y si te digo que además esta Tesis ha sobrevivido a dos mudanzas, con obras y traslados de laboratorio incluidos? Y, por si fuera poco…una pandemia. Con estos antecedentes comprenderás que estoy orgullosa de poder finalmente escribir estas líneas, y triste porque esta etapa se termina. Tengo mucho que agradecer, por eso pido perdón desde ya por si me olvido de alguien.

María, gracias por dedicar mucho de tu tiempo y energía a mis victorias y a mis fracasos (más de los últimos que de los primeros). Por corregirme cuando algo no estaba bien hecho, y por aportar soluciones a los callejones sin salida. Admiro tu capacidad para lidiar con mil frentes a la vez y que nunca tengas una mala palabra para nadie, incluso tras horas de música y conversaciones no fácilmente digeribles... Gracias por la confianza y la manga ancha con los habitantes del 206. Por enseñarme a pensar de manera más crítica, creo que voy por el buen camino. Infinitas gracias por todo lo que me llevo.

Luisa, muchas gracias por estar siempre dispuesta a aportar un punto de vista distinto y por tener un *paper* preparado en la recámara. Por animarme a seguir formándome en todos los ámbitos. Admiro que seas capaz de almacenar tantísima información y darle forma al rompecabezas para que todo tenga sentido. Me sorprende que a pesar de todos los años que le has dedicado a la ciencia, sigues manteniendo la pasión y las ganas de mejorar. Muchas gracias por todo.

Adela, gracias por la alegría que vas repartiendo, las anécdotas y los consejos. Siempre que ha estado en tu mano has intentado ayudarme, muchas gracias. Me faltó jamón para haber sido tu ahijada… Disfruta mucho de la etapa que viene, te has ganado las "vacaciones".

A **Soco**, por ser mi tutora de Tesis y atenderme siempre con la mejor predisposición.

Al Dr. **Henri** Batoko y a la gente del ISV. Por darme la oportunidad de aprender mucho sobre proteínas, aunque la nuestra sea una puñetera. Fueron 3 meses intensos y una experiencia muy recomendable, ¡qué bonita es Bélgica!

A mis **TF-leches** y gente de paso por el *lab*, María, J.A, Marina, Fran, Espe, Bashma "Batman", Víctor, Natalia "holaaa" (leer con acento adecuado), Oriana, Wided. **Laura** "ventresca", ojalá y podamos vernos pronto en Italia o en Granada, pero con comida de por medio. **Manuel**, "el argentino que quiere ser un andaluz buenorro", una pena que no coincidiéramos en persona para unirme a las risas con vos. Gracias por compartir memes y arte, ¡tengo pendiente una visita por tu tierra! **Jesús**, a pesar de que eres un voyeur en el grupo, sabes que te aprecio. Gracias por acogernos en CR y enseñarnos esa "bonita" ciudad. Sé que siempre nos reencontraremos en nuestra cita anual de libertinaje en Madrid. Mucha suerte en esta nueva etapa. Y por favor, no fumes más cosas de colores.

¿Qué decir de **mis bichas**, de mis flamencas lab! Tengo claro que esta Tesis no habría podido ver la luz sin vosotras, gracias de corazón AMIGAS. ¡Buenos días **Eliana**! Perfectas aliadas en limpieza y organización, gracias por hacer que me guste el rosa un poco más. Pequeña malafollá, ha sido un placer enorme trabajar contigo, te irá bien y te seguirás quejando, pero hay que quererte así. Espero volver a coincidir contigo, ya sea barriendo calles, contratadas para emitir sonidos propios de animales o con

suerte, en un laboratorio. Me alegro mucho de haber compartido chapas varias, canciones desafinadas, bricomanías, ataques de risa, secretos, fiestas, litros de aceite y algún que otro experimento… Hemos llegado a tal punto, que con una mirada nos lo decimos todo. ¡Eres lo más muack! Mil gracias por la ayuda desinteresada, pequeña.

La tercera pata del banco ¡mi puchi **Lau**!, gracias por hablar bien de mí para que me contrataran. Nadie coloniza espacios de trabajo tan bien como tú. Eres pura dedicación, y prueba de ello son las 300 cajas, tuppers, tarros, bolsas y toda clase de recipientes con muestras que nos has dejado en el lab. No tengo palabras para explicar tooooro lo que has hecho por mí. He aprendido infinito contigo, y he aprendido muy bien. Aunque los p-value del RNA-seq y las troleadas de Excel y R sigan sin tener sentido. Sé que te esperan cosas muy buenas, porque te lo mereces. Pero por favor intenta sentarte mejor. Un besi para ti también Casi.

He disfrutado mucho dentro y fuera del lab con vosotras. Para nosotras quedan los "días internacionales de…", los "niña, ¡baja la radio!" los experimentos malditos, los motes, las carcajadas que se oyen en otros edificios, los desayunos, las confesiones, los audios-cotilleo, salir a las tantas… ha sido un inmenso placer trabajar con vosotras, GRACIAS.

A **mis niñicos**, que han hecho esta etapa más amena, por surtirme con comida, *bullying* y ánimos, memes infinitos, pero sobretodo momentos para el recuerdo.

Rubén "retrasado", no puedo decir que seas un buen guía insular pero sí que eres buena gente a pesar de ser canario y de inventarte que tienes padres. Ojalá más visitas a la fábrica de Arehucas, más festivales, muñecos de "nieve" oscura y atardeceres. Gracias por tanto almogrote, mojo, chorizo, tirmas, canela, audios de telenovela… Han sido muchas horas y copas de Yllera para el recuerdo. Y no, no me pico.

Edu "*Arabidipsis*", tengo la espalda destrozada (guiño, guiño). Ojalá volver a los ataques de risas falsas. Te agradezco mucho tus masajes y tu apoyo moral, siempre ofreciendo ayuda a quien la necesitara. Seguro que encuentras un trabajo donde valoren lo meticuloso que eres. Y si no, ya sabes que tienes voz radiofónica. Te quiero, aunque creas que el mejor chocolate viene de Almería…

Au, espero que no te dejes el pelo largo más, ni te vuelvas a afeitar (¡por favor!) y que sigas troleando a la gente y abriendo debates incómodos, son mis favoritos. Y no traigas más piñonate, que si no estoy yo no se lo va a comer nadie… Espero que tengas suerte y acabes tu Tesis pronto para poder dedicarte a tu verdadera pasión, el *jugger*. Mil gracias por ayudar siempre que te lo he pedido. Y deja de renegar de tu tierra, ¡especialito!

Álex (bien de tilde), no puedo elegir un solo mote para ti, "no ha nacido quién". Sabes que has sido y eres un proyecto personal. Me alegro inmensamente de haber coincidido contigo, eres una (uuuuufffaaaaaaa) persona especial y me has aportado muchísimo. Tienes que mejorar la tolerancia a los micro infartos, pero vas por muy buen camino. Espero seguir recibiendo karaokes y memes. Como científico no hay duda de que vales mil, y de que esto es lo tuyo. Mi "último" consejo es que no intentes ser tan cuadriculado y que disfrutes del doctorado, porque ¡el tiempo pasa volando! Sé que echarás de menos los trombitos y las aperturas de ojos.

No puedo olvidarme de la Veneno, Octodecanona, Brasero, Horse, Waterparties, los infernillos, los "en celo", "aquí huele a tostada", tacones, putrefacciones, #ustésecuide, "el confesionario está abierto", fuegotes, bien de etanol, casi matagatos, Lores y Macus, plutones, cianuro, Sandro Rey, #quesoylaxinniloco, desatranques Jandro, anuncios de seguros, llamadas a seguridad, 2-nonenal, purgaciones, #eeeeerleee los viernes, tómbola antojitos… casi 5 años dan para mucho.

Felipe, gracias por echarme una mano en la última etapa. Te deseo mucha suerte con tu Tesis y en el grupo. Espero que pronto haya más findes de playa, y barbacoas en Villa Pokémon. Y por favor, reduce tu ingesta de sal.

Ana, mi acaricida favorita, mil gracias por tu indispensable ayuda con la molecular, y a tu grupo por su generosidad. No sé cuántas fotos, audios, semillas y plásmidos tuyos me han salvado la vida. Gracias por ser tan buena gente. Ojalá volver pronto a Villa Amparo o a otro *escape room* distinto, pero culminar con fuego real esta vez… PD: me debes una boda.

A toda la gente generosa de la EEZ. No puedo nombrarlos a todos, pero sí quiero destacar a nuestros vecinos de la primera planta (**Mariam**, **Antonio, Pao**…) por donarnos plásmidos, reactivos, protocolos y consejos. A **Silvia**, **Patri** y ***Pasheco***, por ser infinitamente generosos. Aunque reconozco que prefería ir a pedir cuando no estaba LA jefa, nunca me habéis negado nada. Gracias por la ayuda con los embrollos moleculares, por las risas y los consejos. A **M. José Soto** por inculcarme el gusanillo y por seguir ayudando siempre que ha estado en su mano. A **Ricardo**, por sacarme la vena psicóloga que tanto me gusta y por MARUMARI, ¡sopa! Me alegro mucho de que una charla de ciencia hiciera que nos conociéramos. Gracias por los buenos ratos, ¡nos quedan muchos más! **Salva**, mi archienemigo doctoral… encantada de haber recibido tus visitas, ya fuera para echarnos unas risas y criticar (en la mayoría de los casos), para pedir algo o simplemente por aburrimiento. **Leyre** "¿a quién no le va a gustar un baptisterio romano del siglo primero?", una pena no haber coincidido más tiempo. Espero que estés mejorando tu asento cubano, mami. Tengo pendiente una ruta por tu País. A **María Sanz** por los ánimos de los comienzos. A **Coral** por su contribución con la bioinformática. A todos los habitantes de la **EEZ** que intentan hacer la vida más fácil al resto (administración, informática, limpieza, mantenimiento…).

Mi agradecimiento también a **Dolo** (UGR) por la donación de hormonas, y a los servicios del **CIC** (David) por las horas de microscopio. A **Edu** (IPBLN) por la ayuda con el análisis del RNA-seq.

A mis **amigos** de toda la vida, Barbarie y Pescarios, imposible nombrarlos a todos. Gracias por distraerme con tantos y tan variados planes, aunque os he maldecido muchas veces cuando preguntabais "qué, ¿cómo va la tesis?". Sé que nunca habéis entendido realmente lo que hacía en el laboratorio, pero los ánimos me llegaban igual, gracias.

A San Antonio y Santa Rita porque al final, y a pesar de los maltratos, me han ayudado a acabar la Tesis. A Alexandra Elbakyan, por hacernos la vida un poco más fácil y barata, *because scientific knowledge belongs to humanity.* A los sacos de Brooklyn Fitboxing, a Hans Zimmer, a Two Steps from Hell, a Tagus, Netflix, HBO, Chuy y compañía por los ratos de no ciencia.

A mi **peque**, mi *Marío*, por ser mi otra mitad desde hace ya más años de los que puedo contar con 2 manos. El que se ha llevado algún que otro momento malo y me ha animado a seguir adelante. Gracias por haberme hecho el camino mucho más fácil, por no cuestionar, o por cuestionar cuando tocaba. No podría haber encontrado mejor compañero de vida, admiro lo cabezón que eres y que siempre quieras aspirar a más. Espero poder seguir mejorando juntos, sea donde sea. Te quiero INFINITO.

A mi **familia**: a mis padres, porque son las personas a las que más admiro y por enseñarme que las cosas hay que ganárselas. Porque habéis apoyado a "la niña" en todo lo que ha querido hacer y os seguís esforzando para darme siempre lo mejor. A mis hermanos, por confiar en mí, por los buenos ratos y por darme a los soles que tengo por sobrinos. OS QUIERO.

A la ciencia, porque como escribió Mary Shelley "quien no haya experimentado la seducción que la ciencia ejerce sobre una persona, jamás comprenderá su tiranía».

Trust I seek and I find in you
every day for us something new
open mind for a different view
and nothing else matters.

Nothing Else Matters (Metallica)

Index

Summary

There are numerous environmental conditions that are continuously changing and that affect all organisms, including plants. As an evolutionary adaptation, plants have developed specific mechanisms that allow them to cope with these adverse conditions. Environmental changes cause stress in plants and their response usually begins with the perception of the stress, followed by changes in metabolism and accompanied by gene expression alterations and protein modifications. All these processes are expected to induce an efficient response to the stress. Key players in orchestrating this response are reactive oxygen and nitrogen species (ROS/RNS), which build signalling networks with external and internal signals. ROS/RNS are generated during cell metabolism. Under normal conditions antioxidant system controls ROS/RNS production, however at high or uncontrolled concentrations, a rapid accumulation takes place, leading to cellular damage. One of the main sites for ROS/RNS generation in the cell are peroxisomes. These organelles are highly dynamic and metabolically active and are found in almost all eukaryotic cells. Peroxisomes are closely linked to mitochondria and chloroplasts, sharing metabolic pathways, as well as the import and transport of proteins. Organelles/compartments-dependent signalling communication to the nucleus, termed retrograde signalling, from mitochondria and chloroplast in stress response are better understood than in peroxisomes. Different types of stresses and the subsequent response of the plant are studied in our group, being the common link the peroxisome and the production of the signal molecules ROS/RNS. Thus, the present Thesis aims to elucidate peroxisomal-dependent signalling in plant response to abiotic stress as general objective.

In **Chapter 1**, we have analyzed plant response to the synthetic auxin 2,4-dichlorophenoxyacetic acid (2,4-D). This auxin is used as an herbicide at high concentrations, and induces ROS production in plant cells and an epinastic phenotype. We found that acyl CoA oxidase 1 (ACX1), the first enzyme in the fatty acid β-oxidation occurring in the peroxisome, is one of the main sources of ROS production after 2,4-D treatment. Transcriptomic analyses of WT plants exposed to this stress revealed two different responses. An early response, in which a ROS-related peroxisomal footprint was detected and later responses, in which other organelles, such as mitochondria and chloroplasts, are involved. We also determined that peroxisomal ROS derived from ACX1

regulated a large number of genes previously associated with epinasty and also the expression of the auxin receptor AUXIN SIGNALLING F-BOX 3 (AFB3) at early times. AFB3 together with the SCF (ASK-cullin-F-box) E3 ubiquitin ligase complexes, was shown to mediate auxins degradation by the 26S proteasome downstream of ACX1, and we have found that AFB3 in an ACX1-dependent way, is involved in the epinastic phenotype induced by 2,4-D. Later ACX1-dependent genes in plant response to 2,4-D are related with proteasome, which we have shown to be also involved in epinasty development.

Adjustments in gene expression are essential to trigger a suitable response to environmental cues, being the peroxisomes a key source of signalling molecules. In **Chapter 2**, and given the scarcity of information related to retrograde signalling of the peroxisome under stress conditions, we carried out a meta-analysis to try to bring some light on this topic. After collecting data from different public and in-house transcriptomes with mutants and/or stresses leading to disturbances of peroxisomal-dependent ROS production, we identified a data set of common and peroxisomal-specific genes regulated by ROS from this organelle, under different conditions. Thus, we found 101 and 86 genes commonly regulated at short-time and long-time stress treatments, respectively. Enrichment analysis with early peroxisomal-dependent genes showed their involvement in response to stress/stimulus, and a high co-expression, suggesting an early coordinated peroxisomal-dependent plant response to stress. In particular, these genes clustered in two main nodes related to heat shock factors (HSFs) and jasmonic acid (JA) biosynthesis and signalling. Genes commonly regulated at long-time were enriched in terms also related to stress and clustered in a gene network related to JA biosynthesis, suggesting that peroxisomal retrograde signalling is a coordinated response to avoid damages in the cell and to protect proteins under stress conditions.

Plasticity of peroxisomes enables them to adapt their morphology, number and movement to changes in their surroundings. Although peroxisomal proliferation has been described for a long time, many aspects of this process remain undiscovered. Peroxins 11a-e (PEX11a-e) proteins are involved in the first stage of peroxisomal proliferation. Furthermore, *PEX11a* have been shown to be essential for peroxules production, very dynamic extensions produced by peroxisomes and regulated by ROS and NO in response to cadmium (Cd). However, functionality of PEX11a and therefore, of peroxules, is not well

known. In **Chapters 3 and 4** we have tried to expand the knowledge about functionality of peroxules under control and stress conditions. For this purpose, we have generated mutant lines: 1) by CRISPR/Cas9 altering *PEX11a* gene *(pex11a-CR)* and 2) by cross-polination, generating double mutants with a T-DNA insertion in PEX11a locus and with a CFP *(px-ck)* located in peroxisomes *(pex11a-SKI x px-ck)*. As a result of changes in protein sequences, a fragment in the C-terminal is absent in both *pex11a* mutants, being the functional protein shorter in *pex11a-CR* lines. Despite of peroxisomal phenotype observed in each mutant was different, both *pex11a* mutants were unable to produce peroxules in response to Cd, confirming PEX11a involvement in peroxules formation and fast response to stress. An *in silico* analysis of PEX11a expression, regulation and putative posttranslational modifications (PTMs) of the protein was carried out. We suggest that the presence or not of target aminoacids for different PTMs in *pex11a-CR* and *pex11a-SKI x px-ck* sequence, could explain the differences observed in the peroxisomal phenotype between them. We also carried out a phenotypical characterization revealing that early germination was altered in *pex11a-CR*, which could be due to changes in fatty acid metabolism. Lateral roots, as well as foliar area, were reduced in *pex11a-CR* mutants. Furthermore, we checked Cd response in *pex11a* mutants using confocal microscopy and histochemistry, confirming proliferation of these organelles in response to Cd in *px-ck* seedlings. Curiously, *pex11a*-CR lines did not display a statistically significant peroxisomes increment in the presence of Cd by laser microscopy but different results were observed by histochemistry.

To take a deep insight into the role of PEX11a in plant response to Cd stress, we performed transcriptomic analysis included in **Chapter 4**. *px-ck* and *pex11a-CR* seedlings were treated with Cd (100 μM) for 1 h and 24 h. Functional annotation analysis of genes differentially expressed (DEGs) revealed numerous alterations related to morphology and metabolism of chloroplasts in *pex11a-CR* under control conditions. In addition, DEGs in *pex11a-CR* in non-treated plants were assigned to pathways such as photosynthesis, porphyrin and chlorophyll metabolism, glutathione metabolism and starch and sucrose metabolism. Experimental data of pigment content and organelle ultrastructure confirmed transcriptional results, showing alterations of thylakoid/stroma rate and reduction of chlorophylls and carotenoids content in the mutants, respect to the WT background. Under control conditions we also determined a reduction in starch

accumulation. In response to Cd 1h we found a higher number of DEGs in *pex11a-CR* compared to *px-ck* (6,192 vs. 3,485). We filtered the early *PEX11a*-dependent genes regulated after Cd 1 h, and their enrichment showed categories related to iron homeostasis and transport. Enrichment of the later transcriptional response to Cd (24 h) displayed a link with nucleus, ribosomes, translation and peptide metabolic and biosynthetic processes.

These results together support the key function for peroxisomes in plant development and plant response to stress being able to regulate different processes such as protein protection networks under stress, hormonal-dependent signalling and biosynthesis, such as for AUX and JA, nutrition and development.

Resumen

Las condiciones ambientales cambian continuamente, afectando a todos los organismos, incluidas las plantas. Evolutivamente las plantas han desarrollado mecanismos específicos que les permiten hacer frente a las condiciones adversas. Los cambios en el entorno provocan estrés en las plantas y su respuesta empieza con la percepción del estrés, seguida de cambios en el metabolismo y acompañada de alteraciones en la expresión génica y modificaciones en proteínas. Todos estos procesos están dirigidos a dar una respuesta eficaz al estrés, en la que las especies reactivas de oxígeno y nitrógeno (ROS/RNS) son fundamentales. Las ROS/RNS se generan en células vegetales como consecuencia del metabolismo celular y participan como moléculas señal. En condiciones normales, los sistemas antioxidantes controlan la producción de ROS/RNS, sin embargo, si se acumulan de forma no controlada, se provoca daño celular. Uno de los principales compartimentos celulares donde se producen las ROS/RNS son los peroxisomas. Estos orgánulos son muy dinámicos y metabólicamente activos y se encuentran en casi todas las células eucariotas. Los peroxisomas están estrechamente relacionados con las mitocondrias y los cloroplastos, ya que comparten vías metabólicas, así como el importe y transporte de proteínas. La comunicación/señalización entre los distintos compartimentos y el núcleo se denomina señalización retrógrada. En mitocondrias y cloroplastos y en respuesta a estrés, esta señalización se ha estudiado ampliamente mientras que en peroxisomas la información disponible es escasa. En nuestro grupo se estudia la respuesta de la planta a diferentes tipos de estreses, siendo el nexo común el peroxisoma y el papel señalizador de las ROS/RNS. Por tanto, la presente Tesis tiene como objetivo general dilucidar la señalización dependiente de peroxisomas en la respuesta de las plantas al estrés abiótico.

En el **Capítulo 1**, analizamos la respuesta de las plantas a la auxina sintética ácido 2,4-diclorofenoxiacético (2,4-D). Esta auxina se utiliza como herbicida a altas concentraciones, e induce la producción de ROS en la célula y un fenotipo de epinastia. Describimos cómo la enzima acil CoA oxidasa 1 (ACX1), que participa en la β-oxidación de los ácidos grasos en el peroxisoma, es una de las principales fuentes de producción de ROS tras el tratamiento con 2,4-D. Los análisis transcriptómicos de plantas WT expuestas a este herbicida revelaron diferentes vías de producción de ROS. En una

respuesta temprana, intervenía principalmente el peroxisoma, y en una respuesta posterior, estaban más involucrados las mitocondrias y los cloroplastos. También determinamos que las ROS peroxisomales derivadas de ACX1 regulaban una gran cantidad de genes previamente asociados con la epinastia, y también la expresión del receptor de auxinas AUXIN SIGNALLING F-BOX 3 (AFB3) a tiempos cortos. Se demostró que AFB3 junto con el complejo de ubiquitinación SCF median la degradación de auxinas por el proteasoma 26S aguas abajo de ACX1, y que está involucrado en el fenotipo de epinastia inducido por 2,4-D. Los genes dependientes de ACX1 a tiempos posteriores están relacionados en parte, con el proteasoma, que hemos demostrado también está relacionado con el desarrollo de la epinastia.

Los ajustes en la expresión génica son esenciales para desencadenar una respuesta adecuada a las señales ambientales, siendo los peroxisomas una fuente clave de moléculas de señalización. En el **Capítulo 2**, y dada la escasez de información relacionada con la señalización retrógrada del peroxisoma en condiciones de estrés, realizamos un meta-análisis para intentar aportar algo de luz. Recopilamos datos de transcriptomas publicados y de nuestro grupo, sobre mutantes y/o condiciones que alteran los niveles de ROS peroxisomal. Se identificó un conjunto de genes comunes y específicos regulados por ROS peroxisomal. Concretamente, encontramos 101 genes regulados a tiempos cortos y 86 a tiempos largos. El enriquecimiento funcional de los genes de tiempos cortos demostró su presencia en categorías relacionadas con percepción y respuesta a estímulos. Además, se encontró una alta co-expresión entre estos genes, lo que sugiere una respuesta temprana coordinada de la planta dependiente del peroxisoma. En particular, estos genes se agruparon en dos nodos principales relacionados con proteínas de choque térmico y de biosíntesis y señalización de JA. En los genes regulados por ROS peroxisomal a tiempos largos también se encontraron categorías relacionadas con el estrés y biosíntesis de JA. Estos resultados sugieren que la señalización retrógrada peroxisomal es una respuesta coordinada para evitar daños en la célula y proteger a las proteínas en condiciones de estrés.

La plasticidad de los peroxisomas les permite adaptar su morfología, número y dinámica a los cambios en su entorno. Aunque la proliferación peroxisomal se ha descrito ampliamente, muchos aspectos de este proceso aún se desconocen. Las proteínas peroxinas 11a-e (PEX11a-e) están involucradas en la primera etapa de la proliferación

peroxisomal. Además, se ha demostrado que PEX11a es esencial en la producción de peróxulos. Se trata de unas extensiones muy dinámicas producidas por los peroxisomas y que están reguladas por ROS y NO en respuesta al cadmio (Cd). Sin embargo, no se conoce bien la funcionalidad de PEX11a ni la de los peróxulos. Para abordar estos interrogantes, en los **Capítulos 3 y 4** se han generado líneas mutantes mediante tecnología CRISPR/Cas9 alterando el gen PEX11a *(pex11a-CR)* y dobles mutantes con una inserción de T-DNA en el locus PEX11a y con un marcaje CFP *(px-ck)* en los peroxisomas *(pex11a-SKI x px-ck).* Como resultado de los cambios en las secuencias de la proteína, en ambos mutantes un fragmento del extremo C-terminal se pierde siendo la proteína funcional más corta aún en el mutante *pex11a-CR*. Determinamos que ninguna de las líneas mutantes producía peróxulos en respuesta al Cd, sino que se formaban yemas en su lugar, lo que confirma la participación de PEX11a en la respuesta rápida a este estrés. Curiosamente, el fenotipo de los peroxisomas observado era distinto en cada mutante. Por otro lado, se llevó a cabo un análisis *in silico* sobre la expresión y regulación de *PEX11a*, como de las modificaciones post-traduccionales (PTMs) de la proteína. Sugerimos que la presencia o no de aminoácidos diana para diferentes PTM en las secuencias *pex11a-CR* y *pex11a-SKI x px-ck*, podría explicar las diferencias observadas en el fenotipo peroxisomal entre ellos. También realizamos una caracterización fenotípica que reveló que el inicio de la germinación temprana estaba alterado en *pex11a-CR*, lo que podría deberse a cambios en el metabolismo de los ácidos grasos. Se observó que las raíces laterales y el área foliar se reducían en este mutante. Además, se comprobó la respuesta de los mutantes al Cd mediante microscopía confocal e histoquímica, confirmando la proliferación de estos orgánulos en respuesta a Cd en plántulas *px-ck* previamente descrita. Curiosamente, las líneas *pex11a-CR* no mostraron un incremento significativo de peroxisomas en presencia de Cd por microscopía confocal, pero se observaron resultados diferentes por histoquímica.

Para profundizar en la función de PEX11a en la respuesta de la planta al estrés por Cd, se realizó un análisis transcriptómico incluido en el **Capítulo 4**. Las plántulas de *px-ck* y *pex11a-CR* se trataron durante 1 h y 24 h con Cd (100 µM). El enriquecimiento funcional de los genes diferencialmente expresados (DEGs) reveló numerosas alteraciones en *pex11a-CR* relacionadas con la morfología y el metabolismo de los cloroplastos en condiciones de control. Además, el análisis de las categorías KEGG de los

DEGs en muestras control de *pex11a-CR* mostró su implicación en fotosíntesis, metabolismo de porfirinas y clorofilas, glutatión, almidón y sacarosa. Los datos experimentales de contenido de pigmentos y la ultraestructura de estos orgánulos confirmaron los resultados de transcriptómica. Se encontró un contenido más bajo de clorofilas y carotenoides, así como de almidón, además de alteraciones en la distribución de los tilacoides. En respuesta a Cd 1 h, se encontró un mayor número de DEGs en *pex11a-CR* en comparación con *px-ck* (6.192 frente a 3.485). Tras filtrar los genes dependientes de *PEX11a* regulados después del tratamiento con Cd 1 h, se realizó un enriquecimiento que los asociaba a procesos de homeostasis y transporte de hierro. La misma aproximación se hizo con los genes regulados en el mutante a las 24 h y se halló la posible vinculación con núcleo, ribosomas, traducción y procesos metabólicos y biosintéticos de péptidos.

Estos resultados apoyan la importancia de los peroxisomas como orgánulos clave el desarrollo de la planta y en su respuesta al estrés, estando relacionado con diferentes procesos como la protección de las proteínas, la biosíntesis y señalización dependiente de hormonas como el JA y las AUX, la nutrición y el desarrollo.

General Introduction

A. Stress in plants

Being sessile organisms, plants must sense and respond to a variety of stresses such as high/low temperature, high/low light, and the presence of heavy metals, herbicides or pathogens occurring within a very short time period. Thus, plants have developed a series of specific mechanisms that allow them to grow and adapt to changeable adverse conditions, enabling them to acclimate, survive and reproduce (Zandalinas *et al.*, 2019; Fichman and Mittler, 2020).

Traditionally, plant response to stress includes four phases (based on Lichtenthaler 1998): (1) response phase, at the beginning of stress and is represented by an alarm reaction accompanied by a decrease in conventional physiological functions; (2) restitution or resistance phase, composed by resistance of adaptation processes, repair processes, as well as reactivation processes, which occur as the stress continues; (3) final phase or long-term stress, when the stress intensity is too high and the adaptation capacity is overloaded, the stage of exhaustion leads to chronic disease or death; and (4) regeneration phase, the stressor is removed and the regeneration of the physiological function can be partial or full. When stress exceeds the limits of tolerance and adaptability, the plant can be permanently damaged or even die (Sade *et al.*, 2018; Hasanuzzaman *et al.*, 2020); however, if this point is not reached, stress cause destabilization in the plant, followed by normalization and improved resistance in some cases (Kollist *et al.*, 2019), boosting a faster evolution (Karanja *et al.*, 2019).

From another point of view, the stress response might be classified as local or systemic, taking into account which part of the plant senses the stress. Perception of alterations of environmental conditions might occur at the whole-plant level (systemic response), or more often, only a small part of the plant (local response) senses the change before the rest of the plant (Choudhury *et al.*, 2017; Zandalinas *et al.*, 2019). Therefore, the sensing tissue will generate a systemic signal that will travel to other parts of the plant, triggering acclimation and defence mechanisms, even if they did not yet sense the stress or the change in environmental conditions (Kollist *et al.*, 2019). Systemic signalling from local to systemic tissues enables the plant to rapidly acclimate to the coming change in the environment and to survive it better. Thereby, this kind of response has been

reported for biotic and abiotic stresses (Choudhury *et al.*, 2017; Katano *et al.*, 2018; Kollist *et al.*, 2019; Xie *et al.*, 2019; Fichman and Mittler, 2020; Romero-Puertas *et al.*, 2021).

Plant signalling operates at the level of cell compartments, whole cells, tissues, organs or even plant communities. The aim is to organise adequate physiological responses such as modification of enzyme activity, cytoskeleton structure or gene expression in response to external and internal signals. To achieve this, plants have evolved a network of signalling proteins including plasma membrane receptors and ion transporters, cascades of kinases and other enzymes, as well as several second messengers such as reactive oxygen/nitrogen species (ROS/RNS), cytosolic calcium (Ca^{2+}), or cyclic nucleotides (cAMP and cGMP) among others (**Fig. 1**; (Sandalio and Romero-Puertas, 2015*a*; Demidchik *et al.*, 2018; Romero-Puertas *et al.*, 2021).

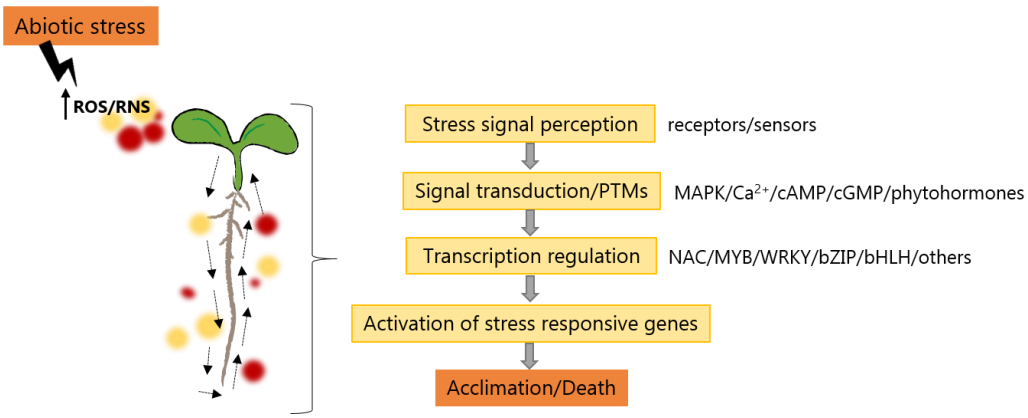

Figure 1. Scheme of general plant abiotic stress response. *The reactive oxygen and nitrogen species (ROS/RNS) are important signal molecules in plants and key regulators of a variety of processes, including abiotic stress response. Abiotic stress causes overproduction of ROS and RNS in cells so a tight regulation between ROS/RNS generation and elimination is necessary to allow plant acclimation.*

A.1 Cadmium (Cd) in the environment

Despite the natural occurrence within the earth's crust of many natural chemical elements, most of which are essential to life, others like mercury (Hg), aluminium (Al), lead (Pb) and cadmium (Cd) are potentially toxic when they accumulate (Genchi *et al.,* 2020; Balali-Mood *et al.*, 2021). Approximately 70 metallic chemical elements are classified as heavy metals and metalloids, which have relatively high density compared to water and whose concentrations in the earth's crust range from less than 0.1 % to less than 0.01 %

(Tchounwou *et al.*, 2012; Hurdebise *et al.*, 2015). Some of these non-essential metal(oid)s may be highly toxic even at low concentrations, such as Cd, Hg, Pb and arsenic (As; (Mustafa and Komatsu, 2016; Fu and Xi, 2020).

Some geogenic processes such as the rock weathering are responsible for heavy metals accumulation in soil (Wang *et al.*, 2021). Additionally, anthropogenic activities like agricultural activities (irrigation, limestone amendments, as well as inorganic fertilizers, pesticides and sewage sludge), electricity generated from coal and oil, industrial activities (smelting operations, electroplating or chemical products), mining or houlsehod waste, contribute to environmental pollution and human exposure to these toxic metals (**Fig. 2;** (Shahid *et al.*, 2018; Kumar *et al.*, 2019; Deng *et al.*, 2020; Okereafor *et al.*, 2020).

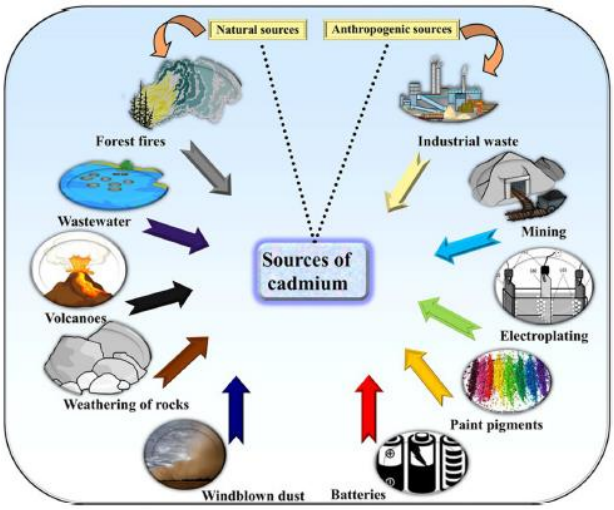

Figure 2. Sources of cadmium in agricultural soils. *Scheme of the main natural and anthropogenic sources of the heavy metal cadmium (from Shahid et al., 2018).*

Excess of heavy metals has become a dangerous problem to agriculture, the environment and human health. When heavy metals are accumulated, the soil quality decrease and contaminate plants, coupled with erosion and vegetal cover loss, which lead to the transport of pollutants to subterranean and superficial water. Moreover, they can enter into the food chain, causing severe health concerns to (Sahay and Gupta, 2017). Plant roots can upload Cd where is mainly retained but it also may be translocated to others organs, entering into the food chain (Shahid *et al.*, 2018; Wang *et al.*, 2021). In fact, Cd has been found in a wide range of food samples, such as cereals, vegetables, nuts, tubers, or tea, with concentrations ranging from 0.01 to 0.39 mg/kg dry weight (Oymak

et al., 2009; Clemens *et al.*, 2013; Zhong *et al.*, 2016). The European Food Safety Authority (EFSA) established a provisional tolerable monthly intake of 2.5 µg/kg body weight and european countries are close to or slightly exceeding this limit (EFSA, 2012). High intake of Cd is considered a significant health risk to humans, and it has been associated with various diseases such as cancer, hypertension, cardiovascular and pulmonary disorders, skin and eye damages and neurodegenerative problems, among others (Fu and Xi, 2020; Unsal *et al.*, 2020).

The heavy metal Cd has been listed as one of the top 10 hazardous substances (Agency for Toxic Substances and Disease Registry-ATSDR, 2019). This heavy metal is not believed to play a role in higher biologic systems or human nutrition (Mehri, 2020), although it has been described a biological role for Cd in marine diatoms (Lane and Morel, 2000). The bioavailability of Cd is highly dependent on soil structure, organic matter and pH (Clemens and Ma, 2016). The main routes through which Cd increase its presence in the environment are mining, industrial activity and phosphate fertilizers used in agriculture (Clemens *et al.*, 2013).

A.1.1 Cadmium toxicity in plant cells

Cd is highly toxic to plants partly due to its chemical similarity to essential elements such as iron (Fe), manganese (Mn), zinc (Zn) and Ca, which enable Cd to enter the plant and replace these elements in a variety of biological processes (Nordberg *et al.*, 2018; Meng *et al.*, 2019). Metals with no known function as Cd use the specific transporters through which plants take up nutrient metals (Clemens *et al.*, 2013). Therefore, Cd could enter plant cells via cation transporters of minerals such as Fe, Ca and Zn (Aravind and Prasad, 2005; Terrón-Camero *et al.*, 2019; Chaffai and Cherif, 2020) and once inside, this metal can be immobilized in the vacuole or can be translocated to the upper side of the xylem through apoplast or symplastic routes (Socha and Guerinot, 2014).

The main effects of Cd-induced toxicity in plants are showed in **Fig 3**: 1) macro- and micro-nutrient imbalance, which is one of the first symptoms. Particularly, it occurs with Fe and Ca due to the Cd similarity to nutrient cations, resulting in competition for absorption at the root (Sandalio *et al.,* 2001; Loix *et al.*, 2017; Sahay and Gupta, 2017;

Chaffai and Cherif, 2020); 2) imbalance in the redox status causing oxidative stress as a consequence of alterations in antioxidant defences, the indirect triggering of Fenton reactions and the respiratory chain impairment. ROS generation provokes damage to macromolecules (Romero-Puertas *et al.*, 1999; Cuypers *et al.*, 2016; Gupta *et al.*, 2017) and 3) enzyme inactivation when Cd replaces essential metals, changing their structure or function (Schützendübel *et al.*, 2002). As a result of these effects, inhibition of seed germination, decrease in plant growth and yield occurs, and even genotoxicity and plant death (Kalaivanan and Ganeshamurthy, 2016; Mustafa and Komatsu, 2016; Ayangbenro and Babalola, 2017; Tiwari and Lata, 2018).

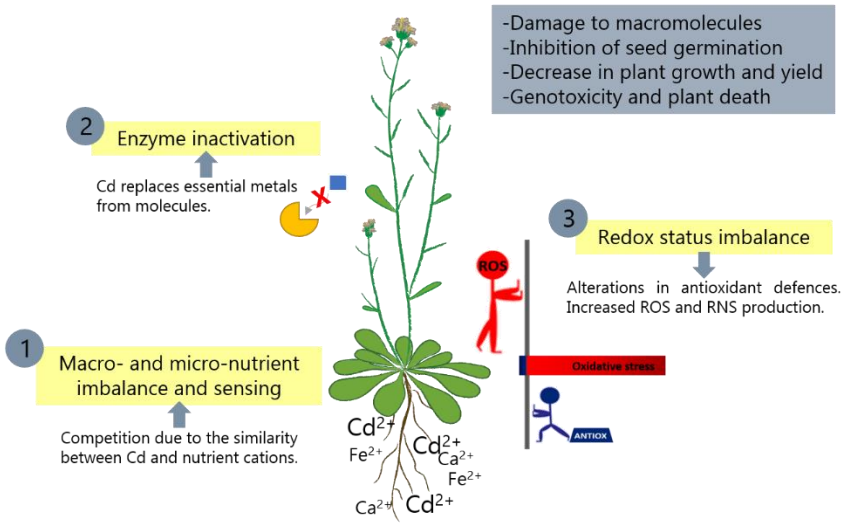

Figure 3. Overview of cadmium effects in the plant cell. *Cd interferes with the entry and transport of nutrients and causes oxidative stress and inactivation of enzymatic activities. General effects of Cd are showed in the blue rectangle.*

A.2 2,4-dichlorophenoxyacetic acid (2,4-D)-mediated stress in plants

The 2,4-dichlorophenoxy acetic acid (2,4-D) was the first synthetic auxin analogue to indole-3-acetic acid (IAA, natural auxin) used in agriculture as herbicide for the control of broadleaf weeds in the 1940s. It was developed during the World War II and its low cost has led to continued usage today and it remains one of the most commonly used herbicides in the world (Song, 2014; Zuanazzi *et al.*, 2020).

Chemical characteristics of 2,4-D as well as its extensive use favor its widespread occurrence in the environment (Islam *et al.*, 2018). Contamination of soil and water with

2,4-D can affect environment and human health. In fact, the toxic effects of this herbicide have been associated with endocrine disruption, reproductive disorders, genetic alterations, carcinogenic effects or neurodegenerative disease (Zuanazzi *et al.*, 2020).

The dose dependent mode of action of 2,4-D causes different effects on sensitive species. Thus, at low concentrations 2,4-D stimulates growth and developmental processes and at high concentrations act as herbicide, disturbing the normal growth and provoking lethal damage in the plant (Grossmann, 2000; Pazmiño *et al.*, 2014; Song, 2014). 2,4-D induces ROS over-accumulation and oxidative stress as well as disturbances in actin cytoskeleton structures. Actin disturbances increases epinasty and alterations in the dynamics of organelles such as peroxisomes and mitochondria (Rodríguez-Serrano *et al.*, 2014), which are involved in ROS/RNS metabolism. 2,4-D-dependent oxidative effects in plants have been widely studied, although the signalling mechanisms and the role of ROS in regulating plant responses to 2,4-D it is not clear.

A.3 Reactive Oxygen Species (ROS) and Reactive Nitrogen Species (RNS) as signalling molecules in response to stress

Oxygen (O_2) is an essential element of life for most of all multicellular organisms including plants and animals, and the rapid accumulation of this molecule in the atmosphere in the Earth's distant past, was an important event for life evolution (Zhou *et al.*, 2020). Moreover, many anaerobic organisms also generate ROS and are armed with ROS scavenging systems. Therefore, the evolution of both prokaryotic and eukaryotic organisms could proceed in the presence of ROS long before an oxygenic atmosphere appeared (Czarnocka and Karpiński, 2018).

Gradual reduction of O_2 by high-energy exposure or electron-transfer reactions leads to the production of highly reactive ROS. When O_2 is present, the cellular processes characterized by high-speed electron or energy transport inevitably result in the leakage of electrons or energy from molecular oxygen, thereby producing ROS with a higher chemical activity than O_2 (Khorobrykh *et al.*, 2020).

It has been estimated that about 1-2 % of O_2 consumed by plants is diverted to produce ROS, hence they are continuously generated during the respiratory pathway of aerobic organisms and in many other biochemical reactions (Mhamdi and Van

Breusegem, 2018; Waszczak *et al.*, 2018; Farooq *et al.*, 2019). ROS can be classified as radical, when contain free unpaired electrons, and non-radical species if there are no unpaired electrons. Among radicals are superoxide anion ($O_2^{\bullet-}$), hydroperoxyl ($HO_2^{\bullet}$), hydroxyl radical (•OH), peroxyl radical ($ROO^{\bullet}$) and alkoxyl radical ($RO^{\bullet}$); and among non-radicals there are singlet oxygen ($^1O_2$), hydrogen peroxide (H_2O_2) and ozone (O_3). Apart from these common ROS, some others are also found in plants such as hypochlorous acid (HOCl), hydroperoxides (ROOH), and excited carbonyls (RO*). In addition, some acids like hypobromous acid (HOBr), hypoiodous acid (HOI) and radicals like carbonate radical ($CO_3^{\bullet-}$) and semiquinone ($SQ^{\bullet-}$), are also incorporated into ROS group (Hasanuzzaman *et al.*, 2020; Khorobrykh *et al.*, 2020).

The most commonly produced ROS are $O_2^{\bullet-}$, H_2O_2, •OH and $^1O_2$ (Farooq *et al.*, 2019). ROS stability, apart from their short half-time, are linked to their reactivity: H_2O_2 and $O_2^{\bullet-}$ are the most stable forms of ROS, having a long lifetime-from milliseconds to seconds, whereas the lifetime of $^1O_2$ and •OH is shorter, ranging from nanoseconds to microseconds (Waszczak *et al.*, 2018; Farooq *et al.*, 2019; Khorobrykh *et al.*, 2020). Being chemically unstable, ROS can only oxidize compounds in their close vicinity (Mielecki *et al.*, 2020). $^1O_2$ is extremely unstable in cells and has a great impact on photosynthesis (Hasanuzzaman *et al.*, 2020). $O_2^{\bullet-}$ is the precursor of various ROS such as H_2O_2, because of its instability and strong oxidation/reducibility capacity (Mhamdi and Van Breusegem, 2018). •OH can be formed when the O−O double bond in H_2O_2 cleaves and usually acts very near its production site. •OH is the most reactive ROS, being able to react with all biological molecules (Huang *et al.*, 2019). Among all ROS, H_2O_2 is often put forward as the most attractive signalling molecule because of its relatively low toxicity, stability and long lifespan, and in addition it can diffuse through biological membranes travelling between organelles and cells (Cuypers *et al.*, 2016; Khorobrykh *et al.*, 2020). At the low physiological levels in the nanomolar range, H_2O_2 is considered the major agent signalling through specific protein targets, which engage in metabolic regulation and stress responses to support cellular adaptation to changes in the environment (Nazir *et al.*, 2020).

ROS are generated in both unstressed and stressed plant cells. It is known that when plants are subjected to different abiotic and/or biotic stresses a rapid accumulation of ROS (mainly H_2O_2) and other important signalling molecules such as RNS takes place

(Sandalio and Romero-Puertas, 2015*b*). The term RNS includes molecules derived from the reduction of nitrogen compounds, including the free radical nitric oxide ($NO^{\bullet}$), which coexist with molecules with an energetically more favourable electron structure, the nitrosonium cation (NO^{+}) and the nitroxyl anion (NO^{-}; Neill *et al.*, 2003; del Río, 2015; Corpas, 2016; Astier *et al.*, 2018). In addition, NO and ROS can react, generating mainly higher nitrogen oxides compounds (NO_2, N_2O_3, and N_2O_4) and peroxynitrite ($ONOO^{-}$), which is one of the most potent oxidant molecules in the cell; and with lipid peroxyl radicals ($LOO^{\cdot}$) through a still unknown mechanism, to produce nitro-fatty acids (NO_2-FA; (Rubbo, 2013; Astier *et al.*, 2018; Mata-Pérez *et al.*, 2020). NO acts as an inter- and intracellular signalling molecule, and may be able of regulate gene transcription and activate secondary messengers. NO has been linked with multiple processes in plants, such as seed germination, pollen tube growth, cell wall lignification, auxin-induced root organogenesis, establishment and functioning of the legume-*Rhizobium* symbiosis, flowering, fruit ripening, leaf senescence, and biotic and abiotic stress responses (Astier *et al.*, 2018; Del Castello *et al.*, 2019; Hancock and Neill, 2019; Kohli *et al.*, 2019; León and Costa-Broseta, 2020; Terrón-Camero *et al.*, 2020; Manrique-Gil *et al.*, 2021). In particular, it has been described that NO is involved in plant Cd responses in a time- and dose-dependent way (Besson-Bard *et al.*, 2009; Romero-Puertas *et al.*, 2019). pre-treatment with NO protects against Cd toxicity by increasing antioxidant capacity and heavy-metal stress tolerance in plants (Kopyra *et al.*, 2006; Noriega *et al.*, 2007; Terrón-Camero *et al.*, 2019).

ROS and RNS play the double role as "Dr. Jekyll and Mr. Hyde". These two molecular families are prone to uncontrolled overproduction under stressful circumstances, causing cellular nitro-oxidative damage mainly due to the reaction with lipids, proteins and nucleic acids (Romero-Puertas and Sandalio, 2016; Hancock and Neill, 2019; Kohli *et al.*, 2019); on the contrary and under normal physiological conditions, low concentration or high levels but relatively short-lived and/or controlled levels of ROS and RNS, act as signalling molecules in a variety of fundamental processes, including growth and development, ion transport, defence, and cell death (Romero-Puertas and Sandalio, 2016; Turkan, 2018; Choudhary *et al.*, 2020). In this regard, a finely tuned balance between ROS and RNS scavenging and production is necessary; **Fig 4**). This balance is firmly controlled by the entire redox-sensing and signalling networks that regulate the cellular

ROS levels spatially and temporally by modifying the ROS/RNS generation and scavenging mechanisms.

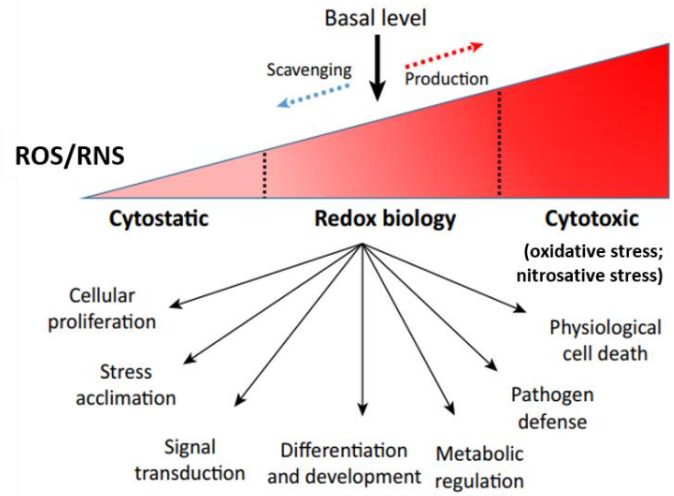

Figure 4. Redox homeostasis occurring in plant cell*. Balance between reactive oxygen species (ROS) and reactive nitrogen species (RNS) production and scavenging is finely tuned in plant cells. When ROS levels are too low (cytostatic state) or when ROS levels are too high (cytotoxic state) cell is not able of working properly. Basal level of ROS are required in many biological processes (modified from Mittler, 2017).*

In this regulation, the so-called retrograde signalling (communication between the organelles and the nucleus) as well as the so-called anterograde signalling (nucleus to organelle communication), are essential to direct the energy use correctly during stress exposure (Crawford *et al.*, 2018; Farooq *et al.*, 2019). The retrograde signalling employs oxidants and antioxidants as flexible integrators of redox signals that are translated into acclimation responses (Farooq *et al.*, 2019). Consequently, plants must re-program gene expression and cellular metabolism to divert energy from processes such as growth and development to stress responses. In order to restore cellular energy homeostasis after the stress exposition, the activities of the organelles must be tightly co-ordinated with the transcriptional re-programming in the nucleus (Crawford *et al.*, 2018). Retrograde signals from mitochondria and chloroplast in stress response are better understood (Pfannschmidt *et al.*, 2020; Wang *et al.*, 2020) than in peroxisomes. Recently, retrograde signals originated from peroxisomes have been connected with the inhibition of catalases (CATs), and the role of peroxisome-derived H_2O_2 in the induction of programmed cell death (PCD) has been established (Mielecki *et al.*, 2020).

Recently and using transcriptomic techniques, it has been identified important stress-responsive signalling molecules, such as mitogen-activated protein kinases (MAPKs) and phosphatases, involved in ROS metabolism (Huang *et al.*, 2019; Kohli *et al.*, 2019). Ca^{2+} is actively involved in intra- and extra-cellular signalling networks as well as plant MAPK signalling networks. Ca^{2+} and ROS signalling interactions are considered to be bidirectional, as Ca^{2+} is necessary for ROS production, while ROS is primarily required for the regulation of cellular Ca^{2+} (Jalmi and Sinha, 2015; Kawasaki *et al.*, 2017; Huang *et al.*, 2019; Kohli *et al.*, 2019). In addition, ROS and RNS are capable to self-regulation and regulating its partners affecting production and elimination of these molecules (Romero-Puertas and Sandalio, 2016).

B. ROS and RNS production in plant cells

In animals, mitochondria and plasma membrane-bound nicotinamide adenine dinucleotide phosphate oxidases (NADPH) are the major source of ROS (Czarnocka and Karpiński, 2018). In plants however, the primary cellular ROS generation sites are chloroplasts, mitochondria, peroxisomes, the apoplast, and plasma membrane (Singh *et al.*, 2019; Hasanuzzaman *et al.*, 2020).

In animal systems, most of the NO produced is due to the enzyme nitric oxide synthase (NOS; EC 1.14.13.39) which catalyses the oxygen- and NADPH-dependent oxidation of L-arginine to NO and citrulline. NOS has a dual location in cytosol and peroxisomes of hepatocytes (Stolz *et al.*, 2002; Pacher *et al.*, 2007). However, in plants, although a nitric oxide like activity (NOS-l) has been reported no gene associated has been identified (Astier *et al.*, 2019; León and Broseta, 2020), and the only genes orthologous to animal NOS found in plants are the ones from some green algae (Foresi *et al.*, 2015; Jeandroz *et al.*, 2016; Santolini *et al.*, 2017; Astier *et al.*, 2018; Tejada-Jiménez *et al.*, 2019). In addition, different NO sources have been described although our current knowledge of the metabolic sources of NO and the mechanisms involved in NO scavenging in plants is incomplete (Sandalio and Romero-Puertas, 2015*a*; León and Broseta, 2020).

B.1 ROS and RNS generation in organelles

The three main sources of plant ROS/RNS are the chloroplastic photosynthesis, the mitochondrial respiration and the peroxisomal photorespiration cycle. ROS/RNS can be generated in the cell wall, the apoplast, the plasma membrane and the vacuole. Chloroplasts have a high metabolic activity accompanied with intensive formation of redox active compounds, which are able to react with O_2 to produce ROS (Khorobrykh *et al.*, 2020). Chloroplasts and peroxisomes are the main sources of ROS in the presence of light, whilst the mitochondria are the major source under dark conditions (Xie *et al.*, 2019). Photorespiration is responsible for 70 % of total H_2O_2 production in C3 plants, but this reaction runs in peroxisomes outside of the chloroplast (Foyer and Noctor, 2020; Khorobrykh *et al.*, 2020).

Table 1. Main plant subcellular compartments and major pathways involved in reactive oxygen and nitrogen species production. *Elaborated from Kohli et al., 2019, Janku et al., 2019, Choudhary et al., 2020 and* ***annex I.***

Site of production	ROS/RNS produced	Metabolism/pathway involved
Cell wall	$O_2^{\bullet-}$, H_2O_2, •OH, NO	Class III peroxidases (POXs), oxidized NADH and diamino oxidases
Apoplast	H_2O_2, NO	Superoxide dismutase (SOD), thiol-disulphite network, Cys rich kinases and polyamines catabolism, nitrate reduction
Plasma membrane	$O_2^{\bullet-}$, H_2O_2	RBOHs
Vacuole (tonoplast)	H_2O_2	ROS metabolism (antioxidants action)
Mitochondria	$O_2^{\bullet-}$, H_2O_2, •OH, NO, $ONOO^-$	Mitochondrial electron transport chain (complexes I and III), nitrate reduction
Chloroplast	$O_2^{\bullet-}$, H_2O_2, •OH, $^1O_2$, NO, $ONOO^-$	Photosynthetic (PSI and II) and Fenton reactions, SOD, NOS-l
Peroxisome	$O_2^{\bullet-}$, H_2O_2, •OH, NO, $ONOO^-$	β-oxidation, photorespiration, sulfite detoxification, purine and polyamine metabolism, NOS-l

a) Chloroplast

In chloroplast, O_2 produced during photosynthesis accepts electrons, which pass through the photosystems, originating $O_2^{\bullet-}$ and H_2O_2 in the photosystem I (PSI). Under stress conditions, an overload on electron transport chain occurs, which results in electron

leakage from ferredoxin to molecular O_2 producing $O_2^{\bullet-}$ via Mehler reaction. H_2O_2 production in chloroplast results from the action of chloroplastic SOD on $O_2^{\bullet-}$ and subsequently conversion to H_2O by ascorbate-glutathione (AsA-GSH) cycle (Choudhary *et al.*, 2020). Accumulation of H_2O_2 can lead to the generation of •OH via Fenton reactions if the scavenging of H_2O_2 by the antioxidant enzymes is not fast enough (Khorobrykh *et al.*, 2020). The water-water cycle (electron flow from H_2O at PSII to H_2O at PSI) shortens the lifetime of photoproduced $O_2^{\bullet-}$ and H_2O_2 to suppress the production of •OH radicals, whose interaction with target molecules is thus prevented, leading to photo-inhibition (Asada *et al.*, 2000; Czarnocka and Karpiński, 2018).

In addition to $O_2^{\bullet-}$ and H_2O_2 formation by the photosynthetic electron transport chain, energy transfer within the photosystems leads to $^1O_2$ production (Kohli *et al.*, 2019). $^1O_2$ is generated by lipoxygenase localized in the chloroplast, specifically through the transfer of energy from chlorophyll triplet (^{3}Chl) to the molecular oxygen ($^3O_2$) under low light conditions. $^1O_2$ provokes the inactivation of PSII via dysfunction of D1 polypeptide and pigment destruction (Farooq *et al.*, 2019; Khorobrykh *et al.*, 2020).

NO, which has been detected in chloroplasts, is generated by L-arginine- and NADPH dependent NO synthase like activity and may perform a regulatory function in this organelle (Kohli *et al.*, 2019).

b) Mitochondria

During mitochondrial respiration, electrons can flow from reduced organic substrates to the molecular oxygen through components of the respiratory chain in the inner mitochondrial membrane, leading to ROS production. Two main components of the mitochondrial electron transport chain (mt ETC) that act as electron donor agents in the production of ROS, are Complex I and Complex II (Choudhary *et al.*, 2020).

$O_2^{\bullet-}$ production occurs during normal operation of the respiratory chain, but its rate is highly increased in conditions of decelerated respiratory rates, e.g., by respiratory chain inhibition or limited adenosine diphosphate (ADP) availability, resulting in a highly reduced state of mitochondrial electron transport chain. $O_2^{\bullet-}$ conversion to H_2O_2 and O_2 is strongly accelerated by SOD present in mitochondrial matrix (Farooq *et al.*, 2019; Janku

et al., 2019). Mitochondria generally produce ROS during respiration, but ROS production increases under stress conditions such as photoinhibition (Popov *et al.*, 2021).

In hydrated seeds, mitochondria, is one of the major sources for ROS while in dry seeds, ROS are synthesized primarily via non-enzyme-catalysed reactions (Popov *et al.*, 2021). As a result, $O_2^{\bullet -}$, H_2O_2 and •OH are generated causing an imbalance in the intracellular status of ROS, which potentially results in defective seed germination (Janku *et al.*, 2019). It is worth noting that $O_2^{\bullet -}$ production in plant mitochondria can be ameliorated by several pathways that enable bypassing the electron transport chain. Proton leak across the membrane is facilitated by uncoupling proteins, whereas alternative oxidase (AOX) bypasses proton pumping on Complex III and IV (Kumar *et al.*, 2019; Singh *et al.*, 2019; Popov *et al.*, 2021).

Mitochondria are an important source of NO in plants, and hence likely to be a major target for the actions of NO and other RNS (Igamberdiev *et al.*, 2014). Almost every complex of the mitochondrial ETC can interact with NO, be target of NO, and participate in metabolism of NO (Gupta *et al.*, 2018). The balance between these multiple sources of NO is variable but under hypoxia, mitochondrial NO production increases substantially (Igamberdiev *et al.*, 2014). Complex I regulates NO production and participates in the formation of a supercomplex with complex III under hypoxia. Complex II is a target for NO, which also regulates ROS generation. Complex III is one of the major sites for NO production, and the produced NO participates in the phytoglobin-NO cycle that leads to the maintenance of the redox level and limited energy production under hypoxia. Complex IV is another major site for NO production in mitochondria, which is inhibited by excess of NO. Additionally, the AOX pathway minimizes nitrite-dependent NO synthesis that would arise from enhanced electron leakage in the cytochrome pathway (Gupta *et al.*, 2018; Kumar *et al.*, 2019).

c) Peroxisome

Different ROS including H_2O_2, $O_2^{\bullet -}$ and •OH, as well as RNS like NO, $ONOO^-$, and nitrosoglutatione (GSNO), have been reported to be generated in peroxisomes (Sandalio and Romero-Puertas, 2015*a*; Del Río and López-Huertas, 2016; Kohli *et al.*, 2019; see **annex I**).

H_2O_2 is produced in multiple metabolic processes and in different types of peroxisomes, being the most remarkable enzymes the photorespiratory glycolate oxidase (GOX) reaction (in green tissues), the main enzyme of fatty acid β-oxidation, Acyl-CoA oxidase (ACX), the flavin adenine dinucleotide (FAD)- or flavin mononucleotide (FMN)-dependent oxidases. The spontaneous or enzymatic dismutation of $O_2^{\bullet-}$ produced by different enzymes are also peroxisomal H_2O_2 sources (Del Río and López-Huertas, 2016; Lismont *et al.*, 2019; **annex I**). GOX is involved in the photorespiration, and it is responsible for producing around 70 % of the H_2O_2 in plant cells (Cui *et al.*, 2016). Five GOX proteins have been described in Arabidopsis: GOX1, GOX2 and GOX3, which display narrow substrate specificities against glycolate and L-lactate, and hydroxy acid oxidases HAOX1 and HAOX2, which present broader substrate specificities (Pan *et al.*, 2020). The photorespiratory pathway, allows the photosynthetic CO_2 fixation of plants to occur in the presence of O_2. It is an essential pathway because O_2 can compete with the CO_2-fixing enzyme ribulose 1,5-bisphosphate carboxylase (RuBisCO), forming 2-phosphoglycolate, which can affect negatively the photosynthesis. In the photorespiration participate chloroplasts, peroxisomes, mitochondria and the cytosol. Polyamines catabolism is another source of H_2O_2 in peroxisomes. Different plant species harbour Cu-diamine oxidases (CuAOs) and Flavin-polyamine oxidases (PAOs) in peroxisomes, which are involved in polyamine catabolism and polyamine back-conversion reactions (spermine to spermidine and spermidine to putrescine; Wang *et al.*, 2019).

Ureides metabolism and nucleic acids catabolism are $O_2^{\bullet-}$ sources in peroxisomes. The enzymes responsible for $O_2^{\bullet-}$ generation are xanthine oxidoreductase (XOR) and urate oxidase (or uricase, UO). XOR catalyzes the conversion of hypoxanthine and xanthine into uric acid with the concomitant formation of NADH and $O_2^{\bullet-}$. UO converts the uric acid into allantoin producing $O_2^{\bullet-}$. Furthermore, sulfite oxidation by sulfite oxidase (SO) takes also place in peroxisomes producing $O_2^{\bullet-}$ (**annex I**). Another source of $O_2^{\bullet-}$ in peroxisomes is an electron transport chain located in the peroxisomal membrane (Sandalio and Del Río, 1988; López-Huertas *et al.*, 1999) and composed by three polypeptides (PMP18, PMP32 and PMP29), which uses NADH/NADPH and can transfer electrons to cytochrome C or O_2 outside the peroxisome, releasing $O_2^{\bullet-}$. As a consequence of Fenton-type reactions, •OH can be generated in peroxisomes, and $^1O_2$

has also been reported in peroxisomes (Mor *et al.*, 2014), although their metabolism and signalling have not been yet explored.

NO and RNS are also produced in plant peroxisomes (**annex I**). Therefore, a nitric oxide synthase (NOS)-like activity has been described in peroxisomes (Barroso *et al.*, 1999). Additionally, indole-3-butyric acid to IAA conversion by β-oxidation generates NO (Schlicht *et al.*, 2013) and under anaerobic conditions, the purified peroxisomal enzyme XOR can reduce nitrite to NO (Antonenkov *et al.*, 2010). In addition, polyamine oxidases and amine oxidases might be NO sources in peroxisomes (Agurla *et al.*, 2018). NO can react with $O_2^{\bullet-}$ promoting $ONOO^-$ formation as well as with GSH leading to GSNO production, considered a cellular reservoir of NO (Ortega-Galisteo *et al.*, 2012; Corpas and Barroso, 2014; Sandalio and Romero-Puertas, 2015*a*).

In addition, the presence of hydrogen sulfide (H_2S) has been also detected in peroxisomes (Corpas *et al.*, 2019), being able of inhibit the activity of CAT, suggesting the possible role of H_2S as a novel signalling molecule in plant response to oxidative stress conditions.

d) Other ROS/RNS sources

Plant-specific class III peroxidases, as members of a large multigene family of peroxidases (POXs, EC 1.11.1.7) are localized in the plant cell wall and constitute other important source of apoplastic ROS. POXs are known to be involved in stress signalling under abiotic stress stimuli (Janku *et al.*, 2019). In addition to POXs, others enzymes such as amine oxidase, quinone reductase or oxalate oxidase are responsible for $^{\bullet}OH$, $O_2^{\bullet-}$ and H_2O_2 generation, as well as NO production. The plasma membrane is other source of ROS due to the presence of membrane-bound NADPH oxidase, also known as the respiratory burst oxidase homolog (RBOH). RBOH can transfer free electrons from its intracellular region to molecular oxygen via the apoplast through the plasma membrane (Torres and Dangl, 2005; Kohli *et al.*, 2019).

B.2 Regulation of ROS and RNS production

To regulate ROS levels and oxidative stress, plants have a wide range of antioxidative mechanism that consists on enzymatic and non-enzymatic components

which work synergistically and interactively to balance ROS production and scavenge preventing cellular damage (Sewelam *et al.*, 2016; Nadarajah, 2020; **Fig. 5**).

NADPH is a critical cofactor required by several reductive biosynthetic and detoxification pathways in plant cells. In particular, there are several sources of NADPH in the peroxisome, including: the oxidative pentose phosphate pathway (OPPP), peroxisomal, 6-phosphogluconate dehydrogenase 2 (PGD2), and the NADP-dependent isocitrate de-hydrogenase (pICDH; Pan and Hu, 2018).

B.2.1 Enzymatic antioxidants

The enzymatic system mainly includes SOD, CAT, glutathione peroxidase (GPX) and enzymes in the AsA-GSH cycle such as ascorbate peroxidase (APX), monodehydroascorbate reductase (MDHAR), dehydroascorbate reductase (DHAR), and glutathione reductase (GR; Hasanuzzaman *et al.*, 2020; Khan *et al.*, 2020). In addition, POXs, polyphenol oxidase (PPO), glutathione S-transferase (GST), thioredoxins (TRXs), and peroxiredoxins (PRXs) participate in ROS scavenging and redox regulation (Foyer and Noctor, 2020; Dvořák *et al.*, 2021*a*).

SOD (E.C.1.15.1.1) initiates the first line of defence. In the *Arabidopsis thaliana* genome, three *FeSOD (FSD1*, *FSD2*, and *FSD3)*, one *MnSOD (MSD1),* and three *Cu/ZnSOD (CSD1*, *CSD2*, and *CSD3)* genes have been identified. Individual SOD isozymes are located in mitochondria *(MSD1)*, peroxisomes *(CSD3)*, cytosol *(CSD1* and *FSD1)*, chloroplast *(FSD1*, *CSD2*, *FSD2*, and *FSD3)* and nucleus *(FSD1*; Dvořák *et al.*, 2021*a*,*b*). CAT (EC 1.11.1.6) is located mainly in peroxisomes and catalyses the dismutation of H_2O_2 molecules into O_2 and H_2O, which may be responsible for the bulk removal of H_2O_2 in excess produced under stress conditions (Mittler, 2002). Three genes *(CAT1*, *CAT2*, and *CAT3)* encoding CATs have been found in the Arabidopsis genome (Du *et al.*, 2008). The third most remarkable enzymatic antioxidant system is the enzyme GPX (EC 1.11.1.9). GPX is localized in vacuoles, cell wall, and cytosol and catalyse the reduction of H_2O_2 to alcohols. GPX competes with CAT for H_2O_2 having a protector function against low levels of oxidative stress (Khan *et al.*, 2020; Nadarajah, 2020).

In plant cells, the AsA-GSH or Asada-Halliwell cycle is the major antioxidant defence pathway to detoxify H_2O_2, which consist in non-enzymatic antioxidants AsA and

GSH, as well as four important enzymes APX, MDHAR, DHAR, and GR located in different compartiments (Jiménez *et al.*, 1997). APX (E.C.1.1.11.1) has a higher affinity of binding H_2O_2 compared to CAT and reduces H_2O_2 to H_2O and DHA, using AsA as a reducing agent. Five isoforms of APX are located in the cytosol, mitochondria, peroxisome, and chloroplast (stroma and thylakoids). Thanks to the enzyme MDHAR (E.C.1.6.5.4), the AsA can be regenerated. MDHAR has several isozymes which are present in chloroplast, mitochondria, peroxisomes, cytosol, and glyoxysomes (Gieti, 1992). Regulation of the AsA content in both symplast and apoplast, is essential for maintaining the redox state of the plant cell. Apart from MDHAR, DHAR (M.C.1.8.5.1) reduces dehydroascorbate (DHA) to AsA using GSH as an electron donor. DHAR is found abundantly in seeds, roots and both green and etiolated shoots. GR (E.C.1.6.4.2) is a flavoprotein oxidoreductase predominantly found in chloroplasts with small amounts occurring in peroxisomes, mitochondria and cytosol. GR uses NADPH as a reductant to reduce GSSG to GSH (Das and Roychoudhury, 2014; Huang *et al.*, 2019; Nadarajah, 2020).

B.2.2 Non-enzymatic antioxidants

The non-enzymatic antioxidant system is also involved in alleviating oxidative damage and it is mainly mediated by low molecular mass antioxidants, such as AsA, GSH (both involved in AsA-GSH cycle), carotenoids, tocopherols and phenolics compounds, alkaloids and nonprotein amino acids (Hasanuzzaman *et al.*, 2020; Khan *et al.*, 2020).

AsA is the most abundant water-soluble antioxidant in plants, which serves as a cofactor for enzymes involved in photosynthesis, hormone biosynthesis, and the regeneration of other antioxidants such as α-tocopherol. 90 % of the AsA is concentrated not only in the cytosol, but also substantially in apoplast, becoming into a strong defence against ROS excess. Once used, AsA can be recycled by several different mechanisms. The short-lived MDHA radical, produced following AsA oxidation, can be recycled following reduction by ferredoxin or MDHAR. If MDHA is not reduced immediately to AsA, disproportionates to AsA and DHA, wich can be recycled into AsA by DHAR (Gallie 2012; Smirnoff 2018). DHAR uses reduced glutathione (GSH) to reduce DHA generated from the oxidation of AsA. GSH is a low molecular weight compound which prevent oxidation of thiol groups, and react with different ROS such as $^1O_2$ and •OH acting like a reductant molecule (Das and Roychoudhury, 2014). GSH is found in almost all cellular

compartments such as cytosol, ER, mitochondria, chloroplasts, vacuoles, peroxisomes, and even the apoplast. GSH possess a high reductive potential allowing it to participate in multiple plant processes such as: cell division and differentiation, senescence, enzymatic activity, synthesis of proteins and nucleotides, detoxification of xenobiotics, regulation of synthesis of phytochelatins and stress response (Ulrich and Jakob, 2019; Hasanuzzaman *et al.*, 2017, 2020).

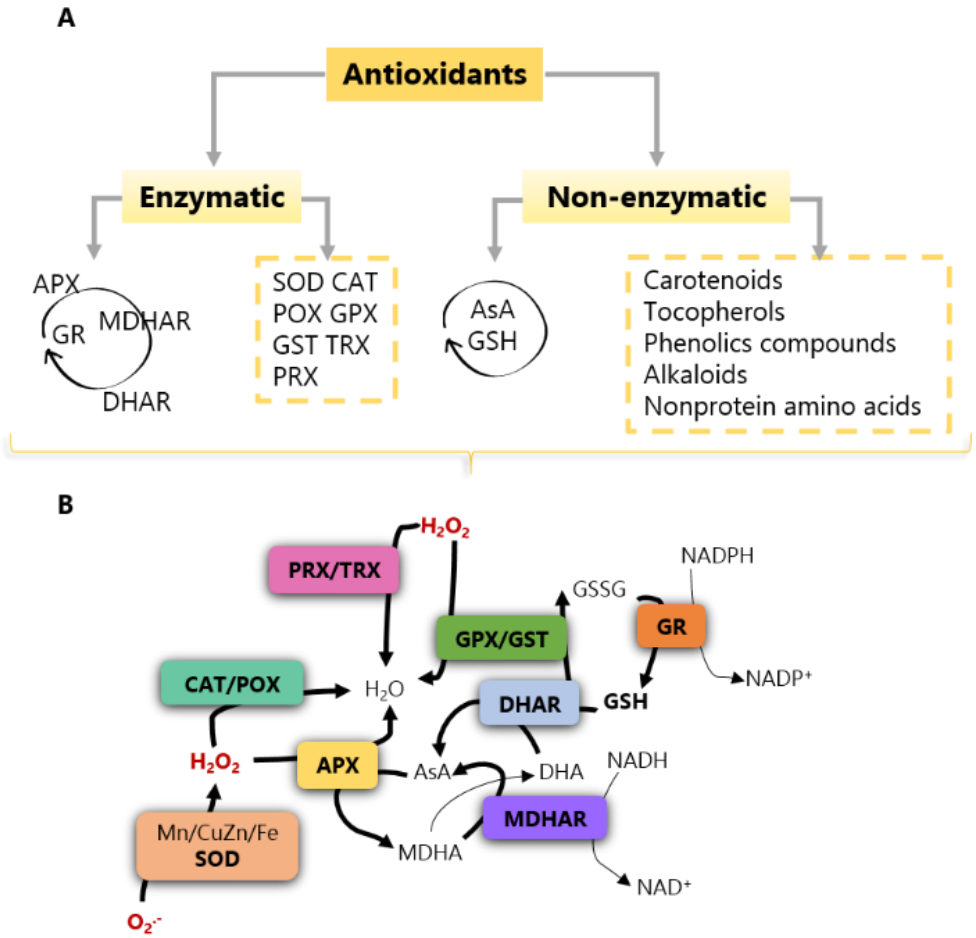

Figure 5. Overview of mechanisms of ROS detoxification by plant antioxidant system. (A) *Main enzymatic and non-enzymatic antioxidants* ***(B)*** *Combined action of antioxidants to cope with ROS generated under stress conditions. APX (ascorbate peroxidase), AsA (ascorbate), CAT (catalase), DHA (dehydroascorbate), DHAR (dehydroascorbate reductase), GPX (glutathione peroxidase), GR (glutathione reductase), GSH (reduced glutathione), GSSG (oxidized glutathione) GST (glutathione S-transferase) H_2O_2 (hydrogen peroxide), MDHA (monodehydroascorbate), MDHAR (monodehydroascorbate reductase) NADPH (nicotinamide adenine dinucleotide*

phosphate), O_2^- (superoxide anion), POX (peroxidases), PRX (peroxiredoxins), SOD (superoxide dismutase), TRX (thioredoxin).

C. Peroxisomes as central players in stress response

In 1954, the Swedish PhD student Johannes Rhodin described "microbodies" in ultrastructural studies of the mouse kidney. Later on, Christian De Duve and colleagues isolated peroxisomes from rat liver, and proposed the functional term of "peroxisomes" due to the presence of several enzymes involved in the production and degradation of H_2O_2 (De Duve and Baudhuin, 1966; Gabaldón, 2010). Despite being one of the last major organelles to be discovered, peroxisomes have been gaining importance and currently are considered a multifunctional global player with high relevance for cell functionality and for perception and response to changes in their environment in both animal and plant organisms (Sandalio and Romero-Puertas, 2015*a*; Fransen and Lismont, 2019; **annex I**).

One of the characteristic of peroxisomes is its high plasticity, being able to adapt their number, morphology, size, movement and metabolic pathways in response to environmental changes. However, the signal or molecules which trigger these responses, when these modifications take place, and the functionality of peroxisomal dynamic changes in term of tolerance are not well understood. Several evidences demonstrated that changes in peroxisomal dynamics are regulated by ROS and NO (López-Huertas *et al.*, 2000; Sinclair *et al.*, 2009; Rodríguez-Serrano *et al.*, 2016*a*; Ebeed *et al.*, 2018; Calero-Muñoz *et al.*, 2019; Terrón-Camero *et al.*, 2020). Disturbances in any of the processes in which peroxisomes take part, could trigger transitory changes in ROS an NO production which can be perceived by the cell as an alarm promoting a fast response (Sandalio *et al.*, 2019; **annexes I** and **II**). A "ROS/RNS signature", which is specific for localization, levels and timing of ROS/RNS production, is capable of triggering a specific response, although the mechanisms and components involved in recognizing and transducing the information to the nucleus are unclear (Mittler, 2011); nonetheless, peroxisomes appear to play an important role in this whole process (Rosenwasser *et al.*, 2011; Sewelam *et al.*, 2014).

Peroxisomes are one of the main sites of H_2O_2 generation in plant cells, and it has been hypothesized that H_2O_2 signalling could result in two kinds of responses: (1) the

signalling induced by H_2O_2 is integrated regardless of the origin of H_2O_2 or (2) H_2O_2-induced signalling is dependent on the production site of H_2O_2 (Sewelam *et al.*, 2014; Su *et al.*, 2019).

On the other hand, it has been reported that peroxisome related metabolic functions are essential for pathogenic development of plant pathogenic fungi: foliar plant pathogens need lipid and fatty acid metabolisms for supporting initial growth and development into the leaf tissue; they also require lipid mobilization, acetyl CoA, and the glyoxylate cycle to enter its host. In these processes, ROS and NO are involved, thereby peroxisomes has pivotal roles in the development of fungal pathogenesis as a source of signalling molecules (Kubo, 2013).

It is clear that peroxisomes are essential in the perception and response to stress conditions such as 2,4-D or Cd. However, very little has been described to date about the elements involved in the signalling process that has to occur in the cell to respond appropriately, and in which the peroxisome actively participates.

C.1 Plant Peroxisomes

The proteome of plant peroxisomes changes across developmental stages, and according to Hayashi and Nishimura (2006), five types of peroxisomes can be found in higher plants: 1) leaf peroxisomes, which participate in photorespiration and the light-mediated developmental process called photomorphogenesis; 2) the so-called glyoxysomes, which are closely associated with the lipid metabolism and the gyoxylate cycle and are located in germinating seeds; 3) root nodule peroxisomes in legumes, which are involved in nitrogen fixation by biosynthesis of ureide; 4) gerontosomes, which are located in senescent tissues, using glyoxysomal enzymes to catabolize lipids; 5) unspecialized peroxisomes, which are relatively undifferentiated peroxisomes located throughout the whole plant.

The peroxisomal specialization observed in plants may actually suggest that plants contain multiple layers of regulation that are much more complex than those observed in yeast and mammals, which would allow for the coordination of tissue specific peroxisome biogenesis observed in plants. Interestingly, all peroxisomes from such different organisms have a feature in common: detoxification of ROS (Mullen and Trelease, 2006). In addition, the versatility and capacity showed by peroxisomes to

produce such fast metabolic changes can be partly explained by post-translational modifications (PTMs; Sandalio *et al.*, 2019, see **annex II**).

C.1.1 Morphological and structural characteristics

Peroxisomes are commonly referred to as small organelles, nevertheless they are 0.1-1 μm in diameter (Smith and Aitchison, 2013), size not so different from mitochondria. While the dimension varies between different organisms, studies have shown them to also vary in size within the same organism. These organelles have a spherical or oval morphology and are composed of a dense matrix. They contain as basic enzymatic constituents CAT and H_2O_2-producing flavin oxidases. In plants, peroxisomes usually contain a granular matrix but they can have crystalline or amorphous inclusions composed of oxidized CAT. Peroxisomes are delimited by a single lipid bilayer, and contain neither DNA nor elements of a translation system (Del Río and López-Huertas, 2016; Kao *et al.*, 2018*a*; Olmedilla and Sandalio, 2019; Pan *et al.*, 2020). Consequently, all proteins necessary for the assembly and biogenesis of peroxisomes, such as matrix or membrane-associated proteins are encoded in the nucleus, and thought to be synthesized on free cytosolic ribosomes (Agrawal *et al.*, 2011; Kim and Hettema, 2015) and imported into the peroxisomes (Kunze, 2020).

Peroxisomes can be found in all eukaryotes except the *Archaezoa* (Wayne, 2019), and thus are likely to derive from an ancestral peroxisome in the last eukaryotic common ancestor (LECA; Gabaldón 2018). Peroxisomes are an example of functional organization to match oxidative metabolism and functionality, playing a key role in the evolution of metabolic networks of photosynthetic organisms by connecting oxidative and biosynthetic pathways operating in different compartments (**annex I**).

C.1.2 Main metabolic functions

Peroxisomes have a wide-range of metabolic pathways and an intricate metabolic connection with other organelles. In single cell organisms such as the yeast *Hansenula polymorpha,* these organelles participate in methanol oxidation as well as the metabolism of alkylated amine or alkane (Veenhuis *et al.*, 1985; Brown and Baker, 2008). In fungi it has been demonstrated that peroxisomes are required for penicillin biosynthesis (Meijer *et al.*, 2010). *Trypanosoma* and *Leishmania* parasites

compartmentalize glycolysis in a specialized peroxisomes called glycosomes (Bauer and Morris, 2017). In mammals, key enzymes are found in peroxisomes, involved in cholesterol, bile acids, and plasmalogen synthesis (etherlipids, such as plasmalogens, are important constituents of the neuronal myelin sheaths in the brain; Brown and Baker, 2008). In humans, peroxisomes are crucial and this is exemplified by the occurrence of inborn errors that cause severe diseases and are often lethal. Moreover, roles in non-metabolic processes such as ageing, anti-viral defence and cancer have been connected with peroxisomes in humans (Islinger *et al.*, 2018; Kim, 2020; Jansen *et al.*, 2021).

In plants, the main functions of peroxisomes are associated with metabolic pathways such as fatty acid β-oxidation, photorespiration, glyoxylate cycle, ureide metabolism, auxins (IAA), JA and salicylic acid (SA) biosynthesis, polyamine and amino acid catabolism, and sulfur metabolism (Sandalio and Romero-Puertas, 2015*b*; Kao *et al.*, 2018*b*; Olmedilla and Sandalio, 2019). Recent studies have linked more metabolic pathways to peroxisomes, adding to the complexity of plant peroxisomal metabolism essential anabolic processes, such as biosynthesis of biotin, ubiquinone, phylloquinone, isoprenoids and benzoic acid (BA) derivatives (Reumann and Bartel, 2016; Kao *et al.*, 2018*b*; Pan and Hu, 2018; Pan *et al.*, 2020). The main metabolic pathways in which peroxisomes participate, as well as the production of ROS and RNS, are shown in **Fig. 6** (**annex I**).

C.1.2.1 Lipid Metabolism: Fatty acid β-oxidation and Glyoxylate cycle

In plants, lipids and mainly triacylglycerols are stored in so-called oil bodies located in cells of the endosperm and cotyledons and used as energy and carbon source for germination. In germinating seeds, oil bodies are degraded rapidly by glyoxysomes, which are unique peroxisomes for fatty acid β-oxidation and the glyoxylate cycle (Shimada *et al.*, 2018).

FA degradation is an important part of plant primary metabolism, which can affect other carbon metabolic processes and lipid homeostasis when blocked. In plants, the degradation of all FA into acetyl-CoA takes place in peroxisomes. Each β-oxidation cycle is a four-step cascade catalyzed by three enzymes: ACX producing H_2O_2, multifunctional protein (MFP)-which catalyzes both a hydration and an oxidation step,

and 3-ketoacyl-CoA thiolase (KAT), producing an acetyl-CoA and an FA-CoA that is shortened by two carbons and subjected to the next round of β-oxidation (Poirier *et al.*, 2006). These three enzymes act in saturated FA metabolism, and auxiliary enzymes are required for unsaturated FA (Li *et al.*, 2019). Although β-oxidation takes place mainly in glyosxysomes, it is also found in green tissues being involved in important processes including synthesis of IAA, JA, ubiquinone, and secondary metabolites such as BA and phenylpropanoids (Pan *et al.*, 2020).

In plants, the end product of β-oxidation, acetyl-CoA, enters into the glyoxylate cycle, producing 4-carbon metabolites that can be consumed by gluconeogenesis and mitochondrial respiration (Rinaldi *et al.*, 2016). Some key peroxisomal enzymes participate in the glyoxylate cycle: aconitase (ACO), malate dehydrogenase (MDH), citrate synthase (CSY), isocitrate lyase (ICL) and malate synthase (MLS). Apart from glyoxysomes, glyoxylate activity also occurs in senescent leaf, cotyledons and flowers as well as in pollen, indicating a developmental and metabolic control of the key enzymes involved in these processes (Kunze and Hartig, 2013; Paudyal *et al.*, 2017; Su *et al.*, 2019).

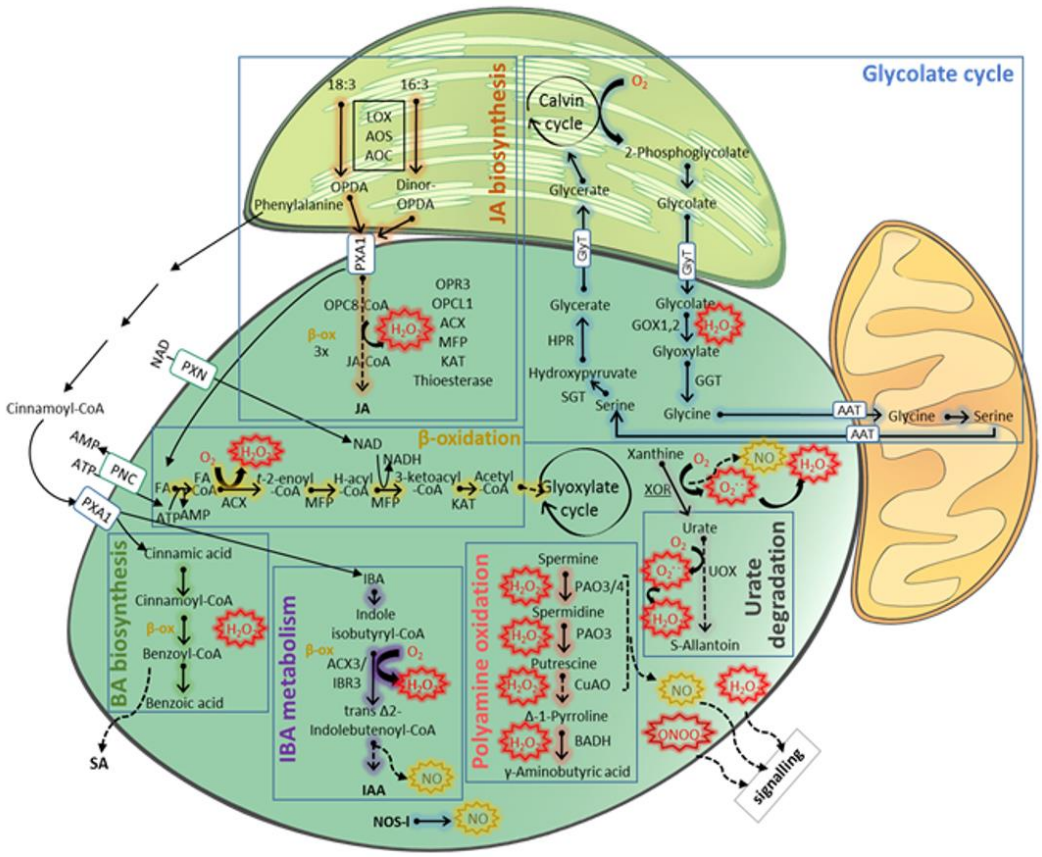

Figure 6. Principal peroxisomal metabolic pathways associated with peroxisomal ROS and NO production. ROS are produced in metabolic pathways such as b-oxidation, photorespiration, ureides metabolism, and polyamine oxidation, and in a small electron transport chain associated with the membrane (peroxisomal membrane proteins, PMP18 and PMP29). NO is produced in peroxisomes by NOS-like (NOS-l) activity, although other sources, such as XOR, polyamine oxidation, and IBA metabolism, could also be involved. ROS, NO, and other RNS may leak out of the peroxisome (dashed arrows) and act as signal molecules that regulate cell metabolism and gene expression. AAT, amino acid translocator; AOC, allene oxide cyclase; AOS, allene oxide synthase; BADH, betaine aldehyde dehydrogenase; CuAO, copper amine oxidase1; GOX1,2, glycolate oxidase1,2; GGT, glutamate–glyoxylate aminotransferase; GlyT, glycerate–glycolate translocator; H-acyl-CoA, 3-hydroxyacyl-CoA; HPR, hydroxypyruvate reductase; IAA, indole-3-acetic acid; IBA, indole-3-butyric acid; IBR3, acyl-coA dehydrogenase/oxidase-like IBR3; KAT, L-3-ketoacyl-CoA-thiolase; LOX, lipoxygenase; MFP, multifunctional protein; OPCL1, OPC-8:0 CoA ligase1; NOS-l, NO synthase-like; OPR3, OPDA reductase3; PAO3, polyamine oxidase3; PAO3/4, polyamine oxidase 3/4; PNC, peroxisomal ATP carrier; PXA1, peroxisomal ABC-transporter1; PXN, peroxisomal NAD carrier; SGT, serin–glyoxylate aminotransferase; UOX, urate oxidase. Figure taken from **annex I**.

C.1.2.2 Photorespiration and the Glycolate pathway

During oil seed germination, the glyoxylate cycle enzymes are replaced by photorespiration enzymes (Pan *et al.*, 2020). The photorespiration pathway consists in the phosphoglycolate recycling, using O_2 and releasing CO_2. Photorespiration spans multiple subcellular compartments, with peroxisomes at the center of this pathway (Kaur *et al.*, 2009). The glycolate pathway is initiated in the chloroplast by the oxygenase activity of RuBisCO, a key enzyme of CO_2 fixation in photosynthesis, which can bind O_2 instead of CO_2, generating the toxic product 2-phosphoglycolate. This product is converted by the phosphoglycolate phosphatase (PGLP1) into glycolate, which enters into leaf peroxisomes. The peroxisome localized photorespiratory enzymes such as GOX, glutamate: glyoxylate aminotransferase (GGAT), serine: glyoxylate aminotransferase (SGAT) and hydroxypyruvate reductase 1 (HPR1), while the NADH-producing enzyme MDH and the H_2O_2-degrading enzyme CAT are indirectly involved (Dellero *et al.*, 2016). Glycolate is converted into the amino acid glycine in the peroxisome and then is transported into mitochondria where it is converted to serine. Last steps in this cycle include: serine re-entering into the leaf peroxisomes where it is converted into glycerate and then transported into chloroplast. The glycerate is then phosphorylated to 3-phosphoglycerate and enters the Calvin-Benson cycle, closing the glycolate pathway (Hagemann and Bauwe, 2016). Arabidopsis has five GOX proteins (GOX1, GOX2 and GOX3) and mutants and gene expression analyses in Arabidopsis showed that GOX1 and

GOX2 function in photorespiration, whereas GOX3 is more involved in metabolizing l-lactate to sustain low concentrations of l-lactate in roots (Engqvist *et al.*, 2015).

Even though photorespiration affects negatively photosynthetic activity and therefore often decreases plant growth, it is suggested to play a role in multiple signalling pathways, especially in plant hormone responses controlling growth and environmental and defence responses (Foyer *et al.*, 2009; Müller and Munné-Bosch, 2021).

C.1.2.3 Biosynthesis of phytohormones

Plant hormones are a group of naturally occurring substances which influence almost every physiological process in plants. They occur in very low concentrations and mainly affect the growth and development of plants at specific time points. They are essential for the appropriate growth of plants and also influence cell death. So far, peroxisomes have been shown to play a role in the biosynthesis of three plant hormones: JA, auxins (IAA) and SA, which are essential key players in a various number of metabolic and developmental processes (Kaur *et al.*, 2009; Pan *et al.*, 2020; Devireddy *et al.*, 2021).

a) Auxins

IBA is an endogenous auxin precursor that is converted into the active auxin IAA in peroxisomes. It has been demonstrated that IBA and its chemical analog 2,4-DB, undergo a two-carbon shortening (a hallmark of β-oxidation reactions) to release IAA or 2,4-D, suggesting the bioactivation of proto-auxins such as IBA and 2,4-DB through β-oxidation (Kaur *et al.*, 2009).

Peroxisome-originated auxin plays important regulatory roles in the development of lateral root, cotyledon, root hair and apical hook in seedlings. So far, four naturally occurring auxins in plants are known: IAA, IBA, the 4-chloroindole-3-acetic acid (4-Cl-IAA) and the 2-phenylacetic acid (PAA; Adham *et al.*, 2005; Kao *et al.*, 2018*b*).

b) Jasmonates

The group of jasmonates includes JA and methyl jasmonate (MeJA). These oxylipins are signalling molecules capable of regulating genes involved in cell growth and biotic and abiotic stress responses (Zander *et al.*, 2020).

Both the chloroplast and the peroxisome are involved in the biosynthesis of JA: the chloroplast-synthesized JA precursors 12-oxo-phytodienoic acid (OPDA) and

dnOPDA which are transported via an ABC transporter (PAX1) through the peroxisomal membrane into their matrix. OPDA is reduced by OPDA reductase (OPR) to 3-oxo-2-cyclopentane-1-octanic acid (OPC:8), followed by 3 rounds of β-oxidation and conversion into JA. Similarly, dnOPDA is reduced to 3-oxo-2-(20-pentenyl)-cyclopentane-1-hexanoic acid (OPC6) and activated to OPC-6:0-CoA (Liu and Timko, 2021). A recent study in Arabidopsis discovered an OPR3-independent JA biosynthetic pathway, in which OPDA directly enters β-oxidation to produce 4,5-didehydro-JA that can be directly converted to JA by the cytosolic OPR2 (Chini *et al.*, 2018; Pan and Hu, 2018).

c) Salicylic acid

BA is a precursor of SA, hormone involved in growth and defence. Despite the importance of SA, its biosynthesis is not well understood: even though the main site of SA biosynthesis is probably located in chloroplasts being synthesized via the shikimate pathway, there is evidence indicating that peroxisome are maybe also involved in the biosynthesis of SA; other possible pathway for the biosynthesis of SA could be by processing of phenylalanine, derived from the shikimate pathway, to a *trans*-cinnamic acid. The further processing of the cinnamic acid to SA involves the reduction of two carbons via a β-oxidation, suggesting that this step is localized in peroxisomes (Kaur *et al.*, 2009; Sharma *et al.*, 2020).

C.1.2.4 Other metabolic functions

Peroxisomes, in collaboration with other organelles, are also involved in the biosynthesis of several crucial cofactors, such as phylloquinone (or vitamin K1), biotin (or vitamin B7), coenzyme A (CoA) and ubiquinone (coenzyme Q; Reumann *et al.*, 2009; Tanabe *et al.*, 2011). Several enzymes involved in the mevalonic acid (MVA) pathway, which is one of the two major routes in generating precursors for the biosynthesis of isoprenoids, are located in peroxisomes (Pulido *et al.*, 2012).

Peroxisomes also participate in the degradation of many bioactive or toxic metabolites, such as polyamines (PA), urate, pseudouridine, sulfite and methylglyoxal. PA, including putrescine (Put), spermidine (Spd) and spermine (Spm) are important in plant development and stress response and it has been suggested to play a critical signalling role through its ability to control H_2O_2 production (Qu *et al.*, 2017; Chen *et al.*, 2019). In

addition, peroxisomes are able to degrade amino acids such as valine, leucine and isoleucine. Although the synthesis of the branched-chain amino acids commonly occurs in chloroplasts, it has been reported that the first enzyme in their synthesis (acetolactate synthase) interact with enzymes dually localized to peroxisomes and chloroplast (ALS-interacting protein 1 and 3; Pan and Hu, 2018).

C.1.3 ROS and RNS scavenging in peroxisomes

Under normal conditions, peroxisomal ROS concentration is adequately controlled. However, to counteract ROS/RNS accumulation and to keep peroxisomal ROS homeostasis, these organelles are armed with a set of ROS and RNS scavengers: antioxidant enzymes (see antioxidants section) such as CuZn-SOD, Mn-SOD, CAT, enzymes of the AsA-GSH cycle (APX, MDHAR, DHAR, GR); and non-enzymatic antioxidants like AsA and GSH (Sandalio and Romero-Puertas, 2015*b*; **Fig. 5** and **annex I**).

Despite H_2O_2 being rapidly removed by both CAT and APX, the scavenging mechanisms could be regulated to allow H_2O_2 to act as a second messenger. Simultaneous mutations of all three CATs in Arabidopsis resulted in severe redox disturbance, growth defects and transcriptional changes, suggesting that H_2O_2 may play a role in retrograde signalling (Su *et al.*, 2018, 2019).

In addition, glutathione S-transferases (GST tau 5, GST PHI 9 and GST PH1 10; GST lambda 2 and GST THETA 1-3) recently identified in peroxisomal proteomic analyses (Pan and Hu, 2018) could support peroxides regulation in these organelles. Other antioxidants and redox proteins present in mammal peroxisomes such as peroxiredoxin or glutaredoxins (Fransen and Lismont, 2019), have not been identified by proteomic or genetic analysis so far in plant peroxisomes. Moreover, accumulating evidence showed that NO could scavenge ROS by regulating the enzyme antioxidant system and the non-enzymatic antioxidant system to enhance the tolerance to heavy metal stress in plants (Wei *et al.*, 2020).

All these peroxisomal metabolic functions share ROS and/or NO as "orchestra conductors": disturbances in any of these metabolic processes can trigger transitory changes in ROS/RNS production which can regulate peroxisomal metabolism leading to

peroxisomal-dependent signalling, triggering a specific cell response (Sandalio and Romero-Puertas, 2015*b*; Kao *et al.*, 2018*b*; Olmedilla and Sandalio, 2019; **annex II**).

C.1.4 Peroxisomal biogenesis

Peroxisome biogenesis is a contentious topic with two overarching proposed mechanisms: 1) "endoplasmatic reticulum (ER) vesiculation" model: de novo synthesis from the ER or 2) "grow and division" model: fission from pre-existing peroxisomes. The prevailing model during the early 70s was the synthesis from the ER, where the organelles were believed to be derived from the rough ER. Later on, this model was then replaced by the "growth and division" model (Lazarow and Fujiki, 1985; **Fig. 7**) in which peroxisomal proteins were synthesized on free polyribosomes in the cytosol. Moreover, in this second model proposed, a post-translational import of peroxisomal proteins occurs, which are responsible to induce growth and fission of mature pre-existing peroxisomes. Since the 80s this "growth and division" model has been generally accepted. Later on, it was proposed an "ER semi-autonomous peroxisome and replication" model in plant peroxisome biogenesis (Mullen and Trelease, 2006; Hu *et al.*, 2012; **Fig. 7**). It now seems, and although it is still heavily debated (Williams *et al.*, 2015; Wróblewska *et al.*, 2017), that the generation of peroxisomes includes de novo biogenesis, during which pre-peroxisomal vesicles fuse to form a new peroxisome or fuse with pre-existing peroxisomes. These peroxisomes grow until mature organelles, which can divide into new peroxisomes (Su *et al.*, 2019).

Christian de Duve proposed that peroxisomes may have been the first endosymbionts (allowing the cells to cope with the rising free molecular oxygen in the Earth's atmosphere) which subsequently lost their DNA (Joshi and Subramani, 2013). Since peroxisomes are devoid of a genome, the entire peroxisome proteome is nuclear-encoded and imported into the organelle mainly by the peroxin proteins (PEX). In 1996, Distel and colleagues described the term peroxin as "proteins involved in peroxisome biogenesis" (inclusive of peroxisomal matrix protein import, membrane biogenesis, peroxisome proliferation, and peroxisome inheritance; Distel *et al.*, 1996).

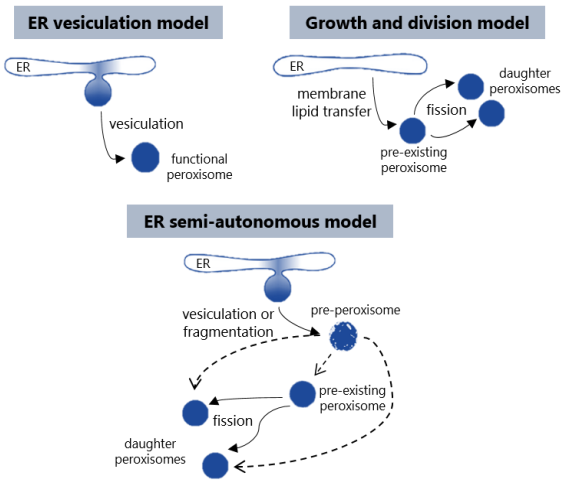

Figure 7. Models for plant peroxisomes biogenesis. *Three models have been proposed to date. In the "ER vesiculation" model a specialized region of the ER can produce functional peroxisomes "de novo". By contrast in the "growth and division" model daughter peroxisomes arise from preexisting peroxisomes by fission. The "ER semi-autonomous" model involves "de novo" formation (vesiculation or fragmentation) and growth of pre-existing peroxisomes. Adapted from Hu et al., 2012.*

To date, 37 PEX proteins have been described (Mast *et al.*, 2020). Some are highly conserved across kingdoms, whereas others only occur in a limited number of species (Hu *et al.*, 2012; Sibirny, 2016; Pan and Hu, 2018; Jansen *et al.*, 2021). These proteins can be divided into three groups depending on their different function:

a) PEX proteins involved in the formation of peroxisomal membrane.

Two classes of peroxisomal membrane proteins (PMPs) are known: Class I and Class II PMPs. Class II PMPs (like AtPEX3 and AtPEX19) are synthesized on free cytosolic ribosomes and are then subsequently imported into the peroxisomal membrane leading to the growth of pre-existing mature peroxisomes. In contrast, Class I PMPs (AtPEX16, AtPEX10 and APX) after being translated in the cytosol, travel through the ER membrane towards a specialised region of the ER, the so-called peroxisomal ER (pER; Kim and Hettema, 2015; Walter and Erdmann, 2019). Then, nascent ER-vesicle are formed and released into the cytoplasm, and mature into an intermediate sorting compartment (ERPIC). In plant cells these ERPICs can be transported and fused to pre-existing mature peroxisomes, delivering the PMPs as well as membrane lipids to the peroxisomes (Kaur *et al.*, 2009; Kalel and Erdmann, 2018). The insertion of peroxisomal membrane proteins is facilitated by PEX3, PEX16, and PEX19: PEX19, acting as the chaperone for PMPs; PEX3,

the membrane anchor for PEX19, and PEX16, which recruits PEX3 to the ER before the formation of pre-peroxisomes. Arabidopsis PEX16 also recruits PMPs to the ER in a PEX3/PEX19-independent manner (Baker *et al.*, 2016; Pan *et al.*, 2020).

b) PEX proteins involved in the import of peroxisomal matrix proteins

Four steps are required for the peroxisomal matrix protein import: (1) binding of receptors to peroxisomal matrix proteins; (2) docking of receptor complex to the peroxisomal membrane proteins; (3) translocation of receptor complex into the peroxisomal matrix; and (4) recycling of the receptors (Kim and Hettema, 2015). With some exceptions, peroxisomal matrix proteins usually contain a C-terminal tripeptide so called "Peroxisomal Targeting Signal" type 1 (PTS1), or a nonapeptide PTS2 in the N-terminal region. Besides the peroxisomal targeting signals, cytosolic receptors are essential for a proper transport of these proteins to peroxisomes. Both peroxisomal matrix proteins containing PTS1 or PTS2, are recognized and bound by the soluble receptors PEX5 (for PTS1) and PEX7 (for PTS2) in the cytosol, and then docked to peroxisomal membrane by the complex PEX13- PEX14 (Baker *et al.*, 2016; Reumann and Chowdhary, 2018; **Fig. 8**). In *Arabidopsis* it has been shown that PEX13, binds to the PEX7-PEX5 complex via the PTS2 pathway, whereas PEX14 binds directly to PEX5. The mechanism underlying the translocation of the proteins across the peroxisomal membrane and their release into the lumen of the peroxisomes is still unknown. The current knowledge suggests that RING-domain-containing PEX2, PEX10 and PEX12 allow a translocation of the receptor-cargo complex through the peroxisomal membrane (Cross *et al.,* 2016; **Fig. 8**).

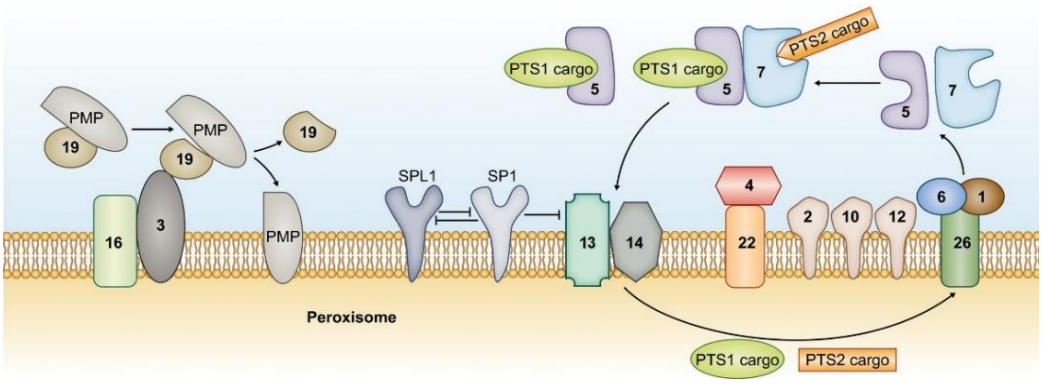

Figure 8. Model for protein import in Arabidopsis peroxisomes. *Cytosolic PEX5 and PEX7 recognize their cargo proteins with a PTS (PTS1 and PTS2). Cargo-loaded PEX5 associates with the membrane via interactions with PEX13 and PEX14. After cargo release, the receptors are recycled back into the cytosol through two protein complexes, PEX2-PEX10-PEX12 and PEX6-PEX1-PEX26. PEX4 is anchored by PEX22. Destabilization of PEX13 by the RING-type E3 ubiquitin ligase SP1 (suppressor of plastid protein import locus 1) regulates peroxisomal matrix proteins import. In addition, PEX19 acts as a chaperone for peroxisomal membrane proteins (PMPs), with the aid of PEX3 and PEX16 (from Pan et al., 2020).*

PEX5 is recycled from the peroxisomal matrix back to the cytosol, by the ubiquitin conjugating enzyme PEX4 and its membrane anchor PEX22, three RING-type ubiquitin ligases, PEX2, PEX10 and PEX12; and two AAA ATPases, PEX1 and PEX6, which are tethered to their membrane anchor PEX26/APEM9 (Kao *et al.*, 2018*b*; Pan *et al.*, 2020). In yeast and mammal cells PEX5 has been described as a redox-sensitive protein (Ma *et al.*, 2013; Apanasets *et al.*, 2014). Thus, in mammal cells the import of CAT into the peroxisome is regulated by PEX5 redox changes, retaining CAT in the cytosol under stress conditions (Walton *et al.*, 2017). In plants, the target zone for redox changes in PEX5 is conserved suggesting a similar mechanism operating in plant peroxisomes (Su *et al.*, 2019).

c) PEX proteins involved in the proliferation machinery.

An important process regulating the size and number of peroxisomes in eukaryotic cells is the so-called proliferation. PEX11 family play an important role in the enlargement and elongation steps during proliferation (see next section).

D. Peroxisomal dynamics: division, proliferation and pexophagy

Eukaryotic cells are able to regulate the number, area and size of their organelles allowing the cells to quickly react upon environmental changes like herbicides or heavy metals among others. Plant peroxisome abundance is governed by (1) biogenesis, associated with physiological processes and division (fission) of a preexisting peroxisome (see **section C.1.4**), (2) proliferation, which is related to stress responses, and (3) pexophagy, a selective degradation mechanism of peroxisomes (Olmedilla and Sandalio, 2019; **annex I**).

When plants suffer a stress, the peroxisome number increases through a complex process called proliferation, consisting of several partially overlapping steps: 1) elongation of peroxisome, 2) membrane constriction and 3) fission process (Schrader *et al.*, 2016; Jansen *et al.*, 2021). In general, PEX proteins are involved in peroxisome biogenesis and maintenance and among them, PEX11 have an important role in the first stage of the peroxisome proliferation (Orth, 2007; Lingard and Trelease, 2006; Terrón-Camero *et al.*, 2020; **annex I**). In human and mammals, three members of the PEX11 family have been described (PEX11α, PEX11β and PEX11γ); yeast also have three members (PEX11, PEX25 and PEX27); and five members have been reported in Arabidopsis (PEX11a, PEX11b, PEX11c, PEX11d and PEX11e; Orth, 2007).

Several studies about the induction of peroxisome proliferation have been published. In yeast such as *Sacharomyces cerevisiae*, peroxisome proliferation is induced by FA like oleic acid (Hiltunen *et al.*, 2003). The oleate responsive elements (ORE) localized in the promoter region of several genes encoding peroxisomal proteins can be recognised by the transcription factors OAF1 and OAF2 (also named PIP2; Trzcinska-Danielewicz *et al.*, 2008; Turcotte *et al.*, 2010). Peroxisome proliferation seems to be governed by H_2O_2 in animals and plants (López-Huertas *et al.*, 2000; Rodríguez-Serrano *et al.*, 2016*b*; Ebeed *et al.*, 2018; Calero-Muñoz *et al.*, 2019). Recently, it has been shown that peroxisome proliferation can be affected by different levels of NO (Terrón-Camero *et al.*, 2020). In mammals, the peroxisome proliferator activator receptor α (PPARα) participate in the regulation of genes involved in lipid homeostasis, including all peroxisomal β-oxidation genes. Apart from PPARα, two additional isoforms PPARδ/β and

PPARγ, induced during proliferation, have been found in mammal cells (Schrader *et al.*, 2016).

In plants, no genes were found coding for PPAR or OAF1/PIP2 homolog proteins (León, 2008; Kaur *et al.*, 2009). Peroxisome proliferation has been observed in response to several abiotic stresses conditions. Desai and Hu (2008) described that in response to far red light, peroxisome can proliferate in plant cells, requiring phytochrome A (phyA) and the up-regulation of the *AtPEX11b* gene, mediated by the bZIP transcription factor HY5 HOMOLOG (HYH). It has been also reported proliferation triggered by other stressors: ozone (Oksanen *et al.*, 2004), clofibrate (Nila *et al.*, 2006; Castillo *et al.*, 2008), salinity (Mitsuya *et al.*, 2010), drought, ABA (Ebeed *et al.*, 2018), Cd (Romero-Puertas *et al.*, 1999; Rodríguez-Serrano *et al.*, 2016*a*), hypoxia (Li and Hu, 2015), and senescence (Pastori and Río, 1997). In fact, salinity upregulated *PEX11e* in tobacco plants (Mitsuya *et al.*, 2010), and *PEX11a* and *PEX11c* in *A. thaliana* (Fahy *et al.*, 2017). *PEX11a* and *PEX11e* were upregulated in response to Cd exposure in Arabidopsis plants (Rodríguez-Serrano *et al.*, 2016*b*). *PEX11b*, *PEX11c* and *PEX11d* were up-regulated by hypoxia (Li and Hu, 2015), while transcription of *PEX11c* correlated with higher peroxisome abundance under drought, or combination of heat and drought stress (Hinojosa *et al.*, 2019). Others factors inducing ROS accumulation, such as the herbicide 2,4-D (Pazmiño *et al.*, 2014; Bernat *et al.*, 2018) and wounding do not alter the number of peroxisomes, while jasmonic acid treatment reduces the number of peroxisomes and increased their size (Castillo *et al.*, 2008).

To maintain ROS homeostasis in the cell, it is necessary to control the proliferation of peroxisomes by eliminating excess or damaged peroxisomes. Autophagy is a catabolic process, which allows to remove, degrade, and recycle damaged and unnecessary cells components and organelles (Lee *et al.*, 2014). Selective authophagy of peroxisome is called pexophagy (Avin-Wittenberg *et al.*, 2018; Olmedilla and Sandalio, 2019). The capability of maintaining redox homeostasis and quality control/abundance of peroxisomes could determine the successful plant adaptation to adverse conditions.

It has been speculated that plant peroxisome proliferation could be considered a protective response against ROS overflow in cell compartments due to their high efficient enzymatic and non-enzymatic antioxidant defences. Thus, peroxisome proliferation could balance ROS homeostasis during protoplast transition from G0 to G1,

where an oxidative burst take place with a slightly inversely correlation between ROS levels and peroxisome abundance (Tiew *et al.*, 2015).

On the other hand, gene co-expression analysis in Arabidopsis plants under drought stress showed correlation between photorespiratory genes and peroxisome number, suggesting the coordination of photorespiration and peroxisomal proliferation, probably through the H_2O_2 generation (Li and Hu, 2015). This result is supported by the absence of peroxisome proliferation in *gox2* Arabidopsis mutants exposed to Cd (Calero-Muñoz *et al.*, 2019). A genome analysis of *Physcomitrella*, *Arabidopsis thaliana* and wheat *(Triticum aestivum)*, concluded that peroxisome proliferation and upregulation of β-oxidation genes is a conserved response to drought, dehydration and ABA, as well as increased and differential expression of *PEX11* (Ebeed *et al.*, 2018). These evidences suggest that peroxisomal H_2O_2 may participate in environmental changes perception and adaptation through differential *PEX11* regulation (**annex I**).

Apart from proliferation, peroxisomes have been reported to have the capacity to produce peroxules under certain stress conditions. The term "peroxule" was coined by Scott et al. (2007) to refer to dynamic extensions observed in peroxisomes. This name was chosen due to the similarity with other transient tubular prolongations that had been observed earlier in chloroplast called stromules (Köhler and Hanson, 2000), and in mitochondria, known as matrixules (Logan, 2006). Until now, peroxules formation has not yet been described in mammals. However, it is tempting to speculate that a similar mechanism also exists in mammalian cells to regulate redox communication between peroxisomes and other cell organelles (Fransen and Lismont, 2019). Peroxules formation is transient as they characteristically extended and retracted. In general, these dynamic extensions may be construed as part of a ROS responsive machinery aimed at relieving subcellular stress created by toxic ROS (Sinclair *et al.*, 2009). Sinclair et al. (2009) showed that, after a few minutes of treatment with H_2O_2, peroxisomes produce peroxules, which progress over time with peroxisome elongation and further proliferation.

D.1 The peroxin 11 *(PEX11)* gene family

PEX11 protein family members are peroxisomal integral membrane proteins, which seem to share α-helical transmembrane domains and both termini exposed to the cytosol (Charton *et al.*, 2019). PEX11 proteins are involved in the peroxisome elongation,

where participate in membrane remodelling. After elongation, several proteins collaborate to divide the peroxisome, although not much is known about the control of the constriction step, whereas several proteins have been revealed to be involved in the fission steps during proliferation: the dynamin-related proteins (DRPs) and FISSION1 (FIS1; Kaur *et al.*, 2009; Baker *et al.*, 2016; Kao *et al.*, 2018*b*; **Fig. 9**).

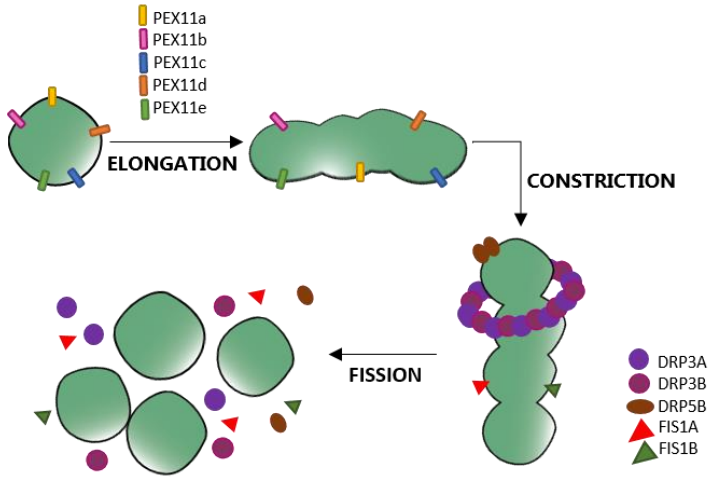

Figure 9. Scheme of plant peroxisome proliferation. *First stage of peroxisome proliferation is the elongation of the organelle, followed by the constriction and finally the division stage. In plants PEX11a-e proteins are involved in the elongation. By the contrary, proteins that regulate constriction are unknown. Dynamin-related proteins (DRPs: DRP3A, DRP3B) and FISSION1 (FIS1: FIS1A, FIS1B) proteins participate in the final step. Figure inspired from Pan et al., 2020.*

In yeast and mammals, FIS1 acts as an adaptor for the dynamin-like protein DLP1 (mammals) or the dynamin-related protein Vps1p VSP18 (yeast), by recruiting them to peroxisomes and mitochondria, which leads to membrane fission (Koch et al., 2005). Human PEX11β recruits DRP1 to the peroxisomal membrane (Koch and Brocard, 2011), and both *S. cerevisiae* PEX11 and human PEX11β have been reported to function as GTPase activating protein (GAP) for Dnm1 (DRP1; Williams *et al.*, 2015).

Peroxisomal fission shares several components with the mitochondrial fission machinery. In *Arabidopsis* two homologues of FIS1, FIS1A and FIS1B, have been identified and both are shared during peroxisome and mitochondria division. Moreover, three different DRPs have been reported (DRP3A, DRP3B, and DRP5B), having DRP3A and B functions in peroxisomal and mitochondrial fission whereas DRP5B supports fission of peroxisomes and chloroplasts (Kao *et al.*, 2018*b*; Su *et al.*, 2019). AtPEX11a to e have been

demonstrated to interact physically with FIS1B, whereas no interaction has been found with FIS1A or DRP3A (Lingard *et al.*, 2008).

Apart from the role in proliferation, several functions have been attributed to proteins of the PEX11 family: in the yeast *Ogataea polymorpha* PEX11 has been implicated in peroxisome segregation during cell division (Krikken *et al.*, 2009). *Saccharomyces cerevisiae* PEX11 is involved in peroxisome-mitochondria contact sites (Shai *et al.*, 2018), while *O. polymorpha* PEX11 has been implicated in peroxisome-ER contact sites (Wu *et al.*, 2020). *S. cerevisiae* PEX11 has also been proposed to act as a pore-forming protein (Mindthoff *et al.*, 2016) and has been implicated in medium chain FA oxidation as well (Van Roermund *et al.*, 2000). In mammals, PEX11γ has been suggested to coordinate peroxisomal growth and division via heterodimerization with PEX11 paralogs and interaction with Mff and FIS1 (Schrader *et al.*, 2016).

Over-expression of PEX11 family proteins from yeast, plants and mammalian systems results in the formation of long tubules that have been called juxtaposed elongated peroxisomes (JEPs), and tubular peroxisomal accumulations (TPAs; Delille et al., 2010; Koch *et al.*, 2010; Joshi *et al.*, 2012).

Attending to the amino acid sequence, PEX11 proteins from plants can be divided into groups: Class I *(AtPEX11c,* -*d* and -*e)*, which display a high similarity to each other (75 % average identity and 92 % average similarity), and Class II *(AtPEX11a* and -*b)*, which are more divergent (exhibit 31 % identity and 51 % similarity to each other; Lingard and Trelease, 2006). Lingard and Trelease (2006) studied the transitory expression of PEX11a-e in Arabidopsis and tobacco BY-2 suspension cells, and reported that in cells transformed with AtPEX11c or AtPEX11d, peroxisomes elongated without subsequent fission, whereas PEX11e leads to an increase in peroxisomal number without elongation. In AtPEX11b-transformed cells, peroxisomes were aggregated and rounded. Cells transformed with myc-AtPEX11a show a significant difference regarding the amount of elongated peroxisomes over a time period of 72 h. After over-expression of the CFP-PEX11c, CFP-PEX11e and CFP-PEX11d fusion proteins in Arabidopsis, peroxisomal clustering and an increased number of peroxisomes was reported by Orth and colleagues (2007). In this work and after analysing RNAi silencing plants, it was shown that AtPEX11 proteins are in part redundant for regulation of peroxisome proliferation, being the isoform b the less important in this process (Orth *et al.*, 2007). Additionally, in cells where PEX11c, PEX11d

and PEX11e were silenced simultaneously, peroxisomes were enlarged, but not elongated, suggesting that these proteins act in peroxisome growth, but not in tubulation (Lingard *et al.*, 2008).

D.1.2 Peroxisomal dynamics under stress: Cd as a case of study

Cd is one of the stresses that induces peroxisome proliferation in Arabidopsis. Time course analyses of peroxisomes in responses to Cd by confocal microscopy have allowed to stablish differential changes in peroxisome dynamics, starting with fast peroxules formation (15-30 min), peroxisome elongation, and proliferation (3 h; Rodríguez-Serrano *et al.*, 2016*b*; **Fig. 10**). While longer treatment periods (24 h) considerably increase peroxisomal speed. The increase of movement was regulated by ROS produced by NADPH oxidases and Ca^{2+} ions (Rodríguez-Serrano *et al.*, 2009). The increase of peroxisomal movement could improve antioxidant defences in places where Cd or other factors promote ROS accumulation and could help in signalling transduction and metabolite exchange in different parts of the cell (Rodríguez-Serrano *et al.*, 2009).

Due to the fast induction of peroxules in response to H_2O_2 (Sinclair *et al.*, 2009) and Cd (Rodríguez-Serrano *et al.*, 2016*b*) and the absence of significant changes in *PEX11a* expression in *nox1* mutants (Terrón-Camero *et al.*, 2020), it is reasonable to assume that PEX11a could be regulated by specific ROS and NO-dependent PTMs. However, PTMs peroxisomal proteomic analyses have reveal that *PEX11a* is a putative target of phosphorylation in Arabidopsis (Kataya *et al.*, 2019; Sandalio *et al.*, 2019; see **annex II**), although other redox modification cannot be rule out. In fact, the activation of yeast Pex11p depends on redox changes in its cysteins (Knoblach and Rachubinski, 2010; Schrader *et al.*, 2012).

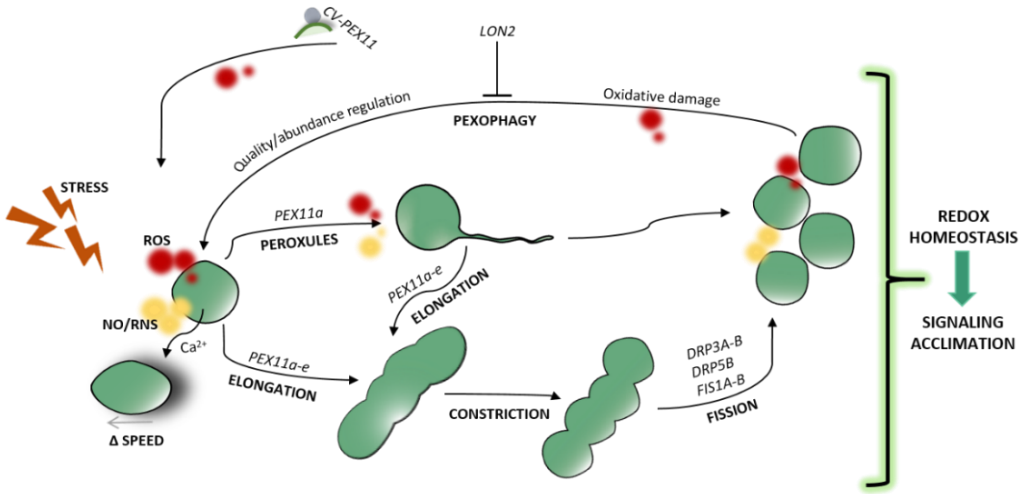

Figure 10. Scheme of plant peroxisome proliferation. *Hypothetical scheme showing changes in peroxisomal dynamics and their regulation, as well as their contribution to cell responses to abiotic stresses such as metal toxicity. Cd stress promotes the generation of ROS which activate PEX11a and PEX11e, probably by ROS-/NO-dependent PTMs. PEX11a promotes the formation of peroxules, which could control ROS/NO accumulation and ROS-dependent gene expression. Peroxisomal elongation, constriction and proliferation, which are also regulated by ROS and NO, were later observed. Longer exposure periods increase the speed of peroxisome movement, which is also controlled by ROS. The number of peroxisomes, as well as oxidized, damaged peroxisomes, can be regulated by pexophagy or via a process independent of autophagy involving chloroplast vesicles interactions with PEX11, both of which processes are regulated by ROS. Red color, ROS; yellow color, NO. Figure taken from* ***annex I****.*

D.1.3. Peroxules formation and *PEX11a*

Although their function is not clear, it has been suggested that peroxules might serve as a platform for the connection of peroxisomes with other organelles to facilitate the exchange of metabolites such as ROS/RNS and proteins during stress response (Jaipargas *et al.*, 2016; Foyer *et al.*, 2020; Pan *et al.*, 2020). When producing peroxules, peroxisomes are immobile, suggesting that they are tethered to another organelle, with PEX11a representing a good candidate for mediating inter-organellar docking (Rodríguez-Serrano *et al.*, 2016*b*; **annex I**). Accumulating evidence has revealed convincingly that peroxules are key to the interaction of peroxisomes with organelles known to have close metabolic and physical ties with peroxisomes, including the ER, oil bodies, mitochondria and chloroplasts (Sinclair *et al.*, 2009; Thazar-Poulot *et al.*, 2015; Gao *et al.*, 2016; Jaipargas *et al.*, 2016; Rodríguez-Serrano *et al.*, 2016*b*). According to Mathur (2020) recurrent changes in shape and organelle interactivity may increase its

efficiency for metabolic exchange, may trigger defence response pathways or allow more efficient retrieval and resource recycling. In spite of peroxule-dependent ROS signalling, there is not any evidence that peroxules could participate in H_2O_2 transfer between organelles. However, stromules have been reported to be involved in transfer H_2O_2 from chloroplasts to nuclei as a part of retrograde signalling (Caplan *et al.*, 2015; Kumar *et al.*, 2018). As far as we know, the connection of peroxisomes with nuclei throughout peroxules has not been demonstrated. Peroxules are also involved in protein transport such as the transfer of the sugar dependent 1 (SDP1) lipase from the peroxisomal membrane to the lipid body (Thazar-Poulot *et al.*, 2015). It is worth noting that the percentage of peroxisome producing peroxules under Cd toxicity has been reported to be 20-40 % (Rodríguez-Serrano *et al.*, 2016*b*; Terrón-Camero *et al.*, 2020), which suggest the existence of different populations of peroxisomes in the cell differing in tethering to other organelles and probably their functions.

Peroxules have been associated with peroxisome proliferation (Sinclair *et al.*, 2009), although Rodríguez-Serrano et al. (2016) suggested that they do not always cause proliferation and may be involved in regulating ROS accumulation and ROS-dependent signalling transduction (Rodríguez-Serrano *et al.*, 2016*b*; Terrón-Camero *et al.*, 2020). In fact, Arabidopsis *drp3a* mutants displayed enlarged peroxisomes and peroxules (Rinaldi *et al.*, 2016) suggesting that blocking fission machinery promote peroxules formation, supporting the idea that this process is not only a previous step to peroxisome proliferation.

Peroxules formation in response to Cd and As is dependent on *PEX11a*, and *pex11a* Arabidopsis mutants show altered ROS-dependent signalling network (Rodríguez-Serrano *et al.*, 2016*b*). However, recently Terrón-Camero et al. (2020) have demonstrated that peroxules regulation also depends on NO in response to Cd. These findings demonstrate that PEX11a and peroxules formation play a key role in regulating stress perception and rapid cell responses to environmental cues (Rodríguez-Serrano *et al.*, 2016*b*; Terrón-Camero *et al.*, 2020). PEX11a function however is far to be well known

Objectives

The mechanisms involved in plant response to stress with special interest in the role of reactive oxygen species (ROS) and nitric oxide (NO), as signal molecules, is one of the main goals of the group "Reactive Oxygen and Nitrogen Species Signalling under Stress Conditions in Plants", from the Department of Biochemistry, Molecular and Cellular Biology of Plants, in the Estación Experimental del Zaidín-CSIC, Granada.

Plant response to different abiotic stresses such as the herbicide 2,4-D or the heavy metal cadmium (Cd) have been largely analysed in the group, focused mainly in the role of ROS as essential signalling molecules in plant adaptation and survival. In particular, special interest has been paid to the peroxisome as sensor of redox changes and cellular redox homeostasis regulator. Originally, peroxisomes were regarded as an H_2O_2 sink, nonetheless recent biochemical, transcriptomic and proteomic studies have revealed that these organelles are much more complex and there is much to discover. Critical metabolic pathways are hosted in plant peroxisomes such as, β-oxidation, photorespiration, biosynthesis of phytohormones and ROS/RNS metabolism. Therefore, peroxisomes are a source of signalling molecules, which are essential for the regulation of development processes and plant response to stress. Very little is known however, about peroxisomal downstream signalling networks.

Although peroxisomal proliferation has been described for a long time, in recent years, our knowledge about peroxisomal dynamics has increased. Dynamic peroxisomal extensions, called peroxules, have been described after application of ROS and NO donors and in plant response to stress. Among others, the Arabidopsis proteins Peroxin 11a-e (PEX11a-e) are involved in the first stage of peroxisomal proliferation, being the PEX11a essential to produce peroxules in response to Cd. Although PEX11a and peroxules formation play a key role in regulating stress perception and fast cell responses to environmental cues, the underlying signalling mechanisms are not well known.

With this background, this Thesis aims to elucidate peroxisomal dependent signalling in plant response to abiotic stress as general objective. To achieve this, three specific objectives were defined and addressed, as follow:

1. To identify the peroxisomal ROS-dependent signalling in plant response to the herbicide 2,4-D. For this purpose, we carried out a transcriptomic analysis with

WT and *acx1* mutants, affected in the peroxisomal enzyme Acyl-CoA oxidase (ACX), which is one of the main sources for H_2O_2 production after 2,4-D treatment.

2. To identify a data set of common and specific genes regulated by peroxisomal ROS under different conditions. For this, we carried out a meta-analysis of different, public and in-house transcriptomes, with mutants and/or stresses leading to peroxisomal-dependent ROS levels altered.

3. To evaluate, by a genetic approach, the role of the peroxin 11a (PEX11a) in plant development and plant response to Cd stress. To meet the objective, we generated CRISPR-Cas9 mutants affected in PEX11a and evaluated their phenotype under developmental and stress conditions. In addition, a transcriptomic analysis has been made with these mutants under control and Cd stress.

Chapter 1

Insights into ROS-dependent signalling underlying transcriptomic plant responses to the herbicide 2,4-D

Adapted from:

Romero-Puertas, M. C., **Peláez-Vico, M. A.**, Pazmiño, D., Rodríguez-Serrano, M., Terrón-Camero, L. C., Bautista, R., Gómez-Cadenas, A., Claros, M., León, J. and Sandalio, L. M. 2021.
Accepted in Plant, Cell and Environment.

Insights into ROS-dependent signalling underlying transcriptomic plant responses to the herbicide 2,4-D

María C. Romero-Puertas[1]*, M. Ángeles Peláez-Vico[1], Diana M. Pazmiño[1], María Rodríguez-Serrano[1#], Laura Terrón-Camero[2], Rocío Bautista[3], Aurelio Gómez-Cadenas[4], M. Gonzalo Claros[3,5,6], José León[7], Luisa M. Sandalio[1]*

[1]*Departamento de Bioquímica, Biología Celular y Molecular de Plantas, EEZ, CSIC, C/ Prof. Albareda, 18008 Granada, Spain*
[2] *Bioinformatics Unit, IPBLN, CSIC, Granada, Spain.*
[3]*Plataforma Andaluza de Bioinformática-SCBI, Universidad de Málaga, C/Severo Ochoa 34, 29590 Málaga, Spain*
[4]*Department Ciències Agràries i del Medi Natural, Universitat Jaume I, E-12071, Castelló de la Plana, Spain*
[5]*Departamento de Biología Molecular y Bioquímica, Ciencias, Univ. de Málaga, Campus de Teatinos s/n, 29071, Málaga, Spain*
[6]*Institute for Mediterranean and Subtropical Horticulture "La Mayora" (IHSM-UMA-CSIC), Av. Louis Pasteur, 49. 29010 Málaga, Spain*
[7]*Instituto de Biología Molecular y Celular de Plantas (CSIC-Univ. Valencia), CPI Edificio 8E, Avda. Ingeniero Fausto Elio s/n, 46022 Valencia, Spain*
[#] *Current address: Education Faculty, University of Granada, Melilla, Spain*

*Authors for correspondence:
Dr. Luisa M. Sandalio
Telephone: +34958181600 Ext. 316
e-mail: luisamaria.sandalio@eez.csic.es

Dr. María C. Romero-Puertas
Telephone: +34958181600 Ext. 175
e-mail: maria.romero@eez.csic.es

Running title: H_2O_2 signalling under 2,4-D treatment

Key words: 2,4-D; Acyl-CoA oxidase; auxin; peroxisomes; reactive oxygen species; signalling; transcriptome

ABSTRACT

The synthetic auxin 2,4-dichlorophenoxyacetic acid (2,4-D) functions as an agronomic weed control herbicide. High concentrations of 2,4-D induce plant growth defects, particularly leaf epinasty and stem curvature. Although the 2,4-D-triggered ROS production, little is known about its signalling. In this study, by using a null mutant in peroxisomal acyl CoA oxidase 1 *(acx1-2)*, we identified ACX1 as one of the main sources of ROS production and, in part, also causing the epinastic phenotype following 2,4-D application. Transcriptomic analyses of WT plants after treatment with 2,4-D revealed a ROS-related peroxisomal footprint in early plant responses, while other organelles, such as mitochondria and chloroplasts, are involved in later responses. Interestingly, a group of 2,4-D-responsive ACX1-dependent transcripts previously associated with epinasty is related to auxin biosynthesis, metabolism and signalling. We found that the auxin receptor AUXIN SIGNALLING F-BOX 3 (AFB3), a component of SCF (ASK-cullin-F-box) E3 ubiquitin ligase complexes, which mediates AUX/IAA degradation by the 26S proteasome, acts downstream of ACX1 and is involved in the epinastic phenotype induced by 2,4-D. We also found that protein degradation associated with ubiquitin E3-RING and E3-SCF-FBOX in ACX1-dependent signalling in plant responses to 2,4-D is significantly regulated over longer treatment periods.

1. INTRODUCTION

2,4-dichlorophenoxyacetic acid (2,4-D) is one of the most commonly used auxinic herbicides in agriculture (Burns and Swaen, 2012). In fact, new 2,4-D-resistant crops have been approved by the U.S. Department of Agriculture in the previous ten years (Egan *et al.*, 2011), suggesting current contamination of soil and water that can affect the environment and even human health (Teixeira *et al.*, 2007; Zuanazzi *et al.*, 2020; Li *et al.*, 2021). 2,4-D is a synthetic analogue of natural auxins, which at high concentrations induces plant growth defects, particularly stem curvature, leaf epinasty, senescence and root growth inhibition (Grossmann *et al.*, 2001; Romero-Puertas *et al.*, 2004a; Pazmiño *et al.,* 2012).

Auxin modulates the expression of genes regulated by the interplay of auxin response factors (ARFs) and auxin/indole acetic acid (AUX/IAA) repressors. At low auxin concentrations, AUX/IAA repress ARFs activators and block auxin-regulated gene expression; however, higher concentrations of auxin promote the binding of auxin to Transport Inhibitor Response1/Auxin Signalling F-Box (TIR1/AFB) receptors; this leads to degradation of AUX/IAA repressors by the 26S proteasome, which promotes auxin-dependent gene expression (Eyer *et al.*, 2016; Sandalio *et al.*, 2016). It has been suggested that 2,4-D acts via TIR1/AFB auxin-mediated signalling (Parry *et al.*, 2009; Eyer *et al.*, 2016). The TIR1/AFB gene family consists of six receptors: TIR1 and five AFB homologs (Prigge *et al.*, 2016). Analysis of Arabidopsis mutant lines of TIR and AFB has demonstrated that these receptors are indeed essential for the plant perception and specificity of auxin herbicides (McCauley *et al.*, 2020).

A close relationship between reactive oxygen species (ROS) has been established in both auxin-dependent cell growth and 2,4-D mode of action. Hydroxyl radicals (·OH) are involved in the cleavage of covalent bonds in the cell wall during plant growth (Liszkay *et al.*, 2004), and ROS have been shown to affect auxin homeostasis and conjugation, with the degradation, distribution and relocation of IAA giving rise to morphological changes (reviewed in Sandalio *et al.*, 2016). ROS over-accumulation and oxidative stress are two of the main effects of the herbicide 2,4-D, which also increases lipid and protein oxidation and induces proteolysis (Romero-Puertas *et al.*, 2004a; Pazmiño *et al.*, 2011, 2012). 2,4-D has been shown to affect actin cytoskeleton structures, probably due to the *S*-nitrosylation and carbonylation of actin; these post-translational modifications (PTMs)

disrupt actin polymerization and cytoskeleton structures, leading to increased epinasty and alterations in the dynamics of organelles such as peroxisomes and mitochondria (Rodríguez-Serrano *et al.*, 2014). The dysfunction of these organelles may contribute to the accumulation of ROS, as was observed following treatment of pea and Arabidopsis plants with 2,4-D (Romero-Puertas *et al.*, 2004a; Pazmiño *et al.*, 2011; Rodríguez-Serrano *et al.*, 2014). The peroxisomal enzymes xanthine oxidase (XOD) and Acyl-CoA oxidase (ACX) have been suggested as possible sources of ROS following 2,4-D treatment (Romero-Puertas *et al.*, 2004a; Pazmiño *et al.*, 2011, 2014), indicating that peroxisomes are key organelles in plant responses to this herbicide. Peroxisomes, which can produce and remove ROS efficiently, have the capacity to regulate oxidative metabolism (Sandalio and Romero-Puertas, 2015; Sandalio *et al.,* 2021). Peroxisomes, whose metabolism and dynamic plasticity enable changes to be made in their enzymatic composition, size, shape, number and motility under different situations, play a key decision-making role in the cell (Kao *et al.*, 2018; Sandalio *et al.,* 2021).

Fatty acid β-oxidation is one of the main sources of ROS, particularly H_2O_2, in peroxisomes (Pan *et al.*, 2020). ACX, the first enzyme in the pathway, catalyzes the oxidation of Acyl-CoA to trans-2-enoyl-CoA, leading to the production of H_2O_2 in the reaction (Rinaldi *et al.*, 2016). This pathway, which provides energy from fats stored in oil bodies, is highly active at the initial stage of seedling growth (Rinaldi *et al.*, 2016). β-oxidation, which is involved in the synthesis of key metabolites, including hormones such as indole acetic acid (IAA) (Zolman *et al.*, 2008) and jasmonic acid (JA) (Castillo *et al.,* 2004; Afitlhile *et al.,* 2005; Delker *et al.,* 2007), also occurs in green tissues (Pan *et al.*, 2020; Sandalio *et al.,* 2021).

Although 2,4-D-dependent oxidative effects in plants have been widely characterized, little is known about their underlying signalling mechanisms and the role of ROS in regulating plant responses to 2,4-D. Previous results have suggested ACX as one of the H_2O_2 sources in plant response to 2,4-D. In this study, we have got a deeper insight into ACX1 role in plant response to 2,4-D. Thus, we observed an increase in H_2O_2 production in WT plants in response to the herbicide, which is lacking in the T-DNA insertion *acx1-2* mutant. Furthermore, epinastic phenotype, which has been previously shown to be ROS-dependent, induced by the herbicide in WT plants is hardly observed in *acx1* mutants. By analyzing transcriptomic responses in Arabidopsis plants, WT and

acx1-2, we found that H_2O_2 produced during β-oxidation regulates several sets of early genes related to IAA homeostasis, transport and signalling, leading to regulation of leaf epinasty. Longer exposure to 2,4-D involved other organelles such as mitochondria and chloroplast in regulating ROS-dependent 2,4-D effect. In addition, at this time point, protein degradation related to the E3-RING ubiquitin ligase and proteasome complex is significantly regulated in ACX1-dependent genes, suggesting a key role for this process in 2,4-D epinasty development.

2. MATERIALS AND METHODS

2.1. Plant Material and 2,4-D treatment

All the Arabidopsis seeds used in this study were in the Col-0 genetic background. T-DNA insertion *acx1-2* (SALK 041464; Adham *et al.,* 2005), *acx1-4* (SALK 145527) and *afb3-4* (SALK 068787C) were obtained from Nottingham Arabidopsis Stock Centre (NASC). Seeds were sown in moistened soil and grown in 16 h light and 8 h dark photoperiod cycles at 22 and 20 ºC, respectively, under 120 µmol m^{-2} s^{-1} and at 60 % relative humidity. Genomic DNA PCR analysis of *acx1-4* and *afb3-4* lines was carried out to verify homozygosity in T-DNA insertions with the appropriate primers (**Suppl. Table S1; Suppl. Fig. S1 A-B**; **Fig. 6**). The effect of 2,4-dichlorophenoxyacetic acid (2,4-D) on Arabidopsis plants was analysed by spraying 23 mM 2,4-D solution (prepared in 0.05 % dimethyl sulfoxide, DMSO and 0.05 % EtOH), and plant leaves were collected after 1 and 72 h post treatment (hpt). Control plants were sprayed with 0.05 % DMSO and 0.05 % EtOH. Before 2,4-D spraying, pre-infiltration with 0.1 mM MG132 prepared in 0.05 % DMSO and 0.05 % EtOH or control (0.05 % DMSO/0.05 % EtOH) were made when indicated. 2,4-D treatment times, concentrations and techniques used in this study had been previously optimised (Romero-Puertas *et al.,* 2004a; Pazmiño *et al.,* 2014; Rodríguez-Serrano *et al.,* 2014).

2.2. H_2O_2 quantification and localization

Hydrogen peroxide (H_2O_2) was quantified by spectrofluorimetry using horseradish peroxidase and homovanillic acid (excitation: 315 nm; emission: 425 nm) in 50 mM HEPES pH 7.5 (Romero-Puertas *et al.*, 2004b). A standard curve with known concentrations of commercial H_2O_2 was used to quantify samples. H_2O_2 accumulation was

also imaged by confocal laser scanning microscopy (CLSM) using 2',7'-dichlorodihydrofluorescein diacetate (DCF-DA) in 10 mM Tris-HCl (pH 7.4). Leaf sections (2 mm^2) were incubated for 30 min with DCF-DA and were then embedded in 30% (w/v) polyacrylamide blocks. Leaf sections were cut using a vibratome (Rodríguez-Serrano *et al.*, 2009) and analysed with the aid of a confocal laser scanning microscope (Leica TCS SL; Leica Microsystems), at 485 nm excitation and 530 nm emission. Chlorophyll-induced autofluorescence was also detected (excitation at 633 nm and emission at 680 nm).

2.3. Hormonal Analysis

Hormone extraction and analysis were carried out mainly as described in Balfagón et al. (2019). Before hormonal extraction, a mixture containing 50 ng of [$^2H_6$]-ABA, [^{13}C]-SA and dihydrojasmonic acid was added to 0.1 g of dry tissue as internal controls and hormones were quantified using a TQ-S Micro Triple Quadrupole Mass Spectrometer. Standard curves for each compound were used to quantify endogenous concentrations.

2.4. Microarray Data Bioinformatics and Statistical Analysis

2,4-D- and DMSO/EtOH (control)-sprayed leaves of similar sizes and developmental stages were sampled at 1 and 72 h. For microarray analysis, three independent biological replicates, each composed of leaves pooled from at least 5 different plants, were used per experimental condition. As described previously (Rodríguez-Serrano *et al.*, 2009), isolated total RNA was treated with deoxyribonuclease I (DNaseI; Turbo DNA free, Thermo Fisher Scientific) and cleaned on RNeasy Mini columns (Qiagen). These RNA samples were used to perform chip hybridization and analysis of transcriptional measures (Arabidopsis ATH1 chips; Affymetrix, Santa Clara, CA, US) at the *Centro Nacional de Biotecnología* (CSIC, Madrid). Expression data were normalized using the Robust Multi-Array Average (RMA) algorithm implemented in the affyPLM package. Differential gene expression was based on linear models for analysing microarray data (LIMMA) (Smyth and Speed, 2003). Both affyPLM and LIMMA are part of the Bioconductor project (Gentleman *et al.,* 2004). Differentially expressed (DE) genes were obtained by paired comparisons, with two independent comparisons carried out for each combination of treated samples vs. control for each genotype. Only genes with a fold-change (FC) over

1.5 (|log2(FC)| > 0.58496) and an adjusted $P < 0.05$ (adjusted using the false discovery rate; FDR) method developed by Benjamini-Hochberg (1995) were considered for further investigation. The non-overlapping genes between the data sets of interest were computed using the Venny algorithm (http://bioinfogp.cnb.csic.es/tools/venny/). Array data were deposited in Gene Expression Omnibus (GEO) repository (GSE179303).

Gene expression of relevant genes was confirmed by quantitative real-time polymerase chain reaction (qRT-PCR) as described elsewhere (Terrón-Camero *et al.*, 2020), where the relative expression of each gene was normalized to that of *TUB4*, and fold changes were calculated as $2^{-\Delta\Delta Ct}$. Primers used in this study are described in **Suppl. Table S1.** RNA amplification, labelling and slide hybridization were essentially carried out as described in Adie et al. (2007).

2.5. ROSMETER and bioinformatic analyses

The ROSMETER platform was used to identify transcriptomic imprints in plant responses to 2,4-D on the basis of ROS type and origin (Rosenwasser *et al.*, 2013). ROS-producing treatments compiled in the ROSMETER platform are detailed in Rosenwasser et al. (2013). Significantly enriched ($P < 0.05$) Gene Ontology (GO) terms from data sets of interest were analysed using Mapman software (https://mapman.gabipd.org/), which displays large datasets in diagrams of metabolic pathways, and the classification SuperViewer tool on the BAR website (http://bar.utoronto.ca/ntools/cgi-bin/ntools classification superviewer.cgi), with automatically derived functional GO classifications, as of March 31, 2019, downloaded from the TAIR website (ATH GO GOSLIM.txt.gz, file ATH GO GOSLIM.txt). For functional protein association networks, the String database (https://string-db.org/) was used. Functional enrichment of differentially ACX1-dependent regulated genes after 2,4-D application in *A. thaliana* leaves (1h and 72h) was performed by PlantGSEA plants (http://systemsbiology.cau.edu.cn/PlantGSEA/analysis.php). Gene expression (log FC) of regulated genes of interest belonging to GO terms related to oxidative stress (26 terms) were represented by a heatmap using the pheatmap package (version 1.0.12).

2.6. Epinasty degree analysis

Epinasty was quantified by analysing the angle (α) between the central nerve and the lateral edges in leaf sections of 1-2 mm^2 from leaves untreated and treated with 2,4-D.

2.7. Statistical analysis

Mean values for the quantitative experiments described above were obtained from at least three independent experiments, with no less than three independent samples per experiment. Statistical analyses were performed using a one- or two-way ANOVA test when necessary followed by a Student´s t-test (p-value < 0.05) or Tukey multiple comparison test (p-value < 0.05), respectively. The analyses were carried out with the aid of IBM SPPS Statistics 24 and GraphPad Prism 6. Error bars representing standard error (SEM) are shown in the figures.

3. RESULTS

3.1. ACX1: a principal source of ROS following 2,4-D treatment in Arabidopsis

In a previous study carried out in our laboratory, concentrations of herbicide 2,4-D were optimized (Romero-Puertas *et al.*, 2004a; Rodríguez-Serrano *et al.*, 2014), with 23 mM 2,4-D being selected. ROS production has previously been found to increase after 72 h 2,4-D treatment, with some evidence suggesting that ACX, the enzyme catalysing the first step of β-oxidation, is an important source of 2,4-D-induced ROS (Pazmiño *et al.*, 2011). We firstly determined, in control and 2,4-D-treated WT plants, the expression levels of *ACX1*, which is induced under different abiotic stress and hormone supply conditions (Castillo *et al.*, 2004). The induction of *ACX1* in WT indicates that this enzyme may play a role in ROS production after herbicide treatment (**Fig. 1 A**). To further study the role of ROS in plant responses to 2,4-D, we focused on the *acx1* mutants which are impaired in *ACX1* (*acx1-2* described in Adham *et al.*, 2005 and *acx1-4* genotyped in **Suppl. Fig. S1**). Phenotype after 2,4-D treatment was characterized in WT and *acx1-2* and *acx1-4* plants (**Fig. 1 B-D**). The spraying of Arabidopsis WT plants with 23 mM 2,4-D produced pronounced epinasty in rosette leaves and leaf turgidity loss, reaching maximum levels after 72 h of treatment, as described elsewhere (Rodríguez-Serrano *et al.*, 2014; **Fig. 1 B-D**). Epinasty degree was less severe in the *acx1-2* and *acx1-4* mutants than in WT (**Fig. 1 B-D**). These results suggest that part of the phenotype observed in WT plants treated

with 2,4-D may be due to *ACX1* and we will use *acx1-2* mutant from now on. A progressive increase in H_2O_2 in 2,4-D-treated WT plants as compared to untreated plants was fluorimetrically observed, which reached a statistically significant increase after 1 h of treatment although the highest accumulation took place after 72 h of treatment (**Fig. 2 A).** *acx1-2* mutant failed to accumulate H_2O_2 in response to 2,4-D, with a similar pattern being observed in control plants (**Fig. 2 A**). Confocal microscopic detection of H_2O_2, by using DCF-DA (green fluorescence), corroborated these findings, with a considerable increase in H_2O_2-dependent fluorescence being observed after 72 h of 2,4-D treatment in WT plants, while *acx1-2* failed to accumulate H_2O_2 in response to 2,4-D (**Fig. 2 B-C**).

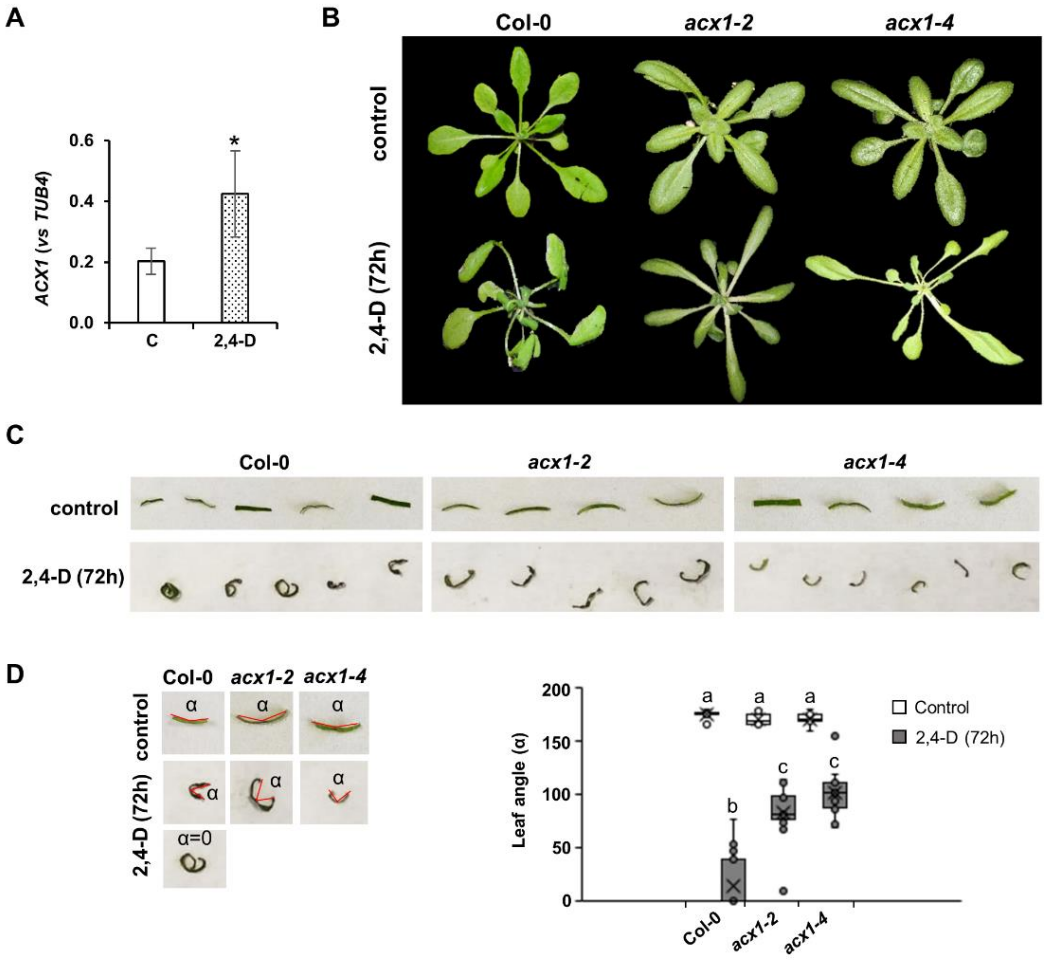

Figure 1. Effect of 2,4-D on plant phenotype. (A) *Quantitative RT-PCR analysis of ACX1 transcript in WT leaves after 1 h of spraying with 2,4-D.* ***(B)*** *WT, acx1-2 and acx1-4 plants were foliarly treated*

with 23 mM 2,4-D, whose phenotypic impact is shown (72 h). ***C)*** *WT, acx1-2 and acx1-4 leaf strips from leaves treated or not with 2,4-D (72 h).* ***D)*** *Leaves were sliced after 72 h of 2,4-D spraying and curvature was analysed by calculating the angle (α) of each strip with the tool angle from ImageJ software. The angle of the fully curved strips was considered 0. Asterisks in A) denote significant differences between 2,4-D treated and control (sprayed with DMSO/EtOH) plants according to the Student's t-test (p-value < 0.05). Different letters denote in D) significant differences between values obtained by Tukey multiple comparison tests (p-value < 0.05).*

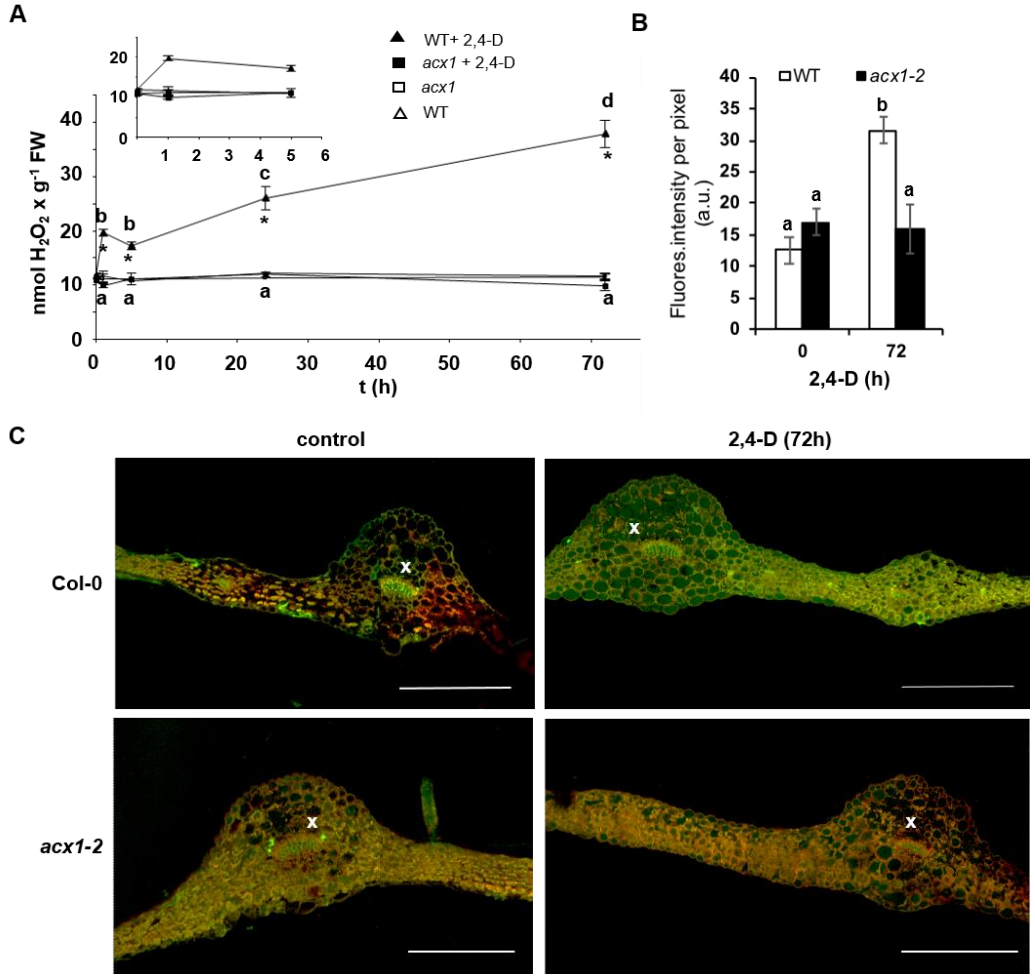

Figure 2*.* ***ROS production after 2,4-D treatment. (A)*** *H_2O_2 content assayed by fluorimetry in acid extracts from WT and acx1-2 leaves after plant spraying with 2,4-D (1 h-72 h). Values are means ± SEM of at least three experiments with three independent extracts each;* ***(B)*** *Quantification of fluorescence across the section tissue showed in C), in arbitrary units using ImageJ software;* ***(C)*** *Confocal laser scanning microscopy (CLSM) imaging of H_2O_2 accumulation in green colour, in cross-sections of Arabidopsis leaves using DCF-DA (Ex/Em: 485/530 nm). Images are maximal projections from several optical sections and are representative of at least 15 leaf sections from four different experiments. Asterisks in A) denote significant differences between treated acx1-2 and WT plants at each time point according to the Student's t-test (p-value < 0.05). The absence of an asterisk*

denotes no significant differences between acx1-2 and WT plants under control conditions. Different letters denote in B) significant differences between values, obtained using Tukey multiple comparison tests (p-value < 0.05). x, xylem. Bar= 300 µm

3.2. The herbicide 2,4-D generates an early transcriptome footprint related to peroxisomal stress

Although part of the 2,4-D effect appears to be ROS-dependent (Grossmann *et al.*, 2001; Rodríguez-Serrano *et al.*, 2014; De *et al.*, 2016; Sandalio *et al.*, 2016), not much is known about the molecular mechanism underlying ROS-dependent regulation. Taking into account the clear relationship between H_2O_2 accumulation and the *acx1-2* phenotype in response to 2,4-D, we performed a time-course microarray analysis of WT and *acx1-2* Arabidopsis plants treated with 2,4-D to identify genes differentially regulated in both lines in response to the herbicide. We analysed the transcriptomes at 1 hpt, which corresponds to the early increase of H_2O_2 in WT plants, and at 72 hpt, when 2,4-D effects on plants can be observed such as epinasty and repair mechanisms were shown to be activated in pea plants (Rodríguez-Serrano *et al.*, 2014). We then investigated the occurrence of ROS-related transcriptomic signatures in our transcriptome using the ROSMETER bioinformatics platform related to ROS type and origin (Rosenwasser *et al.*, 2013). Significantly, the highest transcriptome correlation values after 1 h of 2,4-D treatment were found in relation to the transcriptomes of catalase mutants *(cat2)* exposed to 3 and 8 h high light, in which peroxisomal H_2O_2 is accumulated (Vanderauwera *et al.*, 2005; **Fig. 3 A**). High correlation was observed also with the transcriptome obtained after treatment of WT with the catalase inhibitor 3-aminotriazole (AT), which also led to an increase in peroxisomal H_2O_2 (Gechev *et al.*, 2005; **Fig. 3 A**). The early transcriptome also showed significant correlation, although at lesser extent with those obtained following direct applications of H_2O_2 in Arabidopsis seedlings (Davletova *et al.*, 2005), methyl viologen (MV; Kilian *et al.*, 2007), and the mitochondrial complex I inhibitor rotenone (Garmier *et al.*, 2008; **Fig. 3 A**). The correlation values for the *cat2* signature declined over time (72 h), while those related with another ROS origin increased (**Fig. 3 B**). Because MV and rotenone triggers ROS production in chloroplasts and mitochondria, the contribution of these organelles in 2,4-D-induced ROS production likely occurs at a later stage (**Fig. 3 B**).

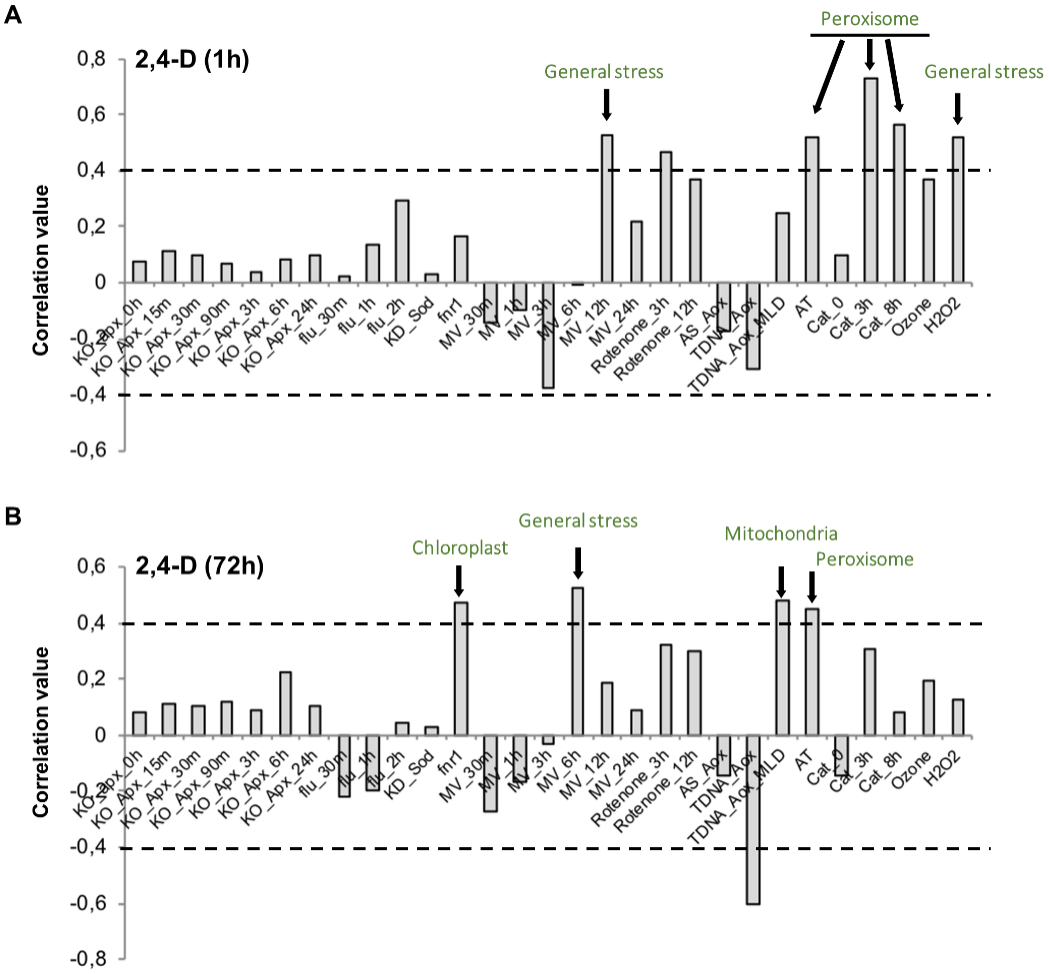

Figure 3. Analysis of 2,4-D transcriptome using the ROSMETER platform. *Correlation values of changes in the transcriptome in WT Arabidopsis plants treated with 2,4-D for 1 h* ***(A)*** *and 72 h* ***(B)*** *generated by the ROSMETER platform. Correlation values (y axis ordinate) were obtained as described by Rosenwasser et al. (2011, 2013) from the 2,4-D transcriptome and transcriptomes of the individual ROS-producing treatments compiled in the ROSMETER platform (x axis abscissa) detailed in Suppl. Table S1 from Rosenwasser et al. (2013). 1 indicates complete correlation. Positive and negative data correspond to positive and negative correlation, respectively, between the transcriptomes. 0 indicates no correlation. Correlation values above 0.4 (discontinuous line) can be considered significant correlation values that provide biological insights (Rosenwasser et al., 2013). Higher correlation values (arrows) at 1 h relate to peroxisomal stress (AT, aminotriazole treatment) cat 3h and cat 8h, cat2-2 mutants under 3 and 8 h high light stress, respectively. Higher correlation values (arrows) at 72 h relate to peroxisomal stress (AT, aminotriazole treatment), general stress (methyl viologen, MV 6h treatment), chloroplast stress (fnr1 mutants) and mitochondrial stress (aox mutants).*

3.3. ACX1-dependent genes in early plant responses to 2,4-D

Peroxisomes appear to be one of the main targets for H_2O_2 accumulation in early plant responses to 2,4-D, with ACX1 appearing to be one of the principal sources of this accumulation. Transcriptome analysis thus provides a deeper insight into both WT and *acx1-2* mutant by identifying peroxisomal-dependent genes that regulate plant responses to the herbicide. Large sets of transcripts responded to 2,4-D treatment in the leaves of WT and *acx1-2* mutant at both time points analysed (**Suppl. Fig. S2 and S3**). After 1 h treatment, 3,600 genes were regulated in WT plants (1,764 up and 1,836 down), and 3,619 genes were regulated in *acx1-2* (1,503 up and 2,116 down). When comparing genes regulated in WT and *acx1-2* in response to 2,4-D at 1 h, we found 698 genes up-regulated and 644 genes down-regulated in WT but not in *acx1-2* mutant, which we consider early ACX1-dependent genes (**Suppl. Fig. S2 A-B**; **Suppl. Table S2**). After 72 h treatment, 7,442 genes were regulated in WT plants (4,113 up and 3,329 down), and 8,309 genes were regulated in *acx1-2* (4,543 up and 3,766 down). When comparing genes regulated in WT and *acx1-2* in response to 2,4-D at 72 h, we found 841 genes up-regulated and 857 genes down-regulated in WT but not in *acx1-2* mutant, which we consider late ACX1-dependent genes (**Suppl. Fig. S3 A-B**; **Suppl. Table S2**).

A significant enrichment in GO functional categories related to signal transduction, transport, stress-response pathways, cell organization and biogenesis, mainly related to the endoplasmic reticulum (ER) and Golgi apparatus was found among early ACX1-dependent up-regulated transcripts (**Suppl. Fig. S2 C**). Among ACX1-dependent down-regulated transcripts a significant over-representation of GO categories related to transcription, developmental processes, in addition to up-regulated pathways, signal transduction, as well as cell organization and biogenesis, mainly related to the chloroplast and plastid was observed (**Suppl. Fig. S2 D**). At a later stage, ACX1-dependent up-regulated transcripts included a significant representation of stress-response pathways, transcription, and other biological and developmental processes, which are mainly associated with the cell wall and plasma membrane (**Suppl. Fig. S3 C**). Down-regulated transcripts at 72 hpt included DNA and RNA metabolism, cell organization and biogenesis, as well as electron transport and energy pathways and other cellular processes, mainly associated with ribosomes and cytosol (**Suppl. Fig. S3 D**). Interestingly, the category responses to abiotic and biotic stimulus is significantly

represented in both, up and down-regulated genes. Quantitative real-time polymerase chain reaction (qRT-PCR) was used to verify the expression pattern of selected genes of interest belonging to different categories: *ATP24a*, *HSP, PR-1* and the *peroxisomal Ca-dependent solute carrier*. Similar results were obtained through microarray and qRT-PCR analyses, thus demonstrating the reliability of microarray analysis (**Suppl. Fig. S4**). *ATP24a* encoding a peroxidase was upregulated in WT plants by 2,4-D, while an opposite pattern was observed in *acx1-2* mutants; *HSP* encoding a heat shock protein (HSP) was upregulated in WT, but less up-regulated in *acx1-2* mutant. At 72 hpt, similar results described at 1 hpt were observed for *ATP24a* and *HSP,* while *PR-1* was upregulated in WT and to a lesser extent in *acx1-2*. The *peroxisomal Ca-dependent solute carrier* was down-regulated in WT and slightly up-regulated in *acx1-2* mutant.

To check whether ACX1-dependent genes in plant response to 2,4-D were related with ROS and/or redox metabolism we further analysed these genes by PlantGSEA considering up and down regulated genes together. We found the categories of interest: hydrogen peroxide metabolic process, response to hydrogen peroxide, response to reactive oxygen species and response to oxidative stress significantly represented after 1h treatment (**Fig. 4**; **Suppl. Table S3**). After 72 h treatment, categories significantly represented were regulation of hydrogen peroxide metabolic process, regulation of oxygen and reactive oxygen species metabolic process, hydrogen peroxide metabolic process and oxygen and reactive oxygen species metabolic process (**Fig. 4**; **Suppl. Table S3**). We further analyzed our transcriptomic results and look for genes related to the categories glutathione/ascorbate/redox metabolism although these categories were not significantly overrepresented. A heat map with genes related with the categories of interest is shown in **Fig. 4** (**Suppl. Table S4**).

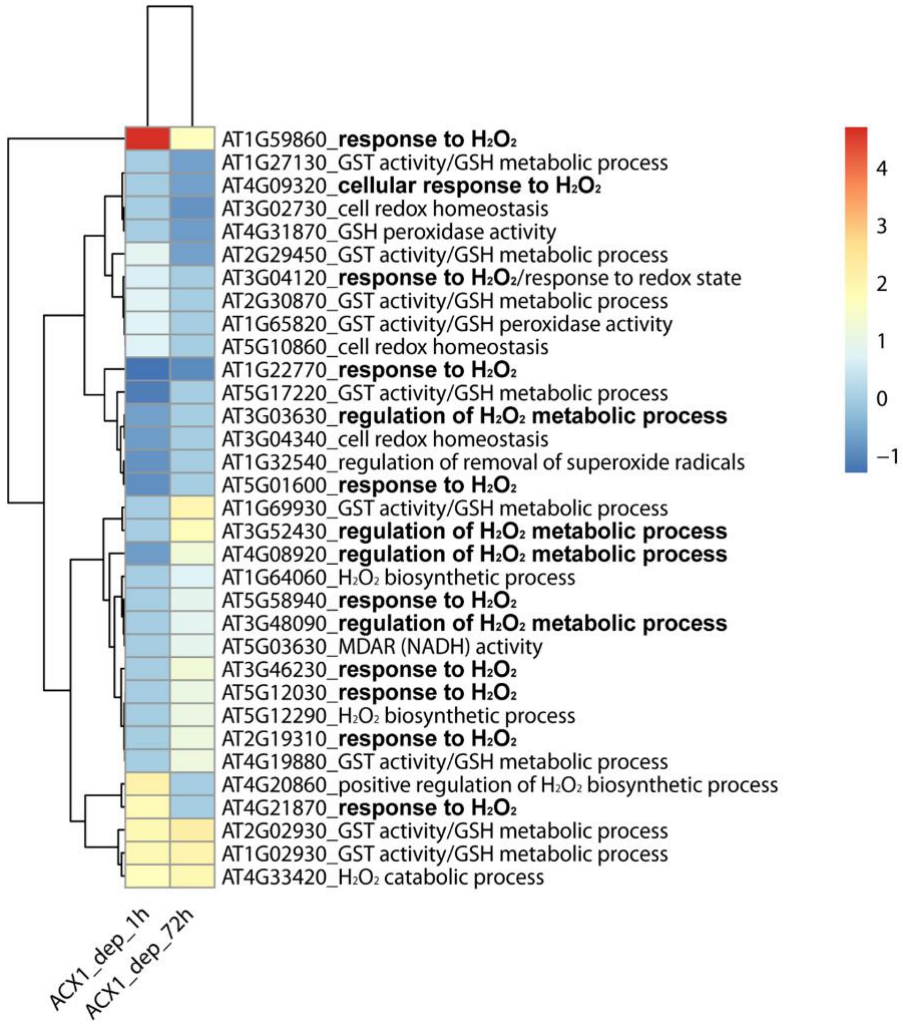

Figure 4: Analysis of ACX1-dependent genes in plant response to 2,4-D related with ROS/GSH/AsA and redox. *Heatmap of the ACX1-dependent differentially regulated genes (p-value<0.05) in plant response to 2,4-D, within the ROS/GSH/AsA and redox-related GO categories. Significantly over-represented functional categories obtained by PlantGSEA are presented in bold (**Suppl. Table S3**). Locus identifiers (**Suppl. Table S4**) have been accompanied by Gene Ontology category related to oxidative metabolism. Glutathione transferase activity/glutathione metabolic process:GO:0004364/GO:0006749, response to hydrogen peroxide:GO:0042542, regulation of removal of superoxide radicals:GO:2000121, glutathione transferase activity/glutathione peroxidase activity:GO:0004364/GO:0004602, regulation of hydrogen peroxide metabolic process:GO:0010310, response to hydrogen peroxide/response to redox state:GO:0042542/GO:0051775, cell redox homeostasis:GO:0045454, positive regulation of hydrogen peroxide biosynthetic process:GO:0010729, hydrogen peroxide catabolic process:GO:0042744, hydrogen peroxide biosynthetic process:GO:0050665, cellular response to hydrogen peroxide:GO:0070301, glutathione peroxidase activity:GO:0004602, monodehydroascorbate reductase (NADH) activity:GO:0016656.*

3.4. Hormone levels in plant responses to 2,4-D

Epinasty is regulated by hormonal cross-talk (Sandalio *et al.*, 2016) and peroxisomal β-oxidation is required for the biosynthesis of certain hormones such as IAA and jasmonic acid (JA) (reviewed in Raghavan *et al.*, 2006; Sandalio and Romero-Puertas, 2015). We therefore further analysed different hormones in leaves from WT and *acx1-2* Arabidopsis plants treated or not with 2,4-D. Abscisic acid (ABA), which has been reported to be involved in 2,4-D toxicity (Raghavan *et al.*, 2006) and to regulate epinasty and hyponasty (Cox *et al.*, 2004), increased in plant responses to 2,4-D with the period of treatment, although no significant differences were observed in relation to *acx1-2* as compared to WT plants (**Fig. 5 A**). A significant increase in salicylic acid (SA) content was observed after 72 h of 2,4-D treatment, with slightly higher levels observed in *acx1-2* mutant than in WT (**Fig. 5 B**). On the other hand, we observed a significant decrease in JA concentrations in WT plants in response to 2,4-D treatment after 72 h, whereas no changes in JA content were observed in *acx1-2* mutant after treatment (**Fig. 5 C**). Lower levels of JA in *acx1-2* compared to WT in all cases is expected, as β-oxidation involving ACX1 is required for JA synthesis to occur (Castillo *et al.*, 2004). These findings suggest that JA may not be a key molecule for triggering epinasty following herbicide treatment. Further experiments showed that treatment of WT plants with ABA, SA and JA does not induce an epinastic phenotype in our hands (**Suppl. Fig. S5**).

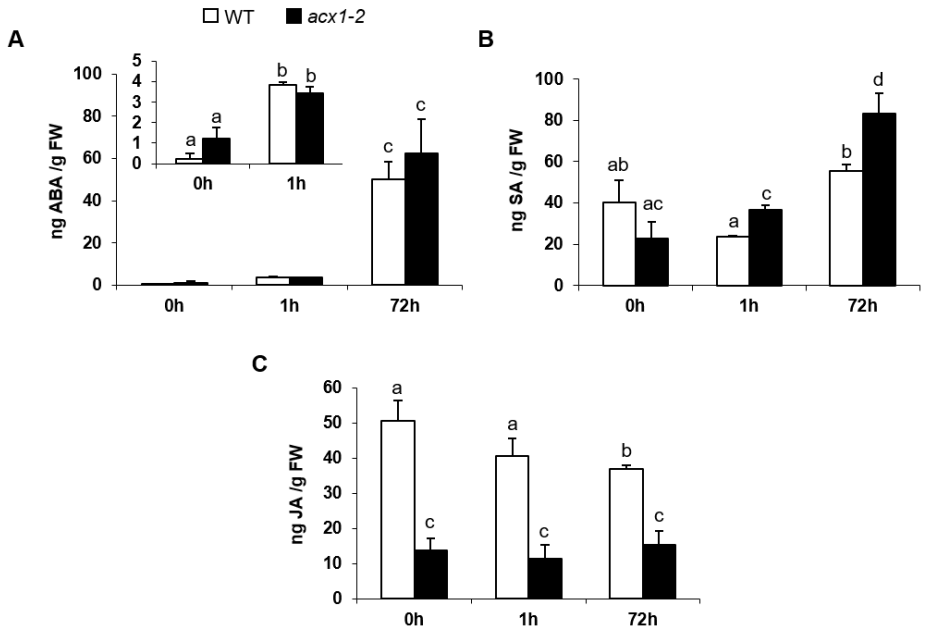

Figure 5. Effect of 2,4-D on plant hormone production. (A) *ABA,* ***(B)*** *SA and* ***(C)*** *JA production in WT and acx1-2 plants after 2,4-D spraying at 1 h and 72 h. The inset is an amplification of the graph at 0 and 1 h treatment in A). Bars represent the mean ± SEM of at least 4 replicates. Different letters denote significant differences between the different values obtained using Tukey multiple comparison tests (p-value < 0.05).*

3.5. Auxin signalling in plant responses to 2,4-D is ACX1-dependent

Within the principal categories significantly represented in ACX1-dependent genes regulated by 2,4-D stress, we found genes associated with auxin biosynthesis, metabolism and signalling (**Table 1**). To obtain a deeper insight, we looked for available mutants affected in genes potentially regulated by peroxisomal ACX1-dependent H_2O_2 in response to 2,4-D, associated with auxins (**Table 1**) in the 6,760 T-DNA mutant collection from the SALK Institute (NASC, ID: N27941). We found 21 mutants available (**Table 1**) and after 2,4-D treatment as described in material and method section, the SALK 068787C mutant showed the most similar epinastic phenotype to that of *acx1-2* mutant (**Fig. 6**). SALK 068787C mutant has a T-DNA insertion in the At1g12820 gene coding for protein AUXIN SIGNALLING F-BOX 3 (AFB3; **Fig. 6 A**), and it has been previously described as *afb3-4* (Parry *et al.,* 2009). *AFB3* expression in WT and *acx1-2* mutants after 2,4-D treatment was validated by qRT-PCR, which showed a significant inhibition in WT after 1 h treatment, with no significant changes observed in *acx1-2* mutant (**Suppl. Table S2**; **Fig. 6 C**; **Suppl. Fig. S4**). We then determined the homozygosity of *afb3-4* (**Fig. 6 B**) and analysed *AFB3* expression under 2,4-D treatment conditions in this mutant (**Fig. 6 B-C**). We performed semiquantitative RT-PCR, which found no *AFB3* expression in *afb3-4* seedlings under our experimental conditions (**Fig. 6 C**). The AFB3 component of SCF (ASK-cullin-F-box) E3 ubiquitin ligase complexes acts as an auxin receptor that mediates AUX/IAA protein proteasomal degradation. Following StringDB enrichment analysis, setting no more than 10 interactors in the first shell and five interactors in a second shell, AFB3 was found to be linked to auxin-regulated gene transcription and directly connected to the S-phase kinase-associated proteins (Skp) (**Fig. 7 A**, **Table 2**), which acts as an adapter that connects the F-box protein to CULLIN (CUL) proteins.

In addition, ubiquitin-dependent degradation was significantly represented after 2,4-D treatment in ACX1-dependent genes, at later time (72 h), as imaged by Mapman software (**Fig. 7 B**, **Suppl. Table S5**). Moreover, pre-infiltration of leaves with the

proteasome inhibitor MG132 decrease significantly epinastic phenotype in WT leaves (**Fig. 7 C**) supporting the key role for proteasome in development of epinasty. We further used a genetic approach, by using *cul4cs* mutants (Chen *et al.,* 2006), showing downregulation of CUL4, which is involved in protein degradation (Fonseca and Rubio, 2019) and observed that development of epinasty after 2,4-D treatment is drastically affected in this mutant, supporting previous results.

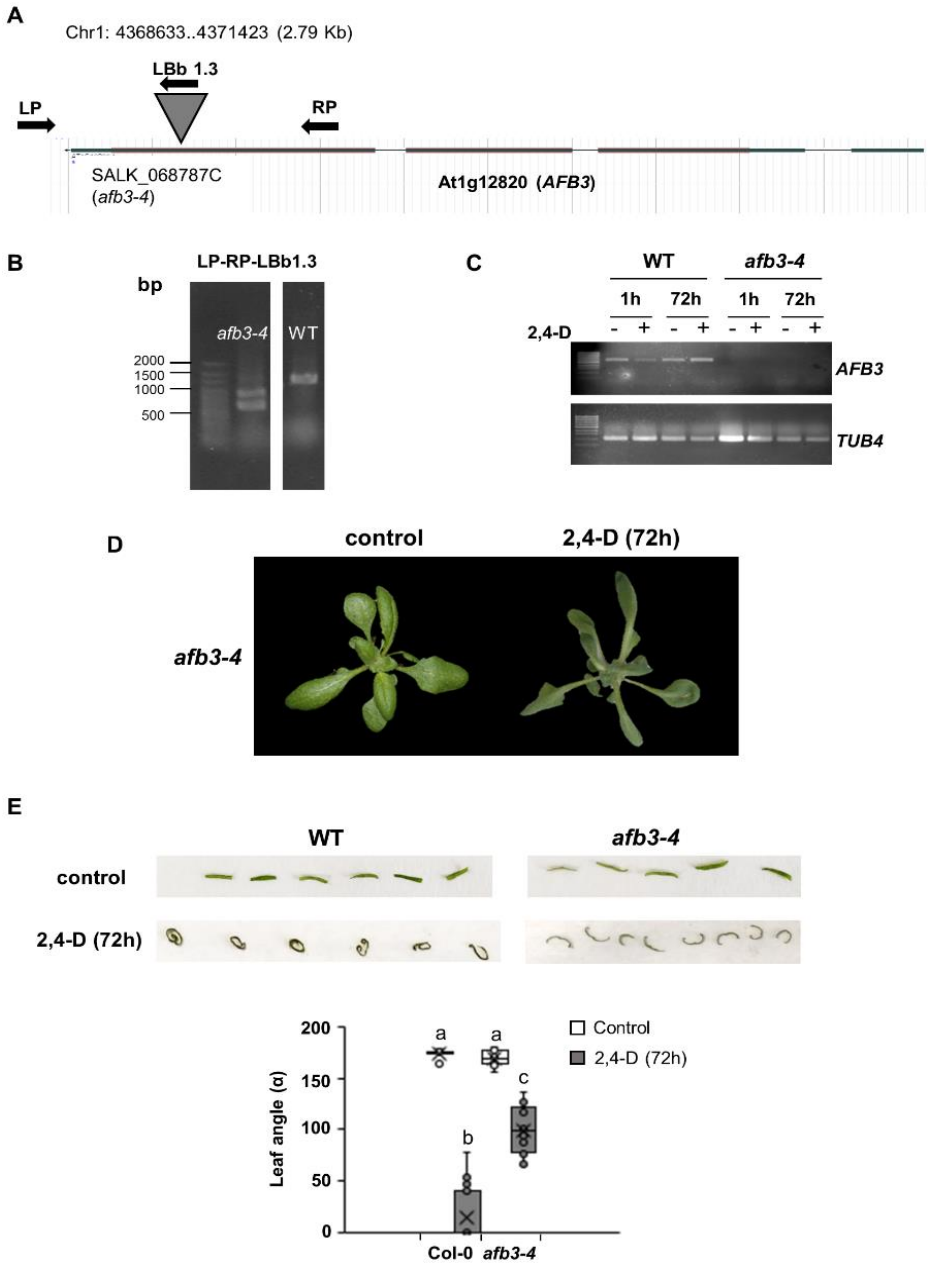

Figure 6. afb3-4 genotyping and phenotype after 2,4-D treatment. (A) *Diagram showing the position of the T-DNA insertion and primers used (LP, RP and LBb1.3) for genotyping afb3-4 mutants.* ***(B)*** *PCR-based genotyping of WT and mutant plants. Ethidium bromide stained amplicons obtained when using LP, RP and LBb1.3 primers; several repetitions for afb3-4 mutants have been removed from the gel.* ***(C)*** *Two gels with semi-quantitative RT-PCR analysis of AFB3 and TUB4 transcripts, respectively, in WT and afb3-4 leaves after 1 and 72 h of spraying with 2,4-D. No amplification of the transcript was observed following quantitative analysis of afb3-4 mutants.* ***(D)*** *WT and afb3-4 plants were foliarly treated with 23 mM 2,4-D, whose effect on leaves phenotype is shown.* ***(E)*** *Leaves were sliced after 72 h of 2,4-D spraying and curvature was analyzed by calculating the angle (α) of each strip with the tool angle from ImageJ software. Different letters denote significant differences between the different values obtained using Tukey multiple comparison tests (p-value < 0.05).*

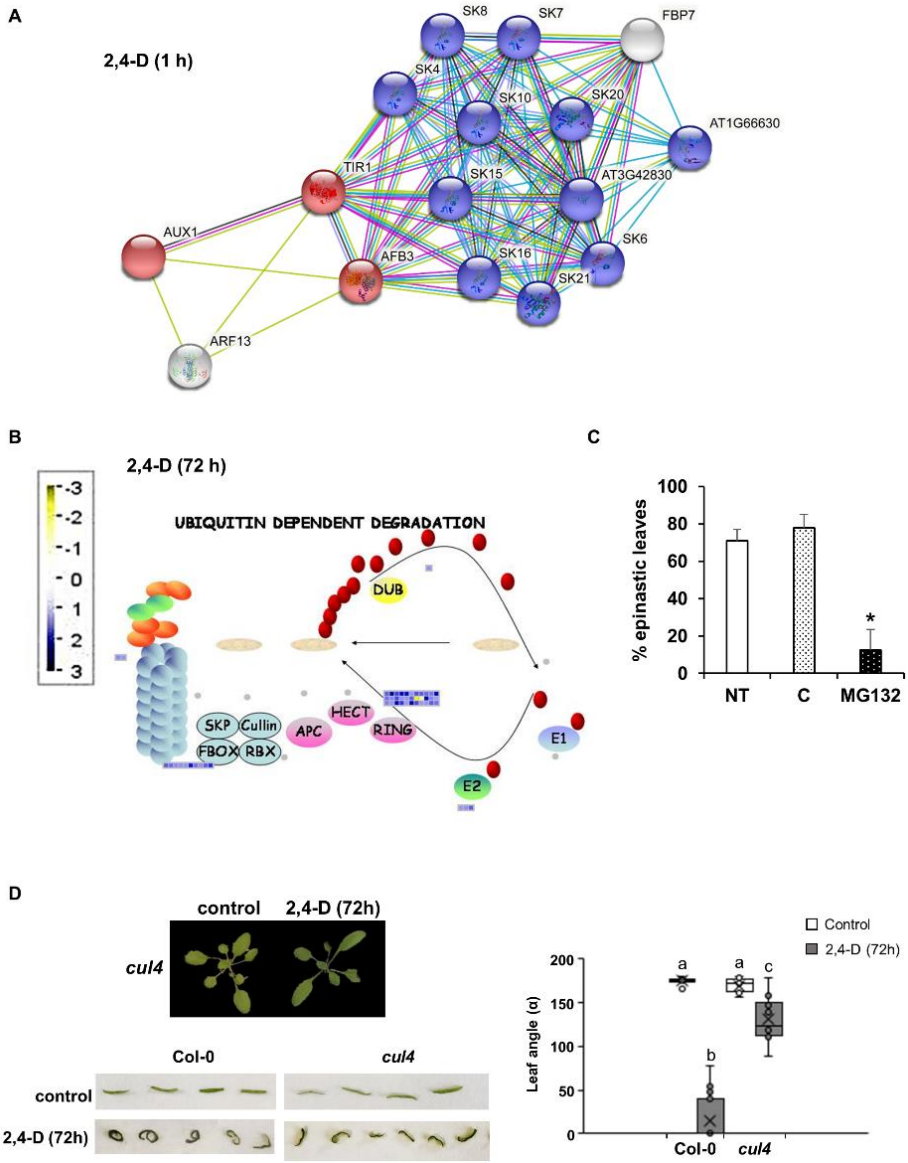

Figure 7. Functional partners of AFB3 and ACX1-dependent genes regulated in response to 2,4-D related to proteasomal degradation. (A) *StringDB tool (https://string-db.org/) following the selection of no more than 10 interactors including five interactors in a second shell predicted functional partners for AFB3. Partners are represented by SKP1-like proteins involved in ubiquitination and subsequent proteasomal degradation of target proteins related with auxin signalling.* ***(B)*** *Diagram of ACX1-dependent genes regulated in response to 2,4-D related with ubiquitin-dependent degradation using MapMan after 72 h of 2,4-D treatment. At this time point, protein degradation related to E3-RING and E3-SCF-FBOX ubiquitin categories (Suppl. Table S5), was significantly regulated.* ***(C)*** *Percentage of epinastic leaves in plants after 2,4-D treatment in not pre-treated leaves (NT), pre-treated with DMSO/EtOH (C) and pre-treated with the inhibitor of proteasome, MG132, prepared in DMSO/EtOH.* ***(D)*** *WT and cul4cs plants were foliarly treated with 23 mM 2,4-D, whose effect on leaves phenotype is shown; leaves were sliced after 72 h of 2,4-D spraying and curvature was analyzed by calculating the angle (α) of each strip with the tool angle from ImageJ software. Different letters denote significant differences between the different values obtained using Tukey multiple comparison tests (p-value < 0.05). In C) asterisks denote significant differences between MG132 and C plants according to the Student's t-test (p-value < 0.05). The absence of an asterisk denotes no significant differences between C and NT plants.*

4. DISCUSSION

The action mode of auxinic herbicides such as 2,4-D is beginning to be understood more clearly. At high concentrations, 2,4-D has an inhibitory effect on growth and development, as well as growth abnormalities such as epinasty, leaf abscission and senescence (Grossmann, 2000; Pazmiño *et al.*, 2011; Sandalio *et al.*, 2016). Although most analysis of 2,4-D toxicity has focused on the event cascade involving ET and ABA induction, ROS has been reported to play a central role in the development of the main effects of 2,4-D, including epinasty and senescence (Pasternak *et al.*, 2005; Pazmiño *et al.*, 2011; Sandalio *et al.*, 2016). In fact, the tolerance of *Salvinia natan* to 2,4-D is related to its capacity to cope with oxidative stress (Dolui *et al.*, 2021). Although the 2,4-D-dependent phenotype and certain biochemical issues have been characterized in different plant species, less information is available at the molecular level. Transcriptomic analyses of short-term treatment of Arabidopsis plants with 2,4-D (1 h) have revealed significant changes in the transcription levels of genes belonging to the functional categories of transcription, metabolism, cellular communication, signal transduction, subcellular localisation, transport facilitation, protein fate, proteins with binding functions or cofactor requirements, as well as cellular environmental regulation/interactions (Raghavan *et al.*, 2005). As described by Raghavan et al. (2005, 2006), 2,4-D not only modulates the expression of auxin, ET and ABA pathways but also regulates a wide variety

of other cellular processes including rescue, defence and pathogen-related gene functions (Raghavan *et al.*, 2005). Comparative analyses of IAA- and 2,4-D-induced transcriptomes have shown similar differential gene expression patterns (Pufky *et al.*, 2003; Raghavan *et al.*, 2005, 2006; McCauley *et al.*, 2020). Most of these studies have focused on genes associated with the metabolism and signalling of other plant hormones including ABA and ET, which are assumed to play a fundamental role in triggering plant death following auxin herbicide treatment (Raghavan *et al.*, 2005, 2006; Gaines *et al.*, 2020; McCauley *et al.*, 2020). However, whether and how H_2O_2 modulates auxin and 2,4-D transcriptional responses, as well as the sources of ROS involved, have not been elucidated. Some evidence suggests that ACX is an important source of ROS induced by the herbicide 2,4-D (Pazmiño *et al.*, 2011). In Arabidopsis, ACX is a family of six enzymes with overlapping specificities for Acyl-CoA substrates of various chain lengths, ACX1-ACX6 (Schilmiller *et al.*, 2007; Khan *et al.*, 2012). In this study, *acx1* mutants showed a noteworthy reduction in epinasty in response to 2,4-D (**Fig. 1**). In addition, analysis and imaging of H_2O_2 accumulation clearly show that peroxisomal ACX1 is one of the main sources of ROS under 2,4-D treatment conditions (**Fig. 2**). It is therefore possible to conclude that part of the epinastic phenotype is mainly associated with ACX1-dependent H_2O_2 in accordance with the 2,4-D-dependent induction of ACX activity previously observed in pea leaves (Pazmiño *et al.*, 2011) and *ACX1* induction observed in this study (**Fig. 1**).

In a previous analysis, epinasty was shown to be the result of differential ROS accumulation in leaves and of changes in the actin cytoskeleton caused by ROS- and NO-dependent posttranslational modifications of actin (Rodríguez-Serrano *et al.*, 2014). The reduction of H_2O_2 in *acx1-2* mutant respect to WT, in plant exposed to 2,4-D, could therefore explain the considerable reduction in epinasty observed in this Arabidopsis line. H_2O_2 is a signalling molecule involved in the regulation of cell responses to biotic and abiotic stress conditions (Fichman and Mittler, 2020). Interestingly, time course analysis of H_2O_2 in WT leaf extracts showed an increase after 1 h treatment and further increases during the period of 2,4-D exposure. We therefore analysed gene expression after 1 hpt and 72 hpt in both WT and *acx1-2* mutant to identify genes differentially regulated in early and long-term responses to 2,4-D. Analysis of the transcriptome in WT using the bioinformatic tool ROSMETER shows a high correlation with peroxisomal H_2O_2 production

during the first hour of treatment, thus suggesting that peroxisomal ACX1-dependent H_2O_2 plays an important role as a signalling molecule in the regulation of rapid responses to the herbicide. Other peroxisomal sources however, may have a role in plant response to 2,4-D, such as XOD as it has been previously shown (Romero-Puertas *et al.*, 2004a; Pazmiño *et al.*, 2011, 2014) or glycolate oxidase (GOX) although this activity has been shown to decrease in pea plants treated with the herbicide (Pazmiño *et al.,* 2011) and the main genes for this activity, *GOX1* and *GOX2* showed no significant changes with the treatment in our transcriptomic data.

Longer periods of treatment reduce the correlation with peroxisomal ROS, while the correlation with other sources such as mitochondria and chloroplasts was found to increase (**Fig. 3**); this result suggests the generation of progressive waves of different types of ROS involving different organelles, which also stimulates multiple signal sources. Oxidative stress characterized by ROS over accumulation and lipid peroxidation has been associated with 2,4-D-dependent leaf epinasty and senescence symptoms in different plant species (Karuppanapandian *et al.*, 2011; Pazmiño *et al.*, 2011), although the contribution of different sources of ROS and organelles have not been explored in great depth.

The specific induction of genes at the early stage of 2,4-D exposure constitutes the primary response which can even regulate cellular events induced at a later stage. A similar number of early genes regulated by 2,4-D was observed in WT and *acx1-2* mutant, and the *ACX1*-dependent transcripts identified were related to signal transduction, transport, stress-response pathway, cell organization and biogenesis categories. The results obtained by transcriptomic analyses were verified by qRT-PCR analysis of several genes belonging to different categories, with similar results obtained by both approaches. Among the early-response genes analysed, peroxidase-encoding *ATP24a* was down-regulated by 2,4-D in *acx1-2* mutant. *ATP24a* is involved in removing H_2O_2, toxic reductant oxidation, lignin biosynthesis, degradation, suberization, auxin catabolism and responses to environmental stresses such as wounding, pathogen attack and oxidative stress, although these functions might be dependent on each isozyme/isoform in each plant tissue (https://www.genscript.com/protein-database/per62 arath). Changes in the peroxidase pattern induced by 2,4-D have been reported in the cotyledon cell suspension cultures of bush bean, while peroxidase activity, which has been suggested to correlate

with cell wall expansion, may play a role in cell growth (Arnison and Boll, 1976). *HSP* and *PR-1* were down-regulated in *acx1-2* mutant but upregulated in WT after treatment with 2,4-D. *HSPs* were differentially expressed at the transcriptional level, and protein content was up-regulated after 24 and 72 hpt in citrus fruits under 2,4-D treatment (Ma *et al.*, 2014). HSPs could prevent irreversible protein inactivation and aggregation and, acting as chaperonins, could favour protein transport (Pazmiño *et al.*, 2011). *HSP71.2* and *PRP4A* expression was up-regulated in pea plants in response to 2,4-D and both genes were regulated by ROS (Pazmiño *et al.*, 2011), thus supporting differential expression in *acx1-2.*

Further datamining on ACX1-dependent genes regulated in response to 2,4-D showed different GO categories related with H_2O_2 metabolism and signalling significantly over represented supporting our previous results (**Fig. 4**). Although 2,4-D promoted an increase of total GSH in pea plants (Pazmiño *et al.,* 2011), GO categories related with this molecule were not significantly over-represented within ACX1-dependent genes suggesting an ACX1-independent role for GSH. Several glutathione-S-transferase (GST) genes have been found regulated however (**Suppl. Table S4**), indicating that GSH may have a key role in detoxification through GST activity, which has been shown highly induced in plant response to 2,4-D (Romero-Puertas *et al.*, 2004a).

Evidences at the biochemical and molecular levels have demonstrated that high exogenous concentrations of 2,4-D alter plant hormone levels, contributing to the epinastic phenotype and senescence (Raghavan *et al.*, 2005, 2006; Sandalio *et al.*, 2016). ABA levels increased with the treatment but at similar levels in WT and *acx1-2* mutant suggesting that may not have a key role in *acx1-2* phenotype. A higher increase in SA levels was observed after 72 h treatment in *acx1-2* respect to WT, suggesting that this hormone may have a role in *acx1-2* phenotype, at least at later stages of the treatment, which needs further analyses. Although *acx1-2* always showed decreased levels of JA as expected, this hormone only decreases significantly after 72 h treatment in WT plants. Although lower levels of JA in the mutant did not induced an epinastic/hyponastic phenotype under control conditions and spraying of these hormones on WT plants do not develop epinasty under our experimental conditions, a role for JA in plant response to 2,4-D cannot be discarded.

We then focused our attention on auxin-related genes (**Table 1**). Early-response genes up-regulated by 2,4-D specifically in WT and not in *acx1-2* mutant (*ACX1*-dependent genes) are involved in auxin stimulus (i.e.: *IAA10*, *IAA26* and *RCE1 RUB1 conjugating enzyme 1)*, and in the cellular response to auxin stimulus (i.e: *SGT1A* phosphatase-like proteins; **Table 1**). On the other hand, *ACX1*-dependent genes down-regulated by 2,4-D included genes related to polar and basipetal auxin transport (i.e.: *HSL1 HAESA-like 1; ABCB14 and D6PK*) and regulation of auxin mediated signalling pathways (i.e.: *PIF5 PIL6 phytochrome interacting factor 3-like 6, TIR1 F-box/RNI-like superfamily protein, AFB5 auxin F-box protein 5, AFB3 auxin signalling F-box 3, SAUR*; **Table 1**). Most of these genes have been identified as early auxin-response genes in different plant species (Abel and Theologis, 1996), such as Arabidopsis (Raghavan *et al.*, 2005, 2006) and citrus fruits (Ma *et al.*, 2014) exposed to 2,4-D. These results demonstrate that 2,4-D acts through auxin-signalling pathways and that peroxisomal ACX1 plays an important role in regulating early auxin-signalling responses to 2,4-D involved in the epinastic phenotype. Interestingly, longer exposure to 2,4-D (72 h) affected twice the number of genes as compared to early responses, with the highest numbers observed in *acx1-2. ACX1*-dependent genes regulated after long periods of 2,4-D exposure are associated with stress-response pathways, transcription and developmental processes and are mainly related to the cell wall and plasma membrane; this suggests that longer periods of treatment preferentially activate repair and defence mechanisms to cope with damage induced by the herbicide. However, long term 2,4-D exposure also up-regulates auxin-related genes, most of which correlate with the response to auxin stimulus (i.e.: MYB domain proteins, *MYB6 and MYB109*, *arginine decarboxylase 2 ADC2 and SGT1 phosphatase-related protein),* and down-regulated auxin-related genes including the SAUR-like auxin-responsive protein family and *IAA8*.

2,4-D has been reported to be a poor substrate for ABP1, a disputed potential auxin receptor (Gao *et al.*, 2015), whose action mode is thought to be through the nuclear-localized TIR1/AFB auxin receptors, which promote the degradation of AUX/IAA transcriptional repressors in an auxin-dependent manner via the ubiquitin-proteasome system (UPS; Parry *et al.*, 2009; Eyer *et al.*, 2016). In fact, 2,4-D has been reported to have an inhibitory effect on plant growth via the TIR1/AFB auxin-mediated signalling pathway (Eyer *et al.*, 2016). SCF TIR1/AFB contains interchangeable F-box proteins (FBPs) which

determine the specificity to the E3 protein through direct physical interactions with the targets to be degraded (Hua and Vierstra, 2011). At high IAA levels, TIR1/AFB 1–5 increase the affinity for the AUX/IAA degron through direct IAA binding, resulting in AUX/IAA ubiquitylation and further degradation, thus ensuring ARF derepression and auxin-induced transcriptional changes (Calderón Villalobos *et al.*, 2012; **Fig. 8**). Screening of available mutants related to *ACX1*-dependent genes in plant responses to 2,4-D (**Table 1**) showed that *afb3-4,* with a T-DNA insertion in *AFB3,* which has a similar phenotype to that of *acx1-2* and *acx1-4* in response to 2,4-D, appears to play a key role in developing epinasty and it is ACX1-dependent. In addition, analysis of AFB3 using the STRING database shows a close relationship with genes directly connected with auxin signalling. Several studies have highlighted the distinct biochemical properties and biological functions of AFBs, with TIR1/AFB2 showing stronger interactions with AUX/IAA than AFB1 and AFB3; AFB3 has been shown to play a role in responses to nitrate and salinity (Calderón Villalobos *et al.*, 2012; Garrido Vargas *et al.*, 2020). Our results show that AFB3 expression is ACX1-dependent whose silencing could interfere with AUX/IAA ubiquitynilation and degradation and reduce the epinastic phenotype as observed in *acx1* mutants. This finding is corroborated by the similar phenotype observed in *afb3-4* mutants. The silencing of AFB3 does not completely prevent leaf epinasty, suggesting that other complex factors may contribute (Calderón-Villalobos *et al.*, 2010). It has been shown however that phenotype of tir1 and afb1 to 3 single mutants differs in root response to 2,4-D showing that these proteins do not contribute equally (Parry *et al.*, 2009).

Later plant response to 2,4-D showed protein degradation related to the E3-RING ubiquitin ligases as significantly regulated in ACX1-dependent genes (**Fig. 7 B** and **Suppl. Table S5**). In fact, pre-treatment with proteasome inhibitor MG132, highly prevents epinasty in leaves after 2,4-D treatment (**Fig. 7 C**). Furthermore, *cul4cs* mutants, affected in CUL4 (Chen *et al.*, 2006), which is a recruiting protein for the Cullin F-box E3-ligase complex involved in protein degradation, and it has been involved in key processes of the plant such as photomorphogenesis, germination and auxin response, decreased drastically epinastic phenotype after 2,4-D treatment supporting results obtained with MG132 (**Fig. 7 D**).

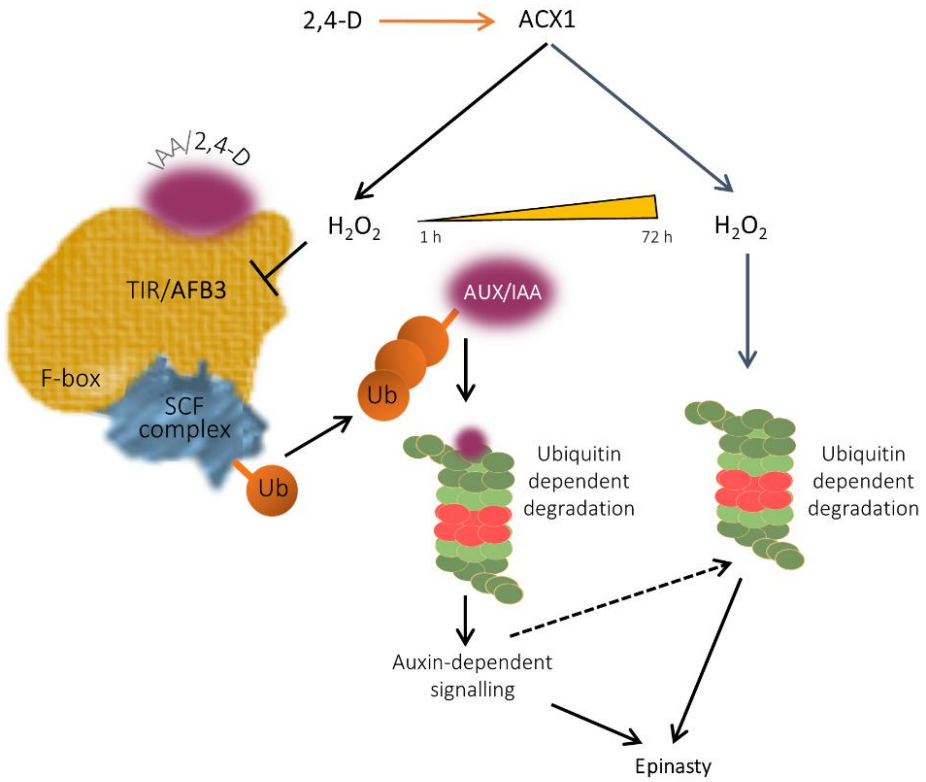

Figure 8. Scheme showing the possible mechanistic effects of 2,4-D in Arabidopsis plants. *2,4-D treatment induces H_2O_2 mainly dependent on ACX1, as acx1-2 mutants showed no increase after the herbicide treatment. At early time point, 2,4-D triggers ACX1-dependent inhibition of AFB3, as in acx1-2 mutants no significant changes in AFB3 transcript was observed. AFB3 is involved in AUX/IAA ubiquitination and further degradation of auxin responsive factors repressors. Changes in AFB3 level leads to deregulation of auxin-dependent signalling, which is involved in epinastic phenotype induced by 2,4-D. Transcriptomic analyses on later ACX1-dependent genes in plant response to 2,4-D showed enrichment of the E3-RING and E3-SCF-FBOX ubiquitin-dependent degradation, which is involved in development of epinastic phenotype induced by the herbicide. Pre-treatment with proteasome inhibitor MG132, highly prevents epinasty in leaves after 2,4-D treatment similarly to the observed in cul4cs mutants, affected in CUL4, which is a recruiting protein for the Cullin F-box E3-ligase complex, part of the ubiquitin dependent degradation process. Discontinuous line shows possible pathway.*

5. CONCLUSIONS

Reactive oxygen species (ROS) are involved in the toxicity of auxinic 2,4-D herbicide and most of the characteristic phenotypes associated with this herbicide. However, peroxisomal ROS derived from ACX1 also play an important role in signalling in response to 2,4-D and regulate a large number of genes, such as peroxidases, HSP and

PRPs, involved in primary responses to 2,4-D. Additionally, ACX1-dependent H_2O_2, which regulates *AFB3* expression, can modulate AUX/IAA ubiquitination and degradation and thereby the expression of auxin-responsive genes at early plant response to the herbicide (**Fig. 8**). However, later response to 2,4-D treatment produce different waves of ROS production associated with chloroplasts and mitochondria which regulate stress-response pathways, transcription and developmental processes. At this stage, within ACX1-dependent genes, protein degradation related to the E3-RING ubiquitin ligases is significantly regulated and involved in epinastic phenotype.

Acknowledgements

This study was funded by the Spanish Ministry of Science, Innovation and Universities (MCIU), the State Research Agency (AEI) and FEDER grant PGC2018-098372-B-I00. MAP-V was supported by MCIU Research Personnel Training (FPI) grant BES-2016-076518. The authors also wish to thank Michael O'Shea for proofreading the manuscript.

6. Supplementary Material

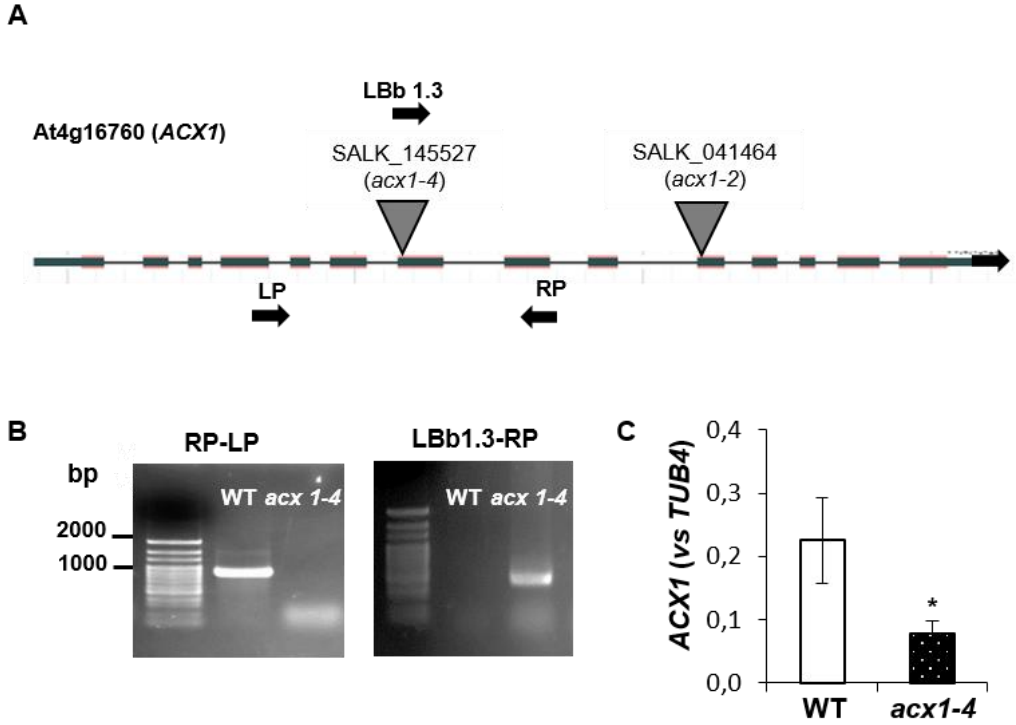

Suppl. Fig. S1*. *acx1-4 genotype. (A) *Diagram showing the position of the T-DNA insertion and primers used (LP, RP and LBb1.3) for genotyping acx1-4 mutants.* ***(B)*** *PCR-based genotyping of WT and mutant plants. Ethidium bromide-stained amplicons obtained when using LP, RP and LBb1.3 primers.* ***(C)*** *Quantitative RT-PCR analysis of ACX1 transcript in WT and acx1-4 leaves.*

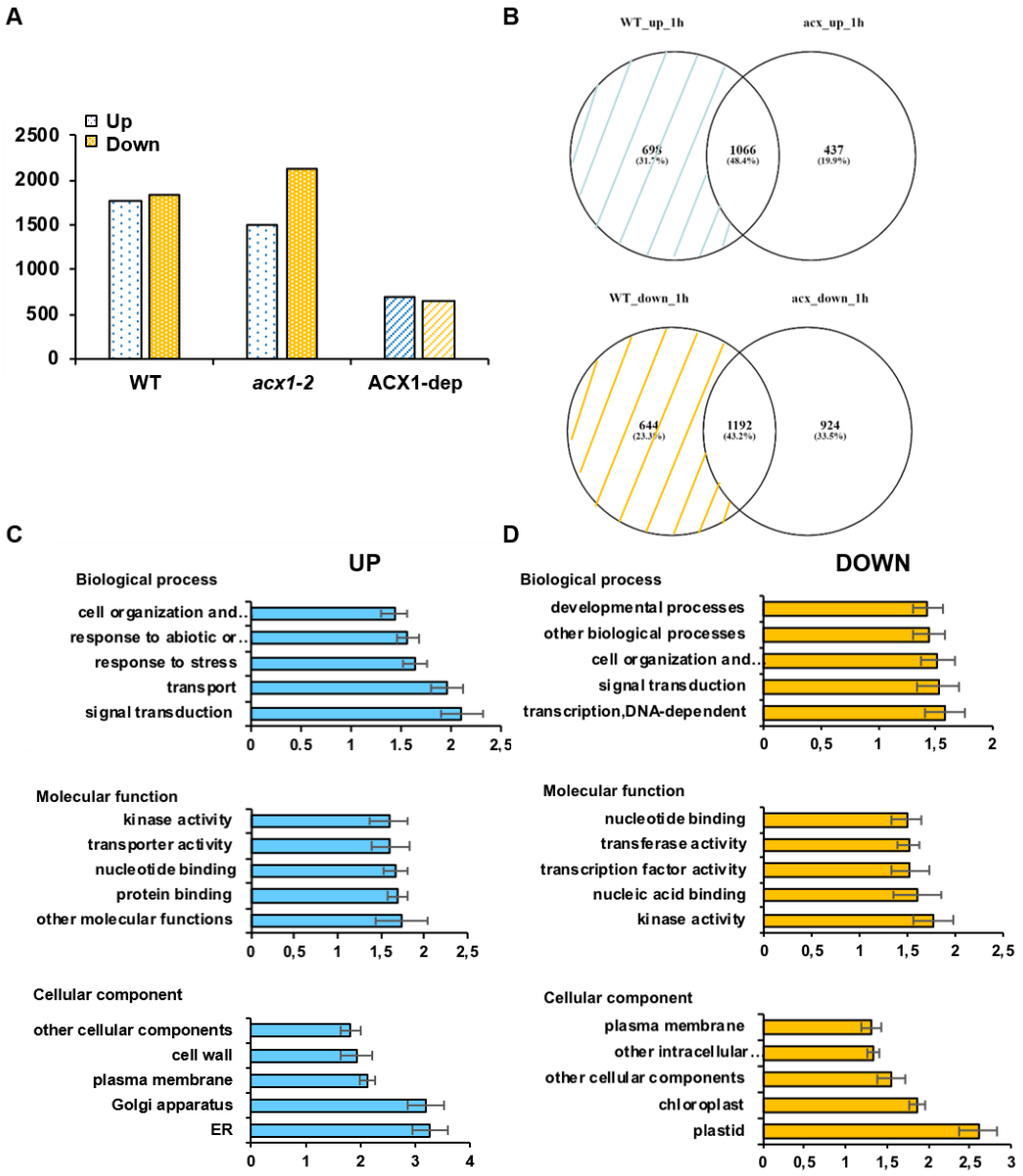

Suppl. Fig. S2. Changes in global transcript expression in the acx1-2 mutant compared to wild type (WT) in response to short-term 2,4-D treatment. (A) *Number of up- and down-regulated genes in WT and acx1-2 mutants after 1 h of 2,4-D spraying, and Venn diagrams* ***(B)*** *showing the overlap between gene expression changes in WT and acx1-2 mutants after 1 h of 2,4-D spraying; upregulated transcripts at the top and downregulated transcripts at the bottom. Transcript expression altered in the leaves of WT plants, but not of acx1-2 mutants (ACX1-dependent) is marked by blue (up-regulated) and orange (down-regulated) coloured stripes. Five main categories after gene ontology (GO) enrichment of ACX1-dependent up-* ***(C)*** *and down-* ***(D)*** *regulated transcripts after 1h of 2,4-D spraying. Normed to frequency of class over all ID numbers on x axes.*

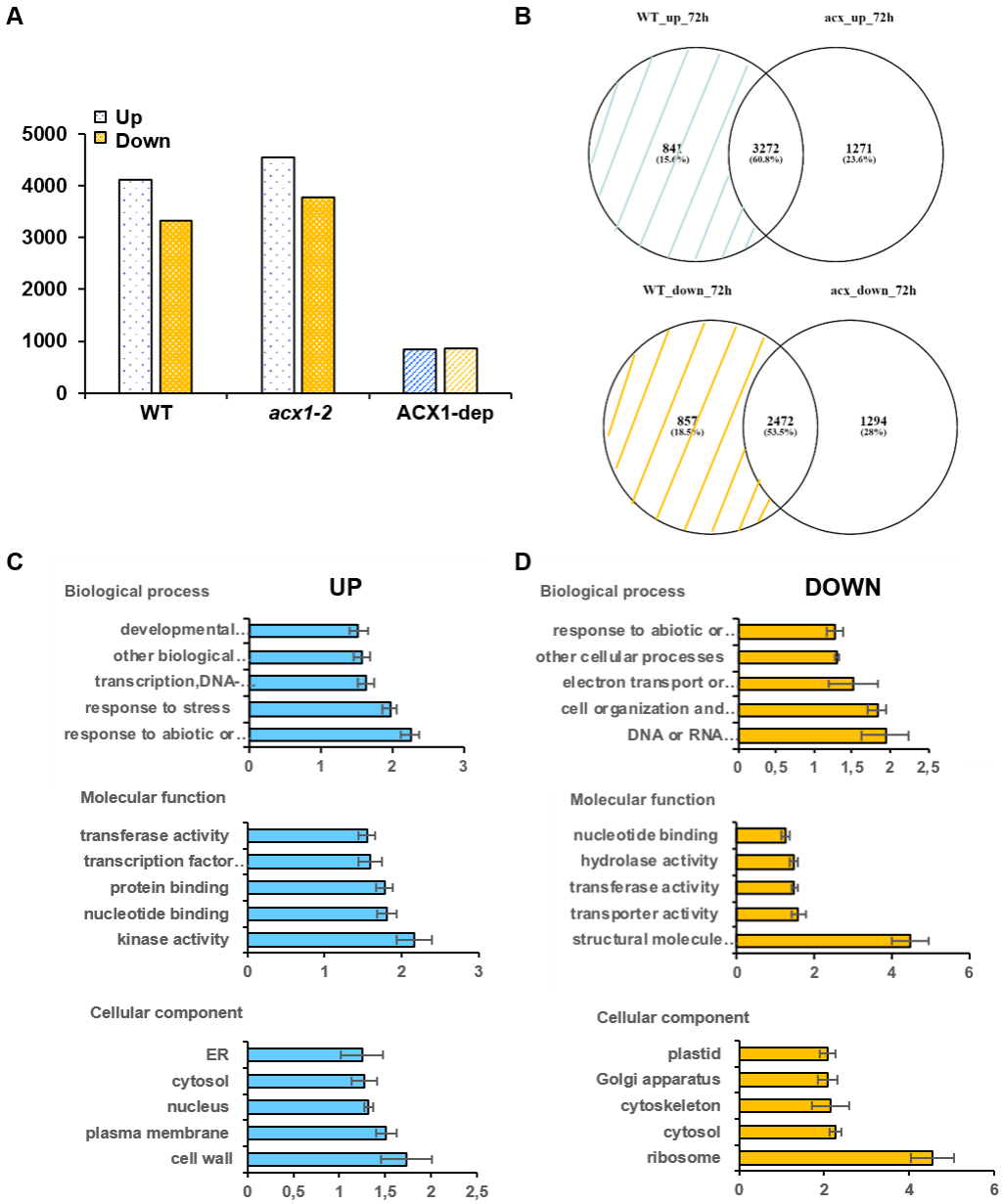

Suppl. Fig. S3. Changes in global transcript expression in the acx1-2 mutant as compared to wild type (WT) in response to long-term 2,4-D treatment. (A) *Number of up- and down-regulated genes in WT and acx1-2 mutants after 72 h of 2,4-D spraying, and Venn diagrams* ***(B)*** *showing the overlap between gene expression changes in WT and acx1-2 mutants after 72 h of 2,4-D spraying; up-regulated transcripts on top and down-regulated transcripts on bottom. Transcript expression altered in leaves of WT plants, but not in acx1-2 mutants (ACX1-dependent), is marked by blue (up-regulated) and orange (down-regulated) coloured stripes. Five main categories after gene ontology (GO) enrichment of ACX1-dependent up-* ***(C)*** *and down-* ***(D)*** *regulated transcripts after 72 h of 2,4-D spraying. Normed to frequency of class over all ID numbers on x axes.*

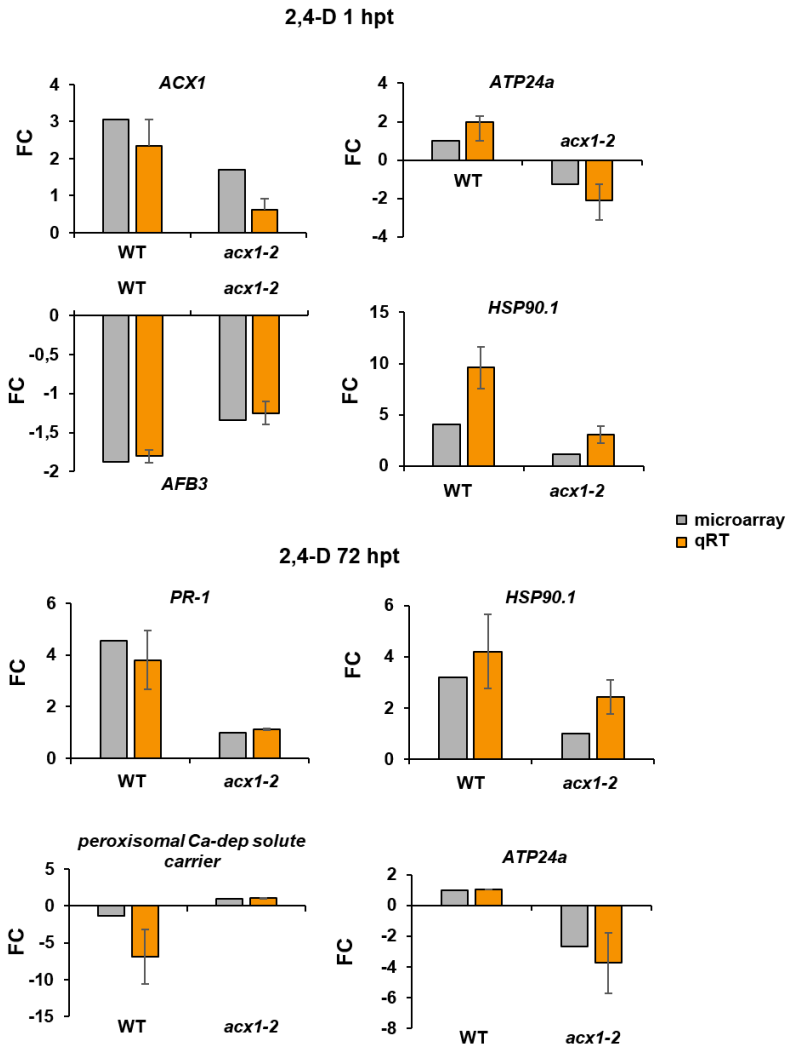

Suppl. Fig. S4. Validation of microarray results. *Quantitative real-time PCR compared with fold change (FC) data obtained by microarray analyses of genes related to different categories. FCs using qRT-PCR were calculated as* $2^{-\Delta\Delta Ct}$ *(n= 3). Primers used are described in Suppl. Table S1. Each gene was normalized against TUB4 expression.*

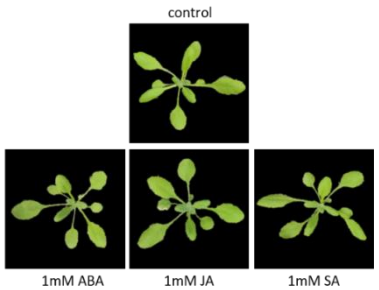

Suppl. Fig. S5. Plant phenotype after hormone treatment. *Representative images of plants after 48 h of being sprayed with jasmonic acid (JA, 1mM), salicylic acid (SA; 1mM) or abscisic acid (ABA; 1mM).*

Suppl. Table S1. *Reverse transcription quantitative PCR and genotyping primers.*

Gene	Primer sequence	ID
protein kinase-s	AGCTCAATTGCTCTCGCAGTTCC	At3g45860
protein kinase-as	ATCGACTGAACAAAGAGCGGACG	
PR1-s	TCCGCCGTGAACATGTGGGTTAG	At2g14610
PR1-as	CCCACGAGGATCATAGTTGCAACTGA	
bZIP-TF-s	TTCTCCAGACACTACAAGCAGCC	At5g28770
bZIP-TF-as	GATCCCCAACGCTTCGAATAC	
peroxidase ATP24a-s	GGCTAACTCTTGTTCAAGGGC	At5g39580
peroxidase ATP24a-as	CCACCAAGTCAAACCGAAAG	
HSP90.1-s	TGAGACAGCTTTGTTGACGTCTGG	At5g52640
HSP90.1-as	GGCATATCACCATCTTCCTCAACG	
Perox Ca-dep solute carrier-s	GCATGGGCCAAGAGTTTCTG	At5g61810
Perox Ca-dep solute carrier-as	CGAAATGCTTGCGGAAGG	
AFB3-s	TGATAAACTTTACCTCTACCGAACAG	At1g12824
AFB3-as	CCTAACATATGGTGGTGCATCTT	
SALK_041464-LP	CATGGCAACCAATTGTTCTGGA	
SALK_041464-RP	ACTATTGGGTGCAGGATGGCA	
SALK_145527-LP	GCACTTGGATCCTCAGAGAAACG	
SALK_145527-RP	TCCTCTCTCTTTGCCTTTCGG	
SALK_068787C-LP	TCATGTTGCTTACAAATTGCG	
SALK_068787C-RP	TCTGCAAACAGATGACAAACG	

Suppl. Table S2. *ACX1-dependent genes regulated after 2,4-D treatment at 1 and 72 hpt (**in CD**).*

Suppl. Table S3: *ACX1-dependent genes in plant response to 2,4-D 1 h and 72 h were categorized by PlantGSEA and significantly overrepresented GOs categories related with ROS and/or redox metabolism are shown.*

1 h:

Standard Gene Set Name	**HYDROGEN_PEROXIDE_METABOLIC_PROCESS**
Full Description/Abstract	GO:0042743 hydrogen peroxide metabolic process, GOslim:biological_process
Organization of contributer	The Arabidopsis Information Resource (TAIR)
External URL	http://amigo.geneontology.org/cgi-bin/amigo/term_details?term=GO:0042743

Standard Gene Set Name	**RESPONSE_TO_HYDROGEN_PEROXIDE**
Full Description/Abstract	GO:0042542 response to hydrogen peroxide, GOslim:biological_process
Organization of contributer	The Arabidopsis Information Resource (TAIR)
External URL	http://amigo.geneontology.org/cgi-bin/amigo/term_details?term=GO:0042542

Standard Gene Set Name	**RESPONSE_TO_REACTIVE_OXYGEN_SPECIES**

Full Description/Abstract	GO:0000302 response to reactive oxygen species, GOslim:biological_process
Organization of contributer	The Arabidopsis Information Resource (TAIR)
External URL	http://amigo.geneontology.org/cgi-bin/amigo/term_details?term=GO:0000302

Standard Gene Set Name	**RESPONSE_TO_OXIDATIVE_STRESS**
Full Description/Abstract	GO:0006979 response to oxidative stress, GOslim:biological_process
Organization of contributer	The Arabidopsis Information Resource (TAIR)
External URL	http://amigo.geneontology.org/cgi-bin/amigo/term_details?term=GO:0006979

72 h:

Standard Gene Set Name	**HYDROGEN_PEROXIDE_METABOLIC_PROCESS**
Full Description/Abstract	GO:0042743 hydrogen peroxide metabolic process, GOslim:biological_process
Organization of contributer	The Arabidopsis Information Resource (TAIR)
External URL	http://amigo.geneontology.org/cgi-bin/amigo/term_details?term=GO:0042743

Standard Gene Set Name	**REGULATION_OF_HYDROGEN_PEROXIDE_METABOLIC_PROCESS**
Full Description/Abstract	GO:0010310 regulation of hydrogen peroxide metabolic process, GOslim:biological_process
Organization of contributer	The Arabidopsis Information Resource (TAIR)
External URL	http://amigo.geneontology.org/cgi-bin/amigo/term_details?term=GO:0010310

Standard Gene Set Name	**REGULATION_OF_OXYGEN_AND_REACTIVE_OXYGEN_SPECIES_METABOLIC_PROCESS**
Full Description/Abstract	GO:0080010 regulation of oxygen and reactive oxygen species metabolic process, GOslim:biological_process
Organization of contributer	The Arabidopsis Information Resource (TAIR)
External URL	http://amigo.geneontology.org/cgi-bin/amigo/term_details?term=GO:0080010

Standard Gene Set Name	**OXYGEN_AND_REACTIVE_OXYGEN_SPECIES_METABOLIC_PROCESS**
Full Description/Abstract	GO:0006800 oxygen and reactive oxygen species metabolic process, GOslim:biological_process
Organization of contributer	The Arabidopsis Information Resource (TAIR)
External URL	http://amigo.geneontology.org/cgi-bin/amigo/term_details?term=GO:0006800

Suppl. Table S4: *ACX1-dependent genes in plant response to 2,4-D in categories related with ROS/glutathione/ascorbate/redox metabolism represented in Fig. 4.*

1 h:

Gene	logFC	GO	Category
AT3G04340	-0.714230921	GO:0045454	cell redox homeostasis
AT5G10860	0.730518451	GO:0045454	cell redox homeostasis
AT1G02930	1.897105456	GO:0004364/ GO:0006749	glutathione transferase activity/glutathione metabolic process
AT2G02930	1.931366848	GO:0004364/ GO:0006749	glutathione transferase activity/glutathione metabolic process
AT2G29450	0.841213567	GO:0004364/ GO:0006749	glutathione transferase activity/glutathione metabolic process
AT2G30870	0.767210115	GO:0004364/ GO:0006749	glutathione transferase activity/glutathione metabolic process
AT5G17220	-1.125895774	GO:0004364/ GO:0006749	glutathione transferase activity/glutathione metabolic process
AT1G65820	0.725260581	GO:0004364/ GO:0004602	glutathione transferase activity/glutathione peroxidase activity
AT4G33420	1.706245656	GO:0042744	hydrogen peroxide catabolic process
AT4G20860	2.079525253	GO:0010729	positive regulation of hydrogen peroxide biosynthetic process
AT3G03630	-0.668235613	GO:0010310	regulation of hydrogen peroxide metabolic process
AT4G08920	-0.721057373	GO:0010310	regulation of hydrogen peroxide metabolic process
AT1G32540	-0.833621127	GO:2000121	regulation of removal of superoxide radicals
AT1G22770	-1.303566844	GO:0042542	response to hydrogen peroxide
AT1G59860	4.700560417	GO:0042542	response to hydrogen peroxide
AT4G21870	1.86518917	GO:0042542	response to hydrogen peroxide
AT5G01600	-0.919736423	GO:0042542	response to hydrogen peroxide
AT3G04120	0.654296803	GO:0042542/ GO:0051775	response to hydrogen peroxide/response to redox state

72 h:

Gene	loGFC	GO	Category
AT1G02930	2.000782041	GO:0004364/ GO:0006749	glutathione transferase activity/glutathione metabolic process
AT1G22770	-0.959535067	GO:0042542	response to hydrogen peroxide
AT1G27130	-0.674885525	GO:0004364/ GO:0006749	glutathione transferase activity/glutathione metabolic process
AT1G59860	1.666471789	GO:0042542	response to hydrogen peroxide
AT1G64060	0.71861369	GO:0050665	hydrogen peroxide biosynthetic process
AT1G69930	1.93972882	GO:0004364/ GO:0006749	glutathione transferase activity/glutathione metabolic process
AT2G02930	2.235423995	GO:0004364/ GO:0006749	glutathione transferase activity/glutathione metabolic process
AT2G19310	1.141231576	GO:0042542	response to hydrogen peroxide
AT2G29450	-0.692530866	GO:0004364/ GO:0006749	glutathione transferase activity/glutathione metabolic process
AT3G02730	-0.839836207	GO:0045454	cell redox homeostasis
AT3G46230	1.314925394	GO:0042542	response to hydrogen peroxide
AT3G48090	0.813987754	GO:0010310	regulation of hydrogen peroxide metabolic process

AT3G52430	1.78001666	GO:0010310	regulation of hydrogen peroxide metabolic process
AT4G08920	1.237668109	GO:0010310	regulation of hydrogen peroxide metabolic process
AT4G09320	-0.67543874	GO:0070301	cellular response to hydrogen peroxide
AT4G19880	1.121625021	GO:0004364/ GO:0006749	glutathione transferase activity/glutathione metabolic process
AT4G31870	-0.758843696	GO:0004602	glutathione peroxidase activity
AT4G33420	1.92078688	GO:0042744	hydrogen peroxide catabolic process
AT5G03630	0.858140231	GO:0016656	monodehydroascorbate reductase (NADH) activity
AT5G12030	1.081205062	GO:0042542	response to hydrogen peroxide
AT5G12290	1.084923343	GO:0050665	hydrogen peroxide biosynthetic process
AT5G58940	0.907052251	GO:0042542	response to hydrogen peroxide

Suppl. Table S5. *ACX1-dependent categories and genes regulated after 2,4-D treatment at 72 hpt related to ubiquitin-dependent degradation (Fig. 7 B).*

bin	name	elements	p-value
29.5.11.4.2	**protein.degradation.ubiquitin.E3.RING**	**33**	**3.3997946535802E-6**
29.5.11.4.3.2	**protein.degradation.ubiquitin.E3.SCF.FBOX**	**10**	**0.0076764921382881**
29.5.11.3	protein.degradation.ubiquitin.E2	3	0.35398455493209546
29.5.11.20	protein.degradation.ubiquitin.proteasom	2	0.588201554399896
29.5.11.5	protein.degradation.ubiquitin.ubiquitin protease	1	0.7232133500380811

Protein degradation ubiquitin E3 RING genes:

ID	name	FC
at3g47550	zinc finger (C3HC4-type RING finger) family protein | chr3:17523458-17525540 FORWARD	1.917
at3g43430	zinc finger (C3HC4-type RING finger) family protein | chr3:15354535-15355304 REVERSE	1.78
at5g01160	e-cadherin binding protein-related | chr5:54010-55856 FORWARD	1.697
at5g22920	zinc finger (C3HC4-type RING finger) family protein | chr5:7664991-7667265 FORWARD	3.094
at3g05670	PHD finger family protein | chr3:1653264-1657159 FORWARD	1.64
at2g15580	zinc finger (C3HC4-type RING finger) family protein | chr2:6797638-6798939 FORWARD	1.552
at3g13430	zinc finger (C3HC4-type RING finger) family protein | chr3:4367281-4368820 FORWARD	2.104
at1g79380	copine-related | chr1:29860491-29863316 FORWARD	2.04
at4g28270	zinc finger (C3HC4-type RING finger) family protein | chr4:14007539-14009019 REVERSE	2.818
at1g22500	zinc finger (C3HC4-type RING finger) family protein | chr1:7949476-7950900 FORWARD	2.599
at5g47050	protein binding / zinc ion binding | chr5:19106340-19108348 FORWARD	1.592
at5g18650	zinc finger (C3HC4-type RING finger) family protein | chr5:6217912-6220702 FORWARD	2.144
at4g27470	zinc finger (C3HC4-type RING finger) family protein | chr4:13734999-13736518 FORWARD	2.44
at3g47990	zinc finger (C3HC4-type RING finger) family protein | chr3:17713144-17716308 REVERSE	1.532
at1g79810	Symbols: TED3, PEX2, ATPEX2 | TED3 (REVERSAL OF THE DET PHENOTYPE 3); protein binding / zinc ion binding | chr1:30019744-30022486 FORWARD	1.514
at2g30580	Symbols: DRIP2 | DRIP2 (DREB2A-INTERACTING PROTEIN 2); protein binding / ubiquitin-protein ligase/ zinc ion binding | chr2:13026000-13030661 FORWARD	1.542
at1g76410	Symbols: ATL8 | ATL8; protein binding / zinc ion binding | chr1:28668848-28669646 FORWARD	1.918
at3g05200	Symbols: ATL6 | ATL6; protein binding / zinc ion binding | chr3:1476982-1478730 FORWARD	2.89
at2g42350	zinc finger (C3HC4-type RING finger) family protein | chr2:17639152-17639998 FORWARD	2.015
at3g61550	zinc finger (C3HC4-type RING finger) family protein | chr3:22776401-22777225 FORWARD	-2.5
at2g02960	zinc finger (C3HC4-type RING finger) family protein | chr2:862087-864359 REVERSE	2.034
at4g33940	zinc finger (C3HC4-type RING finger) family protein | chr4:16266023-16267786 FORWARD	1.931

at1g63170	zinc finger (C3HC4-type RING finger) family protein | chr1:23425352-23427311 FORWARD	-1.608
at2g26000	zinc finger (C3HC4-type RING finger) family protein | chr2:11081302-11085350 FORWARD	1.517
at1g18470	zinc finger (C3HC4-type RING finger) family protein | chr1:6356131-6360192 REVERSE	1.858
at2g42360	zinc finger (C3HC4-type RING finger) family protein | chr2:17640798-17641790 FORWARD	2.696
at2g44950	Symbols: RDO4, HUB1 | HUB1 (HISTONE MONO-UBIQUITINATION 1); protein binding / protein homodimerization/ ubiquitin-protein ligase/ zinc ion binding | chr2:18542213-18548591 REVERSE	1.554
at5g22000	Symbols: RHF2A | RHF2A (RING-H2 GROUP F2A); protein binding / zinc ion binding | chr5:7277322-7280255 FORWARD	1.753
at1g67530	armadillo/beta-catenin repeat family protein / U-box domain-containing family protein | chr1:25307658-25311308 FORWARD	1.661
at2g28830	binding / structural constituent of ribosome / ubiquitin-protein ligase | chr2:12366748-12370684 REVERSE	1.94
at1g49210	zinc finger (C3HC4-type RING finger) family protein | chr1:18201889-18202764 FORWARD	2.684
at5g58580	Symbols: ATL63 | ATL63 (ARABIDOPSIS TÓXICOS EN LEVADURA); protein binding / zinc ion binding | chr5:23676906-23677832 REVERSE	1.503
at3g15070	zinc finger (C3HC4-type RING finger) family protein | chr3:5070134-5073317 REVERSE	1.803

Protein.degradation.ubiquitin.E3.SCF.FBOX genes:

at1g11270	Transcript	F-box family protein | chr1:3785507-3786990 REVERSE	1.923
at3g06240	Transcript	F-box family protein | chr3:1887043-1888750 FORWARD	1.837
at5g57360	Transcript	Symbols: ZTL, LKP1, ADO1, FKL2 | ZTL (ZEITLUPE); protein binding / ubiquitin-protein ligase | chr5:23241427-23244590 FORWARD	1.613
at1g55270	Transcript	kelch repeat-containing F-box family protein | chr1:20617954-20620136 REVERSE	1.59
at5g65850	Transcript	F-box family protein | chr5:26346314-26347610 FORWARD	1.559
at4g21510	Transcript	F-box family protein | chr4:11445849-11447163 REVERSE	2.337
at1g76920	Transcript	F-box family protein (FBX3) | chr1:28892062-28893676 FORWARD	1.793
at1g06630	Transcript	FUNCTIONS IN: molecular_function unknown;	1.567
at1g70590	Transcript	F-box family protein | chr1:26618321-26620388 FORWARD	1.917
at5g27920	Transcript	F-box family protein | chr5:9941905-9944778 REVERSE	2.239

Table 1. ACX1-dependent genes related to auxin metabolism and signalling. *Transcripts regulated in WT but not in acx1-2 muta to auxin metabolism and signalling.*

	Transcript ID	mutant	GO clasification	Target Description
1 h-up	At1g04100		[GO:0009733] response to auxin stimulus	IAA10 indoleacetic acid-indu
	At1g75500		[GO:0090355] positive regulation of auxin metabolic process	WAT1 Walls Are Thin 1
	At2g34650		[GO:0009733] response to auxin stimulus	ABR PID Protein kinase supe
	At3g16500		[GO:0009733] response to auxin stimulus	IAA26 PAP1 phytochrome-as
	At3g28910	SALK 027644C	[GO:0009733] response to auxin stimulus	ATMYB30 MYB30 myb doma
	At3g63420		[GO:0010541] acropetal auxin transport	AGG1 ATAGG1 GG1 Ggamm
	At4g23570	SALK 122139C	[GO:0071365] cellular response to auxin stimulus	SGT1A phosphatase-related
	At4g36800		[GO:0009733] response to auxin stimulus	RCE1 RUB1 conjugating enzy
	At5g35735		[GO:0031348] negative regulation of defense response	Auxin-responsive family prot
	At5g35570		[17.2.2] hormone metabolism.auxin.signal transduction	O-fucosyltransferase family p
	At1g68370	SALK 031635C	[17.2.2] hormone metabolism.auxin.signal transduction	ARG1 Chaperone DnaJ-dom
	At1g14000		response to auxin stimulus GO:0009733	VIK VH1-interacting kinase
	At5g45710	SALK 138256C	response to auxin stimulus	AT-HSFA4C HSFA4C RHA1 w
	At5g54490		response to auxin stimulus	PBP1 pinoid-binding protein
1 h-down	At1g12820	SALK 068787C	[GO:0000394] RNA splicing, via endonucleolytic cleavage and ligation	AFB3 auxin signalling F-box
	At1g28010	SALK 026876C	[GO:0010315] auxin efflux	ABCB14 ATABCB14 MDR12 P
	At1g28010		[GO:0010540] basipetal auxin transport	ABCB14 ATABCB14 MDR12 P
	At1g28440	SALK 141756C	[GO:0009926] auxin polar transport	HSL1 HAESA-like 1
	At2g21210	SALK 050249C	[GO:0015995] chlorophyll biosynthetic process	SAUR-like auxin-responsive p
	At2g22670		[GO:0009733] response to auxin stimulus	IAA8 indoleacetic acid-induc
	At2g33860	SALK 005658C	[GO:0009855] determination of bilateral symmetry	ARF3 ETT TF B3 family protei
	At2g47750		[GO:0009733] response to auxin stimulus	GH3.9 putative indole-3-ace
	At3g02260	SALK 105495C	[GO:0009826] unidimensional cell growth	ASA1 BIG CRM1 DOC1 LPR1
	At3g59060		[GO:0010928] regulation of auxin mediated signalling pathway	PIF5 PIL6 phytochrome inter
	At3g62980	SALK 151603C	[GO:0009734] auxin mediated signalling pathway	AtTIR1 TIR1 F-box/RNI-like s
	At4g25960		[GO:0010540] basipetal auxin transport	ABCB2 PGP2 P-glycoprotein
	At5g48900		[GO:0009926] auxin polar transport	Pectin lyase-like superfamily
	At5g49980		[GO:0007165] signal transduction	AFB5 auxin F-box protein 5
	At5g53590		[GO:0009733] response to auxin stimulus	SAUR-like auxin-responsive p

Table 1 (cont.). ACX1-dependent genes related to auxin metabolism and signalling.

	At5g55910		GO:0010540] basipetal auxin transport	D6PK D6 protein kinase
1 h-down	At1g60690		[17.2.3] hormone metab aux.induced-regulated-responsive-activated	NAD(P)-linked oxidoreduct
	At5g53588		hormone metabolism.auxin.signal transduction	CPuORF50 conserved pept SAUR-like aux-responsive
	At4g37260		[GO:0009733] response to auxin stimulus	ATMYB73 MYB73 myb dom
	At2g46830		[GO:0009733] response to auxin stimulus	AtCCA1 CCA1 circadian clo
	At2g37630		[GO:0009733] response to auxin stimulus	AS1 ATMYB91 ATPHAN MY regulator family protein
72 h-up	At1g80680	SALK 135920C	[GO:0009870] defense response signalling pathway	MOS3 NUP96 PRE SAR3 SU
	At5g65940	SALK 102725C	[GO:0009733] response to auxin stimulus	CHY1 beta-hydroxyisobuty
	At4g16420		[GO:0009733] response to auxin stimulus	ADA2B PRZ1 homolog of y
	At2g26740		[GO:0009733] response to auxin stimulus	ATSEH SEH soluble epoxide
	At3g09980		[GO:0009733] response to auxin stimulus	Family of unknown functio
	At4g34710		[GO:0009733] response to auxin stimulus	ADC2 ATADC2 SPE2 arginin
	At5g64890		[GO:0009733] response to auxin stimulus	PROPEP2 elicitor peptide 2
	At4g33940	SALK 142877C	[GO:0009733] response to auxin stimulus	RING/U-box superfamily pr
	At5g02840	SALK 137617C	[GO:0009733] response to auxin stimulus	LCL1 LHY/CCA1-like 1
	At1g80680		[GO:0032502] developmental process	MOS3 NUP96 PRE SAR3 SU
	At3g16640		[GO:0010252] auxin homeostasis	TCTP translationally control
	At1g80680		[GO:0031965] nuclear membrane	MOS3 NUP96 PRE SAR3 SU
	At3g59060		[GO:0010600] regulation of auxin biosynthetic process	PIF5 PIL6 phytochrome inte
	At5g54140		[GO:0009850] auxin metabolic process	ILL3 IAA-leucine-resistant (
	At1g28440	SALK 141756C	[GO:0009926] auxin polar transport	HSL1 HAESA-like 1
	At4g23570	SALK 122139C	[GO:0071365] cellular response to auxin stimulus	SGT1A phosphatase-related
	At3g16640		[GO:0009734] auxin mediated signalling pathway	TCTP translationally control
	At3g59060		[GO:0010928] regulation of auxin mediated signalling pathway	PIF5 PIL6 phytochrome inte
	At3g15450		hormone metabolism.auxin.synthesis-degradation	Aluminium induced protein
	At3g55730	SALK 148462C	[GO:0009733] response to auxin stimulus	AtMYB109 MYB109 myb do
	At4g09460		[GO:0009733] response to auxin stimulus	AtMYB6 MYB6 myb domain
	At3g09600	SALK 016333C	[GO:0009733] response to auxin stimulus	LCL5 RVE8 Homeodomain-
	At2g26740		[GO:0009733] response to auxin stimulus	ATSEH SEH soluble epoxide

Table 1 (cont.). ACX1-dependent genes related to auxin metabolism and signalling.

72 h-down	At2g21050		[GO:0006865] amino acid transport	LAX2 like AUXIN RESISTAN
	At2g22670		[GO:0009733] response to auxin stimulus	IAA8 indoleacetic acid-ind
	At2g26730		[GO:0009926] auxin polar transport	Leucine-rich repeat protei
	At2g34680	SALK 113677C	[GO:0009733] response to auxin stimulus	AIR9 Outer arm dynein lig
	At2g47750		[GO:0009733] response to auxin stimulus	GH3.9 putative indole-3-a
	At4g12410	SALK 152759C	[GO:0009733] response to auxin stimulus	SAUR-like auxin-responsiv
	At4g25960		[GO:0010540] basipetal auxin transport	ABCB2 PGP2 P-glycoprote
	At5g48900		[GO:0009926] auxin polar transport	Pectin lyase-like superfam
	At1g17350		auxin response	NADH:ubiquinone oxidore
	At1g14020		auxin response	O-fucosyltransferase famil
	At1g60690		auxin response	NAD(P)-linked oxidoreduc
	At1g74430		[GO:0009733] response to auxin stimulus	ATMYB95 ATMYBCP66 MY

Table 2. Enrichment analysis of AFB3 using the String database. *GO categories related to biological process (BP), molecular fu*
pathways obtained following enrichment analysis of AFB3 using the String database, when no more than 10 interactors were selected

BP	#term ID	term description	observed gene count
	GO:0016567	protein ubiquitination	10
	GO:0006511	ubiquitin-dependent protein catabolic process	9
	GO:0009987	cellular process	11
	GO:0048527	lateral root development	2
	GO:0021700	developmental maturation	2
	GO:0009734	auxin-activated signalling pathway	2
MF	GO:0010011	auxin binding	2
CC	GO:0019005	SCF ubiquitin ligase complex	10
	GO:0005634	nucleus	10
	GO:0043231	intracellular membrane-bounded organelle	11
	GO:0005623	cell	11
KEGG pathways	ath04120	ubiquitin-mediated proteolysis	7
	ath04141	protein processing in endoplasmic reticulum	7

7. REFERENCES

Abel S, Theologis A. 1996. Early genes and auxin action. *Plant Physiology* **111**, 9–17.

Adham AR, Zolman BK, Millius A, Bartel B. 2005. Mutations in *Arabidopsis* Acyl-CoA oxidase genes reveal distinct and overlapping roles in β-oxidation. *Plant Journal* **41**, 859–874.

Adie BAT, Pérez-Pérez J, Pérez-Pérez MM, Godoy M, Sánchez-Serrano JJ, Schmelz EA, Solano R. 2007. ABA is an essential signal for plant resistance to pathogens affecting JA biosynthesis and the activation of defenses in *Arabidopsis*. *Plant Cell* **19**, 1665–1681.

Afitlhile MM, Fukushige H, Nishimura M, Hildebrand DF. 2005. A defect in glyoxysomal fatty acid beta oxidation reduces jasmonic acid accumulation in Arabidopsis. *Plant Physiology Biochemistry* **43**, 603–609.

Arnison PG, Boll WG. 1976. The effect of 2,4-D and kinetin on peroxidase activity and isoenzyme pattern in cotyledon cell suspension cultures of bush bean (*Phaseolus vulgaris* cv. Contender). *Canadian Journal of Botany* **54**, 1857–1867.

Balfagón D, Sengupta S, Gómez-Cadenas A, Fritschi FB, Azad RK, Mittler R, Zandalinasc SI. 2019. Jasmonic acid is required for plant acclimation to a combination of high light and heat stress. *Plant Physiology* **181**, 1668–1682.

Benjamini, Y, Hochberg Y. 1995. Controlling the false discovery rate: A practical and powerful approach to multiple testing. *Journal of the Royal Statistical Society* **57**, 289–300.

Burns CJ, Swaen GMH. 2012. Review of 2,4-dichlorophenoxyacetic acid (2,4-D) biomonitoring and epidemiology. *Critical Reviews in Toxicology* **42**, 768–786.

Calderón-Villalobos LI, Tan X, Zheng N, Estelle M. 2010. Auxin perception-structural insights. *Cold Spring Harbor Perspectives in Biology* **2**, 1–16.

Calderón-Villalobos LI, Lee S, De Oliveira C, Ivetac A, Brandt W, Armitage L, Sheard LB, Tan X, Parry G, Mao H, Zheng N, Napier R, Kepinski S, Estelle M. 2012. A combinatorial TIR1/AFB-AUX/IAA co-receptor system for differential sensing of auxin, *Nature Chemical Biology* **8**, 477–485.

Castillo MC, Martínez C, Buchala A, Métraux JP, Léon J. 2004. Gene-specific involvement of β-oxidation in wound-activated responses in *Arabidopsis*. *Plant Physiology* **135**, 85–94.

Chen H, Shen Y, Tang X, Yu L, Wang J, Guo L, Zhang Y, Zhang H, Feng S, Strickland E, Zheng N, Deng XW. 2006. *Arabidopsis* CULLIN4 forms an E3 ubiquitin ligase with RBX1 and the CDD complex in mediating light control of development. *The Plant Cell* **18**, 1991–2004.

Cox MCH, Benschop JJ, Vreeburg RAM, Wagemaker CAM, Moritz T, Peeters AJM, Voesenek LACJ. 2004. The roles of ethylene, auxin, abscisic acid, and gibberellin in the hyponastic growth of submerged *Rumex palustris* petioles. *Plant Physiology* **136**, 2948–2960.

Davletova S, Rizhsky L, Liang H, Shengqiang Z, Oliver DJ, Coutu J, Shulaev V, Schlauch K, Mittler R. 2005. Cytosolic ascorbate peroxidase 1 is a central component of the reactive oxygen gene network of *Arabidopsis*. *Plant Cell* **17**, 268–281.

De AK, Dey N, Adak MK. 2016. Some physiological insights of 2,4-D sensitivity in an aquatic fern: *Azolla pinnata* R.Br. *Journal of Biotechnology and Biomaterials* **6**, 235.

Delker C, Zolman BK, Miersch O, Wasternack C. 2007. Jasmonate biosynthesis in *Arabidopsis thaliana* requires peroxisomal β-oxidation enzymes–Additional proof by properties of *pex6* and *aim1*. Phytochemistry **68**, 1642–1650.

Dolui D, Saha I, Adak MK. 2021. 2,4-D removal efficiency of *Salvinia natans* L. and its tolerance to oxidative stresses through glutathione metabolism under induction of light and darkness. *Ecotoxicology and Environmental Safety* **208**, 111708.

Egan JF, Maxwell BD, Mortensen DA, Ryan MR, Smith RG. 2011. 2,4-dichlorophenoxyacetic acid (2,4-D)-resistant crops and the potential for evolution of 2,4-D-resistant weeds. *Proceedings of the National Academy of Sciences of the United States of America* **108**, E37.

Eyer L, Vain T, Pařízková B, Oklestkova J, Barbez E, Kozubíková H, Pospíšil T, Wierzbicka1 R, Kleine-Vehn J, Fránek1 M, Strnad M, Robert S, Novak O. 2016. 2,4-D and IAA amino acid conjugates show distinct metabolism in *Arabidopsis*. *PLoS ONE* **11**, 1–18.

Fichman Y, Mittler R. 2020. Rapid systemic signalling during abiotic and biotic stresses: Is the ROS wave master of all trades? *Plant Journal* **102**, 887–896.

Fonseca S, Rubio V. 2019. *Arabidopsis* CRL4 complexes: Surveying chromatin states and gene expression. *Frontiers in Plant Science* **10**, 1095.

Gaines TA, Duke SO, Morran S, Rigon CAG, Tranel PJ, Anita Küpper, Dayan FE. 2020. Mechanisms of evolved herbicide resistance. *Journal of Biological Chemistry* **295**, 10307–10330.

Gao Y, Zhang Y, Zhang D, Dai X, Estelle M, Zhao Y. 2015. Auxin binding protein 1 (ABP1) is not required for either auxin signalling or *Arabidopsis* development. *Proceedings of the National Academy of Sciences of the United States of America* **112**, 2275–2280.

Garmier M, Carroll AJ, Delannoy E, Vallet C, Day DA, Small ID, Millar AH. 2008. Complex I dysfunction redirects cellular and mitochondrial metabolism in *Arabidopsis*. *Plant Physiology* **148**, 1324–1341.

Garrido-Vargas F, Godoy T, Tejos R, O'Brien JA. 2020. Overexpression of the auxin receptor AFB3 in *Arabidopsis* results in salt stress resistance and the modulation of NAC4 and SZF1, *International Journal of Molecular Sciences* **21**, 1–15.

Gechev TS, Minkov IN, Hille J. 2005. Hydrogen peroxide-induced cell death in *Arabidopsis*: Transcriptional and mutant analysis reveals a role of an oxoglutarate-dependent dioxygenase gene in the cell death process. *IUBMB Life* **57**, 181–188.

Gentleman RC, Carey VJ, Bates DM, Bolstad B, Dettling M, Dudoit S, Ellis B, Gautier L, Ge Y, Gentry J, Hornik K, Hothorn T, Huber W, Iacus S, Irizarry R, Leisch F, Li C, Maechler M, Rossini AJ, Sawitzki G *et al.* 2004. Bioconductor: Open software development for computational biology and bioinformatics. *Genome Biology*. **5**, R80.

Grossmann K. 2000. Mode of action of auxin herbicides: A new ending to a long, drawn out story. *Trends in Plant Science* **5**, 506–508.

Grossmann K, Kwiatkowski J, Tresch S. 2001. Auxin herbicides induce H_2O_2 overproduction and tissue damage in cleavers (*Galium aparine* L.). *Journal of Experimental Botany* **52**, 1811–1816.

Hua Z, Vierstra RD. 2011. The cullin-RING ubiquitin-protein ligases. *Annual Review of Plant Biology*, **62**, 299–334.

Kao YT, Gonzalez KL, Bartel B. 2018. Peroxisome function, biogenesis, and dynamics in plants. *Plant Physiology* **176**, 162–177.

Karuppanapandian T, Wang HW, Prabakaran N, Jeyalakshmi K, Kwon M, Manoharan K, Kim W. 2011. 2,4-dichlorophenoxyacetic acid-induced leaf senescence in mung bean (*Vigna radiata* L. Wilczek) and senescence inhibition by co-treatment with silver nanoparticles. *Plant Physiology and Biochemistry* **49**, 168–177.

Khan BR, Adham AR, Zolman BK. 2012. Peroxisomal Acyl-CoA oxidase 4 activity differs between Arabidopsis accessions. *Plant Molecular Biology* **78**, 45–58.

Kilian J, Whitehead D, Horak J, Wanke D, Weinl S, Batistic O, D'Angelo C, Bornberg-Bauer E, Kudla J, Harter K. 2007. The AtGenExpress global stress expression data set: Protocols, evaluation and model data analysis of UV-B light, drought and cold stress responses. *Plant Journal* **50**, 347–363.

Li ZF, Dong JX, Vasylieva N, Cui YL, Wan DB, Hua XD, Huo JQ, Yang DC, Gee SJ, Hammock BD. 2021. Highly specific nanobody against herbicide 2,4-dichlorophenoxyacetic acid for monitoring of its contamination in environmental water. *Science of the Total Environment* **753**, 141950.

Liszkay A, Van Der Zalm E, Schopfer P. 2004. Production of reactive oxygen intermediates ($O_2^{\cdot-}$, H_2O_2, and $^{\cdot}OH$) by maize roots and their role in wall loosening and elongation growth. *Plant Physiology* **136**, 3114–3123.

Ma Q, Ding Y, Chang J, Sun X, Zhang L, Wei Q, Cheng Y, Chen L, Xu J, Deng X. 2014. Comprehensive insights on how 2,4-dichlorophenoxyacetic acid retards senescence in post-harvest citrus fruits using transcriptomic and proteomic approaches. *Journal of Experimental Botany* **65**, 61–74.

McCauley CL, McAdam SAM, Bhide K, Thimmapuram J, Banks JA, Young BG. 2020. Transcriptomics in *Erigeron canadensis* reveals rapid photosynthetic and hormonal responses to auxin herbicide application. *Journal of Experimental Botany* **71**, 3701–3709.

Pan R, Liu J, Wang S, Hu J. 2020. Peroxisomes: Versatile organelles with diverse roles in plants. *New Phytologist* **225**, 1410–1427.

Parry G, Calderón-Villalobos LI, Prigge M, Peret B, Dharmasiri S, Itoh H, Lechner E, Gray WM, Bennett M, Estelle M. 2009. Complex regulation of the TIR1/AFB family of auxin receptors. *Proceedings of the National Academy of Sciences of the United States of America* **106**, 22540–22545.

Pasternak T, Potters G, Caubergs R, Jansen MAK. 2005. Complementary interactions between oxidative stress and auxins control plant growth responses at plant, organ, and cellular level. *Journal of Experimental Botany* **56**, 1991–2001.

Pazmiño DM, Rodríguez-Serrano M, Romero-Puertas MC, Archilla-Ruiz A, del Río LA, Sandalio LM. 2011. Differential response of young and adult leaves to herbicide 2,4-dichlorophenoxyacetic acid in pea plants: Role of reactive oxygen species. *Plant Cell and Environment* **34**, 1874–1889.

Pazmiño DM, Romero-Puertas MC, Sandalio LM. 2012. Insights into the toxicity mechanism of and cell response to the herbicide 2,4-D in plants. *Plant Signalling and Behavior* **7**, 425–427.

Pazmiño DM, Rodríguez-Serrano M, Sanz M, Romero-Puertas MC, Sandalio LM. 2014. Regulation of epinasty induced by 2,4-dichlorophenoxyacetic acid in pea and Arabidopsis plants. *Plant Biology* **16**, 809–818.

Prigge MJ, Greenham K, Zhang Y, Santner A, Castillejo C, Mutka AM, O'Malley RC, Ecker JR, Kunkel BN, Estelle M. 2016. The Arabidopsis auxin receptor F-box proteins AFB4 and AFB5 are required for response to the synthetic auxin picloram. *G3: Genes, Genomes, Genetics* **6**, 1383–1390.

Pufky J, Qiu Y, Rao MV, Hurban P, Jones AM. 2003. The auxin-induced transcriptome for etiolated Arabidopsis seedlings using a structure/function approach. *Functional and Integrative Genomics* **3**, 135–143.

Qin G, Gu H, Zhao Y, Ma Z, Shi G, Yang Y, Pichersky E, Chen H, Liu M, Chen Z, Qu LJ. 2005. An indole-3-acetic acid carboxyl methyltransferase regulates Arabidopsis leaf development. *Plant Cell* **17**, 2693–2704.

Raghavan C, Ong EK, Dalling MJ, Stevenson TW. 2005. Effect of herbicidal application of 2,4-dichlorophenoxyacetic acid in *Arabidopsis*. *Functional and Integrative Genomics* **5**, 4–17.

Raghavan C, Ong EK, Dalling MJ, Stevenson TW. 2006. Regulation of genes associated with auxin, ethylene and ABA pathways by 2,4-dichlorophenoxyacetic acid in *Arabidopsis*. *Functional and Integrative Genomics* **6**, 60–70.

Rinaldi MA, Patel AB, Park J, Lee K, Strader LC, Bartel B. 2016. The roles of β-oxidation and cofactor homeostasis in peroxisome distribution and function in *Arabidopsis thaliana*. *Genetics* **204**, 1089–1115.

Rodríguez-Serrano M, Romero-Puertas MC, Sparkes I, Hawes C, del Río LA, Sandalio LM. 2009. Peroxisome dynamics in *Arabidopsis* plants under oxidative stress induced by cadmium. *Free Radical Biology and Medicine* **47**, 1632–1639.

Rodríguez-Serrano M, Pazmiño DM, Sparkes I, Rochetti A, Hawes C, Romero-Puertas MC, Sandalio LM. 2014. 2,4-Dichlorophenoxyacetic acid promotes *S*-nitrosylation and oxidation of actin affecting cytoskeleton and peroxisomal dynamics. *Journal of Experimental Botany* **65**, 4783–4793.

Romero-Puertas MC, McCarthy I, Gómez M, Sandalio LM, Corpas FJ, del Río LA, Palma JM. 2004a. Reactive oxygen species-mediated enzymatic systems involved in the oxidative action of 2,4-dichlorophenoxyacetic acid. *Plant Cell and Environment* **27**, 1135–1148.

Romero-Puertas MC, Rodríguez-Serrano M, Corpas FJ, Gómez M, del Río LA, Sandalio LM. 2004b. Cadmium-induced subcellular accumulation of $O_2^{\cdot-}$ and H_2O_2 in pea leaves. *Plant, Cell and Environment* **27**, *1122 – 1134*.

Rosenwasser S, Rot I, Sollner E, Meyer AJ, Smith Y, Leviatan N, Fluhr R, Friedman H. 2011. Organelles contribute differentially to reactive oxygen species-related events during extended darkness. *Plant Physiology* **156**, 185–201.

Rosenwasser S, Fluhr R, Joshi JR, Leviatan N, Sela N, Hetzroni A, Friedman H. 2013. ROSMETER: A bioinformatic tool for the identification of transcriptomic imprints related to reactive oxygen species type and origin provides new insights into stress responses. *Plant Physiology* **163**, 1071–1083.

Sandalio LM, Romero-Puertas MC. 2015. Peroxisomes sense and respond to environmental cues by regulating ROS and RNS signalling networks. *Annals of Botany* **116**, 475–485.

Sandalio LM, Rodríguez-Serrano M, Romero-Puertas MC. 2016. Leaf epinasty and auxin: A biochemical and molecular overview. *Plant Science* **253**, 187–193.

Sandalio LM, Peláez-Vico MA, Molina-Moya E, Romero-Puertas MC. 2021. Peroxisomes as redox-signalling nodes in intracellular communication and stress responses. *Plant Physiology*, kiab060.

Schilmiller AL, Koo AJK, Howe GA. 2007. Functional diversification of acyl-coenzyme A oxidases in jasmonic acid biosynthesis and action. *Plant Physiology* **143**, 812–824.

Smyth GK, Speed T. 2003. Normalization of cDNA microarray data. *Methods* **31**, 265–273.

Teixeira MC, Duque P, Sá-Correia I. 2007. Environmental genomics: mechanistic insights into toxicity of and resistance to the herbicide 2,4-D. *Trends in Biotechnology* **25**, 363–370.

Terrón-Camero LC, Peláez-Vico MA, del-Val C, Sandalio LM, Romero-Puertas MC. 2019. Role of nitric oxide in plant responses to heavy metal stress: Exogenous application versus endogenous production. *Journal of Experimental Botany* **70,** 4477–4488.

Terrón-Camero LC, Rodríguez-Serrano M, Sandalio LM, Romero-Puertas MC. 2020. Nitric oxide is essential for cadmium-induced peroxule formation and peroxisome proliferation. *Plant Cell and Environment* **43**, 2492–2507.

Ueda J, Miyamoto K, Góraj-Koniarska J, Saniewski M. 2018. Petiole bending in detached leaves of *Bryophyllum calycinum*: Relevance to polar auxin transport in petioles. *Acta Biologica Cracoviensia Series Botanica* **60**, 25–33.

Vanderauwera S, Zimmermann P, Rombauts S, Vandenabeele S, Langebartels C, Gruissem W, Inzé D, Van Breusegem F. 2005. Genome-wide analysis of hydrogen peroxide-regulated gene expression in *Arabidopsis* reveals a high light-induced transcriptional cluster involved in anthocyanin biosynthesis. *Plant Physiology* **139**, 806–821.

Zolman BK, Martinez N, Millius A, Adham AR, Bartel B. 2008. Identification and characterization of Arabidopsis indole-3-butyric acid response mutants defective in novel peroxisomal enzymes. *Genetics* **180**, 237–251.

Zuanazzi NR, Ghisi NC, Oliveira EC. 2020. Analysis of global trends and gaps for studies about 2,4-D herbicide toxicity: A scientometric review. *Chemosphere* **241**, 125016.

Chapter 2

Gene network downstream plant stress response modulated by peroxisomal H_2O_2

Terrón-Camero, L. C., **Peláez-Vico, M. A.**, Rodríguez-González, A., Del Valʹ C., Sandalio, L. M. and Romero-Puertas, M. C.

Gene network downstream plant stress response modulated by peroxisomal H_2O_2

Laura C. Terrón-Camero[1]*, M. Ángeles Peláez-Vico[1]*, A. Rodríguez-González, Coral del Val[2,3], Luisa M. Sandalio[1], María C. Romero-Puertas[1#]

[1]*Department of Biochemistry and Molecular and Cellular Biology of Plants, Estación Experimental del Zaidín (EEZ), Consejo Superior de Investigaciones Científicas (CSIC), Apartado 419, 18080 Granada, Spain*
[2]*Department of Artificial Intelligence, University of Granada, 18071 Granada, Spain*
[3]*Andalusian Data Science and Computational Intelligence (DaSCI) Research Institute, University of Granada, 18071 Granada, Spain*

*The authors contributed equally to this study

[#]Author for correspondence:
María C. Romero-Puertas,
Estación Experimental del Zaidín (CSIC),
Department of Biochemistry and Molecular and Cellular Biology of Plants,
Apartado de correos 419,
18080 Granada, SPAIN
Tel: + 34 958 181600 ext. 175
e-mail: maria.romero@eez.csic.es

Running title: peroxisomal retrograde signalling

Key words: jasmonic acid; peroxisome; ROS; signalling; abiotic stress

ABSTRACT

Reactive oxygen species (ROS) act as secondary messengers that can be sensed by specific redox sensitive proteins responsible for the activation of a signal transduction culminating in altered gene expression. ROS have different activities and hence elicit different protein modifications, which might be manifested in eliciting different gene expression. The subcellular site in which the modification in ROS/oxidation state occurs can also serve as a specific signal of a cellular redox network. Actually, the chemical identity of ROS and its subcellular origin will leave a specific imprint on the transcriptome response. In the last years, a number of transcriptomic data related with altered ROS metabolism in peroxisomes have been carried out. In this work, we have made a meta-analysis with these transcriptomic data which determined and identified common transcriptional footprints for peroxisomal-dependent signalling at early and later time points. These footprints revealed the regulation of various metabolic pathways and gene families, which are in common with plant responses to several abiotic stresses. Main peroxisomal-dependent genes are related with protein and endoplasmic reticulum protection at later stages of stress while earlier ones are related with hormone biosynthesis and signalling regulation. Peroxisomal footprints provide a valuable resource for assessing and support key peroxisomes function within cell metabolism under control and stress situations.

1. INTRODUCTION

Eukaryotic cells evolved to organellar compartmentalization to increase efficiency of metabolic processes and protect cellular components from products, such as reactive oxygen and nitrogen species (ROS/RNS), which may be harmful in excess (Gabaldón, 2018). Peroxisomes are small organelles found in most eukaryotes that are delimited by a single lipid membrane and have a close relationship with other organelles such as, chloroplasts and mitochondria (Kao *et al.,* 2018). Initially, these organelles were regarded as a H_2O_2 sink produced by different sources both inside and outside peroxisomes, degraded by catalases and other ROS-inactivating enzymes (Sandalio and Romero-Puertas, 2015; Cross *et al.,* 2016). In recent years however, biochemical, transcriptomic and proteomic approaches have demonstrated that these organelles are much more complex and perform functions hitherto unknown (Reumann *et al.,* 2016; Sandalio *et al.,* 2021). In fact, the metabolic diversity and plasticity of peroxisomes is remarkable, and unexpected functions of plant peroxisomes continue to be discovered (Reumann *et al.,* 2016). Key metabolic pathways are hosted in plant peroxisomes such as, β-oxidation pathway and photorespiration, which is shared with chloroplast and mitochondria. In addition, the biosynthesis of phytohormones jasmonic acid (JA), auxin IAA and salicylic acid (SA) together with ROS/RNS metabolism makes peroxisomes a source of signalling molecules being essential for the regulation of development processes and plant response to stress (Sandalio *et al.,* 2021).

Although other organelles/compartments-dependent signalling communication to the nucleus, termed retrograde signalling, which have a key role in cell response to environmental cues and organelle assembly and metabolism, is better identified, knowledge about peroxisomes-dependent retrograde signalling is just beginning. Adjustments in the transcriptome is essential to trigger both, early and late responses to environmental cues were peroxisomes has a key role as source of signalling molecules. Chemical properties of H_2O_2 such as, stability and diffusibility, makes this ROS a molecule easier to follow and analyse than other ROS. Specificity for H_2O_2-dependent signalling

produced in different organelles have been shown previously and in particular, for H_2O_2 produced in peroxisomes induced either by chemical treatment (Gechev *et al.,* 2005) or by using different mutants (Takahashi *et al.,* 1997; Chaouch *et al.,* 2010; Queval *et al.,* 2007; Sewelam *et al.,* 2014; Su *et al.,* 2018). Therefore, transcriptional changes have been analysed in mutants affected in catalase (CAT) activity, one of the main peroxisomal antioxidants, under different stress conditions such as high or continuous light, CO_2 shift and photorespiratory stress (Vanderauwera *et al.,* 2005; Mhamdi *et al.,* 2010; Queval *et al.,* 2012, Sewelam *et al.,* 2014; Waszczak *et al.,* 2016; Kerchev *et al.,* 2016). Transcriptome of the triple mutant *cat1 cat2 cat3*, which showed redox disorders under control conditions, was also analysed (Su *et al.,* 2018). Excess of H_2O_2 in this triple mutant affected genes involved in growth regulation, plant response to stress and MAPK cascades (Su *et al.,* 2018). Transcriptomes of other mutants, affected in glycolate oxidase (GOX), one of the main enzymes involved in peroxisomal located photorespiration and H_2O_2-producing, have been analysed under control and stress situations (Kerchev *et al.,* 2016). All these analysis point to H_2O_2 produced in peroxisomes as one of the molecules able to change, direct and/or indirectly gene expression. The structure of gene networks and identification of downstream responses induced by peroxisomal H_2O_2 is far to be well known however. In particular, main outstanding questions for peroxisome research are the role of peroxisome-derived ROS, how environmental signals and internal metabolic states of the organelle are translated at the molecular level (Sandalio and Romero-Puertas, 2015; Rodríguez-Serrano *et al.,* 2016; Cross *et al.,* 2016; Kao *et al.,* 2018).

Meta-analysis of different transcriptomes offers a straightforward method to identify common and specific groups of transcriptomic changes. Previous meta-analyses showed specific signatures for different ROS sources (Rosenwasser *et al.,* 2013; Willems *et al.,* 2016). However, the presence of robust marker transcripts related to peroxisomal-dependent signalling is scarce. Analysis of the peroxisomal ROS-dependent transcripts generated in different laboratories would help to obtain marker genes for this organelle-dependent signalling. In this study, we have examined both in-house and public data sets

derived from the profiling of Arabidopsis gene expression in mutants and treatments with peroxisomal-dependent ROS levels altered in order to identify a data set of common and specific genes regulated by peroxisomal ROS under different conditions. This analysis will enable us to gain a deeper understanding of the role played by peroxisomes as stress sensors and regulators of cellular responses to adverse conditions resulting in plant acclimation and resistance.

2. MATERIALS AND METHODS

2.1. Plant material and growth conditions

Arabidopsis ecotype Columbia-0 (Col-0) constitutes the genetic background for all plants used in this study. Col-0 and *cat2-2* seeds were surface disinfected and stratified for 24-48 h at 4 ºC and then sown on Murashige and Skoog (MS) 0.5x solid medium (Murashige and Skoog, 1962) grown at 22 ºC in 16 h light and 8 h darkness for 14 d. Plants were then transferred to petri dishes containing 0.5x liquid MS medium and grown for 24 h. To study the effect of cadmium on gene expression, the solution was supplemented with 100 µM $CdCl_2$ and seedlings were analysed after 1 and 3 h of treatment.

2.2. RNA isolation from seedlings

Total RNA was isolated from seedlings by the acid guanidine thiocyanate-phenol-chloroform method (Chomczynski and Sacchi 1987), using the Trizol reagent (Thermo Fisher Scientific) according to the manufacturer's instructions. RNA was reverse transcribed with the aid of the PrimeScript RT Master Mix (Takara) following the instructions of the commercial company.

2.3. RT-PCR analysis of gene expression

Each 20 µl reaction contained either 1 µl cDNA or a dilution, 200 nM of each primer, and 1x TB Green Premix Ex Taq (Takara). Quantitative real-time PCR was performed on an iCycler iQ5 (Bio-Rad). The samples were initially denatured by heating

at 95 °C for 3 min followed by 35-cycle amplification and a quantification program (95 °C for 30 s, 55 °C for 30 s, and 72 °C for 45 s). A melting curve was conducted to ensure amplification of a single product. The amplification efficiency of primers was calculated using the formula E = [10 (1/a) -1] x 100, where a is the slope of the standard curve. The relative expression of each gene was normalized to that of *TUB4*, and the results were analyzed using the relative expression ratio according to the Pfaffl method (Pfaffl, 2001). Primers used are described in **Suppl. Table S1**.

2.4. Microarray data

In total, twenty-one lists of genes (profiles) from six independent studies showing disrupted peroxisomal H_2O_2 metabolism, were collected from available repository Gene Expression Omnibus (https://www.ncbi.nlm.nih.gov/geo/), from published data (**Fig. 1; Suppl. Table S2**) and from two transcriptomes conducted in-house (**Fig. 1; Suppl. Table S2**; GSE179303).

2.5. Data processing, cross comparison and data analysis

Genes differentially expressed (DEGs) respect their control provided by authors were organized in a database according to treatment, timing and mutant (blue colour in gene selection column from **Suppl. Table S3**) and different groups were compared by Venny 2.0 (http://bioinfogp.cnb.csic.es/tools/venny/index.html) and Bioinformatics and evolutionary genomics app (http://bioinformatics.psb.ugent.be/webtools/Venn/) software to obtain common and specific genes in the different groups (blue colour in Venn diagram comparison in gene selection column from **Suppl. Table S3**). Among the 11 short-time profiles, we selected DEGs from at least, 5 stressed peroxisome profiles and in the case of 9 long-time profiles we selected DEGs from at least, 4 stressed peroxisome profiles. Classification in different Gen Ontology (GO) categories and functional class enrichment of DEGs of interest was analysed with "Classification Super Viewer" (http://bar.utoronto.ca/ntools/cgi-bin/), StringDB (https://string-db.org/), GeneMania (https://genemania.org/), Mapman (https://mapman.gabipd.org/), and KEGG (https://www.genome.jp/kegg/) using the background for *Arabidopsis thaliana* and running on default parameters. PlantGSEA tool

(http://systemsbiology.cau.edu.cn/PlantGSEA/analysis.php; *Yi et al.,* 2013) was used to perform functional enrichment of the 101 and 86 genes from short and long times, respectively. The analysis was carried out using the Plant Ontology gene sets database (by TAIR), comparing our dataset with the complete Arabidopsis genome. The statistical test employed was Yekutieli (FDR<0.05). Graphs of the most significant GO terms have also been made focusing on biological processes and cellular components using R programming (http://systemsbiology.cau.edu.cn/PlantGSEA/analysis.php; Yi *et al.,* 2013).

2.6. Statistical Analysis

Mean values for the quantitative experiments described above were obtained from at least three independent experiments, with no less than three independent samples per experiment. Statistical analyses were performed using a one-way ANOVA test followed by a Student´s t-test (p-value < 0.05). The analyses were carried out with the aid of IBM SPPS Statistics 24. Error bars representing standard error (SEM) are shown in the figures.

3. RESULTS

3.1. Peroxisomal-ROS perturbed transcriptomic data sets

We compiled the data from six independent public transcriptomic results related with mutants having altered peroxisomal H_2O_2 metabolism in *A. thaliana* with different experimental setups (**Fig. 1; Suppl. Table S2**). Genetic modifications involved peroxisomal antioxidant enzymes such as, catalase (CAT; *cat2-2* mutants) or peroxisomal ROS-producing enzymes such as, glycolate oxidase (GOX; *gox1, gox2* mutants) and Acyl-CoA oxidase (ACX; *acx1* mutants). Two double mutants from above genotypes were also included *(cat2-2 gox1 and cat2-2 gox2).* All transcriptomic analyses were organized in a profile database according to treatments, timing and mutants leading to twenty-one datasheets (**Fig. 1**). We found five categories according to the stress applied: Cd (four profiles), 2,4-D (two profiles), CO_2 shift (ten profiles), high light (one profile), and combined CO_2 and high light (four profiles) as described in published works (**Suppl.**

Table S2). Six genetic backgrounds were distributed in different profiles: *gox2* (two profiles); *35S::GOX2* (two profiles); *cat2* (thirteen profiles); *cat2gox1* (one profile); *cat2gox2* (one profile) and *acx1* (two profiles). To identify early and late peroxisomal-dependent genes we divided our meta-analysis in three categories depending on the timing of the treatment analysed: short-term (0.5 to 3 h, nine profiles); long-term (1 to 4 d, eleven profiles) and mid-term (3 to 24 h treatment, one profile).

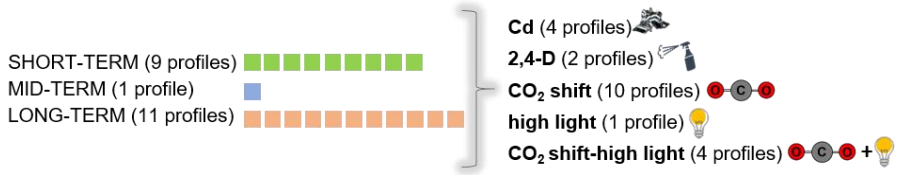

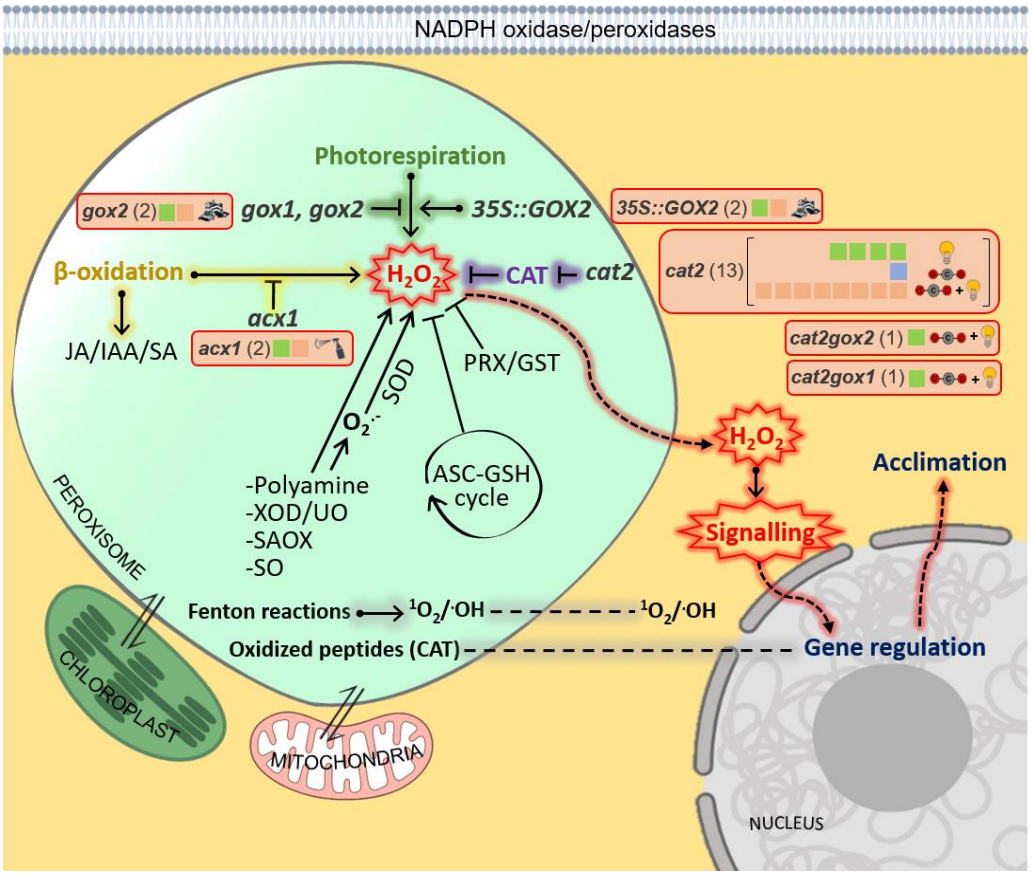

Fig. 1. Peroxisomal transcriptional profiles perturbation categories and timing. *Transcriptional profiles monitoring peroxisomal H_2O_2 perturbations were classified following genetic backgrounds used (italics text), chemical treatments/environmental stresses (bold text) and timing used (capital*

*letters) detailed in **Suppl. Table S2**. For each perturbation category, the number of transcriptional profiles is given. 35S::GOX2: mutants with glycolate oxidase 2 overexpression; gox1/2: mutants affected in glycolate oxidase 1/2; acx1: mutants affected in acyl Co-A oxidase1; cat2-2: mutants affected in catalase 2.*

3.2. Identifying peroxisomal-ROS dependent transcriptional changes

DEGs were defined in each datasheet, resulting in a number ranging from 6266 to only four (**Suppl. Table S3, in CD**). Interestingly, the lowest number of DEGs were described in comparisons *cat2* vs *cat2gox2* and *cat2* vs *cat2gox1* as showed by authors (Kerchev *et al.,* 2016). A large majority of datasheets containing DEGs (18 out of 21) had more than one hundred (**Suppl. Table S3, in CD**). After short-term profiles comparison, we selected DEGs present in a minimum of five transcriptional profiles, 55 % of the profiles analysed, originating from at least four independent works. These conditions fit with our objective to find out commons footprints for peroxisomal dependent signalling from different origin. For long-term profiles comparison however, we selected DEGs present in a minimum of four transcriptional profiles, as we found a small number of DEGs common to five profiles, probably due to side effects of the application of different stresses for a longer time, which may interfere in obtaining common genes due to a persistent stress situation. With these criteria, we found 101 genes (about 1 % of the 9,452 DEGs analysed) commonly regulated at short-time treatments (**Fig. 2 A; Suppl. Table S4**) and 86 genes (about 1 % of the 8,620 DEGs analysed) at long-time treatments (**Fig. 2 B; Suppl. Table S5**). Only six genes were in common between short- and long-term selected genes (**Suppl. Table S4**). As we only found one profile for mid-time treatments, no longer analyses were made at this timing.

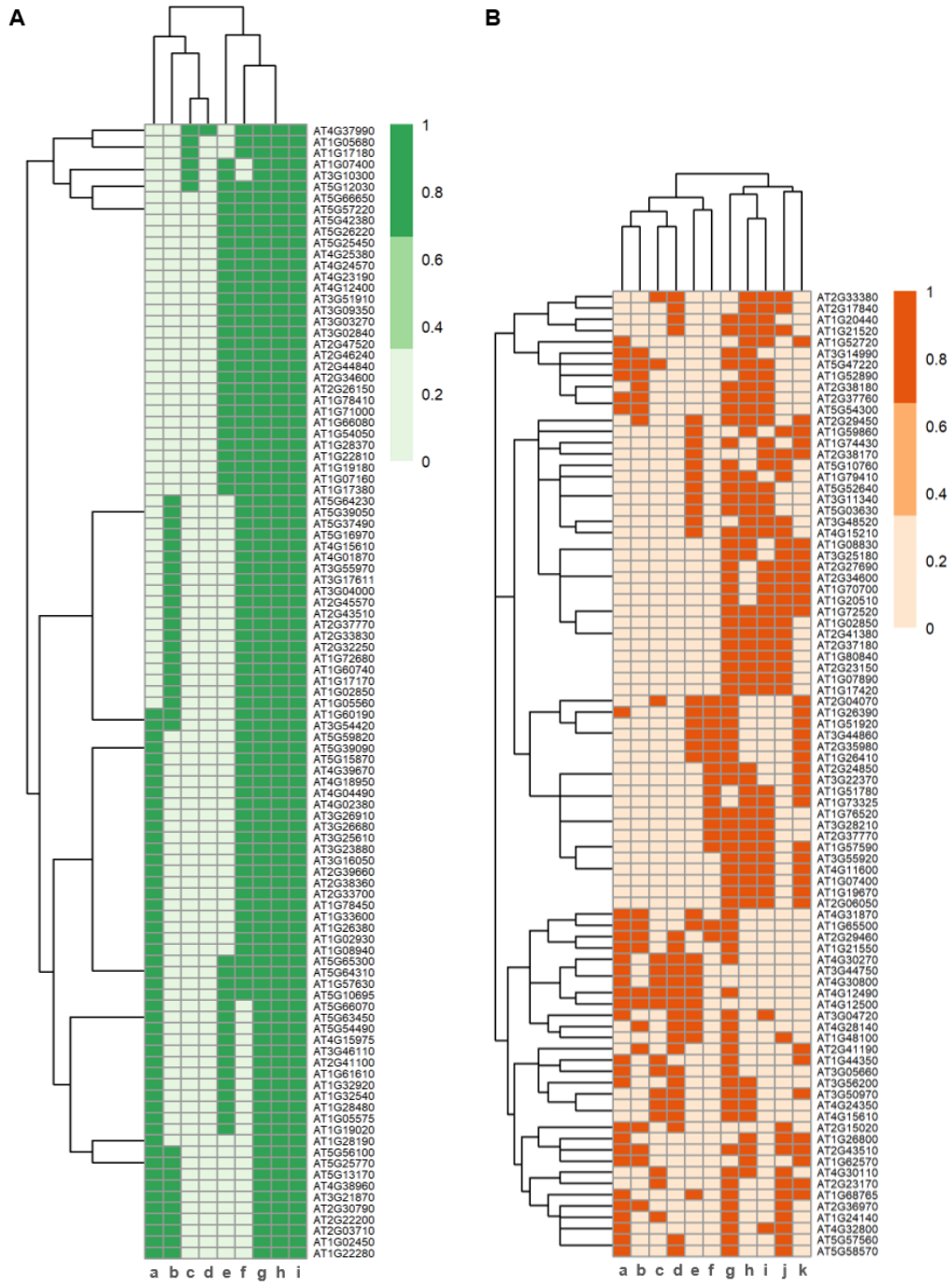

Figure 2. Peroxisomal-ROS dependent transcriptional changes. *Heatmap of DEGs selected from transcriptional profiles related to peroxisomal-dependent signalling at short-time* ***(A)*** *and long-time* ***(B)****. 1 means presence of a gene in a specific profile and 0 no presence. In (A) genes selected are present in at least 5 different profiles and in (B) at least in four. X axis profiles code in (A): (a) 2,4-D metabolism-dependent acx 1-2 60 min; (b) Cd metabolism-dependent 35S::GOX2 30 min; (c)*

cat2 vs. cat2gox1; (d) cat2 vs. cat2gox2; (e) Cd metabolism-dependent gox2-1 30 min, (f) cat2-dependent high light 180 min; (g) CO_2 high light cat2gox2 180 min; (h) CO_2 high light cat2 180 min; (i) CO_2 high light cat2gox1 180 min. X axis profiles code in (B): (a) CO_2 cat2 2880 min short day; (b) CO_2 cat2 5760 min short day b; (c) CO_2 cat2 2880 min long day; (d) CO_2 cat2 5760 min long day b; (e) 2,4-D metabolism-dependent acx1-2 4320 min; (f) Cd metabolism-dependent gox2 1440 min; (g) cat2-dependent CO_2; (h) CO_2 cat2 5760 min short day a; (i) CO_2 cat2 5760 min long day a; (j) Cd metabolism-dependent 35S::GOX2 Cd 1440 min; (k) cat2-dependent CO_2 high light 1440 min.

3.3. Early peroxisomal-dependent transcriptional regulation of pathways and gene families

To determine the different biological processes regulated by the early peroxisomal-dependent transcriptional footprints we made a gene set enrichment exploration for Gene Ontology (GO) and KEGG (Kyoto Encyclopedia of Genes and Genomes) pathways, and protein family gene groups using "Classification Super Viewer" from BAR website, StringDB, GeneMania, PlantGSEA and Mapman tools. Several gene groups were significantly overrepresented ($p < 0.05$ and FDR < 0.05) within the early peroxisomal-dependent genes (**Fig. 3; Suppl. Fig. S1**). As expected, the GO group termed "Response to Stress" and "Response to Stimulus" were enriched in different tools used such as, Classification Super Viewer, StringDB and PlantGSEA. Representative number of genes and normed frequency obtained by Classification Super Viewer tool, related with biological processes (BP), is presented for these GO groups in **Fig. 3** (**A**). Furthermore, relationships between gene sets "Response to Stimulus" (GO:0050896) and "Response to Chemical Stimulus" (GO:0042221) and other significant gene sets in category GO_BP, such as responses to different stimuli (abiotic, biotic, endogenous, etc.), response to stress and immune response, have been found by PlantGSEA tool (http://systemsbiology.cau.edu.cn/PlantGSEA/; **Fig. 3 C**). Interestingly, almost 45 % of the early peroxisomal-dependent genes are localized in the nucleus (**Fig. 3 B**) following results obtained by Classification Super Viewer tool related with cellular component (CC).

This result is in accordance to the significant GO categories "Signal Transduction" and "Transcription DNA-dependent" at this timing found in this study (**Fig. 3 A**).

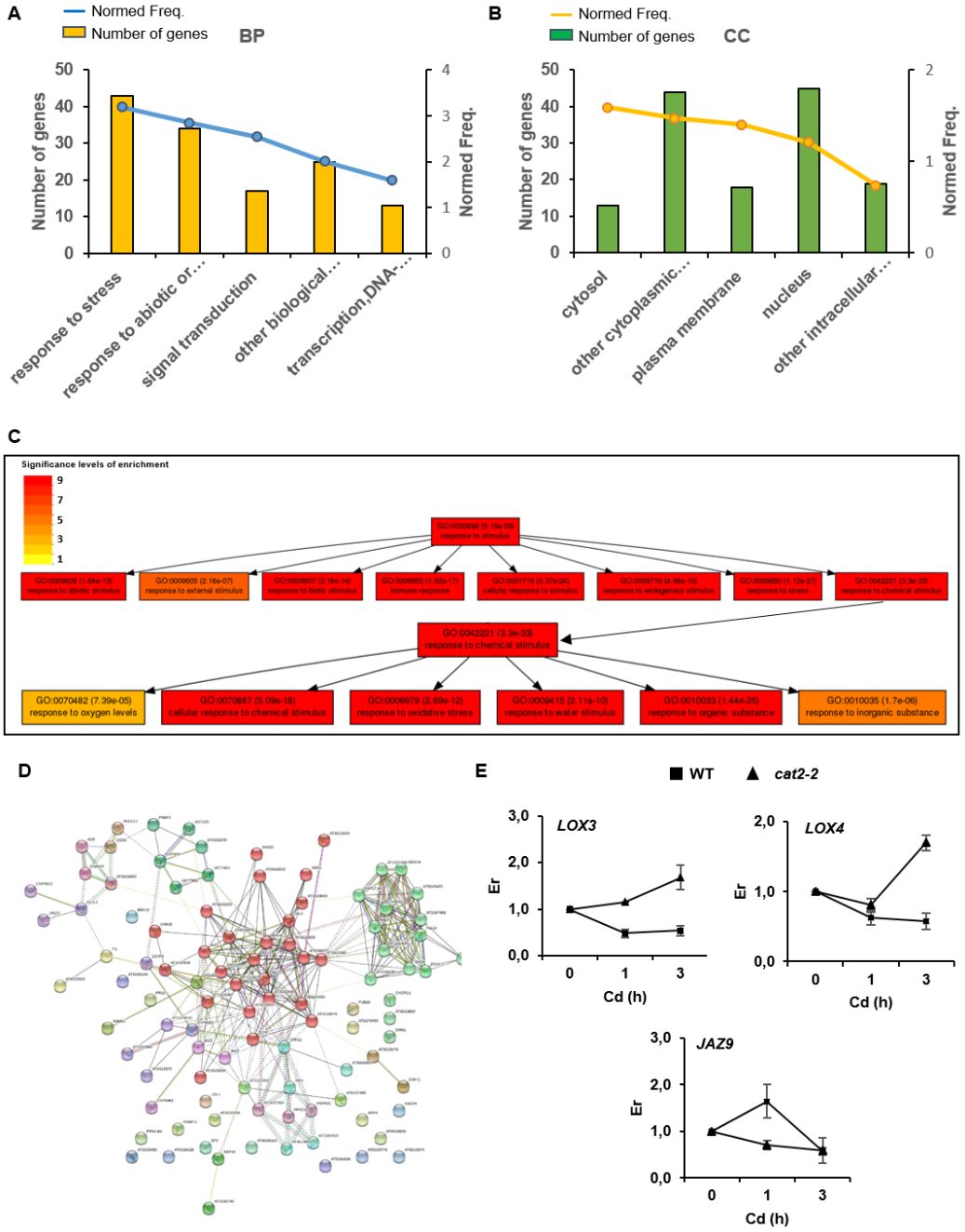

Figure 3. Early peroxisomal-dependent genes classification. *Five main significant GO categories related with biological processes (BP; **A**) and cellular components (CC; **B**) obtained by Classification Super Viewer tool (http://bar.utoronto.ca/ntools/cgi-bin/). The relationship between the selected*

gene sets Response to Stimulus (GO:0050896) and Response to Chemical Stimulus (GO:0042221) and other significant gene sets in category GO_BP ***(C)*** *obtained by PlantGSEA tool (http://systemsbiology.cau.edu.cn/PlantGSEA/). StringDB analysis of early peroxisomal- dependent genes (****D****) showed two main clusters: 1) Heat shock transcription factors and proteins (chaperones) in green and 2) Initial signalling cascades with phosphatases 2C, MAPK, ERF transcription factor and JAZ proteins, in red.* ***E****) JA biosynthetic genes, lipoxygenases 3 and 4 (LOX3 and LOX4) and JA-dependent signalling gene JAZ9, expression in WT and cat2-2 mutants in seedlings response to Cd stress. Er, relative expression respect control conditions (0 h), which was considered as 1. Values represent means ±SEM. * denote significant differences between Cd treatment and control within each genotype (p < 0,05; Student's t-test).*

Analysis of Plant Ontology gene sets resulted in 90 % of the genes related with stamen, and 80-85 % related with different reproductive organs such as, sepals and flowers (**Suppl. Fig. S2**). Vascular leaf tissue is also highly represented with an 82 % of the genes having this location in the plant (**Suppl. Fig. S2**). In addition, within the early peroxisomal-dependent genes we found significant number of genes targets of HY5 and AtbHLH (PIF1) TFs (**Suppl. Table S6**). Analysis by StringDB organized early peroxisomal-dependent genes in two main clusters: 1) Heat shock transcription factors and proteins (chaperones) and 2) Initial signalling cascades with phosphatases 2C, MAPK, ERF transcription factor and JA biosynthesis and signalling genes (**Fig. 3 D; Suppl. Table S7**). We analysed two genes involved in JA biosynthesis, such as *LOX3* and *LOX4* in plant response to Cd stress after short-time treatment in WT and *cat2-2* mutants and meanwhile we observed a significant repression of these genes in WT plants, in *cat2-2* no significant changes were found (**Fig. 3 E**). At the same conditions *JAZ9* involved in JA-dependent signalling is induced in WT after 1 h treatment, but no changes were observed in *cat2-2* mutants (**Fig. 3 E**).

Interestingly, early peroxisomal-dependent genes presented almost a 93 % of co-expression obtained by GeneMania analysis, where a group of twenty proteins appears to regulate the network between them (**Fig. 4 A**). Most of these proteins are HSPs/chaperones and well-known transcription factors related with plant response to stress.

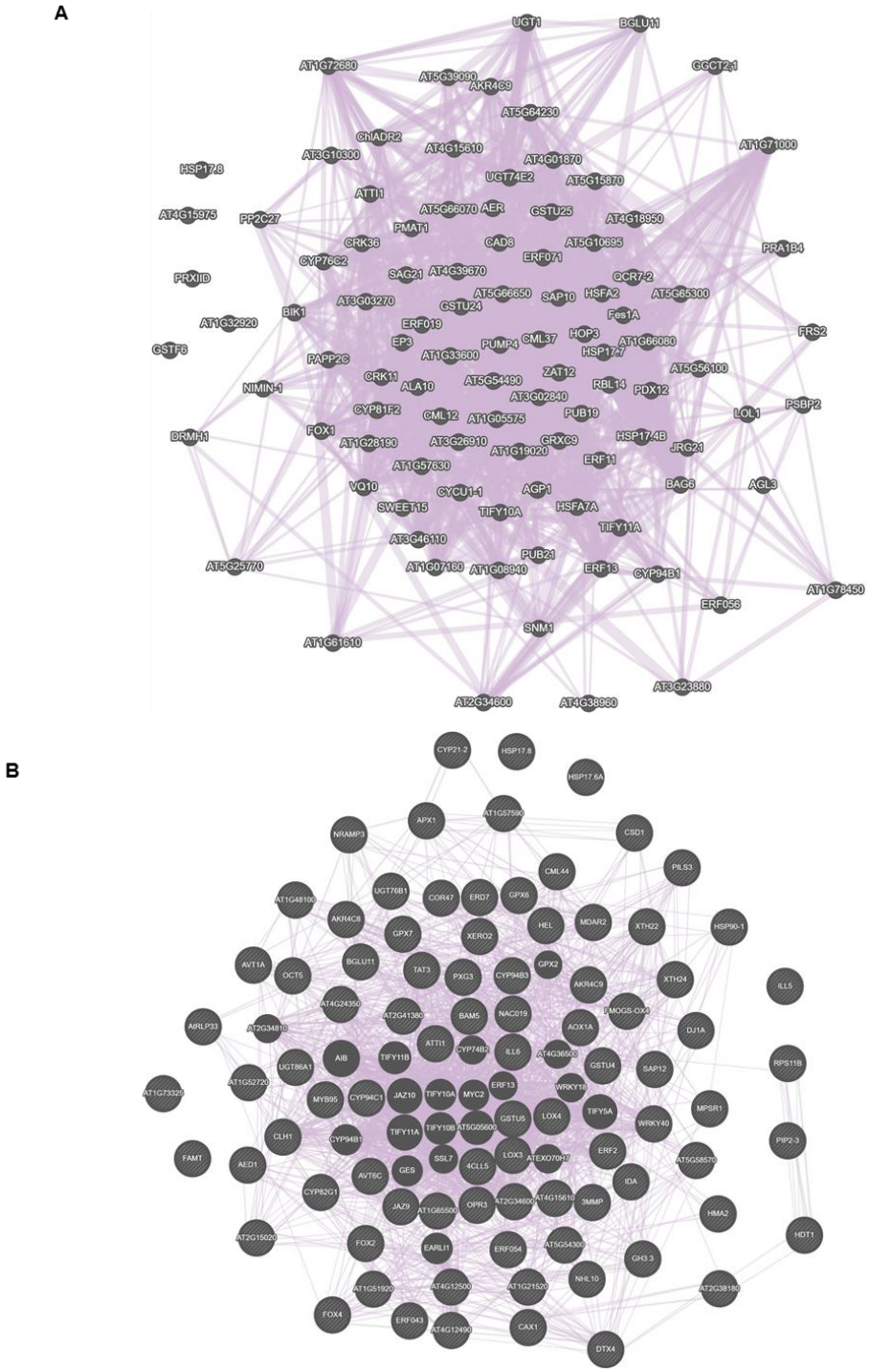

Figure 4. Co-expression analysis for early peroxisomal-dependent genes. *Co-expression analysis by GeneMania showed a high percentage within the early peroxisomal-dependent genes* ***(A)*** *and within late peroxisomal-dependent genes* ***(B)****.*

3.4. Late peroxisomal-dependent transcriptional regulation of pathways and gene families

We followed a similar analysis to stablish late peroxisomal-dependent transcriptional footprints. Several gene groups were significantly overrepresented ($p < 0.05$ and FDR < 0.05) within the late peroxisomal-dependent genes (**Fig. 5; Suppl. Fig. S3**). Representative number of genes and normed frequency obtained by Classification Super Viewer tool, related with BP, is presented for these GO groups in **Fig. 5 A**. Although we found only six genes in common between short- and long-term peroxisomal-dependent genes, the GO group termed "Response to Stress" and "Response to abiotic and biotic stress" persist over time (**Fig. 3 A** and **5 A**). Relationships between gene sets "Response to Stimulus" (GO:0050896) and "Response to Chemical Stimulus" (GO:0042221) and other significant gene sets in category GO_BP, such as responses to different stimuli (abiotic, biotic, endogenous, etc.), response to stress and immune response, obtained by PlantGSEA tool is also maintained (http://systemsbiology.cau.edu.cn/PlantGSEA/analysis.php; **Fig. 5 C**). At this timing however, higher normed frequency is related with cell wall, ER and extracellular locations, being the highest number of genes presented in the extracellular one (**Fig. 5 B**) instead of being the nucleus as founded at early times (**Fig. 3 B**).

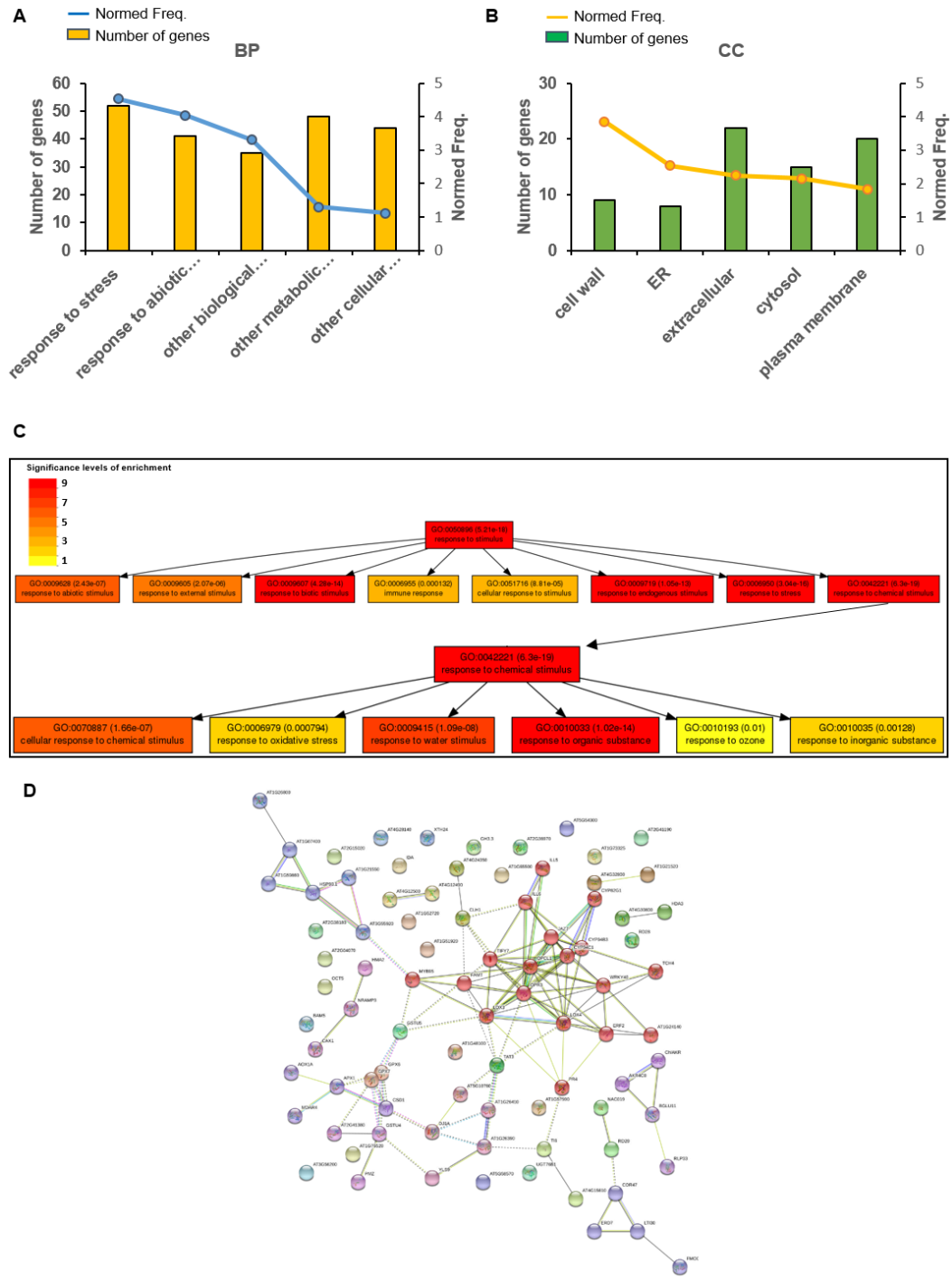

Figure 5. Late peroxisomal-dependent genes classification. *Five main significant GO categories related with biological processes (BP; **A**) and cellular components (CC; **B**) obtained by Classification Super Viewer tool (http://bar.utoronto.ca/ntools/cgi-bin/). The relationship between the selected gene sets Response to Stimulus (GO:0050896) and Response to Chemical Stimulus (GO:0042221) and other significant gene sets in category GO_BP* ***(C)*** *obtained by PlantGSEA tool*

*(http://systemsbiology.cau.edu.cn/PlantGSEA/analysis.php). StringDB analysis of early peroxisomal-dependent genes **(D)** showed one main cluster related with JA signalling and alpha-Linolenic acid metabolism and two smaller ones, related with GSH metabolism and heat shock proteins (HSPs).*

These changes in location may be related with the changes in BP with a higher normed frequency, other than "responses to stress", found at this timing respect to early responsive genes, which are "other metabolic and cellular processes" (**Fig. 5 A**). Analysis of Plant Ontology gene sets at this timing is similar to the one made at early time, showing the vascular tissue the highest number of genes (almost 90 %), followed closely by stamen and sepals (**Suppl. Fig. S4**). Interestingly, we also found a significant number of genes targets of HY5 TF within the late peroxisomal-dependent genes (**Suppl. Table S6**). Analysis by StringDB showed one main cluster for late peroxisomal-dependent genes related with JA signalling and alpha-Linolenic acid metabolism and two smaller ones, related with GSH metabolism and HSPs (**Fig. 5 D; Suppl. Table S8**). Similarly to early peroxisomal-dependent genes, late responses presented almost a 88 % of co-expression obtained by GeneMania analysis, where a group of twenty proteins appears to regulate the network between them (**Fig. 4 B**). Most of these proteins in this case are transcription factors related with hormonal signalling.

3.5. Peroxisome transcriptional footprints are found in environmental stress-triggered transcriptional responses

We used peroxisome transcriptional footprints to retrieve perturbations with similar transcriptional changes. As different GO groups related with responses to a diversity of stresses were enriched, with the highest normed frequency, within peroxisomal transcriptional footprints (**Fig. 3** and **Fig. 5**), we compared them with transcriptional changes observed after applying four representative abiotic stress conditions for a short-time period (heat, salt, excess light, and oxidative stress imposed by the herbicide paraquat), in a very recent analysis (Zandalinas *et al.,* 2021). Interestingly, 73 genes (72 %) of the early peroxisomal transcriptional footprints were in common with all four stresses (**Fig. 6; Suppl. Table S9, in CD**) and 85 % of them (62 genes), were up regulated in the different stresses (**Suppl. Fig. S5**). Individual comparisons resulted in 83 common genes (82.1 %) with heat stress, 90 genes (89.1 %) with salt stress and 93 genes (92 %) with paraquat and high light (**Fig. 6**), and only three genes are not in common with any of the stresses compared. Enrichment of the common 73 genes resulted in

significant GO_BP such as response to chitin, to organonitrogen compound, to oxidative stress, to toxic substance and to endoplasmic reticulum (ER) stress, among others (**Fig. 7 B**). Main GO related with molecular function (MF) are calcium ion binding, GST activity and cofactor binding (**Fig. 7 B**). KEGG pathways significantly represented are GSH metabolism and response to endoplasmic reticulum (ER) stress (**Suppl. Table S10, in CD**).

Figure 6. Early peroxisomal dependent genes and abiotic stress responses. (A) *Comparison by*

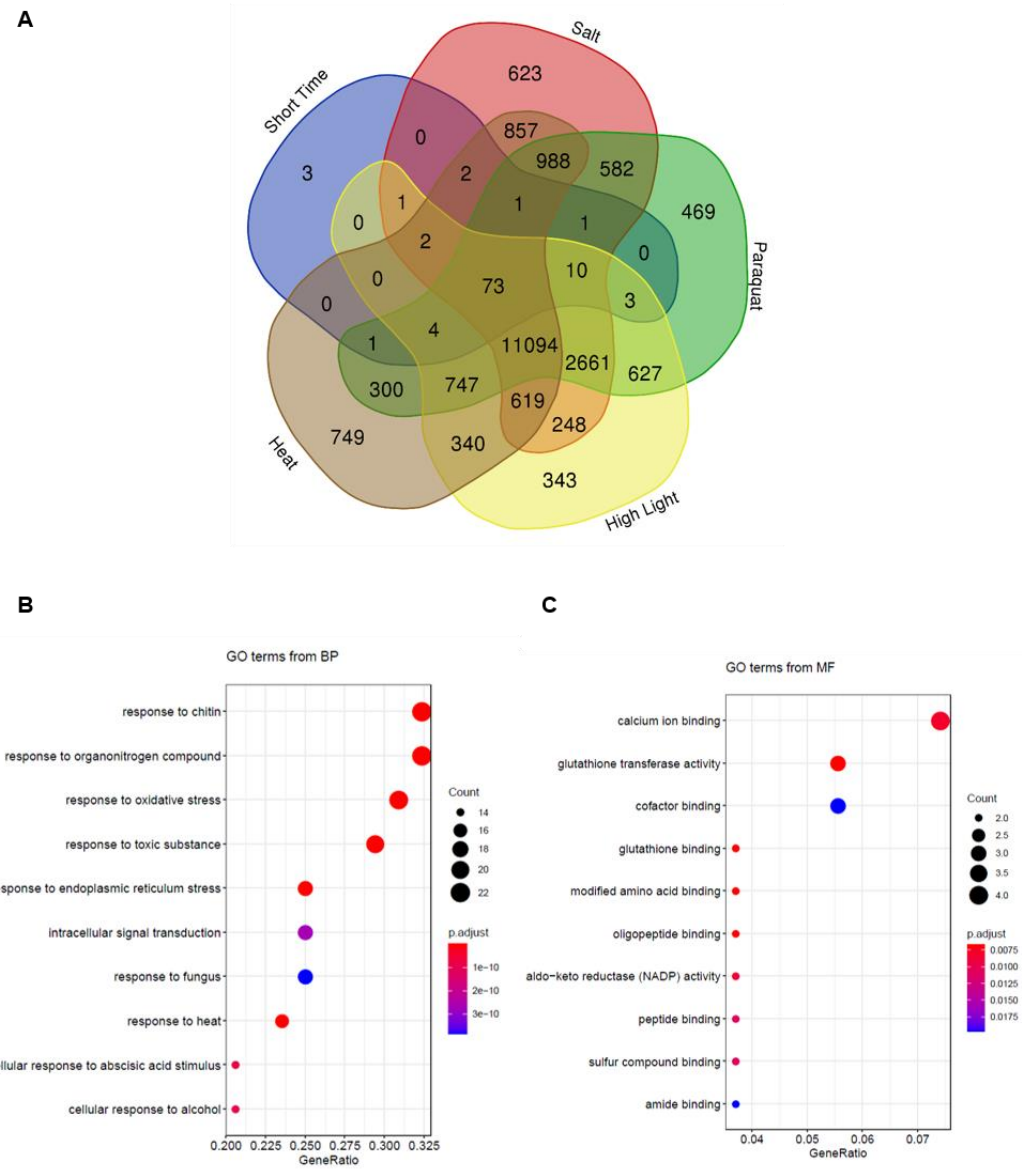

Venny algorithm (http://bioinfogp.cnb.csic.es/tools/venny/) of early peroxisomal dependent genes with transcriptional changes after applying abiotic stress conditions (heat, salt, excess light, and

paraquat). ***(B)*** *Enrichment of common genes obtained in A) showing significant GO terms in Biological Process (BP) and in* ***(C)*** *Molecular Function (MF).*

3.6. Peroxisome transcriptional footprint relation with ROS and other organelles-dependent transcriptional responses

As peroxisome transcriptional footprint (PTF) is based on transcriptomic data from mutant and/or treatments related with peroxisomal H_2O_2 metabolism and "response to oxidative stress" is one of the GO_BP found to be significantly overrepresented we compared PTF with different transcriptomic data related with ROS. Firstly, we compared early PTF with the different clusters obtained in the ROS wheel, which resulted from the analysis of 79 microarray studies related with redox homeostasis perturbations (Willems *et al.,* 2016). We did not found any common gene in early TPF with clusters I, II and VIII. Cluster I could be considered as a representation for plastid retrograde signalling (related with gun mutants; Willems *et al.,* 2016; **Fig. 7**). Cluster II consisted of transcript triggered by HL exposure ranging from 3 to 8 h, which is not in the timing considered for early PTM in our analysis. Similarly, cluster VIII consisted in late timing oxidative stress treatments and constitutively redox perturbations. Comparison with the other clusters resulted in 18 genes in common with cluster III, which is related with short exposures to HL and it has been included in our analysis as *cat2* mutants have been used. Five genes in common with cluster IV, which involves mitochondria and H_2O_2 treatment of cell cultures. Three genes in common with cluster V and three genes with cluster VI, involving different ROS inducers and early UV and $^1O_2$-regulated genes, respectively. Finally, five genes resulted in common with cluster VII, which is related with the impact of RBOHF on a *cat2* background. There are practically no genes in common between genes from the late-PTF and the different groups from the ROS wheel analysis. We found only five, three and one genes in common with groups III, IV and VI, respectively (**Fig. 7**).

	long time (86)	Cluster I-GUN retrograde (102)	Cluster II-HL late (27)	Cluster III-HL early (442)	Cluster IV-ROS CC (52)	Cluster V-ROS (10)	Cluster VI-$^1O_2$-UVB early (21)	Cluster VII-RBOHF (11)	Cluster VIII-ROS acclimation (12)
short time (101)	6	0	0	18	5	3	3	5	0
long time (86)		0	0	5	3	0	1	0	0

Figure 7. Peroxisomal-dependent genes and other ROS footprints. *Comparison by multiple list comparator (https://www.molbiotools.com/listcompare.php) of early (short-time;* ***A****) and late (long-*

*time; **B**) peroxisomal dependent genes with transcriptional changes with different clusters obtained in the ROS wheel (Willems et al., 2016).*

In addition to comparison of PTF with the group I from the ROS wheel related with plastids, we compared transcriptomic data from a mutant altered in mitochondrial ROS metabolism such as *aox1* (Giraud *et al.,* 2008) and did not found any gene in common under control or stress conditions.

4. DISCUSSION

To properly control organelles function and hence, cellular metabolism, different regulatory mechanisms should exist between the nucleus and organelles allowing mutual information exchange. Retrograde signalling is considered a mechanism by which specific signalling molecules that organelles use to transfer information to the nucleus about their physiological and developmental state, trigger a consequently regulation of nuclear genes. Retrograde signalling from plastids is better characterized from the initial analysis of the GUN proteins, as major players, and more recent elements such as metabolites and transcription factors (Kleine and Leister, 2016; Wu and Bock, 2021). Mitochondrial retrograde signalling has also been assessed in the last years (Law *et al.,* 2014) and although the signal element transmitting information is not known, multiple upstream regulatory elements have been identified such as TFs from the NAC family (De Clercq *et al.,* 2013; Ng *et al.,* 2014). It has been proposed that ROS-produced in chloroplast and mitochondria might play a role as key elements for retrograde signalling of these organelles (Sun *et al.,* 2011; Huang *et al.,* 2016; Wagner *et al.,* 2018).

Although different analysis with mutants/treatments leading to peroxisomal altered metabolism showed specific changes in the transcriptome, our knowledge on peroxisomal retrograde signalling is scarce (Su *et al.,* 2019). Wide-scale peroxisomal-dependent signalling was initiated by transcriptomic analysis of treatments/mutants that affect one of the major antioxidants in the organelle, catalase, disturbing peroxisomal H_2O_2 metabolism. Thus, treatment with the catalase inhibitor 3-aminotriazole (AT), was initially used (Gechev *et al.,* 2005), as well as *cat2* mutants, affected in the main gene coding for CAT, under control and stress conditions (Vanderawera *et al.,* 2005; Queval *et al.,* 2007; Chaouch *et al.,* 2010; Mhamdi *et al.,* 2010; Queval *et al.,* 2012; Sewelam *et al.,*

2014; Waszczak *et al.,* 2016). In addition, we have used transcriptomic analysis with mutants affected in *ACX1* and *GOX2*, which are main sources for peroxisomal H_2O_2, from the β-oxidation and photorespiration pathways, respectively (Romero-Puertas *et al.,* 2021). Analyses with double mutants affecting *CAT2* and *GOX1/2* are also available (Kerchev *et al.,* 2016). We carried out a meta-analysis of the different transcriptomes available for mutants affected in peroxisomal ROS metabolism, which let us to identify a common group of genes that respond to peroxisomal stress. Thus, we found 101 and 86 genes commonly regulated at short-time and long-time stress treatments, respectively. Enrichment analysis with early peroxisomal-dependent genes showed GO terms related with response to stress/stimulus (**Fig. 3**) accordingly with the conditions analyzed. GeneMania analysis showed a high percentage of co-expression within the 101 genes suggesting an early coordinated peroxisomal-dependent plant response to stress. In fact, comparing these genes with transcripts regulated after different abiotic stress (Zandalinas *et al.,* 2021), we found a high percentage of them regulated after any of the stress analyzed (**Fig. 6**). Individual comparisons resulted from 82.1 % in common with transcriptomic response to heat stress and 92 % with paraquat and high light. Interestingly, 72 % of the early peroxisomal-dependent genes are shared by the four abiotic stresses analyzed being the associated KEGG pathways related with: 1) GSH metabolism, mainly GST activity, which is related with detoxification and 2) with the response to ER stress. In fact, different abiotic stresses can disturb the correct folding of proteins in the ER leading to the so-called ER stress (Vitale and Boston, 2008; Liu and Howell, 2010). ER stress activates a response system, the unfolded protein response (UPR) to re-establish ER homeostasis (Angelos *et al.,* 2017), which involves the induction of different proteins such as molecular chaperones (Angelos *et al.,* 2017). Although other ROS such as the chloroplast singlet oxygen signalling pathway has been involved in the ER-dependent protein response (Beaugelin *et al.,* 2020), the mechanism underlying peroxisomal H_2O_2-dependence and the ER stress response needs further investigation.

Further StringDB analysis clustered early peroxisomal-dependent genes in two groups related with HSFs and chaperones and different TFs and JA biosynthesis and signalling (**Fig. 3**). Previous independent analyses with *cat2-2* mutants showed that an increase of H_2O_2 produced in peroxisomes induced transcripts involved in protein repair responses (Queval *et al.,* 2007; Sewelam *et al.,* 2014) suggesting that peroxisomes could

regulate part of the mechanisms leading to protein protection in plant response to stress. On the other hand, nuclear localization of about half of the peroxisomal-dependent genes at early time points suggests a peroxisomal-dependent regulation of transcription. Most of TFs and signalling molecules obtained in our meta-analysis were not described however by Sewelam and co-workers (2014), probably due to a later timing of sampled analyzed (8 h) in that work. A large proportion of TFs differentially regulated was found however, in double *(cat2/3)* and triple *(cat1/2/3)* catalase mutants involving practically all TFs families (Su *et al.,* 2018). Comparison with different transcriptomic data related with ROS showed no common genes with plastid retrograde signalling represented by GUN proteins (Sewelam *et al.,* 2014), neither with mitochondrial *aox1*-dependent signalling (Giraud *et al.,* 2008), suggesting that ROS signals derived from peroxisomes are different from the chloroplast and mitochondria, although we cannot discard that ROS signals derived from the different organelles can be interconnected (Sewelam *et al.,* 2014; Su *et al.,* 2018). Thus, it has been reported in Arabidopsis plants that peroxisomal polyamine-dependent ROS production promotes the induction of NADPH oxidase activity which in its turn induces the increase of oxygen consumption by the mitochondrial alternative oxidase pathway (Andronis *et al.,* 2014). Jasmonic acid produced in peroxisome can also modulate transcriptional and enzymatic changes of plasma membrane NADPH oxidases in rice plants in response to thiocyanate (Yu *et al.,* 2021). The upregulation of CAT and GOX in Arabidopsis *rboh* mutants in response to Cd (Gupta *et al.,* 2017) supports a close relationship between peroxisomal ROS and NADPH oxidase-dependent ROS production which could be a key point in cellular redox homeostasis and signalling.

Although few peroxisomal-dependent genes persist over the time, GO terms such as "response to stress" and similar are maintained, suggesting that one of the main functions for peroxisomal retrograde signalling is a coordinated response to avoid damages in the cell and to protect proteins under stress conditions. Therefore, GeneMania analysis showed a high percentage of co-expression within the 85 genes in peroxisomal-dependent plant response to stress at later time responses. Interestingly, in early peroxisomal-dependent signalling, genes associated with the nucleus are one of the main groups, meanwhile at later time responses the main gene groups are associated to extracellular and plasma membrane. Similarly to that occurs at early times, StringDB analysis cluster a group of genes related with JA, which biosynthesis goes through

peroxisomes being ACX1 one of the primary enzymes involved in JA biosynthesis (Castillo *et al.,* 2004). In its turn, JA regulates the number and size of peroxisomes in Arabidopsis plants, by repressing *PEX11b* and *PEX11d* (Castillo *et al.,* 2008). Although JA was considered initially as a key hormone involved in plant response to biotic stress, nowadays it has been clear that it is also involved in abiotic stresses such as, salinity, wounding, heavy metals and UV (Rodríguez-Serrano *et al.,* 2006; Ghorbel *et al.,* 2021). Regulating biosynthesis and signalling events of hormones signalling molecules produced in peroxisomes could be the most natural and efficient way to recover these organelles from stress. We have found that both, JA biosynthesis and JA-dependent signalling are affected in *cat2* mutants in plant response to Cd stress linking organellar ROS production with JA. GSH metabolism and HSPs are two small groups also clustered supporting peroxisomal-dependent role for cell redox homeostasis and protein protection. Recently, the involvement of HSPs and co-chaperones associated have been involved in the regulation of JA-dependent responses linking both peroxisomal-dependent clusters (Di Donato and Geisler, 2019).

Interestingly, HY5 and PIF1 target genes are overrepresented at early peroxisomal-dependent signalling being maintained HY5 at later times. HY5 is a bZIP TF, which directly regulates a wide range of genes mediating plant responses to hormones and abiotic stress responses, such as cold and UV-B (Ulm *et al.,* 2004; Lau and Deng, 2010; Catalá *et al.,* 2011). PIF1 belongs to a small family of bHLH TFs, that play multiple functions, they are mainly accumulated in the dark and induce skotomorphogenesis and facilitate the seedling greening process (Shen *et al.,* 2005; Stephenson *et al.,* 2009). Recently, it has been shown that PIF1 regulates expression of multiple ROS-dependent genes and that PIF1/PIF3 interact physically with HY5/HYH (HY5 homolog) giving rise to transcriptional modules that directly bind ROS signalling genes to regulate their expression in a coordinated way (Chen *et al.,* 2013). Within ROS-dependent genes regulated by PIF/HY5, there are different TFs, such as ethylene-responsive transcription factors (ERF), regulatory proteins (ZAT), HSPs, such as HSP17 and HSP90 and MAPKs. Therefore, PIF1/PIF3-HY5/HYH has been suggested as a rheostat to fine-tune ROS-dependent signalling pathways (Chen *et al.,* 2013). We have found ERF13, ZAT12 and HSP17 among others, as targets for PIF/HY5 within the early peroxisomal-dependent genes and HSP90 within the late peroxisomal-dependent genes. Previous result showed

PIF/HY5 and peroxisomal dynamic and signalling relation. Therefore, HYH transcription factor has been linked to peroxisomal proliferation by activation of the peroxin 11b (PEX11b), through a phytochrome A-dependent pathway (Orth *et al.,* 2007). In addition, PIF1/PIF3-HY5/HYH is a master regulator of plant responses to light conditions, which have been shown to regulates transcription of a number of peroxisomal genes involved in seeds development and photosynthesis processes (Kaur *et al.,* 2013).

In summary, we have found a number of genes regulated commonly in different mutants and stresses where ROS metabolism in peroxisomes is altered, which we have considered as peroxisomal-dependent genes. These genes are highly co-expressed between them and they are shared with transcriptomic responses to several abiotic stresses. Late peroxisomal-dependent genes clustered in groups related with HSFs and proteins, response to ER-stress and GSTs, mainly involved in proteins protection and detoxification. Different transcription factors and hormone-dependent biosynthesis and signalling, mainly related with JA, are within early peroxisomal-dependent genes, suggesting that initial peroxisomal stress may regulate different signalling pathways involved in plant response to stress.

5. Supplementary Material

Suppl. Table S1. *Reverse transcription quantitative PCR primers.*

Gene	Primer sequence (5′ → 3′)	ID
Tubulin beta 4-F	GAGGGAGCCATTGACAACATCTT	AT5G44340
Tubulin beta 4-R	GCGAACAGTTCACAGCTATGTTCA	
lipoxygenase 3 (LOX3)-F	CACTGCAATTCACAAGCAACC	AT1G17420
lipoxygenase 3 (LOX3)-R	CAAAGGAGGAATCGGAGAAGC	
lipoxygenase 4 (LOX4)-F	TGGGTTCTCGTCTAATCTTCGAG	AT1G72520
lipoxygenase 4 (LOX4)-F	AGGGTTGATGGAGAACTGTGTTC	
JASMONATE-ZIM-DOMAIN PROTEIN 9 (JAZ9)-F	CGTTGCTGCGACTAATGCAA	AT1G70700
JASMONATE-ZIM-DOMAIN PROTEIN 9 (JAZ9)-F	CCAAGAACCGAGCCAAGGAT	

Suppl. Table S2. *Works used in the meta-analysis.*

Code	Mutant	Tissue	Treatment	Conditions	Time (min)	Ref
1	KO *cat2*	adult leave	high light	long day	180	Van
2	KO *acx1-2*	adult leave	2,4-D	long day	60	Rom
3	KO *acx1-2*	adult leave	2,4-D	long day	4320	Rom
4	*35S::GOX2*	seedling	Cd (100 µM)	long day	1440	Not
5	*35S::GOX2*	seedling	Cd (100 µM)	long day	30	Not
6	*gox2-1*	seedling	Cd (100 µM)	long day	1440	Not
7	*gox2-1*	seedling	Cd (100 µM)	long day	30	Not
8	KO *cat2*	adult leave	high CO2 and later normal air	short day	5760	Mha
9	KO *cat2*	adult leave	high CO2 and later normal air	long day	5760	Mha
10	KO *cat2*	adult leave	high CO2 and later normal air (short day)	short day	2880	Que
11	KO *cat2*	adult leave	high CO2 and later normal air (short day)	short day	5760	Que
12	KO *cat2*	adult leave	high CO2 and later normal air (long day)	short day	2880	Que
13	KO *cat2*	adult leave	high CO2 and later normal air (long day)	short day	5760	Que
14	KO *cat2*	adult leave	high CO2 and later normal air (long day)	long day	480	Sew
15	KO *cat2*	adult leave	high light, high CO2 and later normal air	long day	180	Kero
16	*cat2-2gox1-1*	adult leave	high light, high CO2 and later normal air	long day	180	Kero
17	*cat2-2gox2-1*	adult leave	high light, high CO2 and later normal air	long day	180	Kero
18	*cat2 vs. cat2-2gox1-1*	adult leave	high CO2 and later normal air	long day	180	Kero
19	*cat2 vs. cat2-2gox2-1*	adult leave	high CO2 and later normal air	long day	180	Kero
20	KO *cat2*	adult leave	high light, high CO2 and normal air	long day	1440	Was
21	KO *cat2*	adult leave	high CO2 and normal air	long day	1440	Was

SHORT TIME (9 profiles): 1, 2, 5, 7, 15, 16, 17, 18, 19
MEDIUM TIME (1 profile) 14
LONG TIME (11 profiles): 3, 4, 6, 8, 9, 10, 11, 12, 13, 20, 21

Suppl. Table S3. *Datasheets used in the meta-analysis (**in CD**).*

Suppl. Table S4. *Early peroxisomal-dependent transcripts.*

	AGI ID	Annotation
1	AT1G72680	ATCAD1_CAD1__cinnamyl-alcohol dehydrogenase
2	AT3G51910	AT-HSFA7A_HSFA7A__heat shock transcription factor A7A
3	AT2G46240	ATBAG6_BAG6__BCL-2-associated athanogene 6
4	AT4G12400	Hop3__stress-inducible protein, putative
5	AT4G25380	AtSAP10_SAP10__stress-associated protein 10
6	AT3G09350	Fes1A__Fes1A
7	AT1G54050	HSP20-like chaperones superfamily protein
8	AT1G28370	ATERF11_ERF11__ERF domain protein 11
9	AT4G38960	BBX19__B-box type zinc finger family protein
10	AT4G24570	DIC2__dicarboxylate carrier 2
11	AT2G41100	ATCAL4_TCH3__Calcium-binding EF hand family protein
12	AT1G28480	GRX480_roxy19__Thioredoxin superfamily protein
13	AT1G19180	AtJAZ1_JAZ1_TIFY10A__jasmonate-zim-domain protein 1
14	AT1G02930	ATGST1_ATGSTF3_ATGSTF6_ERD11_GST1_GSTF6__glutathione S-transferase 6
15	AT2G45570	CYP76C2__cytochrome P450, family 76, subfamily C, polypeptide 2
16	AT2G03710	AGL3_SEP4__K-box region and MADS-box transcription factor family protein
17	**AT2G43510**	ATTI1_TI1__trypsin inhibitor protein 1
18	AT1G78410	VQ motif-containing protein
19	AT3G02840	ARM repeat superfamily protein
20	AT4G39670	Glycolipid transfer protein (GLTP) family protein
21	AT5G59820	AtZAT12_RHL41_ZAT12__C2H2-type zinc finger family protein
22	AT5G54490	PBP1__pinoid-binding protein 1
23	AT1G17380	JAZ5_TIFY11A__jasmonate-zim-domain protein 5
24	AT2G44840	ATERF13_EREBP_ERF13__ethylene-responsive element binding factor 13
25	AT4G18950	Integrin-linked protein kinase family
26	AT1G57630	Toll-Interleukin-Resistance (TIR) domain family protein
27	AT1G26380	FAD-binding Berberine family protein
28	AT3G03270	Adenine nucleotide alpha hydrolases-like superfamily protein
29	AT1G02450	NIMIN-1_NIMIN1__NIM1-interacting 1
30	AT1G19020	
31	AT4G04490	CRK36__cysteine-rich RLK (RECEPTOR-like protein kinase) 36
32	AT4G02380	AtLEA5_SAG21__senescence-associated gene 21
33	AT1G33600	Leucine-rich repeat (LRR) family protein
34	AT5G13170	AtSWEET15_SAG29_SWEET15__senescence-associated gene 29
35	AT2G26150	ATHSFA2_HSFA2__heat shock transcription factor A2
36	**AT2G37770**	AKR4C9_ChlAKR__NAD(P)-linked oxidoreductase superfamily protein
37	**AT2G34600**	JAZ7_TIFY5B__jasmonate-zim-domain protein 7
38	AT2G33700	PP2CG1__Protein phosphatase 2C family protein
39	AT1G71000	Chaperone DnaJ-domain superfamily protein
40	AT1G66080	
41	**AT1G07400**	HSP20-like chaperones superfamily protein
42	AT3G16050	A37_ATPDX1.2_PDX1.2__pyridoxine biosynthesis 1.2
43	AT2G47520	AtERF71_ERF71_HRE2__Integrase-type DNA-binding superfamily protein
44	AT4G37990	ATCAD8_CAD-B2_ELI3_ELI3-2__elicitor-activated gene 3-2
45	AT5G57220	CYP81F2__cytochrome P450, family 81, subfamily F, polypeptide 2
46	AT2G32250	FRS2__FAR1-related sequence 2
47	AT1G05680	UGT74E2__Uridine diphosphate glycosyltransferase 74E2
48	AT1G32920	
49	AT1G32540	LOL1__lsd one like 1

50	AT2G39660	BIK1__botrytis-induced kinase1
51	AT5G10695	
52	AT5G12030	AT-HSP17.6A_HSP17.6_HSP17.6A__heat shock protein 17.6A
53	AT5G42380	CML37__calmodulin like 37
54	AT3G10300	Calcium-binding EF-hand family protein
55	AT1G22280	PAPP2C__phytochrome-associated protein phosphatase type 2C
56	AT4G23190	AT-RLK3_CRK11__cysteine-rich RLK (RECEPTOR-like protein kinase) 11
57	AT3G54420	ATCHITIV_ATEP3_CHIV_EP3__homolog of carrot EP3-3 chitinase
58	AT5G25770	alpha/beta-Hydrolases superfamily protein
59	AT1G60190	AtPUB19_PUB19__ARM repeat superfamily protein
60	AT3G21870	CYCP2;1__cyclin p2;1
61	AT1G28190	
62	AT1G08940	Phosphoglycerate mutase family protein
63	AT1G05560	UGT1_UGT75B1__UDP-glucosyltransferase 75B1
64	AT2G30790	PSBP-2__photosystem II subunit P-2
65	AT1G17170	ATGSTU24_GST_GSTU24__glutathione S-transferase TAU 24
66	AT1G05575	
67	AT5G63450	CYP94B1__cytochrome P450, family 94, subfamily B, polypeptide 1
68	AT5G16970	AER_AT-AER__alkenal reductase
69	AT4G01870	tolB protein-related
70	**AT4G15610**	Uncharacterised protein family (UPF0497)
71	AT1G17180	ATGSTU25_GSTU25__glutathione S-transferase TAU 25
72	AT3G26910	hydroxyproline-rich glycoprotein family protein
73	AT2G22200	Integrase-type DNA-binding superfamily protein
74	AT1G22810	Integrase-type DNA-binding superfamily protein
75	AT3G26680	ATSNM1_SNM1__DNA repair metallo-beta-lactamase family protein
76	AT5G65300	
77	AT5G37490	ARM repeat superfamily protein
78	AT1G61610	S-locus lectin protein kinase family protein
79	AT5G15870	glycosyl hydrolase family 81 protein
80	AT5G25450	Cytochrome bd ubiquinol oxidase, 14kDa subunit
81	AT3G04000	NAD(P)-binding Rossmann-fold superfamily protein
82	AT5G39090	HXXXD-type acyl-transferase family protein
83	AT2G38360	PRA1.B4__prenylated RAB acceptor 1.B4
84	AT3G55970	ATJRG21_JRG21__jasmonate-regulated gene 21
85	AT4G15975	RING/U-box superfamily protein
86	AT5G66070	RING/U-box superfamily protein
87	AT5G39050	PMAT1__HXXXD-type acyl-transferase family protein
88	AT5G56100	glycine-rich protein / oleosin
89	AT5G64230	
90	AT5G26220	AtGGCT2;1_GGCT2;1__ChaC-like family protein
91	AT3G23880	F-box and associated interaction domains-containing protein
92	AT2G33830	AtDRM2_DRM2__Dormancy/auxin associated family protein
93	AT3G46110	Domain of unknown function (DUF966)
94	AT3G25610	ATPase E1-E2 type family protein / haloacid dehalogenase-like hydrolase family protein
95	AT5G64310	AGP1_ATAGP1__arabinogalactan protein 1
96	AT5G66650	Protein of unknown function (DUF607)
97	AT1G60740	Thioredoxin superfamily protein
98	AT1G07160	Protein phosphatase 2C family protein
99	**AT1G02850**	BGLU11__beta glucosidase 11
100	AT1G78450	SOUL heme-binding family protein
101	AT3G17611	ATRBL10_ATRBL14_RBL10_RBL14__RHOMBOID-like protein 14

Suppl. Table S5. *Late peroxisomal-dependent genes.*

	AGI ID	Annotation
1	AT3G44750	ATHD2A_HD2A_HDA3_HDT1__histone deacetylase 3
2	AT1G68765	IDA__Putative membrane lipoprotein
3	AT3G48520	CYP94B3__cytochrome P450, family 94, subfamily B, polypeptide 3
4	AT2G38180	SGNH hydrolase-type esterase superfamily protein
5	AT1G52890	ANAC019_NAC019__NAC domain containing protein 19
6	AT1G72520	ATLOX4_LOX4__PLAT/LH2 domain-containing lipoxygenase family protein
7	AT1G07890	APX1_ATAPX01_ATAPX1_CS1_MEE6__ascorbate peroxidase 1
8	AT4G30800	Nucleic acid-binding, OB-fold-like protein
9	AT1G17420	ATLOX3_LOX3__lipoxygenase 3
10	AT2G35980	ATNHL10_NHL10_YLS9__Late embryogenesis abundant (LEA) hydroxyproline-rich glycoprotein family
11	AT3G11340	UGT76B1__UDP-Glycosyltransferase superfamily protein
12	AT5G47220	ATERF-2_ATERF2_ERF2__ethylene responsive element binding factor 2
13	AT4G32800	Integrase-type DNA-binding superfamily protein
14	AT1G74430	ATMYB95_ATMYBCP66_MYB95__myb domain protein 95
15	AT4G28140	Integrase-type DNA-binding superfamily protein
16	AT1G70700	JAZ9_TIFY7__TIFY domain/Divergent CCT motif family protein
17	AT1G20510	OPCL1__OPC-8:0 CoA ligase1
18	AT1G44350	ILL6__IAA-leucine resistant (ILR)-like gene 6
19	AT5G57560	TCH4_XTH22__Xyloglucan endotransglucosylase/hydrolase family protein
20	AT1G79410	AtOCT5_OCT5__organic cation/carnitine transporter5
21	AT5G10760	Eukaryotic aspartyl protease family protein
22	AT1G19670	ATCLH1_ATHCOR1_CLH1_CORI1__chlorophyllase 1
23	AT4G15210	AT-BETA-AMY_ATBETA-AMY_BAM5_BMY1_RAM1__beta-amylase 5
24	AT2G43510	ATTI1_TI1__trypsin inhibitor protein 1
25	AT4G12490	Bifunctional inhibitor/lipid-transfer protein/seed storage 2S albumin superfamily protein
26	AT3G50970	LTI30_XERO2__dehydrin family protein
27	AT3G28210	PMZ_SAP12__zinc finger (AN1-like) family protein
28	AT2G23150	ATNRAMP3_NRAMP3__natural resistance-associated macrophage protein 3
29	AT1G26410	FAD-binding Berberine family protein
30	AT3G04720	AtPR4_HEL_PR-4_PR4__pathogenesis-related 4
31	AT2G38170	ATCAX1_CAX1_RCI4__cation exchanger 1
32	AT1G08830	CSD1__copper/zinc superoxide dismutase 1
33	AT4G31870	ATGPX7_GPX7__glutathione peroxidase 7
34	AT1G51780	ILL5__IAA-leucine resistant (ILR)-like gene 5
35	AT1G80840	ATWRKY40_WRKY40__WRKY DNA-binding protein 40
36	AT2G33380	AtCLO3_CLO-3_CLO3_RD20__Caleosin-related family protein
37	AT2G34600	JAZ7_TIFY5B__jasmonate-zim-domain protein 7
38	AT2G27690	CYP94C1__cytochrome P450, family 94, subfamily C, polypeptide 1
39	AT2G24850	TAT_TAT3__tyrosine aminotransferase 3
40	AT2G37770	AKR4C9_ChlAKR__NAD(P)-linked oxidoreductase superfamily protein
41	AT2G06050	AtOPR3_DDE1_OPR3__oxophytodienoate-reductase 3
42	AT2G37760	AKR4C8__NAD(P)-linked oxidoreductase superfamily protein
43	AT2G17840	ERD7__Senescence/dehydration-associated protein-related
44	AT3G22370	AOX1A_ATAOX1A_AtHSR3_HSR3__alternative oxidase 1A
45	AT2G37180	PIP2;3_PIP2C_RD28__Aquaporin-like superfamily protein
46	AT5G03630	ATMDAR2__Pyridine nucleotide-disulphide oxidoreductase family protein
47	AT1G20440	AtCOR47_COR47_RD17__cold-regulated 47
48	AT1G07400	HSP20-like chaperones superfamily protein
49	AT3G05660	AtRLP33_RLP33__receptor like protein 33
50	AT1G59860	HSP20-like chaperones superfamily protein
51	AT4G11600	ATGPX6_GPX6_LSC803_PHGPX__glutathione peroxidase 6
52	AT5G52640	ATHS83_ATHSP90.1_HSP81-1_HSP81.1_HSP83_HSP90.1__heat shock protein 90.1

53	AT1G73325	Kunitz family trypsin and protease inhibitor protein
54	AT1G26390	FAD-binding Berberine family protein
55	AT4G24350	Phosphorylase superfamily protein
56	AT1G48100	Pectin lyase-like superfamily protein
57	AT3G25180	CYP82G1__cytochrome P450, family 82, subfamily G, polypeptide 1
58	AT3G55920	Cyclophilin-like peptidyl-prolyl cis-trans isomerase family protein
59	AT2G29460	ATGSTU4_GST22_GSTU4__glutathione S-transferase tau 4
60	AT2G41380	S-adenosyl-L-methionine-dependent methyltransferases superfamily protein
61	AT4G15610	Uncharacterised protein family (UPF0497)
62	AT3G14990	AtDJ1A_DJ-1a_DJ1A__Class I glutamine amidotransferase-like superfamily protein
63	AT1G76520	PILS3__Auxin efflux carrier family protein
64	AT1G62570	FMO GS-OX4__flavin-monooxygenase glucosinolate S-oxygenase 4
65	AT2G15020	
66	AT2G29450	AT103-1A_ATGSTU1_ATGSTU5_GSTU5__glutathione S-transferase tau 5
67	AT1G24140	Matrixin family protein
68	AT2G04070	MATE efflux family protein
69	AT4G30270	MERI-5_MERI5B_SEN4_XTH24__xyloglucan endotransglucosylase/hydrolase 24
70	AT4G30110	ATHMA2_HMA2__heavy metal atpase 2
71	AT2G41190	Transmembrane amino acid transporter family protein
72	AT3G56200	Transmembrane amino acid transporter family protein
73	AT2G23170	GH3.3__Auxin-responsive GH3 family protein
74	AT1G21550	Calcium-binding EF-hand family protein
75	AT5G54300	Protein of unknown function (DUF761)
76	AT3G44860	FAMT__farnesoic acid carboxyl-O-methyltransferase
77	AT1G52720	
78	AT1G65500	
79	AT5G58570	
80	AT2G36970	UDP-Glycosyltransferase superfamily protein
81	AT4G12500	Bifunctional inhibitor/lipid-transfer protein/seed storage 2S albumin superfamily protein
82	AT1G57590	Pectinacetylesterase family protein
83	AT1G02850	BGLU11__beta glucosidase 11
84	AT1G51920	
85	AT1G26800	RING/U-box superfamily protein
86	AT1G21520	

Suppl. Table S6. *TFs for early and late peroxisomal-dependent genes.*

Early

Gene Set Name (NO. Genes)	Description	Category	NO. Genes in Overlap (k)	p-value	FDR
HY5_CONFIRMED (221)	Confirmed target genes of transcription factor: HY5	TF	8	1.48E-06	4.35E-05
HY5_CONFIRMED_AND_ UNCONFIRMED (260)	Confirmed and Unconfirmed target genes of transcription factor: HY5	TF	8	4.76E-06	6.97E-05
ATBHLH15_CONFIRMED _AND_UNCONFIRMED (749)	Confirmed and Unconfirmed target genes of transcription factor: AtbHLH15	TF	9	1.37E-03	0.0134
ATBHLH15_CONFIRMED (189)	Confirmed target genes of transcription factor: AtbHLH15	TF	4	4.77E-03	0.0349

Late

Gene Set Name (NO. Genes)	Description
HY5_CONFIRMED_AND_UNCONFIRMED (260)	Confirmed and Unconfirmed target genes of transcription factor: HY5
HY5_CONFIRMED (221)	Confirmed target genes of transcription factor: HY5

Suppl. Table S7. *StringDB analysis for early peroxisomal-dependent genes.*

Cluster color	Gene count	Protein name	Protein identifier
Red	18	CYP94B3	3702.AT3G48520.1
Red	18	JAZ7	3702.AT2G34600.1
Red	18	MYB95	3702.AT1G74430.1
Red	18	CYP94C1	3702.AT2G27690.1
Red	18	ERF2	3702.AT5G47220.1
Red	18	AT1G24140	3702.AT1G24140.1
Red	18	LOX3	3702.AT1G17420.1
Red	18	OPCL1	3702.AT1G20510.1
Red	18	CYP82G1	3702.AT3G25180.1
Red	18	TCH4	3702.AT5G57560.1
Red	18	LOX4	3702.AT1G72520.1
Red	18	TIFY7	3702.AT1G70700.1
Red	18	ILL5	3702.AT1G51780.1
Red	18	WRKY40	3702.AT1G80840.1
Red	18	OPR3	3702.AT2G06050.1
Red	18	FAMT	3702.AT3G44860.1
Red	18	ILL6	3702.AT1G44350.1
Red	18	PR4	3702.AT3G04720.1
Blue	6	AT1G59860	3702.AT1G59860.1
Blue	6	HSP90.1	3702.AT5G52640.1
Blue	6	AT1G07400	3702.AT1G07400.1
Blue	6	AT3G55920	3702.AT3G55920.1
Blue	6	AT1G21550	3702.AT1G21550.1
Blue	6	AT1G26800	3702.AT1G26800.1
Red	26	ERF11	3702.AT1G28370.1
Red	26	AT5G10695	3702.AT5G10695.1
Red	26	AT1G26380	3702.AT1G26380.1
Red	26	AT4G39670	3702.AT4G39670.1
Red	26	AT1G05575	3702.AT1G05575.1
Red	26	AT1G28190	3702.AT1G28190.1
Red	26	AT3G10300	3702.AT3G10300.3
Red	26	CRK36	3702.AT4G04490.1
Red	26	ERF13	3702.AT2G44840.1
Red	26	AT5G66650	3702.AT5G66650.1
Red	26	AT1G32920	3702.AT1G32920.1
Red	26	AT3G25610	3702.AT3G25610.1
Red	26	AT1G19020	3702.AT1G19020.1
Red	26	JAZ1	3702.AT1G19180.1
Red	26	At5g54490	3702.AT5G54490.1

Red	26	AT5G65300	3702.AT5G65300.1
Red	26	AT1G08940	3702.AT1G08940.1
Red	26	RHL41	3702.AT5G59820.1
Red	26	AGP1	3702.AT5G64310.1
Red	26	TCH3	3702.AT2G41100.1
Red	26	AT5G66070	3702.AT5G66070.2
Red	26	AT3G02840	3702.AT3G02840.1
Red	26	CML37	3702.AT5G42380.1
Red	26	SAG21	3702.AT4G02380.1
Red	26	AT1G57630	3702.AT1G57630.1
Red	26	dic-02	3702.AT4G24570.1
Light Green	13	HSFA2	3702.AT2G26150.1
Light Green	13	Hop3	3702.AT4G12400.2
Light Green	13	HSP17.6A	3702.AT5G12030.1
Light Green	13	RBL14	3702.AT3G17611.1
Light Green	13	BAG6	3702.AT2G46240.1
Light Green	13	AT1G07400	3702.AT1G07400.1
Light Green	13	HSFA7A	3702.AT3G51910.1
Light Green	13	PDX1.2	3702.AT3G16050.1
Light Green	13	Fes1A	3702.AT3G09350.1
Light Green	13	AT1G54050	3702.AT1G54050.1
Light Green	13	AT1G66080	3702.AT1G66080.1
Light Green	13	AT5G25450	3702.AT5G25450.1
Light Green	13	AT1G71000	3702.AT1G71000.1

Suppl. Table S8. *StringDB analysis for late peroxisomal-dependent genes.*

Cluster color	Gene count	Protein name	Protein identifier
Red	18	CYP94B3	3702.AT3G48520.1
Red	18	JAZ7	3702.AT2G34600.1
Red	18	MYB95	3702.AT1G74430.1
Red	18	CYP94C1	3702.AT2G27690.1
Red	18	ERF2	3702.AT5G47220.1
Red	18	AT1G24140	3702.AT1G24140.1
Red	18	LOX3	3702.AT1G17420.1
Red	18	OPCL1	3702.AT1G20510.1
Red	18	CYP82G1	3702.AT3G25180.1
Red	18	TCH4	3702.AT5G57560.1
Red	18	LOX4	3702.AT1G72520.1
Red	18	TIFY7	3702.AT1G70700.1
Red	18	ILL5	3702.AT1G51780.1
Red	18	WRKY40	3702.AT1G80840.1
Red	18	OPR3	3702.AT2G06050.1
Red	18	FAMT	3702.AT3G44860.1
Red	18	ILL6	3702.AT1G44350.1
Red	18	PR4	3702.AT3G04720.1
Blue	6	AT1G59860	3702.AT1G59860.1
Blue	6	HSP90.1	3702.AT5G52640.1
Blue	6	AT1G07400	3702.AT1G07400.1

Blue	6	AT3G55920	3702.AT3G55920.1
Blue	6	AT1G21550	3702.AT1G21550.1
Blue	6	AT1G26800	3702.AT1G26800.1
Medium Purple	4	APX1	3702.AT1G07890.1
Medium Purple	4	CSD1	3702.AT1G08830.1
Medium Purple	4	MDAR4	3702.AT3G27820.1
Medium Purple	4	AOX1A	3702.AT3G22370.1

Suppl. Table S9. *Common genes obtained in Fig. 7A (**in CD**)*

Suppl. Table S10. *KEGG pathways significantly represented in common genes obtained in Fig. 7A (**in CD**).*

Normed to Freq. in arabidopsis set (± *bootstrap StdDev*, p-value)

Biological process

3.19	*0.403*	**3.238e-13**	response to stress (Input set freq.: 0.42; 0.13)
2.85	*0.383*	**4.834e-09**	response to abiotic or biotic stimulus (Input set freq.: 0.33; 0.11)
2.54	*0.559*	**2.204e-04**	signal transduction (Input set freq.: 0.16; 0.06)
2.01	*0.316*	**2.488e-04**	other biological processes (Input set freq.: 0.24; 0.12)
1.59	*0.438*	**0.031**	transcription,DNA-dependent (Input set freq.: 0.12; 0.08)
1.31	*0.742*	0.256	electron transport or energy pathways (Input set freq.: 0.01; 0.01)
1.24	*0.121*	**6.673e-03**	other cellular processes (Input set freq.: 0.56; 0.45)
1.13	*0.114*	**0.042**	other metabolic processes (Input set freq.: 0.48; 0.42)
1.12	*0.303*	0.111	developmental processes (Input set freq.: 0.11; 0.1)
0.91	*0.701*	0.369	pollination (Input set freq.: 0; 0.01)
0.83	*0.222*	0.086	protein metabolism (Input set freq.: 0.13; 0.16)
0.76	*0.231*	0.101	cell organization and biogenesis (Input set freq.: 0.07; 0.1)
0.68	*0.243*	0.099	transport (Input set freq.: 0.05; 0.08)
0.47	*0.386*	0.254	DNA or RNA metabolism (Input set freq.: 0; 0.02)
0.38	*0.108*	**1.020e-04**	unknown biological processes (Input set freq.: 0.08; 0.23)

Molecular function

1.67	*0.574*	**0.039**	transcription factor activity (Input set freq.: 0.09; 0.05)
1.66	*0.273*	**2.238e-03**	protein binding (Input set freq.: 0.26; 0.16)
1.59	*0.193*	**1.714e-03**	other enzyme activity (Input set freq.: 0.31; 0.19)
1.32	*0.203*	**0.014**	other binding (Input set freq.: 0.34; 0.26)
1.3	*0.283*	0.052	transferase activity (Input set freq.: 0.17; 0.13)
1.14	*0.485*	0.156	kinase activity (Input set freq.: 0.05; 0.05)
1.08	*0.277*	0.112	hydrolase activity (Input set freq.: 0.12; 0.11)
1	*0.517*	0.200	nucleic acid binding (Input set freq.: 0.03; 0.03)
0.97	*0.392*	0.180	transporter activity (Input set freq.: 0.04; 0.05)
0.88	*0.304*	0.129	nucleotide binding (Input set freq.: 0.08; 0.1)
0.79	*0.232*	0.082	DNA or RNA binding (Input set freq.: 0.11; 0.14)
0.65	*0.439*	0.222	other molecular functions (Input set freq.: 0.01; 0.03)
0.49	*0.123*	**1.109e-03**	unknown molecular functions (Input set freq.: 0.11; 0.23)

Cellular component

1.59	*0.387*	**0.031**	cytosol (Input set freq.: 0.12; 0.08)
1.47	*0.159*	**9.560e-04**	other cytoplasmic components (Input set freq.: 0.43; 0.29)
1.4	*0.307*	**0.034**	plasma membrane (Input set freq.: 0.17; 0.12)
1.21	*0.137*	**0.021**	nucleus (Input set freq.: 0.44; 0.36)
1.15	*0.473*	0.171	Golgi apparatus (Input set freq.: 0.04; 0.04)
1.15	*0.239*	0.072	chloroplast (Input set freq.: 0.21; 0.18)
1.09	*0.642*	0.225	cell wall (Input set freq.: 0.02; 0.02)
1.08	*0.493*	0.197	ER (Input set freq.: 0.03; 0.03)
1.05	*0.177*	0.087	other membranes (Input set freq.: 0.25; 0.24)
0.79	*0.193*	0.082	mitochondria (Input set freq.: 0.11; 0.14)
0.74	*0.126*	**0.032**	other intracellular components (Input set freq.: 0.18; 0.25)
0.68	*0.499*	0.341	cytoskeleton (Input set freq.: 0; 0.01)
0.66	*0.292*	0.131	other cellular components (Input set freq.: 0.03; 0.05)
0.6	*0.228*	**0.049**	extracellular (Input set freq.: 0.06; 0.11)
0.17	*0.16*	**0.016**	plastid (Input set freq.: 0; 0.05)
0.14	*0.115*	**6.821e-03**	unknown cellular components (Input set freq.: 0; 0.06)

Absolute values (± *bootstrap StdDev*, p-value)

Biological process

57	*5.4*	**6.673e-03**	other cellular processes (nr. in set: 13044)
49	*4.9*	**0.042**	other metabolic processes (nr. in set: 12333)
43	*5.3*	**3.238e-13**	response to stress (nr. in set: 3826)
34	*4.5*	**4.834e-09**	response to abiotic or biotic stimulus (nr. in set: 3387)
25	*3.8*	**2.488e-04**	other biological processes (nr. in set: 3525)
17	*3.6*	**2.204e-04**	signal transduction (nr. in set: 1901)
14	*3.7*	0.086	protein metabolism (nr. in set: 4771)
13	*3.5*	**0.031**	transcription,DNA-dependent (nr. in set: 2322)
12	*3.1*	0.111	developmental processes (nr. in set: 3034)
9	*2.5*	**1.020e-04**	unknown biological processes (nr. in set: 6705)
8	*2.4*	0.101	cell organization and biogenesis (nr. in set: 2994)
6	*2*	0.099	transport (nr. in set: 2482)
2	*1.1*	0.256	electron transport or energy pathways (nr. in set: 433)
1	*0.8*	0.254	DNA or RNA metabolism (nr. in set: 604)
1	*0.7*	0.369	pollination (nr. in set: 312)

Molecular function

35	*5.3*	**0.014**	other binding (nr. in set: 7504)
32	*3.8*	**1.714e-03**	other enzyme activity (nr. in set: 5724)
27	*4.3*	**2.238e-03**	protein binding (nr. in set: 4623)
18	*3.8*	0.052	transferase activity (nr. in set: 3923)
13	*3.2*	0.112	hydrolase activity (nr. in set: 3405)
12	*3.4*	0.082	DNA or RNA binding (nr. in set: 4293)
12	*2.9*	**1.109e-03**	unknown molecular functions (nr. in set: 6879)
10	*3.3*	**0.039**	transcription factor activity (nr. in set: 1699)
9	*3*	0.129	nucleotide binding (nr. in set: 2879)
6	*2.5*	0.156	kinase activity (nr. in set: 1486)
5	*1.9*	0.180	transporter activity (nr. in set: 1458)
4	*2*	0.200	nucleic acid binding (nr. in set: 1137)
2	*1.3*	0.222	other molecular functions (nr. in set: 865)

Cellular component

45	*5*	**0.021**	nucleus (nr. in set: 10525)
44	*4.7*	**9.560e-04**	other cytoplasmic components (nr. in set: 8504)
26	*4.3*	0.087	other membranes (nr. in set: 7037)
22	*4.4*	0.072	chloroplast (nr. in set: 5407)
19	*3.1*	**0.032**	other intracellular components (nr. in set: 7235)
18	*3.8*	**0.034**	plasma membrane (nr. in set: 3639)
13	*3.1*	**0.031**	cytosol (nr. in set: 2321)
12	*2.9*	0.082	mitochondria (nr. in set: 4298)
7	*2.6*	**0.049**	extracellular (nr. in set: 3278)
5	*2*	0.171	Golgi apparatus (nr. in set: 1235)
4	*1.7*	0.131	other cellular components (nr. in set: 1724)
4	*1.8*	0.197	ER (nr. in set: 1051)
3	*1.7*	0.225	cell wall (nr. in set: 780)
1	*0.7*	0.341	cytoskeleton (nr. in set: 414)
1	*0.9*	**0.016**	plastid (nr. in set: 1640)
1	*0.7*	**6.821e-03**	unknown cellular components (nr. in set: 1912)

Suppl. Fig. S1. Enrichment analysis for early peroxisomal-dependent genes. *Significantly over-represented categories obtained by BAR website (http://bar.utoronto.ca/ntools/cgi-bin/).*

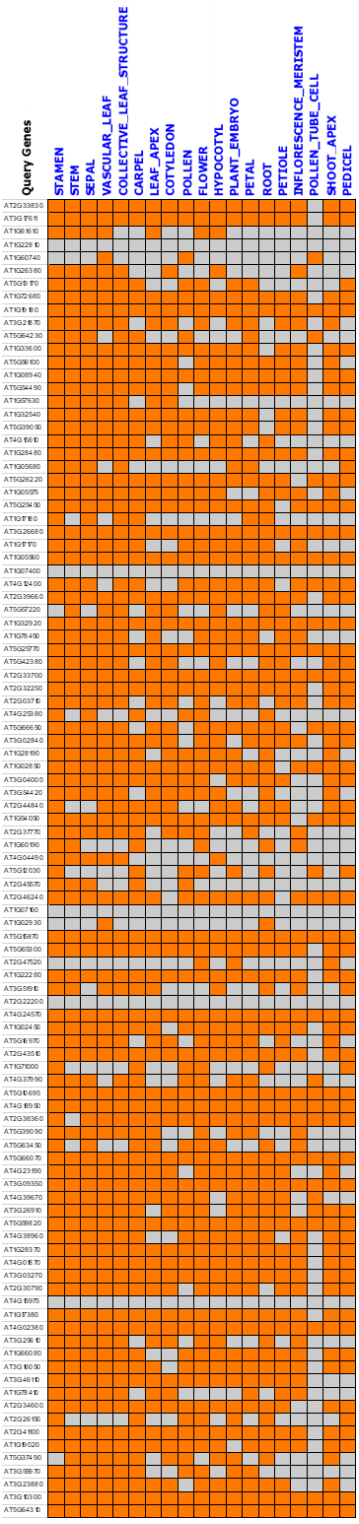

Suppl. Fig. S2. *Plant Ontology analysis for early peroxisomal-dependent genes.*

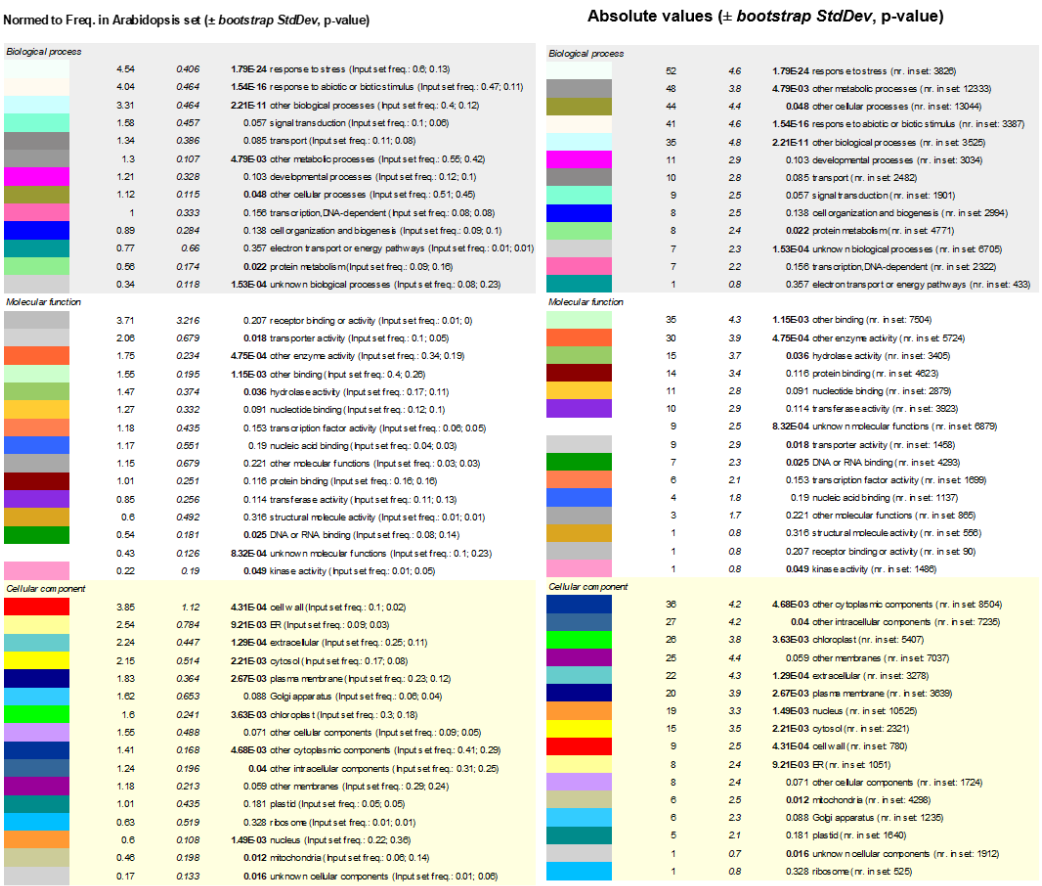

Suppl. Fig. S3. Enrichment analysis for late peroxisomal-dependent genes. *Significantly over-represented categories obtained by BAR website (http://bar.utoronto.ca/ntools/cgi-bin/).*

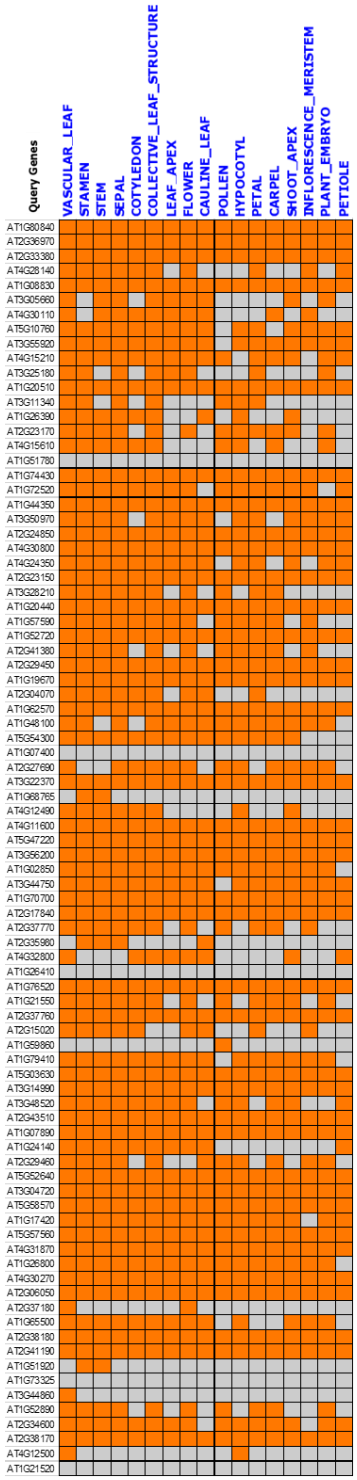

Suppl. Fig. S4. *Plant Ontology analysis for early peroxisomal-dependent genes.*

6. REFERENCES

Andronis, E. A., Moschou, P. N., Toumi, I., and Roubelakis-Angelakis, K. A. (2014). Peroxisomal polyamine oxidase and NADPH-oxidase cross-talk for ROS homeostasis which affects respiration rate in *Arabidopsis thaliana*. Front. Plant Sci. 5: 1–10.

Angelos, E., Ruberti, C., Kim, S.J., and Brandizzi, F. (2017). Maintaining the factory: The roles of the unfolded protein response in cellular homeostasis in plants. Plant J. 90: 671–682.

Beaugelin, I., Chevalier, A., D'Alessandro, S., Ksas, B., and Havaux, M. (2020). Endoplasmic reticulum-mediated unfolded protein response is an integral part of singlet oxygen signalling in plants. Plant J. 102: 1266–1280.

Castillo, M.C., Martínez, C., Buchala, A., Métraux, J.P., and León, J. (2004). Gene-specific involvement of β-oxidation in wound-activated responses in Arabidopsis. Plant Physiol. 135: 85–94.

Castillo, M.C., Sandalio, L.M., del Río, L.A. and León, J. (2008), Peroxisome proliferation, wound-activated responses and expression of peroxisome-associated genes are cross-regulated but uncoupled in *Arabidopsis thaliana*. Plant, Cell and Environ. 31: 492-505.

Catalá, R., Medina, J., and Salinas, J. (2011). Integration of low temperature and light signalling during cold acclimation response in Arabidopsis. Proc. Natl. Acad. Sci. U.S.A. 108: 16475–16480.

Chaouch, S., Queval, G., Vanderauwera, S., Mhamdi, A., Vandorpe, M., Langlois-Meurinne, M., Van Breusegem, F., Saindrenan, P., and Noctor, G. (2010). Peroxisomal hydrogen peroxide is coupled to biotic defense responses by ISOCHORISMATE SYNTHASE1 in a daylength-related manner. Plant Physiol. 153: 1692–1705.

Chaouch, S., Queval, G., and Noctor, G. (2012). AtRbohF is a crucial modulator of defence-associated metabolism and a key actor in the interplay between intracellular oxidative stress and pathogenesis responses in Arabidopsis. Plant J. 69: 613–27.

Chen, D., Xu, G., Tang, W., Jing, Y., Ji, Q., Fei, Z., and Lin, R. (2013). Antagonistic basic helix-loop-helix/bZIP transcription factors form transcriptional modules that integrate light and reactive oxygen species signalling in Arabidopsis. Plant Cell. 25: 1657–1673.

Chomczynski, P., and Sacchi, N. (1987). Single step method of RNA isolation by acid guanidinium thiocyanate-phenol-chloroform extraction. Anal. Biochem. 162: 156–159.

Cross, L.L., Ebeed, H.T., and Baker, A. (2016). Peroxisome biogenesis, protein targeting mechanisms and PEX gene functions in plants. Biochim. Biophys. Acta. Mol. Cell. Res. 1863: 850–862.

De Clercq, I., Vermeirssen, V., Van Aken, O., Vandepoele, K., Murcha, M.W., Law, S.R., Inzé, A., Ng, S., Ivanova, A., Rombaut, D., van de Cotte, B., Jaspers, P., Van der Peer, Y., Kangasjärvi, J., Whelan, J., and Van Breusegem, F. (2013). The membrane-bound NAC transcription factor ANAC013 functions in mitochondrial retrograde regulation of the oxidative stress response in Arabidopsis. Plant Cell. 25: 3472–3490.

Di Donato, M., and Geisler, M. (2019). HSP90 and co-chaperones: a multitaskers' view on plant hormone biology. FEBS Lett. 593: 1415–1430.

Gabaldón, T. (2018). Evolution of the peroxisomal proteome. In: del Río, L.A. and Schrader, M., ed. Proteomics of peroxisomes. Identifying novel functions and regulatory networks. Subcellular Biochemistry, 89. Springer, Germany. pp. 221–233.

Gechev, T.S., Minkov, I.N., and Hille, J. (2005). Hydrogen peroxide-induced cell death in Arabidopsis: Transcriptional and mutant analysis reveals a role of an oxoglutarate-dependent dioxygenase gene in the cell death process. IUBMB Life. 57: 181–188.

Ghorbel, M., Brini, F., Sharma, A., and Landi, M. (2021). Role of jasmonic acid in plants: The molecular point of view. Plant Cell Rep. 40: 1471–1494.

Giraud, E., Ho, L.H., Clifton, R., Carroll, A., Estavillo, G., Tan, Y.F., Howell, K.A., Ivanova, A., Pogson, B.J., Millar, A.H., Whelan, J. (2008). The absence of ALTERNATIVE OXIDASE1a in Arabidopsis results in acute sensitivity to combined light and drought stress. Plant Physiol. 147: 595–610.

Gupta, D.K., Pena, L.B., Romero-Puertas, M.C., Hernández, A., Inouhe, M., and Sandalio L.M. (2017). NADPH oxidases differentially regulate ROS metabolism and nutrient uptake under cadmium toxicity. Plant, Cell and Environ. 40: 509–526.

Huang, S., Aken, O.V., Schwarzländer, M., Belt, K., and Millar, A.H. (2016). The roles of mitochondrial reactive oxygen species in cellular signalling and stress response in plants. Plant Physiol. 171: 1551–1559.

Kao, Y.T., Gonzalez, K.L., and Bartel, B. (2018). Peroxisome function, biogenesis, and dynamics in plants. Plant Physiol. 176: 162–177.

Kaur, N., Li, J., and Hu, J. (2013). Peroxisomes and photomorphogenesis. In: del Río L.A. ed. Peroxisomes and their key role in cellular signalling and metabolism. Subcellular Biochemistry, 69. Springer, Dordrecht. pp. 195–211.

Kerchev, P., Waszczak, C., Lewandowska, A., Willems, P., Shapiguzov, A., Li, Z., Alseekh, S., Mühlenbock, P., Hoebrichts, F., Huang, J. J., Van der Kelen, K., Kangasjärvi, J., Fernie, A.R., De Smet, R., Van de Peer, Y., Messens, J., and Van Breusegem, F. (2016). Lack of GLYCOLATE OXIDASE1, but not GLYCOLATE OXIDASE2, attenuates the photorespiratory phenotype of CATALASE2-deficient Arabidopsis. Plant Physiol, 171: 1704–1719.

Kleine, T., and Leister, D. (2016). Retrograde signalling: Organelles go networking. Biochim. Biophys. Acta, Bioenerg. 1857:1313-1325.

Lau, O.S., and Deng, X.W. (2010). Plant hormone signalling lightens up: Integrators of light and hormones. Curr. Opin. Plant Biol. 13: 571–577.

Law, S.R., Narsai, R., and Whelan, J. (2014). Mitochondrial biogenesis in plants during seed germination. Mitochondrion. 19: 214–221.

Liu, J.X., and Howell, S.H. (2010). Endoplasmic reticulum protein quality control and its relationship to environmental stress responses in plants. Plant Cell. 22: 2930–2942.

Mhamdi, A., Hager, J., Chaouch, S., Queval, G., Han, Y., Taconnat, L., Saindrenan, P., Gouia, H., Issakidis-Bourguet, E., Renou, J.P., and Noctor, G. (2010). Arabidopsis GLUTATHIONE REDUCTASE1 plays a crucial role in leaf responses to intracellular hydrogen peroxide and in ensuring appropriate gene expression through both salicylic acid and jasmonic acid signalling pathways. Plant Physiol. 153: 1144–1160.

Murashige, T., and Skoog, F. (1962). A revised medium for rapid growth and bio assays with tobacco tissue cultures. Physiol. Plant. 15: 473–497.

Ng, S., De Clercq, I., Van Aken, O., Law, S.R., Ivanova, A., Willems, P., Giraud, E., Van Breusegem, F., and Whelan, J. (2014). Anterograde and retrograde regulation of nuclear genes encoding mitochondrial proteins during growth, development, and stress. Mol. Plant. 7: 1075–1093.

Orth, T., Reumann, S., Zhang, X., Fan, J., Wenzel, D., Quan, S., and Hu, J. (2007). The PEROXIN11 protein family controls peroxisome proliferation in Arabidopsis. Plant Cell. 19: 333–350.

Pfaffl, M. W. (2001). A new mathematical model for relative quantification in real-time RT-PCR. Nucleic Acids Res. 29: 2002–2007.

Queval, G., Issakidis-Bourguet, E., Hoeberichts, F.A., Vandorpe, M., Gakière, B., Vanacker, H., Miginiac-Maslow, M., Van Breusegem, F., and Noctor, G. (2007). Conditional oxidative stress responses in the Arabidopsis photorespiratory mutant *cat2* demonstrate that redox state is a key modulator of daylength-dependent gene expression, and define photoperiod as a crucial factor in the regulation of H_2O_2-induced cell death. Plant J. 52: 640–657.

Queval, G., Neukermans, J., Vanderauwera, S., Van Breusegem, F., and Noctor, G. (2012). Day length is a key regulator of transcriptomic responses to both CO_2 and H_2O_2 in Arabidopsis. Plant, Cell and Environ. 35: 374–387.

Reumann, S., and Bartel, B. (2016). Plant peroxisomes: Recent discoveries in functional complexity, organelle homeostasis, and morphological dynamics. Curr. Opin. Plant Biol. 34: 17–26.

Rodríguez-Serrano, M., Romero-Puertas, M.C., Zabalza, A., Corpas, F.J., Gómez, M., del Río, L.A. and Sandalio, L.M. (2006). Cadmium effect on oxidative metabolism of pea (*Pisum sativum* L.) roots. Imaging of reactive oxygen species and nitric oxide accumulation in vivo. Plant, Cell and Environ. 29: 1532–1544.

Rodríguez-Serrano, M., Romero-Puertas, M.C., Sanz-Fernández, M., Hu, J., and Sandalio, L.M. (2016). Peroxisomes extend peroxules in a fast response to stress via a reactive oxygen species-mediated induction of the peroxin PEX11a. Plant Physiol. 171: 1665–1674.

Romero-Puertas M.C., Peláez-Vico M.A., Pazmiño D.M., Rodríguez-Serrano M., Terrón-Camero L.C., Bautista R., Gómez-Cadena A., Claros M.G., León J., Sandalio L.M. (2021). Insights into ROS-dependent signalling underlying transcriptomic plant responses to the herbicide 2,4-D. Accepted in Plant, Cell and Environment

Rosenwasser, S., Fluhr, R., Joshi, J.R., Leviatan, N., Sela, N., Hetzroni, A., and Friedman, H. (2013). ROSMETER: A bioinformatic tool for the identification of transcriptomic imprints related to reactive oxygen species type and origin provides new insights into stress responses. Plant Physiol. 163: 1071–1083.

Sandalio, L.M., and Romero-Puertas, M.C. (2015). Peroxisomes sense and respond to environmental cues by regulating ROS and RNS signalling networks. Ann. Bot. (Oxford, U.K.). 116: 475–485.

Sandalio, L.M., Peláez-Vico, M.A., Molina-Moya, E., and Romero-Puertas, M.C. (2021). Peroxisomes as redox-signalling nodes in intracellular communication and stress responses. Plant Physiol. 186: 22–35.

Sewelam, N., Jaspert, N., Van Der Kelen, K., Tognetti, V.B., Schmitz, J., Frerigmann, H., Stahl, E., Zeier, J., Van Breusegem, F., and Maurino, V.G. (2014). Spatial H_2O_2 signalling specificity: H_2O_2 from chloroplasts and peroxisomes modulates the plant transcriptome differentially. Mol. Plant. 7: 1191–1210.

Shen, H., Moon, J., and Huq, E. (2005). PIF1 is regulated by light-mediated degradation through the ubiquitin-26S proteasome pathway to optimize photomorphogenesis of seedlings in Arabidopsis. Plant J. 44: 1023–1035.

Stephenson, P.G., Fankhauser, C., and Terry, M.J. (2009). PIF3 is a repressor of chloroplast development. Proc. Natl. Acad. Sci. U.S.A. 106: 7654–7659.

Su, T., Wang, P., Li, H., Zhao, Y., Lu, Y., Dai, P., Ren, T., Wang, X., Li, X., Shao, Q., Zhao, D., Zhao, Y., and Ma, C. (2018). The Arabidopsis catalase triple mutant reveals important roles of catalases and peroxisome-derived signalling in plant development. J. Integr. Plant Biol. 60: 591–607.

Su, T., Li, W., Wang, P., and Ma, C. (2019). Dynamics of peroxisome homeostasis and its role in stress response and signalling in plants. Front. Plant Sci. 10: 1–14.

Sun, X., Feng, P., Xu, X., Guo, H., Ma, J., Chi, W., Lin, R., Lu, C., and Zhang, L. (2011). A chloroplast envelope-bound PHD transcription factor mediates chloroplast signals to the nucleus. Nat. Commun. 2: 1–10.

Takahashi, H., Chen, Z., Du, H., Liu, Y., and Klessig, D.F. (1997). Development of necrosis and activation of disease resistance in transgenic tobacco plants with severely reduced catalase levels. Plant J. 11: 993–1005.

Ulm, R., Baumann, A., Oravecz, A., Máté, Z., Adám, E., Oakeley, E.J., Schäfer E., and Nagy, F. (2004). Genome-wide analysis of gene expression reveals function of the bZIP transcription factor HY5 in the UV-B response of Arabidopsis. Proc. Natl. Acad. Sci. U.S.A. 101: 1397–1402.

Vanderauwera, S., Zimmermann, P., Rombauts, S., Vandenabeele, S., Langebartels, C., Gruissem, W., Inzé, D., and Van Breusegem, F. (2005). Genome-wide analysis of hydrogen peroxide-regulated gene expression in Arabidopsis reveals a high light-induced transcriptional cluster involved in anthocyanin biosynthesis. Plant Physiol. 139: 806–821.

Vitale, A., and Boston, R.S. (2008). Endoplasmic reticulum quality control and the unfolded protein response: Insights from plants. Traffic. 9: 1581–1588.

Wagner, S., Van Aken, O., Elsässer, M., and Schwarzländer, M. (2018). Mitochondrial energy signalling and its role in the low-oxygen stress response of plants. Plant Physiol. 176: 1156–1170.

Waszczak, C., Kerchev, P.I., Mühlenbock, P., Hoeberichts, F.A., Van Der Kelen, K., Mhamdi, A., Willems, P., Denecker, J., Kumpf, R.P., Noctor, G., Messens, J., and Van Breusegem, F. (2016). SHORT-ROOT deficiency alleviates the cell death phenotype of the *Arabidopsis catalase2* mutant under photorespiration-promoting conditions. Plant Cell. 28:1844–1859.

Willems, P., Mhamdi, A., Stael, S., Storme, V., Kerchev, P., Noctor, G., Gevaert, K., and Van Breusegem, F. (2016). The ROS wheel: Refining ROS transcriptional footprints. Plant physiol, 171: 1720–1733.

Wu, G.Z., and Bock, R. (2021). GUN control in retrograde signalling: How GENOMES UNCOUPLED proteins adjust nuclear gene expression to plastid biogenesis. Plant Cell. 33: 457–474.

Yi, X., Du, Z., and Su, Z. (2013). PlantGSEA: A gene set enrichment analysis toolkit for plant community. Nucleic Acids Res. 41: 98–103.

Yu, X.Z., Chu, Y.P., Zhang, H., Lin, Y.J., and Tian, P. (2021). Jasmonic acid and hydrogen sulfide modulate transcriptional and enzymatic changes of plasma membrane NADPH oxidases (NOXs) and decrease oxidative damage in *Oryza sativa* L. during thiocyanate exposure. Ecotoxicology. 30: 1511–1520.

Zandalinas, S.I., Sengupta, S., Fritschi, F.B., Azad, R.K., Nechushtai, R. and Mittler, R. (2021). The impact of multifactorial stress combination on plant growth and survival. New Phytol. 230: 1034–1048.

Chapter 3

Generation and characterization of Arabidopsis mutants altered in peroxin 11a *(PEX11a)* gene.

Peláez-Vico, M. A., Molina-Moya, E., Collado-Arenal, A. M., Dagdas, Y., Sandalio, L. M., Romero-Puertas, M. C.

Generation and characterization of *Arabidopsis* mutants altered in peroxin 11a *(PEX11a)* gene

Mª Ángeles Peláez-Vico[1], Eliana Molina-Moya[1], Aurelio M. Collado-Arenal[1], Yasin Dagdas[2], Luisa M. Sandalio[1], María C. Romero-Puertas[1]

[1]*Departamento de Bioquímica, Biología Celular y Molecular de Plantas, Estación Experimental del Zaidín, CSIC, Profesor Albareda 1, E-18008 Granada, Spain*
[2]*Gregor Mendel Institute of Molecular Plant Biology, Dr.-Bohr-Gasse 3, 1030 Vienna, Austria*

Running title: PEX11a role in plant physiology

ABSTRACT

Peroxisomes have a key role in a wide range of cell metabolism and in the perception of and responses to changes in plant environment. Highly dynamic plasticity enables peroxisomes to adapt their morphology, number and movement to changes in their surroundings. Peroxisome proliferation after ROS application or in response to abiotic stress conditions appears to be regulated by specific *PEX11* genes. In particular, *PEX11a* have been shown to be essential for peroxules production, a very dynamic extensions produced by peroxisomes regulated by ROS and NO. Functionality of PEX11a and therefore, of peroxules, however is not well known. In this work, we have used different *in silico* analysis to get a deeper insight into PEX11a expression, regulation and putative posttranslational modifications of the protein. Furthermore, we have generated mutant lines by CRISPR/Cas9 altering *PEX11a* gene *(pex11a-CR)* and double mutants with a T-DNA insertion in *PEX11a* locus and with a CFP located in peroxisomes *(pex11a-SKI x px-ck)*. We have characterized mutants obtained under control conditions and in plant response to Cd stress.

Key words: *Arabidopsis thaliana*, Cd, peroxisomes, proliferation, peroxules, ROS.

1. INTRODUCTION

Peroxisomes are highly dynamic, metabolically active organelles, which play a key role in many aspects of plant development and acclimation to stress conditions. These organelles are also an important source of ROS and RNS being able to sense ROS/redox changes in the cell and then orchestrate a rapid and specific response (Romero-Puertas *et al.*, 2021; **annex II**). When plants suffer a stress, the number of peroxisomes may increase through a complex process called proliferation, including elongation of the peroxisome, membrane constriction and fission (Schrader *et al.*, 2016; Jansen *et al.*, 2021). Peroxisome proliferation has been observed in response to several abiotic stresses such as, ozone (Oksanen *et al.*, 2004), clofibrate (Nila *et al.*, 2006; Castillo *et al.*, 2008), far red light (Desai and Hu, 2008), salinity (Mitsuya *et al.*, 2010), drought (Ebeed *et al.*, 2018), ABA (Ebeed *et al.*, 2018), Cd (Romero-Puertas *et al.*, 1999; Rodríguez-Serrano *et al.*, 2016), hypoxia (Li and Hu, 2015) and senescence (Pastori and Del Río, 1997). Peroxisome proliferation involves elongation, regulated by peroxin 11 (PEX11) and further constriction and fission, mediated by dynamin-related proteins (DRP3A and DRP3B) and fission protein (FIS1A and FIS1B; Pan *et al.*, 2019; **annex I**).

PEX11 family proteins are peroxisomal membrane proteins, which participate in the enlargement and elongation steps during proliferation (Lingard and Trelease, 2006; Orth *et al.*, 2007; Terrón-Camero *et al.*, 2020; **annex I**). PEX11 family in *Arabidopsis thaliana* is composed of five members (PEX11a-e), which can be divided into three clades based on sequence homology: PEX11a, PEX11b, and PEX11c-e (Lingard and Trelease, 2006; Orth *et al.,* 2007). *PEX11a* is expressed at a constitutively low level in all tissues, while *PEX11d* and *PEX11e* are highly expressed in leaf and seed tissue, respectively. *PEX11b* expression is mainly located in cauline leaves (Orth *et al.,* 2007). Despite its conserved role in diverse species, the biochemical function of PEX11 remains elusive. Studies using Arabidopsis RNAi mutants by Orth et al. (2007) suggested that AtPEX11 protein functions are at least partially redundant, because plants with complete or strong silencing of individual *PEX11* genes showed partial reduction in peroxisome number. Plant cells where *PEX11c*, *PEX11d*, and *PEX11e* were silenced simultaneously, showed peroxisomes enlarged, but not elongated, which suggest that this clade of *PEX11* can act in peroxisome growth, but not in the elongation process (Lingard *et al.*, 2008). Ectopic expression of *PEX11* from different origin (plants and yeast) in human cells have

demonstrated an evolutionary conserved mechanism of PEX11 targeting to peroxisomes (Koch *et al.*, 2010).

In addition to proliferate, peroxisomes have the ability to produce dynamic and retractable prolongations called peroxules, which may progress over time with peroxisome elongation and proliferation. In particular, in response to Cd and As it has been described that peroxules production depends on *PEX11a* and is regulated by ROS-dependent signalling network (Rodríguez-Serrano *et al.*, 2016) as well as by NO (Terrón-Camero *et al.*, 2020).

Since PEX11a function is far to be well known, in this study we have examined different mutants altered in *PEX11a* gene, generated by using different technologies in order to gain a deeper understanding into the role of this gene in peroxisomal dynamic and function in plant physiology and in plant response to stress.

2. MATERIALS AND METHODS

2.1. Plant material

All Arabidopsis seeds used in this study were in Col-0 background. Lines used in this work are listened in **Table 1.**

Table 1. *Plant lines used in this work. NASC (Nottingham Arabidopsis Stock Center).*

Line	*Characteristics*	*Supplied by/author*
px-ck	*Line expressing peroxisome-targeted cyan fluorescent protein CFP*	*Nelson et al., 2007 (NASC)*
pex11a-CR9	*Mutant of the PEX11a gene originated by CRISPR/Cas9 technology (px-ck background; C inserted)*	*This work*
pex11a-CR10	*Mutant of the PEX11a gene originated by CRISPR/Cas9 technology (px-ck background; T inserted)*	*This work*
pex11a SK-I	*T-DNA insertion in PEX11a locus mutant (SALK_038574C)*	*NASC*
pex11a SK-II	*T-DNA insertion in PEX11a locus mutant (SALK_006177C)*	*NASC*
pex11a SK-I x px-ck	*T-DNA insertion mutant (SALK_038574C) with peroxisome-targeted (CFP protein) generated by cross fertilization*	*This work*
pPEX11a::GUS 2.4	*Line containing a fragment (1.8 kb) of PEX11a promoter fused to the β-glucuronidase gene in pMDC163 vector (Col-0 background, line 2.4)*	*This work*
pPEX11a::GUS 12.3	*Line containing a fragment (1.8 kb) of PEX11a promoter fused to the β-glucuronidase gene in pMDC163 vector (Col-0 background, line 12.3)*	*This work*

pPEX11a::GUS Ø	*Line containing the empty vector pMDC163 carrying the β-glucuronidase gene*	*This work*
px-ck x mt-yk	*Line expressing peroxisome-targeted cyan fluorescent protein CFP and mitochondrial-targeted yellow protein YFP*	*Rodríguez-Serrano et al., 2014*

2.1.1. Growth in soil

To obtain seeds and for phenotype characterization, different Arabidopsis lines were sown in soil with universal substrate (Compo-Sana) and vermiculite in a 2:1 ratio (substrate: vermiculite). Subsequently, pots were transferred to a growth chamber at 22 °C with photoperiod of 16 h light/8 h dark (long day) or 8 h light/16 h dark (short day) with a light intensity of 120-150 µmol m^{-2} s^{-1} and a relative humidity of 50-60 %. After complete life cycle of the plant, seeds were collected and stored at 4 °C.

2.1.2. In vitro growth cultivation

Arabidopsis seeds were surface disinfected with 70 % ethanol for 2 min. Then, seeds were incubated in a solution containing 50 % sodium hypochlorite for 10 min and finally washed three times with sterilized deionized distilled H_2O (ddH_2O). Subsequently, seeds were stratified in the dark at 4 °C for two days and plated onto 10 cm^2 square plate dishes containing semisolid medium. Murashige and Skoog Medium (MS; Murashige and Skoog, 1962) was used for in vitro experiments. MS medium (0.5 x) contained 2.2 g/l MS (Sigma-Aldrich) including vitamins, 30 g/l sucrose, 8 g/l phytoagar for plates and pH was adjusted to 5.7 with KOH. Media were autoclaved for 20 min at 121 °C and 1 atmosphere of pressure. Arabidopsis seedlings were grown in a growth chamber (Sanyo MLR-351-H, Sanyo, Japan) under control conditions, 20/22 ºC with a long day conditions, 16h/8h day/night photoperiod, light intensity of 100 µmol m^{-2} s^{-1} and 60-65 % relative humidity.

2.2. Confocal microscopy analysis

Arabidopsis leaves were sliced and mounted between a slide and a coverslip in PBS/glycerol (30: 70 %) and the abaxial sections were examined using a confocal laser scanning microscope (TCS SP5 Leica Microsystems, Wetzlar, Germany). At least six confocal images were collected from one leaf of each plant, with at least three plants being used per experiment. At least four experiments were carried out, which means that

thousands of peroxisomes were examined. Peroxisomes were detected by imaging CFP (blue; excitation at 439 nm, emission at 476 nm), chloroplasts were imaged by their autofluorescence (red; excitation at 633 nm, emission at 680 nm) and mitochondria was imaged by YFP fluorescence (yellow, excitation at 508 nm, emission at 524 nm). Images of peroxules formation were acquired in x, y, and t dimensions, and the number of peroxisomes was analyzed using Image J software.

2.3. Generation of *pex11a SK-I x px-ck* mutants by cross fertilization

To obtain double mutants *pex11a SK-I x px-ck*, the mutant line *pex11a* with a T-DNA insertion in At1g47750 locus, and *px-ck* (lines expressing peroxisome-targeted cyan fluorescent protein CFP) were crossed by manual pollination of emasculated flowers. Immediately before from the anthesis stage, the sepals, petals and stamens from flowers of the plants that acted as female were removed with the help of tweezers and magnifying glasses. Later, the mature anthers of the male parent were brought into contact with the pistil of the plant receiving. The mature siliques resulting from these crosses were collected and the resulting seeds constituted the F_1 generation. In this generation all the plants are heterozygous for the two parental loci. F_1 plants were allowed to self-pollinate and the seeds were collected (generation F_2). Due to genetic segregation, in F_2 all genotypes were found. The presence of CFP in peroxisomes was selected by microscopy and homozygosity for the T-DNA insertion was determined by PCR.

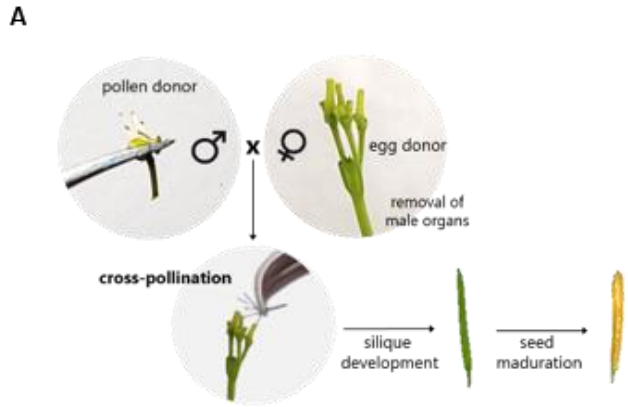

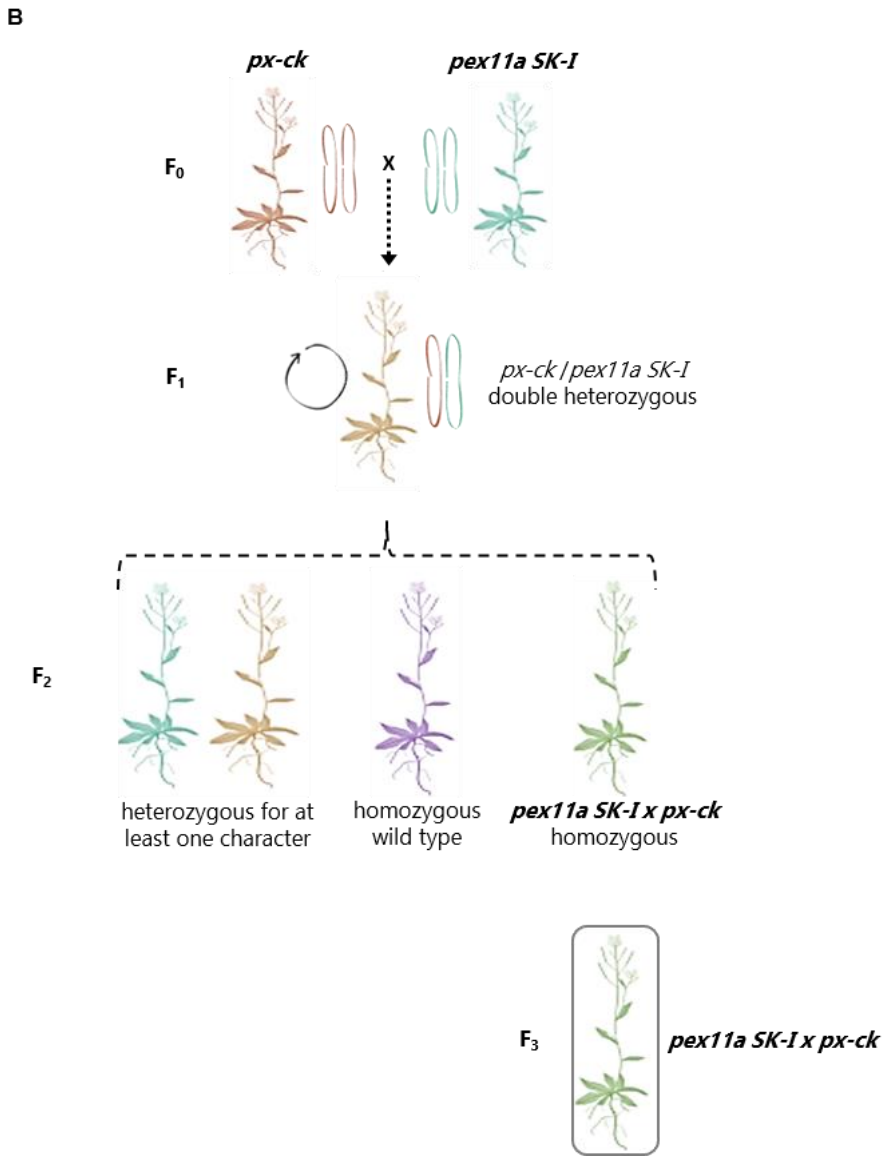

Figure 1. Generation and selection of double homozygous lines pex11a SK-I x px-ck mutants. ***(A)*** *Scheme showing the stages of the cross pollination and* ***(B)*** *selection process of homozygous lines.*

2.3.1. Genomic DNA isolation and conventional Polymerase Chain Reaction (PCR)

Genomic DNA was isolated from Arabidopsis, *px-ck* and mutants. Briefly, extracts from leaves were made by macerating the tissue in extraction buffer (200 mM Tris HCl

pH 7.5, 250 mM NaCl, 25 mM EDTA, 0.5 % SDS). Samples were centrifuged at 13,000 rpm for 5 min and the collected supernatant was mixed with the same volume of isopropanol at RT for 5 min. After that, samples were centrifuged at 13,000 rpm for 5 min and precipitates were allowed to dry. Finally, DNA was dissolved in 100 µl of Tris-EDTA (TE) buffer. The presence and homozygous status of the T-DNA insertion were validated by conventional PCR using Horse-Power™ Red-Taq DNA Polymerase MasterMix (Canvax) and the following conditions: 3 min at 94 °C, followed by 30 cycles of 30 s at 94 °C, 40 s at 55 °C and 1 min 20 s at 72 °C, and finally 7 min at 72 °C. Primer sequences were designed through T-DNA Primer Design Tool (http://signal.salk.edu/tdnaprimers.2.html) powered by Genome Express Browser Server (GEBD) and are listed in **Table 2.**

2.4. Generation of p*PEX11a::GUS* mutants

2.4.1. *PEX11a* promoter (p*PEX11a*) cloning in pGEM-T vector

Region of interest (-1750 to -1) of *PEX11a* promoter was amplified using the AccuPrime Taq DNA polymerase (Invitrogen), which has 5´→ 3´exonuclease activity. PCR reaction was carried out following manufacture's instruction, in a final volume of 25 µl with primers described in **Table 2.** and using genomic DNA as a template. Subsequently, mix solution was initially denatured at 94 °C 2 min, and 30 cycles of denaturation at 94 °C 30 s, annealing at 55 °C 30 s and final extension at 68 °C for 2 min. Amplified 3'-A-tailed PCR product was analysed by agarose gel electrophoresis and ligated into the pGEM-T vector (Promega). This high copy number-plasmid, carrying the *lacZ* gene was employed as an intermediate cloning vector (**Fig. 2**).

Ligation was carried out according to the commercial's instructions employing the T4 DNA ligase in a final volume of 10 µl. The insert was added in a molar ratio 3:1 of insert to vector and reaction was incubated at 4 °C O/N. Competent *E. coli* TOP10 cells (Invitrogen) were transformed by heat shock following manufacturer's recommendations. Briefly, 4 µl of the ligation were mixed with 50 µl of competent cells and incubated on ice for 30 min followed by 30 s at 42 °C and then kept in ice. Successful cloning of an insert into the vector interrupts the coding sequence of β-galactosidase, and recombinants can be identified by blue/white screening (**Fig. 2**). For this purpose, 0.5 mM Isopropyl-β-D-1-thiogalactopyranoside (IPTG) and 80 µg/ml X-Gal were added to Luria Bertani (LB) plates

containing 100 µg/ml ampicillin. The screening of the recombinants was carried out by isolating DNA with the miniprep kit of Quiagen following the company's instructions and the promoter sequence was amplified with primers showed in **Table 2.** DNA sequencing was performed by the DNA Sequencing Service at the López-Neyra Parasitology and Biomedicine Institute (IPBLN-CSIC; Granada, Spain).

Table 2. *List of primers for cloning, genotyping and expression analysis used in this work.*

Gene	ID	Primer sequence (5′ → 3′)	Use
PEX11a-F	AT1G47750	AAGCTTCTTCTCCTAAATTCACC	pPEX11a cloning in pGEM-T vector; screening of CRISPR/Cas9 mutations
PEX11a-R	AT1G47750	CCCGGGTGGAGGAGATGGAGCTT	pPEX11a cloning in pGEM-T vector
PEX11a-F	AT1G47750	GGGGACAAGTTTGTACAAAAAAGCAGG CTTCCTTCTCCTAAATTCACCCATC	Incorporation of attB recombination sites (Gateway technology)
PEX11a-R	AT1G47750	GGGGACCACTTTGTACAAGAAAGCTGGG TCTGGAGGAGATGGAGCTTTTTC	Incorporation of attB recombination sites (Gateway technology)
PEX11a-F	AT1G47750	TCGCGTTAACGCTAGCATGGATCTC	pDONR 207 sequencing check
PEX11a-R	AT1G47750	GTAACATCAGAGATTTTGAGACAC	pDONR 207 sequencing check
LBb1.3		ATTTTGCCGATTTCGGAAC	T-DNA insertion validation
PEX11a-F	AT1G47750	GATTCAAATCACGAGCTCGTC	T-DNA insertion validation (SALK_038574)
PEX11a-R	AT1G47750	AGATCCCAAAATGGGTGAATC	T-DNA insertion validation (SALK_038574)
PEX11a-F	AT1G47750	TCATCGAAAATTCATGCATTG	T-DNA insertion validation (SALK_006177)
PEX11a-R	AT1G47750	TGAAGCCATTTCGAATGTTTC	T-DNA insertion validation (SALK_006177)
TUB4-F	AT5G44340	GAGGGAGCCATTGACAACATCTT	RT-qPCR
TUB4-R	AT5G44340	GCGAACAGTTCACAGCTATGTTCA	RT-qPCR
PEX11a-F	AT1G47750	GATCGTCGAAGCAACACAAC	RT-qPCR
PEX11a-R	AT1G47750	CATAGGTCCACCTTGCTGTA	RT-qPCR; screening of CRISPR/Cas9 mutations
PEX11b-F	AT3G47430	CATTCCAATACGTGGCCAAG	RT-qPCR
PEX11b-R	AT3G47430	TTCGTCTCAGCGCATTGAAC	RT-qPCR
PEX11c-F	AT1G01820	GAACGTGCTGAGATTCTTGG	RT-qPCR
PEX11c-R	AT1G01820	ATTGATGCTGACAGCCTACC	RT-qPCR
PEX11d-F	AT2G45740	GTTCTTGAGTGGTGGACAAC	RT-qPCR
PEX11d-R	AT2G45740	AGGCACAGGACTGATAAGAC	RT-qPCR
PEX11e-F	AT3G61070	GCTGTATCGTGCTAAGCTTC	RT-qPCR
PEX11e-R	AT3G61070	CAGTGACACGAGGACTAATC	RT-qPCR

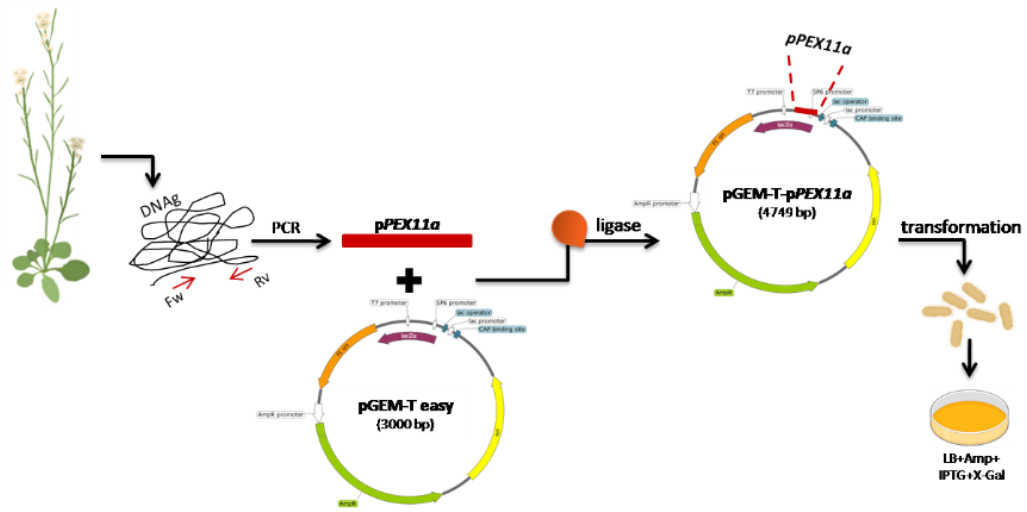

Figure 2. PEX11a promoter cloning in pGEM-T vector*. Maps were obtained from SnapGene Viewer.*

2.4.2. Generation of p*PEX11a::GUS* using Gateway technology

The promoter region of *PEX11a* was amplified from the intermediate cloning vector pGEM-T (see previous section) with the primers indicated in **Table 2.** PCR was performed with iProof High Fidelity DNA Polymerase according to the manufacturer's instructions (BioRad), under the following reaction conditions: 30 s at 98 °C, followed by 30 cycles of 10 s at 98 °C, 30 s at 70 °C, 72 °C for 2 min at 72 °C, and 10 min at 72 °C. BP reaction to clone p*PEX11a* into the pENTRY vector pDONR207 was conducted according to company's instructions. Competent *E. coli* TOP10 cells (Invitrogen) were transformed with the ligation and the selection was carried out in LB plates supplemented with 25 µg/ml gentamycin. Colony PCR and sequencing of cells were carried out to check positive clones. Afterwards, target DNA fragment was transferred into the destination vector pMDC163 with the Gateway™ LR Clonase™ Enzyme mix and the reaction was incubated O/N. The following day, reaction was stopped and *E. coli* competent cells were transformed. Recombinants cells were selected in LB plates containing 50 µg/ml kanamycin. Clones were checked by colony PCR and the DNA was isolated (miniprep Qiagen, Hilden, Germany) to transform *Agrobacterium* (see next section). Plants were then transformed by floral dipping (**section 2.4.4**).

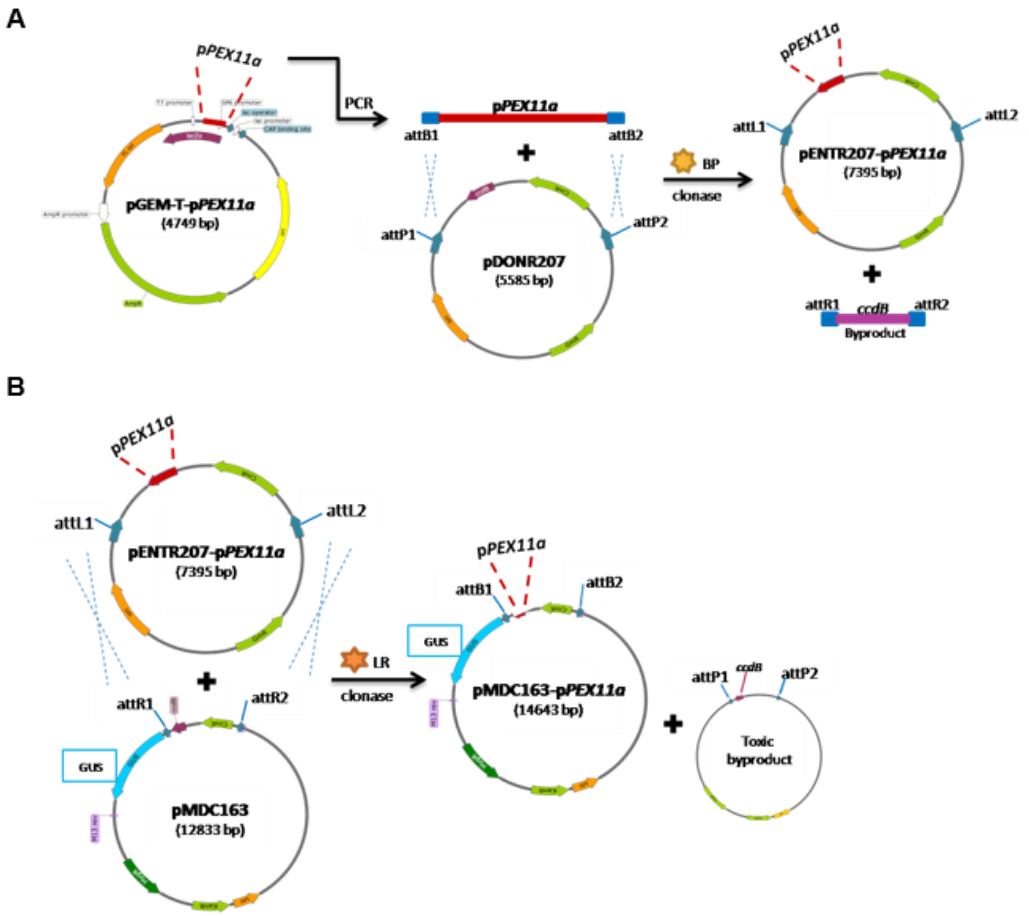

Figure 3. Cloning protocol based in Gateway technology used for pPEX11a::GUS generation. ***(A)*** *BP reaction between the attB recombination sites added to the promotor located in the pGEM-T plasmid and the attP sites from the vector pDONR207.* ***(B)*** *LR reaction occurring between the entry clone and the destination vector.*

2.4.3. Generation and transformation of electro competent *Agrobacterium* cells

Original cells of *Agrobacterium tumefaciens* strain GV31011 were kindly donated by Prof. Isabel Díaz (CBGP UPM-INIA) and new competent cells were produced as follow: 5 ml of LB O/N culture was inoculated with a colony, the following day a 1:50 dilution with the appropriate antibiotic and 0.1 % glucose was grown to an OD_{600} of 0.6-0.7. Then the flask was kept on ice for 30 min. Afterwards the cells were harvested by centrifugation at 4,000 rpm for 15 min at 4 °C. Pellet was washed three times with 1 mM HEPES pH 7 and washed once with 10 % glycerol. Finally, cells were resuspended in 10 % glycerol, shock frozen with liquid nitrogen and stored at -80 °C until use.

For the transformation, 100-500 µg of plasmid DNA (pMDC163-p*PEX11a* or pHEE401E-*PEX11a)* together with 50 µl of competent cells were transferred into dry, cold and sterile electroporation cuvettes. For the electroporation a micro pulser electroporator from BioRad was set to 25 mF, 25 KVol and 200 Ohm for 5 s. Afterwards 900 µl LB was added, incubated at 28 °C for 2 h and plated on LB media with the appropriate antibiotics.

2.4.4. Plant transformation by floral dipping

Agrobacterium-mediated transformation of *Arabidopsis thaliana* plants was performed using the floral dipping method. For this purpose, shoot apexes from 1-month soil-grown plants (F_0 generation) were cut after bolting and plants were transformed five days later. Two days before the plant transformation, *A. tumefaciens* carrying the construction of interest was grown to stationary phase at 28 °C in 10 ml LB medium with the corresponding antibiotics for selection. This culture was used to inoculate 200 ml of medium, which was again incubated for 24 h. Cells were harvested by centrifugation for 10 min at RT at 2,500 g and then resuspended in infiltration medium containing 5 % (w/v) sucrose, 0.22 % MS and 0.02 % (v/v) Silwet L-77 (Lehle Seeds, Round Rock, USA, #VIS-01), adjusted to pH 5.7 and with an OD_{600} of approximately 0.8 prior to use. The above-ground parts of plants were dipped in bacterial solution for 30 s. Then, pots with plants were covered by plastic foil to maintain high humidity and kept them out of direct light in the growth chamber. Twenty-four hours later, plants were transferred to normal growth conditions until F_0 seeds became mature.

2.5. Generation of *pex11a* mutants by CRISPR/Cas9 *(pex11a-CR)*

Guide RNA (gRNA) design and vector construction were carried out in collaboration with Dr. Yasin Dagdas (Gregor Mendel Institute of Molecular Plant Biology). Two 20 bp sequences from *PEX11a* gene (ccaATGGCTACGAAAGCTCC and GCTTCAGAAGATTAGTGCTT) were chosen as targets and inserted in the vector pHEE401E. Competent *E. coli* TOP10 cells were transformed with the construction pHEE401E-g*PEX11a* by heat shock as explained before. After sequencing, DNA was isolated and *Agrobacterium* cells were transformed by electroporation (**section 2.4.3**.).

Agrobacterium-mediated transformation of *Arabidopsis thaliana* was carried out as explained in the previous section.

2.5.1. Mutagenesis analysis

Seed collected from the *px-ck* transformed plants (F_0) were surface disinfected and stratified for 48 h at 4 °C and then sown on MS containing hygromycin (30 mg/l), grown at 22 °C in 16 h light and 8 h darkness for 10 d. Transformants were selected by checking hypocotyl length (hygromycin resistant seedlings display larger hypocotyls) and transferred to soil. A preliminary screening looking for alterations in peroxisomal morphology was carried out using confocal laser scanning microscope (CLSM). Then, genomic DNA of F_1 transgenic plants was extracted using the DNeasy Plant Mini Kit (Qiagen). The fragments surrounding the target sites were amplified using the iProof High-Fidelity PCR kit following conditions from Bio-Rad, to avoid false positive mutations with specific primers (**Table 2**). Bands were cut and purified from agarose gel using QIAquick Gel Extraction Kit (Quiagen) according to manufacturer's instructions. DNA sequencing was performed by the DNA Sequencing Service from IPBLN-CSIC.

Seeds from F_1 generation were collected and plated in medium supplemented with 30 mg/l hygromycin. For the purpose of segregate-out the CRISPR/Cas9 transgene, an inverse selection was performed in F_2 generation: seeds were sown on MS plates containing the selective antibiotic and after hypocotyls elongation, hygromycin sensitive seedlings were selected and transferred to recovery medium plates without antibiotic. Transgene-free plants were confirmed by microscopy and sequencing as explained previously. Additionally, and when it was possible, fragments surrounding the second target site was amplified by PCR and digested with *StyI* HF (New England Biolabs) in a mix consisting of 12,5 µl of PCR product, 2 µl of commercial 10x buffer and 1 µl of *StyI* HF. Restriction mix was incubated at 37 ºC for 3 h and inactivated by incubating at 80 ºC for 20 min. The fragments were checked by agarose electrophoresis.

2.6. Histochemical β-glucuronidase (GUS) assay

Plant material was collected and immersed in GUS staining solution (50 mM sodium phosphate buffer pH 7.2, 2 mM potassium ferrocyanide: $K_4Fe(CN)_6$, 2 mM

potassium ferricyanide: $K_3Fe(CN)_6$, 2 mM 5-bromo-chloro-3-indolyl-ß-glucurinic acid (X-Gluc in DMSO), 0,1 % Triton-x100, 2 mM X-Gluc. To facilitate the penetration of the solution, two cycles of 5 min of vacuum were performed. Samples were then incubated at 37 °C in a light protected environment O/N. Afterwards, GUS staining solution was removed and samples were washed with 99 % ethanol until chlorophyll disappearing.

2.7. Phenotypic analysis of Arabidopsis lines

2.7.1. Germination assay

Seeds were surface disinfected as explained before and plated on solidified MS and stratified at 4 ºC in darkness for 72 h. Radicle protrusion was regarded as seed germination completion. The number of germinated seeds was evaluated from day 0 to day 5. Each germination experiment was performed with at least three replicates (consisting of 100-150 seeds) per genotype.

2.7.2. Root elongation evaluation and lateral roots number

After being disinfected and plated on MS, seeds were grown in Petri dishes arranged in vertical position in order to keep the roots straight. Plants were grown for 10 d under long day conditions and plates randomly disposed in the growth chamber were scanned. Images of each plate were taken by a scanner Epson 3200. Root length as well as lateral roots (LR) were measured at day 10^{th} using Image J software.

2.7.3. Fresh weight and foliar area measurement

Rosette weight was used as growth parameter, and it was evaluated at the end of the 3rd and 4th week of growth period under short and long day conditions. Images from at least 30 plants were taken and the average value for the foliar area was determined by Image J software for each growth condition. After that, plants were harvested and weighed on a Sartorius precision balance (CPA225D) to evaluate fresh weight.

2.7.4. Silique number and seed weight

Siliques located in the main stem as well as in the branches were quantified in plants grown under long day conditions until total development. Weight from at least three replicates of 200 seeds/per experiment was examined. Furthermore, seeds were also embedded for 24 h and their phenotype was evaluated using a Primo Star™ microscope (Zeiss).

2.7.5. Pollen germination assay

Pollen germination on solid surface was carried out according to Daher et al. (2009), with slightly modifications. Briefly, hot agar-containing medium was poured onto a microscope slide to form a layer with a thickness of about 0.5 mm and left to cool. This media contained 18 % sucrose, 0.01 % (1.62 mM) boric acid, 1 mM $CaCl_2$, 1 mM $Ca(NO_3)_2$, 1 mM $MgSO_4$, and 1 mM KCl with a pH adjusted to 7. For solid medium preparation, agar was added to the mix and heated to dissolve it. Fresh pollen was then sprinkled on the cold agar surface tapping the flowers using a fine brush. A stigma was placed nearby to enhance germination and then the slides were placed on top of an empty tip box containing water to keep humidity. Pollen grains were considered germinated when the pollen tube length was greater than the diameter of the pollen grain. Images were taken at 6 h after the beginning of incubation using a Primo Star™ microscope (Zeiss).

2.7.6. Hormones and NaCl treatment

Seeds were surface disinfected as explained above, plated on MS and stratified at 4 ^{o}C in darkness for 48 h. Hormones were added either from the beginning in the media or after 4 d plants growth. Plates were supplemented with: 100 µM 1-aminocyclopropane-1-carboxylic acid (ACC), 10 µM O-(carboxymethyl) hydroxylamine hemihydrochloride (AOA), 3 µM gibberellic acid (GA3), 5 µM indole-3-acetic acid (IAA), 5 µM jasmonic acid (JA; Sigma-Aldrich). Plates containing 100 mM NaCl were also prepared. The length of the main root was determined by growing seedlings vertically for 4 d. Images of each plate were taken by a scanner Epson 3200. Subsequently, the length of the main root was measured by Image J software and the average value of more than 100 seedlings was determined. The effect of the abscisic acid (ABA) in the germination rate was also evaluated in MS plates supplemented with 0, 1, 4 and 10 µM ABA, after 5 d growing.

2.7.7. Cadmium treatment

Seeds were surface disinfected and plated on MS containing 0, 50 or 100 μM $CdCl_2$. Plants were grown for 7 d and plates were scanned to evaluate Cd effects in seedlings. Root length was measured using Image J software. For microscopy, seedlings were plated on MS and growth for 13 d, transferred to liquid MS, grown for 24 h and then treated with 100 μM $CdCl_2$ for different time points (1 h, 24 h and 72 h).

2.7.8. Peroxisome size and number analysis

Peroxisomes were observed in leaves of two-week-old seedlings treated or not with 100 μM $CdCl_2$ by CLSM. Peroxisome size and number were measured through the analysis of high magnification CLSM images taken after 4 h of Cd treatment using the Analyze Particles algorithm implemented in ImageJ and expressed as average size (μm^2). The formation of peroxules was analyzed in high magnification CLSM images after in vivo incubation with 100 μM $CdCl_2$ for 30 min.

2.7.9. Cytochemical identification of peroxisomes

Cytochemical localization of peroxisomes was carried out as described before (Calero-Muñoz *et al.*, 2019) using leaves from plants grown for 15 days. Briefly, Arabidopsis leaves were cut into pieces of approximately 1 mm^2 and initially fixed with 0.5 % glutaraldehyde (v/v), prepared in 50 mM potassium phosphate buffer, pH 6.8, for 2.5 h at RT. After that, samples were washed with the same buffer and incubated in DAB solution (2 mg/ml) prepared in 50 mM Tris-HCl, pH 9.0 for 1.5 h. Samples were incubated in a solution containing DAB and 0.02 % H_2O_2 at 37 °C for 3 h. After that, pieces were washed with 50 % potassium phosphate buffer, pH 6.8, and stained with 1 % (w/v) OsO_4. Samples were then dehydrated in a stepped ethanol series from 30 to 100 %, embedded in Embed 812 resin series (25-100 %; w/v; Electron Microscopy Sciences, Hatfield, PA, USA) and cut into thin (0.5-0.7 mm) or ultra-thin (50-70 nm) sections for further optical and electron microscopy analysis, respectively. Sections were not stained for optical microscopy analysis but were post stained with uranyl acetate for electron microscopy analyses. Final images were analyzed by Image-J software.

2.8. Expression analysis

2.8.1. RNA isolation and cDNA synthesis

Extraction of total RNA from seedlings was carried out using Trizol reagent (MRC). DNase treatment was carried out using DNA-free™ DNA Removal Kit (Invitrogen) according to the manufacturer's protocol. Integrity and concentration of RNA was analyzed by electrophoresis in 1 % agarose gels (w/v) in 45 mM Tris-HCl buffer (pH 8.0), 45 mM glacial acetic acid and 1 mM EDTA (TAE). Agarose was dissolved in TAE buffer and samples were prepared in loading buffer containing 4 % glycerol. After electrophoresis (100 V for 15 min), RNA bands were stained with ethidium bromide 0.5 µg/ml and visualized using a Chemidoc (Bio-Rad) system coupled with a high sensitivity CCD camera. Band intensity was quantified with Image J software. After that, 1 µg RNA was reverse transcribed using 5x PrimeScript RT Reagent Kit (Takara), with the following reaction conditions: 37 °C, 15 min; 85 °C, 5 s (Mastercycler thermal cycler, Eppendorf).

2.8.2. Real–time quantitative polymerase chain reaction (qRT–PCR)

qRT–PCR was used to quantify the expression level of different genes. Reaction mix was composed by 10 µl of TB Green Premix Ex Taq (Takara), 8 µl of MilliQ water, 0.5 µl of each specific primer (10 µM; **Table 2**) and 1 µl cDNA as template. An iCycler iQ5 (Bio-Rad) were used for perform the reaction with the following program: 1 cycle (95 °C, 3 min), 35 cycles (95 °C, 10 s; 45-60 °C, 30 s; 72 °C, 30 s), 1 cycle (72 °C, 10 min). For each reaction a Ct value and a melting curve were obtained. For each quantification assay, at least 3 biological replicates were used. Relative expression of genes respect control or mock samples was calculated with the **Equation 1**, using *TUB4* as endogenous gene.

Equation 1. *Normalized relative expression*

$$Relative\ expression = 2^{-\Delta\Delta Ct}$$

$$\Delta\Delta Ct = (Ct_{target\ gene} - Ct_{endogenous\ gene}) - (Ct_{calibrator\ gene} - Ct_{endogenous\ gene})$$

2.8.3. Oligonucleotides design and primer efficiency

Specific primers used for RT-qPCR assays as well as sequencing and cloning processes were designed through PRIMER3 (http://bioinfo.ut.ee/primer3-0.4.0/) and

synthesized by Sigma-Aldrich. General conditions imposed were a G-C content between 50-60 % and temperatures between 50-60 °C whenever was possible. The approximate alignment temperature (T_a) was calculated depending on the length and composition of the oligonucleotides used, following the formula: $T_a = 2 (A + T) + 4 (G + C)$. Serial dilutions of pooled samples were prepared to calculate the efficiency of the oligonucleotides. Calculations were made from the slopes of the standard curve obtained by the iQ5 program using the formula E = [10 (1/a) -1] x 100, where "a" is the slope. Primer melting curves with 90-105 % efficiency were performed to validate amplification specificity (Bustin *et al.*, 2009). Primer sequences are indicated in **Table 2.**

2.9. Statistical analysis

Mean values for all experiments were obtained from at least three independent experiments with at least three independent biological replicates in each experiment. Mean values for the different treatments were compared using Student's t-test after one-way ANOVA analysis. The complement Real Statistics Resource Pack from Excel was used to perform statistical analysis. Error bars represent standard error (SEM).

3. RESULTS AND DISCUSSION

3.1. PEX11a expression by in silico analysis

In order to know in which stages and organs of the plant *PEX11a* is expressed, an initial *in silico* study was carried out using the tool ePlant (http://bar.utoronto.ca/eplant/). *In silico* expression pattern of *PEX11a* showed higher expression in mature pollen, seeds embedded for 24 h and stamens, while low expression of this gene was found in all organs and stages of development of *A. thaliana* (**Fig. 4 A**). In addition, *PEX11a* expression is higher in some specific tissues of the root such as columella root cap cells and lateral roots (LR) cap cells (**Fig. 4 B**).

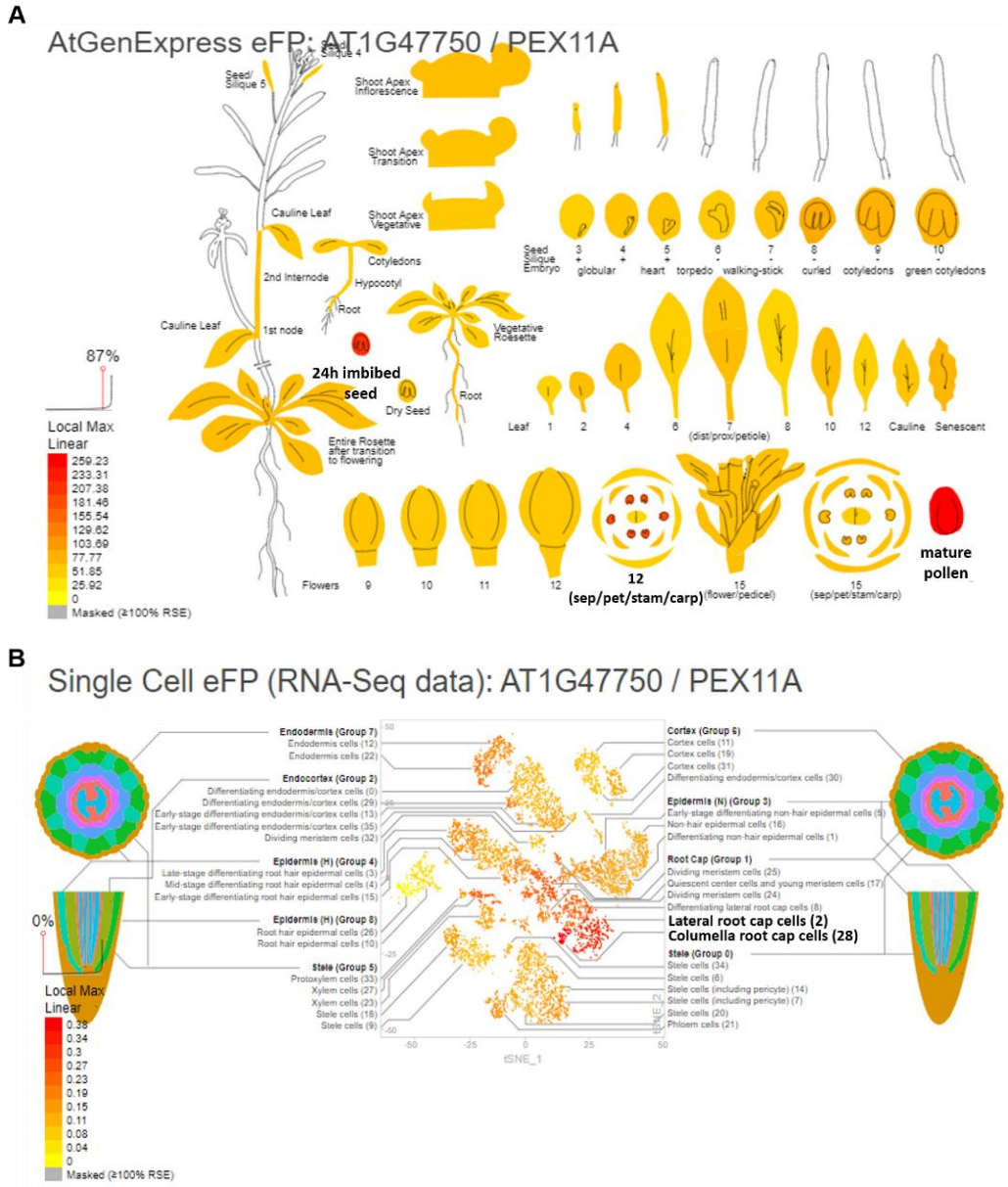

Figure 4. In silico PEX11a expression data available at BAR web site (http://bar.utoronto.ca/eplant/). (A) *Scheme showing the expression level of PEX11a throughout development of A. thaliana.* ***(B)*** *PEX11a expression in a cross section from Arabidopsis root. Red and orange tissues mean higher expression.*

Expression of *PEX11* transcripts in Arabidopsis leaves, roots and suspension cells was analyzed by Lingard and Trelease (2006). Four of the five *PEX11* gene transcripts were expressed in both, tissues and suspension culture cells, but *PEX11a* transcripts were not. However, transcripts for all five genes were detected in silique. Orth et al. (2007) also

analyzed the expression of the five isoforms of *PEX11* in seedling, flower, silique, seed, stem, rosette leaf, cauline leaf, senescent leaf and root. Thus, *PEX11a* was expressed at a constitutively low level in all tissues examined (Orth *et al.*, 2007), which agrees with *in silico* data.

The tool ePlant from BAR website also gathers information about *PEX11a* expression in Arabidopsis plants under stress conditions such as water limitation, hypoxia and selenate treatment showing a decrease in the expression under hypoxia and selenite respect to control plants (**Fig. 5 A**). *In silico* experiments with the elicitors flg22 and Pep1 revealed *PEX11a* expression was located mainly in epidermis and pericycle of control roots while this expression is decreased in response to the elicitors (**Fig. 5 B**).

A

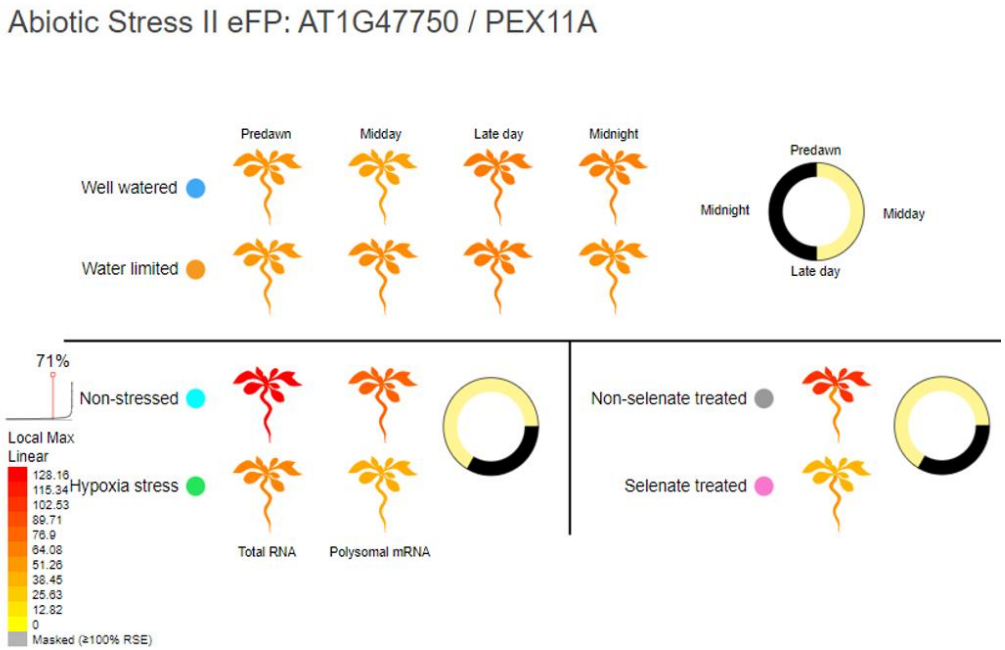

B

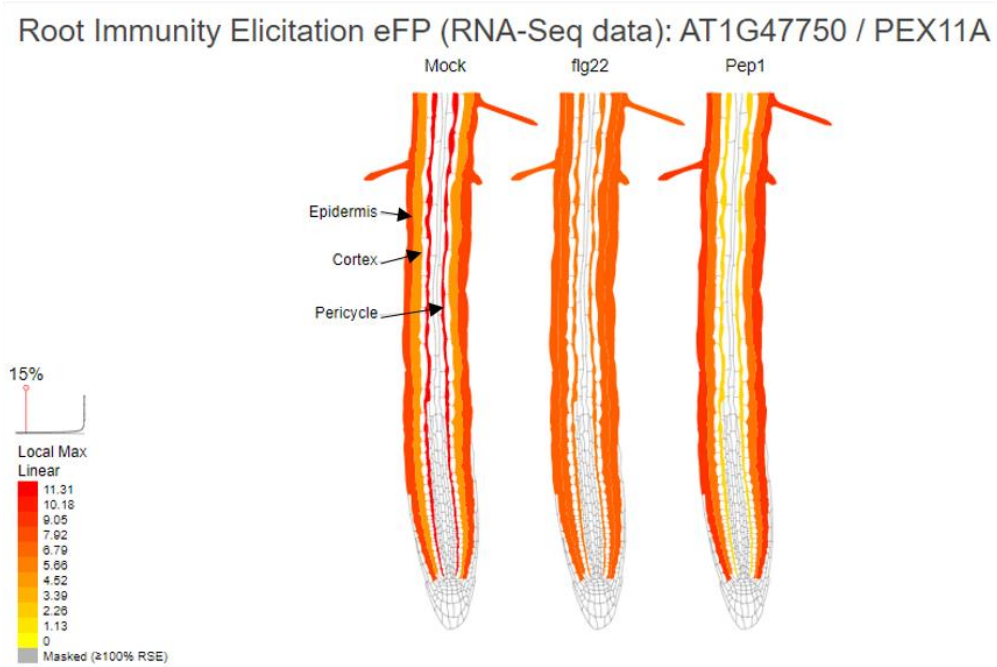

Figure 5. PEX11a expression data under stress conditions at BAR web site (http://bar.utoronto.ca/eplant/). (A) *PEX11a level expression in response to abiotic stress.* ***(B)*** *PEX11a expression in Arabidopsis roots in response to flg22 and Pep1 elicitors. Red and orange tissues mean higher expression.*

Several evidences in the literature suggest that abiotic stress appears to regulate specific *PEX11* genes. Thus, salinity upregulated *PEX11a* and *PEX11c* in WT, but not in the salt-susceptible mutants *fry1-6*, *sos1-14*, and *sos1-15* of *A. thaliana* (Fahy *et al.*, 2017). In a different analysis, salt upregulated in an ABA-dependent manner, *PEX11e* in Arabidopsis plants and both, *PEX11e* overexpression and salt stress increased peroxisome number, although *PEX11e* overexpression did not improve salt tolerance (Mitsuya *et al.*, 2010). Quinoa plants upregulated *CqPEX11c* in response to heat and the combination of heat and drought, while *CqPEX11a* remains constant (Hinojosa *et al.*, 2019). *PEX11a* and *PEX11e* were upregulated in response to Cd exposure in Arabidopsis plants (Rodríguez-Serrano *et al.*, 2016; Terrón-Camero *et al.*, 2020) while *PEX11b*, *PEX11c*, and *PEX11d* were upregulated by hypoxia (Li and Hu, 2015).

Although the involvement of *PEX11a* in plant stress responses has been described, no information is available on its regulation at molecular level. Therefore, a search for regulatory sequences present in a fragment of the promoter (1.8 kb) of this peroxisomal protein was carried out. The tool MatInspector from Genomatix (https://www.genomatix.de/) and PlantRegMap (http://plantregmap.gao-lab.org/) were used for that purpose. We found several families of stress-related transcription factors (TFs) that could bind to regulatory sequences located in *PEX11a* promoter (**Fig. 6**). Among them we can highlight the families WRKY, MYB and the heat stress transcription factor (HSF) family.

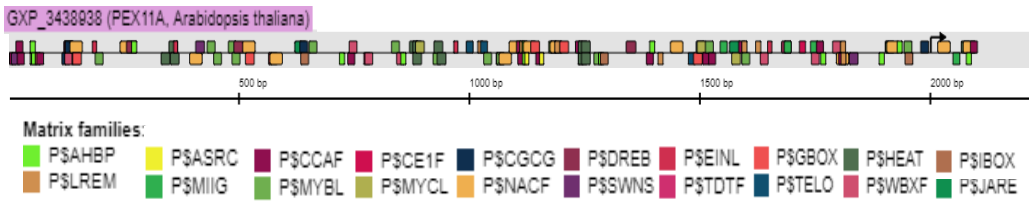

Figure 6. In silico identification of binding sites of transcription factors related to stress in PEX11a promoter. *Different colors represent putative binding sites of the different families of transcription factors located in the promoter generated by MatInspector.*

As previously mentioned, our group has reported the increase of *PEX11a* expression in response to Cd (Rodríguez-Serrano *et al.*, 2016). Therefore, we use stress-related data collected from MatInspector and PlantRegMap and compared the TFs obtained from an *in house* transcriptome in response to Cd (**Fig. 7**). We identified 21 common elements belonging to 5 families: WRKY (12), HSF (4), MYB (3), Homeodomain-leucine zipper (HD-Zip; 1) and Trihelix (1).

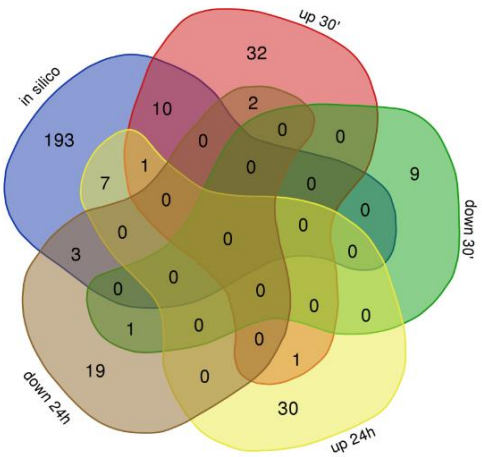

Figure 7. Putative TFs involved in PEX11a regulation after Cd treatment. *Venn diagram displaying common elements between in silico TFs related to stress and data from an in house transcriptome in response to Cd. Information obtained from MatInspector and PlantRegMap was compared with differential expressed genes in WT plant response to Cd 30 min and 24 h.*

WRKY family, name coined from the highly conserved 60 amino acid long WRKY domains of the TFs, has been widely studied and related to different types of biotic and abiotic stresses, as well as in physiological processes including pollen development and functionality and seed development (Zhang and Wang, 2005). HSF family can regulate the expression of stress-responsive genes, such as heat shock proteins (HSPs; Guo *et al.*, 2016). MYB family play regulatory roles in developmental processes and defense responses in plants (Yanhui *et al.*, 2006). HD-Zip TFs are unique to the plant kingdom and participate in the regulation of plant developmental processes, signalling networks and responses to abscisic acid-mediated stress, drought, cold and oxidative stress (Gong *et al.*, 2019). Trihelix family is involved in response to salt and pathogen stresses, the development of perianth organs, trichomes, stomata and the seed abscission layer, and the regulation of late embryogenesis (Kaplan-Levy *et al.*, 2012). Among *PEX11* Arabidopsis genes family, the only regulatory mechanism that has been characterized at molecular level is over *PEX11b*, which transcription has been reported to be induced by the *HY5 HOMOLOG (HYH)* TF in response to light through phytochrome A (phyA), while it was repressed by the nuclear protein Forkhead-Associated Domain Protein 3 (FHA3) (Desai and Hu, 2008; Desai, 2017).

3.2. Localization of *PEX11a* expression through the *GUS* reporter gene

To get a deeper insight into *PEX11a* expression we used plants transformed with its native promoter fused to *β-glucuronidase* gene. Histochemical staining of Col-0 plants containing the construction pMDC163-p*PEX11a*, from seeds to senescent tissues is showed in **Fig. 8**. Both lines p*PEX11a::GUS 2.4* and p*PEX11a::GUS 12.3* showed similar behavior.

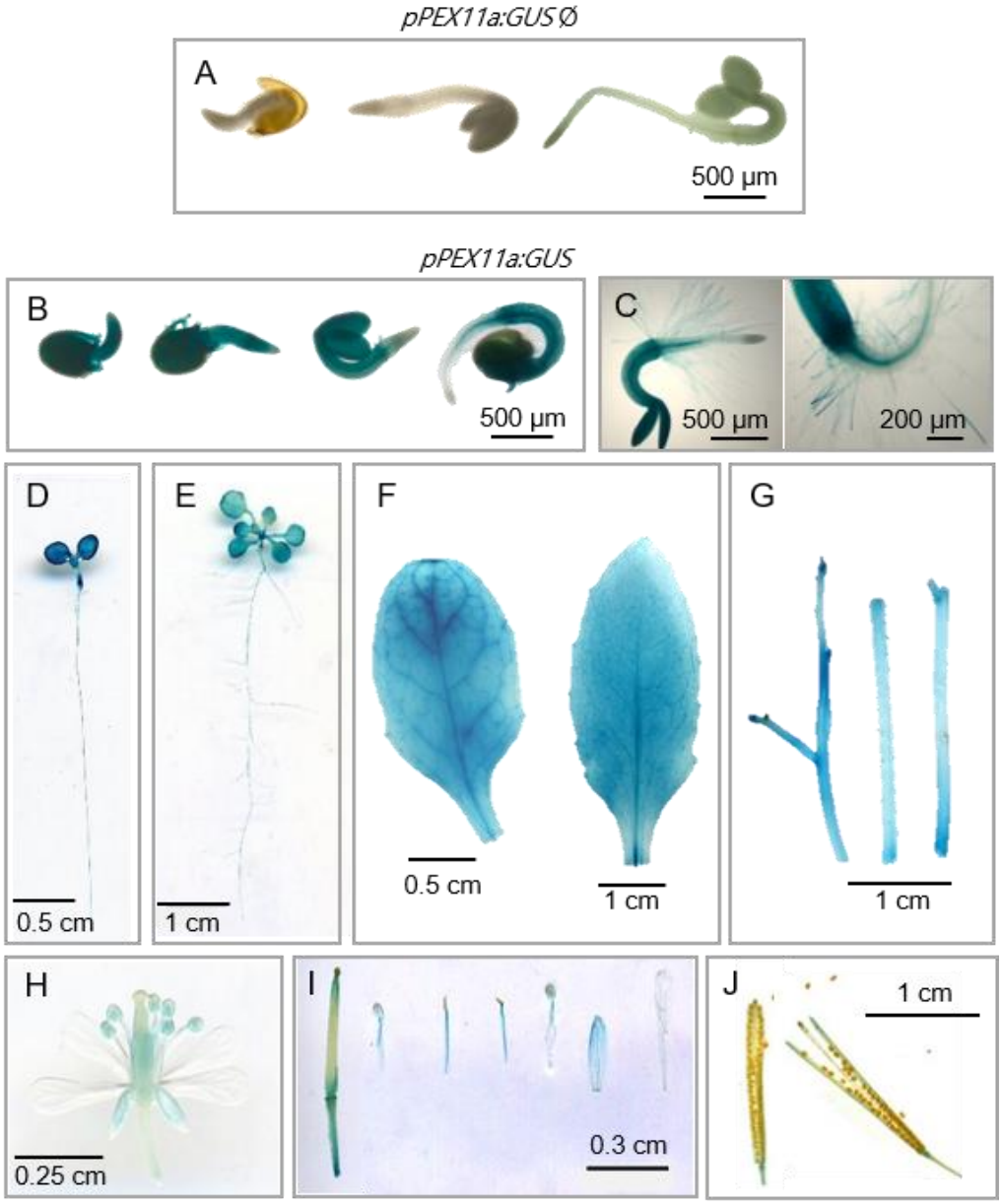

Figure 8. Histochemical analysis of GUS activity in Arabidopsis plants transformed with PEX11a promoter (1.8 kb) fused to the GUS reporter gene in pMDC163 vector. (A) *pPEX11a::GUS Ø used as a control.* ***(B)*** *Seedlings (1 to 3 days),* ***(C)*** *5 days,* ***(D)*** *7 days,* ***(E)****14 days,* ***(F)*** *leaves (4 weeks and 5 weeks),* ***(G)*** *stem of apical, middle and basal zone,* ***(H-I)*** *flower and* ***(J)*** *silique of pPEX11a::GUS 2.4 mutant were analysed by histochemical staining.*

PEX11a expression in the early stages of Arabidopsis development was observed in cotyledons and in vascular tissues (**Fig. 8 B-C**), with higher intensity in root hairs (**Fig. 8 C**). Interestingly, this pattern expression matches with the *in silico* data showed in **Fig.**

4 B and **Fig. 5 B**, being these cells from where the LR emerge. In one and two-week-old seedlings GUS staining was mainly located in the aerial part (**Fig. 8 D-E**) as well as in vascular tissues of 4-weeks-old leaves (**Fig. 8 F**). Furthermore, some parts of the Arabidopsis flower showed *PEX11a* expression and specially sepals and anthers (**Fig. 8 H-I**), which agrees with *in silico* data from Bar Toronto (**Fig. 4 A**). However, no expression was detected in mature seeds in our hands (**Fig. 8 J**).

We have found a remarkably presence of *PEX11a* in the vascular bundle of p*PEX11a*::*GUS* 2.4 and 12.3 lines. Interestingly, it has been reported the propagation of different signals such as electric potential, calcium and ROS waves through the plant vascular bundle during systemic signalling in stress response (Zandalinas *et al.*, 2020; Zandalinas and Mittler, 2021).

3.3. Double T-DNA insertion and CFP-peroxisomal marked mutants generation

RNA interference (RNAi) is a biological mechanism which leads to post transcriptional gene silencing (Younis *et al.,* 2014). At the beginning of this Thesis and working with the Arabidopsis RNAi line *pex11a* (Orth *et al.,* 2007; Rodríguez-Serrano *et al.,* 2016) we observed a decrease in the fluorescence intensity through generations. T-DNA insertion mutants are widely used to elucidate gene functions in genetic analyses of Arabidopsis. Thus, we decided to perform a cross pollination to obtain a new mutant affected in PEX11a between parental T-DNA insertion lines and lines expressing peroxisome-targeted cyan fluorescent protein CFP (*px-ck*; Nelson *et al.,* 2007). Two different *pex11a* T-DNA mutants were available from SALK: *pex11a SK-I*, (SALK_038574C) and *pex11a SK-II* (SALK_006177C). Amplification and analysis of T-DNA flanking sequences was carried out as explained in **section 2.3.1.** Both lines were genotyped to check the presence and the position of the T-DNA inserts. According to TAIR database, the region in which insertion may located is 431 nucleotides for *pex11a SK-I* and 308 for

pex11a SK-II (**Fig. 10 A**). It was found that the LP/LBb1.3 region was amplified but not the LP/RP region, thus confirming the homozygosity for both mutant lines (**Fig. 10 B**).

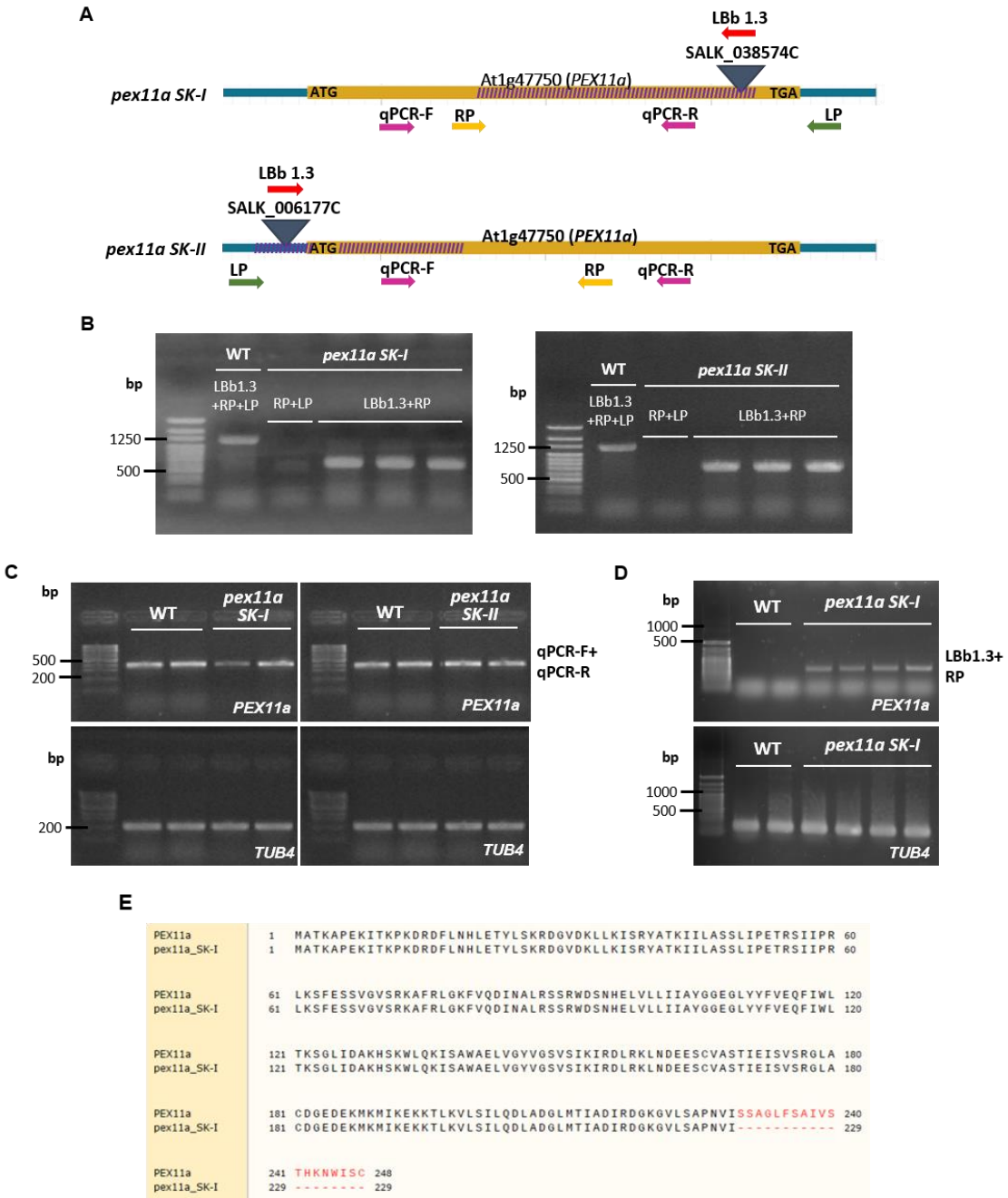

Figure 10. Genotyping and PEX11a expression of pex11a SK mutants. (A) *Scheme showing the insertion flanking position according to TAIR (https://www.arabidopsis.org/) striped in purple, and the position where the T-DNA insertion begins (blue triangle), obtained by sequencing.* ***(B)***

Ethidium bromide stained amplicons are shown using primers LP, RP and LBb1.3 described in ***Table 2*** *to check homozygosity.* ***(C)*** *PEX11a expression (semi- quantitative) in pex11a SK-I and pex11a SK-II mutants using tubulin-4 (TUB4) as reference and primers for expression (****Table 2****) represented as pink arrows in (A).* ***(D)*** *PEX11a expression (semi- quantitative) in pex11a SK-I mutant using tubulin-4 (TUB4) as reference and primers LBb1.3 and RP (****Table 2****).* ***(E)*** *Region of the peptide sequence conserved from the wild type PEX11a protein is displays in black and the region where T-DNA insertion begins in pex11a-SK-I mutant is highlighted in red.*

To corroborate the position of the insert, the flanking regions were sequenced using primers showed in **Table 2.** In the case of *pex11a SK-I* mutant the gene is interrupted at position 688, while the insertion is located upstream of the ATG in *pex11a SK-II* (**Fig. 10 A**). We also checked expression of *PEX11a* in both mutants using primers in the middle of the locus (pink arrows in **Fig. 10 B**). Although we determined the insertion is not interrupting the amplified fragment using qPCR primers in neither of the two mutants, we found a slight decrease in *PEX11a* expression in *pex11a SK-I* but not in *pex11a SK-II* by semi-quantitative RT-PCR (**Fig. 10 C**). In addition, we checked expression using the primers LBb1.3+RP in *pex11a SK-I* (**Fig. 10 D**) finding amplification and expression of this fragment. The resultant PEX11a protein found in *pex11a SK-I* mutant should be shorter than the WT, affecting to the last 19 aa in C-terminal part (**Fig. 10 E**.). Taking into account the insertion position, we decided to cross *pex11a SK-I* mutant, whose T-DNA insertion affects the final part of the gene, with *px-ck* plants, which have CFP targeted peroxisomes

3.4. *pex11a* mutants generation by CRISPR/Cas9: *pex11a-CR*

CRISPR/Cas9 system is a powerful tool for targeted gene editing, and is widely applied in plants. In parallel to obtaining *pex11a SK-I x px-ck* double mutants, we decided to use the Clustered Regularly Interspaced Short Palindromic Repeats (CRISPR)/CRISPR-associated protein 9 (Cas9) system to generate a new mutant affected in *PEX11a* in a *px-ck* background. A scheme with the selection process is showed in **Fig. 11 A.** Screening of the plants to detect the targeted gene modification in F_1 generation was performed, firstly by hygromycin selection and subsequently by microscopy and sequencing, in a total of 36 resistant parental lines. Peroxisomal morphology as well as dynamic were analysed using CLSM in order to detect changes in CRIPSR/Cas9 mutants. Seedlings from 8 lines with altered morphology and/or aberrant dynamic were selected for sequencing to determine if the observed phenotypes were due to mutations in *PEX11a* sequence.

After analysing sequences among the F_1 transformed plants we found in most cases that in mutant lines appeared a single T insertion just one position ahead of the ATG (-1), as well as a single C and/or T insertion in position 416 (**Fig. 11 B**), causing a frame shift leading to a premature stop codon in both cases (**Fig. 11 C**). Final homozygous lines selected consisted in a single C or a single T insertion. Two lines with two different mutations were selected, *pex11a-CR9* (C inserted) and *pex11a-CR10* (T inserted). When a C was inserted, a new target sequence (5'…C/CWWGG…3') for the restriction enzyme *Sty* HF (**Fig. 11 A**) was generated, but not when a T was inserted (**Fig. 11 D**). We did not find changes in peroxisomal morphology and dynamic as a consequence of mutation in position -1.

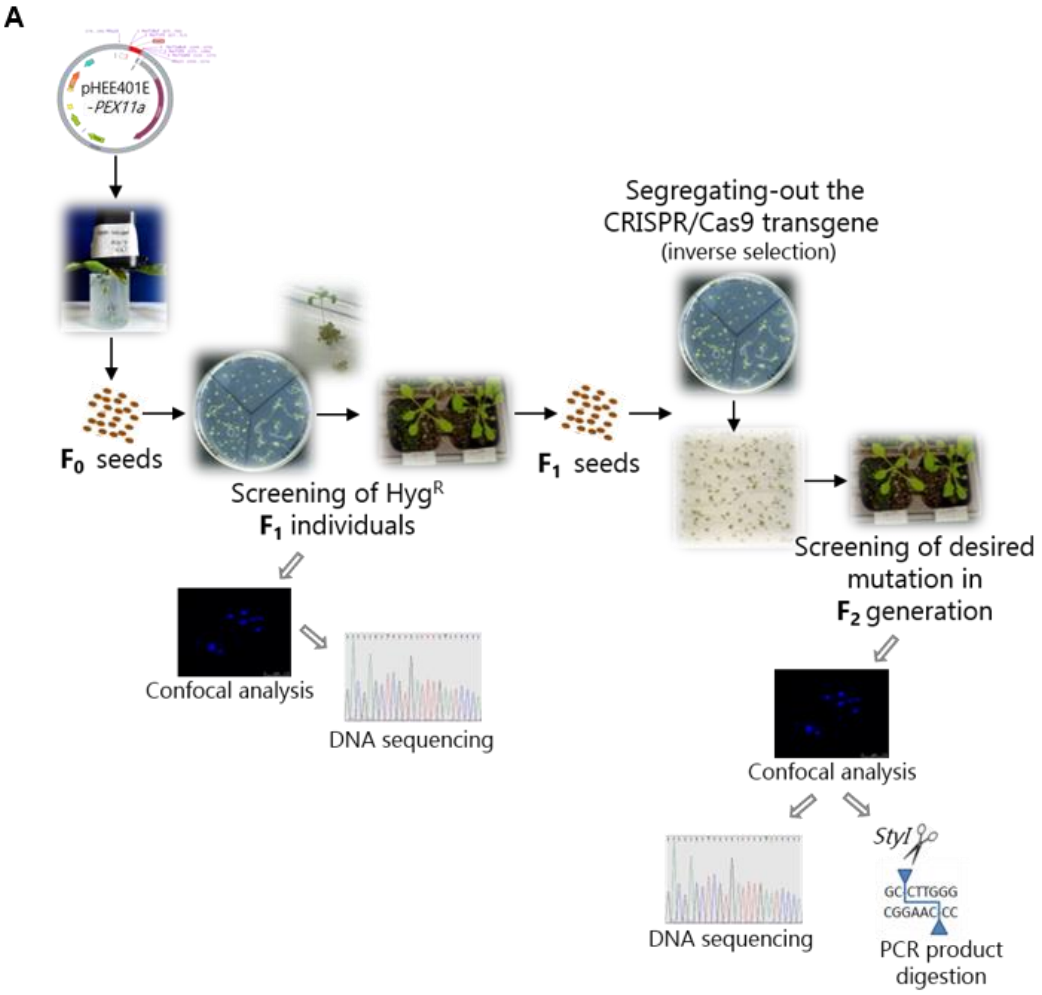
A
pHEE401E
-PEX11a
F0 seeds
Screening of HygR
F1 individuals
Confocal analysis
DNA sequencing
F1 seeds
Segregating-out the
CRISPR/Cas9 transgene
(inverse selection)
Screening of desired
mutation in
F2 generation
Confocal analysis
DNA sequencing
StyI
GCCTTGGG
CGGAACCC
PCR product
digestion

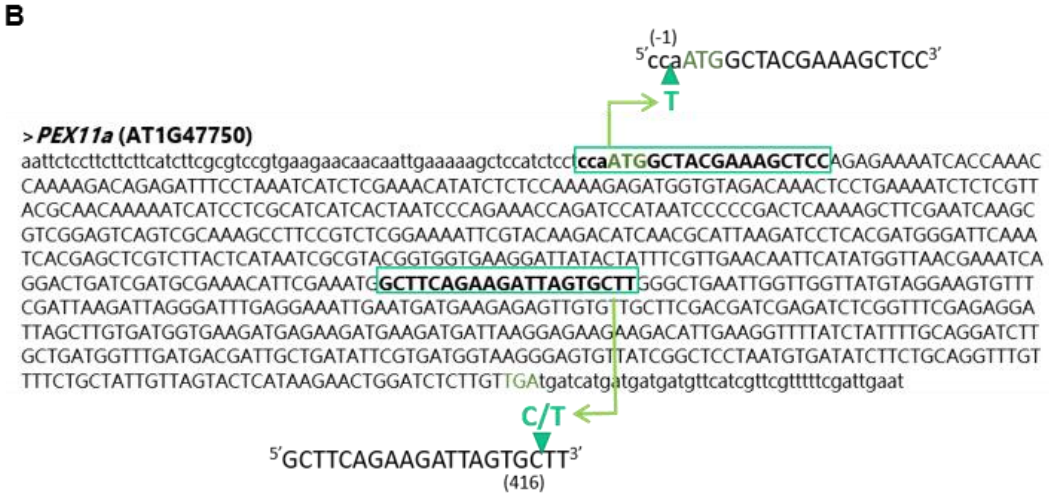
B
(-1)
5'ccaATGGCTACGAAAGCTCC3'
T
>PEX11a (AT1G47750)
aattctccttcttcttcatcttcgcgtccgtgaagaacaacaattgaaaaagctccatctcccccaATGGCTACGAAAGCTCCAGAGAAAATCACCAAAC
CAAAAGACAGAGATTTCCTAAATCATCTCGAAACATATCTCTCCAAAAGAGATGGTGTAGACAAACTCCTGAAAATCTCTCGTT
ACGCAACAAAAATCATCCTCGCATCATCACTAATCCCAGAAACCAGATCCATAATCCCCCGACTCAAAAGCTTCGAATCAAGC
GTCGGAGTCAGTCGCAAAGCCTTCCGTCTCGGAAAATTCGTACAAGACATCAACGCATTAAGATCCTCACGATGGGATTCAAA
TCACGAGCTCGTCTTACTCATAATCGCGTACGGTGGTGAAGGATTATACTATTTCGTTGAACAATTCATATGGTTAACGAAATCA
GGACTGATCGATGCGAAACATTCGAAATGGCTTCAGAAGATTAGTGCTTGGGCTGAATTGGTTGGTTATGTAGGAAGTGTTT
CGATTAAGATTAGGGATTTGAGGAAATTGAATGATGAAGAGAGTTGTGTTGCTTCGACGATCGAGATCTCGGTTTCGAGAGGA
TTAGCTTGTGATGGTGAAGATGAGAAGATGAAGATGATTAAGGAGAAGAAGACATTGAAGGTTTTATCTATTTTGCAGGATCTT
GCTGATGGTTTGATGACGATTGCTGATATTCGTGATGGTAAGGGAGTGTTATCGGCTCCTAATGTGATATCTTCTGCAGGTTTGT
TTTCTGCTATTGTTAGTACTCATAAGAACTGGATCTCTTGTTGATgatcatgatgatgatgttcatcgttcgtttttcgattgaat
C/T
5'GCTTCAGAAGATTAGTGCTT3'
(416)

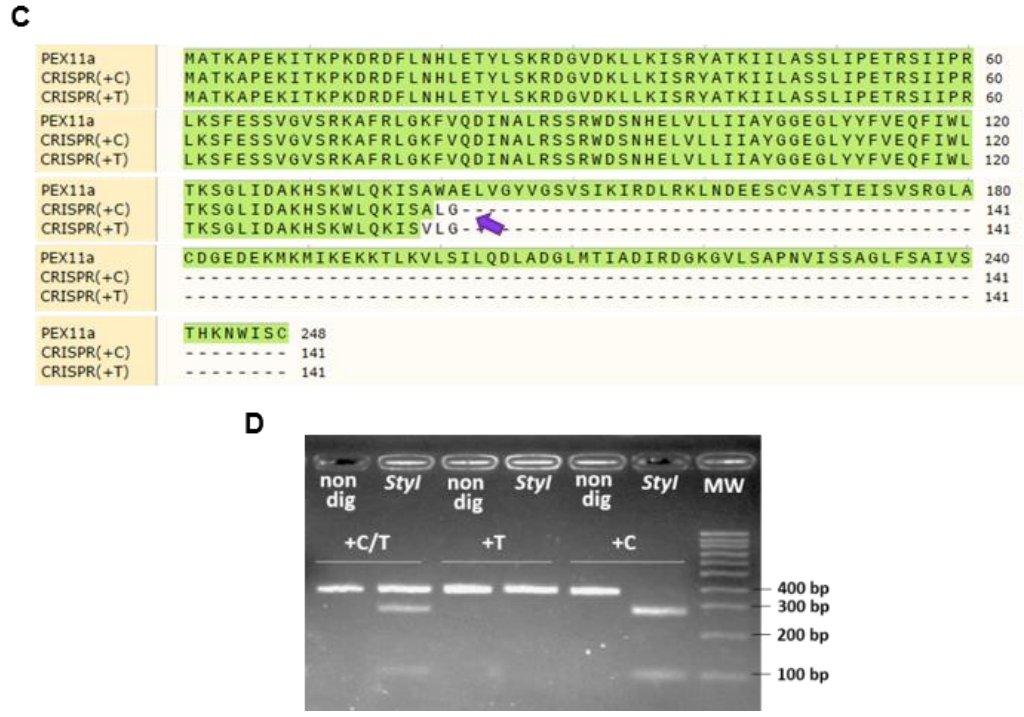

Figure 11. Selection of pex11a mutant lines generated by CRISPR/Cas9 technology. (A) *Scheme showing the process for selection of homozygous mutants carrying a mutation in PEX11a gene.* ***(B)*** *Position and mutations most frequently found among CRISPR/Cas9 lines in T1 and T2 generations. The 20 nt target sequences are framed in green.* ***(C)*** *Truncated protein resulting after the single C/T insertion. The region of the peptide sequence conserved from the wild type PEX11a protein is highlighted in green and the last amino acid is pointed by a purple arrow.* ***(D)*** *1 % agarose gel electrophoresis of the amplified fragment by PCR using PEX11a RT-qPCR primers (**Table 2**). Digestion of the total fragment (379 bp) with the enzime StyI of heterozygous lines generated 3 bands (379, 282 and 97 bp), no digestion in homozygous pex11a-CR10 line and 2 bands (282 and 97 bp) in homozygous pex11a-CR9 line.*

3.5. Phenotypic characterization of *pex11a* lines

3.5.1. Peroxisomal phenotype of mutants altered in *PEX11a*

The appearance of peroxisomes in CLSM microscopy was used as criteria for the selection of the mutant lines. To check peroxisomal phenotype under control conditions, seeds from F_1 and F_2 were plated on MS and grown under long-day conditions for two weeks. Representative high magnification CLSM images of leaves from *px-ck* and *pex11a-CR* lines are shown in **Fig. 12**. Two *pex11a-CR* lines selected using CRISPR/Cas9 technology showed peroxisomes smaller than *px-ck* imaged by CLSM. No differences were found however, on peroxisomal size in *pex11a SK-I x px-ck_double mutants*. In

general, we observed a lower number of peroxisomes in *pex11a-CR* lines compared to *px-ck* (**Fig. 12**). Regarding morphology, *pex11a-CR9* and *pex11a-CR10* peroxisomes showed less circularity than *px-ck* lines while *pex11a SK-I x px-ck* displayed no big differences in the morphology when compared to *px-ck* (**Fig. 12**). It has been described that ectopic expression of PEX11a protein results in the formation of elongated and tubular peroxisomes (Delille *et al.*, 2010; Koch *et al.*, 2010; Joshi *et al.*, 2012). As explained before (**Fig. 10 E** and **Fig. 11 C**), the functional protein fragment for each *pex11a* line is different, which could explain the differences observed in the peroxisomal phenotype.

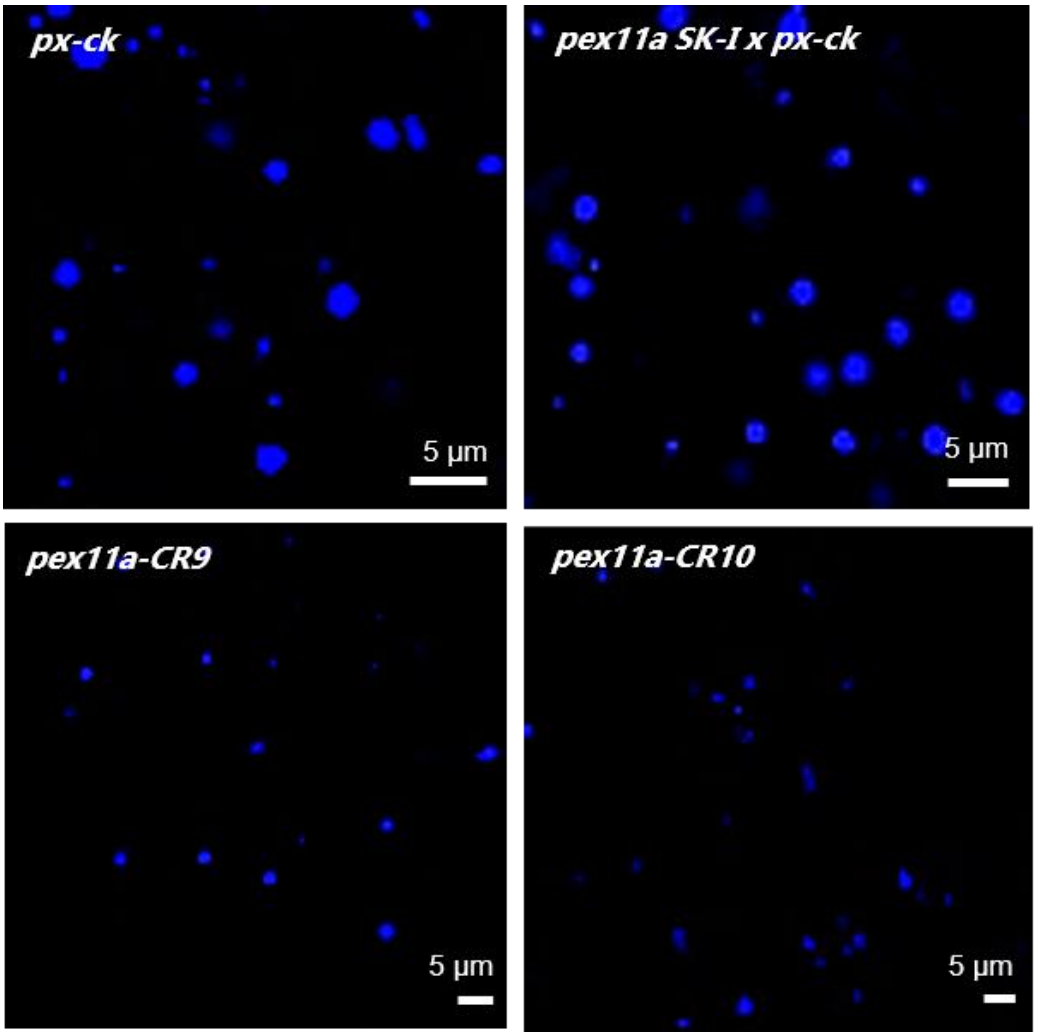

Figure 12. Imaging of peroxisomes from mutants altered in PEX11a. *Confocal image of leaves from untreated two-week seedlings of px-ck, pex11a SK-I x px-ck, pex11a-CR9 and pex11a-CR10 showing peroxisomes in blue. Bar=5 µm.*

3.5.2. Expression of the *PEX11* family in seedlings and adult plants

To investigate whether the alteration of isoform *a* produced change in the expression of the other *PEX11* family genes, the expression of the five isoforms was analyzed at two different points over Arabidopsis development (**Fig. 13**). Among the 5 isoforms analyzed, *PEX11c* and especially *PEX11d*, showed the highest expression in both, seedlings (two weeks) and leaves from adult plants (four weeks). The transcript levels observed at 2 weeks of growth in *px-ck* and *pex11a-CR9* mutant are not significantly different, but for *PEX11d*, which expression is higher in the mutant (**Fig. 13 A-B**). *pex11a-CR10* showed slightly but significant lower *PEX11a, c* and *e* while higher *PEX11d* expression levels in seedlings respect to *px-ck* (**Fig. 13**). For *pex11a SK-I x px-ck* lines, *PEX11a* expression was 3-fold reduced compared to *px-ck* at two and four weeks of growth (**Fig. 13 C**). These results agree with what we observed previously in semi quantitate analysis of *PEX11a* expression in *pex11a SK-I x px-ck*. No changes with respect to *px-ck* were observed for the other members of *PEX11* family in *pex11a SK-I x px-ck*. In 4-week adult *pex11a-CR10* plants, the reduction in the expression levels of *PEX11a* and *c* observed in seedling was maintained, but not for *PEX11e* (**Fig. 13 B**). Expression analysis by Orth et al. (2007) showed the expression of the five isoforms of *PEX11* family in seedling and rosette leaf, finding the higher expression for *PEX11e* and *PEX11d*, which agrees with our results. Although PEX11 isoforms seem to play different roles in peroxisomal proliferation, functional redundancy among various isoforms has been observed (Orth *et al.,* 2007).

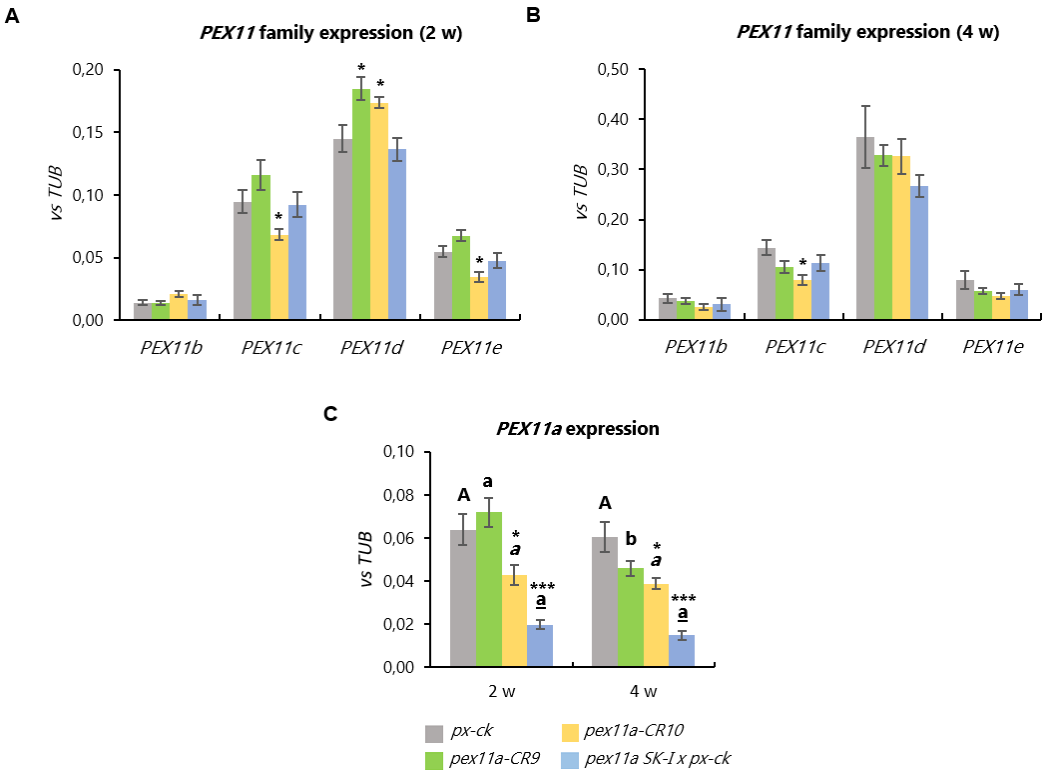

Figure 13. Analysis of PEX11 family expression by* qRT-PCR under control *conditions. (A) *Expression levels of PEX11b-e in two week old seedlings and* ***(B)*** *in adult plant leaves (four weeks).* ***(C)*** *Expression levels of PEX11a isoform in seddlings and adult plant leaves. Primers used are listed in* ***Table 2****. Asterisks denote significant differences between pex11a-CR9, pex11a-CR10 and pex11a SK-I and px-ck, within a PEX11 isoform, according to Student`s t-test (p-value <0.05: *; p-value <0.005: **; p-value <0.001: ***). In (C) different letters denote significant differences between 2 w and 4 w within the same genotype (px-ck: upper case; pex11a-CR9: lower case; pex11a-CR10: italics; pex11a SK-I; underlined) obtained by the Student`s t-test (p-value< 0.05).*

3.5.3. Germination phenotype in *pex11a* lines

In silico data suggest that *PEX11a* could be expressed to a greater extent in seeds, that's why germination rate of *PEX11a* mutants and seedling development in the following days after germination were studied. No differences were found regarding the germination rate at day 5, when comparing the different mutants with *px-ck* (**Fig. 14 A**). There was a delay in germination however, for *pex11a-CR9* and *pex11a-CR10* lines on day 2, finding a significantly lower number of germinated seeds (about half of the seeds) compared with *px-ck* (**Fig. 14 B-C**). *pex11a SK-I x px-ck* showed a germination rate similar to *px-ck*.

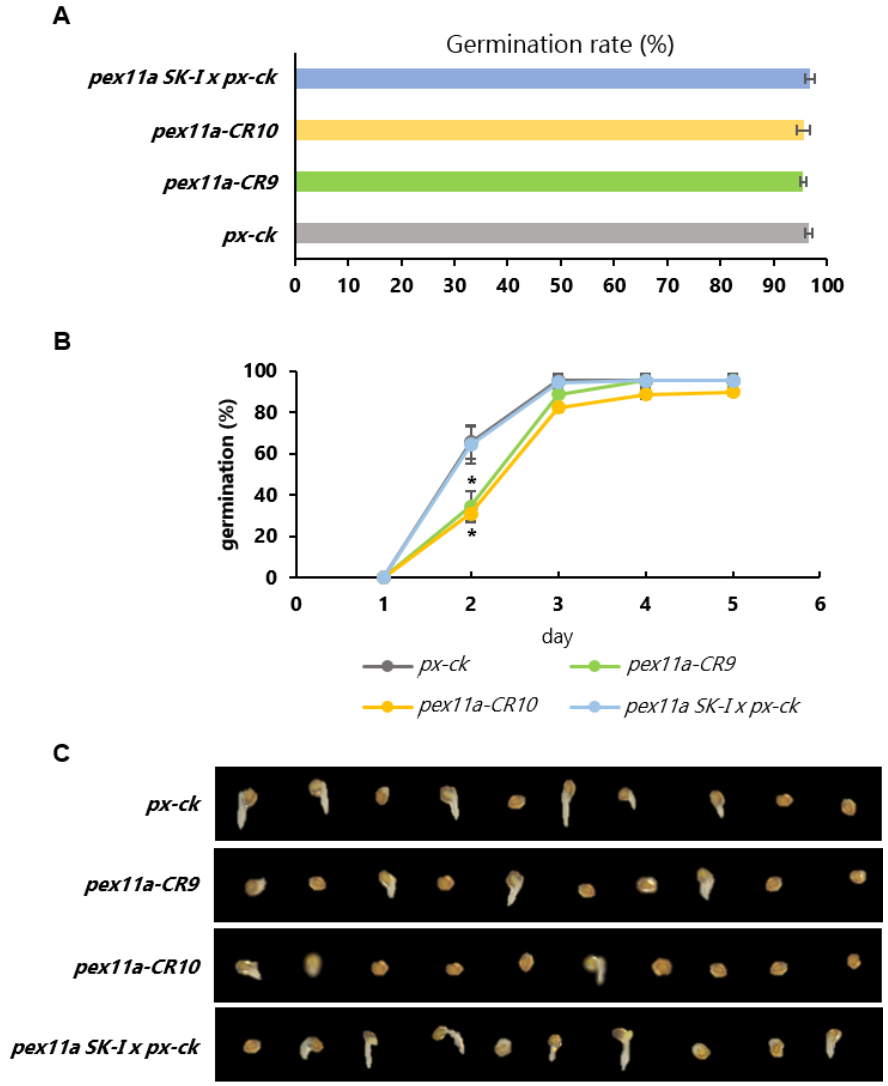

Figure 14. Germination of pex11a mutants under control conditions. (A) *Germination rate after 5 d.* ***(B)*** *Percentage of germinated seeds from day 0 to day 5.* ***(C)*** *Seeds on MS plates after 2 d. Data represent the mean ± SEM of at least three independent experiments, each with three replicates. The asterisks indicate significant differences between each line and px-ck (p-value <0.05: *) according to the Student's t-test.*

Peroxisomal membrane protein Pex11p from *Saccharomyces cerevisiae*, the orthologous of plant PEX11a, has been reported to be involved in medium-chain fatty acid (MCFA) β-oxidation (Van Roermund *et al.*, 2000). Disturbances of PEX11a, which is required to peroxules formation, could also affect β-oxidation because peroxules are

involved in the transfer of the sugar dependent 1 (SDP1) lipase from the peroxisomal membrane to the lipid body (Thazar-Poulot *et al.,* 2015). Therefore, alteration of PEX11a functionality in seeds could affect fatty acid metabolism which is essential for seed germination. In addition, when ROS reached a threshold, seeds dormancy is relieved and the following germination can be initiated being dependent on redox-signalling (Katsuya-Gaviria *et al.*, 2020). Further analysis in ROS/redox metabolism in *pex11a-CR* seeds will let us know if ROS/redox changes in mutant lines are the origin for alterations in germination observed. In addition to this, WRKY and MYB family have been related with seed development and the regulation of late embryogenesis (Kaplan-Levy *et al.*, 2012; Muthamilarasan *et al.*, 2015). Since *PEX11a* is expressed in the early stages of development and some regulatory sequences for TFs from these families have been found in *PEX11a* promoter, a link between them may exist, which deserve further analysis.

3.5.4. Phenotype of *pex11a* lines in response to hormone treatments

The effect on the germination rate in seeds sown in MS plates supplemented with ABA is shown in **Fig. 15 A**. There was a reduction of about 40 % in the three genotypes with 1 µM ABA and no differences were observed comparing mutants with *px-ck* neither with 4 µM nor with 10 µM ABA. In addition, the effects of other hormones and salt stress in *pex11a* mutants were tested. Seedling roots were measured after 4 d growing in plates supplemented with: 1-aminocyclopropane-1-carboxylic acid (ACC), O-(Carboxymethyl) hydroxylamine hemihydrochloride (AOA), gibberellic acid (GA3), indole-3-acetic acid (IAA), jasmonic acid (JA) and NaCl. None of the hormones tested nor the NaCl treatment had significant effects on the root growth of the mutants with respect to *px-ck.* We also evaluated if there was any effect adding the different treatments mentioned above in plants already grown in MS for 5 d, finding no changes in any case. Under control conditions however, a significant decrease of about 22 % in *pex11a-CR9* main root length was observed after 4 d growing in MS respect to *px-ck*, while no changes were detected in *pex11a SK-I x px-ck* (**Fig. 15 C**). These results together with *PEX11a in silico* expression located in epidermis and pericycle of control roots suggest a function for this gene in root development.

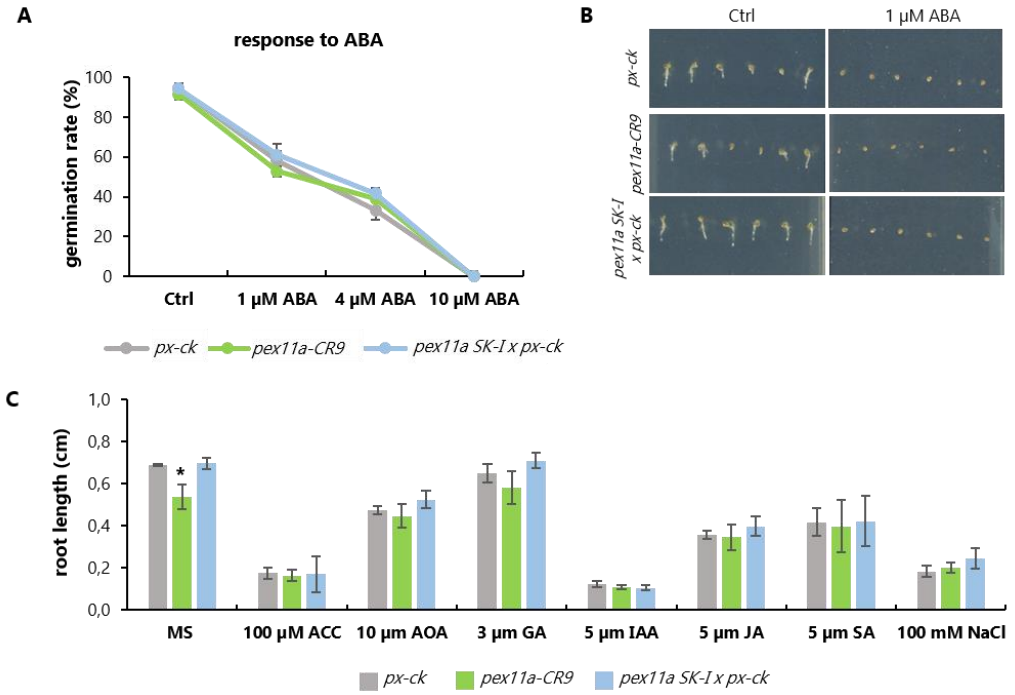

Figure 15. Seed germination and seedling growth in response to hormones and salt treatment. (A) *Seed germination rate after 5 days, in plates containing 1, 4 and 10 µM ABA.* ***(B)*** *Seedling phenotype after 3 days of 1 µM ABA treatment.* ***(C)*** *Root length of Arabidopsis seedlings, 4 days after 100 µM 1-aminocyclopropane-1-carboxylic acid (ACC), 10 µM O-(Carboxymethyl) hydroxylamine hemihydrochloride (AOA), 3 µM gibberellic acid (GA3), 5 µM indole-3-acetic acid (IAA), JA jasmonic acid (JA) and 100 mM NaCl treatment. Asterisks indicate significant differences between each line and px-ck (p-value <0.05: *) according to the Student's t-test.*

Information about the effect of phyto-hormones on PEX11 regulation is very scarce. In Arabidopsis plants ABA treatment upregulated only *PEX11d*, while in wheat plants ABA upregulated three PEX11d isoforms*, d-1*, *d-3 and d-4* in drought tolerant cultivars but not in the sensitive cultivars in which a significant up-regulation of *PEX11b* was observed (Ebeed *et al.*, 2018). In Arabidopsis plants ABA treatment upregulated *PEX11b* and *PEX11d*, meanwhile *PEX11c* was down regulated (Li and Hu, 2015). Therefore, *PEX11a* apparently is not regulated by ABA, and in our hands, effects of ABA on germination rate appears to be PEX11a-independent (**Fig. 15 B**). The absence of changes in root length of PEX11a-related mutants by NaCl treatment suggest that PEX11a has not an important role at least at this stage, in response to salinity, meanwhile *PEX11e* was up-regulated in Arabidopsis under salinity conditions (Mitsuya *et al.*, 2010).

3.5.5. Root phenotype in *pex11a* mutants

To study root architecture, seedlings were grown in plates of MS under long day conditions and after 10 d growing the length of the main root as well as the number of lateral roots (LR) were evaluated. Unlike what was observed in younger seedlings in control conditions (4 d; **Fig. 16 B**), no significant differences were found in the length of the main root at day 10 (**Fig. 16 A**).

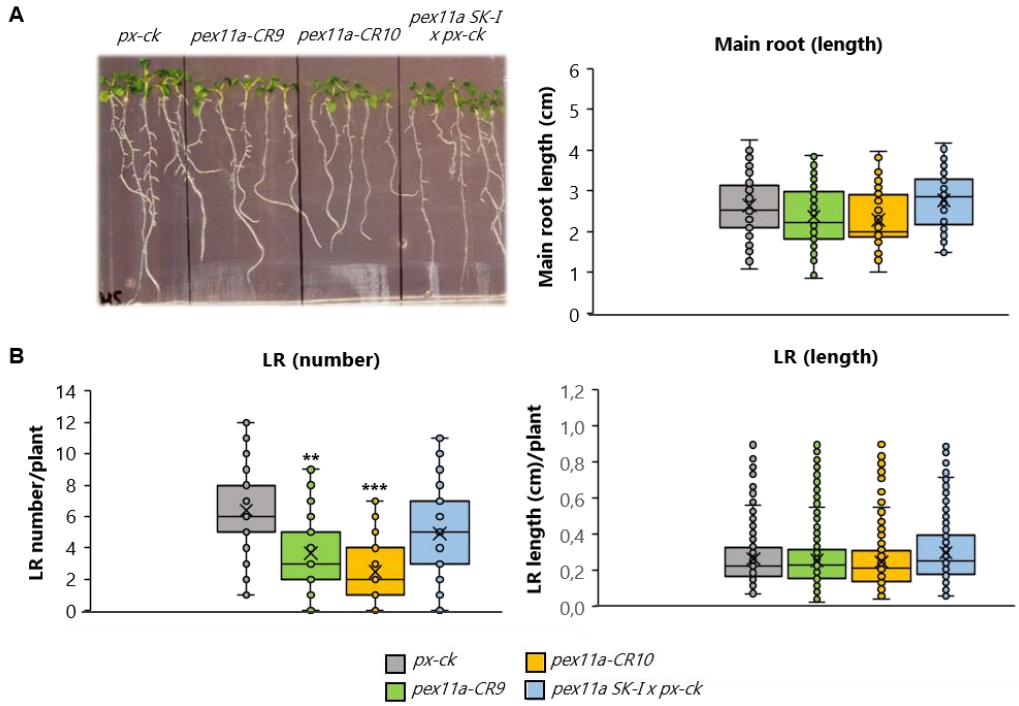

Figure 16. Root phenotype of px-ck seedlings and pex11a lines grown under control conditions. (A) *Phenotype of 10 day old seedlings and length of the main root.* ***(B)*** *Number of LR (n=240-265/phenotype) and length of the LR (n=290-500/genotype). Asterisks denote significant differences of each genotype compared to px-ck according to Student´s t-test (p-value <0.05: *; p-value <0.005: **; p-value <0.001: ***).*

px-ck seedlings showed an average of 6-7 LR per plant, while the value for the mutants *pex11a-CR9* and *pex11a*-CR10 was 2-3 LR. A slight decrease in the number of LR was also observed in *pex11a SK-I x px-ck* compared to *px-ck* seedlings although differences were not significant (**Fig. 16 B**). Regarding the length of the LR, no significant

changes were detected in any of the genotypes (**Fig. 16 B**). Previous *in silico PEX11a* expression observed in LR cap cells support a role for this peroxin in development of LR.

ROS are involved in multiple stages of plant root developmental processes such as meristem maintenance, root elongation, LR formation, root hair, endodermis, and vascular tissue differentiation (Eljebbawi *et al.*, 2021). Therefore, any disturbances in ROS production in *pex11a* mutants could explain the changes observed in LR numbers. In fact, *PEX11a* has been reported to be regulated by ROS (Rodríguez-Serrano *et al.,* 2016).

3.5.6. Plant growth in pex11a mutants

Plants were sown on soil under short- and long-day conditions and after 3 and 4 weeks, rosette area, as well as number of leaves and fresh weight were analyzed (**Fig. 17** and **Fig. 18**). *pex11a-CR9* mutant grown under short-day conditions exhibited a lower number of leaves on average compared to *px-ck* (10-11 vs. 12-13 leaves; **Fig. 17 A-B**), while in the case of *pex11a SK-I x px-ck* this feature was not altered (**Fig. 17 A-B**). Rosette area of the two *pex11a-CR* lines was about 1.5 lower than *px-ck* and in the case of *pex11a SK-I x px-ck* a no significant differences were observed respect to *px-ck* (**Fig. 17 A-C**). These results were supported by a statistically significant decrease (1.4-fold) in fresh weight for *pex11a-CR* lines (**Fig. 17 C**).

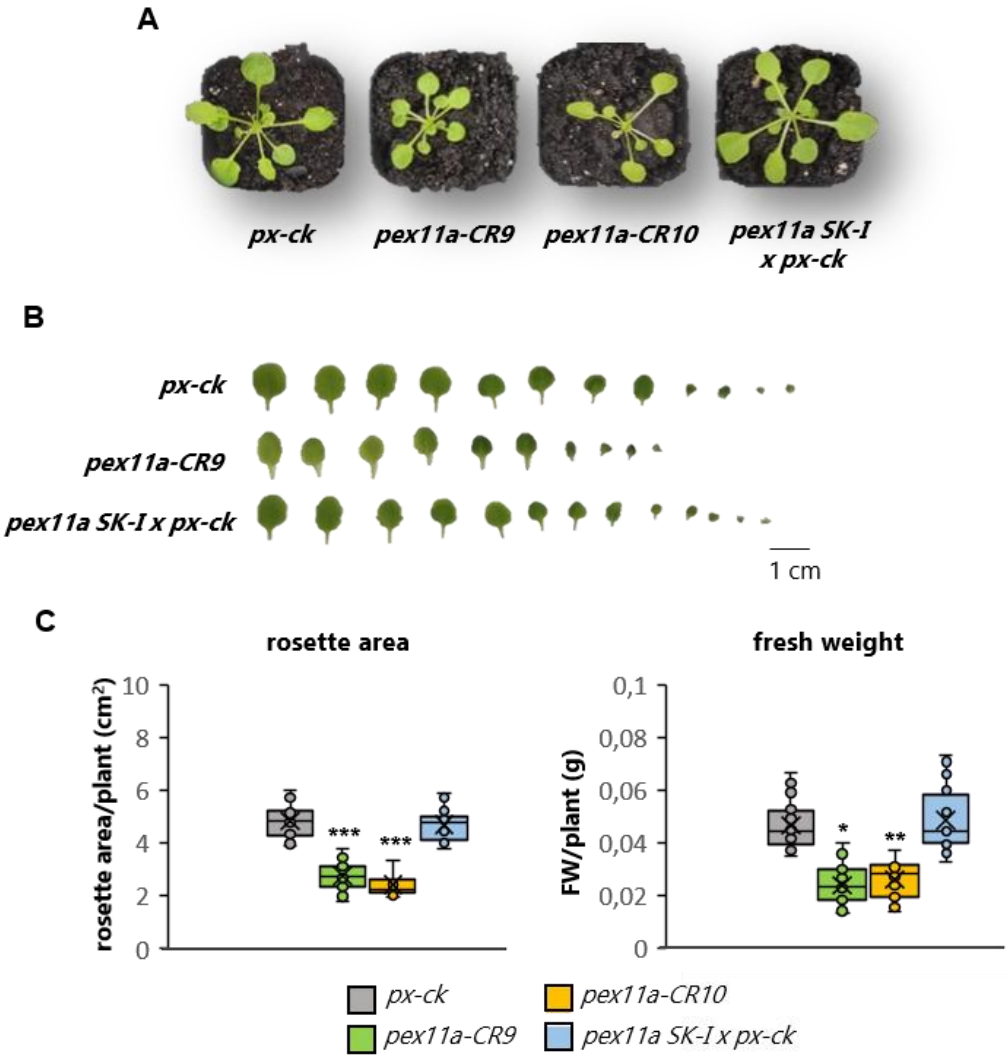

Figure 17. Phenotype and growth parameters of px-ck plants and pex11a mutants under short day conditions. (A) *Rosette leaf phenotype of 3-weeks-old plants.* ***(B)*** *Rosette leaves number of 3-weeks-old plants. Bar=1 cm.* ***(C)*** *Rosette area and fresh weight of px-ck and pex11a lines (n=30-40 plants). Asterisks denote significant differences between each genotype and px-ck according to Student´s t-test (p-value <0.05: *; p-value <0.005: **; p-value <0.001: ***).*

No significant differences were found in the number of leaves under long day conditions (**Fig. 18 A-B**). However, a reduction in the leaf area was measured in *pex11a-CR9* and *pex11a-CR10* plants grown under long-day conditions and the size of the rosette leaves was slightly larger in *pex11a SK-I x px-ck* than in *px-ck* plants (**Fig. 18 A-C**). Similar to short day conditions, a decrease of 1.3-fold of fresh weight was found in *pex11a-CR*

mutants and no significant differences in the fresh weight values of *pex11a SK-I x px-ck* plants compared to *px-ck* were detected (**Fig. 18 C**).

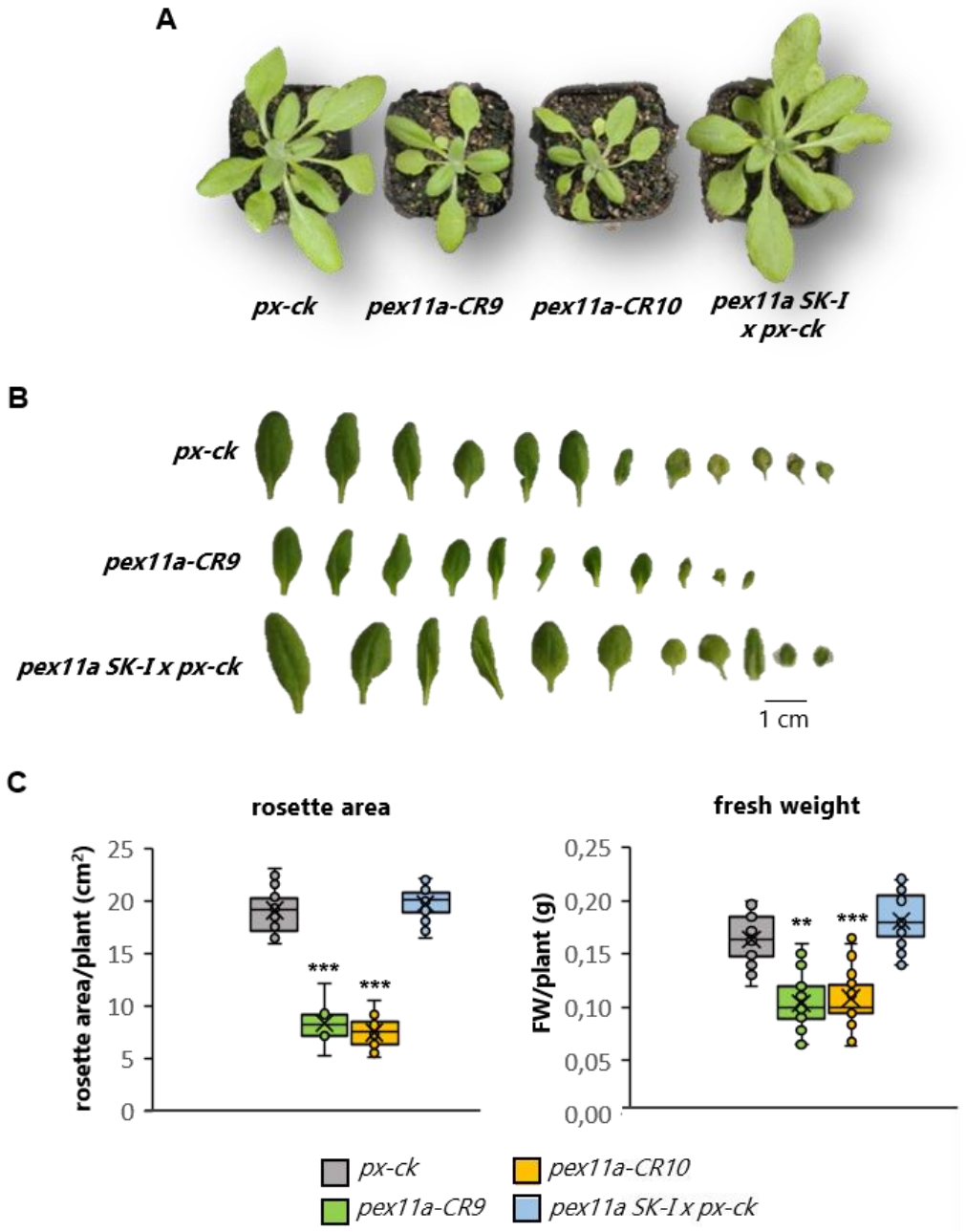

Figure 18. Phenotype and growth parameters of px-ck plants and pex11a mutants under long day conditions. (A) *Rosette leaf phenotype of 4-weeks-old plants.* ***(B)*** *Rosette leaves number of 3-weeks-old plants. Bar=1 cm.* ***(C)*** *Rosette area and fresh weight of px-ck and pex11a lines (n=30-*

*40 plants). Asterisks denote significant differences between each genotype and px-ck according to Student´s t-test (p-value <0.05: *; p-value <0.005: **; p-value <0.001: ***).*

Differences observed in the phenotype of *pex11a-CR9/CR10 and pex11a SK-I x px-ck* lines could be due to the differences in PEX11a sequence obtained in each case which would affect the structure and function of this protein. Furthermore, effects of T-DNA insertion in 3-D structure of the protein is unknown. Thus, *pex11a SK-I x px-ck* contains the Cys166, which apparently could act as a redox sensor, while this Cys is absent in the sequence of *pex11a-CR9* and *CR10*. Cys 166 is a putative target for *S*-nitrosylation following different prediction software such as, GPS-SNO (http://sno.biocuckoo.org/), pCysMod (Li *et al.*, 2021), SNO-site predictor (Li *et al.*, 2019), iSNO-PseAAC (Xu *et al.*, 2013) and Posttranslational Modifications (PTM) viewer (https://www.psb.ugent.be/webtools/ptm-viewer/experiment.php; **Fig. 19 A-C**). Furthermore, Cys 248, which would be absent in both mutants CR lines and *pex11a SK-I x px-ck*, is a putative target for *S*-palmitoylation and *S*-sulfinylation (**Fig. 19 A-C**). Targets for phosphorylation gave us S63 by PTM viewer while multiple aa may be targets for Tyr or Ser/Thr kinases phosphorylation following GPS-kinase predictor (Wang *et al.*, 2020; **Fig. 19 B-C**).

A

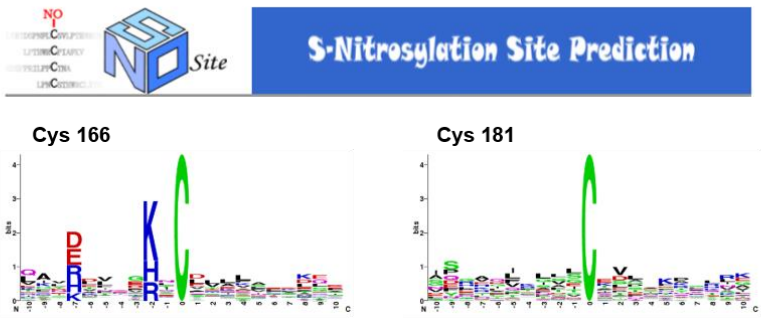

GPS :

Position	Peptide	Score	Cutoff	Cluster
166	KLNDEESCVASTIEI	2,918	2,443	Cluster B

P-CysModPredictRes

ID	Position	Modification	FPR	Peptide
sp|Q9FZF1|PX11A_ARATH	166	S-nitrosylation	0.00%	KLNDEESCVASTIEI
sp|Q9FZF1|PX11A_ARATH	248	S-palmitoylation	0.31%	THKNWISC*******
sp|Q9FZF1|PX11A_ARATH	248	S-sulfinylation	1.29%	THKNWISC*******

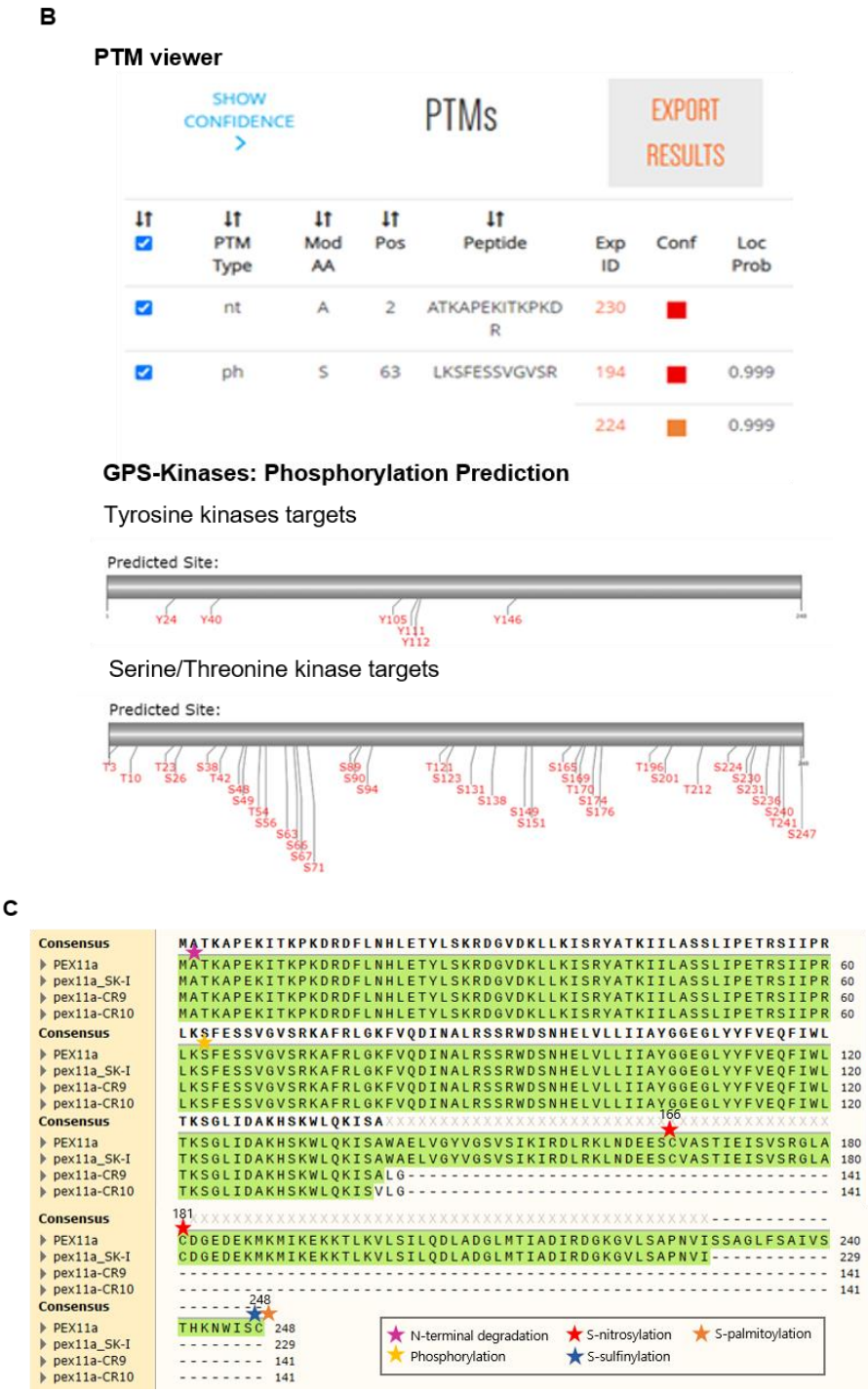

Figure 19. Putative Posttranslational modifications for PEX11a protein. (A) *Target aa prediction for different PTMs such as Cys modifications (S-nitrosylation, S-palmitoylation and S-sulfinylation) and* ***(B)*** *Ser, Thr and Tyr modifications (phosphorylation, ph). The second aa of the*

protein also may suffer N-terminal degradation (nt). ***(C)*** *Location of putative targets for the different PTMs in PEX11a sequence.*

In addition to elongation and proliferation of peroxisomes, PEX11a may have different functions already unknown in plants such as the function of yeast Pex11p in medium-chain fatty acid oxidation previously mentioned (Van Roermund *et al.*, 2000). In yeast Pex11 has been reported to be a pore-forming protein sharing sequence similarity with cation-selective channels melastatin-related transient receptor potential (TRPM) subfamily (Mindthoff *et al.*, 2016). This channel could conduct solutes with molecular mass below 300-400 Da, including β-oxidation metabolites, which would explain changes in the rate of β-oxidation in yeast *pex11* mutants (Van Roermund *et al.*, 2000; Mindthoff *et al.*, 2016). Disturbances in PEX11a protein could also affect the tethering and metabolites exchange between chloroplast-peroxisomes and mitochondria-peroxisomes, which in its turn could affect different metabolic pathways leading to plant developmental problems.

3.5.7. Silique and seed phenotype in *pex11a* lines

The appearance of the seeds as well as the number of siliques were also analyzed as part of the phenotypic characterization of *PEX11a* mutants. A small decrease in the size of the dry seeds was found in *pex11a-CR* mutant, although no significant changes in weight was detected (**Fig. 20 A**). Likewise, the appearance of the seeds was observed after 24 h in water but no alterations were detected (**Fig. 20 B**). The siliques, located in the main stem and in the branches, of plants grown under long day conditions were monitored, finding no differences neither in the number of siliques of the main stem nor in the total number of siliques (**Fig. 20 C**). There were also no changes in the development and appearance of the siliques in the mutants compared to the *px-ck* (**Fig. 20 B**).

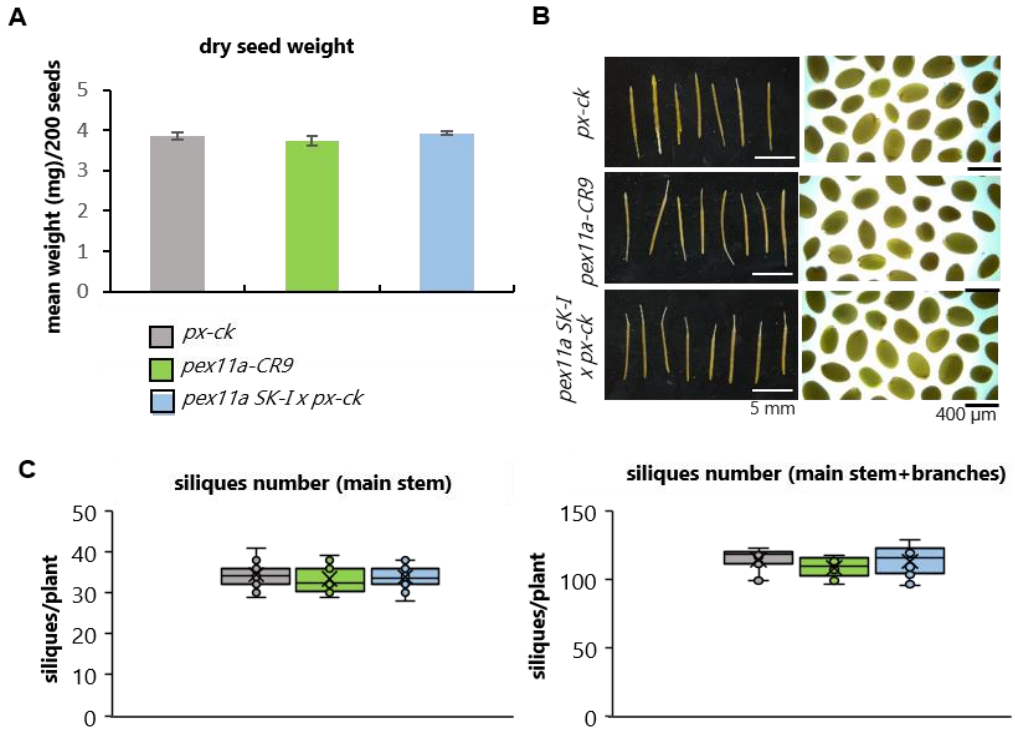

Figure 20. Number of siliques and phenotype of px-ck and pex11a mutant seeds. (A) *Average of dry seed weight (3 replicates with 200 seeds each).* ***(B)*** *Phenotype of seeds after being embedded in water for 24 h (bar=400 µm) and siliques (bar=5 mm).* ***(C)*** *Siliques number found in the main stem and the branches of the plant.*

3.5.8. Pollen germination ability of *pex11a* lines

PEX11a expression is induced in mature pollen according to the information provided by ePlant from BAR website. Therefore, a pollen germination test was carried out in order to observe if the alteration of the *PEX11a* gene was affecting pollen germination. No differences were observed when pollen germination of the mutants was compared to *px-ck* (**Fig. 21**).

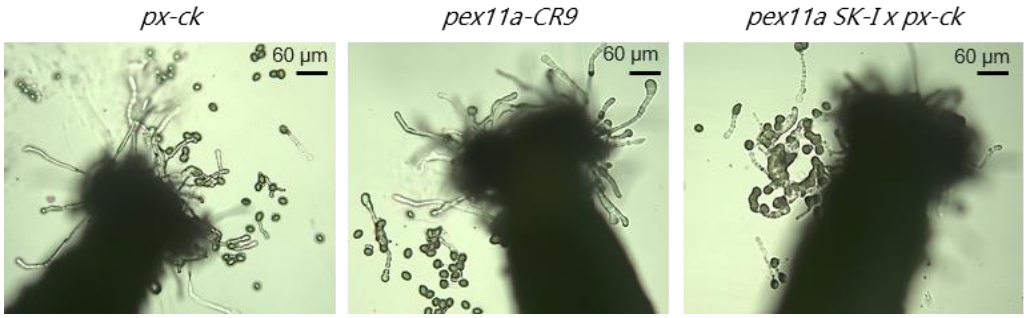

Figure 21. Pollen germination assay for px-ck, pex11a-CR9 and pex11a SK-I x px-ck. *The protocol of Daher et al. 2009 was followed for pollen germination on solid surface and images were taken 6 h after the beginning of incubation. Pistil (in dark) was placed near the pollen grains to facilitate germination. Bar=60 µm.*

Based on these results, and previous results on number of seeds, PEX11a apparently have not an essential function on plant reproduction.

3.6. Analysis of *pex11a* lines in response to Cd

3.6.1. Effect of Cd on root growth

Seeds were plated on MS supplemented with 50 and 100 µM $CdCl_2$ to evaluate the effect of this heavy metal on the growth of mutant seedlings. The main root of *pex11a-CR9* was significantly shorter compared to *px-ck under* control conditions after 7 d growing (**Fig. 22**), showing a reduction of 23 % as we reported before for 4 day old seedlings. This result is in accordance with the reduction of plant size previously mentioned in *pex11a-CR9* under control conditions. In contrast, no changes were found in *pex11a SK-I x px-ck* in control conditions. We observed that Cd strongly inhibits root growth of all genotypes at 7 d, especially at the highest concentration (**Fig. 22**). However, a reduction of 58 % in root length was found in *px-ck* seedlings with 50 µM $CdCl_2$, while this value was 38 % and 64 % for *pex11a-CR9* and *pex11a SK-I x px-ck,* respectively. These results suggest that PEX11a may be involved in Cd-dependent root growth decrease, although disturbances in PEX11a may affect differently to the metal depending on the kind of mutation.

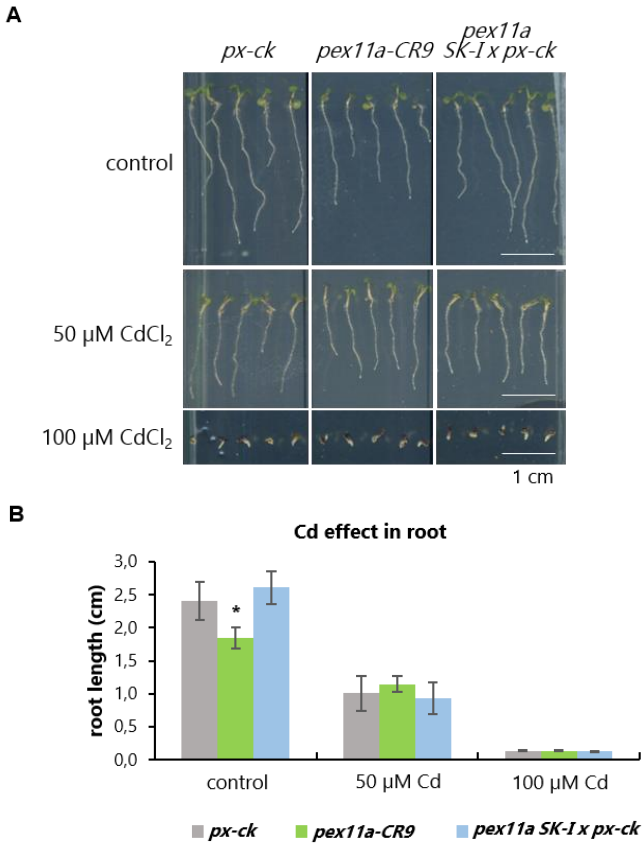

Figure 22. Effects of different Cd concentrations on root growth of px-ck and pex11a mutant seedlings. (A) *Representative images of 7-day-old Arabidopsis seedlings grown in MS medium supplemented with 0, 50, and 100 µM $CdCl_2$.* ***(B)*** *Length of the main root measured at 7 days of $CdCl_2$ treatment (n=120-160).*

3.6.2. Ultrastructure of peroxisomes in *pex11a* mutants

To get a deeper insight into the structure and ultrastructure of peroxisomes and to study additional organelle alterations derived from the treatment with Cd we analyzed the morphology of peroxisomes by optical and electron microscopy at short time (1 h) and long time (72 h) Cd treatment using DAB citochemistry (**Fig. 23**). Interestingly, the number of peroxisomes per cell was 0.2-fold higher in *pex11a-CR9* under control conditions compared to *px-ck* at 1 h (**Fig. 23 A-B**). However, we found a decrease around 0.8-times in peroxisome number in *pex11a-CR9* and also in *pex11a SK-I x px-ck* in control plants at 72 h (**Fig. 23 A-B**). Cd treatment did not affect peroxisome number per cell after 1 h in *px-ck,* while the number was significantly reduced in both *pex11a-CR9* and *pex11a*

SK-I x px-ck (**Fig. 23 B**). Surprisingly, after 72 h of Cd treatment, the number of peroxisomes per cell in *px-ck* decreased, whilst it was higher in the two *pex11a* lines (**Fig. 23 B**). Regarding the size of the organelles, after 1 h of treatment an increase in the peroxisomal area was observed both in *px-ck* and in *pex11a-CR9* but not in *pex11a SK-I x px-ck*. The same trend was found in the long time treatment (**Fig. 23 C**). *pex11a SK-I x px-ck* peroxisomes were found to be significantly larger than those of *px-ck* under control conditions.

A

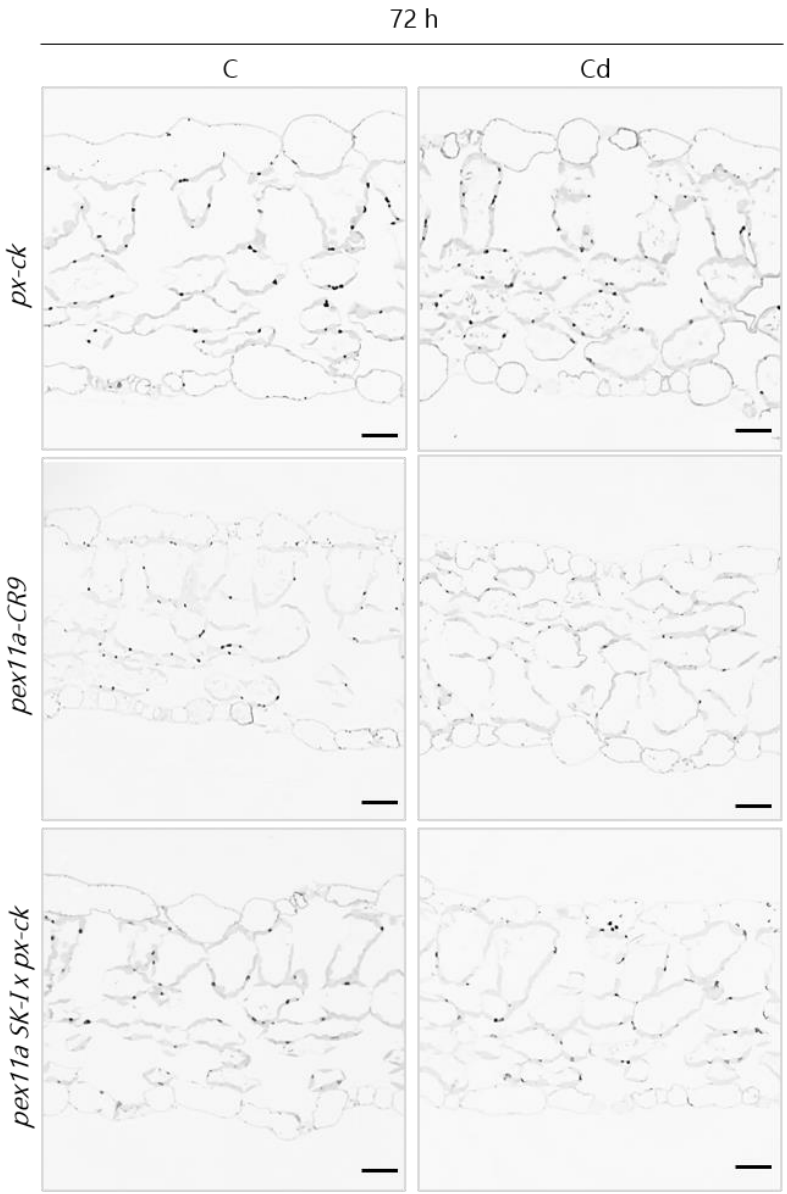

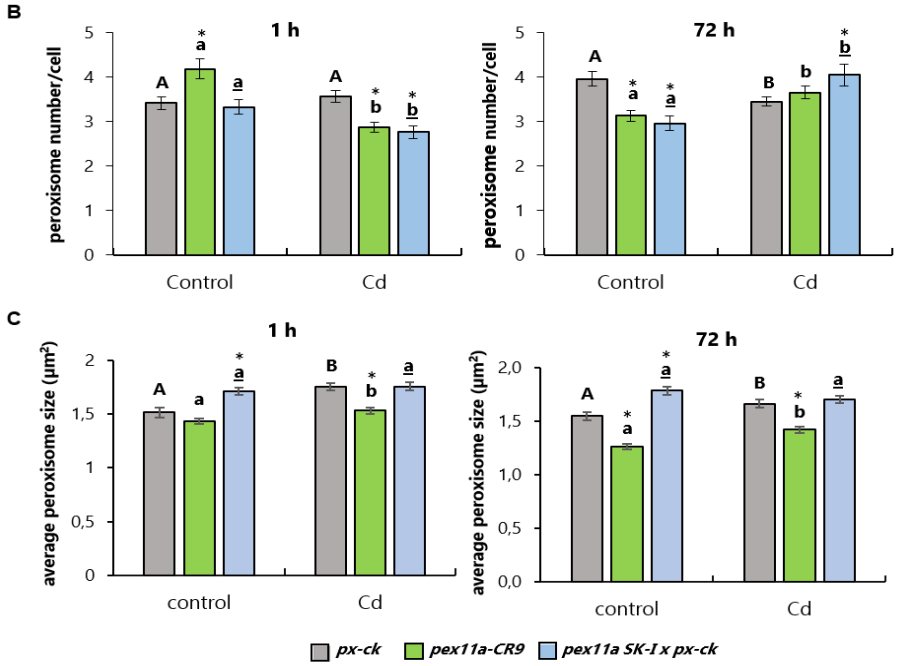

Figure 23. Optical microscopy analysis of catalase-mediated staining of peroxisomes with 3'3-diaminobenzidine (DAB) in thin leaf sections. ***(A)*** *Representative images of thin leaf-sections from seedlings of px-ck, pex11a-CR9 and pex11a SK-I x px-ck treated or not with Cd (72 h). Representative peroxisomes are indicated with arrows. Bar= 20 µM.* ***(B)*** *Count of the number of peroxisomes per cell in thin leaf sections.* ***(C)*** *Average peroxisomes size measured in thin leaf sections. Different letters denote significant differences between Cd treatment and control within the same genotype (px-ck: upper case; pex11a-CR9: lower case; pex11a SK-I; underlined) obtained by the Student`s t-test (p-value< 0.05). Asterisks denote significant differences between pex11a-CR9 or pex11a SK-I and px-ck, within control or treatment, according to Student`s t-test (p-value <0.05).*

These results point to a role for PEX11a in both, division and proliferation under control conditions and in response to Cd stress. Considering that peroxisomal population is regulated by division/proliferation and peroxisomal degradation by specific autophagy termed pexophagy (Calero-Muñoz *et al.*, 2019; Olmedilla and Sandalio, 2019) we cannot exclude that pexophagy could be also altered in *pex11a* mutants. In fact, Calero-Muñoz et al. (2019) have reported that Cd regulate peroxisomal abundance by inducing pexophagy in Arabidopsis leaves (Calero-Muñoz *et al.*, 2019).

3.6.3. Peroxisomal phenotype of *pex11a* lines

It has been previously described that Cd induces peroxisome proliferation after 3 h of treatment (Rodríguez-Serrano *et al.*, 2016). To assess if peroxisome proliferation in response to Cd is affected in *pex11a* mutants we used high magnification CLSM images taken after 4 h of Cd treatment to image and count peroxisomes. A quantification of the number of peroxisomes per leaf area and the size of the organelles were carried out in CLSM images. We observed a marked decrease in the size of peroxisomes in *pex11a-CR* lines but not in *pex11a SK-I x px-ck* compared to *px-ck* control (**Fig. 24 A** and **B**). Interestingly, in *px-ck* plants treated with Cd the average area decreased 1.9 μm^2, while in *pex11a SK-I x px-ck* the reduction was 0.6 μm^2, being this size significantly higher than *px-ck* under Cd conditions. However, in *pex11a-CR* mutants the area of peroxisomes treated and untreated with Cd was very similar (**Fig. 24 A-B**). After analyzing peroxisomal proliferation in response to Cd, we found a significantly higher number of peroxisomes in *px-ck* plants treated with Cd, as previously described (Rodríguez-Serrano *et al.*, 2016; Terrón-Camero *et al.*, 2020). The same trend was found in *pex11a SK-I x px-ck.* Although a slight but not significant increase in the number of peroxisomes was observed in *pex11a-CR* mutants (**Fig. 24 A-C**).

A

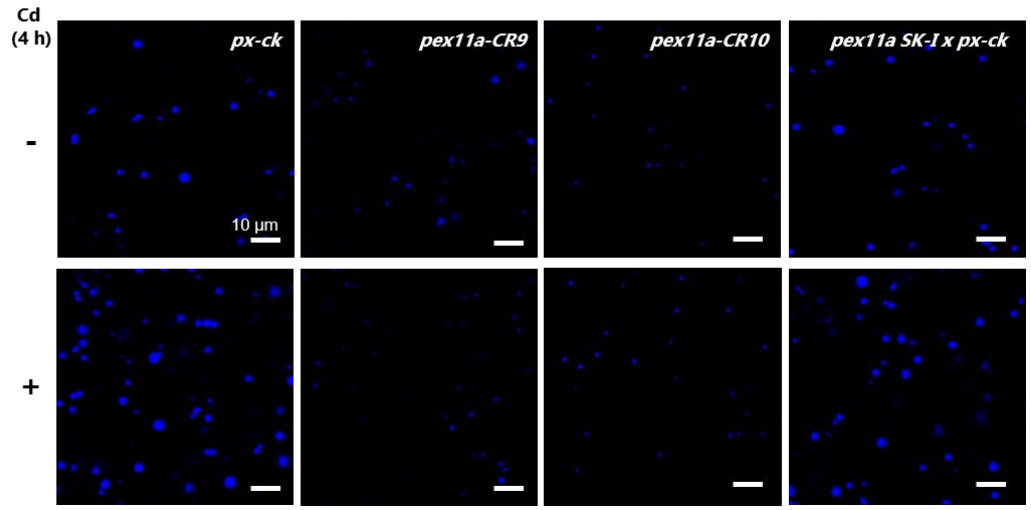

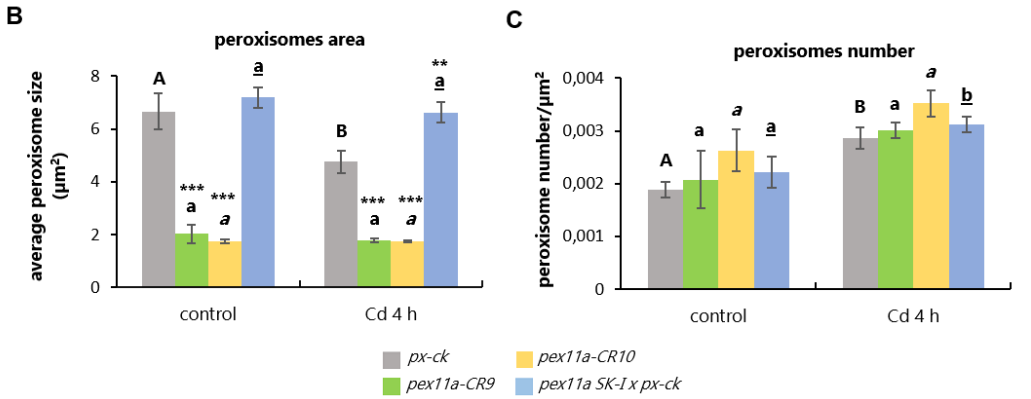

Figure 24. Effect of cadmium on peroxisome proliferation. (A) *Representative CLSM images of leaves from two-week seedlings of px-ck, pex11a-CR9, pex11a-CR10 and pex11a SK-I x px-ck treated or not with 100 µm Cd for 4 h. Bar=10 µm.* ***(B)*** *Average size of peroxisomes (µm²) and* ***(C)*** *Number of peroxisomes/µm². Data represent the mean from at least 3 experiments (images number=20-60). Different letters denote significant differences between Cd treatment and control within the same genotype (px-ck: upper case; pex11a-CR9: lower case; pex11a-CR10: italics; pex11a SK-I; underlined) obtained by the Student`s t-test (p-value< 0.05). Asterisks denote significant differences between pex11a-CR9, pex11a-CR10 or pex11a SK-I and px-ck, within a time-point, according to Student`s t-test (p-value <0.05: *; p-value <0.005: **; p-value <0.001: ***).*

The decrease of peroxisomal area for *pex11a-CR9* and *pex11a-CR10* observed by CLM contrasts with the absence of significant changes between the different lines observed by histochemistry. An explanation could be related with disturbances of CFP-SKL import to peroxisomes due to changes of PEX11a structure. This effect has been previously observed in Arabidopsis lines with disturbances in peroxisomal proteins such as glycolate oxidase and acyl CoA oxidase when crossing with *px-ck* lines. The reduction of peroxisomal size observed in *px-ck* in response to Cd could be due to the proliferation of peroxisomes giving rise smaller peroxisomes originated from constriction of elongated peroxisomes (Rodríguez-Serrano *et al.*, 2016). This fact agrees with the statistically significant increase of peroxisomal population observed in *px-ck* after 4 h treatment. Similar results were obtained in *pex11a SK-I x px-ck*, while apparently CRISPR/Cas9 mutants did not experience significant peroxisome proliferation. Taking into account the data obtained with DAB histochemistry after 72 h of treatment, we can speculate that *pex11a* mutants would be able to proliferate; however, we cannot discard that disturbances in PEX11a could affect pexophagy regulation promoting peroxisomes accumulation after long periods of treatment.

3.6.4. Peroxules production in *px-ck* and *pex11a* lines in response to Cd

It has been previously reported that Cd induces peroxisomal membrane extensions, so-called peroxules, very soon after treatment, followed by elongation of the peroxisomes, with constriction, beading and fragmentation into new peroxisomes during peroxisome proliferation (Rodríguez-Serrano *et al.,* 2016). The analysis of peroxules formation in *px-ck* lines shows that these structures contact with chloroplasts and mitochondria (**Fig. 25 A-B**) as it was previously reported (Rodríguez-Serrano *et al.,* 2016). Interestingly, the length of peroxules is apparently related with the length of cell, as shown in hypocotyls (**Fig. 25 B**). Furthermore, we have also observed peroxules connections with plasma membrane (**Fig. 25 C, video 1 A-B in CD**) suggesting new roles for these extensions yet unexplored. Interestingly, the analysis of vascular tissue in leaves showed that peroxules formation takes place in the direction of cytoplasmic streaming (**Fig. 26, video 2 in CD**), which could be associated to the highest *PEX11a* expression observed in leaf vascular tissue (**Fig 8**). This result support that peroxules formation requires peroxisomal contact with cytoskeleton or endoplasmic reticulum (Mathur, 2021) which in its turn govern cytoplasmic streaming (Ueda *et al.,* 2010; Woodhouse and Goldstein, 2013). Several evidences have demonstrated that cytoskeleton and motor proteins are involved in endoplasmic reticulum and cytoplasmic streaming (Ueda *et al.,* 2010; Woodhouse and Goldstein, 2013), organelles motility and organelle extension production, such as peroxules, matrixules and estromules (see review by Mathur, 2021). However, proteins that may directly link cytoskeleton or ER to organelles extension formation has not been yet identified.

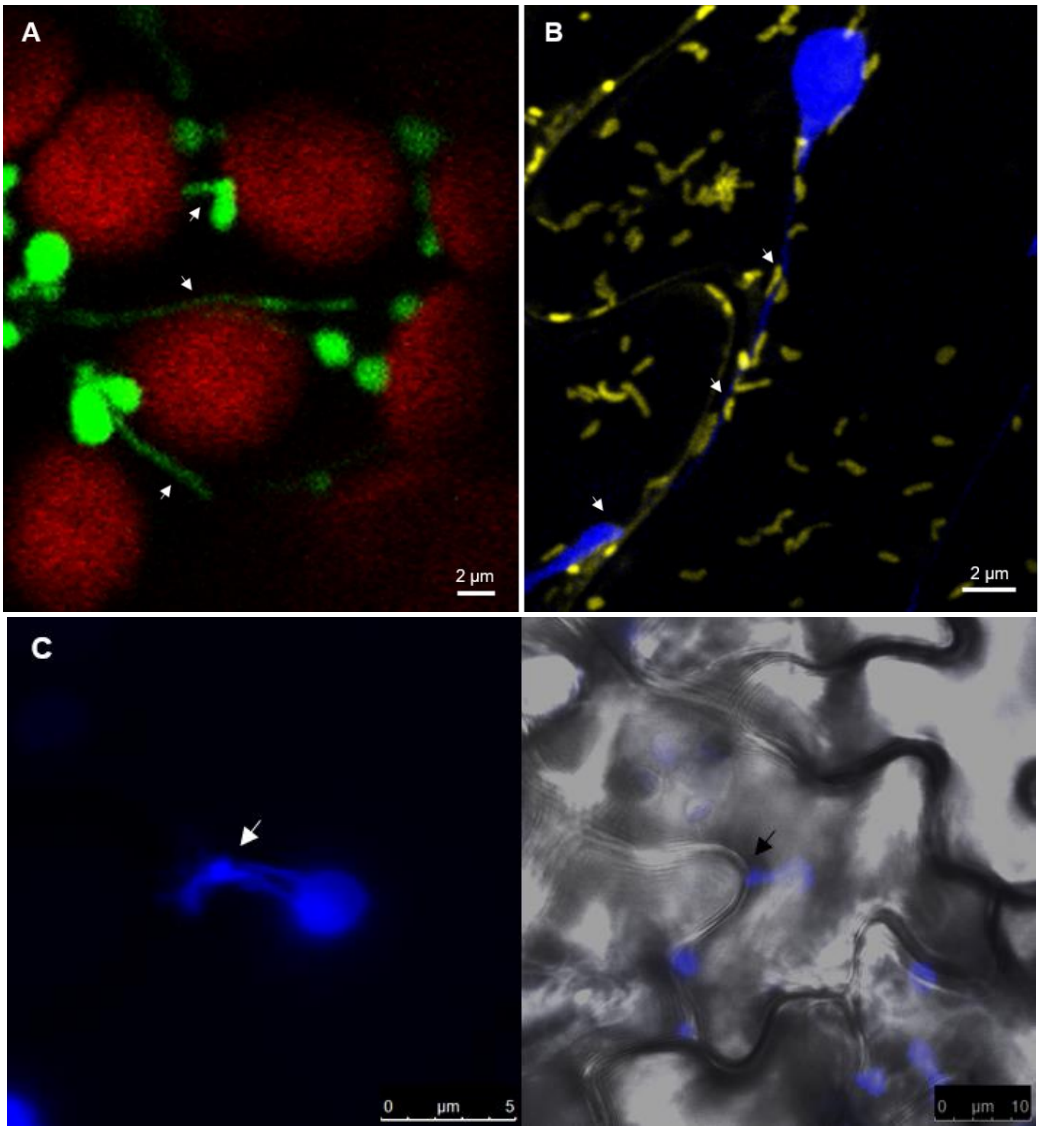

Figure 25. Peroxules contacts with chloroplasts, mitochondria and plasma membrane. *CLSM images of leaves from two-week seedlings of px-gk, px-ck and px-ck x mit-yk treated with 100 µm Cd for 30 min.* ***(A)*** *Mesophyll cells showing peroxisomes (green) and chloroplasts (reed).* ***(B)*** *Hypocotyl cells showing peroxisomes (blue) and mitochondria (yellow).* ***(C)*** *Epidermis cells showing a peroxisome and peroxules (blue).* ***(D)*** *Overlay of image C and bright field showing peroxules contact with plasma endoplasmic membrane. Contact sites of peroxules and other cell compartments are pointed by arrows.*

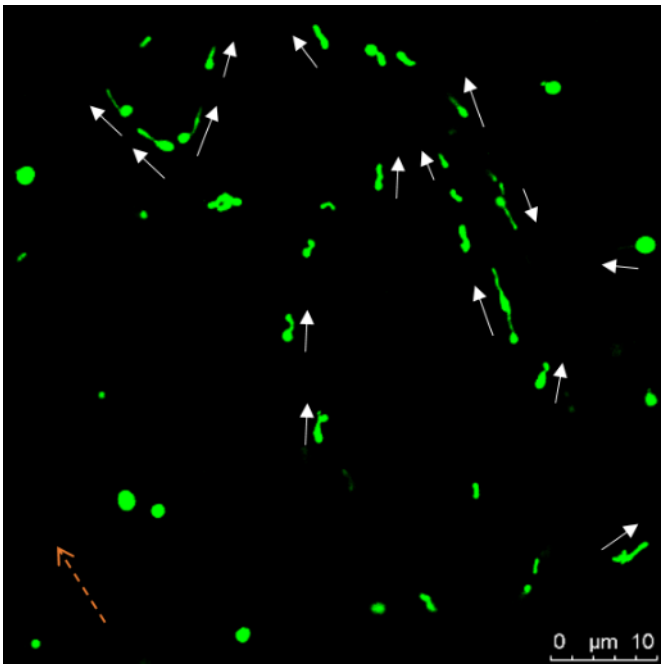

Figure 26. Peroxules observation in vascular tissue. *CLSM image of leaves from two-week seedlings of px-ck treated with 100 µm Cd for 30 min. Peroxisomes are shown in green, and the direction of the cytoplasmic streaming is indicated by the dashed orange arrow. Whites arrows pointed peroxules direction.*

Among the five PEX11 isoforms, *PEX11a* is essential for peroxules production having reported that the highest number of these dynamic extensions in *px-ck* was observed after 30 min of incubation with Cd (Rodríguez-Serrano *et al.,* 2016). We tested the ability to produce peroxules in the different mutants under the same conditions. In the presence of 100 µM Cd, we rarely observed peroxules in *pex11a* lines. Instead of fine, long and highly dynamic extensions, we observed in *pex11a* mutants a barely protrusion from the body of the peroxisome, somewhat similar to buds (**Fig. 27, video 3 in CD**). In *px-ck* plants it has been described that around 30-40 % of peroxisomes per leaf area produce peroxules (Rodríguez-Serrano *et al.,* 2016). Peroxisomal phenotype of *pex11a-CR* lines is similar to those of *pex11a* RNAi mutant and, as previously observed by Rodríguez-Serrano et al. (2016), we have also observed no peroxules in *pex11a-CR* nor in *pex11a SK-I x px-ck* lines in response to Cd. These results corroborate the essential role of PEX11a in peroxules formation and suggest that the sequence of protein lost in both *pex11a* lines would be required for peroxules production. Final Cys 248, absent in *pex11a-CR* and *pex11a SK-I x px-ck*, may be target of redox PTMs, such as *S*-sulfenylation as

predicted by PTM viewer (**Fig. 19**) We cannot discard however, that Cys166, present in *SK-I* but not in *CR* lines, could be necessary for peroxules production, as effects of T-DNA insertion on 3-D structure of PEX11a in *pex11a SK-I x px-ck* mutants is unknown as mentioned before.

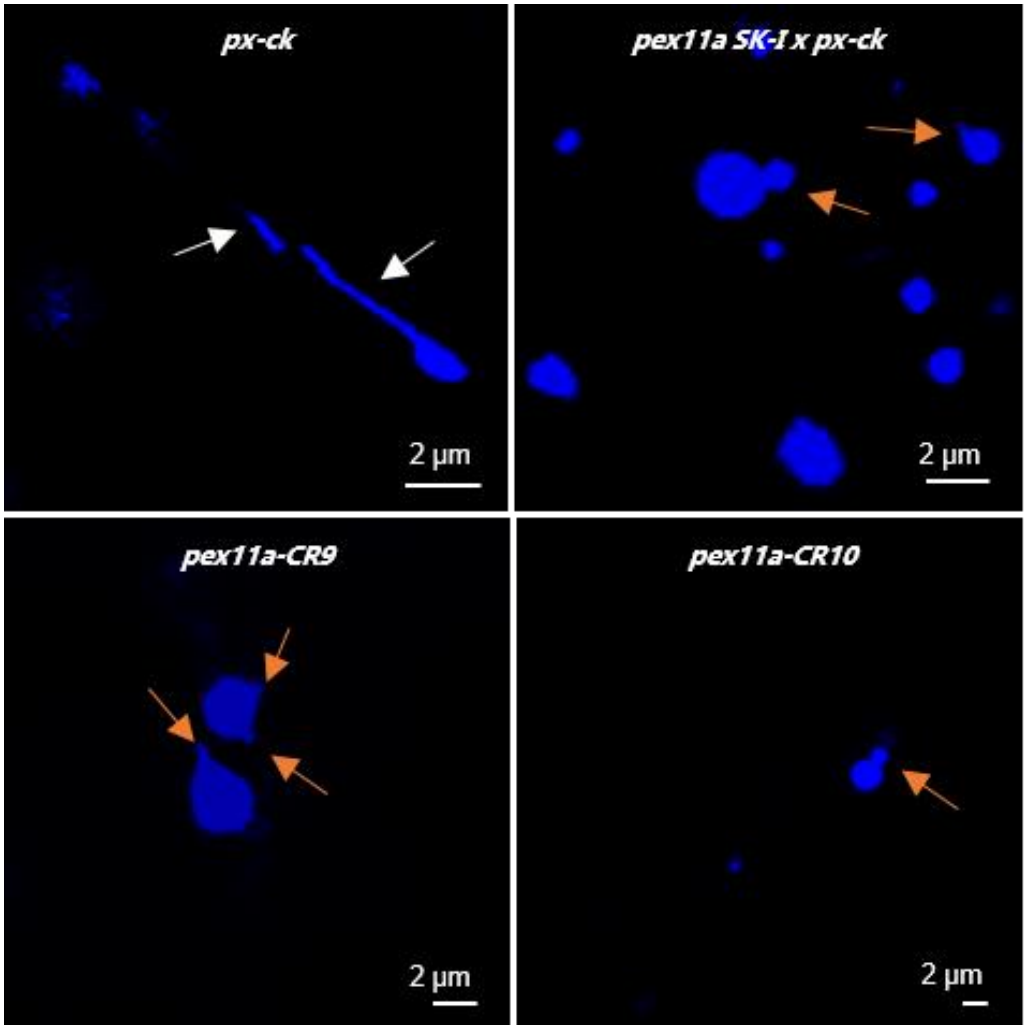

Figure 27. Peroxules production under Cd stress. *Two-weeks-old seedlings leaves of px-ck, pex11a SK-I x px-ck, pex11a-CR9 and pex11a-CR10 were explored in CLSM after 30 min Cd. White arrows denote peroxules and orange arrows buds.*

Rodríguez-Serrano et al. (2016) demonstrated that both peroxules formation and *PEX11a* expression were regulated by ROS production by NADPH oxidases. Then, we can speculate that ROS production induced by different stress conditions could affect PEX11a

structure or functionality by ROS-dependent PTMs. In fact, rapid peroxule induction without significant changes in *PEX11a* expression has been reported in *nox1* Arabidopsis mutants in response to Cd (Terrón-Camero et al., 2020), thus suggesting that PEX11a can be regulated by specific ROS and NO-dependent PTMs. Disturbances inPEX11a structure could disturb PEX11a/DRPs interaction or affect tethering with other organelles such as chloroplasts. Thus, Gao et al. (2016) using near-infrared optical tweezers combined with total-internal-reflection-fluorescence microscopy, were able to demonstrate that chloroplasts and peroxisomes are physically tethered through peroxules. These authors suggest that peroxules could have a role in maintaining peroxisome-organelle interactions in the dynamic environment, highlighting a crucial role for organelle interactions for essential biochemistry and physiological processes such as fatty acid β-oxidation and photorespiration (Gao *et al,* 2016). In addition, Rodríguez-Serrano et al. (2016) demonstrated that peroxules could participate in ROS-dependent signalling and/or ROS homeostasis in the cell and therefore have a key role in regulating stress perception and fast cell responses to environmental cues. However, no connection between peroxules and nuclei has been established so far, although chloroplasts extensions termed stromules, participate in H_2O_2 transfer from chloroplast to nucleus, and therefore are involved in retrograde signalling processes (Caplan *et al.,* 2015; Kumar *et al.,* 2018). Deciphering the mechanism of peroxule-dependent signalling process is a challenging which will require a combined molecular and cellular efforts.

4. REFERENCES

Bustin SA, Benes V, Garson JA, et al. 2009. The MIQE guidelines: Minimum information for publication of quantitative real-time PCR experiments. Clinical Chemistry **55**, 611–622.

Calero-Muñoz N, Expósito-Rodríguez M, Collado-Arenal AM, et al. 2019. Cadmium induces reactive oxygen species-dependent pexophagy in Arabidopsis leaves. Plant, Cell and Environment **42**, 2696–2714.

Caplan JL, Kumar AS, Park E, Padmanabhan MS, Hoban K, Modla S, Czymmek K, Dinesh-Kumar SP. 2015. Chloroplast stromules function during innate immunity. Developmental Cell **155**, 3–12.

Castillo MC, Sandalio LM, Del Río LA, León J. 2008. Peroxisome proliferation, wound-activated responses and expression of peroxisome-associated genes are cross-regulated but uncoupled in Arabidopsis thaliana. Plant, Cell and Environment **31**, 492–505.

Delille HK, Agricola B, Guimaraes SC, Borta H, Lüers GH, Fransen M, Schrader M. 2010. Pex11pβ-mediated growth and division of mammalian peroxisomes follows a maturation pathway. Journal of Cell Science **123**, 2750–2762.

Desai M, Pan R, Hu J. 2017. Arabidopsis Forkhead-Associated Domain Protein 3 negatively regulates peroxisome division. Journal of Integrative Plant Biology **7**, 235–236.

Desai M, Hu J. 2008. Light induces peroxisome proliferation in Arabidopsis seedlings through the photoreceptor phytochrome A, the transcription factor HY5 homolog, and the peroxisomal protein peroxin11b. Plant Physiology **146**, 1117–1127.

Ebeed HT, Stevenson SR, Cuming AC, Baker A. 2018. Conserved and differential transcriptional responses of peroxisome associated pathways to drought, dehydration and ABA. Journal of Experimental Botany **69**, 4971–4985.

Eljebbawi A, Rondón-Guerrero YDC, Dunand C, Estevez JM. 2021. Highlighting reactive oxygen species as multitaskers in root development. iScience **24**, 1–23.

Fahy D, Sanad MNME, Duscha K, et al. 2017. Impact of salt stress, cell death, and autophagy on peroxisomes: Quantitative and morphological analyses using small fluorescent probe N-BODIPY. Scientific Reports **7**, 1–17.

Gao H, Metz J, Teanby NA, Ward AD, Botchway SW, Coles B, Pollard MR, Sparkes I. 2016. In vivo quantification of peroxisome tethering to chloroplasts in tobacco epidermal cells using optical tweezers. Plant Physiology **1**: 263-72.

Gong S, Ding Y, Hu S, Ding L, Chen Z, Zhu C. 2019. The role of HD-Zip class I transcription factors in plant response to abiotic stresses. Physiologia Plantarum **167**, 516–525.

Guo M, Liu JH, Ma X, Luo DX, Gong ZH, Lu MH. 2016. The plant heat stress transcription factors (HSFS): Structure, regulation, and function in response to abiotic stresses. Frontiers in Plant Science **7**, 114.

Hinojosa L, Sanad MNME, Jarvis DE, Steel P, Murphy K, Smertenko A. 2019. Impact of heat and drought stress on peroxisome proliferation in quinoa. Plant Journal **99**, 1144–1158.

Jansen RLM, Santana-Molina C, Van Den Noort M, Devos DP, Van Der Klei IJ. 2021. Comparative genomics of peroxisome biogenesis proteins: Making sense of the PEX proteins. Frontiers in Cell and Developmental Biology **20**, 654163.

Joshi S, Agrawal G, Subramani S. 2012. Phosphorylation-dependent Pex11p and Fis1p interaction regulates peroxisome division. Molecular Biology of the Cell **23**, 1307–1315.

Kaplan-Levy RN, Brewer PB, Quon T, Smyth DR. 2012. The trihelix family of transcription factors-light, stress and development. Trends in Plant Science **17**, 163–171.

Katsuya-Gaviria K, Caro E, Carrillo-Barral N, Iglesias-Fernández R. 2020. Reactive Oxygen Species (ROS) and nucleic acid modifications during seed dormancy. Plants **9**, 1–14.

Koch J, Pranjic K, Huber A, Ellinger A, Hartig A, Kragler F, Brocard C. 2010. PEX11 family members are membrane elongation factors that coordinate peroxisome proliferation and maintenance. Journal of Cell Science **123**, 3389–3400.

Kumar AS, Park E, Nedo A, et al. 2018. Stromule extension along microtubules coordinated with actin-mediated anchoring guides perinuclear chloroplast movement during innate immunity. eLife **7**, 1–33.

Li J, Hu J. 2015. Using co-expression analysis and stress-based screens to uncover Arabidopsis peroxisomal proteins involved in drought response. PLoS ONE **10**, 1–13.

Li T, Song R, Yin Q, Gao M, Chen Y. 2019. Identification of *S*-nitrosylation sites based on multiple features combination. Scientific Reports **9**, 1–14.

Li S, Yu K, Wu G, Zhang Q, Wang P, Zheng J, Liu ZX, Wang J, Gao X, Cheng H. 2021. pCysMod: Prediction of multiple cysteine modifications based on deep learning framework. Frontiers in Cell and Developmental Biology **9**, 1–10.

Lingard MJ, Gidd SK, Bingham S, Rothstein SJ, Mullen RT, Trelease RN. 2008. Arabidopsis PEROXIN11c-e, FISSION1b, and DYNAMIN-RELATED PROTEIN3A cooperate in cell cycle-associated replication of peroxisomes. Plant Cell **20**, 1567–1585.

Lingard MJ, Trelease RN. 2006. Five Arabidopsis peroxin 11 homologs individually promote peroxisome elongation, duplication or aggregation. Journal of Cell Science **119**, 1961–1972.

Mathur J. 2021. Organelle extensions in plant cells. Plant Physiology **185**, 593–607.

Mindthoff S, Grunau S, Steinfort LL, Girzalsky W, Hiltunen JK, Erdmann R, Antonenkov VD. 2016. Peroxisomal Pex11 is a pore-forming protein homologous to TRPM channels. Biochimica et Biophysica Acta-Molecular Cell Research **1863**, 271–283.

Mitsuya S, El-Shami M, Sparkes I, Charlton WL, Lousa CDM, Johnson B, Baker A. 2010. Salt stress causes peroxisome proliferation, but inducing peroxisome proliferation does not improve NaCl tolerance in *Arabidopsis thaliana*. PloS ONE **5**, e9408.

Muthamilarasan M, Bonthala VS, Khandelwal R, Jaishankar J, Shweta S, Nawaz K, Prasad M. 2015. Global analysis of WRKY transcription factor superfamily in *Setaria* identifies potential candidates involved in abiotic stress signalling. Frontiers in Plant Science **6**, 1–15.

Nelson BK, Cai X, Nebenführ A. 2007. A multicolored set of in vivo organelle markers for co-localization studies in Arabidopsis and other plants. The Plant Journal **6**, 1126-1136.

Nila AG, Sandalio LM, López MG, Gómez M, Del Río LA, Gómez-Lim MA. 2006. Expression of a peroxisome proliferator-activated receptor gene (xPPARα) from *Xenopus laevis* in tobacco (*Nicotiana tabacum*) plants. Planta **224**, 569–581.

Oksanen E, Häikiö E, Sober J, Karnosky DF. 2004. Ozone-induced H_2O_2 accumulation in field-grown aspen and birch is linked to foliar ultrastructure and peroxisomal activity. New Phytologist **161**, 791–799.

Olmedilla A, Sandalio LM. 2019. Selective autophagy of peroxisomes in plants: From housekeeping to development and stress responses. Frontiers in Plant Science **10**, 1–7.

Orth T, Reumann S, Zhang X, Fan J, Wenzel D, Quan S, Hu J. 2007. The PEROXIN11 protein family controls peroxisome proliferation in Arabidopsis. The Plant Cell **19**, 333–350.

Pan R, Liu J, Wang S, Hu J. 2020. Peroxisomes: Versatile organelles with diverse roles in plants. New Phytologist **225**, 1410–1427.

Pastori GM, Del Río LA. 1997. Natural senescence of pea leaves. Plant Physiology **113**, 411–418.

Rodríguez-Serrano M, Pazmiño DM, Sparkes I, Rochetti A, Hawes C, Romero-Puertas MC, Sandalio LM. 2014. 2,4-Dichlorophenoxyacetic acid promotes *S*-nitrosylation and oxidation of actin affecting cytoskeleton and peroxisomal dynamics. Journal of Experimental Botany **17**, 4783–4793.

Rodríguez-Serrano M, Romero-Puertas MC, Sanz-Fernández M, Hu J, Sandalio LM. 2016. Peroxisomes extend peroxules in a fast response to stress via a reactive oxygen species-mediated induction of the peroxin PEX11a. Plant Physiology **171**, 1665–1674.

Romero-Puertas MC, McCarthy I, Sandalio LM, Palma JM, Corpas FJ, Gómez M, Del Río LA. 1999. Cadmium toxicity and oxidative metabolism of pea leaf peroxisomes. Free Radical Research **31**, Suppl:S25–31.

Romero-Puertas MC, Terrón-Camero LC, Peláez-Vico MÁ, Molina-Moya E, Sandalio LM. 2021. An update on redox signals in plant responses to biotic and abiotic stress crosstalk: Insights from cadmium and fungal pathogen interactions. Journal of Experimental Botany **72**, 5857–5875.

Sandalio LM, Peláez-Vico MA, Romero-Puertas MC. 2020. Peroxisomal metabolism and dynamics at the crossroads between stimulus perception and fast cell responses to the environment. Frontiers in Cell and Developmental Biology **8**, 2014–2018.

Schrader M, Costello JL, Godinho LF, Azadi AS, Islinger M. 2016. Proliferation and fission of peroxisomes-An update. Biochimica et Biophysica Acta-Molecular Cell Research **1863**, 971–983.

Terrón-Camero LC, Rodríguez-Serrano M, Sandalio LM, Romero-Puertas MC. 2020. Nitric oxide is essential for cadmium-induced peroxule formation and peroxisome proliferation. Plant, Cell and Environment **43**, 2492–2507.

Thazar-Poulot N, Miquel M, Fobis-Loisy I, Gaude T. 2015. Peroxisome extensions deliver the Arabidopsis SDP1 lipase to oil bodies. Proceedings of the National Academy of Sciences of the United States of America 112, 4158–4163.

Ueda H, Yokota E, Kutsuna N, Shimada T, Tamura K, Shimmen T, Hasezawa S, Dolja VV, Hara-Nishimura I. 2010. Myosin-dependent endoplasmic reticulum motility and F-actin organization in plant cells. PNAS USA **15**: 6894–6899.

Van Roermund CWT, Tabak HF, Van den Berg M, Wanders RJA, Hettema EH. 2000. Pex11p plays a primary role in medium-chain fatty acid oxidation, a process that affects peroxisome number and size in *Saccharomyces cerevisiae*. Journal of Cell Biology **150**, 489–497.

Wang C, Xu H, Lin S, Deng W, Zhou J, Zhang Y, Shi Y, Peng D, Xue Y. 2020. GPS 5.0: An update on the prediction of kinase-specific phosphorylation sites in proteins. Genomics, Proteomics and Bioinformatics **18**, 72–80.

Woodhouse FG, Goldstein RE. 2013. Cytoplasmic streaming in plant cells emerges naturally by microfilament selforganization. PNAS USA **35**, 14132–14137.

Xu Y, Ding J, Wu LY, Chou KC. 2013. iSNO-PseAAC: Predict cysteine *S*-nitrosylation sites in proteins by incorporating position specific amino acid propensity into pseudo amino acid composition. PLoS ONE **8**, 1–7.

Yanhui C, Xiaoyuan Y, Kun H, et al. 2006. The MYB transcription factor superfamily of Arabidopsis: Expression analysis and phylogenetic comparison with the rice MYB family. Plant Molecular Biology **60**, 107–124.

Younis A, Siddique MI, Kim CK, Lim KB. 2014. RNA Interference (RNAi) induced gene silencing: A promising approach of Hi-Tech plant breeding. International Journal of Biological Sciences **10**, 1150-1158.

Zandalinas SI, Fichman Y, Mittler R. 2020. Vascular bundles mediate systemic reactive oxygen signalling during light stress. Plant Cell **32**, 3425–3435.

Zandalinas SI, Mittler R. 2021. Vascular and nonvascular transmission of systemic reactive oxygen signals during wounding and heat stress. Plant Physiology **186**, 1721–1733.

Zhang Y, Wang L. 2005. The WRKY transcription factor superfamily: Its origin in eukaryotes and expansion in plants. BMC Evolutionary Biology **5**, 1–12.

Chapter 4

Peroxin 11a (PEX11a) function in Arabidopsis plants under control and stress conditions: a transcriptomic approach.

Peláez-Vico, M. A., Terrón-Camero, L. C, Molina-Moya, E., Collado-Arenal, A. M., Andrés León, E., Sandalio, L. M., Romero-Puertas, M. C.

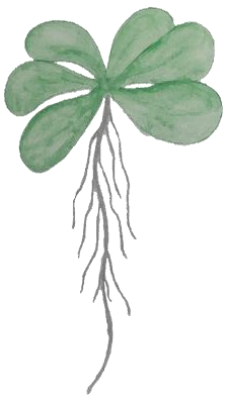

Peroxin 11a (PEX11a) function in Arabidopsis plants under control and stress conditions: a transcriptomic approach

Mª Ángeles Peláez-Vico, Laura C. Terrón-Camero, Eliana Molina-Moya, Aurelio M. Collado-Arenal, Andrés León, E., Luisa M. Sandalio, María C. Romero-Puertas

Departamento de Bioquímica, Biología Celular y Molecular de Plantas, Estación Experimental del Zaidín, CSIC, Profesor Albareda 1, E-18008 Granada, Spain

Running title: PEX11a role in plant biology

ABSTRACT

Peroxin 11a (PEX11a) has been recently involved in peroxules production in plant response to the heavy metal cadmium (Cd). Its role in plant redox maintenance and peroxules, and therefore, peroxisomal-dependent signalling in response to Cd has been suggested. The molecular mechanism underlying PEX11a-dependent signalling however, are completely unknown. In this work, we have used a mutant affected in PEX11a, generated by CRISPR-Cas9 technology (pex11a-CR) to analyse transcriptomic changes under Cd stress at two time points, 1 and 24 h. In addition, we obtained a deeper insight in transcriptomic changes observed in the mutant under normal conditions to unravel new PEX11a functions in plant biology. Our results suggest that PEX11a may regulate chloroplast metabolism and structure, chlorophylls and starch biosynthesis under normal conditions pointing to a key role in organelles crosstalk. Transcriptomic data point to PEX11a-dependent regulation of iron and ion metabolism and transport at early time, while ribosome and spliceosome metabolism at later time in plant response to Cd.

1. INTRODUCTION

Cadmium (Cd) is one of the most toxic nonessential elements for plants and not only inhibits plant growth and development, but it also accumulates in the human body over time via the food chain (Genchi *et al.,* 2021). In plants, Cd stress markedly induces reactive oxygen species (ROS) accumulation being peroxisomes one of the main sources. These organelles have a central role in the coordination of the signalling processes that occur in the plant response to stress (Sandalio and Romero-Puertas, 2015; Pan *et al.,* 2020; Su *et al.,* 2019; Sandalio *et al.,* 2020, 2021).

In peroxisomes of pea plants Cd increases H_2O_2 concentration, disturbs antioxidants enzymes, and causes oxidative modification of peroxisomal proteins (Romero-Puertas *et al.,* 1999, 2002). In addition, this heavy metal also affects peroxisomal dynamics, producing a significant increase in peroxisome speed after 24 h of treatment, which dependent on endogenous ROS and Ca^{2+} (Rodríguez-Serrano *et al.,* 2016). Peroxisomal proliferation has been described under certain stress conditions such as Cd (Rodríguez-Serrano *et al.,* 2016; Calero-Muñoz *et al.,* 2019; Terrón-Camero *et al.,* 2020). The first stage of this process consists on the elongation/tubulation of the peroxisome, which is mediated among others by PEX11 protein family members. After that, membrane is constricted and finally fission occurs mediated by dynamin-related proteins DRP3A, DRP3B and DRP5B together with FISSION proteins FIS1A and FIS1B (Kaur *et al.,* 2009; Pan *et al.,* 2020). Recently, dynamic peroxisomal extensions, called peroxules, have been observed after application of H_2O_2 (Sinclair *et al,* 2009), Cd (Rodríguez-Serrano *et al.,* 2016) and NO donors (Terrón-Camero *et al.,* 2020). In Arabidopsis exposed to Cd, peroxules were initially observed followed by peroxisome proliferation, with peroxisomes number finally returning to those recorded under control conditions (Rodríguez-Serrano *et al.,* 2016) which was regulated by pexophagy (Calero-Muñoz *et al.,* 2019). Among the five PEX11 isoforms found in Arabidopsis, PEX11a-e, we have described the involvement of PEX11a in peroxules production under Cd and As treatment (Rodríguez-Serrano *et al.,* 2016; and this work). Although PEX11a and peroxules formation play a key role in regulating stress perception and fast cell responses to environmental cues, very little is known about the molecular mechanism underlying. Deciphering the functionality of peroxules at molecular level is one of the most interesting challenges in cell biology. To

get a deep insight in this subject, we have investigated the early transcriptional response of Arabidopsis *px-ck* and a mutant affected in *PEX11a* gene *(pex11a-CR)* generated in a *px-ck* background, under high Cd (100 µM) exposure for 1 h and 24 h and normal growth conditions through Illumina sequencing. Here, we report the identification of *PEX11a* dependent genes and pathways in Arabidopsis seedlings under normal conditions and in response to Cd stress. The identification of these genes and pathways may help to uncover the molecular mechanism of peroxisomes and more specifically, of peroxules in fast stress response and *PEX11a* functionality.

2. MATERIALS AND METHODS

2.1. Sample collection and preparation

Arabidopsis seeds of *px-ck* and *pex11a-CR9* were surface- disinfected and stratified for 24-48 h at 4 °C and then sown on Murashige and Skoog (MS) 0.5x solid medium (Murashige and Skoog, 1962), grown at 22 °C in 16 h light and 8 h darkness for 13 d. Seedlings were then transferred to petri dishes containing 0.5x liquid MS medium and grown for 24 h. Seedlings were treated with 100 µM $CdCl_2$ for 1 h and 24 h (Fig. 1). Regarding the treatment, samples were noted as control (C) or Cd_1h or Cd_24h. Three independent biological replicates each treatment, with a total of 18 RNA samples were extracted with Trizol reagent (MRC) and treated using DNA-free™ DNA Removal Kit (Invitrogen) following manufacturer's instructions.

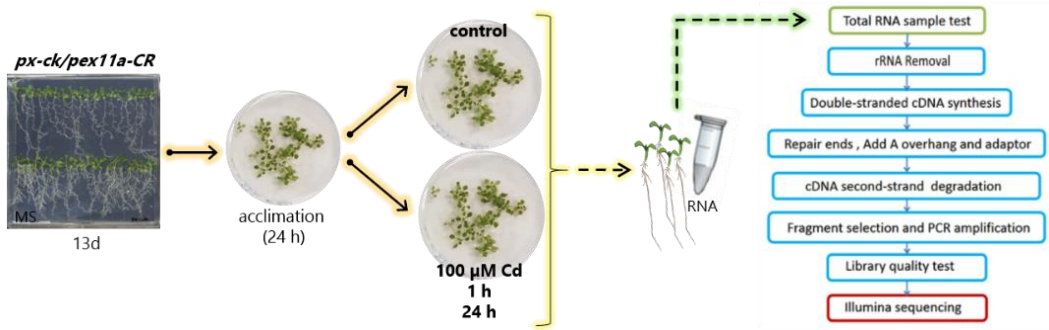

***Figure 1*. Sample preparation and overview of RNA-seq process.** *Modified from scheme supplied by Novogene Corporation Inc.*

2.2. RNA quality and quantification

Total RNA quality was verified by Nanodrop to test RNA purity (OD_{260}/OD_{280}) and agarose gel electrophoresis to test RNA integrity and potential contamination. Further RNA integrity and quantitation were assessed using the RNA Nano 6000 Assay Kit of the Bioanalyzer 2100 system (Agilent Technologies, CA, USA).

2.3. RNA-seq analysis

RNA sequencing (RNA-seq) was performed by the company Novogene (Cambridge, UK). Bioinformatics analysis were carried out by the Genomics and Bioinformatics Unit at the *Instituto de Parasitología y Biomedicina López-Neyra* (IPBLN-CSIC; Granada, Spain).

2.3.1. Construction and sequencing of the mRNA library

A total amount of 2 μg RNA per sample was used as input material for the RNA sample preparations. Firstly, ribosomal RNA was removed by Epicentre Ribo-zeroTM rRNA Removal Kit (Epicentre, USA), and rRNA free residue was cleaned up by ethanol precipitation. Subsequently, sequencing libraries were generated using the rRNA-depleted RNA by NEBNext® UltraTM Directional RNA Library Prep Kit for Illumina® (NEB, USA) following manufacturer's recommendations. Briefly, fragmentation was carried out using divalent cations under elevated temperature in NEBNext First Strand Synthesis Reaction Buffer (5x). First strand cDNA was synthesized using random hexamer primer and M-MuLV Reverse Transcriptase (RNaseH-). Second strand cDNA synthesis was subsequently performed using DNA Polymerase I and RNase H. In the reaction buffer, dNTPs with dTTP were replaced by dUTP. Remaining overhangs were converted into blunt ends via exonuclease/polymerase activities. After adenylation of 3′ ends of DNA fragments, NEBNext Adaptor with hairpin loop structure were ligated to prepare for hybridization. The average insert size for the paired-end libraries was 300 bp (±50 bp) and fragments were purified with AMPure XP system (Beckman Coulter, Beverly, USA). Then, 3 μl USER Enzyme (NEB, USA) was used with size-selected, adaptor-ligated cDNA at 37 °C for 15 min followed by 5 min at 95 °C before PCR. Subsequently, PCR was performed with Phusion High-Fidelity DNA polymerase, Universal PCR primers and Index(X) Primer. At last, products were purified (AMPure XP system) and library quality was assessed on the Agilent Bioanalyzer 2100 system. A total of 18 RNA libraries consisted

of three control libraries and three Cd-treated libraries for each genotype and time were analyzed.

2.3.2. Quality assessment and pre-processing

The original raw data from Illumina were transformed to Sequenced Reads by base calling. Raw data are recorded in a FASTQ file, which contains sequence information (reads) and corresponding sequencing quality information. Raw reads are filtered to remove reads with adapter contamination or reads with low quality. Only clean reads were used in the downstream analyses.

2.3.3. RNA-seq reads mapping

Reads obtained from the sequencer were positioned in the reference genome by nucleotide homology. For this alignment, the HISAT2 aligner was used resulting in a 97.5 % on average of properly aligned reads (Kim *et al.,* 2015). Arabidopsis thaliana TAIR10 was used as reference genome and annotation was conducted using TAIR10 v47 annotation file (www.arabidopsis.org). After that, featureCounts software (Liao *et al.,* 2014) was used to assign sequence reads to genes.

2.3.4. Transcript abundance estimation and differential expression testing

In this process, all reads co-localized in protein-coding exons are summarize and associated to genes. As a consequence, we obtain the raw and unnormalized expression values (usually identified as counts) for each gene within each sample. After the statistical processing, these values can be used to measure changes in expression. To evaluate the differential expression analysis, edgeR package was used (Nikolayeva and Robinson, 2014). Low expressed genes were removed and remaining genes were normalized by the trimmed mean of M-values (TMM) method (Robinson and Oshlack, 2010). Counts per million (CPM) and log2-counts per million (log-CPM) were used for exploratory plots (Nikolayeva and Robinson, 2014) to check the consistency of the replicates. Furthermore, we calculated reads per kilo base per million mapped reads (RPKM) per gene on each sample. Principal component analysis (PCA) and Hierarchical Clustering of normalized samples were used to explore data and to get a general overview on the similarity of RNA-sequencing samples (Reeb *et al.,* 2015; Ritchie *et al.,* 2015). After that, three samples (px-ck_C_2, px-ck_Cd_24h_1 and pex11a-CR_Cd24h_2) were discarded because it did not

cluster correctly and its outlier behavior. Differentially expressed genes (DEGs) were calculated between control and Cd-treated seedling for each genotype as well as *pex11a-CR* versus *px-ck*, through False Discovery Rate (FDR) value <0.05 and log2FC to evaluate the significance and the change in expression of a gene.

2.3.5. Gene annotation, classification, and metabolic pathway analysis

In order to identify the effects of differential gene expression, we carry out a functional enrichment study using the clusterProfiler Bioconductor package (Yu *et al.*, 2012). For this purpose, DEGs were compared against all expressed genes in the RNA-seq assay. Therefore, Gene Ontology (GO) enrichment analysis was evaluated for Biological Process (BP), Molecular Function (MF) and Cellular Component (CC) ontology terms. Finally, the DEGs selected above were compared to the Kyoto Encyclopedia of Genes and Genomes (KEGG) pathway database. PlantGSEA tool was used to perform functional enrichments. The analysis was carried out using the Plant Ontology gene sets database (by TAIR), comparing our dataset with the complete Arabidopsis genome. The statistical test employed was Yekutieli (FDR<0.05).

2.4. Chlorophyll and carotenoids content

Chlorophyll and carotenoids content of samples prepared by 80 % acetone extraction, was measured by spectrophotometry. Leaves from plants grown under short day conditions (4 w) and long day conditions (3 w) were weighed and incubated with 80 % acetone solution in a proportion 1:2 (w/v). Samples were incubated in rotation for 24 h at 4 ºC. After that, samples were centrifuged for 10 min at 15,000 g. The supernatant was collected for analysis by spectrophotometry. Optical densities were recorded at 663, 646, 470 y 750 nm to determine the concentrations (µg/mg fresh weight) of chlorophyll a, chlorophyll b, chlorophyll (a + b) and carotenoids. Values were calculated using the formula described by Lichtenthaler and Welburn (1983).

2.5. Histological detection of starch

To detect starch granules, rosettes of 3- and 4-week-old plants grown under long day and short day were depigmented with 70 % ethanol at 37 ºC for a minimum of 24 h to remove chlorophylls. Leaves were then stained with a solution of lugol (Sigma-Aldrich) at RT for 5-10 min. Samples were washed and scanned at high resolution. For the

quantification of intensity/pixel by ImageJ software, squares of 0.2 x 0.2 cm (long day plants) and 0.06 x 0.06 cm (short day plants) were used.

2.7. Light stress assays

Four different light responses were tested in Arabidopsis mutants. To evaluate the response to low light intensity, seedlings were plated in MS for 7 d in short day and long day conditions, and they were transferred to pots and grown 3 weeks with low light intensity. To reduce light intensity, the upper part of the greenhouses was covered with two layers of white silk paper that allowed half of the light (70 µmol m^{-2} s^{-1}) to pass through. Fresh weight (FW) was measured in 4-week-old plants. On the other hand, the response to red and blue light was also evaluated. Seeds were sown in soil and subjected to 16 h of red light/8 h of darkness using a led plant grow light (80 W) and the germination rate was measured after 7 d. In addition, to evaluate the response to high light intensity, seedlings were grown in soil for 3 weeks under long day conditions and 600 µmol m^{-2} s^{-1} of light intensity. Germination rate as well as foliar area were measured in these conditions.

2.8. Chloroplast ultrastructure analysis

Arabidopsis leaves were cut into pieces of approximately 1 mm^2 and initially fixed with 0.5 % glutaraldehyde (v/v), prepared in 50 mM potassium phosphate buffer, pH 6.8, for 2.5 h at RT. After that, samples were washed with the same buffer and incubated in DAB solution (2 mg/ml) prepared in 50 mM Tris-HCl, pH 9.0 for 1.5 h. Samples were incubated in a solution containing DAB and 0.02 % H_2O_2 at 37 °C for 3 h. After that, pieces were washed with 50 % potassium phosphate buffer, pH 6.8, and stained with 1 % (w/v) OsO_4. Samples were then dehydrated in a stepped ethanol series from 30 to 100 %, embedded in Embed 812 resin series (25-100 %; w/v; Electron Microscopy Sciences, Hatfield, PA, USA). Samples were cut into ultra-thin (50-70 nm) sections and stained with uranyl acetate for electron microscopy analysis (Calero-Muñoz *et al.,* 2019). Measurement of thylakoid-free stroma region was carried out with ImageJ software.

3. RESULTS

3.1. Transcriptome sequencing of control and Cd-treated seedlings

To get a deeper insight into *PEX11a* function under control conditions and in plant response to Cd, we carried out an RNA-seq in order to identify the differently expressed genes (DEGs) in *px-ck* (background with CFP-marked peroxisomes) and *pex11a-CR* (line CR9) mutants (in a px-ck background), affected in peroxules production. We analyzed two time points, one just after the peak of peroxules production under Cd treatment, 1 h and the other after 24 h, when the number of peroxisomes is similar to the control conditions although velocity is higher (Rodríguez-Serrano *et al.,* 2016). The raw Illumina sequencing reads were qualified and adapter trimmed to yield a total of 135-233 million clean short reads. Over 98.4 % of the clean reads had quality scores at the Q20 level and over 95 % of the clean reads had scores at the Q30 level. Clean reads number multiply read length of samples, saved in G unit were 20-27.4 (**Sup. Table S1**). A high proportion of the valid, clean reads (97-98.6 %) were readily mapped onto the Arabidopsis reference genome sequence after the different treatments (**Sup. Table S2 A-B**). The transcriptional abundance of the genes was measured as RPKM and a total of 22,504 transcripts were expressed in our samples. Expression distribution in samples is showed in boxplots in **Fig. 2**. Distribution of unnormalised and normalised data were not identical but still not very different.

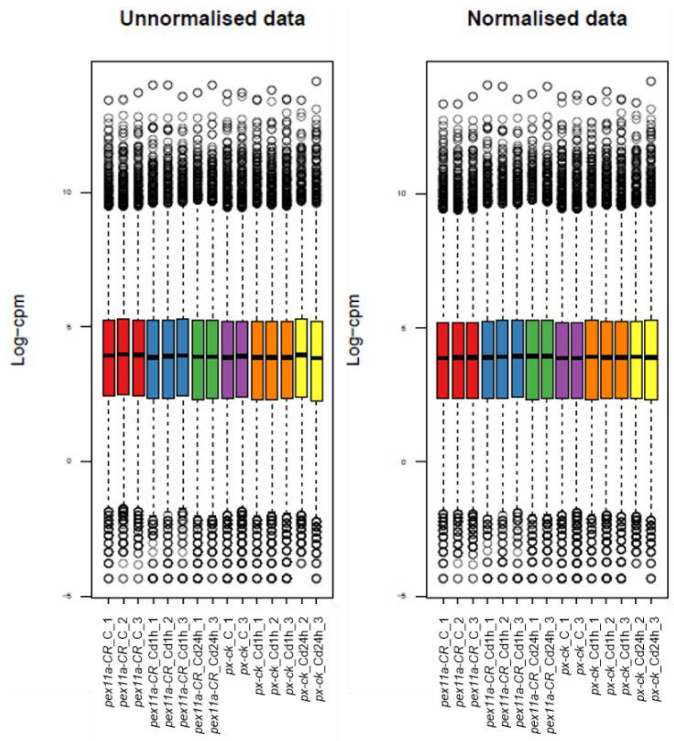

Figure 2. Boxplots of log-CPM (log counts per million) values showing expression distributions. *Non filtered (unnormalised) data and filtered (normalized) data for each sample is showed. Boxes colored with the same color correspond to biological replicates. The line dividing the box represents the median of the data and top and bottom of the box shows the upper and lower quartiles respectively. Outliers are show as circles.*

The plot dimension 2 (dim 2) in **Fig. 3** illustrates that replicates of *pex11a-CR* treated with Cd 1h (pex11a-CR_Cd_1h), in blue, belong to an independent cluster and the same occurs with samples treated for 24 h (pex11a-CR_Cd_24h), in green. *px-ck* seedlings treated for 24 h are located in a different and independent cluster (px-ck_Cd_24h), in yellow. Surprisingly, *pex11a-CR* control samples (pex11a-CR_C), in red, highly clustered with *px-ck* samples treated with Cd 1 h (px-ck_Cd_1h), in orange. *px-ck* control samples showed certain dispersion among replicates, in purple.

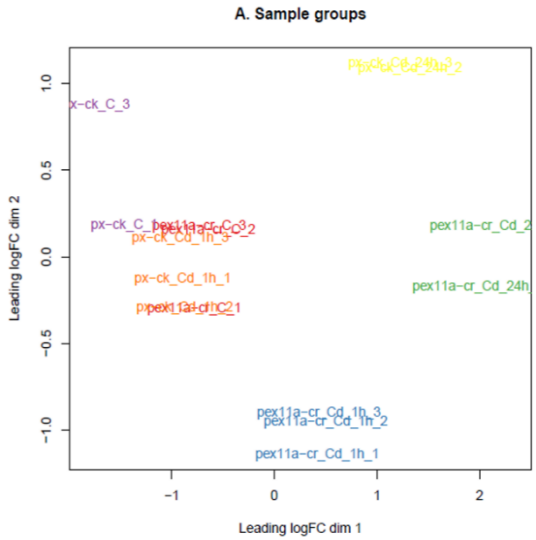

Figure 3. Multidimensional scaling (MDS) plot showing variation among samples based on normalized data*. Each point represents 1 sample, and the distance between 2 points reflects the leading logFC of the corresponding RNA-Seq samples. The leading logFC (base 2 logarithm of fold change) is the average of the largest absolute logFC between each pair of samples.*

3.2. Identification of Differentially Expressed Genes (DEGs) in *pex11a-CR* under control conditions.

In the present study, a FDR ≤ 0.05 and the absolute value of log2FC were set as the thresholds to determine the significance of differences in gene expression. Volcano plot enables quick visual identification of gene expression alterations, being the upregulated genes towards the right (blue dots), while downregulated genes are towards

the left (yellow dots). The most statistically significant genes are towards the top. Volcano plot from the comparison pex11a_CR vs px-ck is shown in **Fig. 4 A**, with a total of 1,994 significant DEGs: 1,106 genes up-regulated and 888 genes down-regulated under control conditions (**Fig. 4 B**).

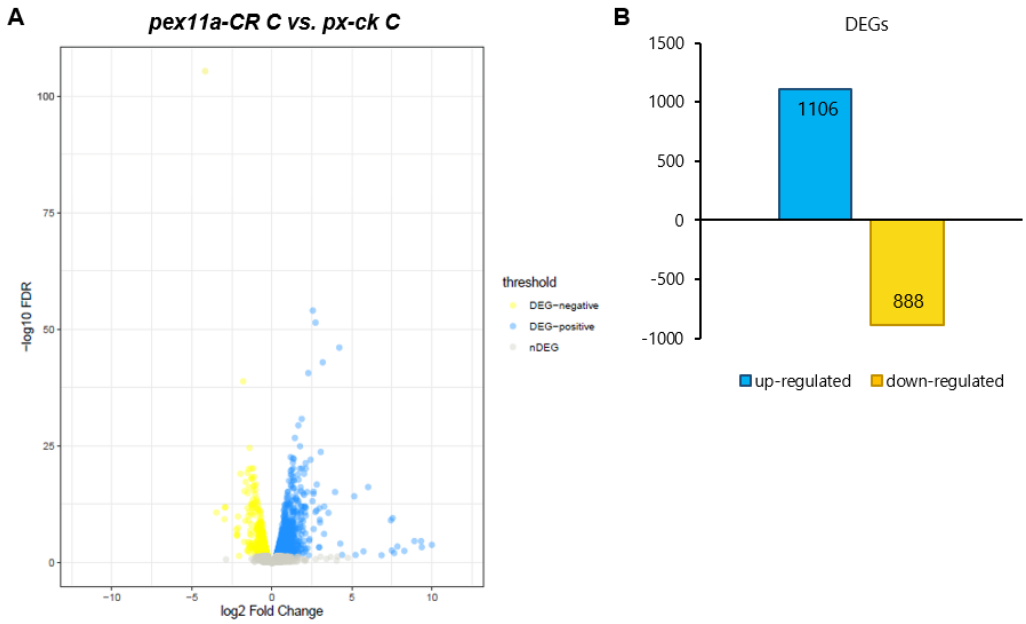

Figure 4. Screening of differentially expressed genes (DEGs) in pex11a-CR vs px-ck. (A) *Volcano plot showing log2 fold change (log2FC) on the x-axis and -log10 FDR (p-value) on the y-axis of gene expression alterations found using edgeR in control conditions (pex11a-CR C vs. px-ck C). Up regulated genes are blue dots while yellow dots represent down regulated genes. Genes not significantly regulated (nDEGs) are grey dots.* ***(B)*** *Number of significantly up-regulated and down-regulated genes in control conditions.*

3.3. Functional annotation analysis of DEGs

We classified DEGs into gen ontology (GO) categories to obtain useful information about differentially regulated metabolic processes in pex11a_CR. The first ten categories of DEGs from Cellular Component (CC), Biological Process (BP) and Molecular Function (MF) are reported in **Figures 5, 6** and **7** (**Sup. Table S3, S4** and **S5**) respectively. Surprisingly, GO terms from CC, with 1,709 DEGs annotated in 28 categories (**Sup. Table S3**), were all enriched components located in chloroplasts, regardless of the FC threshold applied (**Fig. 5**). Main CC terms, with (log2FC)>1 or <-1 were related with thylakoids, photosynthetic membrane, light-harvesting complex and plastoglobuli (**Fig. 5**).

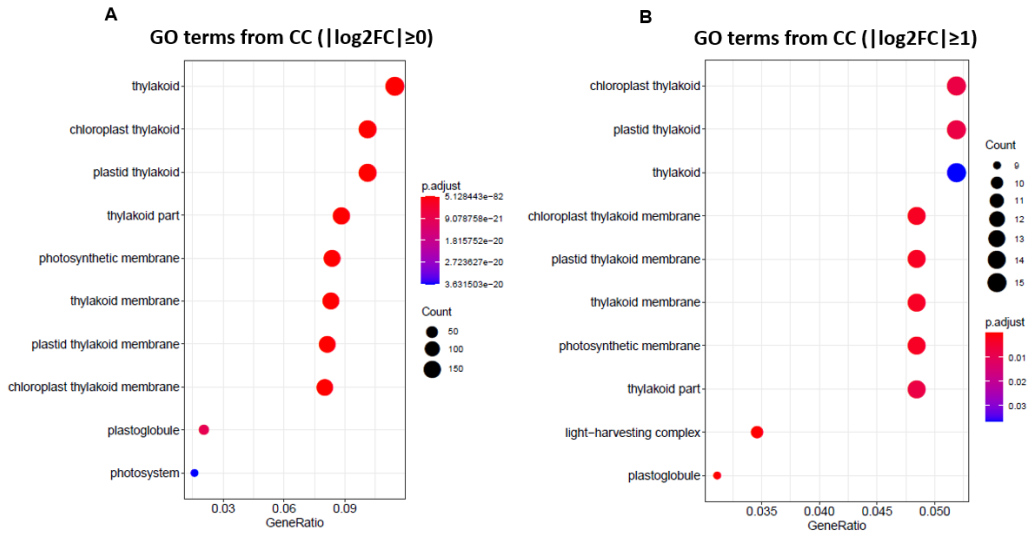

Figure 5. Cellular Component (CC) from Gene Ontology (GO) analysis of differently expressed genes in A. thaliana pex11a-CR vs px-ck under control conditions. (A) *Filtered enrichment |log2FC|≥0 and,* ***(B)*** *|log2FC|≥1.*

We found 398 GO categories in the BP ontology (1,563 DEGs; **Sup. Table S4**). The main enriched terms were: photosynthesis and light reactions, response to organonitrogen compound, response to chitin, plastid organization and isopentenyl diphosphate (including biosynthesis and metabolism) among others (**Fig. 6 A**). Applying the cut off |log2FC|≥1 some new enriched terms were annotated such as response to ethylene, response to chitin, response to extracellular stimulus, toxin metabolic process and cellular response to hypoxia (**Fig. 6 B**). The category lipid localization (including cellular response to lipid, lipid transport and lipid storage) was significantly annotated in data filtered with |log2FC|≥2. Additionally, cellular response to abscisic acid stimulus and response to freezing were annotate considering this filter. A large number of enriched terms related to cellular response to decreased oxygen levels were also found using the most restraining filter (**Fig. 6 C**).

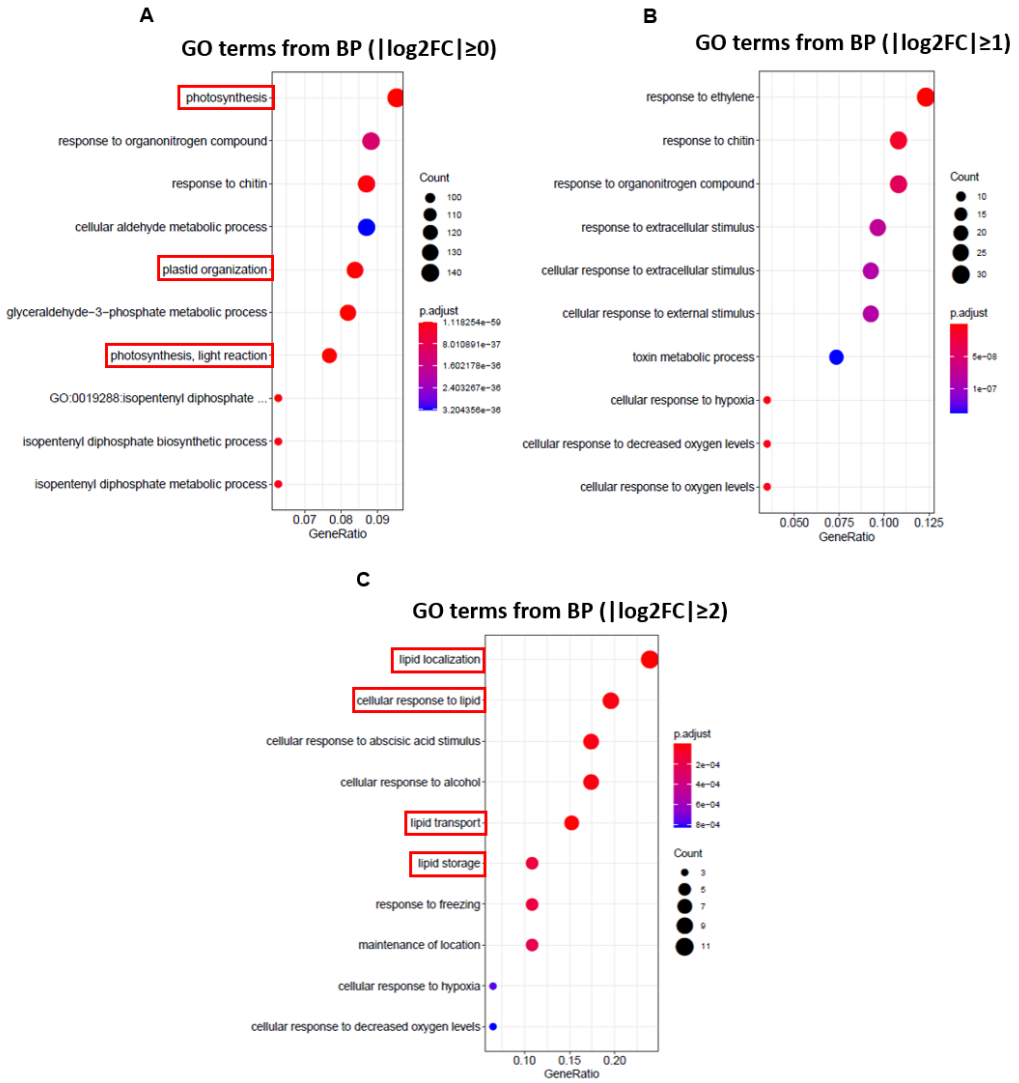

Figure 6. Biological Process (BP) from Gene Ontology (GO) analysis of differently expressed genes in A. thaliana pex11a-CR vs px-ck under control conditions. (A) *Filtered enrichment |log2FC|≥0,* ***(B)*** *|log2FC|≥ 1 and* ***(C)*** *|log2FC|≥2.*

In the MF ontology, 1,496 DEGs could be enriched in 23 different categories (**Sup. Table S5**). Among the main enriched terms (**Fig. 7 A**) we found different enzymatic activities related to sugars metabolism and O-glycosidic bond, such as hydrolase, transferase and aldo-keto reductase activity. Others enriched terms were oxygen binding, chlorophyll binding and nutrient reservoir activity (**Fig. 7 A** and **7 B**). The number of categories decreased when we used a higher threshold (|log2FC|≥2), finding just 4

significant terms related to nutrient reservoir activity, lipid binding, oxygen binding and hydrolase activity (**Fig. 7 C**).

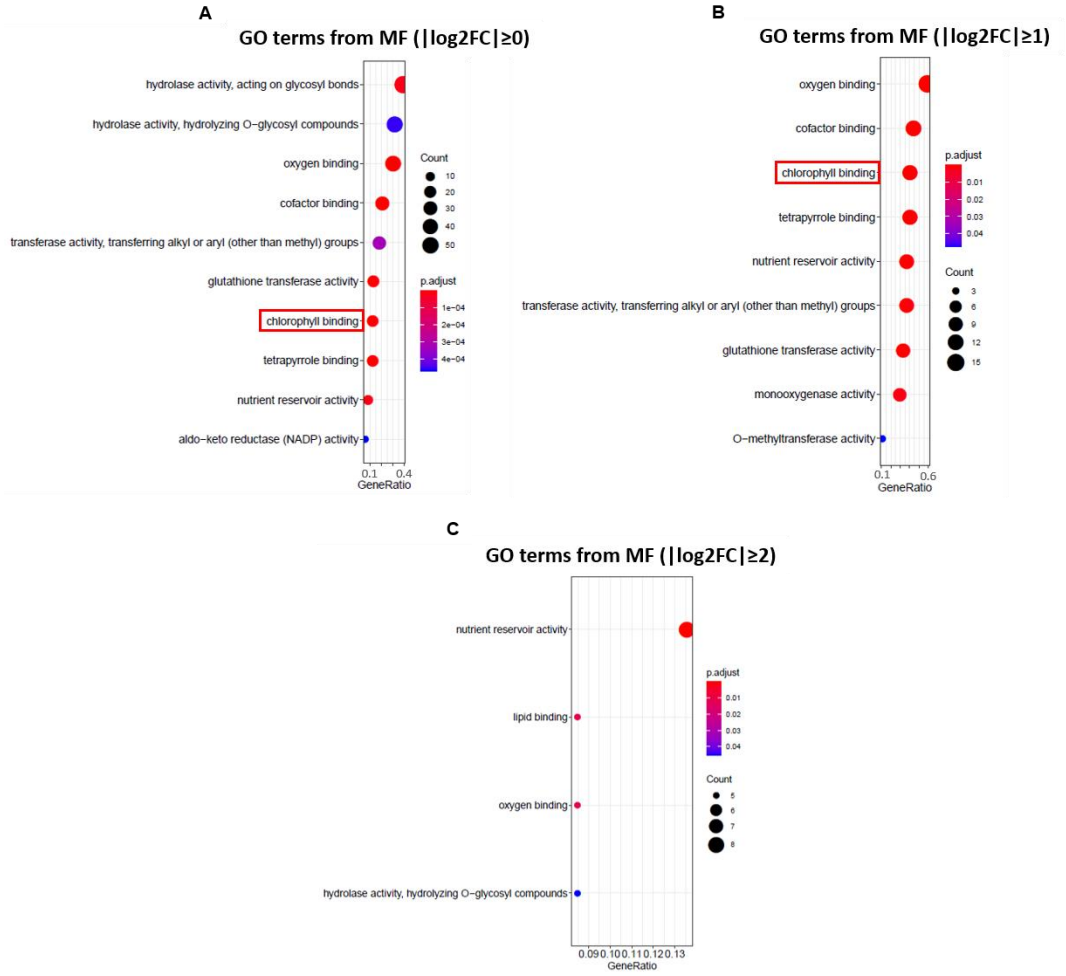

Figure 7. Molecular Function (MF) from Gene Ontology (GO) analysis of differently expressed genes in A. thaliana pex11a-CR vs px-ck under control conditions. (A) *Filtered enrichment |log2FC|≥0,* ***(B)*** *|log2FC|≥ 1 and* ***(C)*** *|log2FC|≥2.*

3.4. KEGG pathway analysis of DEGs

Metabolic pathway analysis could be used to further understand the biological function of genes. DEGs obtained for *pex11a-CR vs px-ck* samples under control conditions were mapped to the reference canonical pathways in KEGG. We found a total of 484 DEGs annotated in the KEGG database that were assigned to 11 KEGG pathways. The most significant pathways were photosynthesis, porphyrin and chlorophyll

metabolism, and glutathione metabolism followed by starch and sucrose metabolism and MAPK signalling pathway (**Table 1**).

Table 1. Main KEGG pathways changed in *pex11a-CR vs px-ck* under control conditions. Count indicates the number of DEGs enriched in this pathway.

ID	Description	p.adjust	Count
ath00196	Photosynthesis - antenna proteins	2,78E-01	19
ath00860	Porphyrin and chlorophyll metabolism	4,67E+03	25
ath00195	Photosynthesis	7,58E+03	30
ath00480	Glutathione metabolism	1,31E+09	27
ath00500	Starch and sucrose metabolism	0.010747	30
ath04016	MAPK signalling pathway - plant	0.017748	25
ath04075	Plant hormone signal transduction	0.020541	43
ath00460	Cyanoamino acid metabolism	0.022732	15
ath00940	Phenylpropanoid biosynthesis	0.041134	28
ath00941	Flavonoid biosynthesis	0.049508	7
ath00630	Glyoxylate and dicarboxylate metabolism	0.049508	15

3.5. Chloroplast-related parameters analyzed in *pex11a-CR* mutants

As chloroplast metabolism appears to be a key target in *pex11a-CR* mutants, we analyzed different parameters related with this organelle in two different lines *(pex11a-CR9 and pex11a-CR10)*.

3.5.1. Chloroplast ultrastructure in *pex11a-CR* under control conditions

Since it appears that chloroplasts metabolism in *pex11a-CR* could be affected according to a large number of terms from GO enrichment under control conditions, and this organelle is a target for damage under Cd stress, we decided to check ultrastructure of these organelles by electron microscopy. Representative TEM images (**Fig. 8 A**) showed a homogeneous distribution of thylakoids in the chloroplasts of two-week-old seedlings in px-ck, meanwhile *pex11a-CR9* showed higher stroma area without thylakoids. The stromal region measured in *pex11a-CR9* line represented 23 % of the total area of the chloroplast, while in *px-ck,* it was 12 %, which demonstrate differences in the ratio thylakoids/stroma in both lines (**Fig. 8 B**).

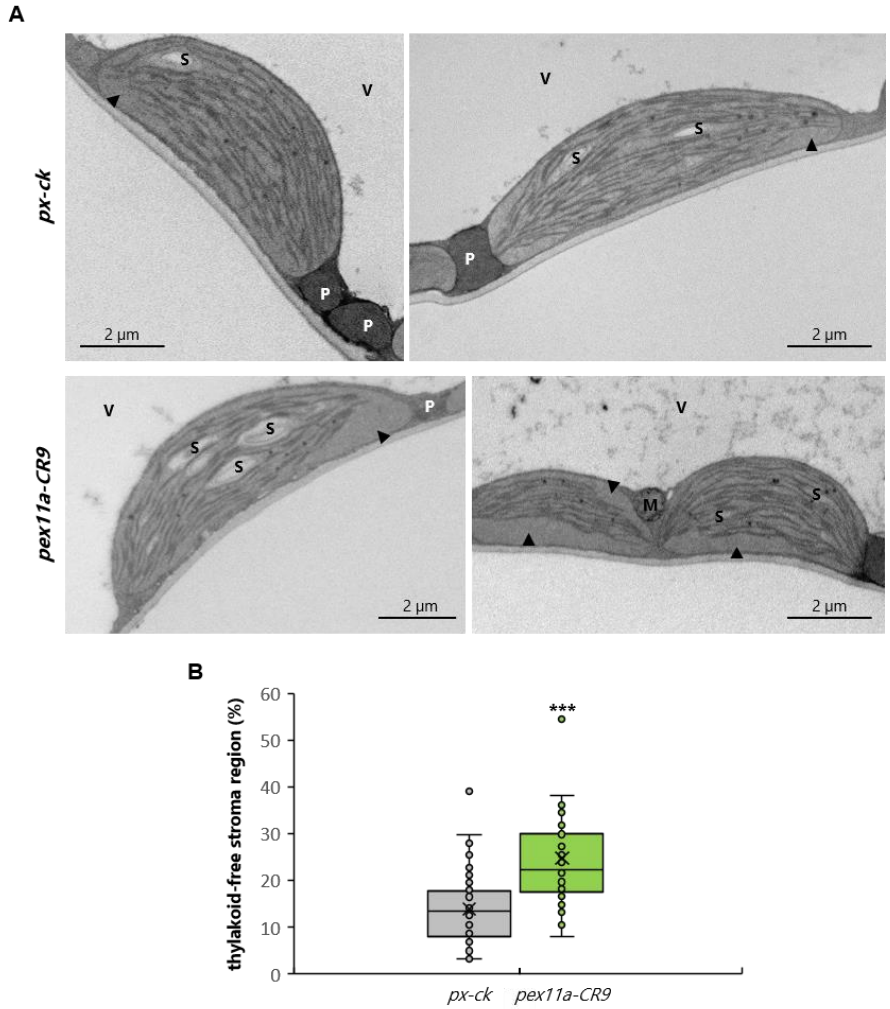

Figure 8. Chloroplast ultrastructure in Arabidopsis seedlings under control conditions. (A) *Representative transmission electron micrographs of chloroplasts from 2-weeks-old px-ck and pex11-CR seedlings. Arrowheads indicate thylakoid-free area in stroma chloroplast. M, mitochondria; P, peroxisome; S, starch; V, vacuole. Scale bar: 2 µm.* ***(B)*** *Measurement of thylakoid-free stroma region (%) in untreated seedlings. Data are means, distributions and whiskers (maximum and minimum) of at least three independent experiments. Different letters denote significant differences between different treatments according to the Student´s t-test (p-value < 0.05).*

3.5.2. Chlorophyll and carotenoids content in *pex11a-CR* lines

An overview of DEGs for *pex11a-CR* mutant related with photosynthesis and antenna proteins is showed in **Fig. 9.** Interestingly, almost all the light-harvesting chlorophyll protein complex (LHC) were repressed under control conditions in the mutant *pex11a-CR vs px-ck*.

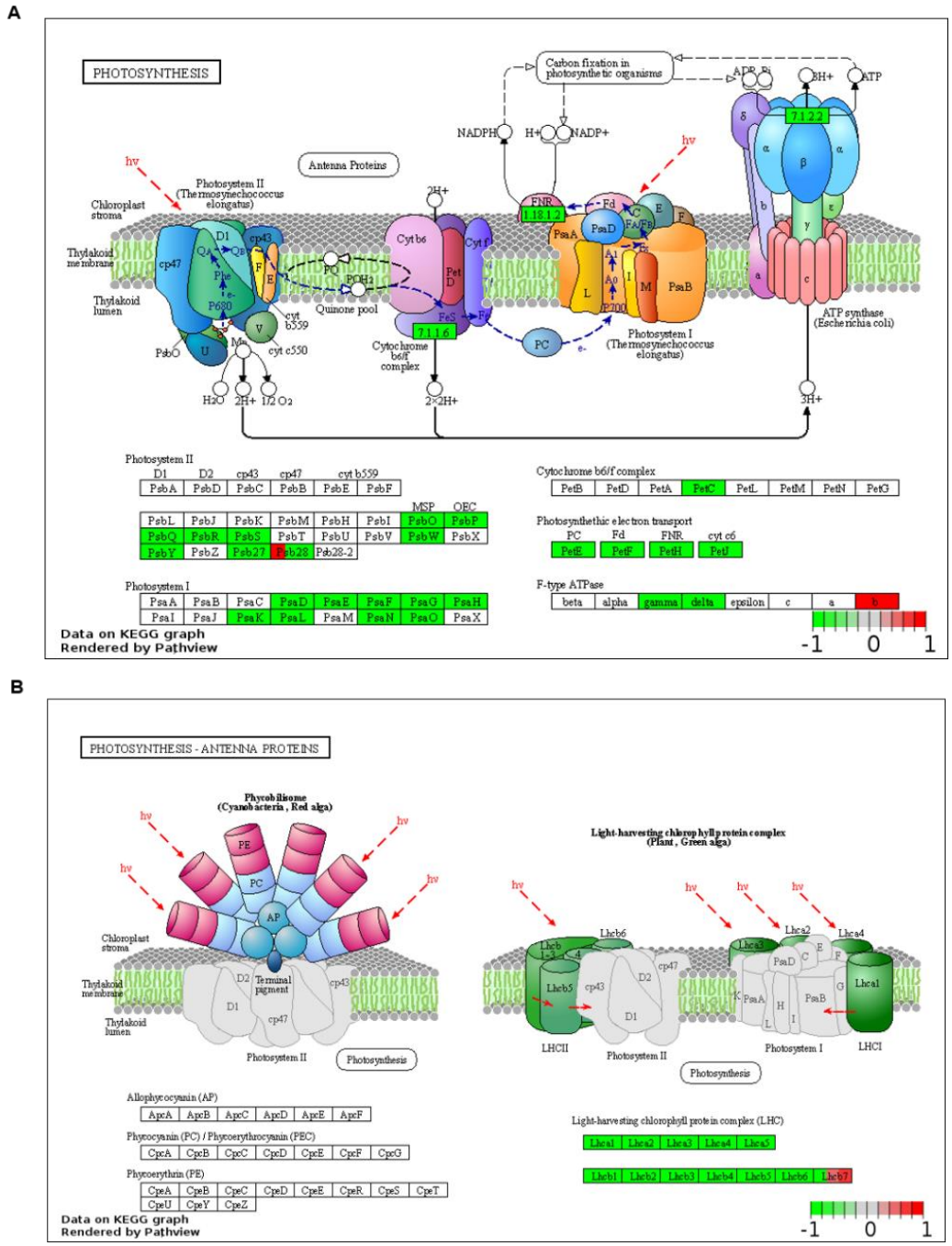

Figure 9. Photosynthesis pathway analysis of differently expressed genes in A. thaliana pex11a-CR mutant under control conditions. *Red boxes mean up-regulated genes and green mean down-regulated genes.* ***(A)*** *Photosynthesis and* ***(B)*** *Antenna proteins. The pathway frames are from the KEGG database.*

The same trend was also observed in the proteins from photosystem I and II. In addition, a heatmap with DEGs related with porphyrin and chlorophyll metabolism is shown in **Fig. 10**. Mostly DEGs from this category were also down-regulated (yellow) in *PEX11a* mutant.

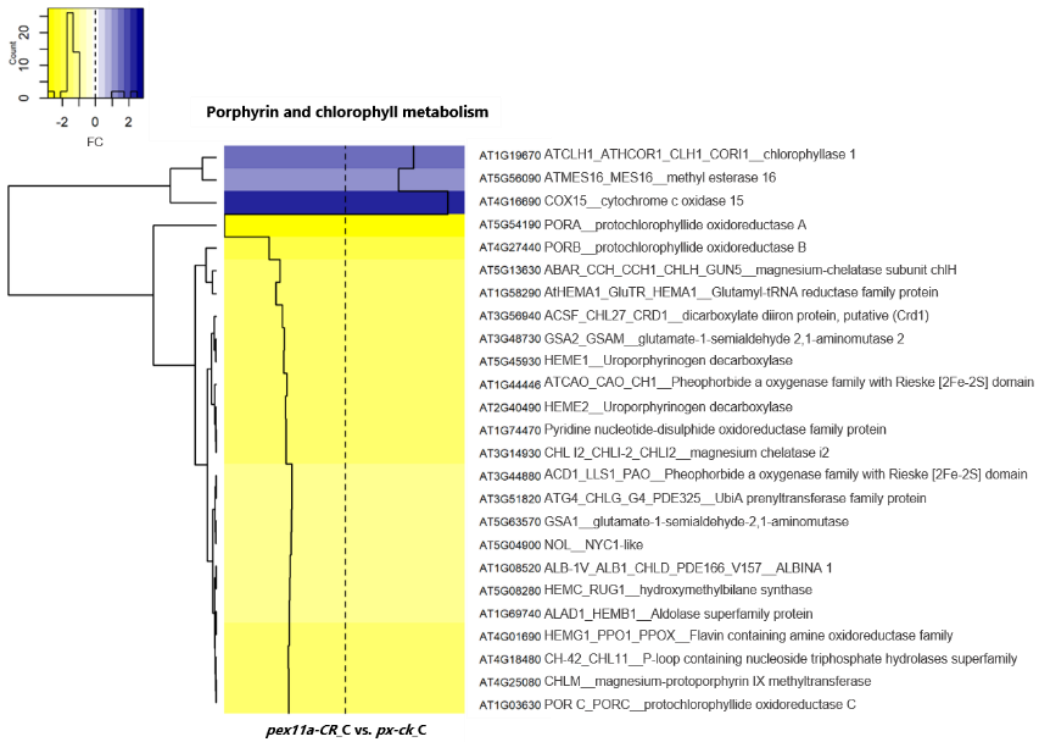

Figure 10. Transcriptional changes in genes from porphyrin and chlorophyll metabolism category in pex11a-CR vs px-ck. *Transcriptional profile represented as a heatmap to highlight genes significantly upregulated (blue) or downregulated (yellow) in pex11a-CR compared to px-ck. Gene expression changes are represented as FC (continuous black line). Count indicates the number of DEGs enriched in this pathway.*

As a first approach to evaluate if pigment abundance is altered in the mutant, chlorophyll a, chlorophyll b, and carotenoids content were measured on 3-weeks leaves of *px-ck* and two different lines of *pex11a-CR (pex11a-CR9* and *pex11a-CR10)* plants grown under short-day conditions, and on 4-weeks leaves of plants grown under long-day conditions (**Fig. 11**). We did not find significant differences in chlorophyll content in plants grown in short day conditions. In these conditions the two different lines of *pex11a-CR* showed a decrease, although not significant, in the carotenoids content (**Fig. 11 A**). However, there were important changes in pigments content in plants grown under

long-day conditions. In both *pex11a-CR* lines, chlorophyll a and b were drastically reduced. In terms of carotenoids content in long-day conditions, *pex11a-CR* mutants showed a slight reduction although significant (**Fig. 11 B**).

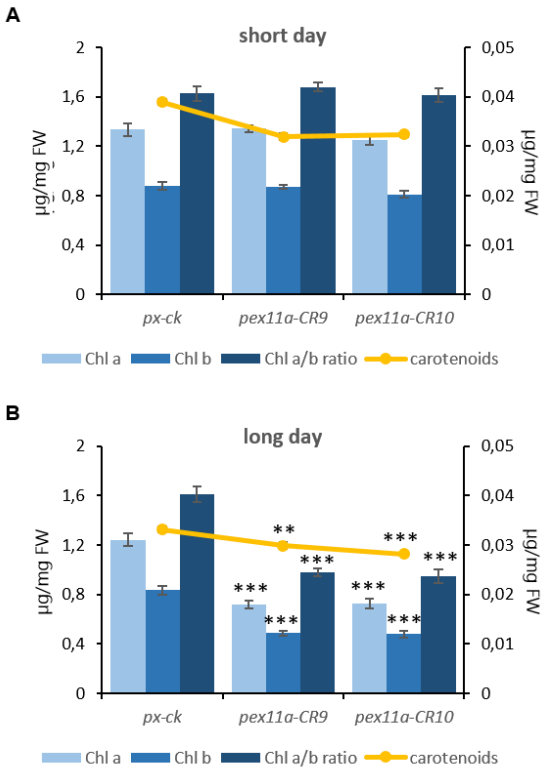

Figure 11. Pigment content of leaves of px-ck and pex11a mutants. (A) *Chlorophyll (Chl) a, Chl b and carotenoids content in plants grown under short day conditions for 3 w.* ***(B)*** *Chl a, Chl b and carotenoids content in leaves in plants grown under long day conditions for 4 w. Main y axis represents µg of Chl/mg FW and secondary y axis indicates µg of carotenoids/mg of FW. Data are mean values of at least 6 replicates ± SEM. Asterisks denote significant differences compared to px-ck according to Student´s t-test (p-value <0.05: *; p-value <0.005: **; p-value <0.001: ***).*

3.5.3. Light stress response

In order to study if quality of light affect *pex11a-CR* phenotype, we analyzed the influence of red and blue light on *px-ck* and *pex11a-CR* on germination. A decrease in the germination rate in response to blue light and a moderate decrease in response to red light were found in all genotypes. In *px-ck* seedlings, the germination rate was 4.5 % and 5.6 % lower respect to control conditions, in response to red and blue light, respectively. No significant changes were found between genotypes under the tested

conditions, although an important decrease was observed in *pex11a-CR* in response to blue light (**Sup. Figure S1**).

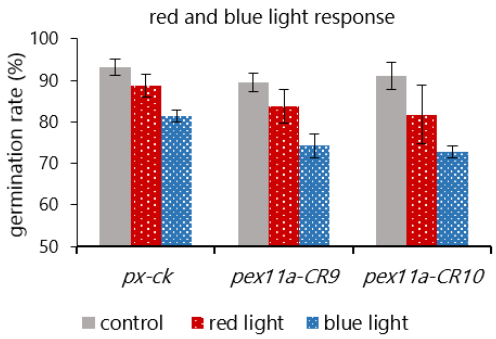

Supplemental Figure S1. Effect of red light and blue light on the germination of px-ck and pex11a-CR seedlings grown in soil. *Data are mean values of at least 2 experiments with 3 replicates ± SEM.*

The effect of low light intensity (70 µmol m^{-2} s^{-1}) on FW of adult plants was also analyzed. FW of 4-week-old plants was measured under short-day and long-day conditions. *pex11a-CR* control plants showed significantly less FW than *px-ck* plants. In *px-ck* plants grown under short day conditions with low light, FW decreased about 79 % while the decrease in *pex11a-CR* was 74 %. Similar trend, was observed under long day conditions (**Sup. Figure S2**).

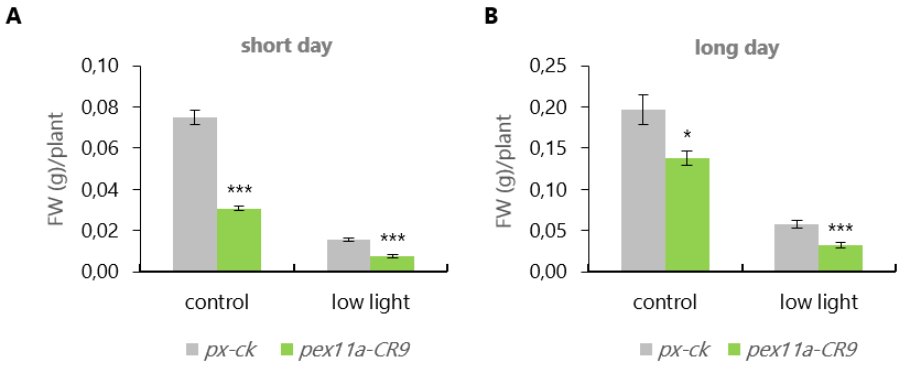

Supplemental Figure S2. Fresh weight (FW) of px-ck and pex11a-CR mutant grow under low intensity light conditions. *Seedlings were grown in MS plates for 7 days and then they were transferred to pots and after 3 weeks growing with low light intensity, FW was measured in short-day conditions* ***(A)*** *and in long-day conditions* ***(B)****. Data are mean values of at least 2 experiments with 6 replicates ±SEM. Asterisks denote significant differences compared to px-ck according to Student´s t-test (p-value <0.05: *; p-value <0.005: **; p-value <0.001: ***).*

In order to analyze high light effects in *pex11a-CR* phenotype we study germination rate and foliar area in plat grown with 600 µmol m^{-2} s^{-1}. A reduction of the number of germinated seed was found in all genotypes. In *px-ck* plants grown under high light conditions germination rate decreased about 31 % while the decrease in *pex11a-CR10* line was 37 %. The most significant change was observed in *pex11a-CR9* line with a reduction of 48 % in the germination rate (**Sup. Figure S3 A**). We measured alterations in the foliar area in plants in response to high light stress after 2 and 3 weeks growing under stress conditions. Both *pex11a-CR* lines showed a significant decrease of rosette area after 14 d and the same trend was observed after 21 d (**Sup. Figure S3 B**).

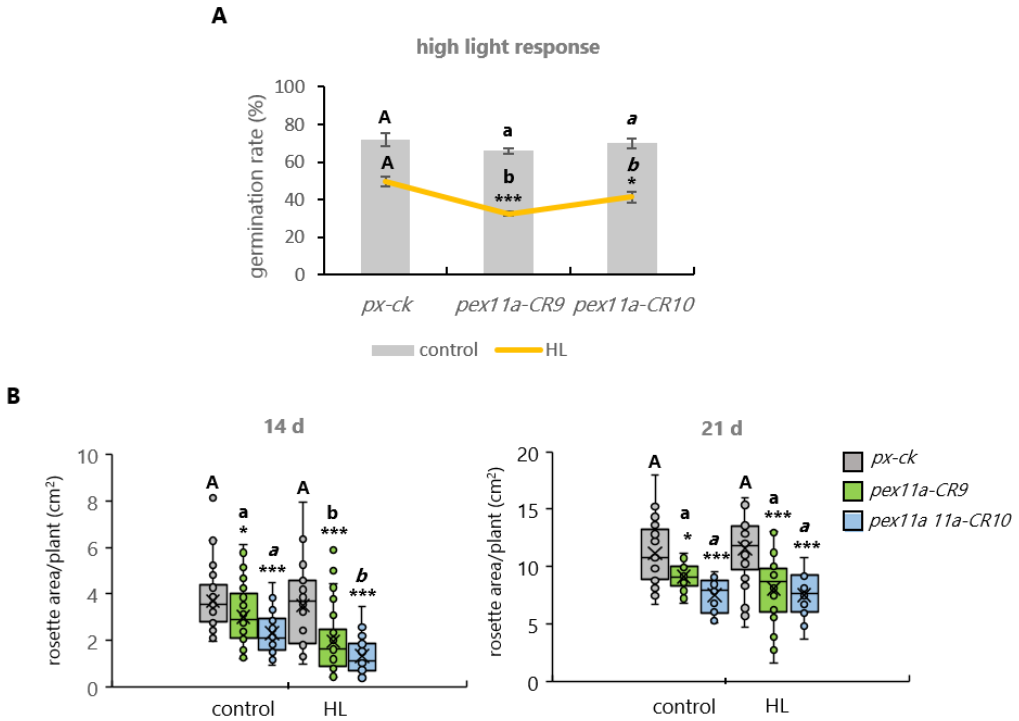

Supplemental Figure S3. px-ck and pex11a-CR lines response to high light (HL) stress. (A) *Germination rate of 5 days old seedlings grown in soil with HL intensity and long day conditions.* ***(B)*** *Foliar area was measured after 14 d and 21 d growing under HL conditions. Asterisks denote significant differences between pex11a-CR9 and pex11a-CR10 and px-ck, within the treatment, according to Student`s t-test (p-value <0.05: *; p-value <0.005: **; p-value <0.001: ***). Different letters denote significant differences between control and HL within the same genotype (px-ck: upper case; pex11a-CR9: lower case; pex11a-CR10: italics; pex11a SK-I; underlined) obtained by the Student`s t-test (p-value< 0.05).*

3.5.4. Analysis of starch metabolism pathway

According to the results of KEGG analysis, "starch and sucrose metabolism pathway" appears to be altered in *pex11a-CR* under control conditions. An overview of genes down and up regulated in this pathway is showed in **Fig. 12.** We found both, induced and repressed DEGs, although most of the genes involved in this pathway were up regulated (blue). To evaluate whether starch metabolism was affected in the mutant, we evaluated starch distribution at the end of the day and at the end of the night in Arabidopsis plants growth under short and long day conditions (**Fig. 13**). Under short day conditions, we found a significant decrease in starch content in *pex11a-CR* at the end of the day and also at the end of the night. The same trend was detected in plants grown under long day conditions, being the starch content in *pex11-CR* significantly lower vs *px-ck* (**Fig. 13**).

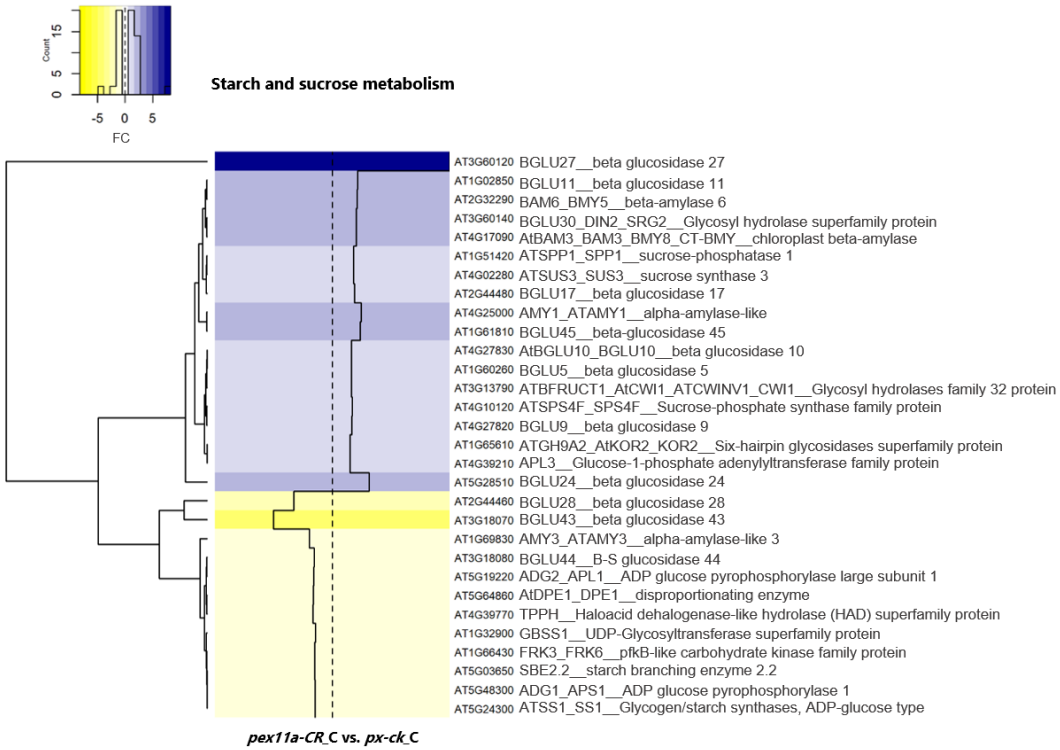

Figure 12. Transcriptional changes in genes from starch and sucrose metabolism in pex11a-CR. *Transcriptional profile represented as a heatmap to highlight genes significantly upregulated (blue) or downregulated (yellow) in pex11a-CR compared to px-ck. Gene expression changes are represented as FC (continuous black line). Count indicates the number of DEGs enriched in this pathway.*

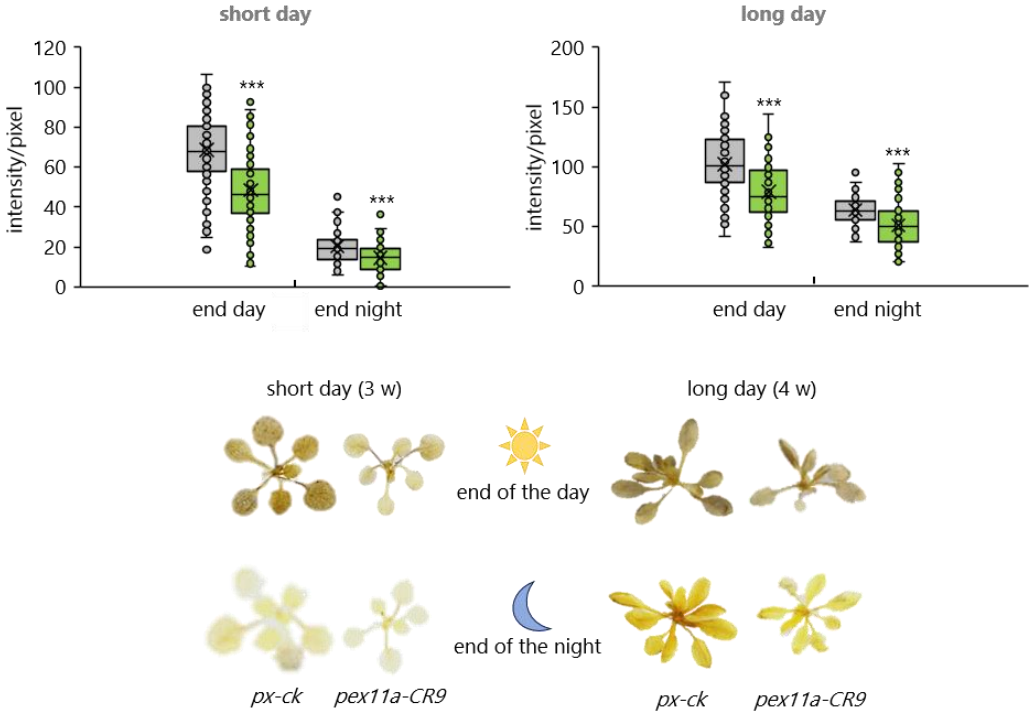

Figure 13. Analysis of starch accumulation in px-ck and pex11a-CR9 rosettes. *3-weeks-old and 4-weeks-old rosettes were collected at the end of the day and the end of the night in short and long day conditions. Rosettes were depigmented and stained with Lugol's solution for starch location. Intensity was measured using ImageJ. Data are mean values of 3 independent experiments with at least 20 measures ± SEM. Asterisks denote significant differences compared to px-ck according to Student´s t-test (p-value <0.05: *; p-value <0.005: **; p-value <0.001: ***).*

3.6. *PEX11a*-dependent genes regulated in plant response to Cd

Volcano plots from the comparisons in each genotype after Cd treatments 1 and 24 h vs. control are shown in **Fig. 14** and **16**. Large sets of DEGs responded to Cd treatment in the leaves of *px-ck* and *pex11-CR* mutant at both time points analysed (**Fig. 14** and **16**). After 1 h treatment, 3,485 genes were regulated in *px-ck* plants (2,560 up and 925 down; **Fig. 14 A**), and 6,192 genes were regulated in *pex11-CR* (3,761 up and 2,431 down; **Fig. 14 B**).

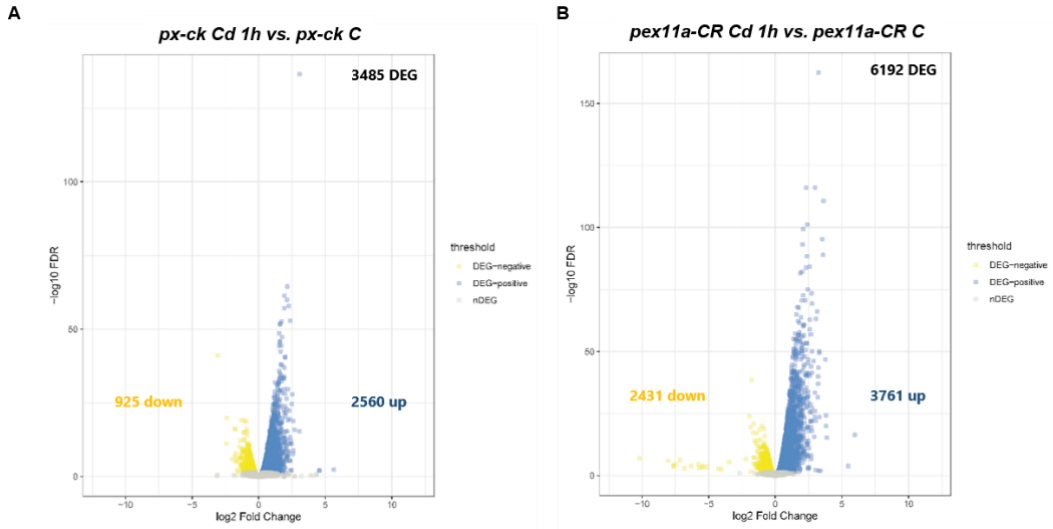

Figure 14. Changes in global transcript expression in pex11a-CR and px-ck in response to short-term Cd treatment. *Volcano plot showing log2 fold change (log2FC) on the x-axis and-log10 FDR (p-value) on the y-axis of gene expression alterations found using edgeR.* ***(A)*** *Cd-treated px-ck seedlings,* ***(B)*** *Cd-treated pex11a-CR seedlings. Number of up- (blue dots) and down-regulated (yellow dots) genes (FDR > 0.05) in px-ck and pex11a-CR after 1 h of Cd treatment. Genes not significally regulated (nDEGs) are grey dots.*

When comparing genes regulated in *px-ck* and *pex11-CR* in response to Cd at 1 h, we found 750 genes regulated in *px-ck* but not in *pex11-CR* mutant, which we consider early *PEX11a*-dependent genes (**Fig. 15 A**; **Sup. Table S6**). Increasing astringency decreased the number of *PEX11a*-dependent genes as expected, being 193 and 28 when applying |log2FC|≥1 and |log2FC|≥2, respectively (**Fig. 15 A**; **Sup. Table S7**). After analyzing the 750 early *PEX11a*-dependent genes we found GO categories in the BP related with ion and in particular, with iron homeostasis and transport (**Fig. 15 B**; **Sup. Table S8 A**). It has been widely studied that iron and in general, ion metabolism is a key process in plant response to Cd. We represented *PEX11a*-dependent genes related with iron metabolism and transport in a heatmap (**Fig. 17**). After 1 h of Cd treatment, most genes were up-regulated and and curiously, after Cd 24 h we only found one gene that was also up-regulated. Further enrichment analysis by Plant GSEA showed plant response to stress/stimulus as categories significantly overrepresented (**Fig. 15 B**; **Sup. Table S9**). The only MF found as significantly overrepresented in *PEX11a*-dependent DEGs in early plant response to Cd is polygalacturonase activity (**Sup. Table S8 B**).

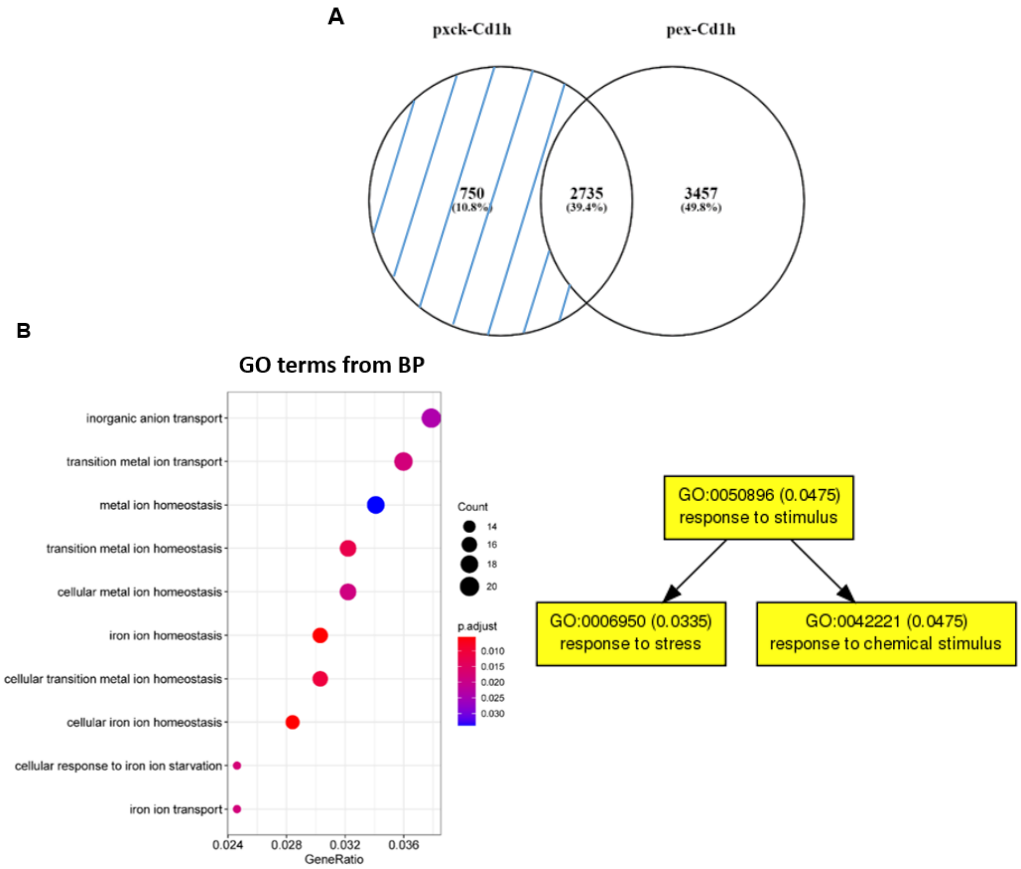

Figure 15. Changes in global transcript expression in pex11a-CR mutant compared to px-ck in response to short-term Cd treatment. (A) *Venn diagrams showing overlap and specificity between gene expression changes in each genotype after 1 h of treatment. DEGs in px-ck seedlings, but not pex11a-CR (PEX11a-dependent) is marked by blue.* ***(B)*** *Main categories after gene ontology (GO) enrichment of PEX11a-dependent DEGs after 1 h of Cd treatment.*

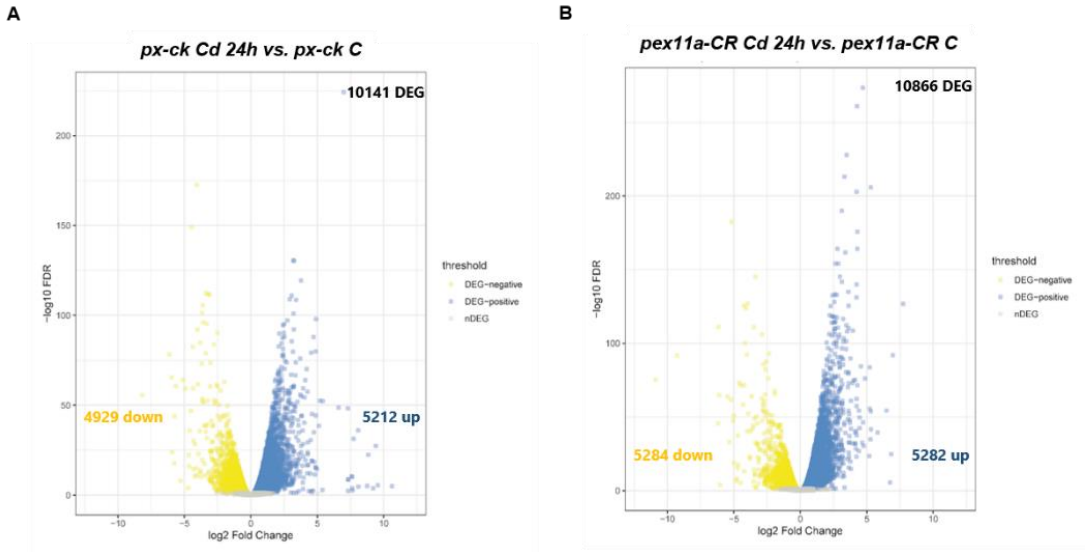

Figure 16. Changes in global transcript expression in pex11a-CR and px-ck in response to long-term Cd treatment. *Volcano plot showing log2 fold change (log2FC) on the x-axis and-log10 FDR (p-value) on the y-axis of gene expression alterations found using edgeR.* ***(A)*** *Cd-treated px-ck seedlings,* ***(B)*** *Cd-treated pex11a-CR seedlings. Number of up- (blue dots) and down-regulated (yellow dots) genes (FDR > 0.05) in px-ck and pex11a-CR mutants after 24 h of Cd treatment. Genes not significally regulated (nDEGs) are grey dots.*

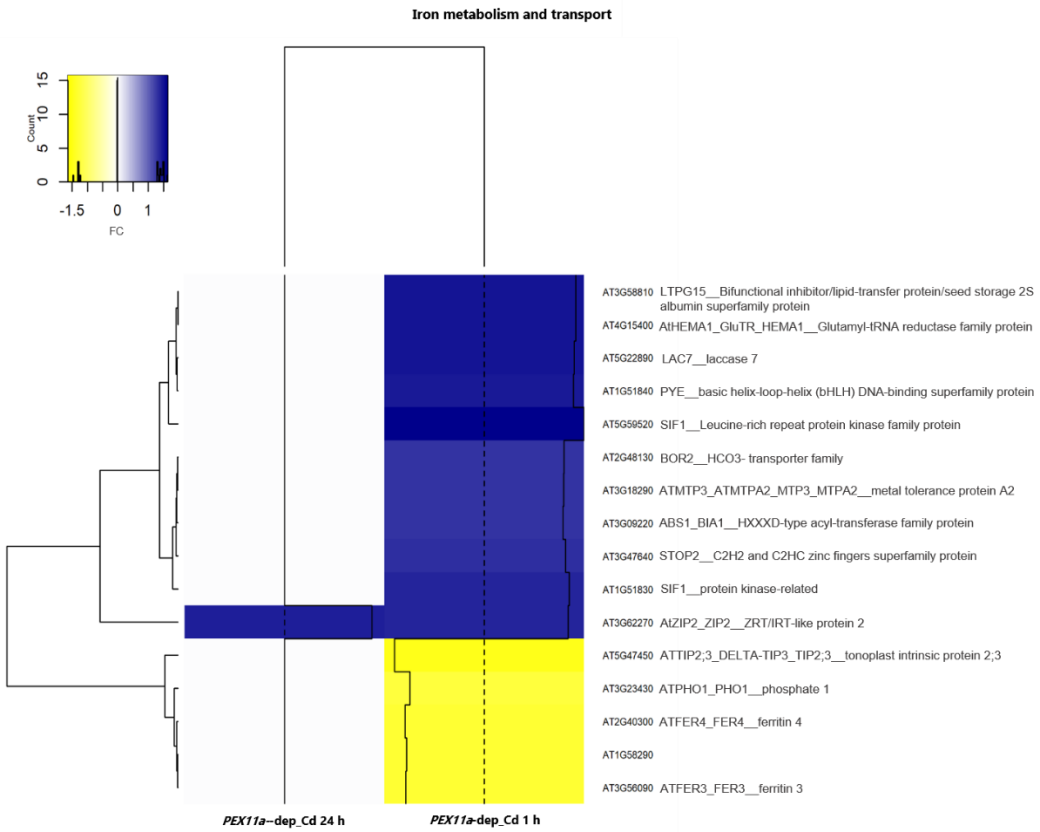

Figure 17. Transcriptional changes for PEX11a-dependent genes related with iron metabolism and transport after 1 h and 24 h of Cd treatment. *Transcriptional profile represented as a heatmap to highlight genes significantly upregulated (blue) or downregulated (yellow) in px-ck but not in pex11a-CR in plant response to Cd. Gene expression changes are represented as FC (continuous black line). Count indicates the number of DEGs enriched in this pathway.*

After 24 h treatment, 10,141 genes were regulated in *px-ck* plants (5,212 up and 4,929 down), and 10,866 genes were regulated in *pex11-CR* (5,582 up and 5,284 down; **Fig. 17**). When comparing genes regulated in *px-ck* and *pex11-CR* in response to Cd at 24 h, we found 3,595 genes regulated in *px-ck* but not in *pex11-CR* mutant, which we consider later *PEX11a*-dependent genes (**Fig. 18**; **Sup. Table S10**). Increasing astringency

decreased the number of *PEX11a*-dependent genes as expected being 957 and 235 when applying |log2FC|≥1 and |log2FC|≥2, respectively (**Fig. 18 A**; **Sup. Table S11**). We further considered the threshold of |log2FC|≥1 at this time point, and then analysed enrichment terms of the 957 *PEX11a*-dependent genes. We found 17 GO categories in the BP ontology with main enriched terms being peptide metabolic and biosynthetic processes, different glycosylation related categories and translation (**Fig. 18 B**; **Sup. Table S12 A**). Three MF categories were overrepresented within *PEX11a*-dependent genes after 24 h Cd treatment: structural molecule activity, structural constituent of ribosome, and peptidyl-prolyl cis-trans isomerase activity (**Fig. 18 B**; **Sup. Table S12 B**). Plant GSEA however, showed nutrient reservoir activity as the only MF overrepresented significantly (**Sup. Table S13**), which is similar to the results obtained by StringDB. Interestingly, most of CC categories significantly overrepresented are related with ribosomes and nucleus (**Fig 18 B**; **Sup. Table S12 C**).

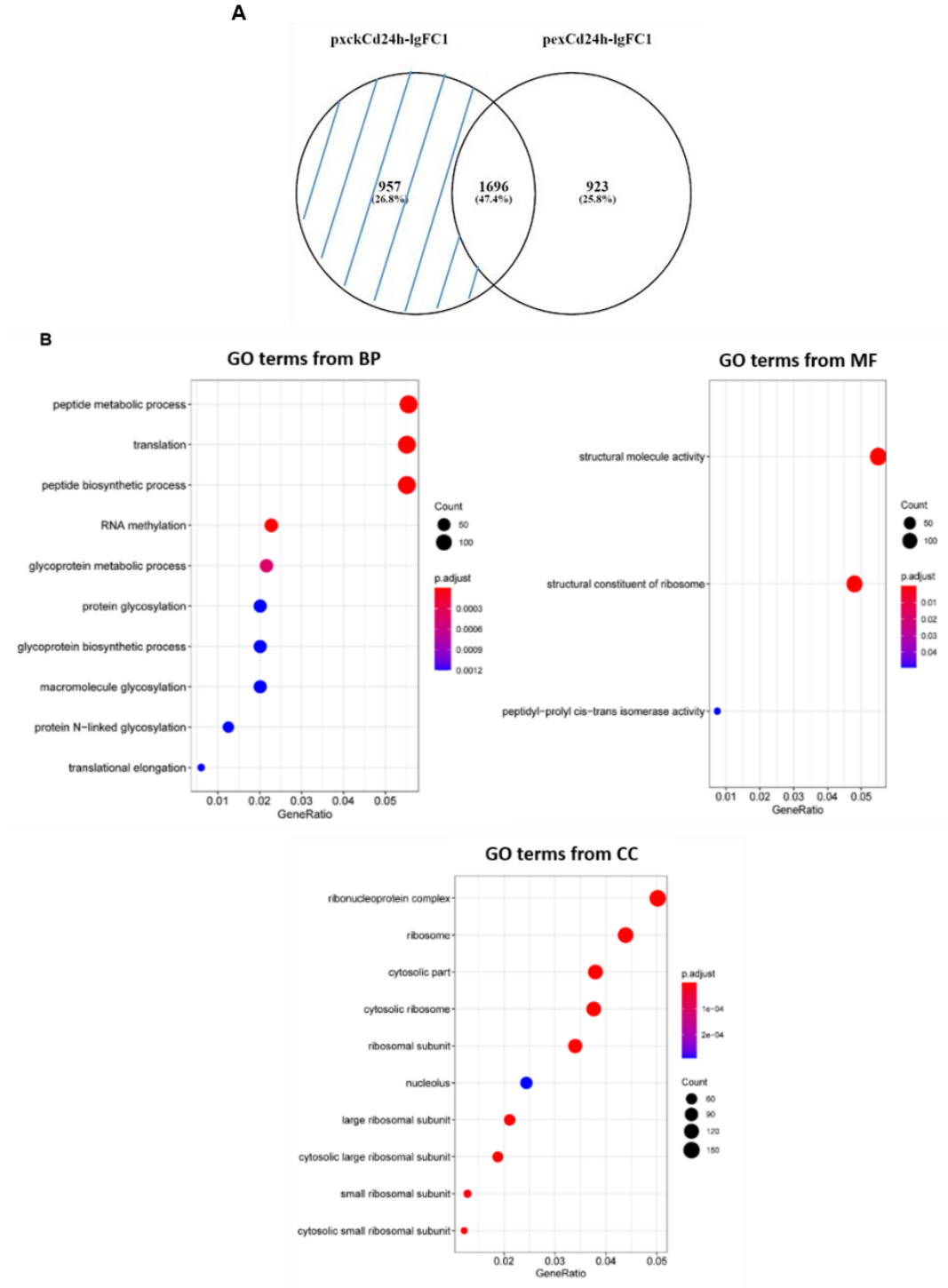

Figure 18. Changes in global transcript expression in the pex11a-CR mutant compared to px-ck in response to long-term Cd treatment. (A) *Venn diagrams showing overlap and specific DEGs*

between pex11a-CR and px-ck after 24 h of Cd treatment. DEGs in px-ck seedlings, but not in pex11a-CR (PEX11a-dependent) is marked by blue. ***(B)*** *Main categories after gene ontology (GO) enrichment of PEX11a-dependent DEGs after 24 h of Cd treatment and |log2FC|≥1.*

Accordingly, enrichment analysis showed ribosome and the nuclear spliceosome (a large ribonucleoprotein complex) as significant KEGG pathways within PEX11a-dependent genes, in plant response to Cd after 24 h treatment (**Fig. 19; Sup. Table S14**).

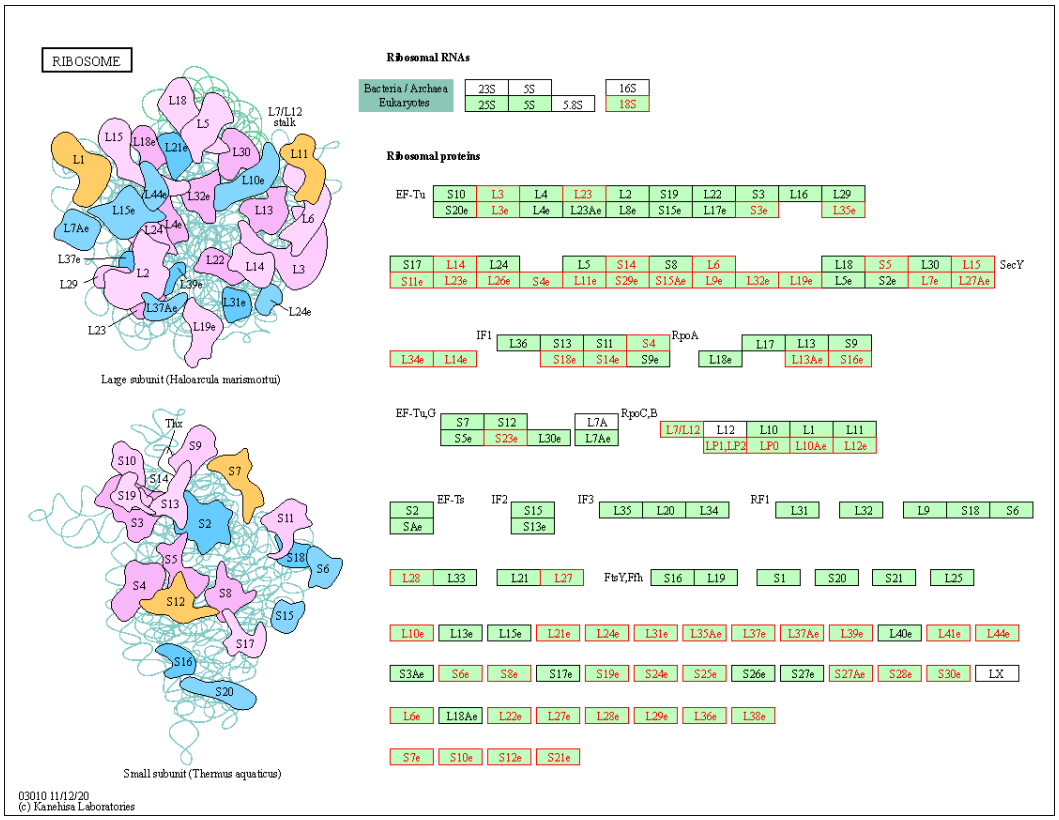

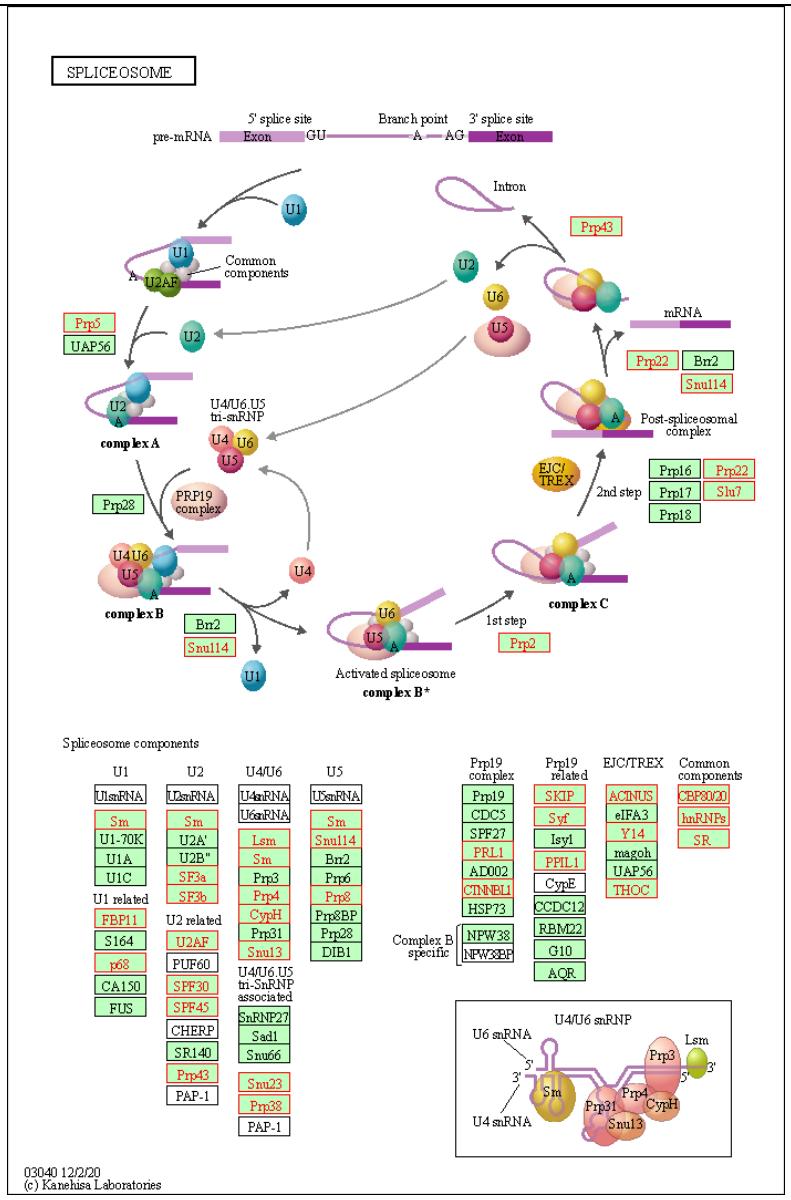

Figure 19. PEX11a-dependent genes in plant response to Cd 24 h within Ribosome and Spliceosome pathways. *Red boxes mean up-regulated genes and green boxes mean down-regulated genes in px-ck. The pathway frames are from the KEGG database.*

4. DISCUSSION

This study investigated early (1 h) and later (24 h) effects of cadmium (Cd) treatment in the transcriptome of *px-ck* and *pex11a-CR* seedlings, which is affected in peroxules production. Previous transcriptomic studies reporting the effect of Cd are focused on metal tolerance and accumulation in plants, rather than signalling and stress response (Takahashi *et al.,* 2011; Derakhshani *et al.,* 2020). The general objective of our study was to get a deeper insight into *PEX11a* function under control conditions and in plant response to Cd, since the implication of this protein in the rapid response to stress has been previously described (Rodríguez-Serrano *et al.,* 2016; Terrón-Camero *et al.,* 2020).

The analysis of variation among samples showed that control replicates clustered well and independently, however *pex11a-CR* control samples highly clustered with *px-ck* samples after 1 h Cd treatment, suggesting a great alteration of the mutant under normal conditions. In fact, a total of 1,994 significant DEGs being 1,106 up-regulated and 888 down-regulated were found under control conditions in the mutant vs *px-ck*. Results of phenotypic characterization of *pex11a-CR* lines showed in chapter 3 support this high number of differentially expressed transcripts. After the functional annotation analysis of DEGs altered in control conditions, all the categories enriched in cellular components were related to chloroplast. In particular, thylakoids, photosynthetic membrane, and light-harvesting complex as well as chlorophyll binding. We measured chlorophyll content in leaves of *pex11a-CR* mutants finding a remarkably decrease, and the ratio thylakoid/stroma was also reduced in *pex11a-CR*, which support transcriptomic data. Cd toxicity affects many aspects of plant metabolism like growth and root length, enzyme activity and photosynthesis (Sandalio *et al.,* 2001; Qadir *et al,* 2014; Haider *et al.,* 2021) being chloroplast one of the main targets under Cd treatment. Supply of cadmium chloride (0.5 mM) inhibited chlorophyll formation in pea and maize leaf (Sandalio *et al.,* 2001; Jain *et al.,* 2007). Furthermore, chloroplast from Cd treated pea after two weeks showed disorganized thylakoids, and a higher number and size of plastoglobuli and starch grains (Sandalio *et al.,* 2001). As *pex11a-CR* mutants already showed altered chloroplast phenotype under normal conditions, it would be interesting to analyze in depth if Cd treatment emphasize this phenotype. Chloroplast phenotype in *pex11a-CR* under normal conditions may be part of the reasons for transcriptomic clustering with

px-ck treated with Cd 1 h. On the other hand, in leaves, an early induction of several genes encoding enzymes involved in the biosynthesis of phenylpropanoids was observed in Arabidopsis in response to Cd (Herbette *et al,* 2006).

Starch and sugar metabolism was also disturbed in *pex11a-CR* mutants as shown in the transcriptomic analysis with starch synthases being down regulated, while β-amylases were up-regulated, giving rise a reduction of starch accumulation. Disturbances of photosynthesis rate and carbohydrates could explain the reduction of size and biomass observed in *pex11a-CR* mutants as it has been shown in mutants lacking chloroplast fructose-1,6-bisphosphatase (FBPase), involved in the Calvin-Benson cycle (Rojas *et al.*, 2015). Therefore, PEX11a loss of function interfere with chloroplasts metabolism and structure. Several evidences in the literature support an intimate relationship between peroxisome and chloroplast metabolisms although the molecular mechanism have not been well stablished. Thus, Chlamydomonas mutants deficient in peroxisomal NAD^+-dependent malate dehydrogenase 2 (MDH2) show disturbances in the reverse coupling of redox/H_2O_2 signals from peroxisomes to chloroplasts (Kong *et al.,* 2018). In Arabidopsis plants the peroxisomal $NAD(P)^+$/NAD(P)H rate regulates photosynthesis performance to meet the demand for reducing equivalents under fluctuating light (Li *et al.,* 2019). In addition, the peroxisomal H_2O_2 basal levels affect considerably the antioxidative defense regulation in both cytosol and chloroplasts, as it was reported in peroxisomal *apx4* knockdown rice plants (Sousa *et al.,* 2018). The inhibition of catalase (CAT) activity in *apx4* rice mutants affected considerably the photosynthetic performance under adverse conditions, thus promoting oxidative stress and favouring antioxidant enzyme accumulation in cytosol and chloroplasts (Sousa *et al.,* 2018). The use of optical tweezers has allowed to demonstrate the interaction between peroxisomes and chloroplasts which are tethered through peroxules in vivo in epidermal cells of tobacco leaf (Gao *et al.* 2016). However, the structure involved in tethering has not been described. Based on our results, PEX11a could participate in this issue regulating redox homeostasis, metabolites transport and signalling processes in chloroplasts. These results illustrate the coordination of chloroplasts and peroxisomes in retrograde signal pathways. Further analysis however, are needed to confirm this hypothesis.

Between the early PEX11a-dependent genes regulated after Cd 1 h the category of iron and metal transition homeostasis and transport is stand outs suggesting a

connection between peroxules and heavy metal homeostasis in plant cells and a new function for peroxisomes. Cd, is a no-essential heavy metal, which shares chemical properties with iron and it has long been known that it is able to enter in root cells by using iron uptake transporters (Korshunova *et al.,* 1999; Guerinot, 2000). Therefore, Cd compete with iron for transporters and Cd induces a transcriptional program in part overlapping with transcription induced by Fe deficiency. High H_2O_2 level however, may regulate iron homeostasis under Cd stress conditions (McInturf *et al.,* 2021). In addition, several evidences outline an important role of ROS on the regulation of ion/metal transporters (Gupta *et al.,* 2017; Huang et al., 2019). Therefore, disturbances of ROS homeostasis and ROS-dependent signalling derived of PEX11a (Rodríguez-Serrano *et al.,* 2016), could explain transcriptional changes observed in some genes grouped in iron and metal transition observed in this work.

Wide range of translational changes usually take place in response to different stress conditions (Merchant *et al.,* 2017). Under Cd stress, cells have to reorganize their protein production at both quantitative and qualitatively level to cope with the pleiotropic cellular stress induced by the metal. One of gene categories more represented in response to Cd in Arabidopsis cells in response to Cd in plants is 'Translation, ribosomal structure and biogenesis" suggesting that translation exerts a homeostatic role to maintain essential cell functions (Sormani *et al.,* 2011; Ma *et al.,* 2018; Romero-Puertas *et al.,* 2019). In our work, the enrichment of the later transcriptional response to Cd (24 h) in PEX11a-dependent genes displayed a link with nucleus, ribosomes, translation and peptide metabolic and biosynthetic processes, suggesting PEX11a-dependent regulation of not only transcription but also translation. Splicing is a fundamental RNA-processing step for eukaryotic gene expression involved in the removal of introns and the joining of different exons together, thus generating mature transcripts (Laloum *et al.,* 2018). This process allows quantitative and qualitative regulation of gene expression sequences of pre-mRNA. Splicing reaction occurs in the spliceosome, a large ribonucleoprotein complex which is composed of five small nuclear ribonucleoproteins (snRNPs) and a number of non-snRNP associated proteins (Laloum *et al.,* 2018). The activation of spliceosome by Cd treatment has been reported in yeast as a mechanism to increases the efficiency of general splicing thus adjusting gene expression landscape required for heavy metal detoxification (Chanarat and Svasti, 2020). In Arabidopsis plants mutation of

splicing factor SR34b reduces cadmium tolerance by regulating IRT1 (Zhang *et al.,* 2014). Spliceosome has been also associated to ABA and sugar signalling in development and under stress conditions (Laloum *et al.,* 2018). No data as far as we know has been shown related with PEX11 family and splicing regulation, pointing transcriptomic data to a new possible function for PEX11a in plant biology which need further analysis.

5. Supplementary Material

Suppl. Table S1. *Data quality control summary.*

sample	raw_reads	clean_reads	raw_data(G)	clean_data(G)	error_rate(%)	Q
px-ck1_C	80638437	79939991	24.2	24.0	0.02	9
px-ck2_C	85258405	83748613	25.6	25.1	0.02	9
px-ck3_C	83910673	83025514	25.2	24.9	0.02	9
px-ck1_Cd1h	80351447	79568473	24.1	23.9	0.02	9
px-ck2_Cd1h	69696364	68889303	20.9	20.7	0.02	9
px-ck3_Cd1h	67565421	66530251	20.3	20.0	0.02	9
px-ck1_Cd24h	68590992	67828750	20.6	20.3	0.02	9
px-ck2_Cd24h	85274104	84535418	25.6	25.4	0.02	9
px-ck3_Cd24h	72036630	70459429	21.6	21.1	0.02	9
pex11a-CR1_C	78329498	77056828	23.5	23.1	0.02	9
pex11a-CR2_C	85635405	84229123	25.7	25.3	0.02	9
pex11a-CR3_C	68879402	67999811	20.7	20.4	0.02	9
pex11a-CR1_Cd1h	92755941	91331699	27.8	27.4	0.02	9
pex11a-CR2_Cd1h	75954938	74790219	22.8	22.4	0.02	9
pex11a-CR3_Cd1h	91918968	90897159	27.6	27.3	0.02	9
pex11a-CR1_Cd24h	74747674	73930730	22.4	22.2	0.02	9
pex11a-CR2_Cd24h	70588998	69778668	21.2	20.9	0.03	9
pex11a-CR3_Cd24h	78319156	77220947	23.5	23.2	0.02	9

Suppl. Table S2 A. *Data quality control summary for px-ck samples.*

Sample name	px-ck1_C	px-ck2_C	px-ck3_C	px-ck1_Cd1h	px-ck2_Cd1h	px-ck3_Cd1h	px-ck
Total reads	159879982	167497226	166051028	159136946	137778606	133060502	1356
Total mapped	156326125 (97.78%)	163513903 (97.62%)	162247767 (97.71%)	154460808 (97.06%)	134547732 (97.66%)	129638367 (97.43%)	1332 (98
Multiple mapped	8808239 (5.51%)	16845176 (10.06%)	9315679 (5.61%)	8671005 (5.45%)	6890560 (5.00%)	7731575 (5.81%)	665 (4.
Uniquely mapped	147517886 (92.27%)	146668727 (87.56%)	152932088 (92.10%)	145789803 (91.61%)	127657172 (92.65%)	121906792 (91.62%)	1265 (93
Read-1	73834339 (46.18%)	73401237 (43.82%)	76541113 (46.09%)	72972931 (45.86%)	63983050 (46.44%)	60969335 (45.82%)	632 (46
Read-2	73683547 (46.09%)	73267490 (43.74%)	76390975 (46.00%)	72816872 (45.76%)	63674122 (46.21%)	60937457 (45.80%)	633 (46
Reads map to '+'	73736754 (46.12%)	73311599 (43.77%)	76453023 (46.04%)	72878179 (45.80%)	63815182 (46.32%)	60936064 (45.80%)	632 (46
Reads map to '-'	73781132 (46.15%)	73357128 (43.80%)	76479065 (46.06%)	72911624 (45.82%)	63841990 (46.34%)	60970728 (45.82%)	633 (46
Non-splice reads	112290349 (70.23%)	116457972 (69.53%)	120305274 (72.45%)	112149454 (70.47%)	98999818 (71.85%)	95774234 (71.98%)	960 (70
Splice reads	35227537 (22.03%)	30210755 (18.04%)	32626814 (19.65%)	33640349 (21.14%)	28657354 (20.80%)	26132558 (19.64%)	305 (22

Suppl. Table S2 B. *Data quality control summary for pex11a-CR samples.*

Sample name	pex11a-CR1_C	pex11a-CR2_C	pex11a-CR3_C	pex11a-CR1_Cd1h	pex11a-CR2_Cd1h	pex11a-CR3_Cd1h	pex CR1
Total reads	154113656	168458246	135999622	182663398	149580438	181794318	1478
Total mapped	151943631 (98.59%)	165906449 (98.49%)	133564254 (98.21%)	178059542 (97.48%)	145092095 (97.00%)	176960510 (97.34%)	1455 (98
Multiple mapped	8603490 (5.58%)	9504370 (5.64%)	7849223 (5.77%)	9837739 (5.39%)	8024881 (5.36%)	10951474 (6.02%)	752 (5.
Uniquely mapped	143340141 (93.01%)	156402079 (92.84%)	125715031 (92.44%)	168221803 (92.09%)	137067214 (91.63%)	166009036 (91.32%)	1380 (93
Read-1	71738403 (46.55%)	78209913 (46.43%)	62866933 (46.23%)	84147114 (46.07%)	68543656 (45.82%)	83017549 (45.67%)	690 (46
Read-2	71601738 (46.46%)	78192166 (46.42%)	62848098 (46.21%)	84074689 (46.03%)	68523558 (45.81%)	82991487 (45.65%)	690 (46
Reads map to '+'	71644383 (46.49%)	78163041 (46.40%)	62837446 (46.20%)	84081572 (46.03%)	68509617 (45.80%)	82973427 (45.64%)	689 (46
Reads map to '-'	71695758 (46.52%)	78239038 (46.44%)	62877585 (46.23%)	84140231 (46.06%)	68557597 (45.83%)	83035609 (45.68%)	690 (46
Non-splice reads	105572514 (68.50%)	117159310 (69.55%)	94596841 (69.56%)	124574867 (68.20%)	102142318 (68.29%)	123547305 (67.96%)	1004 (67
Splice reads	37767627 (24.51%)	39242769 (23.30%)	31118190 (22.88%)	43646936 (23.89%)	34924896 (23.35%)	42461731 (23.36%)	375 (25

6. REFERENCES

Calero-Muñoz N, Expósito-Rodríguez M, Collado-Arenal AM, et al. 2019. Cadmium induces reactive oxygen species-dependent pexophagy in Arabidopsis leaves. Plant, Cell and Environment **42**, 2696–2714.

Chanarat S, Svasti J. 2020. Stress-induced upregulation of the ubiquitin-relative Hub1 modulates pre-mRNA splicing and facilitates cadmium tolerance in *Saccharomyces cerevisiae*. Biochimica et Biophysica Acta-Molecular Cell Research **2**, 118565.

Derakhshani, B., Jafary, H., Zanjani, B. M., Hasanpur, K., Mishina, K., Tanaka, T., et al. 2020. Combined QTL mapping and RNA-Seq profiling reveals candidate genes associated with cadmium tolerance in barley. PLoS ONE 15, 1–19.

Gao H, Metz J, Teanby NA, Ward AD, Botchway SW, Coles B, Pollard MR, Sparkes I. 2016. In vivo quantification of peroxisome tethering to chloroplasts in tobacco epidermal cells using optical tweezers. Plant Physiology **170**, 263–272.

Genchi G, Sinicropi MS, Lauria G, Carocci A, Catalano A. 2020. The effects of cadmium toxicity. International Journal of Environmental Research and Public Health **17**, 1–24.

Guerinot, M.L. 2000. The ZIP family of metal transporters. Biochimica et Biophysica Acta **1465**, 190–198.

Gupta DK, Pena LB, Romero-Puertas MC, Hernández A, Inouhe M, Sandalio LM. 2017. NADPH oxidases differentially regulate ROS metabolism and nutrient uptake under cadmium toxicity. Plant, Cell and Environment **40**, 509–526.

Haider FU, Liqun C, Coulter JA, Cheema SA, Wu J, Zhang R, Wenjun M, Farooq M. 2021. Cadmium toxicity in plants: Impacts and remediation strategies. Ecotoxicology and Environmental Safety **211**, 111887.

Herbette S, Taconnat L, Hugouvieux V, Piette L, Magniette ML, Cuine S, Auroy P, Richaud P, Forestier C, Bourguignon J et al. 2006**.** Genome-wide transcriptome profiling of the early cadmium response of Arabidopsis roots and shoots. Biochimie **11**, 1751–65.

Huang H, Ullah F, Zhou DX, Yi M, Zhao Y. 2019. Mechanisms of ROS regulation of plant development and stress responses. Frontiers in Plant Science **10**, 1–10.

Jain M, Pal M, Gupta P, Gadre R. 2007. Effect of cadmium on chlorophyll biosynthesis and enzymes of nitrogen assimilation in greening maize leaf segments: Role of 2-oxoglutarate. Indian Journal of Experimental Biology **45**, 385-389.

Kaur N, Reumann S, Hu J. 2009. Peroxisome biogenesis and function. The Arabidopsis Book **7**, e0123.

Kim D, Langmead B, Salzberg SL. 2015. HISAT: a fast spliced aligner with low memory requirements. Nature Methods **12**, 357–360.

Kong F, Burlacot A, Liang Y, Légeret B, Alseekh S, Brotman Y, Fernie AR, Krieger-Liszkay A, Beisson F, Peltier G et al. 2018. Interorganelle communication: Peroxisomal MALATE DEHYDROGENASE2 connects lipid catabolism to photosynthesis through redox coupling in Chlamydomonas. Plant Cell **8**, 1824–1847.

Korshunova YO, Eide D, Clark WG, Guerinot ML, Pakrasi HB. 1999. The IRT1 protein from Arabidopsis thaliana is a metal transporter with a broad substrate range. Plant Molecular Biology **1**, 37–44.

Laloum T, Martín G, Duque P. 2018. Alternative splicing control of abiotic stress responses. Trends in Plant Science **2**, 140–150.

Li J, Tietz S, Cruz JA, Strand DD, Xu Y, Chen J, Kramer DM, Hu J. 2019. Photometric screens identified Arabidopsis peroxisome proteins that impact photosynthesis under dynamic light conditions. The Plant Journal **97**, 460–474.

Liao Y, Smyth GK, Shi W. 2014. featureCounts: an efficient general purpose program for assigning sequence reads to genomic features. Bioinformatics **30**, 923–930.

Lichtenthaler HK, Wellburn RA. 1983. Determinations of total carotenoids and chlorophylls a and b of leaf extracts in different solvents. Biochemical Society Transactions **11**, 591–592.

Ma JQ, Jian HJ, Yang B, Lu K, Zhang AX, Liu P, Li JN. 2018. Genome-wide analysis and expression profiling of the HMA gene family in oilseed rape (*Brassica napus*). Gene **620**, 36–45.

McInturf SA, Khan MA, Gokul A, Castro-Guerrero NA, Hohner R, Li J, Marjault HB, Fichman Y, Kunz HH, Goggin FL et al. 2021. Cadmium interference with iron sensing reveals transcriptional programs sensitive and insensitive to reactive oxygen species. Journal of Experimental Botany, erab393.

Merchante C, Stepanova AN, Alonso JM. 2017. Translation regulation in plants: an interesting past, an exciting present and a promising future. The Plant Journal **90**, 628–653.

Murashige T, Skoog F. 1962. A revised medium for rapid growth and bio assays with tobacco tissue cultures. Physiol. Plant. **15**: 473–497.

Nikolayeva O, Robinson MD. 2014. edgeR for differential RNA-seq and ChIP-seq analysis: an application to stem cell biology. Methods in Molecular Biology **1150**, 45–79.

Pan R, Liu J, Wang S, Hu J. 2020. Peroxisomes: Versatile organelles with diverse roles in plants. New Phytologist **225**,

1410–1427.

Qadir S, Jamshieed S, Rasool S, Ashraf M, Akram NA, Ahmad P. 2014. Modulation of plant growth and metabolism in cadmium-enriched environments. Reviews of Environmental Contamination and Toxicology **229**, 51–88.

Reeb PD, Bramardi S, Steibel JP. 2015. Assessing Dissimilarity Measures for Sample- Based Hierarchical Clustering of RNA Sequencing Data Using Plasmode Datasets. PLoS ONE **10**, 1–18.

Ritchie ME, Phipson B, Wu D, Hu Y, Law CW, Shi W, Smyth GK. 2015. limma powers differential expression analyses for RNA-sequencing and microarray studies. Nucleic Acids Research **43**, e47.

Robinson MD, Oshlack A. 2010. A scaling normalization method for differential expression analysis of RNA-seq data. Genome Biology **11**, R25.

Rodríguez-Serrano M, Romero-Puertas MC, Sanz-Fernández M, Hu J, Sandalio LM. 2016. Peroxisomes extend peroxules in a fast response to stress via a reactive oxygen species-mediated induction of the peroxin PEX11a. Plant Physiology **171**, 1665–1674.

Rojas-González JA, Soto-Súarez M, García-Díaz Á, Romero-Puertas MC, Sandalio LM, Mérida Á, Thormählen I, Geigenberger P, Serrato AJ, Sahrawy M. 2015. Disruption of both chloroplastic and cytosolic FBPase genes results in a dwarf phenotype and important starch and metabolite changes in *Arabidopsis thaliana*. Journal of Experimental Botany **9**, 2673–89.

Romero-Puertas MC, McCarthy I, Sandalio LM, Palma JM, Corpas FJ, Gómez M, Del Río LA. 1999. Cadmium toxicity and oxidative metabolism in pea leaf peroxisomes. Free Radical Research **31**, S25–31.

Romero-Puertas MC, Palma JM, Gómez M, Del Río LA, Sandalio LM. 2002. Cadmium causes the oxidative modification of proteins in pea plants. Plant, Cell and Environment **25**, 677–686.

Romero-Puertas MC, Terrón-Camero LC, Peláez-Vico MÁ, Olmedilla A, Sandalio LM. 2019. Reactive oxygen and nitrogen species as key indicators of plant responses to Cd stress. Environmental and Experimental Botany **161**, 107–119.

Sandalio LM, Dalurzo, HC, Gómez M, Romero-Puertas MC, Del Río LA. 2001. Cadmium-induced changes in the growth and oxidative metabolism of pea plants. Journal of Experimental Botany **364**, 2115–2126.

Sandalio LM, Romero-Puertas MC. 2015. Peroxisomes sense and respond to environmental cues by regulating ROS and RNS signalling networks. Annals of Botany **116**, 475–485.

Sandalio LM, Peláez-Vico MA, Romero-Puertas MC. 2020. Peroxisomal metabolism and dynamics at the crossroads between stimulus perception and fast cell responses to the environment. Frontiers in Cell and Developmental Biology **8**, 1–5.

Sandalio LM, Peláez-Vico MA, Molina-Moya E, Romero-Puertas MC. 2021. Peroxisomes as redox-signalling nodes in intracellular communication and stress responses. Plant Physiology **186**, 22–35.

Sinclair AM, Trobacher CP, Mathur N, Greenwood JS, Mathur J. 2009. Peroxule extension over ER-defined paths constitutes a rapid subcellular response to hydroxyl stress. Plant Journal **59**, 231–242.

Sormani R, Delannoy E, Lageix S, Bitton F, Lanet E, Saez-Vasquez J, Deragon JM, Renou JP, Robaglia C. 2011. Sublethal cadmium intoxication in *Arabidopsis thaliana* impacts translation at multiple levels. Plant and Cell Physiology **2**, 436–447.

Sousa RHV, Carvalho FEL, Lima-Melo Y, Alencar VTCB, Daloso DM, Margis-Pinheiro M, Komatsu S, Silveira JAG. 2018. Impairment of peroxisomal APX and CAT activities increases protection of photosynthesis under oxidative stress. Journal of Experimental Botany **35**: 627–639.

Su T, Li W, Wang P, Ma C. 2019. Dynamics of peroxisome homeostasis and its role in stress response and signalling in plants. Frontiers in Plant Science **10**, 705.

Takahashi R, Ishimaru Y, Senoura T, Shimo H, Ishikawa S, Arao T, et al. 2011. The OsNramp1 iron transporter is involved in Cd accumulation in rice. J Exp Bot. **14**: 4843–4850.

Terrón-Camero LC, Rodríguez-Serrano M, Sandalio LM, Romero-Puertas MC. 2020. Nitric oxide is essential for cadmium-induced peroxule formation and peroxisome proliferation. Plant, Cell and Environment **43**, 2492–2507.

Yu G, Wang LG, Han Y, He QY. 2012. clusterProfiler: an R package for comparing biological themes among gene clusters. OMICS **16**, 284–287.

Zhang W, Du B, Liu D, Qi X. 2014. Splicing factor SR34b mutation reduces cadmium tolerance in Arabidopsis by regulating iron-regulated transporter 1 gene. Biochemical and Biophysical Research Communications **3**, 312–317.

General Discussion

Peroxisomes play crucial roles in several phases of plant lifecycle and plant responses to stress (Kao *et al.,* 2018; Su *et al.,* 2019). Although in the last years, our knowledge of plant peroxisome biology has been increased, outstanding questions remains to be elucidated. One of the main questions are: what are the roles for ROS produced in peroxisomes? How peroxisomes sense environmental signals and internal metabolic state and translate this information at molecular and metabolic level? How interorganellar crosstalk is carried out and regulated?

In this Thesis, we have investigated by transcriptomic analysis peroxisomal-dependent molecular changes, in particular, ACX1-dependent downstream responses in plant response to the herbicide 2,4-D (Chapter 1). In addition, we have carried out a meta-analysis comprising transcriptomic data available at public databases related with mutants/treatments with altered peroxisomal H_2O_2 metabolism to obtain the structure of gene networks and to identify a footprint underlying peroxisomal-stress dependent signalling (Chapter 2). Both chapters involve altered ROS metabolism inside peroxisomes and hence, the information obtained is close related to the peroxisomal internal-state translation to the nucleus (**Fig. 1**). On the other hand, transcriptomic analyses on mutants affected in the peroxisomal peroxin 11a (PEX11a), led us to obtain information on genes underlying peroxisomal-dependent signalling in response to changes in ROS production in different organelles induced by stress (Chapters 3 and 4; **Fig. 1**). *PEX11a* induction has been shown to be dependent in part, on NADPH oxidases (RBOH D and F; Rodríguez-Serrano *et al.,* 2016), which are involved in producing ROS in the plasma membrane and in sensing external stress. In fact, Arabidopsis RBOH D and RBOH F have been shown to be essential for a rapid systemic signal in plant response to stress, which is involved in cell-to-cell, long-distance communication (Miller *et al.,* 2009; Zandalinas *et al.,* 2020). Recently, a core set of genes has been associated with this ROS-dependent systemic signal, which prime systemic leaves and allow them to acclimate to a particular stress (Zandalinas *et al.,* 2019. The integration of ROS, Ca^{2+}, electric and hydraulic signals, during systemic acquired acclimation has been suggested to occurs at the vascular bundles (Zandalinas *et al.,* 2020). In this work, we have observed peroxules connections with plasma membrane where RBOHs are located and in the vascular tissue. Further analysis comparing PEX11a- and RBOHD-dependent genes, recently deposited in public

databases, will let us to know the percentage of overlapping and specific signalling between these two proteins, and possible role for PEX11a in systemic acquired acclimation.

When comparing ACX1-dependent genes in plant response to 2,4-D at early time point (1 h), with early peroxisomal-dependent genes, we obtained 49 genes in common, almost 50 % of the early peroxisomal-dependent genes. The result support data obtained in chapter 1, by the ROSMETER bioinformatics platform related to ROS type and origin (Rosenwasser *et al.,* 2013), which suggest an initial stress in peroxisomes after the herbicide treatment. ACX1-dependent genes at a later response to the herbicide compared with late-peroxisomal-dependent genes showed 28 genes in common, a 34 % of late-peroxisomal-dependent genes, accordingly with the declining of the correlation values for peroxisomal stress over time, obtained in chapter 1 by the ROSMETER platform. Enrichment analysis for common early genes for ACX-dependent and peroxisomal-dependent results in GOs related with signal transduction, response to stress and response to abiotic and biotic stimulus, already associated to peroxisomal-dependent signalling in chapter 2. In fact, peroxisomal dependent signalling obtained from our meta-analysis, suggested a key role for peroxisomes in regulating transcription, initially focused on prevention of protein damage through regulation of heat shock factors and later focused on proteins protection through regulation of heat shock proteins and chaperones. Results obtained at later responses agree with results obtained previously in a comparative signalling pathways study between peroxisomes and chloroplast (Sewelam *et al.,* 2014). Additionally, Sewelam et al. (2014) showed that part of the H_2O_2 responses produced in peroxisomes was independent of the location of ROS production as they were regulated by ROS originated by different organelles/location. Peroxisomal-dependent genes obtained by our meta-analysis however, appear to be peroxisomal-specific as showed no genes in common with chloroplast retrograde signalling represented by cluster I in the ROS wheel (Willems *et al.,* 2016), nor with mitochondrial AOX1-dependent signalling (Giraud *et al.,* 2008), supporting the functionality of meta-analysis for obtaining specific genes commonly regulated in different experimental conditions. Therefore, in this work, we have obtained a group of specific genes, at early and later times, which may be regulated by ROS-derived from peroxisomes (peroxisomal

footprint). Contrary to chloroplasts and mitochondria, retrograde signalling related with peroxisomes has been scarcely covered. Peroxisomal footprint obtained in this work, is highly coordinated and related with plant stress response, showing a high correlation with different abiotic stress responses (Zandalinas *et al.,* 2021). We have identified different TFs related with early plant response to stress, HSFs, mainly related to protein protection. Biosynthesis of the hormone JA, which is produced in peroxisomes and JA-dependent signalling, appears to be also target of peroxisomal-dependent signalling (**Fig. 1**), suggesting that peroxisomal stress resort to signalling molecules produced inside the organelle to deal with the stress. In fact, JA is able to regulated peroxisomal homeostasis (Castillo *et al.,* 2008). Furthermore, we have shown in chapter 1 that ROS from peroxisomal ACX1 regulates IAA-dependent signalling, another hormone produced inside the organelle. Involvement of protein degradation related to the E3-RING ubiquitin ligases, which is devoted to elimination of damaged proteins has been shown to be dependent on peroxisomal ACX1 in later plant response to 2,4-D. In chapter 2, later peroxisomal-dependent genes have been associated with other cellular locations, in particular with ER and have been associated with ER-stress, focused again in protein protection. Further characterization of peroxisomal-dependent genes obtained in this work will uncover new mechanisms related with peroxisomal stress translation into metabolic/proteomic changes within the cell.

Comparison of PEX11a-dependent genes in plant response to Cd at early time point (1 h) with early peroxisomal-dependent genes obtained in chapter 2, gave rise only five genes in common. Similarly, comparison of PEX11a-dependent genes in plant response to Cd at later time point (24 h) with late peroxisomal-dependent genes results in only five genes in common too. These results point to the previous hypothesis suggesting that may be PEX11a-dependent signalling is not so related with an intrinsic peroxisomal stress, but with an external stress. Interestingly, enrichment analysis of DEGs in *pex11a-CR* mutants vs *px-ck* under control conditions, point to chloroplasts as the main organelle affected by *PEX11a* mutation, especially related with thylakoids, photosynthetic membrane, light-harvesting complex and plastoglobuli. KEGG pathways associated with PEX11a-dependent genes are related also with chlorophyll, glutathione, and starch and sucrose metabolism (**Fig. 1**). These results suggest a key role for PEX11a in chloroplast

metabolism and structure maintenance. Electron microscopy on *pex11a-CR* mutants showed altered ratio thylakoids/stroma within chloroplasts, and biochemical and histochemical analyses showed lower pigment and starch content in the mutants with respect to *px-ck*, supporting a role for PEX11a in chloroplast metabolism. Effects of PEX11a mutation on chloroplast metabolism may be part of the reason for the lower mutant growth respect to *px-ck*, differences that are enhanced under high light conditions. Further analyses on photosynthetic efficiency in *pex11a* mutants will allow us to confirm this hypothesis. Later transcriptional response to Cd showed ribosomes and spliceosome as key pathways regulated by PEX11a. Conversion of precursors mRNA, expressed in most eukaryotic genes, to mRNA by splicing, and later translation to proteins are main functions for spliceosome and ribosomes, respectively. Recent PEX11a interactome made in our group showed possible interaction of the protein with two translation initiation factors that may explain part of these results. How PEX11a may take action on ribosome and spliceosome metabolisms however, need further experimental support.

Enrichments related with *Cellular Components* for PEX11a-dependent genes point to a function for other organelles/location regulation instead of peroxisomes. We cannot discard however, that PEX11a has a key function within peroxisomes also, as we have found that peroxisomal homeostasis may be altered in plant response to Cd stress and a more specific analysis for peroxisomal metabolome and proteome will help to uncover this issue.

Physiological and biochemical characterization of *pex11a* mutants showed possible functions for PEX11a not only in plant response to stress but also in developmental processes such as, germination and lateral root formation (**Fig. 1**). As previously discussed, alteration of PEX11a could affect fatty acid metabolism in seeds, which is essential for seed germination or differential ROS/redox state in the mutants could alter seed dormancy relieve that is dependent of ROS. Interestingly, six of the seven more induced genes in *pex11a-CR* vs *px-ck*, are involved in seed development and metabolism, being more than two hundred times induced all of them. Different mutants affected in these genes showed defective seed development and/or germination process (Tukagoshi *et al.,* 2007; Tang *et al.,* 2012). The remaining gene of seven is a receptor kinase

involved in auxin-mediated lateral root development under phosphate starvation (Deb *et al.,* 2014). Further in depth analysis of transcriptomic data and experimental work will help to unravel PEX11a and therefore, peroxisomal role in plant development processes.

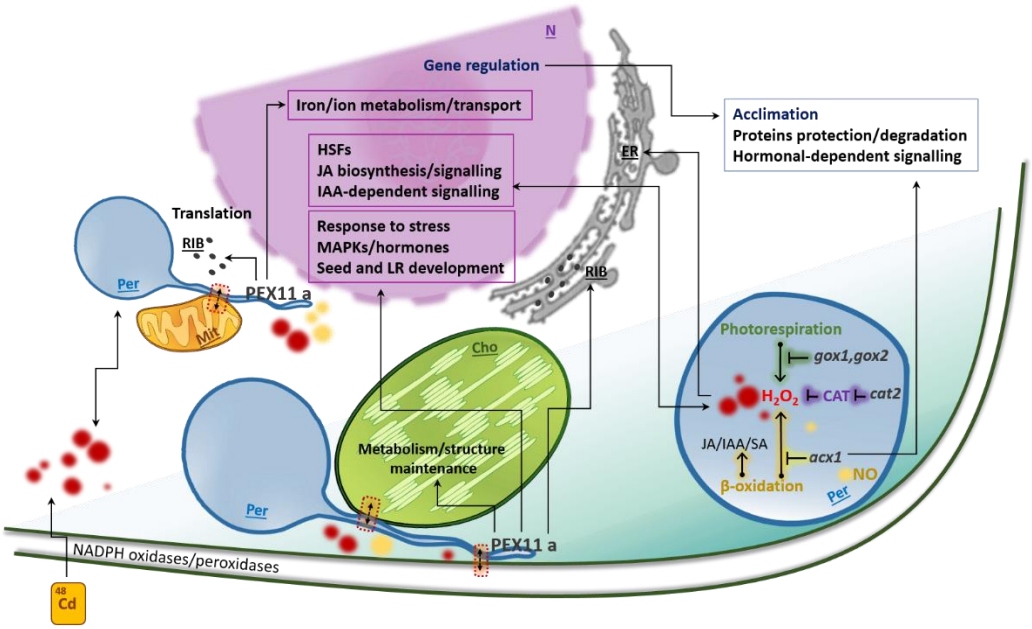

Figure 1. Scheme showing peroxisomal-dependent signalling processes under normal and stress conditions. *ACX-dependent ROS produced inside of peroxisomes, regulate IAA-dependent signaling and protein degradation. Reticulum endoplasmic could also be target of peroxisomal-dependent signalling during a later response to stress. Peroxisomes collaborate and communicate with other organelles or cell locations, such as mitochondria, chloroplasts and plasma membrane (rectangles with red dashed line). Chloroplasts appears to be the main organelle affected by PEX11a mutation, altering structure and several pathways occurring in this organelle. Cd stress promotes the generation of ROS, which activate PEX11a, in a ROS and NO-dependent way. PEX11a promotes the formation of peroxules, which could control ROS/NO accumulation and ROS-dependent gene expression. Iron/ion metabolism and transport is regulated by PEX11a after short-term cadmium treatment. Later transcriptional response to Cd showed ribosomes and spliceosome as key pathways regulated by PEX11a. Cho (chloroplast), ER (endoplasmic reticulum), Mit (mitochondria), N (nuclei), Per (peroxisome), RIB (ribosome). Red spheres, ROS; yellow spheres, NO.*

Conclusions

1. 2,4-D induced a ROS-related peroxisome footprint in early plant responses. Peroxisomal ACX1 is one of the main sources of ROS production and is associated to epinastic phenotype following 2,4-D application in plants. ACX1-dependent signalling in plant responses to 2,4-D regulate a large number of genes, such as peroxidases, HSP and PRPs, involved in primary responses to 2,4-D. In particular, ACX1-dependent H_2O_2, can regulate AUX/IAA ubiquitination and degradation and thereby the expression of auxin-responsive genes at the early plant response to the herbicide while at later stages, protein degradation related to the E3-RING ubiquitin ligases is significantly regulated being both responses involved in epinastic phenotype.

2. Meta-analysis of available data sets derived from the profiling of Arabidopsis gene expression in mutants and treatments with peroxisomal-dependent ROS levels altered let us to identify early and late peroxisomal footprint as common and specific genes regulated by peroxisomal ROS under different stress conditions. Different transcription factors related with heat shock factors and hormone-dependent biosynthesis and signalling, mainly related with JA, are within early peroxisomal-dependent genes. Late peroxisomal-dependent genes clustered in groups related with heat shock factors and proteins, response to ER-stress and GSTs. Peroxisomal-dependent genes are highly co-expressed between them and they are shared with transcriptomic responses to several abiotic stresses, they appear to be mainly devoted to proteins protection and detoxification.

3. Characterization of mutants affected in peroxisomal peroxin11a (PEX11a), *pex11a* confirmed that this protein is essential for peroxules observation in plant response to stress and probably for peroxisome homeostasis within the cell. Novel additional roles for PEX11a has been suggested in plant development such as germination, lateral root development and plant growth.

4. Transcriptomic data from mutants affected in peroxisomal peroxin11a (PEX11a), *pex11a-CR* under normal conditions point to a key role for PEX11a in chloroplast metabolism maintenance, involving mainly chlorophyll and starch, and in chloroplast structure, mainly related with thylakoids, suggesting that this protein is essential for peroxisome and chloroplast crosstalk. Under Cd stress, transcriptomic data suggest a role for PEX11a mainly related with iron and ion transport and metabolism at early time while involvement in ribosome and spliceosome metabolism at later stages

General References

Adham AR, Zolman BK, Millius A, Bartel B. 2005. Mutations in Arabidopsis Acyl-CoA oxidase genes reveal distinct and overlapping roles in β-oxidation. Plant Journal **41**, 859–874.

Agrawal G, Joshi S, Subramani S. 2011. Cell-free sorting of peroxisomal membrane proteins from the endoplasmic reticulum. Proceedings of the National Academy of Sciences of the United States of America **108**, 9113–9118.

Agurla S, Gayatri G, Raghavendra AS. 2018. Polyamines increase nitric oxide and reactive oxygen species in guard cells of Arabidopsis thaliana during stomatal closure. Protoplasma **255**, 153–162.

Antonenkov VD, Grunau S, Ohlmeier S, Hiltunen JK. 2010. Peroxisomes are oxidative organelles. Antioxidants and Redox Signalling **13**, 525–537.

Apanasets O, Grou CP, Van Veldhoven PP, Brees C, Wang B, Nordgren M, Dodt G, Azevedo JE, Fransen M. 2014. PEX5, the shuttling import receptor for peroxisomal matrix proteins, is a redox-sensitive protein. Traffic **15**, 94–103.

Aravind P, Prasad MNV. 2005. Modulation of cadmium-induced oxidative stress in *Ceratophyllum demersum* by zinc involves ascorbate-glutathione cycle and glutathione metabolism. Plant Physiology and Biochemistry **43**, 107–116.

Asada K, Allen J, Foyer CH, Matthijs HCP. 2000. The water-water cycle as alternative photon and electron sinks. Philosophical Transactions of the Royal Society B: Biological Sciences **355**, 1419–1431.

Astier J, Gross I, Durner J. 2018. Nitric oxide production in plants: An update. Journal of Experimental Botany **69**, 3401–3411.

Astier J, Mounier A, Santolini J, Jeandroz S, Wendehenne D. 2019. The evolution of nitric oxide signalling diverges between animal and green lineages. Journal of Experimental Botany **70**, 4355–4364.

Avin-Wittenberg T, Baluška F, Bozhkov PV, *et al.* 2018. Autophagy-related approaches for improving nutrient use efficiency and crop yield protection. Journal of Experimental Botany **69**, 1335–1353.

Ayangbenro AS, Babalola OO. 2017. A new strategy for heavy metal polluted environments: A review of microbial biosorbents. International Journal of Environmental Research and Public Health **14**, 1–16 .

Baker A, Hogg TL, Warriner SL. 2016. Peroxisome protein import: A complex journey. Biochemical Society Transactions **44**, 783–789.

Balali-Mood M, Naseri K, Tahergorabi Z, Khazdair MR, Sadeghi M. 2021. Toxic mechanisms of five heavy metals: Mercury, lead, chromium, cadmium, and arsenic. Frontiers in Pharmacology **12**, 1–19.

Barroso JB, Corpas FJ, Carreras A, Sandalio LM, Valderrama R, Palma M, Lupiáñez JA, Del Río LA. 1999. Localization of nitric-oxide synthase in plant peroxisomes. Journal of Biological Chemistry **274**, 36729–36733.

Bauer S, Morris MT. 2017. Glycosome biogenesis in trypanosomes and the de novo dilemma. PLoS Neglected Tropical Diseases **11**, 1–13.

Bernat P, Nykiel-Szymańska J, Stolarek P, Słaba M, Szewczyk R, Różalska S. 2018. 2,4-dichlorophenoxyacetic acid-induced oxidative stress: Metabolome and membrane modifications in *Umbelopsis isabellina*, a herbicide degrader. PLoS ONE **13**, 1–18.

Besson-Bard A, Gravot A, Richaud P, Auroy P, Duc C, Gaymard F, Taconnat L, Renou JP, Pugin A, Wendehenne D. 2009. Nitric oxide contributes to cadmium toxicity in Arabidopsis by promoting cadmium accumulation in roots and by up-regulating genes related to iron uptake. Plant Physiology **149**, 1302–1315.

Brown LA, Baker A. 2008. Shuttles and cycles: Transport of proteins into the peroxisome matrix. Molecular Membrane Biology **25**, 363–375.

Calero-Muñoz N, Expósito-Rodríguez M, Collado-Arenal AM, *et al.* 2019. Cadmium induces reactive oxygen species-dependent pexophagy in Arabidopsis leaves. Plant, Cell and Environment **42**, 2696–2714.

Caplan JL, Kumar AS, Park E, Padmanabhan MS, Hoban K, Modla S, Czymmek K, Dinesh-Kumar SP. 2015. Chloroplast stromules function during innate immunity. Developmental Cell **155**, 3–12.

Castillo MC, Sandalio LM, Del Río LA, León J. 2008. Peroxisome proliferation, wound-activated responses and expression of peroxisome-associated genes are cross-regulated but uncoupled in *Arabidopsis thaliana*. Plant, Cell and Environment **31**, 492–505.

Chaffai R, Cherif A. 2020. The cadmium-induced changes in the polar and neutral lipid compositions suggest the involvement of triacylglycerol in the defense response in maize. Physiology and Molecular Biology of Plants **26**, 15–23.

Charton L, Plett A, Linka N. 2019. Plant peroxisomal solute transporter proteins. Journal of Integrative Plant Biology **61**, 817–835.

Chen D, Shao Q, Yin L, Younis A, Zheng B. 2019. Polyamine function in plants: Metabolism, regulation on development, and roles in abiotic stress responses. Frontiers in Plant Science **9**, 1–13.

Chini A, Monte I, Zamarreño AM, *et al.* 2018. An OPR3-independent pathway uses 4,5-didehydrojasmonate for jasmonate synthesis. Nature Chemical Biology **14**, 171–178.

Choudhary A, Kumar A, Kaur N. 2020. ROS and oxidative burst: Roots in plant development. Plant Diversity **42**, 33–

43.

Choudhury FK, Rivero RM, Blumwald E, Mittler R. 2017. Reactive oxygen species, abiotic stress and stress combination. Plant Journal **90**, 856–867.

Clemens S, Aarts MGM, Thomine S, Verbruggen N. 2013. Plant science: The key to preventing slow cadmium poisoning. Trends in Plant Science **18**, 92–99.

Clemens S, Ma JF. 2016. Toxic heavy metal and metalloid accumulation in crop plants and foods. Annual Review of Plant Biology **67**, 489–512.

Corpas FJ, Barroso JB. 2014. Peroxynitrite ($ONOO^-$) is endogenously produced in Arabidopsis peroxisomes and is overproduced under cadmium stress. Annals of Botany **113**, 87–96.

Corpas FJ. 2016. Reactive Nitrogen Species (RNS) in plants under physiological and adverse environmental conditions: Current View. Progress in Botany **78**, 97–119.

Corpas FJ, Barroso JB, González-Gordo S, Muñoz-Vargas MA, Palma JM. 2019. Hydrogen sulfide: A novel component in Arabidopsis peroxisomes which triggers catalase inhibition. Journal of Integrative Plant Biology **61**, 871–883.

Crawford T, Lehotai N, Strand Å. 2018. The role of retrograde signals during plant stress responses. Journal of Experimental Botany **69**, 2783–2795.

Cross LL, Ebeed HT, Baker A. 2016. Peroxisome biogenesis, protein targeting mechanisms and PEX gene functions in plants. Biochimica et Biophysica Acta-Molecular Cell Research **1863**, 850–862.

Cui L, Lu Y, Li Y, Yang C, Peng X, Lines TR. 2016. Overexpression of glycolate oxidase confers improved photosynthesis under high light and high temperature in rice. Frontiers in Plant Science **7**, 1–12.

Cuypers A, Hendrix S, Dos Reis RA, *et al.* 2016. Hydrogen peroxide, signalling in disguise during metal phytotoxicity. Frontiers in Plant Science **7**, 470.

Czarnocka W, Karpiński S. 2018. Friend or foe? Reactive oxygen species production, scavenging and signalling in plant response to environmental stresses. Free Radical Biology and Medicine **122**, 4–20.

Das K, Roychoudhury A. 2014. Reactive oxygen species (ROS) and response of antioxidants as ROS-scavengers during environmental stress in plants. Frontiers in Environmental Science **2**, 1–13.

De Duve C, Baudhuin P. 1966. Peroxisomes (microbodies and related particles). Physiological reviews **46**, 323–357.

Deb S, Sankaranarayanan S, Wewala G, Widdup E, Samuel MA. 2014. The *S*-domain receptor kinase Arabidopsis receptor kinase2 and the U box/armadillo repeat-containing E3 ubiquitin ligase9 module mediates lateral root development under phosphate starvation in Arabidopsis. Plant Physiology **4**: 1647–1656.

Del Castello F, Nejamkin A, Cassia R, Correa-Aragunde N, Fernández B, Foresi N, Lombardo C, Ramirez L, Lamattina L. 2019. The era of nitric oxide in plant biology: Twenty years tying up loose ends. Nitric Oxide-Biology and Chemistry **85**, 17–27.

Del Río LA. 2015. ROS and RNS in plant physiology: An overview. Journal of Experimental Botany **66**, 2827–2837.

Del Río LA, López-Huertas E. 2016. ROS generation in peroxisomes and its role in cell signalling. Plant and Cell Physiology **57**, 1364–1376.

Delille HK, Dodt G, Schrader M. 2010. Pex11pβ-mediated maturation of peroxisomes. Communicative and Integrative Biology **4**, 51–54.

Dellero Y, Jossier M, Schmitz J, Maurino VG, Hodges M. 2016. Photorespiratory glycolate-glyoxylate metabolism. Journal of Experimental Botany **67**, 3041–3052.

Demidchik V, Maathuis F, Voitsekhovskaja O. 2018. Unravelling the plant signalling machinery: An update on the cellular and genetic basis of plant signal transduction. Functional Plant Biology **45**, 1–8.

Deng M, Zhu Y, Shao K, Zhang Q, Ye G, Shen J. 2020. Metals source apportionment in farmland soil and the prediction of metal transfer in the soil-rice-human chain. Journal of Environmental Management **260**, 110092.

Desai M, Hu J. 2008. Light induces peroxisome proliferation in Arabidopsis seedlings through the photoreceptor phytochrome A, the transcription factor HY5 HOMOLOG, and the peroxisomal protein PEROXIN11b. Plant Physiology **146**, 1117–1127.

Devireddy AR, Zandalinas SI, Fichman Y, Mittler R. 2021. Integration of reactive oxygen species and hormone signalling during abiotic stress. Plant Journal **105**, 459–476.

Distel B, Erdmann R, Gould SJ, *et al.* 1996. A unified nomenclature for peroxisome biogenesis factors. Journal of Cell Biology **135**, 1–3.

Du YY, Wang PC, Chen J, Song CP. 2008. Comprehensive functional analysis of the catalase gene family in *Arabidopsis thaliana*. Journal of Integrative Plant Biology **50**, 1318–1326.

Dvořák P, Krasylenko Y, Ovečka M, Basheer J, Zapletalová V, Šamaj J, Takáč T. 2021*a*. Invivo light-sheet microscopy resolves localisation patterns of FSD1, a superoxide dismutase with function in root development and osmoprotection. Plant, Cell and Environment **44**, 68–87.

Dvořák P, Krasylenko Y, Zeiner A, Šamaj J, Takáč T. 2021*b*. Signalling toward reactive oxygen species-scavenging

enzymes in plants. Frontiers in Plant Science **11**, 618835.

Ebeed HT, Stevenson SR, Cuming AC, Baker A. 2018. Conserved and differential transcriptional responses of peroxisome associated pathways to drought, dehydration and ABA. Journal of Experimental Botany **69**, 4971–4985.

Engqvist MKM, Schmitz J, Gertzmann A, Florian A, Jaspert N, Arif M, Balazadeh S, Mueller-Roeber B, Fernie AR, Maurino VG. 2015. GLYCOLATE OXIDASE3, a glycolate oxidase homolog of yeast L-lactate cytochrome c oxidoreductase, supports L-lactate oxidation in roots of Arabidopsis. Plant Physiology **169**, 1042–1061.

Fahy D, Sanad MNME, Duscha K, *et al.* 2017. Impact of salt stress, cell death, and autophagy on peroxisomes: Quantitative and morphological analyses using small fluorescent probe N-BODIPY. Scientific Reports **7**, 1–17.

Farooq MA, Niazi AK, Akhtar J, Saifullah, Farooq M, Souri Z, Karimi N, Rengel Z. 2019. Acquiring control: The evolution of ROS-Induced oxidative stress and redox signalling pathways in plant stress responses. Plant Physiology and Biochemistry **141**, 353–369.

Fichman Y, Mittler R. 2020. Rapid systemic signalling during abiotic and biotic stresses: Is the ROS wave master of all trades? Plant Journal **102**, 887–896.

Foresi N, Mayta ML, Lodeyro AF, Scuffi D, Correa-Aragunde N, García-Mata C, Casalongué C, Carrillo N, Lamattina L. 2015. Expression of the tetrahydrofolate-dependent nitric oxide synthase from the green alga *Ostreococcus tauri* increases tolerance to abiotic stresses and influences stomatal development in Arabidopsis. Plant Journal **82**, 806–821.

Foyer CH, Bloom AJ, Queval G, Noctor G. 2009. Photorespiratory metabolism: Genes, mutants, energetics, and redox signalling. Annual Review of Plant Biology **60**, 455–484.

Foyer CH, Noctor G. 2020. Redox homeostasis and signalling in a higher-CO_2 world. Annual Review of Plant Biology **71**, 157–182.

Foyer CH, Baker A, Wright M, Sparkes IA, Mhamdi A, Schippers JHM, Breusegem F Van. 2020. On the move: Redox-dependent protein relocation in plants. Journal of Experimental Botany **71**, 620–631.

Fransen M, Lismont C. 2019. Redox signalling from and to peroxisomes: Progress, challenges, and prospects. Antioxidants and Redox Signalling **30**, 95–112.

Fu Z, Xi S. 2020. The effects of heavy metals on human metabolism. Toxicology Mechanisms and Methods **30**, 167–176.

Gabaldón T. 2010. Peroxisome diversity and evolution. Philosophical Transactions of the Royal Society B: Biological Sciences **365**, 765–773.

Gabaldón T. 2018. Evolution of the peroxisomal proteome. Subcellular Biochemistry **89**, 221–233.

Gao H, Metz J, Teanby NA, Ward AD, Botchway SW, Coles B, Pollard MR, Sparkes I. 2016. In vivo quantification of peroxisome tethering to chloroplasts in tobacco epidermal cells using optical tweezers. Plant Physiology **170**, 263–272.

Genchi G, Sinicropi MS, Lauria G, Carocci A, Catalano A. 2020. The effects of cadmium toxicity. International Journal of Environmental Research and Public Health **17**, 1–24.

Gieti C. 1992. Partitioning of malate dehydrogenase isoenzymes into glyoxysomes, mitochondria and chloroplasts. Plant Physiology **100**, 557–559.

Giraud E, Ho LH, Clifton R, Carroll A, Estavillo G, Tan YF, Howell KA, Ivanova A, Pogson BJ, Millar AH, Whelan J. 2008. The absence of ALTERNATIVE OXIDASE1a in Arabidopsis results in acute sensitivity to combined light and drought stress. Plant Physiology **147**: 595–610.

Grossmann K. 2000. Mode of action of auxin herbicides: A new ending to a long, drawn out story. Trends in Plant Science **5**, 506–508.

Gupta DK, Pena LB, Hernández A, Inouhe M, Sandalio LM. 2017. Original Article NADPH oxidases differentially regulate ROS metabolism and nutrient uptake under cadmium toxicity. Plant, Cell and Environment **40**, 509–526.

Gupta KJ, Kumari A, Florez-Sarasa I, Fernie AR, Igamberdiev AU. 2018. Interaction of nitric oxide with the components of the plant mitochondrial electron transport chain. Journal of Experimental Botany **69**, 3413–3424.

Hagemann M, Bauwe H. 2016. Photorespiration and the potential to improve photosynthesis. Current Opinion in Chemical Biology **35**, 109–116.

Hancock JT, Neill SJ. 2019. Nitric oxide: Its generation and interactions with other reactive signalling compounds. Plants **8**, 1–14.

Hasanuzzaman M, Nahar K, Anee TI, Fujita M. 2017. Glutathione in plants: Biosynthesis and physiological role in environmental stress tolerance. Physiology and Molecular Biology of Plants **23**, 249–268.

Hasanuzzaman M, Bhuyan MHMB, Zulfiqar F, Raza A, Mohsin SM, Al Mahmud J, Fujita M, Fotopoulos V. 2020. Reactive oxygen species and antioxidant defense in plants under abiotic stress: Revisiting the crucial role of a universal defense regulator. Antioxidants **9**, 1–52.

Hayashi M, Nishimura M. 2006. *Arabidopsis thaliana*-A model organism to study plant peroxisomes. Biochimica et Biophysica Acta-Molecular Cell Research **1763**, 1382–1391.

Hiltunen JK, Mursula AM, Rottensteiner H, Wierenga RK, Kastaniotis AJ, Gurvitz A. 2003. The biochemistry of peroxisomal β-oxidation in the yeast *Saccharomyces cerevisiae*. FEMS Microbiology Reviews **27**, 35–64.

Hinojosa L, Sanad MNME, Jarvis DE, Steel P, Murphy K, Smertenko A. 2019. Impact of heat and drought stress on peroxisome proliferation in quinoa. Plant Journal **99**, 1144–1158.

Hu J, Baker A, Bartel B, Linka N, Mullen RT, Reumann S, Zolman BK. 2012. Plant peroxisomes: Biogenesis and function. Plant Cell **24**, 2279–2303.

Huang H, Ullah F, Zhou DX, Yi M, Zhao Y. 2019. Mechanisms of ROS regulation of plant development and stress responses. Frontiers in Plant Science **10**, 1–10.

Hurdebise Q, Tarayre C, Fischer C, Colinet G, Hiligsmann S, Delvigne F. 2015. Determination of zinc, cadmium and lead bioavailability in contaminated soils at the single-cell level by a combination of whole-cell biosensors and flow cytometry. Sensors **15**, 8981–8999.

Igamberdiev AU, Ratcliffe RG, Gupta KJ. 2014. Plant mitochondria: Source and target for nitric oxide. Mitochondrion **19**, 329–333.

Islam F, Wang J, Farooq MA, Khan MSS, Xu L, Zhu J, Zhao M, Muños S, Li QX, Zhou W. 2018. Potential impact of the herbicide 2,4-dichlorophenoxyacetic acid on human and ecosystems. Environment International **111**, 332–351.

Islinger M, Voelkl A, Fahimi HD, Schrader M. 2018. The peroxisome: an update on mysteries 2.0. Histochemistry and Cell Biology **150**, 443–471.

Jaipargas EA, Mathur N, Daher FB, Wasteneys GO, Mathur J. 2016. High light intensity leads to increased peroxule-mitochondria interactions in plants. Frontiers in Cell and Developmental Biology **4**, 1–11.

Jalmi SK, Sinha AK. 2015. ROS mediated MAPK signalling in abiotic and biotic stress-striking similarities and differences. Frontiers in Plant Science **6**, 1–9.

Janku M, Luhová L, Petrivalský M. 2019. On the origin and fate of reactive oxygen species in plant cell compartments. Antioxidants **8**, 5.

Jansen RLM, Santana-Molina C, Van Den Noort M, Devos DP, Van Der Klei IJ. 2021. Comparative genomics of peroxisome biogenesis proteins: Making sense of the PEX proteins. Frontiers in Cell and Developmental Biology **20**, 654163.

Jeandroz S, Wipf D, Stuehr DJ, Lamattina L, Melkonian M, Tian Z, Zhu Y, Carpenter EJ, Wong GKS, Wendehenne D. 2016. Occurrence, structure, and evolution of nitric oxide synthase-like proteins in the plant kingdom. Science Signalling **9**, 417.

Jiménez A, Hernández JA, Del Río LA, Sevilla F. 1997. Evidence for the presence of the ascorbate-glutathione cycle in mitochondria and peroxisomes of pea leaves. Plant Physiology **114**, 275–284.

Joshi S, Agrawal G, Subramani S. 2012. Phosphorylation-dependent Pex11p and Fis1p interaction regulates peroxisome division. Molecular Biology of the Cell **23**, 1307–1315.

Joshi S, Subramani S. 2013. Peroxisomes. In Encyclopedia of Biological Chemistry. Lennarz W, Lane M. Eds Elsevier, second edition, 425–430.

Kalaivanan D, Ganeshamurthy AN. 2016. Mechanisms of heavy metal toxicity in plants. In Abiotic Stress Physiology of Horticultural Crops. Rao NKS, Shivashankara KS, Laxman RH. Eds. Springer: India, 85–102.

Kalel VC, Erdmann R. 2018. Unraveling of the structure and function of peroxisomal protein import machineries. Subcellular Biochemistry **89**, 299–321.

Kao YT, Gonzalez KL, Bartel B. 2018. Peroxisome function, biogenesis, and dynamics in plants. Plant Physiology **176**, 162–177.

Karanja AW, Njeru EM, Maingi JM. 2019. Assessment of physicochemical changes during composting rice straw with chicken and donkey manure. International Journal of Recycling of Organic Waste in Agriculture **8**, 65–72.

Katano K, Honda K, Suzuki N. 2018. Integration between ROS regulatory systems and other signals in the regulation of various types of heat responses in plants. International Journal of Molecular Sciences **19**, 3370.

Kataya ARA, Muench DG, Moorhead GB. 2019. A framework to investigate peroxisomal protein phosphorylation in Arabidopsis. Trends in Plant Science **24**, 366–381.

Kaur N, Reumann S, Hu J. 2009. Peroxisome biogenesis and function. The Arabidopsis Book **7**, e0123.

Kawasaki T, Yamada K, Yoshimura S, Yamaguchi K. 2017. Chitin receptor-mediated activation of MAP kinases and ROS production in rice and Arabidopsis. Plant Signalling and Behavior **12**, 4–8.

Khan A, Numan M, Khan AL, Lee IJ, Imran M, Asaf S, Al-Harrasi A. 2020. Melatonin: Awakening the defense mechanisms during plant oxidative stress. Plants **9**, 1–22.

Khorobrykh S, Havurinne V, Mattila H, Tyystjärvi E. 2020. Oxygen and ROS in photosynthesis. Plants **9**, 91.

Kim JA. 2020. Peroxisome Metabolism in Cancer. Cells **9**, 1–19.

Kim PK, Hettema EH. 2015. Multiple pathways for protein transport to peroxisomes. Journal of Molecular Biology **427**, 1176–1190.

Knoblach B, Rachubinski RA. 2010. Phosphorylation-dependent activation of peroxisome proliferator protein PEX11 controls peroxisome abundance. Journal of Biological Chemistry **285**, 6670–6680.

Koch A, Yoon Y, Bonekamp NA, McNiven MA, Schrader M. 2005. A role for Fis1 in both mitochondrial and peroxisomal fission in mammalian cells. Molecular Biology of the Cell **16**, 5077–5086.

Koch J, Pranjic K, Huber A, Ellinger A, Hartig A, Kragler F, Brocard C. 2010. PEX11 family members are membrane elongation factors that coordinate peroxisome proliferation and maintenance. Journal of Cell Science **123**, 3389–3400.

Koch J, Brocard C. 2011. Membrane elongation factors in organelle maintenance: The case of peroxisome proliferation. Biomolecular Concepts **2**, 353–364.

Köhler RH, Hanson MR. 2000. Plastid tubules of higher plants are tissue-specific and developmentally regulated. Journal of Cell Science **113**, 81–89.

Kohli SK, Khanna K, Bhardwaj R, Abd Allah EF, Ahmad P, Corpas FJ. 2019. Assessment of subcellular ROS and NO metabolism in higher plants: Multifunctional signalling molecules. Antioxidants **8**, 641.

Kollist H, Zandalinas SI, Sengupta S, Nuhkat M, Kangasjärvi J, Mittler R. 2019. Rapid responses to abiotic stress: Priming the landscape for the signal transduction network. Trends in Plant Science **24**, 25–37.

Kopyra M, Stachoń-Wilk M, Gwóźdź EA. 2006. Effects of exogenous nitric oxide on the antioxidant capacity of cadmium-treated soybean cell suspension. Acta Physiologiae Plantarum **28**, 525–536.

Krikken AM, Veenhuis M, Van Der Klei IJ. 2009. *Hansenula polymorpha* pex11 cells are affected in peroxisome retention. FEBS Journal **276**, 1429–1439.

Kubo Y. 2013. Function of peroxisomes in plant-pathogen interactions. Subcellular Biochemistry **69**, 329–345.

Kumar AS, Park E, Nedo A, *et al.* 2018. Stromule extension along microtubules coordinated with actin-mediated anchoring guides perinuclear chloroplast movement during innate immunity. eLife **7**, 1–33.

Kumar S, Prasad S, Yadav KK, *et al.* 2019. Hazardous heavy metals contamination of vegetables and food chain: Role of sustainable remediation approaches-A review. Environmental Research **179**, 108792.

Kunze M, Hartig A. 2013. Permeability of the peroxisomal membrane: Lessons from the glyoxylate cycle. Frontiers in Physiology **4**, 1–12.

Kunze M. 2020. The type-2 peroxisomal targeting signal. Biochimica et Biophysica Acta-Molecular Cell Research **1867**, 118609.

Lane TW, Morel FMM. 2000. A biological function for cadmium in marine diatoms. Proceedings of the National Academy of Sciences **97**, 4627–4631.

Lazarow PB, Fujiki Y. 1985. Biogenesis of peroxisomes. Annual Review of Cell Biology **1**, 489–530.

Lee HN, Kim J, Chung T. 2014. Degradation of plant peroxisomes by autophagy. Frontiers in Plant Science **5**, 2012–2015.

León J. 2008. Peroxisome proliferation in Arabidopsis: The challenging identification of ligand perception and downstream signalling is closer. Plant Signalling and Behavior **3**, 671–673.

León J, Costa-Broseta Á. 2020. Present knowledge and controversies, deficiencies, and misconceptions on nitric oxide synthesis, sensing, and signalling in plants. Plant, Cell and Environment **43**, 1.

Li J, Hu J. 2015. Using co-expression analysis and stress-based screens to uncover arabidopsis peroxisomal proteins involved in drought response. PLoS ONE **10**, 1–13.

Li Y, Liu Y, Zolman BK. 2019. Metabolic alterations in the enoyl-coA hydratase 2 mutant disrupt peroxisomal pathways in seedlings. Plant Physiology **180**, 1860–1876.

Lichtenthaler HK. 1998. The stress concept in plants: An introduction. Annals of the New York Academy of Sciences **851**, 187–198.

Lingard MJ, Trelease RN. 2006. Five Arabidopsis peroxin 11 homologs individually promote peroxisome elongation, duplication or aggregation. Journal of Cell Science **119**, 1961–1972.

Lingard MJ, Gidd SK, Bingham S, Rothstein SJ, Mullen RT, Trelease RN. 2008. Arabidopsis peroxin11c-e, fission1b, and dynamin-related protein3A cooperate in cell cycle-associated replication of peroxisomes. Plant Cell **20**, 1567–1585.

Lismont C, Revenco I, Fransen M. 2019. Peroxisomal hydrogen peroxide metabolism and signalling in health and disease. International Journal of Molecular Sciences **20**, 3673.

Liu H, Timko MP. 2021. Jasmonic acid signalling and molecular crosstalk with other phytohormones. International Journal of Molecular Sciences **22**, 1–24.

Logan DC. 2006. Plant mitochondrial dynamics. Biochimica et Biophysica Acta-Molecular Cell Research **1763**, 430–441.

Loix C, Huybrechts M, Vangronsveld J, Gielen M, Keunen E, Cuypers A. 2017. Reciprocal interactions between cadmium-induced cell wall responses and oxidative stress in plants. Frontiers in Plant Science **8**, 1–19.

López-Huertas E, Corpas FJ, Sandalio LM, Del Río LA. 1999. Characterization of membrane polypeptides from pea leaf peroxisomes involved in superoxide radical generation. The Biochemical Journal **337**, 531–536.

López-Huertas E, Charlton WL, Johnson B, Graham IA, Baker A. 2000. Stress induces peroxisome biogenesis genes. EMBO Journal **19**, 6770–6777.

Ma C, Hagstrom D, Polley SG, Subramani S. 2013. Redox-regulated cargo binding and release by the peroxisomal targeting signal receptor, Pex5. Journal of Biological Chemistry **288**, 27220–27231.

Manrique-Gil I, Sánchez-Vicente I, Torres-Quezada I, Lorenzo O. 2021. Nitric oxide function during oxygen deprivation in physiological and stress processes. Journal of Experimental Botany **72**, 904–916.

Mast FD, Rachubinski RA, Aitchison JD. 2020. Peroxisome prognostications: Exploring the birth, life, and death of an organelle. Journal of Cell Biology **219**, 1–13.

Mata-Pérez C, Padilla MN, Sánchez-Calvo B, Begara-Morales JC, Valderrama R, Chaki M, Aranda-Caño L, Moreno-González D, Molina-Díaz A, Barroso JB. 2020. Endogenous biosynthesis of *S*-nitrosoglutathione from nitro-fatty acids in plants. Frontiers in Plant Science **11**, 1–13.

Mathur J. 2020. Organelle extensions in plant cells. Plant Physiology **185**, 593-607.

Meijer WH, Gidijala L, Fekken S, Kiel JAKW, Van Den Berg MA, Lascaris R, Bovenberg RAL, Van Der Klei IJ. 2010. Peroxisomes are required for efficient penicillin biosynthesis in *Penicillium chrysogenum*. Applied and Environmental Microbiology **76**, 5702–5709.

Meng D, Li J, Liu T, *et al.* 2019. Effects of redox potential on soil cadmium solubility: Insight into microbial community. Journal of Environmental Sciences **75**, 224–232.

Mehri A. 2020. Trace elements in human nutrition (II)-An update. International Journal of Preventive Medicine **11**, 1–7.

Mhamdi A, Van Breusegem F. 2018. Reactive oxygen species in plant development. Development **145**, dev164376.

Mielecki J, Gawroński P, Karpiński S. 2020. Retrograde signalling: Understanding the communication between organelles. International Journal of Molecular Sciences **21**, 1–24.

Miller G, Schlauch K, Tam R, Cortes D, Torres MA, Shulaev V, Dangl JL, Mittler R. 2009. The plant NADPH oxidase RBOHD mediates rapid systemic signaling in response to diverse stimuli. Science Signaling **84**: ra45.

Mindthoff S, Grunau S, Steinfort LL, Girzalsky W, Hiltunen JK, Erdmann R, Antonenkov VD. 2016. Peroxisomal Pex11 is a pore-forming protein homologous to TRPM channels. Biochimica et Biophysica Acta-Molecular Cell Research **1863**, 271–283.

Mitsuya S, El-Shami M, Sparkes I a, Charlton WL, Lousa CDM, Johnson B, Baker A. 2010. Salt stress causes peroxisome proliferation, but inducing peroxisome proliferation does not improve NaCl tolerance in *Arabidopsis thaliana*. PloS ONE **5**, e9408.

Mittler R. 2002. Oxidative stress, antioxidants and stress tolerance. Trends in Plant Science **7**, 405–410.

Mittler R, Vanderauwera S, Suzuki N, Miller G, Tognetti VB, Vandepoele K, Gollery M, Shulaev V, Van Breusegem F. 2011. ROS signalling: The new wave? Trends in Plant Science **16**, 300–309.

Mittler R. 2017. ROS are good. Trends in Plant Science **22**, 11–19.

Mor A, Koh E, Weiner L, Rosenwasser S, Sibony-Benyamini H, Fluhr R. 2014. Singlet oxygen signatures are detected independent of light or chloroplasts in response to multiple stresses. Plant Physiology **165**, 249–261.

Mullen RT, Trelease RN. 2006. The ER-peroxisome connection in plants: Development of the 'ER semi-autonomous peroxisome maturation and replication' model for plant peroxisome biogenesis. Biochimica et Biophysica Acta-Molecular Cell Research **1763**, 1655–1668.

Müller M, Munné-Bosch S. 2021. Hormonal impact on photosynthesis and photoprotection in plants. Plant Physiology **185**, 1500–1522.

Mustafa G, Komatsu S. 2016. Toxicity of heavy metals and metal-containing nanoparticles on plants. Biochimica et Biophysica Acta-Proteins and Proteomics **1864**, 932–944.

Nadarajah KK. 2020. ROS homeostasis in abiotic stress tolerance in plants. International Journal of Molecular Sciences **21**, 1–29.

Nazir F, Fariduddin Q, Khan TA. 2020. Hydrogen peroxide as a signalling molecule in plants and its crosstalk with other plant growth regulators under heavy metal stress. Chemosphere **252**, 126486.

Neill SJ, Desikan R, Hancock JT. 2003. Nitric oxide signalling in plants. New Phytologist **159**, 11–35.

Nila AG, Sandalio LM, López MG, Gómez M, Del Río LA, Gómez-Lim MA. 2006. Expression of a peroxisome proliferator-activated receptor gene (xPPARα) from *Xenopus laevis* in tobacco (*Nicotiana tabacum*) plants. Planta **224**, 569–581.

Nordberg GF, Bernard A, Diamond GL, Duffus JH, Illing P, Nordberg M, Bergdahl IA, Jin T, Skerfving S. 2018. Risk assessment of effects of cadmium on human health (IUPAC Technical Report). Pure and Applied Chemistry **90**, 755–808.

Noriega GO, Yannarelli GG, Balestrasse KB, Batlle A, Tomaro ML. 2007. The effect of nitric oxide on heme oxygenase

gene expression in soybean leaves. Planta **226**, 1155–1163.

Okereafor U, Makhatha M, Mekuto L, Uche-Okereafor N, Sebola T, Mavumengwana V. 2020. Toxic metal implications on agricultural soils, plants, animals, aquatic life and human health. International Journal of Environmental Research and Public Health **17**, 1–24.

Oksanen E, Häikiö E, Sober J, Karnosky DF. 2004. Ozone-induced H_2O_2 accumulation in field-grown aspen and birch is linked to foliar ultrastructure and peroxisomal activity. New Phytologist **161**, 791–799.

Olmedilla A, Sandalio LM. 2019. Selective autophagy of peroxisomes in plants: From housekeeping to development and stress responses. Frontiers in Plant Science **10**, 1–7.

Ortega-Galisteo AP, Rodríguez-Serrano M, Pazmiño DM, Gupta DK, Sandalio LM, Romero-Puertas MC. 2012. *S*-nitrosylated proteins in pea (*Pisum sativum* L.) leaf peroxisomes: Changes under abiotic stress. Journal of Experimental Botany **63**, 2089–2103.

Orth T, Reumann S, Zhang X, Fan J, Wenzel D, Quan S, Hu J. 2007. The PEROXIN11 protein family controls peroxisome proliferation in Arabidopsis. The Plant Cell **19**, 333–350.

Oymak T, Tokalioğlu Ş, Yilmaz V, Kartal Ş, Aydin D. 2009. Determination of lead and cadmium in food samples by the coprecipitation method. Food Chemistry **113**, 1314–1317.

Pacher P, Beckman JS, Liaudet L. 2007. Nitric oxide and peroxynitrite in health and disease. Physiological Reviews **87**, 315–424.

Pan R, Hu J. 2018. Proteome of plant peroxisome. In Proteomics of Peroxisomes: Identifying Novel Functions and Regulatory Networks. Del Río LA, Schrader M. Eds. Springer: Singapore, 3–46.

Pan R, Liu J, Wang S, Hu J. 2020. Peroxisomes: Versatile organelles with diverse roles in plants. New Phytologist **225**, 1410–1427.

Pastori GM, Del Río LA. 1997. Natural senescence of pea leaves. Plant Physiology **113**, 411–418.

Paudyal R, Roychoudhry S, Lloyd JP. 2017. Functions and Remodelling of Plant Peroxisomes. eLS, 1–11.

Pazmiño DM, Rodríguez-Serrano M, Sanz M, Romero-Puertas MC, Sandalio LM. 2014. Regulation of epinasty induced by 2,4-dichlorophenoxyacetic acid in pea and Arabidopsis plants. Plant Biology **16**, 809–818.

Pfannschmidt T, Terry MJ, Van Aken O, Quiros PM. 2020. Retrograde signals from endosymbiotic organelles: A common control principle in eukaryotic cells. Philosophical Transactions of the Royal Society B: Biological Sciences **375**, 20190396.

Poirier Y, Antonenkov VD, Glumoff T, Hiltunen JK. 2006. Peroxisomal β-oxidation-A metabolic pathway with multiple functions. Biochimica et Biophysica Acta-Molecular Cell Research **1763**, 1413–1426.

Popov VN, Syromyatnikov MY, Fernie AR, Chakraborty S, Gupta KJ, Igamberdiev AU. 2021. The uncoupling of respiration in plant mitochondria: Keeping reactive oxygen and nitrogen species under control. Journal of Experimental Botany **72**, 793–807.

Pulido P, Perello C, Rodríguez-Concepción M. 2012. New insights into plant isoprenoid metabolism. Molecular Plant **5**, 964–967.

Qu Y, Wang Q, Guo J, Wang P, Song P, Jia Q, Zhang X, Kudla J, Zhang W, Zhang Q. 2017. Peroxisomal CuAOζ and its product H_2O_2 regulate the distribution of auxin and IBA-dependent lateral root development in Arabidopsis. Journal of Experimental Botany **68**, 4851–4867.

Reumann S, Quan S, Aung K, *et al.* 2009. In-depth proteome analysis of arabidopsis leaf peroxisomes combined with in vivo subcellular targeting verification indicates novel metabolic and regulatory functions of peroxisomes. Plant Physiology **150**, 125–143.

Reumann S, Bartel B. 2016. Plant peroxisomes: Recent discoveries in functional complexity, organelle homeostasis, and morphological dynamics. Current Opinion in Plant Biology **34**, 17–26.

Reumann S, Chowdhary G. 2018. Prediction of peroxisomal matrix proteins in plants. Subcellular Biochemistry **89**, 125-138.

Rhodin J.1954. Correlation of ultrastructural organization and function in normal and experimentally changed proximal tubule cells of the mouse kidney. Stockholm, Sweden: Karolinska Instituet.

Rinaldi MA, Patel AB, Park J, Lee K, Strader LC, Bartel B. 2016. The roles of β-oxidation and cofactor homeostasis in peroxisome distribution and function in *Arabidopsis thaliana*. Genetics **204**, 1089–1115.

Rodríguez-Serrano M, Romero-Puertas MC, Sparkes I, Hawes C, Del Río LA, Sandalio LM. 2009. Peroxisome dynamics in Arabidopsis plants under oxidative stress induced by cadmium. Free Radical Biology and Medicine **47**, 1632–1639.

Rodríguez-Serrano M, Pazmiño DM, Sparkes I, Rochetti A, Hawes C, Romero-Puertas MC, Sandalio LM. 2014. 2,4-Dichlorophenoxyacetic acid promotes *S*-nitrosylation and oxidation of actin affecting cytoskeleton and peroxisomal dynamics. Journal of Experimental Botany **65**, 4783–4793.

Rodríguez-Serrano M, Romero-Puertas MC, Sanz-Fernández M, Hu J, Sandalio LM. 2016. Peroxisomes extend peroxules in a fast response to stress via a reactive oxygen species-mediated induction of the peroxin PEX11a.

Plant Physiology **171**, 1665–1674.

Romero-Puertas MC, McCarthy I, Sandalio LM, Palma JM, Corpas FJ, Gómez M, Del Río LA. 1999. Cadmium toxicity and oxidative metabolism of pea leaf peroxisomes. Free Radical Research **31**, Suppl:S25–31.

Romero-Puertas MC, Sandalio LM. 2016. Nitric oxide level is self-regulating and also regulates its ROS partners. Frontiers in Plant Science **7**, 1–5.

Romero-Puertas MC, Terrón-Camero LC, Peláez-Vico MÁ, Olmedilla A, Sandalio LM. 2019. Reactive oxygen and nitrogen species as key indicators of plant responses to Cd stress. Environmental and Experimental Botany **161**, 107–119.

Romero-Puertas MC, Terrón-Camero LC, Peláez-Vico MÁ, Molina-Moya E, Sandalio LM. 2021. An update on redox signals in plant responses to biotic and abiotic stress crosstalk: Insights from cadmium and fungal pathogen interactions. Journal of Experimental Botany **72**, 5857–5875.

Rosenwasser S, Rot I, Sollner E, Meyer AJ, Smith Y, Leviatan N, Fluhr R, Friedman H. 2011. Organelles contribute differentially to reactive oxygen species-related events during extended darkness. Plant Physiology **156**, 185–201.

Rosenwasser S, Fluhr R, Joshi JR, Leviatan N, Sela N, Hetzroni A, Friedman H. 2013. ROSMETER: A bioinformatic tool for the identification of transcriptomic imprints related to reactive oxygen species type and origin provides new insights into stress responses. Plant Physiology **163**, 1071–1083.

Rubbo H. 2013. Nitro-fatty acids: Novel anti-inflammatory lipid mediators. Brazilian Journal of Medical and Biological Research **46**, 728–734.

Sade N, Rubio-Wilhelmi MM, Umnajkitikorn K, Blumwald E. 2018. Stress-induced senescence and plant tolerance to abiotic stress. Journal of Experimental Botany **69**, 845–853.

Sahay S, Gupta M. 2017. An update on nitric oxide and its benign role in plant responses under metal stress. Nitric Oxide-Biology and Chemistry **67**, 39–52.

Sandalio LM, Del Río LA. 1988. Intraorganellar distribution of superoxide dismutase in plant peroxisomes (glyoxysomes and peroxisomes). Plant Physiology **88**, 1215–1218.

Sandalio LM, Dalurzo HC, Gómez M, Romero-Puertas MC, Del Río LA. 2001. Cadmium-induced changes in the growth and oxidative metabolism of pea plants. Journal of Experimental Botany **52**, 2115–2126.

Sandalio LM, Romero-Puertas MC. 2015. Peroxisomes sense and respond to environmental cues by regulating ROS and RNS signalling networks. Annals of Botany **116**, 475–485.

Sandalio LM, Gotor C, Romero LC, Romero-Puertas MC. 2019. Multilevel regulation of peroxisomal proteome by post-translational modifications. International Journal of Molecular Sciences **20**, 4881.

Santolini J, André F, Jeandroz S, Wendehenne D. 2017. Nitric oxide synthase in plants: Where do we stand? Nitric Oxide-Biology and Chemistry **63**, 30–38.

Schlicht M, Ludwig-Müller J, Burbach C, Volkmann D, Baluska F. 2013. Indole-3-butyric acid induces lateral root formation via peroxisome-derived indole-3-acetic acid and nitric oxide. New Phytologist **200**, 473–482.

Schrader M, Bonekamp NA, Islinger M. 2012. Fission and proliferation of peroxisomes. Biochimica et Biophysica Acta-Molecular Basis of Disease **1822**, 1343–1357.

Schrader M, Costello JL, Godinho LF, Azadi AS, Islinger M. 2016. Proliferation and fission of peroxisomes-An update. Biochimica et Biophysica Acta-Molecular Cell Research **1863**, 971–983.

Schützendübel A, Nikolova P, Rudolf C, Polle A. 2002. Cadmium and H_2O_2-induced oxidative stress in Populus x canescens roots. Plant Physiology and Biochemistry **40**, 577–584.

Scott I, Sparkes IA, Logan DC. 2007. The missing link: inter-organellar connections in mitochondria and peroxisomes? Trends in Plants Science. **12**, 380–381.

Sewelam N, Jaspert N, Kelen K Van Der, Tognetti VB, Schmitz J. 2014. Spatial H_2O_2 signalling specificity: H_2O_2 from chloroplasts and peroxisomes modulates the plant transcriptome differentially. Molecular Plant **7**, 1191–1210.

Sewelam N, Kazan K, Schenk PM. 2016. Global plant stress signalling: Reactive oxygen species at the cross-road. Frontiers in Plant Science **7**, 1–21.

Shahid M, Javed MT, Mushtaq A, Akram MS, Mahmood F, Ahmed T, Noman M, Azeem M. 2019. Microbe-mediated mitigation of cadmium toxicity in plants. In Cadmium Toxicity and Tolerance in Plants-From Physiology to Remediation. Hasanuzzaman M, Prasad MNV, Fujita M. Eds. Elsevier, 427–449

Shai N, Yifrach E, Van Roermund CWT, *et al.* 2018. Systematic mapping of contact sites reveals tethers and a function for the peroxisome-mitochondria contact. Nature Communications **9**, 1761.

Sharma P, Jha AB, Dubey RS, Pessarakli M. 2012. Reactive oxygen species, oxidative damage, and antioxidative defense mechanism in plants under stressful conditions. Journal of Botany **2012**, 1–26.

Sharma A, Sidhu GPS, Araniti F, Bali AS, Shahzad B, Tripathi DK, Brestic M, Skalicky M, Landi M. 2020. The role of salicylic acid in plants exposed to heavy metals. Molecules **25**, 1–21.

Shimada TL, Hayashi M, Hara-Nishimura I. 2018. Membrane dynamics and multiple functions of oil bodies in seeds

and leaves. Plant Physiology **176**, 199–207.

Sibirny AA. 2016. Yeast peroxisomes: Structure, functions and biotechnological opportunities. FEMS Yeast Research **16**, 1–14.

Sinclair AM, Trobacher CP, Mathur N, Greenwood JS, Mathur J. 2009. Peroxule extension over ER-defined paths constitutes a rapid subcellular response to hydroxyl stress. Plant Journal **59**, 231–242.

Singh A, Kumar A, Yadav S, Singh IK. 2019. Reactive oxygen species-mediated signalling during abiotic stress. Plant Gene **18**, 100173.

Smith JJ, Aitchison JD. 2013. Peroxisomes take shape. Nature Reviews Molecular Cell Biology **14**, 803–817.

Socha AL, Guerinot ML. 2014. Mn-euvering manganese: The role of transporter gene family members in manganese uptake and mobilization in plants. Frontiers in Plant Science **5**, 1–16.

Song Y. 2014. Insight into the mode of action of 2,4-dichlorophenoxyacetic acid (2,4-D) as an herbicide. Journal of Integrative Plant Biology **56**, 106–113.

Stolz DB, Zamora R, Vodovotz Y, Loughran PA, Billiar TR, Kim YM, Simmons RL, Watkins SC. 2002. Peroxisomal localization of inducible nitric oxide synthase in hepatocytes. Hepatology **36**, 81–93.

Su T, Li W, Wang P, Ma C. 2019. Dynamics of peroxisome homeostasis and its role in stress response and signalling in plants. Frontiers in Plant Science **10**, 705.

Su T, Wang P, Li H, *et al.* 2018. The Arabidopsis catalase triple mutant reveals important roles of catalases and peroxisome-derived signalling in plant development. Journal of Integrative Plant Biology **60**, 591–607.

Tanabe Y, Maruyama JI, Yamaoka S, Yahagi D, Matsuo I, Tsutsumi N, Kitamoto K. 2011. Peroxisomes are involved in biotin biosynthesis in Aspergillus and Arabidopsis. Journal of Biological Chemistry **286**, 30455–30461.

Tang X, Lim MH, Pelletier J, Tang M, Nguyen V, Keller WA, Tsang EW, Wang A, Rothstein SJ, Harada JJ, Cui Y. 2012. Synergistic repression of the embryonic programme by SET DOMAIN GROUP 8 and EMBRYONIC FLOWER 2 in Arabidopsis seedlings. Journal of Experimental Botany **3**: 1391–1404.

Tchounwou PB, Yedjou CG, Patlolla AK, Sutton DJ. 2012. Heavy metal toxicity and the environment. Natural Institute of Health, **101**, 133–164.

Tejada-Jiménez M, Llamas A, Galván A, Fernández E. 2019. Role of nitrate reductase in NO production in photosynthetic eukaryotes. Plants **8**, 56.

Terrón-Camero LC, Peláez-Vico MÁ, Del-Val C, Sandalio LM, Romero-Puertas MC. 2019. Role of nitric oxide in plant responses to heavy metal stress: Exogenous application versus endogenous production. Journal of Experimental Botany **70**, 4477–4488.

Terrón-Camero LC, Rodríguez-Serrano M, Sandalio LM, Romero-Puertas MC. 2020. Nitric oxide is essential for cadmium-induced peroxule formation and peroxisome proliferation. Plant, Cell and Environment **43**, 2492–2507.

Thazar-Poulot N, Miquel M, Fobis-Loisy I, Gaude T. 2015. Peroxisome extensions deliver the Arabidopsis SDP1 lipase to oil bodies. Proceedings of the National Academy of Sciences of the United States of America **112**, 4158–4163.

Tiew TW, Sheahan MB, Rose RJ. 2015. Peroxisomes contribute to reactive oxygen species homeostasis and cell division induction in Arabidopsis protoplasts. Frontiers in Plant Science **6**, 1–16.

Tiwari S, Lata C. 2018. Heavy metal stress, signalling, and tolerance due to plant-associated microbes: An overview. Frontiers in Plant Science **6**, 452.

Torres MA, Dangl JL. 2005. Functions of the respiratory burst oxidase in biotic interactions, abiotic stress and development. Current Opinion in Plant Biology **8**, 397–403.

Trzcinska-Danielewicz J, Ishikawa T, Miciałkiewicz A, Fronk J. 2008. Yeast transcription factor Oaf1 forms homodimer and induces some oleate-responsive genes in absence of Pip2. Biochemical and Biophysical Research Communications **374**, 763–766.

Tsukagoshi H, Morikami A, Nakamura K. 2007. Two B3 domain transcriptional repressors prevent sugar-inducible expression of seed maturation genes in Arabidopsis seedlings. Proceedings of the National Academy of Sciences of the United States of America **7**: 2543–2547.

Turcotte B, Liang XB, Robert F, Soontorngun N. 2010. Transcriptional regulation of nonfermentable carbon utilization in budding yeast. FEMS Yeast Research **10**, 2–13.

Turkan I. 2018. ROS and RNS: Key signalling molecules in plants. Journal of Experimental Botany **69**, 3313–3315.

Ulrich K, Jakob U. 2019. The role of thiols in antioxidant systems. Free Radical Biology and Medicine **176**, 139–148.

Unsal V, Dalkiran T, Çiçek M, Kölükçü E. 2020. The role of natural antioxidants against reactive oxygen species produced by cadmium toxicity: A review. Advanced Pharmaceutical Bulletin **10**, 184–202.

Van Roermund CWT, Tabak HF, Van den Berg M, Wanders RJA, Hettema EH. 2000. Pex11p plays a primary role in medium-chain fatty acid oxidation, a process that affects peroxisome number and size in *Saccharomyces cerevisiae*. Journal of Cell Biology **150**, 489–497.

Veenhuis M, Hoogkamer-Te Niet MC, Middelhoven WJ. 1985. Biogenesis and metabolic significance of microbodies in urate-utilizing yeasts. Antonie van Leeuwenhoek **51**, 33–43.

Walter T, Erdmann R. 2019. Current advances in protein import into peroxisomes. Protein Journal **38**, 351–362.

Walton PA, Brees C, Lismont C, Apanasets O, Fransen M. 2017. The peroxisomal import receptor PEX5 functions as a stress sensor, retaining catalase in the cytosol in times of oxidative stress. Biochimica et Biophysica Acta-Molecular Cell Research **1864**, 1833–1843.

Wang L, Wang C, Liu X, Cheng J, Li S, Zhu JK, Gong Z. 2019. Peroxisomal β-oxidation regulates histone acetylation and DNA methylation in Arabidopsis. Proceedings of the National Academy of Sciences of the United States of America **116**, 10576–10585.

Wang L, Jin Y, Weiss DJ, Schleicher NJ, Wilcke W, Wu L, Guo Q, Chen J, O'Connor D, Hou D. 2021. Possible application of stable isotope compositions for the identification of metal sources in soil. Journal of Hazardous Materials **407**, 124812.

Wang Y, Selinski J, Mao C, Zhu Y, Berkowitz O, Whelan J. 2020. Linking mitochondrial and chloroplast retrograde signalling in plants. Philosophical Transactions of the Royal Society B: Biological Sciences **375**, 20190410.

Waszczak C, Carmody M, Kangasjärvi J. 2018. Reactive oxygen species in plant signalling. Annual Review of Plant Biology **29**, 209–236.

Wayne R. 2019. Peroxisomes. In Plant Cell Biology-From Astronomy to Zoology. Wayne R. Eds. Elsevier, 83–98.

Wei L, Zhang J, Wang C, Liao W. 2020. Recent progress in the knowledge on the alleviating effect of nitric oxide on heavy metal stress in plants. Plant Physiology and Biochemistry **147**, 161–171.

Willems P, Mhamdi A, Stael S, Storme V, Kerchev P, Noctor G, Gevaert K, Van Breusegem F. (2016). The ROS wheel: Refining ROS transcriptional footprints. Plant Physiology **171**: 1720–1733.

Williams C, Opalinski L, Landgraf C, Costello J, Schrader M, Krikken AM, Knoops K, Kram AM, Volkmer R, Van Der Klei IJ. 2015. The membrane remodeling protein Pex11p activates the GTPase Dnm1p during peroxisomal fission. Proceedings of the National Academy of Sciences of the United States of America **112**, 6377–6382.

Wróblewska JP, Cruz-Zaragoza LD, Yuan W, *et al.* 2017. *Saccharomyces cerevisiae* cells lacking Pex3 contain membrane vesicles that harbor a subset of peroxisomal membrane proteins. Biochimica et Biophysica Acta-Molecular Cell Research **1864**, 1656–1667.

Wu F, de Boer R, Krikken AM, Akşit A, Bordin N, Devos DP, Van Der Klei IJ. 2020. Pex24 and Pex32 are required to tether peroxisomes to the ER for organelle biogenesis, positioning and segregation in yeast. Journal of Cell Science **133**, 1–44.

Xie X, He Z, Chen N, Tang Z, Wang Q, Cai Y. 2019. The roles of environmental factors in regulation of oxidative stress in plant. BioMed Research International **2019**, 21–27.

Zandalinas SI, Sengupta S, Burks D, Azad RK, Mittler R. 2019. Identification and characterization of a core set of ROS wave-associated transcripts involved in the systemic acquired acclimation response of Arabidopsis to excess light. Plant Journal **98**, 126–141.

Zandalinas SI, Fichman Y, Mittler R. 2020. Vascular bundles mediate systemic reactive oxygen signaling during light stress. Plant Cell **11**: 3425–3435.

Zandalinas SI, Sengupta S, Fritschi FB, Azad RK, Nechushtai R, Mittler R. 2021. The impact of multifactorial stress combination on plant growth and survival. New Phytologist. **230**: 1034–1048.

Zander M, Lewsey MG, Clark NM, *et al.* 2020. Integrated multi-omics framework of the plant response to jasmonic acid. Nature Plants **6**, 290–302.

Zhong WS, Ren T, Zhao LJ. 2016. Determination of Pb (Lead), Cd (Cadmium), Cr (Chromium), Cu (Copper), and Ni (Nickel) in Chinese tea with high-resolution continuum source graphite furnace atomic absorption spectrometry. Journal of Food and Drug Analysis **24**, 46–55.

Zhou X, Xiang Y, Li C, Yu G. 2020. Modulatory role of reactive oxygen species in root development in model plant of *Arabidopsis thaliana*. Frontiers in Plant Science **11**, 1–13.

Zuanazzi NR, Ghisi N de C, Oliveira EC. 2020. Analysis of global trends and gaps for studies about 2,4-D herbicide toxicity: A scientometric review. Chemosphere **241**, 125016.

Annex I: **Sandalio LM, Peláez-Vico MA, Molina-Moya E, Romero-Puertas MC.** 2021. Peroxisomes as redox-signalling nodes in intracellular communication and stress responses. Plant Physiology **186**, 22–35.

Annex II: **Sandalio LM, Peláez-Vico MA, Romero-Puertas MC**. 2020. Peroxisomal metabolism and dynamics at the crossroads between stimulus perception and fast cell responses to the environment. Frontiers in Cell and Developmental Biology **8**, 1–5.

Annexes

ANNEX I

Adapted from: Sandalio et al., (2021) Plant Physiology 186, 22–35.

Short title: Redox pathways in peroxisomes

PEROXISOMES AS REDOX-SIGNALLING NODES IN INTRACELLULAR COMMUNICATION AND STRESS RESPONSES

Sandalio LM, Peláez-Vico MA, Molina-Moya E, Romero-Puertas MC*

Department of Biochemistry and Molecular and Cellular Biology of Plants,
Estación Experimental del Zaidín-CSIC, Profesor Albareda 1, 18008 Granada, Spain

List of author contributions: L.M.S. conceived the original review focus and wrote the article with input and critical discussion from all the authors; M.A.P. and E.M.M. edited the figures. All authors read and approved the content of the manuscript. L.M.S. has agreed to act as the author responsible for contacts and correspondence.

*Author for correspondence:
Luisa M. Sandalio
phone +34 958181600,
e-mail: luisamaria.sandalio@eez.csic.es
Department of Biochemistry and Molecular and Cellular Biology of Plants, Estación Experimental del Zaidín-CSIC, Profesor Albareda 1, 18008 Granada, Spain

Funding information: This work was funded by MCIU, AEI and FEDER grant PGC2018-098372-B-I00.

Sentence summary: Peroxisomes are redox nodes playing a diverse range of roles in cell functionality and in the perception of and responses to changes in their environment

Abstract

Redox compartmentalization in organelles is an effective evolutionary strategy (Box1). From an evolutionary perspective, peroxisomes, originating from the endoplasmic reticulum (ER), were selected to house a range of metabolic pathways involving the production of certain ROS such as H_2O_2 to avoid toxicity to other organelles such as mitochondria (Gabaldón, 2018). Peroxisomes play a diverse range of roles in cell functionality and in the perception of and responses to changes in their environment (Lismont et al., 2019; Sandalio and Romero-Puertas, 2015). The range of functions associated with plant peroxisomes has increased considerably over the last two decades (Table 1). As most of these pathways produce ROS and NO, disturbances in these metabolic processes trigger transitory changes in ROS/RNS production. These changes regulate peroxisomal metabolism, leading to peroxisome-dependent signalling and organelle crosstalk, which triggers specific cell responses (Sandalio and Romero-Puertas, 2015). The biosynthesis of phytohormones jasmonic acid (JA), auxin IAA and salicylic acid (SA) associated with the β-oxidation pathway contributes to the complex role of peroxisomes in development and stress responses (Kao et al., 2018; Fig 2A). Peroxisomes dynamically regulate their number, shape and protein content in response to changing environmental conditions and remain in close contact with other subcellular compartments such as mitochondria and chloroplasts (Sandalio and Romero-Puertas, 2015; Shai et al., 2016; Sandalio et al., 2020). Peroxisomes play a key role in the evolution of the metabolic networks of photosynthetic organisms by connecting oxidative and biosynthetic pathways operating in different compartments. This review updates our knowledge of peroxisomal redox homeostasis and the role of ROS and NO in the functionality, biogenesis and abundance of these organelles, as well as their role as redox hubs in metabolic regulation, signalling and organelle crosstalk.

Peroxisomes are reactive oxygen species (ROS) and nitric oxide (NO) producers

Peroxisomes produce and scavenge ROS

ROS include an array of molecular oxygen derivatives that occur as a normal attribute of aerobic life (Fig. 1). Peroxisomes are one of the main sources of cellular ROS production and have a complex antioxidant system to balance ROS levels, enabling them to strictly regulate organelle functionality, metabolism and signalling networks. The first step in O_2 univalent reduction, the superoxide radical $O_2^{\bullet -}$ (Fig. 1), is produced in the ureide and nucleic acid catabolism by xanthine oxidoreductase (XOR) and urate oxidase or uricase (UO) reaction (Werner and Witte, 2011; Sandalio et al., 2013; Fig. 2 A); in the sulfite oxidation by sulfite oxidase (SO; Byrne et al., 2009); and in the NADH/NADPH-dependent electron transport chain in the peroxisomal membrane. Superoxide accumulation is regulated by different superoxide dismutases (SOD; reviewed in Sandalio and Romero-Puertas, 2015; Fig. 2B).

Table 1 Plant peroxisome functions

- ROS and RNS metabolism
- H_2O_2 and NO signaling
- Photorespiration
- Phytohormones biosynthesis (JA, IAA, SA)
- Fatty acid β-oxidation
- Glyoxylate cycle
- Polyamine catabolism
- Amino acids metabolism
- Indole glucosinolates metabolism
- Ureide metabolism
- Purine catabolism
- Biotin biosynthesis
- Ubiquinone biosynthesis
- Phylloquinone biosynthesis
- Isoprenoids biosynthesis
- BA derivate biosynthesis
- Sulfite metabolism

ADVANCES

- Peroxisomal H_2O_2 regulates pathogen associated processes, DNA repair systems, cell cycles and phytohormone-dependent signalling.
- Peroxisomes regulate cellular processes in the cytosol and other cell compartments through moonlighting proteins such as CAT3, which is able to transnitrosylate and degrade GSNOR via autophagy.
- Peroxisomes are highly dynamic organelles that are capable of changing their number, size, morphology and speed in response to environmental redox changes.
- Peroxules are ROS- and NO-induced dynamic structures that are regulated by PEX11a, which connects peroxisomes to chloroplasts, mitochondria, ER and lipid bodies.
- Under basal and stress conditions, peroxisomal populations and quality are regulated by selective autophagy (pexophagy) which is controlled by ROS and the peroxisomal protease LON2.

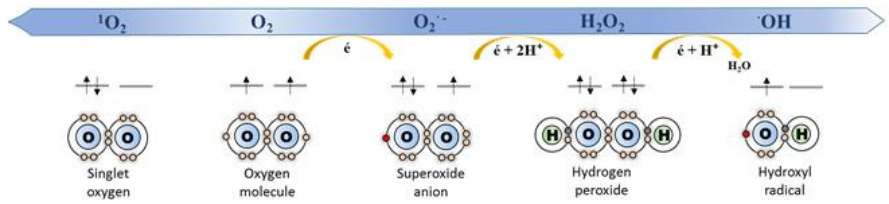

Figure 1. *Sequential reduction of O_2 and ROS production: superoxide ($O_2^{\bullet -}$), hydrogen peroxide (H_2O_2) and hydroxyl (•OH) radicals.*

Box 1 **SUBCELLULAR REDOX COMPARTMENTALIZATION**

As oxygen-dependent redox reactions came to control life after O_2 appeared in the atmosphere, cells developed complex mechanisms to detect and regulate these changes to maintain metabolic functionality. Redox compartmentalization in organelles is an effective evolutionary strategy, which regulates physiological and stress conditions through site-specific footprinting (Jones and Go, 2010). This redox circuit flexibility facilitates rapid responses to changes in intracellular redox equilibrium, which, in turn, favors beneficial signaling and detrimental oxidative stress. Photosynthetic organisms have developed efficient redox control systems using redox signals as the most fundamental forms of information (Foyer and Noctor, 2016). The thiol/disulphide couples GSH/GSSG and Cys/CySS, the ASC/DHA couple and a broad range of redox dependent proteins, which are counterparts of ROS such as H_2O_2 and other oxidants, form the core of the redox state and regulate the cell signaling, structure and activity of proteins and transcription factors. Apart from ROS, RNS are also redox signaling molecules, which include NO and peroxynitrite ($ONOO^-$). Both ROS and RNS regulate covalent, often reversible, modifications, mainly targeting Cys, which regulates metabolic shifts and triggers signaling cell responses (Noctor et al., 2018; Sánchez-Vicente et al., 2019). Although irreversible oxidation products, such as sulfonic acid, carbonylation, and nitration, adversely affect proteins and lipids, they may be also involved in oxidative signaling (Foyer et al., 2017). Analyses of redox potential in plant tissue identified peroxisomes as some of the most oxidized cellular organelles, with a redox potential of approximately −360 mV (Bratt et al., 2016; Smirnoff and Arnaud, 2019).

In photosynthetic tissue, peroxisomes accumulate the highest concentrations of organelle H_2O_2 (the second step in O_2 reduction) with a flux of ~10,000 $nmol^{-2}$ s^{-1} (Foyer and Noctor, 2003). The use of H_2O_2 ratiometric reporter HyperAs targeting peroxisomes has facilitated the imaging of changes in peroxisomal H_2O_2 accumulation in response to Cd treatment (Calero-Muñoz et al., 2019) and the increase in intraperoxisomal Ca^{2+} levels (Costa et al., 2010). The main source of H_2O_2 in peroxisomes in green tissue is GOX in the photorespiration cycle (Fig. 2 A), which contributes up to 70% of total H_2O_2 production in plant cells (Reumann and Weber, 2006; Foyer et al., 2009). Photorespiration requires coordination of the chloroplast, peroxisome, mitochondrion and cytosol; and photorespiration-dependent H_2O_2 production increases considerably under environmental stress conditions such as heat and drought (Walker et al., 2016, Talbi et al., 2015), heavy metal (Gupta et al., 2017), high light (Cui et al., 2016a) and biotic stress (Rojas et al., 2012; Hodges et al., 2016; Yang et al., 2018). Fatty acid β-oxidation, another source of H_2O_2 in peroxisomes by the Acyl-CoA oxidase (ACX), provides energy during the initial stage of seedling growth by oxidizing fats stored as triacylglycerol (TAG) in oil bodies (Rinaldi et al, 2016; Fig. 2 A). Other β-oxidation pathways are active in green tissues, including the synthesis of ubiquinone, hormones such as indole acetic acid (IAA) and jasmonic acid, and secondary metabolites such as benzoic acid (BA) and phenylpropanoids (reviewed in Pan et al., 2020; Fig. 2 A). Polyamine catabolism and sarcosine oxidase (SOX) are additional peroxisomal sources of H_2O_2 (Fig. 2 A; Wang et al.,

2019; Goyer et al., 2004). Peroxisomal H_2O_2 levels are regulated by balancing H_2O_2 generation and scavenging rates (Fig. 2B) by catalase (CAT), which account for 10–25% of total peroxisomal proteins (Reumann et al., 2004; Fig. 2 B). Arabidopsis plants contain three CAT genes, *CAT1*, *CAT2* and *CAT3,* with CAT2 being the most important defense against photorespiratory H_2O_2, accounting for 80% of activity (reviewed in Mhamdi et al., 2012). In fact, physical GOX-CAT interactions regulated by salicylic acid (SA) occur in rice leaves (Zhang et al., 2016). A protective association between CAT and isocitrate lyase has also been observed in castor bean glyoxysomes (Yanik et al., 2005) and CAT2 also interacts with ACX2/ACX3 regulating their activity and therefore the SA-mediated regulation of JA biosynthesis, under biotrophic infection (Yuan et al., 2017). Although the extraordinarily low affinity of CAT for H_2O_2, with a Km of around 43 mM, reduces its efficiency in controlling H_2O_2 the abundance of CAT compensates for this low affinity (Foyer and Noctor, 2016). The peroxisomal ascorbate–glutathione cycle, which, in Arabidopsis, is composed of ascorbate peroxidase *(APX3* and *APX5)*, monodehydroascorbate reductase (*MDHAR1*), dehydroascorbate reductase (*DHAR1*), and glutathione reductase *(GR1)* (reviewed in Mhamdi et al., 2012; Sandalio and Romero-Puertas 2015; Pan et al., 2020; Fig. 2 B) also contribute to H_2O_2 homeostasis. MDHAR and APX are associated with the peroxisomal membrane and the higher affinity for H_2O_2 of APX (100 μM) as compared to CAT, could regulate H_2O_2 leakage from peroxisomes to the cytosol (del Río et al., 2003; Kaur et al., 2009; Eastmond, 2007; Fig. 2 B). Therefore, CAT and APX are positioned to enable H_2O_2 to act as a second messenger. Glutathione S-transferases supports peroxide regulation in these organelles (Pan and Hu, 2018). The ascorbate-glutathion cycle also facilitates regeneration and maintenance of the peroxisomal redox buffers ASC/DHA and GSH/GSSG. The use of ratiometric glutathione redox potential reporters, such as roGFP2, targeting peroxisomes has facilitated the imaging of peroxisome oxidation under extended dark stress and the application of elicitors (Bratt et al., 2016).

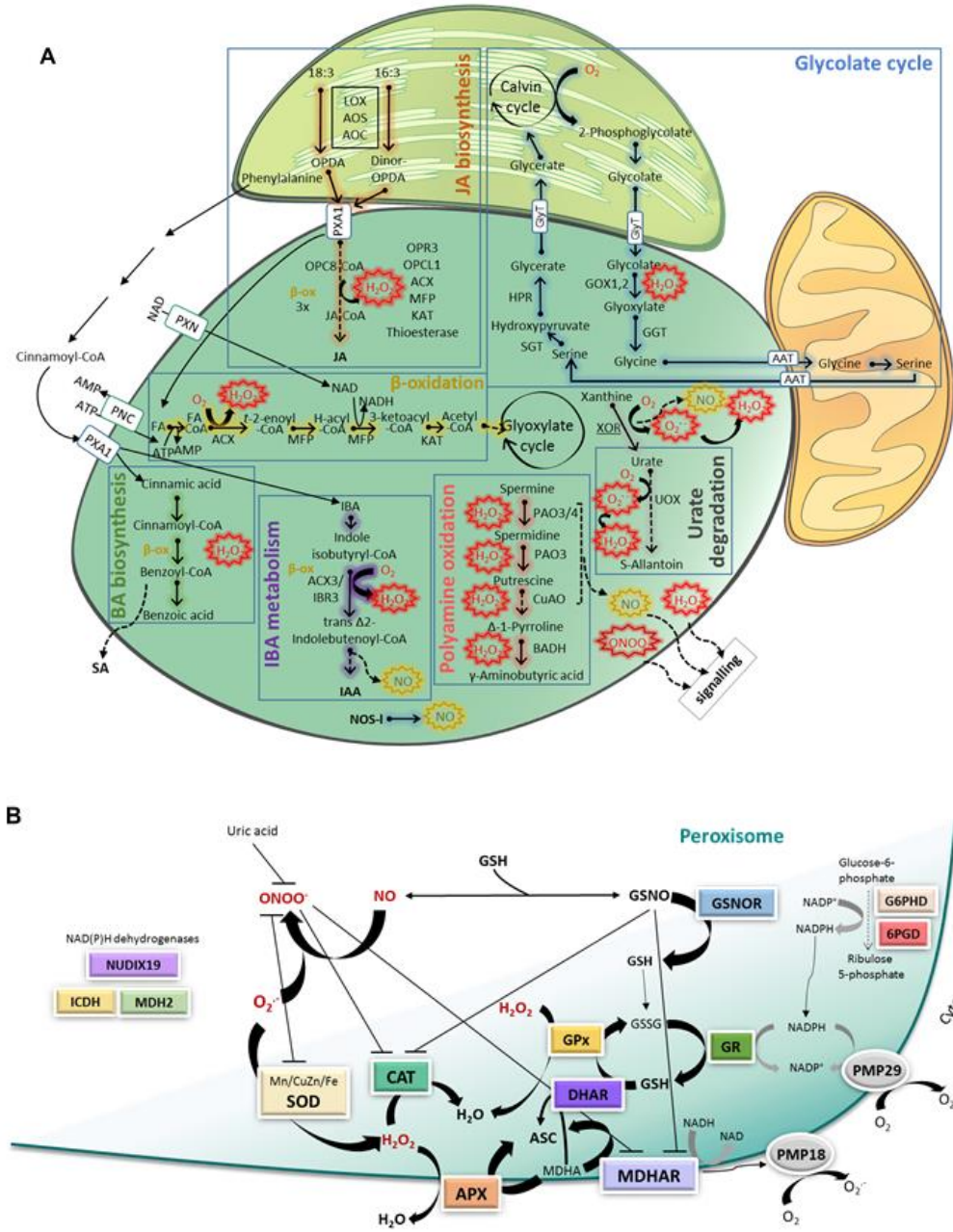

Figure 2. *Oxygen and nitrogen reactive species metabolism in peroxisomes. A, Principal peroxisomal metabolic pathways associated with peroxisomal ROS and NO production. ROS are produced in metabolic pathways such as β-oxidation, photorespiration, ureides metabolism, and polyamine oxidation, and in a small electron transport chain associated with the membrane (peroxisomal membrane proteins, PMP18 and PMP29; Figure 2B). NO is produced in peroxisomes by NOS-like (NOS-l) activity, although other sources, such as XOR, polyamine oxidation, and IBA metabolism, could also be involved. ROS, NO, and other RNS may leak out of the peroxisome (dashed arrows) and act as signal molecules that regulate cell metabolism and gene expression. B,*

Scheme of peroxisomal antioxidant defenses, RNS scavengers, and NAD(P)H supply. $O_2^{\bullet-}$ is regulated by SODs, while H_2O_2 is controlled by CAT, the ASC-GSH cycle, and GPx. Peroxynitrite ($ONOO^-$) and GSNO are produced in peroxisomes by reaction of NO with $O_2^{\bullet-}$ and glutathione (GSH), respectively. GSNO can negatively regulate MDHAR and CAT through S-nitrosylation and nitration, and SOD may be regulated by nitration. SOD may indirectly control $ONOO^-$ by regulating $O_2^{\bullet-}$ levels. Uric acid acts as an ONOO– scavenger. NAD(P)H is supplied by the oxidative pentose phosphate pathway (G6PD; 6PGD), ICDH, MDH, and NUDIX19. 6PGD, 6 phosphogluconate dehydrogenase; AAT, amino acid translocator; AOC, allene oxide cyclase; AOS, allene oxide synthase; APX, ascorbate peroxidase; BADH, betaine aldehyde dehydrogenase; CAT, catalase; CuAO, copper amine oxidase1; DHAR, dehydroascorbate peroxidase; GOX1,2, glycolate oxidase1,2; G6PD, glucose-6-phosphate dehydrogenase; GGT, glutamate–glyoxylate aminotransferase; GlyT, glycerate–glycolate translocator; GR, glutathione reductase; GPx, glutathione peroxidase; H-Acyl-CoA, 3-hydroxyacyl-CoA; HPR, hydroxypyruvate reductase; IAA, indole-3-acetic acid; IBA, indole-3-butyric acid; IBR3, Acyl-coA dehydrogenase/oxidase-like IBR3; ICDH, isocitrate dehydrogenase; KAT, L-3-ketoacyl-CoA-thiolase; LOX, lipoxygenase; MDH2, malate dehydrogenase; MDHAR, monodehydroascorbate peroxidase; MFP, multifunctional protein; OPCL1, OPC-8:0 CoA ligase1; NOS-l, NO synthase-like; NUDIX19, nudix hydrolase homolog 19; OPR3, OPDA reductase3; PAO3, polyamine oxidase3; PAO3/4, polyamine oxidase 3/4; PNC, peroxisomal ATP carrier; PXA1, peroxisomal ABC-transporter1; PXN, peroxisomal NAD carrier; SGT, serin–glyoxylate aminotransferase; UOX, urate oxidase.

Peroxisomal NO/RNS production and scavenging

Although NO is a well-known signalling molecule in plants, its metabolism has not been fully elucidated (León and Costa-Broseta, 2020). Peroxisomal NO production has been associated to a NO synthase-like activity (NOS-l; Fig. 2 A; Barroso et al., 1999), the conversion of IBA to IAA by β-oxidation (Fig. 2 A; Schlicht et al., 2013), polyamine catabolism (Fig. 2 A; Wimalasekera et al., 2011; Agurla et al., 2018) and the XOR reaction (Fig. 2 A; Antonenkov et al., 2010; Wang et al., 2010). Other nitrogen-derived species, such as peroxynitrite ($ONOO^-$), resulting from the $O_2^{\bullet-}$/NO reaction, and nitrosoglutathione (GSNO), resulting from the combination of NO and GSH and considered a cellular NO reservoir, have been detected in peroxisomes (Fig. 2 A; Ortega-Galisteo et al., 2012; Corpas and Barroso, 2014). Peroxisomal SOD could regulate $ONOO^-$ accumulation by controlling $O_2^{\bullet-}$ availability and CAT could degrade it, as reported in animal cells (Gebicka and Didik, 2009), and thus play a key modulatory role at the cross-point between H_2O_2 and NO/$ONOO^-$-mediated signalling pathways (Fig. 2 B). Urate, a well-known peroxynitrite scavenger (Hooper et al., 2000; Alamillo and García-Olmedo, 2001), may contribute also to regulate $ONOO^-$ in peroxisomes (Fig. 2 B). *S*-nitrosoglutathione reductase (GSNOR), which balances NO and *S*-nitrosothiol levels, has been proteomically

identified in plant peroxisomes (reviewed in Sandalio et al., 2019), although this requires validation.

NADH/NADPH regeneration in peroxisomes

The concept of redox stress (oxidative and reductive) reflected by changes in NAD(H)/NADP(H) has gained increasing attention. The NAD(P)H cofactor is required to β-oxidation and antioxidative defenses MDHAR and GR. NAD(P)H regeneration in peroxisome take place by the oxidative pentose phosphate pathway (OPPP; Corpas et al., 1999; Reumann et al., 2007; Lansing et al., 2020; Fig. 2 B), NADP-dependent isocitrate dehydrogenase (ICDH; Corpas et al., 1999; Reumann et al., 2007; Fig. 2 B), NADH phosphorylation by NADH kinase 3 (NADK3) (Waller et al., 2010) and possibly betaine aldehyde dehydrogenase (ALDH19; Hou and Bartels, 2015). The peroxisomal NADH pool is supported by malate dehydrogenase MDH2 (Cousins et al., 2008; Fig.2 B). Peroxisomes also contain pyrophosphatase Nudix Hydrolase Homolog 19 (NUDT19), which hydrolyzes NADPH to NMNH, as well as 2′,5′-ADP and NADH to NMNH and AMP (Lingner et al., 2011).

ROS and NO-dependent PTMs in peroxisomal metabolism regulation

Analysis of peroxisomal proteomes shows that a large number of peroxisomal proteins (35 %) are targeted by multiple PTMs (Sandalio et al., 2019). Peroxisomal-dependent ROS/RNS can fine-tune post-translational redox changes in proteins, regulating stability, activity, location and protein-protein interactions (Hashiguchi and Komatsu, 2016; Duan and Walther, 2015; Sandalio et al., 2019; Foyer et al., 2020) supporting peroxisomes capacity to regulate their metabolism and dynamics in response to environmental changes. Hydrogen peroxide leads to rapid and reversible oxidative protein modifications such as sulfenylation, sulfinylation and intra- and inter-molecular disulfide bond formation, which contribute to coordinated regulation of cellular processes, while overoxidation by sulfonylation appears to be an irreversible process (reviewed in Young et al., 2019; Sandalio et al., 2019; Sies and Jones, 2020). Given their transient nature, these sulfur modifications are regarded as redox switches (Huang et al, 2018). Peroxisomal antioxidant defenses, fatty acid β-oxidation and photorespiration are prone to H_2O_2-dependent redox regulation (reviewed in Sandalio et al., 2019). The

glyoxalase 1 (GLX1) homolog is a putative sulfenylated protein involved in protection against carbonyls (Schmitz et al., 2018).

NO, in turn, modifies proteins through covalent PTMs including *S*-nitrosylation (Martínez-Ruiz et al., 2011). Putative peroxisomal *S*-nitrosylated proteins also include antioxidants and enzymes from the photorespiration cycle (Romero-Puertas and Sandalio, 2016; Sandalio et al., 2019) suggesting that *S*-nitrosylation plays an important role in regulating peroxisomal H_2O_2 concentrations under physiological and stress conditions (Ortega-Galisteo et al., 2012). Recently, the non-canonical catalase CAT3, identified as a "repressor of" GSNOR1 (ROG1), was reported to transnitrosylate GSNOR1 to promote its degradation by autophagy, while CAT1 and CAT2 do not do it, thereby CAT3 positively regulates NO signalling and according Arabidopsis *rog1* mutants are more susceptible to NO than WT (Chen et al., 2020). CAT3 is localized in peroxisomes, the cytoplasm and the plasma membrane (Li et al., 2015; Zou et al., 2015) and is recruited into the nucleus by the cucumber mosaic virus (CMV) 2b protein (Inaba et al., 2011; Murota et al., 2017). Zhan et al. (2018) have reported that *S*-nitrosylation induces selective autophagy of Arabidopsis GSNOR1 during hypoxia responses. CAT3 also interacts with other proteins in the cytosol and plasma membrane, thus increasing the likelihood that these proteins are also substrates of CAT3 transnitrosylase activity (Chen et al., 2020). These findings suggest NO self-regulation and ROS/NO crosstalk. Zhang et al. (2020) have reported that glutathione denitrosylation is required to maintain the up-regulation of GSNOR activity; thus coordinating GSNOR activity with protein *S*-nitrosylation levels to ensure appropriate signalling involving the SA pathway in response to H_2O_2.

Some fatty acid β-oxidation enzymes, including ACX2, 3, may be *S*-nitrosylation targets (Sandalio et al., 2019). OPC-8:0 CoA Ligase1 (OPCL1), involved in activating JA biosynthetic precursors in leaf peroxisomes (Koo et al., 2006), is also a putative target of *S*-nitrosylation, pointing to NO/JA- crosstalk. Proteomic analyses suggest that BRI1 suppressor 1 (BSU1)-like 3 is targeted by *S*-nitrosylation (Sandalio et al., 2019) suggesting NO-dependent brassinosteroids signalling. NO-dependent nitration also inhibits peroxisomal antioxidants such CAT (Lozano-Juste et al., 2011; Chaki et al., 2015) and SOD (Holzmeister et al., 2015). Therefore, NO and ROS, apart from self-regulation (Romero-Puertas and Sandalio, 2016), may also regulate specific proteins and/or metabolic

pathways and metabolite channeling, depending on the redox environment both inside and outside the peroxisome.

Peroxisome-dependent redox regulation of transcriptional responses

ROS act as secondary messengers that are sensed by specific redox-sensitive proteins, which activate signal transduction pathways and alter gene expression (Suzuki et al., 2012; Mittler, 2017). Different ROS trigger different protein modifications, as shown by different gene expression patterns (Møller and Sweetlove, 2010; Mor et al., 2014). The subcellular site, where the ROS/oxidation state is modified, acts as a specific cellular redox network signal (Foyer and Noctor, 2003; König et al., 2012) and leaves a specific imprint on the transcriptome response (Rosenwasser et al., 2011). The selective reactivity, stability and diffusibility of H_2O_2 make it an ideal signalling molecule (Sewelam et al., 2014; Sies and Jones, 2020). Mutants lacking peroxisomal CAT2 *(cat2)* have been extensively studied in Arabidopsis and tobacco plants under control and stress conditions, showing that altering peroxisomal H_2O_2 induces changes in gene expression profiles (Vandenabeele et al., 2003 and 2004; Queval et al., 2012 Chaouch et al., 2010). This profile showed specificity with transcriptional responses that differ from those induced by chloroplast-derived H_2O_2 (Sewelam et al., 2014). Analyses of WT plants grown at specific atmospheric CO_2 levels to boost photorespiration and production of H_2O_2 (Chaouch et al., 2010; Queval et al., 2012) and of WT plants treated with aminotriazole, a catalase inhibitor (Gechev et al., 2005), have also shown that peroxisomal H_2O_2 plays a role in signalling, as a transcriptomic footprint have been linked to peroxisomes (Rosenwasser et al., 2013). However, little is known about how peroxisome-derived H_2O_2 coordinates or relays signalling events. Although peroxisome-dependent gene regulation involves several metabolic categories (reviewed in Sandalio and Romero-Puertas, 2015; Su et al., 2019), those related to protein repair responses under stress conditions are regulated in *cat2* mutants (Queval et al., 2007; Sewelam et al., 2014); suggesting that peroxisomes are involved in acclimation and survival processes under changing environmental conditions. The triple mutant *cat1 cat2 cat3* shows serious redox disturbance and growth defects under physiological conditions, with differentially expressed genes belonging to plant growth regulation, as well as abiotic and biotic stress response categories. Some of these genes belong to transcription factor and receptor-like protein kinase categories (Su et al., 2019). The ROS signals

derived from different cell compartments are proposed to connect in the cytoplasm with MAPK pathway to regulate the expression of nuclear genes (Noctor and Foyer, 2016). Several genes related to MAPK cascade pathways, such as MPK11, MPK13 and serine/threonine kinase oxidative signal inducible 1 (OXI1), are severely altered in the triple *cat* mutant (Su et al., 2019). Thus, peroxisomal H_2O_2 appears to participate in retrograde signalling, although little is known about the underlying molecular mechanisms and crosstalk with ROS from other compartments (Sandalio and Romero-Puertas, 2015; Su et al., 2019).

Redox-dependent regulation of peroxisomal plasticity

Peroxisome biogenesis and proliferation

Their high plasticity enables peroxisomes to adapt their number, morphology, movement and metabolic pathways to changes in their environment (Fig. 3). However, why certain signals and molecules trigger these changes, when these changes occur and how dynamic peroxisomal changes function in relation to tolerance are not well understood. Some evidence shows that peroxisomal proliferation through the division of preexisting peroxisomes is regulated by ROS (López-Huertas et al., 2000; Fig. 3; Box 2). Peroxisome proliferation occurs in response to abiotic stresses associated with ROS production: ozone (Oksanen et al., 2004), clofibrate (Nila et al., 2006; Castillo et al., 2008), salinity (Mitsuya et al., 2010; Fahy et al., 2017), cadmium (Romero-Puertas et al., 1999; Rodríguez-Serrano et al., 2016), drought (Ebeed et al., 2018), ABA (Ebeed et al., 2018) and senescence (Pastori and del Río, 1997). Interestingly, NO has recently been reported to be involved in regulating peroxisome proliferation in response to Cd (Terrón-Camero et al., 2020). Peroxisome proliferation under abiotic stress appears to be regulated by specific PEX11 genes. Thus, salinity upregulated PEX11a and PEX11c in *A. thaliana* (Fahy et al., 2017), while PEX11a and PEX11e were upregulated in response to Cd exposure in Arabidopsis plants (Rodríguez-Serrano et al., 2016; Terrón-Camero et al., 2020), and PEX11b, PEX11c and PEX11d were up-regulated by hypoxia (Li and Hu, 2015). Gene co-expression analysis in Arabidopsis plants under drought conditions shows clustering of photorespiratory genes and peroxisomal abundance, suggesting that H_2O_2 plays a role in peroxisomal abundance regulation (Li and Hu, 2015). This is supported by the absence of

peroxisome proliferation in *gox2* Arabidopsis mutants exposed to Cd (Calero-Muñoz et al., 2019). However, genome analyses of *Physcomitrella*, *Arabidopsis thaliana* and *Triticum aestivum* show up-regulation of β-oxidation in response to drought, dehydration and ABA (Ebeed et al., 2018). Interestingly, PEX11 gene family expression differs between drought-sensitive and resistant wheat genotypes, although the significance or not of these differences for drought tolerance has not been established (Ebeed et al., 2018). These findings suggest that peroxisomal H_2O_2 could be involved in environmental change perception and acclimation through differential PEX11 regulation and peroxisome proliferation. Plant peroxisome proliferation could be a protective response to ROS overflow in cell compartments due to highly efficient peroxisomal antioxidant defenses, as reported during protoplast transition from G0 to G1 (Tiew et al., 2015) and in response to salt stress in Arabidopsis and *Oryza sativa* by reducing both Na^+ accumulation and oxidative stress (Cui et al., 2016b; Fahy et al., 2017). However, in quinoa plants, peroxisome abundance correlates negatively with yields of plants exposed to heat, drought or both (Hinojosa et al., 2019). Therefore, the capacity to maintain H_2O_2 homeostasis and peroxisome quality control/abundance could determine the success of plant adaptation to adverse conditions.

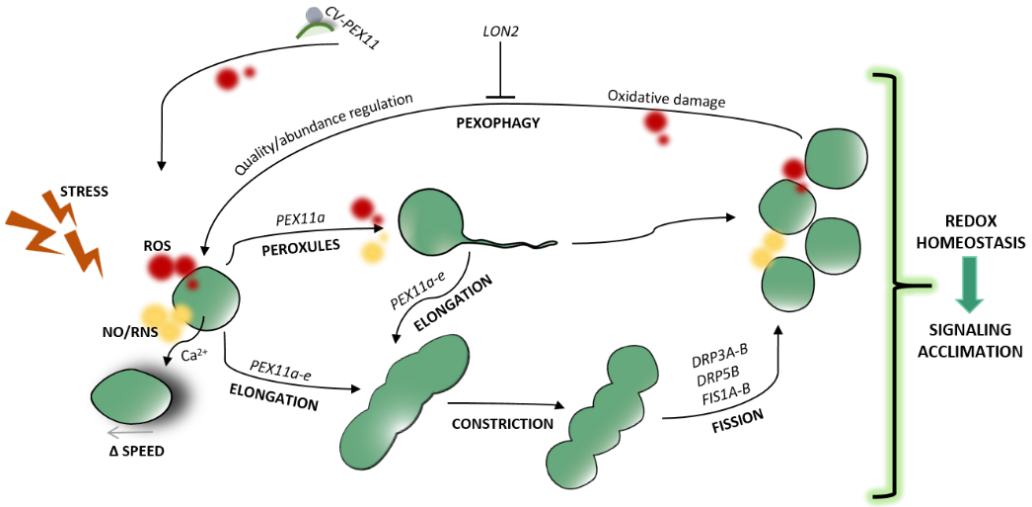

***Figure 3**. Hypothetical scheme showing changes in peroxisomal dynamics and their regulation, as well as their contribution to cell responses to abiotic stresses such as metal toxicity. Cd stress promotes the generation of ROS and NO, which activate peroxins (PEX11a and PEX11e), probably through ROS-/NO-dependent post-translational modifications (PTMs). PEX11a promotes the formation of peroxules, which may control ROS/NO accumulation and ROS-dependent gene expression. Peroxisomal elongation, constriction and proliferation, which are regulated by ROS and*

NO, were later observed. Longer exposure periods increase the speed of peroxisome movement (Δ SPEED), which is also controlled by ROS. The number of peroxisomes, as well as oxidized, damaged peroxisomes, can be regulated by pexophagy or via a process independent of autophagy involving chloroplast vesicle interactions with PEX11 (CV-PEX11), both of which processes are regulated by ROS. All these changes in peroxisomal dynamics may be involved in redox homeostasis and redox-dependent signalling, leading to plant acclimation to the stress. Red color, ROS; yellow color, NO. DRPs: dynamin-related proteins; FIS1A-B: fission protein1A-B; LON2: lon protease homolog 2.

Box 2 PEROXISOME BIOGENESIS AND PROLIFERATION

Plant peroxisome abundance is governed by (1) biogenesis, associated with physiological processes and division (fission) of a preexisting peroxisome, (2) proliferation, which is related to stress responses, and (3) pexophagy, a selective peroxisome degradation mechanism (Kao et al., 2018; Olmedilla and Sandalio, 2019). Proteins involved in peroxisome biogenesis and maintenance are called peroxins (PEXs; Kao et al., 2018). The import of peroxisomal membrane proteins (PMPs) in Arabidopsis involves peroxins PEX19, acting as the chaperone for PMPs, PEX3 acting as the membrane anchor for PEX19, and PEX16, which recruits PEX3 to the ER before the formation of pre-peroxisomes. Arabidopsis PEX16 also recruits PMPs to the ER in a PEX3/PEX19-independent manner (Pan et al., 2020). The import of peroxisomal matrix proteins containing the C-and N-terminal targeting signals PTS1 and PTS2, respectively, take place by the soluble receptors PEX5 (for PTS1) and PEX7 (for PTS2) in the cytosol (Baker et al., 2016; Reumann and Chowdhary, 2018). PEX5 is recycled from the peroxisomal matrix back to the cytosol by the ubiquitin conjugating enzyme PEX4 and its membrane anchor PEX22, three RING-type ubiquitin ligases, PEX2, PEX10 and PEX12, and two AAA ATPases, PEX1 and PEX6 (reviewed in Reumann and Bartel, 2016; Kao et al., 2018).

Peroxisomes proliferate through the division of preexistent peroxisomes, which involves peroxisome elongation regulated by PEX11, organelle constriction and fission, governed by dynamin-related proteins (DRP3A and DRP3B) and fission proteins (FIS1A and FIS 1B; Pan et al., 2020; Su et al., 2019). The PEX11 gene family in Arabidopsis contain five members: PEX11a, PEX11b, PEX11c, PEX11d and PEX11e, (Lingard and Trelease, 2006; Orth et al., 2007). FIS1A and FIS1B are shared by peroxisomes and mitochondria; DRP3A and DRP3B regulate peroxisomal and mitochondrial fission; and DRP5B is involved in peroxisome and chloroplast fission (Kao et al., 2018), indicating a highly coordinated regulation of organelles populations.

ROS/RNS-dependent formation of peroxules

In vivo observation of plant tissues, with fluorescent proteins targeting peroxisomes, reveals the rapid formation of tubular peroxisome extensions called peroxules, induced in response to changes in ROS levels (Fig. 3; Sinclair et al., 2009; Barton et al., 2013; Rodríguez-Serrano et al., 2016). Short periods of Cd exposure (15 min-30 min) induce peroxule formation, which is considerably reduced by H_2O_2 scavengers and in *rboh* mutants, suggesting regulation by external ROS (Rodríguez-Serrano et al., 2016). Confocal images show peroxule contacts with chloroplasts and mitochondria under Cd treatment and high light (Sinclair et al., 2009; Rodríguez-Serrano et al., 2016; Sandalio et al., 2013; Jaipargas et al., 2016). Peroxule formation in response to Cd and As is dependent upon PEX11a, while *pex11a* Arabidopsis mutants show altered ROS-dependent signalling networks (Rodríguez-Serrano et al., 2016). Peroxule production and peroxisome-dependent signalling are compromised in *nia1 nia2* Arabidopsis mutants, which have lower NO levels than wild-type plants in response to Cd treatment, demonstrating the important role of NO in peroxule formation (Terrón-Camero et al., 2020). This could be

due to oxidative changes and *S*-nitrosylation patterns in the antioxidant system (Terrón-Camero et al., 2020), which affect cellular redox balance. PEX11a and peroxule formation therefore play a key role in regulating stress perception and rapid cell responses to environmental cues (Rodríguez-Serrano et al., 2016; Terrón-Camero et al., 2020; Fig. 3). Given rapid peroxule induction and no significant changes in *PEX11a* expression in *nox1* mutants (Terrón-Camero et al., 2020), PEX11a can reasonably be assumed to be regulated by specific ROS and NO-dependent PTMs. Activation of yeast peroxin Pex11p depends on redox changes in its cysteines (Knoblach and Rachubinski, 2010; Schrader et al., 2012).

Although there is no direct evidence, peroxules could participate in the transfer of H_2O_2 and other metabolites to mitochondria and chloroplast (Fig. 4). Stromules, which are dynamic structures similar to peroxules in chloroplasts, transfer H_2O_2 from chloroplasts to nuclei as part of a retrograde signalling process (Caplan et al., 2015; Kumar et al., 2018); however, to our knowledge, no connection between peroxules and nuclei has been established so far. Peroxules could also be involved in protein transport such as the transfer of the sugar dependent 1 (SDP1) lipase from the peroxisomal membrane to the lipid body (Thazar-Poulot et al., 2015; Fig. 4).

Peroxisomal speed is regulated by ROS

Time course analyses of peroxisomes in response to Cd in Arabidopsis seedlings have highlighted a considerable increase in peroxisomal speed after 24 h of treatment which is regulated by ROS produced by RBOHs and Ca^{2+} ions (Fig 3; Rodríguez-Serrano et al., 2009 and 2016). Increased peroxisomal movement could improve antioxidant defenses where Cd and other factors promote ROS accumulation and/or could aid signalling transduction and metabolite exchanges in different parts of the cell (Rodríguez-Serrano et al., 2009). Information on the role of peroxisomal motility under stress conditions is scarce; however, in myosin loss-of-function Arabidopsis mutants and in Arabidopsis treated with the herbicide 2,4-D, inhibition of organelle movement negatively affects plant growth (Rodríguez-Serrano et al., 2014; Ryan and Nebenführ, 2018). Oikawa et al. (2015) found that light-adapted Arabidopsis peroxisomes are much more mobile than dark-adapted peroxisomes (Oikawa et al., 2015) and, by using photorespiratory mutants *shmt1* (defective in serine hydroxymethyltransferase) and *ped2*

(defective in PEX14), they concluded that both, peroxisome mobility and peroxisome-chloroplast interactions observed under light, are regulated by photosynthesis rather than by photoreceptors or photorespiration (Oikawa et al., 2015).

Pexophagy and peroxisomal homeostasis are regulated by oxidative processes.

Excessive numbers of peroxisomes and those containing obsolete or dysfunctional proteins need to be eliminated to control cellular redox homeostasis. Some evidence shows that ROS and oxidative damage to peroxisomes regulate the degradation of oxidized whole peroxisomes by selective autophagy termed pexophagy (Fig. 3; Shibata et al., 2013; Yoshimoto et al., 2014; Olmedilla and Sandalio, 2019). Autophagy-related genes (ATGs) regulate autophagy in all eukaryotic cells including those in plants (Avin-Wittenberg et al., 2018). During photomorphogenesis, several authors have reported pexophagy using Arabidopsis *atg* mutants (Shibata et al. 2013; Farmer et al., 2013; Kim et al., 2013); however, unlike in mammals and yeast, the mechanism in plants is not fully understood. Shibata et al. (2013) have observed high levels of oxidized CAT and clusters of peroxisomes in *atg* mutants. Peroxisomal clusters were also observed in H_2O_2-treated Arabidopsis plants (Yoshimoto et al., 2014) and in *atg5* and *atg7* Arabidopsis mutants exposed to Cd treatment where phagophore and peroxisome colocalization was observed (Calero-Muñoz et al., 2019). Some evidence shows the important role of oxidative processes in pexophagy induction: 1) ubiquitinated CAT is accumulated in Arabidopsis mutants defective in NBR1 *(nbr-1)*, a pexophagy adaptor (Zhou et al., 2013); 2) ATG8/CAT-CAT/NBR1 interactions have been observed in Arabidopsis plants exposed to Cd (Calero-Muñoz et al., 2019); 3) CAT activity is involved in starvation-induced pexophagy (Tyutereva et al., 2018); and 4) clustered peroxisomes in Arabidopsis *atg* mutants mainly accumulate in the aerial parts of plants, where oxidative metabolism is higher than in roots (Yoshimoto et al., 2014; Zhou et al., 2013). Glucose-mediated regulation of root meristem activity requires pexophagy to maintain ROS and auxin cellular homeostasis in Arabidopsis plants (Huang et al., 2019). The chaperone activity of peroxisomal protease LON2 negatively regulates pexophagy (Fig. 3; Farmer et al., 2013; Young and Bartel, 2016). In plants, specific peroxisomal receptors have not been clearly identified, and the role of adaptors, such as NBR1-like proteins, which specifically interact with ubiquitinilated proteins, is under debate (Young et al., 2019; Olmedilla and Sandalio,

2019). The possibility of both NBR1-dependent and independent pexophagy cannot be ruled out. An alternative process independent of autophagy, induced under high CO_2 and increased H_2O_2 conditions, involves chloroplast vesiculation (CV) proteins which interact with PEX11-1 in rice (Fig. 3; Umnajkitikorn et al., 2020).

Peroxisome crosstalk with other organelles

To optimize their multiple functions, peroxisomes collaborate and communicate with other cell organelles by exchanging substrates. Photorespiration is the best example of metabolic cellular interorganelle communication. However, peroxisomes are also cellular redox communication hubs, as well as guardians and modulators of H_2O_2 levels (Fransen and Lismont, 2019) given the following findings: (1) peroxisomes contain enzymes involved in producing and scavenging H_2O_2 and NO; (2) they contain proteins regulated by ROS- and NO-dependent PTMs and therefore act as ROS/NO sensors; (3) they regulate NAD(P)+/NAD(P)H, ASC/DHA and GSH/GSSG pools; and (4) H_2O_2 and NO act as second messengers in a wide range of developmental, physiological and stress processes (Fransen and Lismont, 2019; Sandalio et al., 2020).

There is an intimate relationship between the peroxisomal redox state and changes in the redox state of other organelles. In mammalian systems, H_2O_2 released from peroxisomes into the cytosol diffuses into mitochondria, oxidizing directly or indirectly cysteine residues of mitochondrial proteins (Lismont et al., 2019). Chlamydomonas mutants deficient in peroxisomal NAD^+-dependent MDH2 show that MDH2 plays a key role in the reverse coupling of redox/H_2O_2 signals from peroxisomes to chloroplasts (Kong et al., 2018). Peroxisomal $NAD(P)^+$/NAD(P)H pools in Arabidopsis regulate photosynthesis performance to meet the demand for reducing equivalents under fluctuating light (Li et al., 2019). Peroxisomal basal H_2O_2 levels greatly affect antioxidative defense regulation in cytosol and chloroplasts, as observed in peroxisomal *apx4* knockdown rice plants (Sousa et al., 2018). The inhibition of CAT activity in *apx4* Arabidopsis mutants significantly affected networks involved in photosynthetic performance under adverse conditions promoting oxidative stress and favoring antioxidant enzyme accumulation in cytosol and chloroplasts (Sousa et al., 2018).

Despite the central role of H_2O_2 in peroxisome metabolism and cell functionality, no peroxiporin-like proteins have been identified in the peroxisomal membrane. Although porins are present in plant peroxisomes (Reumann et al., 1997; Corpas et al., 2000; Fig 4), their role in H_2O_2 permeability remains unclear. In yeast, Pex11A, Pex11B and Pex11G have been reported to facilitate the permeation of molecules up to 400 Da (Mindthoff et al., 2016) and could be candidates to diffuse H_2O_2 through the peroxisomal membrane. However, recently, Lismont et al. (2019) provided evidence that neither the porin PXMP2 nor PEX11B is essential for H_2O_2 permeation across the peroxisomal membrane. Throughout membrane contact sites (MCSs), ROS accumulation could directly facilitate inter-organelle signal transmission using as-yet unknown ROS transporters (Fig. 4; Yoboue et al., 2018). Electron microscopy images of leaf cells show physical contact between peroxisome and chloroplasts and, interestingly, H_2O_2 accumulation inside peroxisomes in the contact site with chloroplasts and vacuoles, suggesting a relationship between ROS accumulation and organelle communication (Romero-Puertas et al., 2004). Using femtosecond laser and optic tweezer techniques, tethering between the chloroplast and peroxisomes has been demonstrated (Oikawa et al., 2015; Gao et al., 2016). The area of peroxisomes interacting with chloroplasts increases under light conditions, whereas, in the dark, peroxisomes lost their connection with chloroplasts (Oikawa et al., 2015). The PEX10 Zn RING finger interacts with the chloroplast envelope's outer membrane, which is necessary for full photorespiration functionality and could be a candidate for MCSs in plant peroxisomes (Schumann et al., 2007; Fig. 4). Although the role of PTMs in regulating protein-protein interactions at inter-organelle contact sites remains unexplored, it is reasonable to assume that tethering is regulated by specific PTMs.

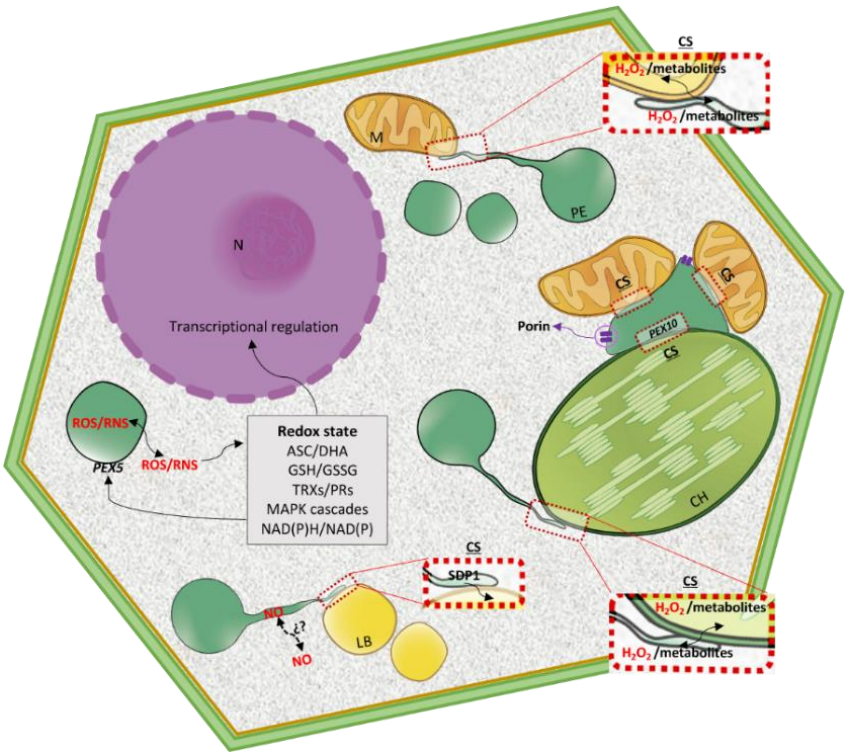

***Figure 4**. Redox-dependent interorganellar crosstalk. Peroxisomes (P) collaborate and communicate with other cellular organelles, mitochondria (M) and chloroplasts (CH) by exchanging molecules such as H_2O_2 and redox metabolites, as well as Ca^{2+} and proteins. These exchanges could take place through porins or membrane contact sites (MCSs). Peroxules formation contributes to ROS/RNS, metabolite and protein exchanges such as the transfer of triacylglycerol lipase sugar-dependent 1 (SDP1) to lipid bodies (LB). ROS/RNS-dependent posttranslational modifications regulate peroxules formation, MCSs, interorganellar crosstalk and signalling transduction. Peroxisomal ROS/RNS interfere with cytosolic redox state and signalling processes and vice versa; the cytosolic redox state regulates peroxisomal protein import by affecting the redox state of peroxin 5 (PEX5). The peroxisomal redox state can also regulate redox changes in the nucleus (N), chloroplasts and mitochondria.*

The translocation of peroxisomal proteins to other cell compartments is part of inter-organelle communication and signalling, although the mechanism(s) by which this occurs is still unknown. Thus, CAT interacts with non-peroxisomal proteins including cytosolic CDPK8 (Zou et al., 2015), plasma membrane-associated OsCPK10 (Bundó and Coca, 2017), cytosolic salt overly sensitive 2 (SOS2; Verslues et al., 2007), lesion simulating disease1 (LSD1; Li et al., 2013), receptor-like cytoplasmic kinase STRK1 (Zhou et al., 2018), chloroplast/cytosolic nucleoside diphosphate kinase 2 (NDPK2), no catalase activity 1 (NCA1; Hackenberg et al., 2013; Li et al., 2015) and nucleoredoxin 1 (NRX1; Kneeshaw et al., 2017) in addition to GSNOR (mentioned above), which are all integral stress-signalling

proteins. It is unclear whether CAT is translocated from peroxisomes by the endoplasmic reticulum (ER)-associated degradation (ERAD)-like system involved in the export of PEX5 from the peroxisome membrane and export of matrix peroxisomal proteins to be degraded (Lingard et al., 2009) or is retained in the cytosol under oxidative conditions as in the case of mammalian cells (Walton et al., 2017). Walton et al. (2017) have reported that Cys-11 of human PEX5 acts as a redox switch that modulates the import of peroxisomal matrix proteins such as CAT. Under oxidative stress conditions, CAT is retained in the cytosol where it can protect against H_2O_2-mediated redox changes and reinforce cellular defenses to prevent oxidative damage out of peroxisomes (Walton et al., 2017). Oxidative and nitrosative stress could enable swift control of CAT localization in compartments, thus helping to regulate redox signalling pathways.

In the case of dual-targeted OPPP enzymes, targeting decisions appear to depend on the cytosolic redox state. This has been suggested in relation to Arabidopsis G6PD1/G6PD4 (Meyer et al., 2011), PGL3 (Hölscher et al., 2014) and PGD2 upon interaction with non-peroxisomal isoforms PGD1 or PGD3, which retain heteromeric enzymes in the cytosol (Lutterbey and von Schaewen, 2016). NADPH-oxidase and peroxisomal AtPAO3 cross-talk to balance intracellular $O_2^{\cdot -}$ /H_2O_2, which in turn, affect the cyt-c/AOX pathways in mitochondria and regulates pollen tube elongation (Wu et al., 2010). As catalase *(cat2)*-deficient Arabidopsis mutants show upregulation of ASC-GSH components in the cytosol (Mhamdi et al., 2010), peroxisomes can interfere with cytosolic redox state. Cytosolic redox changes, in turn, impact the dual targeting of 6-phosphogluconolactonase 3 (PGL3) of chloroplasts and peroxisomes in Arabidopsis leaves, a process requiring thioredoxin m2 (Trxm2) in the cytosol (Hölscher et al., 2014).

FUTURE PERSPECTIVES

One of the most difficult challenges in this field of research is to determine the nature of proteins involved in peroxisomal NO production. We need to amplify our limited knowledge of the mechanisms underlying NO regulation of peroxisome dynamics, metabolism and signalling, together with NO and ROS crosstalk with hormones, such as JA. Additional analyses of the interplay and hierarchy of ROS-, NO-dependent and other peroxisomal PTMs such as phosphorylation and persulfidation are required. Peroxisome-dependent regulatory components also need to be characterized by analysing gene

network structures and by identifying downstream responses induced by peroxisomal ROS and NO. The components of contact sites and the factors involved in peroxule production, as well as the regulatory role of ROS and NO in both these areas, also need to be determined. Analysis of tethering techniques, specific fluorescence proteins and ROS mutants, combined with meta-analyses of organelle proteome data sets, should provide a better understanding of peroxisomal dynamics and inter-organelle interactions. Finally, identification of pexophagy receptors and adaptors and their regulation by ROS, NO and S_2H should enable us to integrate biochemical processes and organelle dynamics into our understanding of cellular regulatory systems.

OUTSTANDING QUESTIONS

- Do carbonylated and nitrated peroxisomal proteins act as signalling messengers?
- Does CAT3 transnitrosylate other proteins in addition to GSNOR? Are other transnitrosylases present in peroxisomes?
- Is S-nitrosylation involved in retrotranslocation of peroxisomal proteins to the cytosol?
- Which pexophagy receptors and adaptors are involved and what role do ROS and NO play in identifying peroxisomes for degradation?
- How do cells balance peroxule production, peroxisome proliferation and changes in peroxisomal speed in response to changes in their environment?
- Which ROS/redox sensor(s) is (are) present in the peroxisomal membrane?

Acknowledgement: The authors wish to thank Michael O'Shea for proofreading the manuscript and to apologize to colleagues whose work has not been cited due to space limitations.

Literature Cited

Agurla S, Gayatri G, Raghavendra AS (2018) Polyamines increase nitric oxide and reactive oxygen species in guard cells of *Arabidopsis thaliana* during stomatal closure. Protoplasma **255**: 153–162

Alamillo JM, García-Olmedo F (2001) Effects of urate, a natural inhibitor of peroxynitrite-mediated toxicity, in the response of *Arabidopsis thaliana* to the bacterial pathogen Pseudomonas syringae. Plant J **25**: 529–540

Antonenkov VD, Grunau S, Ohlmeier S, Hiltunen JK (2010) Peroxisomes are oxidative organelles. Antioxid Redox Signal **13**: 525–537

Avin-Wittenberg T, Baluška F, Bozhkov PV, Elander PH, Fernie AR, Galili G, Hassan A, Hofius D, Isono E, Le Bars R, et al. (2018) Autophagy-related approaches for improving nutrient use efficiency and crop yield protection. J Exp Bot **69**: 1335–1353

Baker A, Hogg TL, Warriner SL (2016) Peroxisome protein import: A complex journey. Biochem Soc Trans **44**: 783–789

Barroso JB, Corpas FJ, Carreras A, Sandalio LM, Valderrama R, Palma M, Lupia A, Rı LA (1999) Localization of nitric-oxide synthase in plant peroxisomes. Int J Biol Chem **274**: 36729–36733

Barton K, Mathur N, Mathur J (2013) Simultaneous live-imaging of peroxisomes and the ER in plant cells suggests contiguity but no luminal continuity between the two organelles. Front Physiol **4**: 1–12

Bratt A, Rosenwasser S, Meyer A, Fluhr R (2016) Organelle redox autonomy during environmental stress.

Plant Cell Environ **39**: 1909–1919

Bundó M, Coca M (2017) Calcium-dependent protein kinase OsCPK10 mediates both drought tolerance and blast disease resistance in rice plants. J Exp Bot **68**: 2963–2975

Burkhart SE, Lingard MJ, BarteL B (2013) Genetic dissection of peroxisome-associated matrix protein degradation in *Arabidopsis thaliana*. Genetics **193**: 125–141

Byrne RS, Ha R, Mendel RR, Hille R (2009) Oxidative half-reaction of *Arabidopsis thaliana* sulfite oxidase generation of superoxide by a peroxisomal enzyme. Int J Bio Chem **284**: 35479–35484

Calero-Muñoz N, Expósito-Rodríguez M, Collado-Arenal AM, Rodríguez-Serrano M, Laureano-Marín AM, Santamaría ME, Gotor C, Díaz I, Mullineaux PM, Romero-Puertas MC, et al. (2019) Cadmium induces reactive oxygen species-dependent pexophagy in Arabidopsis leaves. Plant Cell Environ **42**: 2696–2714

Caplan JL, Kumar AS, Park E, Padmanabhan MS, Hoban K, Modla S, Czymmek K, Dinesh-Kumar SP (2015) Chloroplast stromules function during innate immunity. Dev Cell **34**: 45–57

Castillo MC, Sandalio LM, del Río LA, León J (2008) Peroxisome proliferation, wound-activated responses and expression of peroxisome-associated genes are cross-regulated but uncoupled in *Arabidopsis thaliana*. Plant, Cell Environ **31**: 492–505

Chaki M, Álvarez de Morales P, Ruiz C, Begara-Morales JC, Barroso JB, Corpas FJ, Palma JM (2015) Ripening of pepper (*Capsicum annuum*) fruit is characterized by an enhancement of protein tyrosine nitration. Ann Bot **116**: 637–47

Chaouch S, Queval G, Vanderauwera S, Mhamdi A, Vandorpe M, Langlois-Meurinne M, Van Breusegem F, Saindrenan P, Noctor G (2010) Peroxisomal hydrogen peroxide is coupled to biotic defense responses by ISOCHORISMATE SYNTHASE1 in a daylength-related manner. Plant Physiol **153**: 1692–1705

Chen L, Wu R, Feng J, Feng T, Wang C, Jiliang Hu J, Zhan N, Li Y, Ma X, Ren B, Zhang J, Song C-P, et al. (2020) Transnitrosylation mediated by the non-canonical catalase ROG1 regulates nitric oxide signalling in plants. Dev Cell **53**: 444–457

Corpas FJ, Barroso JB (2014) Peroxynitrite ($ONOO_2^-$) is endogenously produced in Arabidopsis peroxisomes and is overproduced under cadmium stress. Ann Bot **113**: 87–96

Corpas FJ, Barroso JB, Sandalio LM, Palma M, Lupiáñez JA, del Río LA (1999) Characterization and activity regulation during natural senescence. Plant Physiol **121**: 921–928

Corpas FJ, Sandalio LM, Brown MJ, del Río LA, Trelease RN (2000) Identification of porin-like polypeptide(s) in the boundary membrane of oilseed glyoxysomes. Plant Cell Physiol **41**: 1218–1228

Costa A, Drago I, Behera S, Zottini M, Pizzo P, Schroeder JI, Pozzan T, Lo Schiavo F (2010) H_2O_2 in plant peroxisomes: an in vivo analysis uncovers a Ca^{2+}-dependent scavenging system. Plant J **62**: 760–72

Cousins AB, Pracharoenwattana I, Zhou W, Smith SM, Badger MR (2008) Peroxisomal malate dehydrogenase is not essential for photorespiration in Arabidopsis but its absence causes an increase in the stoichiometry of photorespiratory. Plant Physiol **148**: 786–795

Cui L, Lu Y, Li Y, Yang C, Peng X, Lines TR (2016a) Overexpression of glycolate oxidase confers improved photosynthesis under high light and high temperature in rice construction of the GLO -overexpression. Front Plant Sci **7**: 1–12

Cui P, Liu H, Islam F, Li L, Farooq MA, Ruan S, Zhou W (2016b) OsPEX11, a peroxisomal biogenesis factor 11, contributes to salt stress tolerance in *Oryza sativa*. Front Plant Sci **7**: 1–11

Del Río LA, Corpas FJ, Sandalio LM, Palma JM, Barroso JB (2003) Plant peroxisomes, reactive oxygen metabolism and nitric oxide. IUBMB Life **55**: 71–81

Duan G, Walther D (2015) The roles of post-translational modifications in the context of protein interaction networks. PLoS Comput Biol **11**: 1–23

Eastmond PJ (2007) MONODEHYROASCORBATE REDUCTASE4 is required for seed storage oil hydrolysis and postgerminative growth in Arabidopsis. Plant Cell **19**: 1376–1387

Ebeed HT, Stevenson SR, Cuming AC, Baker A (2018) Conserved and differential transcriptional responses of peroxisome associated pathways to drought, dehydration and ABA. J Exp Bot **69**: 4971–4985

Fahy D, Sanad MNME, Duscha K, Lyons M, Liu F, Bozhkov P, Kunz HH, Hu J, Neuhaus HE, Steel PG, et al. (2017) Impact of salt stress, cell death, and autophagy on peroxisomes: Quantitative and morphological analyses using small fluorescent probe N-BODIPY. Sci Rep **7**: 1–17

Farmer LM, Rinaldi MA, Young PG, Danan CH, Burkhart SE, Bartel B (2013) Disrupting autophagy restores peroxisome function to an Arabidopsis lon2 mutant and reveals a role for the LON2 protease in

peroxisomal matrix protein degradation. Plant Cell **25**: 4085–4100

Foyer CH, Baker A, Wright M, Sparkes IA, Mhamdi A, Schippers JHM, Breusegem F Van (2020) On the move: redox-dependent protein relocation in plants. J Exp Bot **71**: 620–631

Foyer CH, Bloom AJ, Queval G, Noctor G (2009) Photorespiratory metabolism: genes, mutants, energetics and redox signalling. Ann rev Plant Bio **60**: 455–484

Foyer CH, Noctor G (2003) Redox sensing and signalling associated with reactive oxygen in chloroplasts, peroxisomes and mitochondria. Physiol Plant **119**: 355–364

Foyer CH, Noctor G (2016) Stress-triggered redox signalling: what 's in prospect? Front Plant Sci **39**: 951–964

Foyer CH, Ruban A V, Noctor G (2017) Viewing oxidative stress through the lens of oxidative signalling rather than damage. Biochem J **474**: 877–883

Fransen M, Lismont C (2019) Redox signalling from and to peroxisomes: Progress, challenges, and prospects. Antioxid Redox Signal **30**: 95–112

Gabaldón T (2018) Evolution of the peroxisomal proteome. Subcell Biochem **89**: 221–233

Gao H, Metz J, Teanby NA, Ward AD, Botchway SW, Coles B, Pollard MR, Sparkes I (2016) In vivo quantification of peroxisome tethering to chloroplasts in tobacco epidermal cells using optical tweezers. Plant Physiol **170**: 263–72

Gebicka L, Didik J (2009) Catalytic scavenging of peroxynitrite by catalase. J Inorg Biochem **103**: 1375–1379

Gechev TS, Minkov IN, Hille J (2005) Hydrogen peroxide-induced cell death in Arabidopsis: transcriptional and mutant analysis reveals a role of an oxoglutarate-dependent dioxygenase gene in the cell death process. IUBMB Life **57**: 181–188

Goyer A, Johnson TL, Olsen LJ, Collakova E, Shachar-Hill Y, Rhodes D, Hanson AD (2004) Characterization and metabolic function of a peroxisomal sarcosine and pipecolate oxidase from Arabidopsis. J Biol Chem **279**: 16947–16953

Gupta DK, Pena LB, Hernández A, Inouhe M, Sandalio LM (2017) NADPH oxidases differentially regulate ROS metabolism and nutrient uptake under cadmium toxicity. Plant Cell Environ **40**: 509–526

Hackenberg T, Juul T, Auzina A, Gwizdz S, Małolepszy A, Van Der Kelen K, Dam S, Bressendorff S, Lorentzen A, Roepstorff P, et al. (2013) Catalase and NO CATALASE ACTIVITY1 promote autophagy-dependent cell death in Arabidopsis. Plant Cell **25**: 4616–4626

Hashiguchi A, Komatsu S (2016) Impact of post-translational modifications of crop proteins under abiotic stress. Proteomes **4**: 42

Hinojosa L, Sanad MNME, Jarvis DE, Steel P, Murphy K, Smertenko A (2019) Impact of heat and drought stress on peroxisome proliferation in quinoa. Plant J **99**: 1144–1158

Hodges M, Dellero Y, Keech O, Betti M, Raghavendra AS, Sage R, Zhu X, Allen DK, Weber APM (2016) Perspectives for a better understanding of the metabolic integration of photorespiration within a complex plant primary metabolism network. J Exp Bot **67**: 3015–3026

Hölscher C, Meyer T, Von Schaewen A (2014) Dual-targeting of Arabidopsis 6-phosphogluconolactonase 3 (PGL3) to chloroplasts and peroxisomes involves interaction with Trx m2 in the cytosol. Mol Plant **7**: 252–255

Holzmeister C, Gaupels F, Geerlof A, Sarioglu H, Sattler M, Durner J, Lindermayr C (2015) Differential inhibition of Arabidopsis superoxide dismutases by peroxynitrite-mediated tyrosine nitration. J Exp Bot **66**: 989–999

Hooper DC, Scott GS, Zborek A, Mikheeva T, Kean RB, Koprowski H, Spitsin S V (2000) Uric acid, a peroxynitrite scavenger, inhibits CNS inflammation, blood-CNS barrier permeability changes, and tissue damage in a mouse model of multiple sclerosis. FASEB J **14**: 691–698

Hou Q, Bartels D (2015) Comparative study of the aldehyde dehydrogenase (ALDH) gene superfamily in the glycophyte *Arabidopsis thaliana* and *Eutrema halophytes*. Ann Bot **22**: 465–479

Huang J, Willems P, Breusegem F Van, Messens J (2018) Pathways crossing mammalian and plant sulfenomic landscapes. Free Radic Biol Med **122**: 193–201

Huang L, Yu LJ, Zhang X, Fan B, Wang FZ, Dai YS, Qi H, Zhou Y, Xie LJ, Xiao S (2019) Autophagy regulates glucose-mediated root meristem activity by modulating ROS production in Arabidopsis. Autophagy **15**: 407–422

Inaba J, Kim BM, Shimura H, Masuta C (2011) Virus-induced necrosis is a consequence of direct protein-protein interaction between a viral RNA-silencing suppressor and a host catalase. Plant Physiol **156**:

2026–2036

Jaipargas EA, Mathur N, Daher FB, Wasteneys GO, Mathur J (2016) High light intensity leads to increased peroxule-mitochondria interactions in plants. Front Cell Dev Biol **4**: 1–11

Jones DP, Go YM (2010) Redox compartmentalization and cellular stress. Diabetes, Obes Metab **12**: 116–125

Kao Y, González KL, Bartel B (2018) Peroxisome function, biogenesis, and dynamics in plants. Plant Physiol **176**: 162–177

Kaur N, Reumann S, Hu J (2009) Peroxisome biogenesis and function. Arabidopsis Book **7**: e0123

Kim J, Lee H, Lee HN, Kim SH, Shin KD, Chung T (2013) Autophagy-related proteins are required for degradation of peroxisomes in Arabidopsis hypocotyls during seedling growth. Plant Cell **25**: 4956–4966

Kneeshaw S, Keyani R, Delorme-Hinoux V, Imrie L, Loake GJ, Le Bihan T, Reichheld JP, Spoel SH (2017) Nucleoredoxin guards against oxidative stress by protecting antioxidant enzymes. Proc Natl Acad Sci **114**: 8414–8419

Knoblach B, Rachubinski RA (2010) Phosphorylation-dependent activation of peroxisome proliferator protein PEX11 controls peroxisome abundance. J Biol Chem **285**: 6670–6680

Kong F, Burlacot A, Liang Y, Légeret B, Alseekh S, Brotman Y, Fernie AR, Krieger-Liszkay A, Beisson F, Peltier G, et al. (2018) Interorganelle communication: Peroxisomal MALATE DEHYDROGENASE2 connects lipid catabolism to photosynthesis through redox coupling in Chlamydomonas. Plant Cell **30**: 1824–1847

König J, Muthuramalingam M, Dietz KJ (2012) Mechanisms and dynamics in the thiol/disulfide redox regulatory network: Transmitters, sensors and targets. Curr Opin Plant Biol **15**: 261–268

Koo AJK, Chung HS, Kobayashi Y, Howe GA (2006) Identification of a peroxisomal acyl-activating enzyme involved in the biosynthesis of jasmonic acid in Arabidopsis. Int J Biol Chem **281**: 33511–33520

Kumar AS, Park E, Nedo A, Alqarni A, Ren L, Hoban K, Modla S, McDonald JH, Kambhamettu C, Dinesh-Kumar SP, Caplan JL (2018) Stromule extension along microtubules coordinated with actin-mediated anchoring guides perinuclear chloroplast movement during innate immunity. Elife **7**: 1–33

Lansing H, Doering L (2020) Analysis of potential redundancy among Arabidopsis 6-phosphogluconolactonase isoforms in peroxisomes. J Exp Bot **71**: 823–836

León J, Broseta ÁC (2020) Present knowledge and controversies, deficiencies, and misconceptions on nitric oxide synthesis, sensing, and signalling in plants. Plant Cell Environ **43**: 1–15

Li J, Hu J (2015) Using co-expression analysis and stress-based screens to uncover Arabidopsis peroxisomal proteins involved in drought response. PLoS One **10**: 1–13

Li J, Liu J, Wang G, Cha JY, Li G, Chen S, Li Z, Guo J, Zhang C, Yang Y, et al. (2015) A chaperone function of NO CATALASE ACTIVITY1 Is required to maintain catalase activity and for multiple stress responses in Arabidopsis. Plant Cell **27**: 908–925

Li J, Tietz S, Cruz JA, Strand DD, Xu Y, Chen J, Kramer DM, Hu J (2019) Photometric screens identified Arabidopsis peroxisome proteins that impact photosynthesis under dynamic light conditions. Plant J **97**: 460–474

Li Y, Chen L, Mu J, Zuo J (2013) LESION SIMULATING DISEASE1 interacts with catalases to regulate hypersensitive cell death in Arabidopsis. Plant Physiol **163**: 1059–1070

Lingard MJ, Monroe-Augustus M, Bartel B (2009) Peroxisome-associated matrix protein degradation in Arabidopsis. Proc Natl Acad **106**: 4561–4566

Lingard MJ, Trelease RN (2006). Five Arabidopsis peroxin 11 homologs individually promote peroxisome elongation, duplication or aggregation. J Cell Sci **119**: 1961–1972

Lingner T, Kataya AR, Antonicelli GE, Benichou A, Nilssen K, Chen X, Siemsen T, Morgenstern B, Meinicke P, Reumann S (2011) Identification of novel plant peroxisomal targeting signals by a combination of machine learning methods and in vivo subcellular targeting analyses. Plant Cell **23**: 1556–1572

Lismont C, Koster J, Provost S, Baes M, Van Veldhoven PP, Waterham HR, Fransen M (2019) Deciphering the potential involvement of PXMP2 and PEX11B in hydrogen peroxide permeation across the peroxisomal membrane reveals a role for PEX11B in protein sorting. Biochim Biophys Acta Biomembr **1861**: 182991

López-Huertas E, Charlton WL, Johnson B, Graham IA, Baker A (2000) Stress induces peroxisome biogenesis genes. EMBO J **19**: 6770–6777

Lozano-Juste J, Colom-moreno R, Valencia D, Ed CPI, Vera C De (2011) In vivo protein tyrosine nitration in *Arabidopsis thaliana*. J Exp Bot **62**: 3501–3517

Lutterbey MC, von Schaewen A (2016) Analysis of homo- and hetero-dimerization among the three 6-phosphogluconate dehydrogenase isoforms of Arabidopsis. Plant Signal Behav **11**: 1–4

Martínez-Ruiz A, Cadenas S, Lamas S (2011) Nitric oxide signalling: Classical, less classical, and nonclassical mechanisms. Free Radic Biol Med **51**: 17–29

Meyer T, Hölscher C, Schwöppe C, Von Schaewen A (2011) Alternative targeting of Arabidopsis plastidic glucose-6-phosphate dehydrogenase G6PD1 involves cysteine-dependent interaction with G6PD4 in the cytosol. Plant J **66**: 745–758

Mhamdi A, Noctor G, Baker A (2012) Plant catalases: Peroxisomal redox guardians. Arch Biochem Biophys **525**: 181–194

Mhamdi A, Queval G, Chaouch S, Vanderauwera S, Van Breusegem F, Noctor G (2010) Catalase function in plants: a focus on Arabidopsis mutants as stress-mimic models. J Exp Bot **61**: 4197–220

Mindthoff S, Grunau S, Steinfort LL, Girzalsky W, Hiltunen JK, Erdmann R, Antonenkov VD (2016) Peroxisomal Pex11 is a pore-forming protein homologous to TRPM channels. Biochim Biophys Acta **1863**: 271–283

Mitsuya S, El-Shami M, Sparkes I, Charlton W L, Lousa CDM, Johnson B, et al. (2010) Salt stress causes peroxisome proliferation, but inducing peroxisome proliferation does not improve NaCl tolerance in *Arabidopsis thaliana*. PLoS ONE **5**: e9408

Mittler R (2017) ROS are good. Trends Plant Sci **22**: 11–19

Møller IM, Sweetlove LJ (2010) ROS signalling – specificity is required. Trends Plant Sci **15**: 370–374

Mor A, Koh E, Weiner L, Rosenwasser S, Sibony-benyamini H, Fluhr R (2014) Singlet oxygen signatures are detected independent of light or chloroplasts in response to multiple stresses. Plant Physiol **165**: 249–261

Murota K, Shimura H, Takeshita M, Masuta C (2017) Interaction between cucumber mosaic virus 2b protein and plant catalase induces a specific necrosis in association with proteasome activity. Plant Cell Rep **36**: 37–47

Nila AG, Sandalio LM, López MG, Gómez M, del Río LA, Gómez-Lim MA (2006) Expression of a peroxisome proliferator-activated receptor gene (xPPARα) from *Xenopus laevis* in tobacco (*Nicotiana tabacum*) plants. Planta **224**: 569–581

Noctor G, Foyer CH (2016). Intracellular redox compartmentation and ROS-related communication in regulation and signalling. Plant Physiol. **171**: 1581–1592

Noctor G, Reichheld J, Foyer CH (2018) ROS-related redox regulation and signalling in plants. Semin Cell Dev Biol **80**: 3–12

Oikawa K, Matsunaga S, Mano S, Kondo M, Yamada K, Hayashi M, Kagawa T, Kadota A, Sakamoto W, Higashi S, Watanabe M, Mitsui T, Shigemasa A, Iino T, Hosokawa Y, Nishimura M (2015) Physical interaction between peroxisomes and chloroplasts elucidated by in situ laser analysis. Nat Plants **1**: 15035

Oksanen E, Häikiö E, Sober J, Karnosky DF (2004) Ozone-induced H_2O_2 accumulation in field-grown aspen and birch is linked to foliar ultrastructure and peroxisomal activity. New Phytol **161**: 791–799

Olmedilla A, Sandalio LM (2019) Selective autophagy of peroxisomes in plants: from housekeeping to development and stress responses. Front Plant Sci **10**: 1–7

Ortega-Galisteo AP, Rodríguez-Serrano M, Pazmiño DM, Gupta DK, Sandalio LM, Romero-Puertas MC (2012) S-Nitrosylated proteins in pea (*Pisum sativum L.*) leaf peroxisomes: changes under abiotic stress. J Exp Bot **63**: 2089–2103

Orth T, Reumann S, Zhang X, Fan J, Wenzel D, Quan S, Hu J (2007) The PEROXIN11 protein family controls peroxisome proliferation in Arabidopsis. Plant Cell **19**: 333–350

Pan R, Hu J (2018) Proteome of Plant Peroxisomes. Subcell Biochem. **89**: 3–45

Pan R, Liu J, Wang S, Hu J (2020) Peroxisomes: versatile organelles with diverse roles in plants. New Phytol **225**: 1410–1427

Pastori GM, del Río LA (1997) Natural senescence of pea leaves. Plant Physiol **113**: 411–418

Queval G, Issakidis-Bourguet E, Hoeberichts FA, Vandorpe M, Gakière B, Vanacker H, Miginiac-Maslow M, Van Breusegem F, Noctor G (2007) Conditional oxidative stress responses in the Arabidopsis photorespiratory mutant *cat2* demonstrate that redox state is a key modulator of daylength-dependent gene expression, and define photoperiod as a crucial factor in the regulation of H_2O_2-induced cell death. Plant J **52**: 640–657

Queval G, Neukermans J, Vanderauwera S, Van Breusegem F, Noctor G (2012) Day length is a key regulator

of transcriptomic responses to both CO_2 and H_2O_2 in Arabidopsis. Plant Cell Environ **35**: 374–387

Reumann S, Babujee L, Ma C, Wienkoop S, Siemsen T, Antonicelli GE, Rasche N, Lüder F, Weckwerth W, Jahn O (2007) Proteome analysis of Arabidopsis leaf peroxisomes reveals novel targeting peptides, metabolic pathways, and defense mechanisms. Plant Cell **19**: 3170–3193

Reumann S, Bartel B (2016) Plant peroxisomes: recent discoveries in functional complexity, organelle homeostasis, and morphological dynamics. Curr Opin Plant Biol **34**: 17–26

Reumann S, Bettermann M, Benz R, Heldt HW (1997) Evidence for the presence of a porin in the membrane of glyoxysomes of castor bean. Plant Physiol **115**: 891–899

Reumann S, Chowdhary G (2018) Prediction of peroxisomal matrix proteins in plants. Subcell Biochem **89**: 125–138

Reumann S, Ma C, Lemke S, Babujee L (2004) AraPerox. A database of putative Arabidopsis proteins. Plan Physiol **136**: 2587–2608

Reumann S, Weber APM (2006) Plant peroxisomes respire in the light: Some gaps of the photorespiratory C_2 cycle have become filled – Others remain. Biochim Biophys Acta **1763**: 1496–1510

Rinaldi MA, Patel AB, Park J, Lee K, Strader LC, Bartel B (2016) The roles of β-oxidation and cofactor homeostasis in peroxisome distribution and function in *Arabidopsis thaliana*. Genetics **204**: 1089–1115

Rodríguez-Serrano M, Pazmiño DM, Sparkes I, Rochetti A, Hawes C, Romero-Puertas MC, Sandalio LM (2014) 2,4-Dichlorophenoxyacetic acid promotes *S*-nitrosylation and oxidation of actin affecting cytoskeleton and peroxisomal dynamics. J Exp Bot **65**: 4783–4793

Rodríguez-Serrano M, Romero-Puertas MC, Sanz-Fernández M, Hu J, Sandalio LM (2016) Peroxisomes extend peroxules in a fast response to stress via a reactive oxygen species-mediated induction of the peroxin PEX11a. Plant Physiol **171**: 1665–1674

Rodríguez-Serrano M, Romero-Puertas MC, Sparkes I, Hawes C, del Río LA, Sandalio LM (2009) Peroxisome dynamics in Arabidopsis plants under oxidative stress induced by cadmium. Free Radic Biol Med **48**: 979

Rojas CM, Senthil-kumar M, Wang K, Ryu C, Kaundal A, Mysore KS, Division PB, Roberts S, Foundation N (2012) Glycolate oxidase modulates reactive oxygen species – mediated signal transduction during nonhost resistance in *Nicotiana benthamiana* and Arabidopsis. Plan Cell **24**: 336–352

Romero-Puertas MC, McCarthy I, Sandalio LM, Palma JM, Corpas FJ, Gómez M, del Río LA (1999) Cadmium toxicity and oxidative metabolism of pea leaf peroxisomes. Free Radic Res **31**: 25–31

Romero-Puertas MC, Rodríguez-Serrano M, Corpas FJ, Gómez M, del Río LA, Sandalio LM (2004) Cadmium-induced subcellular accumulation of $O_2^{\cdot-}$ and H_2O_2 in pea leaves. Plant Cell Environ **27**: 1122–1134

Romero-Puertas MC, Sandalio LM (2016) Nitric oxide level is self-regulating and also regulates its ROS partners. Front Plant Sci **7**: 1–5

Rosenwasser S, Fluhr R, Joshi JR, Leviatan N, Sela N, Hetzroni A, Friedman H (2013) ROSMETER: a bioinformatic tool for the identification of transcriptomic imprints related to reactive oxygen species type and origin provides new insights into stress responses. Plant Physiol **163**: 1071–1083

Rosenwasser S, Rot I, Sollner E, Meyer AJ, Smith Y, Leviatan N, Fluhr R, Friedman H (2011) Organelles contribute differentially to reactive oxygen species-related events during extended darkness. Plant Cell Environ **156**: 185–201

Ryan JM, Nebenführ A (2018) Update on myosin motors: Molecular mechanisms and physiological functions. Plant Physiol **176**: 119–127

Sánchez-Vicente I, Fernández-Espinosa MG, Lorenzo O (2019) Nitric oxide molecular targets: reprogramming plant development upon stress. J Exp Bot **70**: 4441–4460

Sandalio LM, Gotor C, Romero LC, Romero-Puertas MC (2019) Multilevel regulation of peroxisomal proteome by post-translational modifications. Int J Mol Sci **20**: 4881

Sandalio LM, Peláez-Vico MA, Romero-Puertas MC (2020) Peroxisomal metabolism and dynamics at the crossroads between stimulus perception and fast cell responses to the environment. Front Cell Dev Biol **8**: 2014–2018

Sandalio LM, Rodríguez-Serrano M, Romero-Puertas MC, del Río LA (2013) Role of peroxisomes as a source of reactive oxygen species (ROS) signalling molecules. Subcell Biochem **69**: 231–25

Sandalio LM, Romero-Puertas MC (2015) Peroxisomes sense and respond to environmental cues by regulating ROS and RNS signalling networks. Ann Bot **116**: 475–485

Schlicht M, Ludwig-m J, Burbach C, Volkmann D, Baluska F (2013) Indole-3-butyric acid induces lateral root formation via peroxisome-derived indole-3-acetic acid and nitric oxide. New Phytol **200**: 473–482

Schmitz, J, Rossoni AW, Maurino VG (2018) Dissecting the physiological function of plant glyoxalase I and glyoxalase I-like proteins. Front Plant Sci **9**:1618

Schrader M, Bonekamp NA, Islinger M (2012) Fission and proliferation of peroxisomes. Biochim Biophys Acta - Mol Basis Dis **1822**: 1343–1357

Schumann U, Prestele J, O'Geen H, Brueggeman R, Wanner G, Gietl C (2007) Requirement of the C3HC4 zinc RING finger of the Arabidopsis PEX10 for photorespiration and leaf peroxisome contact with chloroplasts. Proc Natl Acad Sci USA **104**: 1069–1074

Sewelam N, Jaspert N, Kelen K Van Der, Tognetti VB, Schmitz J (2014) Spatial H_2O_2 signalling specificity : H_2O_2 from chloroplasts and peroxisomes modulates the plant transcriptome differentially. Mol Plant **7**: 1191–1210

Shai N, Schuldiner M, Zalckvar E (2016) No peroxisome is an island - Peroxisome contact sites. Biochim Biophys Acta - Mol Cell Res **1863**: 1061–1069

Shibata M, Oikawa K, Yoshimoto K, Kondo M, Mano S, Yamada K, Hayashi M, Sakamoto W, Ohsumi Y, Nishimura M (2013) Highly oxidized peroxisomes are selectively degraded via autophagy in Arabidopsis. Plant Cell **25**: 4967–4983

Sies H, Jones DP (2020) Reactive oxygen species (ROS) as pleiotropic physiological signalling agents. Nat Rev Mol Cell Biol. **21**: 363–383

Sinclair AM, Trobacher CP, Mathur N, Greenwood JS, Mathur J (2009) Peroxule extension over ER-defined paths constitutes a rapid subcellular response to hydroxyl stress. Plant J **59**: 231–242

Smirnoff N, Arnaud D (2019) Hydrogen peroxide metabolism and functions in plants. New Phytol **221**: 1197–1214

Sousa RHV, Carvalho FEL, Lima-Melo Y, Alencar VTCB, Daloso DM, Margis-Pinheiro M, Komatsu S, Silveira JAG (2018) Impairment of peroxisomal APX and CAT activities increases protection of photosynthesis under oxidative stress. J Exp Bot **35**: 627–639

Su T, Li W, Wang P, Ma C (2019) Dynamics of peroxisome homeostasis and its role in stress response and signalling in plants. Front Plant Sci **10**: 705

Suzuki N, Koussevitzky S, Mittler RON, Miller GAD (2012) ROS and redox signalling in the response of plants to abiotic stress. Plan Cell Environ **35**: 259–270

Talbi S, Romero-Puertas MC, Hernández A, Terrón L, Ferchichi A, Sandalio LM (2015) Drought tolerance in a Saharian plant Oudneya africana: Role of antioxidant defences. Environ Exp Bot **111**: 114–126

Terrón-Camero LC, Rodríguez-Serrano M, Sandalio LM, Romero-Puertas MC (2020) Nitric oxide is essential for cadmium-induced peroxule formation and peroxisome proliferation. Plant Cell Environ **43**: 2492–2507

Thazar-Poulot N, Miquel M, Fobis-Loisy I, Gaude T (2015) Peroxisome extensions deliver the Arabidopsis SDP1 lipase to oil bodies. Proc Natl Acad Sci USA **112**: 4158–4163

Tiew TW, Sheahan MB, Rose RJ (2015) Peroxisomes contribute to reactive oxygen species homeostasis and cell division induction in Arabidopsis protoplasts. Front Plant Sci **6**: 1–16

Tyutereva EV, Dobryakova KS, Schiermeyer A, Shishova MF, Pawlowski K, Demidchik V, Reumann S, Voitsekhovskaja OV (2018) The levels of peroxisomal catalase protein and activity modulate the onset of cell death in tobacco BY-2 cells via reactive oxygen species levels and autophagy. Funct Plant Biol **45**: 247–258

Umnajkitikorn K, Sade N, Rubio Wilhelmi M del M, Gilbert ME, Blumwald E (2020) Silencing of OsCV (chloroplast vesiculation) maintained photorespiration and N assimilation in rice plants grown under elevated CO_2. Plant Cell Environ **43**: 920–933

Vandenabeele S, Kelen K Van Der, Dat J, Gadjev I, Boonefaes T, Morsa S, Breusegem F Van, Rottiers P, Slooten L, Montagu M Van, et al. (2003) A comprehensive analysis of hydrogen peroxide-induced gene expression in tobacco. Proc Natl Acad Sci **100**: 16113–16118

Vandenabeele S, Vanderauwera S, Vuylsteke M, Rombauts S, Langebartels C, Seidlitz HK, Zabeau M, Van Montagu M, Inzé D, Van Breusegem F (2004) Catalase deficiency drastically affects gene expression induced by high light in *Arabidopsis thaliana*. Plant J **39**: 45–58

Verslues PE, Batelli G, Grillo S, Agius F, Kim Y-S, Zhu J, Agarwal M, Katiyar-Agarwal S, Zhu J-K (2007) Interaction of SOS2 with nucleoside diphosphate kinase 2 and catalases reveals a point of connection between salt stress and H_2O_2 signalling in *Arabidopsis thaliana*. Mol Cell Biol **27**: 7771–7780

Walker BJ, Vanloocke A, Bernacchi CJ, Ort DR (2016) The costs of photorespiration to food production now and in the future. Annu Rev Plant Biol **67**: 107–129

Waller JC, Dhanoa PK, Schumann U, Mullen RT, Snedden WA (2010) Subcellular and tissue localization of NAD kinases from Arabidopsis: Compartmentalization of de novo NADP biosynthesis. Planta **231**: 305–317

Walton PA, Brees C, Lismont C, Apanasets O, Fransen M (2017) The peroxisomal import receptor PEX5 functions as a stress sensor, retaining catalase in the cytosol in times of oxidative stress. Biochim Biophys Acta - Mol Cell Res **1864**: 1833–1843

Wang W, Paschaladis K, Jian-Can F, Jie S, Ji-Hong L (2019) Polyamine catabolism in plants: a universal process with diverse functions. Front Plant Sci **10**: 561

Wang BL, Tang XY, Cheng LY, Zhang AZ, Zhang WH, Zhang FS, Liu JQ, Cao Y, Allan DL, Vance CP, et al. (2010) Nitric oxide is involved in phosphorus deficiency-induced cluster-root development and citrate exudation in white lupin. New Phytol **187**: 1112–1123

Werner AK, Witte C (2011) The biochemistry of nitrogen mobilization: purine ring catabolism. Trends Plant Sci **16**: 381–387

Wimalasekera R, Tebartz F, Scherer GFE (2011) Polyamines, polyamine oxidases and nitric oxide in development, abiotic and biotic stresses. Plant Sci **181**: 593–603

Wu J, Shang Z, Wu J, Jiang X, Moschou PN, Sun W, Roubelakis-Angelakis KA, Zhang S (2010) Spermidine oxidase-derived H_2O_2 regulates pollen plasma membrane hyperpolarization-activated Ca^{2+} -permeable channels and pollen tube growth. Plant J **63**: 1042–53

Yang M, Li Z, Zhang K, Zhang X, Zhang Y, Wang X, Han C, Yu J, Xu K, Li D (2018) Barley stripe mosaic virus cb interacts with glycolate oxidase and inhibits peroxisomal ROS production to facilitate virus infection. Molecular Plant **11**: 338–341

Yanik T, Donaldson RP (2005) A protective association between catalase and isocitrate lyase in peroxisomes. Arch Biochem Biophys **435**: 243–252

Yoboue ED, Sitia R, Simmen T (2018) Redox crosstalk at endoplasmic reticulum (ER) membrane contact sites (MCS) uses toxic waste to deliver messages. Cell Death Dis **9**: 331

Yoshimoto K, Shibata M, Kondo M, Oikawa K, Sato M, Toyooka K, Shirasu K, Nishimura M, Ohsumi Y (2014) Organ-specific quality control of plant peroxisomes is mediated by autophagy. J Cell Sci **127**: 1161–1168

Young PG, Bartel B (2016) Pexophagy and peroxisomal protein turnover in plants. Biochim Biophys Acta **1863**: 999–1005

Young D, Pedre, Ezeriņa D, De Smet B, Lewandowska A, Tossounian MA, Bodra N, Huang J, Astolfi Rosado L, Van Breusegem F, Messens J (2019) Protein promiscuity in H_2O_2 signalling. Antioxid Redox Signal **30**: 1285–1324

Yuan HM, Liu WC, Lu YT (2017) CATALASE2 coordinates SA-mediated repression of both auxin accumulation and JA biosynthesis in plant defenses. Cell Host Microbe **21**: 143–155

Zhan N, Wang C, Chen L, Yang H, Feng J, Gong X, Ren B, Wu R, Mu J, Li Y, Liu Z, Zhou Y, Peng J, Wang K, Huang X, Xiao S, Zuo J (2018) *S*-nitrosylation targets gsno reductase for selective autophagy during hypoxia responses in plants. Mol Cell **71**: 142–154

Zhang T, Ma M, Chen T, Zhang L, Fan L, Zhang W, Wei B, Li S, Xuan W, Noctor G, et al. (2020) Glutathione-dependent denitrosation of GSNOR1 promotes oxidative signalling downstream of H_2O_2. Plant Cell Environ **43**: 1175–1191

Zhang Z, Xu Y, Xie Z, Li X, He Z, Peng X (2016) Association – dissociation of glycolate oxidase with catalase in rice: a potential switch to modulate intracellular H_2O_2 levels. Mol Plant **9**: 737–748

Zhou J, Wang J, Cheng Y, Chi YJ, Fan B, Yu JQ, Chen Z (2013) NBR1-mediated selective autophagy targets insoluble ubiquitinated protein aggregates in plant stress responses. PLoS Genet **9**: e1003196

Zou J, Li X, Ratnasekera D, Wang C, Liu W, Song L, Zhang W, Wu W (2015) Arabidopsis CALCIUM-DEPENDENT PROTEIN KINASE8 and CATALASE3 function in abscisic acid-mediated signalling and H_2O_2 homeostasis in stomatal guard cells under drought stress. Plant Cell **27**: 1445–1460

Zhou YB, Liu C, Tang DY, Yan L, Wang D, Yang YZ, Gui JS, Zhao XY, Li LG, Tang XD, et al. (2018) The receptor-like cytoplasmic kinase STRK1 phosphorylates and activates CatC, thereby regulating H_2O_2 homeostasis and improving salt tolerance in rice. Plant Cell **30**: 1100–1118

ANNEX II

Adapted from: Sandalio et al., (2020) Frontiers in Cell and Developmental Biology 8, 1–5.

PEROXISOMAL METABOLISM AND DYNAMICS AT THE CROSSROADS BETWEEN STIMULUS PERCEPTION AND FAST CELL RESPONSES TO THE ENVIRONMENT

Sandalio L.M., Peláez-Vico M.A., Romero-Puertas M.C.*

Department of Biochemistry and Molecular and Cellular Biology of Plants, Estación Experimental del Zaidín-CSIC, Profesor Albareda 1, 18008 Granada, Spain

Corresponding author: LM Sandalio.
Mail: luisamaria.sandalio@eez.csic.es
Phone +34958181600 ext 316

Keywords: cross-talk, peroxisomes, posttranslational modifications, peroxules, pexophagy, reactive oxygen species, stress

Peroxisomes are highly dynamic, multifunctional plastic organelles whose metabolism, number and phenotype can change depending on developmental, environmental and metabolic requirements. However, the molecular mechanisms governing their plasticity and the role of these changes in development, and stress responses, some of the most challenging areas in the field of biology, are not fully understood. Since their discovery in 1959 by de Duve, information regarding new metabolic pathways associated with these organelles, has increased at an extraordinary rate (Pan et al., 2019). Plant peroxisomes are closely related to other organelles housing metabolic pathways, such as fatty acid β-oxidation, which provide energy during the initial stage of seedling growth by channeling fatty acids from oil bodies to peroxisomal β-oxidation, with Acyl-CoA oxidase being one of the first enzymes involved in this process. Acetyl-CoA from fatty acid β-oxidation is then converted into C4 carboxilic acids by the glyoxylate cycle in seedlings. Fatty acid β-oxidation is also involved in important processes including synthesis of indoleacetic acid (IAA), jasmonic acid, ubiquinone, as well as secondary metabolites such as benzoic acid (BA) and phenylpropanoids (Pan et al., 2019). On the other hand, light triggers a shift in the peroxisomal metabolism and

activates the photorespiration cycle, in which sugars are oxidized to CO_2 in a complex pathway where physical contact between chloroplasts, peroxisomes and mitochondria is required. Other metabolic pathways in peroxisomes include ureide metabolism, polyamine and amino acid catabolism. However, peroxisomes are also an important source of ROS and NO which are associated with these metabolic pathways, in addition to the electron transport chain located in the peroxisomal membrane (Sandalio and Romero-Puertas, 2015). This explains why disturbances in any of these metabolic processes can trigger transitory changes in ROS and NO production which can regulate peroxisomal metabolism and also be perceived by the cell as an alarm, causing a specific rapid response (Sandalio and Romero-Puertas, 2015; Fig. 1 A). This response can be regulated at the post-translational level by NO- and ROS-dependent post-translational protein modifications, which is a very fast, efficient inexpensive strategy to regulate proteins and, therefore, metabolic pathways (Sandalio et al., 2019, Fig. 1A). The transcriptional regulation of cell responses mediated by ROS-dependent peroxisomal sources has also been investigated; hundreds of genes, such as those involved in anthocyanin biosynthesis, pathogenesis, cell death and ubiquitin-dependent protein degradation, as well as those encoding kinases, including MAPKs, and heat shock proteins, have been identified as regulated by H_2O_2 produced during photorespiration (Queval et al., 2007; Chaouch et al. 2010; Sewelam et al., 2014; Su et al., 2018). However, no information is available on peroxisomal NO-dependent regulation of gene expression or on the protein/gene producing NO inside the organelle.

Post-translational modifications regulate the peroxisomal proteome and its metabolism

PTMs can be regarded as an interface between perception of changes in the environment and the rapid cellular responses to these changes. They can regulate protein activity, localization, degradation and inter-protein interactions, giving rise to rapid finely-tuned regulation of protein functionality and, therefore, rapid changes in metabolic pathways and signalling processes (Hashiguchi et al., 2016). This regulation is especially important in plants subjected to changeable environments. Synergistic and antagonistic interplay between PTMs has led to a higher degree of complexity in the regulation of the perception of environmental changes and of specific plant cell responses. Recently, a

meta-analysis of PTMs of the peroxisomal proteome (Sandalio et al., 2019) showed a high degree of possible PTM-dependent regulation of most metabolic pathways in peroxisomes, including phosphorylation, carbonylation, sulfenylation, persulfidation, *S*-nitrosylation, nitration, acetylation and ubiquitination (Sandalio et al., 2019). This multilevel PTM regulation could explain the plasticity of peroxisomes and their capacity to rapidly respond to changes in their environment and to regulate metabolic pathways in organelles sharing metabolites with peroxisomes, such as mitochondria, lipid bodies and chloroplasts (Fig. 1A). Peroxisomal PTMs can even act as on/off switches to channel metabolites to different metabolic pathways (Ortega-Galisteo et al., 2012; Romero-Puertas and Sandalio, 2016). Peroxisomal protein phosphorylation, and its role in regulating different peroxisomal events have been elegantly reviewed by Kataya et al. (2019). The potential peroxisomal targets for ROS- and NO-dependent PTMs have also been studied (Sandalio et al., 2019). However, although different peroxisomal proteins have been identified as potential targets of protein acetylation, which has been receiving much attention in recent years, its precise mechanisms and role played in peroxisomes are little understood (Drazic, et al., 2016; Sandalio et al., 2019). Acetyl-CoA, an essential component in fatty acid β-oxidation commonly found in peroxisomes, could be involved in epigenetic modifications (Fig. 1A). Thus, the Arabidopsis mutant deficient in acyl CoA oxidase 4 (*Atacx4)* shows a decrease in nuclear histone acetylation and an increase in DNA methylation, with similar results being obtained for Arabidopsis mutants deficient in the multifunctional protein MFP2 (*Atmfp2*) and ketoacyl-coenzyme A thiolase (*Atkat2*) (Wang et al., 2019). In mammalian cells, peroxisomal acetyl-CoA also plays a role in mitochondrial protein acetylation (Eisenberg-Bord and Schuldiner, 2017).

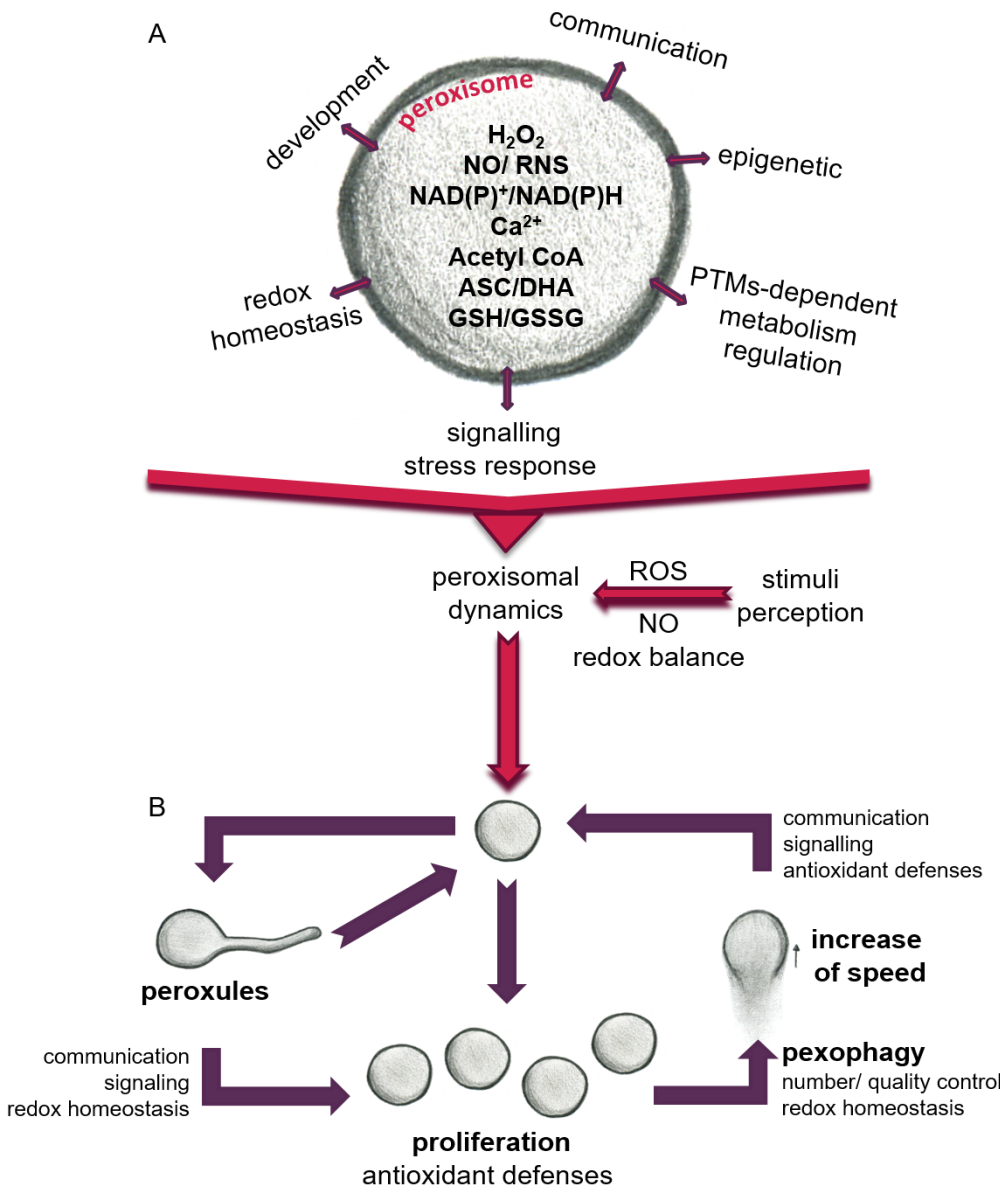

Figure 1. *Scheme showing the role of peroxisomes in the regulation of metabolism, development and plant cell responses to environmental changes. (A)The regulatory role is mediated by ROS, NO, Ca^{+2}, redox balance and other compounds produced in peroxisomes. (B) Changes in peroxisomal dynamics and function in response to environmental stimuli mediated by changes in cellular ROS accumulation.*

Peroxisomal dynamics govern fast responses to stress

Plant peroxisomes can change their size, morphology, number and even speed of movement (Fig. 1B), although why, how and when these changes occur, as well as their advantages and disadvantages in terms of tolerance and acclimation are not well understood. Peroxisomes move along actin filaments (Mathur et al., 2002) which requires myosin motor proteins (Jedd and Chua 2002; Perico and Sparkes 2018). PEROXISOME AND MITOCHONDRIAL DIVISION FACTOR1 (PMD1) acts as an actin-binding protein connecting the peroxisome to the cytoskeleton and is involved in peroxisomal division and the cellular distribution of peroxisomes under stress conditions. Although this connection appears to be regulated by the MPK17 kinase, experimental evidence is yet lacking that PMD1 is a target of MPK17 (Frick and Strader, 2018). In mammalian cells, peroxisomal movement is microtubule-dependent and is mediated by kinesin and dynein motors (Castro et al., 2018). The mitochondrial Rho GTPase 1 (MIRO1) has also been identified as an adaptor for peroxisome motor protein association which regulates the proliferation of peroxisomes and their motility (Castro et al., 2018). In Arabidopsis plants the motility of peroxisomes has also been correlated with the motility of ER (Barton 2013).

Plant peroxisome abundance is governed by 1) biogenesis, associated with physiological processes and division (fission) of a preexisting peroxisome, 2) proliferation, which is related to stress responses and 3) pexophagy, a selective degradation mechanism of peroxisomes by autophagy (Olmedilla and Sandalio, 2019). Proteins involved in peroxisome biogenesis and maintenance are called peroxins (PEXs) (Kao et al., 2018). Peroxisome proliferation involves peroxisome elongation, constriction and fission regulated by PEX11(a-e), GTPases called dynamin-related proteins (DRPs), and fission proteins (e.g., FIS1) (Rodríguez-Serrano et al., 2016; Pan et al., 2019). FIS1A and FIS1B are shared by peroxisomes and mitochondria, and DRP3 regulates peroxisomal and mitochondrial fission, while DRP5B is involved in the fission of peroxisomes and chloroplasts (Kao et al., 2018), indicating a highly coordinated regulation of organelle abundance.

Peroxisome proliferation has been observed in response to several abiotic stresses: high light (Desai and Hu, 2008), ozone (Oksanen et al., 2013), clofibrate (Nila et

al., 2006; Castillo et al, 2008), salinity (Mitsuya et al., 2010), cadmium (Romero-Puertas et al., 1999; Rodríguez-Serrano et al. 2016) and drought (Ebeed et al., 2018); others factors such as the herbicide 2,4-dichlorophenoxyacetic acid (2,4-D) do not alter the number of peroxisomes (McCarthy et al., 2001), while jasmonic acid treatment reduces the number and increased their size (Castillo et al., 2008). Under these stress conditions, plant peroxisome proliferation can be considered a protective response probably to cope with ROS overflow in cell compartments thanks to major enzymatic and non-enzymatic antioxidant defenses in these organelles (Fig. 1B). However, tobacco plants overexpressing the xenopus peroxisome proliferator-activated receptor α (*αPPAR*), regulating fatty acid β-oxidation and peroxisome proliferation, show constitutively larger peroxisome populations (Nila et al., 2006; Mitsuya et al., 2010), although this does not protect against salinity (Mitsuya et al., 2010) or clofibrate (Nila et al., 2006).

The role of changes in peroxisome dynamics under stress conditions can be elucidated by time course analysis of these changes. Sinclair et al (2009) showed that, after a few minutes of treatment with H_2O_2, peroxisomes produce extensions or protrusions called peroxules, which progress over time with peroxisome elongation and further proliferation. Rodríguez-Serrano et al (2016) demonstrated that peroxules were induced after 15 min of Cd treatment (Fig. 1B) due to an increase in ROS production by NADPH oxidases, and peroxules formation was regulated by PEX11a. When producing peroxules, peroxisomes are immobile, suggesting that they are tethered to another organelle, with PEX11a representing a good candidate for mediating inter-organellar docking (Rodríguez-Serrano et al., 2016). The role of ROS in the formation of these structures could be related to changes in membrane elasticity (Sinclair et al, 2009), although PEX11a could also be regulated by redox-dependent PTMs that activate tethering and changes in the peroxisomal membrane. However, proteome analysis showed that PEX11a may be a target of phosphorylation rather than redox PTMs (Sandalio et al., 2019), while the possibility that PEX11a acts as a ROS sensor cannot be ruled out. Peroxules have been associated with peroxisome proliferation (Sinclair et al., 2009; Fig. 1B), although Rodríguez-Serrano et al (2016) suggested that they do not always cause proliferation and may be involved in regulating ROS accumulation and ROS-dependent signalling transduction (Rodríguez-Serrano et al, 2016; Fig. 1B). Therefore,

peroxules could be regarded as part of a strategy to increase the peroxisomal surface favoring metabolite exchange (such as H_2O_2, NO, Ca^{2+}, acetyl CoA and lipids) with other organelles which would explain the physical connection observed with the ER, mitochondria and chloroplasts (Sinclair et al., 2009; Sandalio et al 2013; Rodríguez-Serrano et al, 2016; Mathur et al., 2018). Peroxules are also involved in protein transport such as the transfer of the sugar-dependent 1 (SDP1) lipase from the peroxisomal membrane to the lipid body (Thazar-Poulot et al., 2015).

The components of the tethering complex between peroxisomes and other organelles have not been identified in plants. However, the peroxisomal Zn RING finger of PEX10 in Arabidopsis interacts with the outer membrane of the chloroplast envelope which is necessary for full photorespiration functionality (Schumann et al., 2007). The role of PTMs in the regulation of protein-protein interactions at inter-organellar contact site remains a fascinating and unexplored area of study. It is reasonable to assume that tethering is regulated by specific PTMs. For example, PEX10 is a candidate target for phosphorylation (Sandalio et al., 2019). Although peroxules have not been observed in mammalian cells under control conditions, a similar structure has been reported in PEX5-deficient fibroblasts expressing mitochondrial MIRO1 (Castro et al., 2018).

Following the time course of cell responses to Cd after peroxule formation, peroxisomes elongate, constrict and divide, reaching proliferation after 3 hours of treatment with Cd (Rodríguez-Serrano et al, 2016). Longer treatment periods (24 h) considerably increase the peroxisomal speed of movement which is regulated by ROS produced by NADPH oxidases and Ca^{2+} ions (Rodríguez-Serrano et al., 2009; Fig. 1B). This could improve antioxidant defenses in places where Cd induces ROS accumulation or favors signal transduction and metabolite exchange in different parts of the cell (Rodríguez-Serrano et al., 2009). Although information on the role of peroxisomal motility is scarce, peroxisomal movement has been reported to play an important role in myosin loss-of-function in Arabidopsis mutants where the inhibition of organelle movement negatively affected plant growth (Ryan and Nebenführ, 2018).

Peroxisomal homeostasis is essential for cell viability, and excess, damaged and obsolete peroxisomes need to be degraded by selective autophagy (pexophagy).

Pexophagy could be a solution for regulating basal levels of organelles and after stress-induced proliferation by mainly degrading oxidized peroxisomes (Yoshimoto et al., 2014; Calero et al., 2019; Fig. 1B). Interestingly, the Arabidopsis mutants *Atatg2,* At*atg5 and* At*atg7,* which are deficient in autophagy, accumulate peroxisomes rather than other organelles such as mitochondria, thus confirming the importance of peroxisomal homeostasis (Yoshimoto et al., 2014; Calero et al., 2019; Fig. 1B). Pexophagy also regulates root meristem development by regulating ROS and IAA homeostasis (Huang et al., 2019) and controls guard cell ROS homeostasis, facilitating stomatal opening (Yamauchi et al., 2019).

In summary, peroxisomes perceive changes in their environment, are involved in signalling and crosstalk between other organelles, ROS homeostasis regulation and influence cellular decision-making, involving nuclei, mitochondria and chloroplasts, through small molecules, such as H_2O_2, NO and acetyl-CoA. In adition, the redox couples GSH/GSSG and ASC/DHA could also regulate signalling processes (Foyer an Noctor; 2011). Sequential changes in the morphology, number and velocity of these organelles contribute to these processes in a complex ROS- and probably NO-regulated manner.

Acknowledgement: This study was co-funded by MCIU, AEI, FEDER grant PGC2018-098372-B-I00. The authors acknowledge support of the publication fee by the CSIC Open Access Publication Support Initiative through URICI. MAP-V was supported by Research Personnel Training (FPI) fellowship from the Spanish MCIU (BEJ-2016-076518). The authors also wish to thank Michael O'Shea for proofreading the manuscript.

Conflict of interest: The authors declare no conflict of interest.

References

Barton, K., Mathur, N., and Mathur, J. (2013). Simultaneous live-imaging of peroxisomes and the ER in plant cells suggests contiguity but no luminal continuity between the two organelles. *Front. Physiol.* 4, 1–12. doi: 10.3389/fphys.2013.00196

Calero-Muñoz, N., Expósito-Rodríguez, M., Collado-Arenal, A. M., Rodríguez-Serrano, M., Laureano-Marín, A. M., et al. (2019). Cadmium induces reactive oxygen species-dependent pexophagy in Arabidopsis leaves. *Plant Cell Environ.* 42, 2696–2714. doi: 10.1111/pce.13597

Castillo, M. C., Sandalio, L. M., Del Río, L. A., and León, J. (2008). Peroxisome proliferation, wound-activated responses and expression of peroxisome associated genes are cross-regulated but uncoupled in *Arabidopsis thaliana*. *Plant Cell Environ.* 31, 492–505. doi: 10.1111/j.1365-3040.2008.01780.x

Castro, I. G., Richards, D. M., Metz, J., Costello, J. L., Passmore, J. B., et al. (2018). A role for mitochondrial Rho GTPase 1 (MIRO1) in motility and membrane dynamics of peroxisomes. *Traffic* 19, 229–242. doi: 10.1111/tra.12549

Chaouch, S., Queval, G., Vanderauwera, S., Mhamdi, A., Vandorpe, M., Langlois- Meurinne, M., et al. (2010). Peroxisomal hydrogen peroxide is coupled to biotic defense responses by ISOCHORISMATE SYNTHASE1 in a daylength-related manner. *Plant Physiol.* 153, 1692–1705. doi: 10.1104/pp.110.153957

Desai, M., and Hu, J. (2008). Light induces peroxisome proliferation in Arabidopsis seedlings through the photoreceptor phytochrome A, the transcription factor HY5 homolog, and the peroxisomal protein PEROXIN11b. *Plant Physiol.* 146, 1117–1127. doi: 10.1104/pp.107.113555

Drazic, A., Myklebust, L. M., Ree, R., and Arnesen, T. (2016). The world of protein acetylation. *Biochim. Biophys. Acta-Proteins Proteom.* 1864, 1372–1401.doi: 10.1016/j.bbapap.2016.06.007

Ebeed, H. T., Stevenson, S. R., Cuming, A. C., and Baker, A. (2018). Conserved and differential transcriptional responses of peroxisome associated pathways to drought, dehydration and ABA. *J. Exp. Bot.* 69, 4971–4985. doi: 10.1093/jxb/ery266

Eisenberg-Bord, M., and Schuldiner, M. (2017). Mitochatting – If only we could be a fly on the cell wall. *Biochim. Biophys. Acta-Mol. Cell Res.* 1864, 1469–1480. doi: 10.1016/j.bbamcr.2017.04.012

Foyer, C. H., and Noctor, G. (2011). Ascorbate and glutathione: the heart of the redox hub. *Plant Physiol.* 155, 2–18 doi: 10.1104/pp.110.167569

Frick, E. M., and Strader, L. C. (2018). KinaseMPK17 and the peroxisome division factor PMD1 influence salt-induced peroxisome proliferation. *Plant Physiol.* 176, 340–351. doi: 10.1104/pp.17.01019

Hashiguchi, A., and Komatsu, S. (2016). Impact of post-translational modifications of crop proteins under abiotic stress. *Proteomes* 4, 1–14. doi: 10.3390/proteomes4040042

Huang, L., Yu, L. J., Zhang, X., Fan, B., Wang, F. Z., Dai, Y. S., et al. (2019). Autophagy regulates glucose-mediated root meristem activity by modulating ROS production in Arabidopsis. *Autophagy* 15, 407–422. doi: 10.1080/15548627.2018.1520547

Jedd, G., and Chua, N. H. (2002). Visualization of peroxisomes in living plant cells reveals acto-myosin-dependent cytoplasmic streaming and peroxisome budding. *Plant Cell Physiol.* 43, 384–392. doi: 10.1093/pcp/pcf045

Kao, Y. T., Gonzalez, K. L., and Bartel, B. (2018). Peroxisome function, biogenesis, and dynamics in plants. *Plant Physiol.* 176, 162–177. doi: 10.1104/pp.17.01050

Kataya, A. R. A., Muenchen, D. G., and Moorhead, G. B. (2019). A framework to investigate peroxisomal protein phosphorylation in Arabidopsis. *Trends Plant Sci.* 24, 366–381. doi: 10.1016/j.tplants.2018.12.002

Mathur, J., Mathur, N., and Hulskamp, M. (2002). Simultaneous visualization of peroxisomes and cytoskeletal elements reveals actin and not microtubule based peroxisome motility in plants. *Plant Physiol.* 128, 1031–1045. doi: 10.1104/pp.011018.1

Mathur, J., Shaikh, A., and Mathur, N. (2018). Peroxisome mitochondria inter-relations in plants. *Subcell. Biochem.* 89, 417–433. doi: 10.1007/978-981-13-2233-4_18

McCarthy, I., Romero-Puertas, M. C., Palma, J. M., Sandalio, L. M., et al. (2001). Cadmium induces senescence symptoms in leaf peroxisomes of pea plants. *Plant Cell Environ.* 24, 1065–1073. doi: 10.1046/j.1365-3040.2001.00750.x

Mitsuya, S., El-Shami, M., Sparkes, I., Charlton, W. L., Lousa, C. D. M., Johnson, B., et al. (2010). Salt stress causes peroxisome proliferation, but inducing peroxisome proliferation does not improve NaCl tolerance in Arabidopsis thaliana. *PLoS ONE* 5:e9408. doi: 10.1371/journal.pone.0009408

Nila, A. G., Sandalio, L. M., López, M. G., Gómez, M., Del Río, L. A., and Gómez-Lim, M. (2006). Expression of a peroxisome proliferator activated receptor gene (xPPARa) from *Xenopus laevis* in tobacco (*Nicotiana tabacum*) plants. *Planta* 224, 569–581. doi: 10.1007/s00425-006-0246-8

Oksanen, E., Haikio, E., Sober, J., and Karnosky, D. F. (2003). Ozone induced H_2O_2 accumulation in field-grown aspen and birch is linked to foliar ultrastructure and peroxisomal activity. *New Phytol.* 161, 791–799. doi: 10.1111/j.1469-8137.2003.00981.x

Olmedilla, A., and Sandalio, L. M. (2019). Selective autophagy of peroxisomes in plants: from housekeeping to development and stress responses. *Front. Plant Sci.* 10, 1–7. doi: 10.3389/fpls.2019.01021

Ortega-Galisteo, A. P., Rodríguez-Serrano, M., Pazmiño, D. M., Gupta, D. K., Sandalio, L. M., and Romero-Puertas, M. C. (2012). *S*-Nitrosylated proteins in pea (*Pisum sativum* L.) leaf peroxisomes: changes under abiotic stress. *J. Exp. Bot.* 63, 2089–2103. doi: 10.1093/jxb/err414

Pan, R., Liu, J., Wang, S., and Hu, J. (2019). Peroxisomes: versatile organelles with diverse roles in plants. *New Phytol.* 225, 1410–1427. doi: 10.1111/nph.16134

Perico, C., and Sparkes, I. (2018). Plant organelle dynamics: cytoskeletal control and membrane contact sites. *New Phytol.* 220, 381–394. doi: 10.1111/nph.15365

Queval, G., Issakidis-Bourguet, E., Hoeberichts, F. A., Vandorpe, M., Gakière, B., Vanacker, H., et al. (2007). Conditional oxidative stress responses in the Arabidopsis photorespiratory mutant *cat2* demonstrate that redox state is a key modulator of daylength-dependent gene expression, and define photoperiod as a crucial factor in the regulation of H_2O_2-induced cell death. *Plant J.* 52, 640–657. doi: 10.1111/j.1365-313X.2007.03263.x

Rodríguez-Serrano, M., Romero-Puertas, M. C., Sanz-Fernández, M., Hu, J., and Sandalio, L. M. (2016). Peroxisomes extend peroxules in a fast response to stress via a reactive oxygen species-mediated induction of the peroxin PEX11a. *Plant Physiol.* 171, 1665–1674. doi: 10.1104/pp.16.00648

Rodríguez-Serrano, M., Romero-Puertas, M. C., Sparkes, I., Hawes, C., Del Río, L. A., and Sandalio, L. M. (2009). Peroxisome dynamics in Arabidopsis plants under oxidative stress induced by cadmium. *Free Radic. Biol. Med.* 47, 1632–1639. doi: 10.1016/j.freeradbiomed.2009.09.012

Romero-Puertas, M. C., McCarthy, I., Sandalio, L. M., Palma, J. M., Corpas, F. J., Gómez, M., et al. (1999). Cadmium toxicity and oxidative metabolism in pea leaf peroxisomes. *Free Radic. Res.* 31(Suppl), S25–S31. doi: 10.1080/10715769900301281

Romero-Puertas, M. C., and Sandalio, L. M. (2016). Nitric oxide level is self-regulating and also regulates its ROS partners. *Front. Plant Sci.* 7:316. doi: 10.3389/fpls.2016.00316

Ryan, J. M., and Nebenführ, A. (2018). Update on myosin motors: molecular mechanisms and physiological functions. *Plant Physiol.* 176, 119–127. doi: 10.1104/pp.17.01429

Sandalio, L. M., Gotor, C., Romero, L. C., and Romero-Puertas, M. C. (2019). Multilevel regulation of peroxisomal proteome by post-translational modifications. *Int. J. Mol. Sci.* 20:4881. doi: 10.3390/ijms20194881

Sandalio, L. M., Rodríguez-Serrano, M., Romero-Puertas, M. C., and Del Río, L. A. (2013). "Role of peroxisomes as a source of reactive oxygen species (ROS) signalling molecules," in Peroxisomes and Their Key Role in Cellular Signalling and Metabolism. ed L. A. Del Río (Springer-Verlag, Germany), 231–256.

Sandalio, L. M., and Romero-Puertas, M. C. (2015). Peroxisomes sense and respond to environmental cues by regulating ROS and RNS signalling networks. *Ann. Bot.* 116, 475–485. doi: 10.1093/aob/mcv074

Schumann, U., Prestele, J., O'Geen, H., Brueggeman, R., Wanner, G., and Gietl, C. (2007). Requirement of the C3HC4 zinc RING finger of the Arabidopsis PEX10 for photorespiration and leaf peroxisome contact with chloroplasts. *Proc. Natl. Acad. Sci. U.S.A.* 104, 1069–1074. doi: 10.1073/pnas.0610402104

Sewelam, N., Jasper, T. N., Van Der Kelen, K., Tognetti, V., Schmitz, J., Frerigmann, H., et al. (2014). Spatial H_2O_2 signalling specificity: H_2O_2 from chloroplasts and peroxisomes modulates the plant transcriptome differentially. *Mol. Plant.* 7, 1191–1210. doi: 10.1093/mp/ssu070

Sinclair, A. M., Trobacher, C. P., Mathur, N., Greenwood, J. S., and Mathur, J. (2009). Peroxule extension over ER-defined paths constitutes a rapid subcellular response to hydroxyl stress. *Plant J.* 59, 231–242. doi: 10.1111/j.1365-313X.2009.03863.x

Su, T., Wang, P., Li, H., Zhao, Y., Lu, Y., Dai, P., et al. (2018). The Arabidopsis catalase triple mutant reveals important roles of catalases and peroxisome derived signalling in plant development. *J. Integr. Plant Biol.* 60, 591–607. doi: 10.1111/jipb.12649

Thazar-Poulot, N., Miquel, M., Fobis-Loisy, I., and Gaude, T. (2015). Peroxisome extensions deliver the Arabidopsis SDP1 lipase to oil bodies. *Proc. Natl. Acad. Sci. U.S.A.* 112, 4158–4163. doi: 10.1073/pnas.1403322112

Wang, L., Wang, C., Liu, Y., Cheng, J., Li, S., Zhu, J. K., et al. (2019). Peroxisomal β-oxidation regulates histone acetylation and DNA methylation in Arabidopsis. *Proc. Natl. Acad. Sci. U.S.A.* 116, 10576–10585. doi: 10.1073/pnas.1904143116

Yamauchi, S., Mano, S., Oikawa, K., Hikino, K., Teshima, K. M., et al. (2019). Autophagy controls reactive oxygen species homeostasis in guard cells that is essential for stomatal opening. *Proc. Natl. Acad. Sci. U.S.A.* 116, 19187–19192. doi: 10.1073/pnas.1910886116

Yoshimoto, K., Shibata, M., Kondo, M., Oikawa, K., Sato, M., et al. (2014). Organ specific quality control of plant peroxisomes is mediated by autophagy. *J. Cell Sci.* 127, 1161–1168. doi: 10.1242/jcs.139709

Abbreviations and acronyms

α: angle
%: percentage
°C: celsius
µg: microgram
µl: microliter
µm: microns
µM: micromolar
2 w: 2-week-old
2,4-D: 2,4-dichlorophenoxyacetic acid
ABA: abscisic acid
ABRC: Arabidopsis biological resource centre
ACC: aminocyclopropane-1-carboxylic acid
ACO: aconitase
ACX: acyl-CoA oxidase
ADP: adenosine diphosphate
AFB3: AUXIN SIGNALLING F-BOX 3
Al: aluminium
AOA: O-(carboxymethyl) hydroxylamine hemihydrochloride
AOX: alternative oxidase
APX: ascorbate peroxidase
ARFs: auxin response factors
As: arsenic
AsA/ASC: ascorbate
AT: 3-aminotriazole
ATSDR: agency for toxic substances and disease registry
AUX: auxins
BA: benzoic acid
BP: biological process
Ca: calcium
cAMP: cyclic adenosine monophosphate
CAT: catalase
CC: cellular component
Cd: cadmium
CFP: cyan fluorescent protein
cGMP: cyclic guanosine monophosphate
Chl: chlorophyll
CLSM: confocal laser scanning microscopy
cm: centimetre
CoA: coenzyme A
Col-0: Columbia-0
CPM: counts per million
CRISPR: clustered regularly interspaced short palindromic repeats
CSY: citrate synthase
CuAOs: Cu-diamine oxidases
Cys: cysteine
DAB: 3,3'-*diaminobenzidine*
DCF-DA: 2',7'-dichlorodihydrofluorescein diacetate
DEGs: genes differentially expressed
DHAR: dehydroascorbate reductase
DNA: deoxyribonucleic acid
DRPs: dynamin-related proteins
EDTA: ethylenediaminetetraacetic acid
EFSA: European Food Safety Authority
em: emission
ER: endoplasmic reticulum
ERF: ethylene-responsive transcription factors
ET: ethylene
ETC: electron transport chain
exc: excitation
FA: fatty acid
FAD: adenine dinucleotide
FBPs: F-box proteins
FC: fold change
FDR: false discovery rate
Fe: iron
FIS1: FISSION1 protein
FMN: flavin mononucleotide
Fw: forward
FW: fresh weight
g: grams
GA: gibberellic acid
GEBD: genome express browser server
GEO: gene expression omnibus
GGAT: glutamate: glyoxylate aminotransferase
GO: gene ontology
GOX: glycolate oxidase
GPX: glutathione peroxidase
GR: glutathione reductase
GSH: glutathione
GST: glutathione S-transferase
GUS: β-glucuronidase
h: hour
H_2O_2: hydrogen peroxide
HAOX: hydroxy acid oxidases
Hg: mercury
HL: high light
HPR1: hydroxypyruvate reductase 1
hpt: hour post treatment
HSFs: heat shock factors
HSPs: heat shock proteins
IAA: indole-3-acetic acid
IBA: indole-3-butyric acid
ICL: isocitrate lyase
IPTG: isopropyl-β-D-1-thiogalactopyranoside

JA: jasmonic acid
KAT: 3-ketoacyl-CoA thiolase
KEGG: Kyoto encyclopedia of genes and genomes
LB: Luria Bertani
LHC: light-harvesting chlorophyll protein complex
LP: left primer
LR: lateral roots
M: molar
MAPKs: mitogen-activated protein kinases
MDH: malate dehydrogenase
MDHAR: monodehydroascorbate reductase
MF: molecular function
mg: milligram
min: minute
ml: milliliter
MLS: malate synthase
mM: millimolar
Mn: manganese
MS: Murashige and Skoog medium
MV: methyl viologen
MVA: mevalonic acid
NADPH: nicotinamide adenine dinucleotide phosphate oxidases
NASC: Nottingham Arabidopsis stock centre
nm: nanometer
NO: nitric oxide
NOS: nitric oxide synthase
NT: not treated
O/N: overnight
OD: optical density
OPDA: 12-oxo-phytodienoic acid
OPPP: oxidative pentose phosphate pathway
OPR: OPDA reductase
PAs: polyamines
PAOs: flavin-polyamine oxidases
Pb: lead
PCD: programmed cell death
PCR: polymerase chain reaction
PEX: peroxin
PGD2: 6-phosphogluconate dehydrogenase 2
PGLP1: phosphoglycolate phosphatase
phy A: phytochrome A
pICDH: isocitrate de-hydrogenase
PMPs: peroxisomal membrane proteins
POXs: peroxidases
PPAR: peroxisome proliferator activator receptor
PPO: polyphenol oxidase
PRXs: peroxiredoxins
PS: photosystem
PTF: peroxisome transcriptional footprint
PTMs: posttranslational modifications
PTS: peroxisomal targeting signal
qRT-PCR: quantitative real time PCR
RBOH: respiratory burst oxidase homolog
RNA: ribonucleic acid
RNS: reactive nitrogen species
ROS: reactive oxygen species
RP: right primer
RPKM: reads per kilobase million
RT: room temperature
Rv: reverse
s: second
SA: salicylic acid
SEM: standard error of the mean
SGAT: serine: glyoxylate aminotransferase
SK: SALK
Skp: S-phase kinase-associated proteins
SO: sulfite oxidase
SOD: superoxide dismutase
T-DNA: transfer DNA
TAE: tris acetate-EDTA buffer
TAIR: the Arabidopsis information resource
TFs: transcription factors
TIR1/AFB: transport inhibitor response1/auxin signalling F-Box
TRXs: thioredoxins
UO: uricase
UPS: ubiquitin-proteasome system
UV: ultraviolet
v/v: volume/volume
WT: wild type
XOD: xanthine oxidase
XOR: xanthine oxidoreductase
YFP: yellow fluorescence protein
Zn: zinc

UNIVERSIDAD
DE GRANADA

CSIC
CONSEJO SUPERIOR DE INVESTIGACIONES CIENTÍFICAS

eez